frontiers | Research Topics

Fc-mediated antibody functions and Fc-receptor polymorphism

volume II

Edited by
Guido Ferrari, R. Keith Reeves, Gabriella Scarlatti, Margaret E. Ackerman and Amy W. Chung

Published in
Frontiers in Immunology

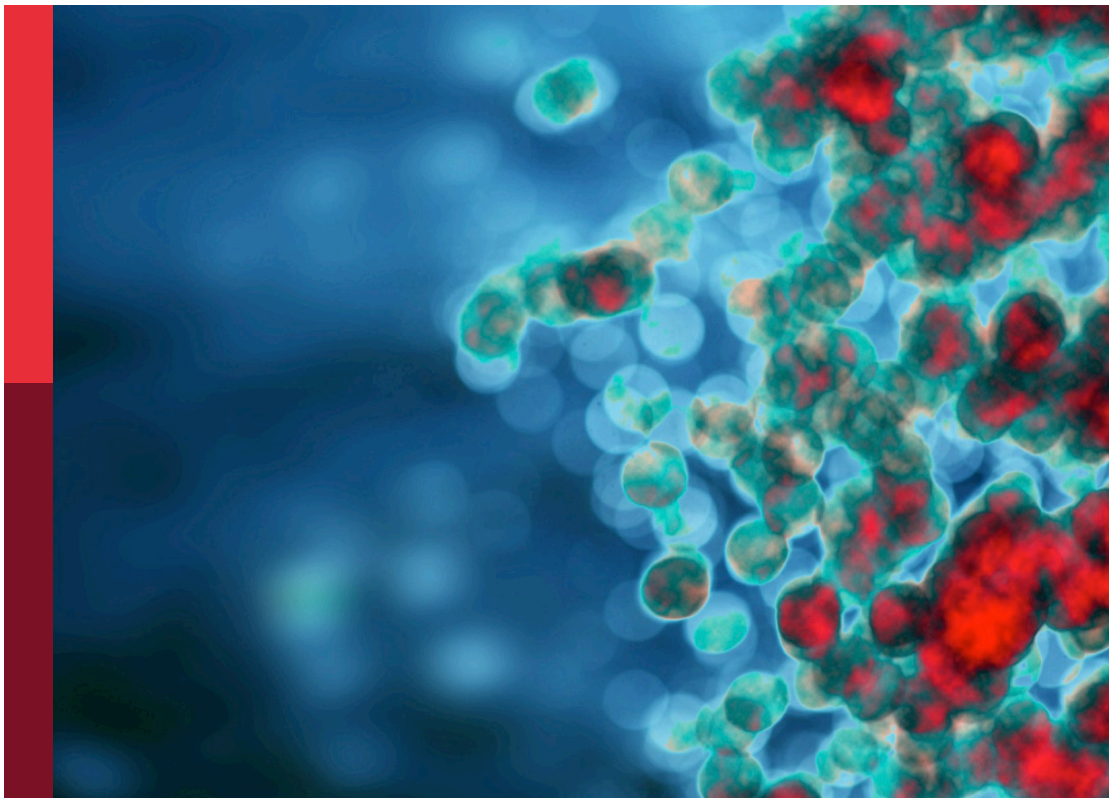

ISSN 1664-8714
ISBN 978-2-8325-2430-5
DOI 10.3389/978-2-8325-2430-5

About Frontiers

Frontiers is more than just an open access publisher of scholarly articles: it is a pioneering approach to the world of academia, radically improving the way scholarly research is managed. The grand vision of Frontiers is a world where all people have an equal opportunity to seek, share and generate knowledge. Frontiers provides immediate and permanent online open access to all its publications, but this alone is not enough to realize our grand goals.

Frontiers journal series

The Frontiers journal series is a multi-tier and interdisciplinary set of open-access, online journals, promising a paradigm shift from the current review, selection and dissemination processes in academic publishing. All Frontiers journals are driven by researchers for researchers; therefore, they constitute a service to the scholarly community. At the same time, the *Frontiers journal series* operates on a revolutionary invention, the tiered publishing system, initially addressing specific communities of scholars, and gradually climbing up to broader public understanding, thus serving the interests of the lay society, too.

Dedication to quality

Each Frontiers article is a landmark of the highest quality, thanks to genuinely collaborative interactions between authors and review editors, who include some of the world's best academicians. Research must be certified by peers before entering a stream of knowledge that may eventually reach the public - and shape society; therefore, Frontiers only applies the most rigorous and unbiased reviews. Frontiers revolutionizes research publishing by freely delivering the most outstanding research, evaluated with no bias from both the academic and social point of view. By applying the most advanced information technologies, Frontiers is catapulting scholarly publishing into a new generation.

What are Frontiers Research Topics?

Frontiers Research Topics are very popular trademarks of the *Frontiers journals series*: they are collections of at least ten articles, all centered on a particular subject. With their unique mix of varied contributions from Original Research to Review Articles, Frontiers Research Topics unify the most influential researchers, the latest key findings and historical advances in a hot research area.

Find out more on how to host your own Frontiers Research Topic or contribute to one as an author by contacting the Frontiers editorial office: frontiersin.org/about/contact

Fc-mediated antibody functions and Fc-receptor polymorphism volume II

Topic editors

Guido Ferrari — Duke University, United States
R. Keith Reeves — Duke University, United States
Gabriella Scarlatti — San Raffaele Hospital (IRCCS), Italy
Margaret E. Ackerman — Dartmouth College, United States
Amy W. Chung — The University of Melbourne, Australia

Citation

Ferrari, G., Reeves, R. K., Scarlatti, G., Ackerman, M. E., Chung, A. W., eds. (2023). *Fc-mediated antibody functions and Fc-receptor polymorphism volume II*. Lausanne: Frontiers Media SA. doi: 10.3389/978-2-8325-2430-5

Table of contents

frontiers in Immunology

ORIGINAL RESEARCH
published: 20 May 2021
doi: 10.3389/fimmu.2021.678511

Functional Homology for Antibody-Dependent Phagocytosis Across Humans and Rhesus Macaques

Justin Pollara[1,2], Matthew Zirui Tay[2†], R. Whitney Edwards[2], Derrick Goodman[2], Andrew R. Crowley[3], Robert J. Edwards[2], David Easterhoff[2†], Haleigh E. Conley[2†], Taylor Hoxie[2†], Thaddeus Gurley[2], Caroline Jones[2], Emily Machiele[2], Marina Tuyishime[1], Elizabeth Donahue[2], Shalini Jha[2], Rachel L. Spreng[2], Thomas J. Hope[4], Kevin Wiehe[2], Max M. He[2], M. Anthony Moody[2], Kevin O. Saunders[1,2], Margaret E. Ackerman[3], Guido Ferrari[1,2‡] and Georgia D. Tomaras[1,2‡]*

[1] Department of Surgery, Duke University School of Medicine, Durham, NC, United States, [2] Human Vaccine Institute, Duke University School of Medicine, Durham, NC, United States, [3] Thayer School of Engineering, Dartmouth College, Hanover, NH, United States, [4] Department of Cell and Developmental Biology, Feinberg School of Medicine, Northwestern University, Chicago, IL, United States

Analyses of human clinical HIV-1 vaccine trials and preclinical vaccine studies performed in rhesus macaque (RM) models have identified associations between non-neutralizing Fc Receptor (FcR)-dependent antibody effector functions and reduced risk of infection. Specifically, antibody-dependent phagocytosis (ADP) has emerged as a common correlate of reduced infection risk in multiple RM studies and the human HVTN505 trial. This recurrent finding suggests that antibody responses with the capability to mediate ADP are most likely a desirable component of vaccine responses aimed at protecting against HIV-1 acquisition. As use of RM models is essential for development of the next generation of candidate HIV-1 vaccines, there is a need to determine how effectively ADP activity observed in RMs translates to activity in humans. In this study we compared ADP activity of human and RM monocytes and polymorphonuclear leukocytes (PMN) to bridge this gap in knowledge. We observed considerable variability in the magnitude of monocyte and PMN ADP activity across individual humans and RM that was not dependent on FcR alleles, and only modestly impacted by cell-surface levels of FcRs. Importantly, we found that for both human and RM phagocytes, ADP activity of antibodies targeting the CD4 binding site was greatest when mediated by human IgG3, followed by RM and human IgG1. These results demonstrate that there is functional homology between antibody and FcRs from these two species for ADP. We also used novel RM IgG1 monoclonal antibodies engineered with elongated hinge regions to show that hinge elongation augments RM ADP activity. The RM IgGs with engineered hinge regions can achieve ADP activity comparable to that observed with human IgG3. These novel modified antibodies will have utility in passive immunization studies aimed at defining the role of IgG3 and ADP in protection from virus challenge or control of disease in RM models. Our results contribute to a better translation of human and macaque antibody and FcR biology, and may help to improve testing accuracy and evaluations of future active and passive prevention strategies.

Keywords: phagocytosis, Fc Receptor, rhesus macaques, antibody function, IgG3

OPEN ACCESS

Edited by:
Fabrizio Ceciliani, University of Milan, Italy

Reviewed by:
Stephen Kent, The University of Melbourne, Australia
Rajeev Gautam, National Institutes of Health (NIH), United States
Silvia Ratto Kim, International Vaccine Institute, South Korea
Simone Irene Richardson, National Institute of Communicable Diseases (NICD), South Africa
Gerrit Koopman, Biomedical Primate Research Centre (BPRC), Netherlands

***Correspondence:**
Justin Pollara
justin.pollara@duke.edu

†Present address:
*Matthew Zirui Tay, Singapore Immunology Network, Agency for Science, Technology and Research (A*STAR), Singapore, Singapore*
David Easterhoff, Moderna Incorporated, Cambridge, MA, United States
Haleigh E. Conley, Department of Clinical Sciences, College of Veterinary Medicine, North Carolina State University, Raleigh, NC, United States
Taylor Hoxie, Nicholas School of the Environment, Duke University, Durham, NC, United States

‡These authors have contributed equally to this work

Specialty section:
This article was submitted to Comparative Immunology, a section of the journal Frontiers in Immunology

Received: *09 March 2021*
Accepted: *28 April 2021*
Published: *20 May 2021*

INTRODUCTION

Fc receptors (FcRs) are cell surface proteins that interact with the Fc domains of antibodies to mediate cell signaling and effector functions (1, 2). Results of immune correlates analyses for the RV144 and HVTN505 clinical trials and preclinical vaccine studies conducted in rhesus macaques (RMs) have identified associations between non-neutralizing FcR-dependent antiviral activities of antibodies and reduced risk of HIV/SHIV infection or control of viremia (3–15). Among the myriad of potential FcR-dependent effector functions, antibody-dependent phagocytosis (ADP) of HIV-1/SIV envelope (Env) protein or virions has emerged as a unifying correlate of reduced infection risk in several vaccine studies conducted in RMs (3, 4, 6, 8), and in *post-hoc* analysis of the human HVTN505 HIV-1 vaccine efficacy trial (16). Despite this commonality, it remains unknown how effectively ADP activity observed in the RM model can predict that in humans.

Outcomes of a signaling event between antibody–antigen immune complexes and FcR are impacted by genetically-determined characteristics of the antibody including isotype, subclass, and allele, as well as characteristics of the FcR such as type, expression level, allele, and isoform (17). In addition, the composition of glycans on the antibody Fc and FcR also impacts interactions between immune complexes and FcR, providing a non-genetic level of control for signaling (18, 19). The downstream cellular response is largely dependent on the type of cell interacting with the immune complex. FcRs are variably expressed on the surface of different types of leukocytes and are therefore among the many clusters of differentiation that are used to define specific types of immune cells. Leukocytes can simultaneously express both activating and inhibitory FcRs, and the balance of these divergent signal pathways is critical to regulation of each potential effector response (1, 20). Although closely related, there are many differences in Fc/FcR biology between humans and RM including antibody subclass diversity (17), antibody structures (21–23), FcR genetic diversity (21, 22), Fc–FcR biophysical interactions (24–26), and cellular expression of FcR (23, 27–29). Thus, there is a need for direct comparisons of ADP between humans and RM to improve our understanding of how to most effectively use and translate results from this important animal model to future human interventions.

In this study, we compared the ADP activity of phagocytes from humans and RM using a panel of monoclonal antibodies (mAbs) specific for the CD4-binding site (CD4bs) of the HIV-1 Env protein that were recombinantly produced as different isotypes and subclasses. Peripheral blood monocytes and polymorphonuclear leukocytes (PMN) were used as sources of phagocytes. Our data demonstrated that, for both human and RM phagocytes, *in vitro* ADP activity was greatest when mediated by human IgG3, followed by RM IgG1, and then human IgG1. ADP activity among the tested antibody isotypes and subclasses was lowest, and often not detectable, when mediated by human IgA mAbs. We also observed considerable variability in the magnitude of monocyte and PMN ADP activity across individual humans and RMs. We found that these differences in human and RM ADP activity were not dependent on FcR alleles, and only modestly impacted by cell-surface levels of FcRs. Notably, we also describe production and characterization of novel RM IgG1 engineered with elongated hinge regions, and demonstrate that elongation of the RM IgG1 hinge to lengths similar to those of human IgG3 improves ADP activity mediated by RM monocytes and PMN. Our data contributes to the creation of a roadmap for effective translation of Fc–FcR biology across species that is needed to effectively evaluate non-neutralizing antibody effector functions in RMs and to make accurate predictions of human outcomes from preclinical studies. Moreover, the novel hinge variant antibodies we describe are expected to be useful surrogates for evaluating the protective or therapeutic potential of IgG3 antibodies of clinical interest in the preclinical RM model.

MATERIALS AND METHODS

Study Samples and Reagents

Peripheral Blood Collection

Peripheral blood was collected by venipuncture, under sedation, from healthy adult RM at the Duke University School of Medicine, prior to allocation into any interventional research study in accordance with a protocol approved by the Duke University Institutional Animal Care and Use Committee. Human peripheral blood samples were collected by venipuncture of healthy consenting adult volunteers in accordance with a protocol approved by the Duke Health Institutional Review Board. Human and RM blood was collected into Acid Citrate Dextrose Vacutainer tubes (BD Biosciences, San Jose, CA) and processed within 4 hours of collection.

Isolation of Monocytes From Human and RM Peripheral Blood

Monocytes were isolated from the peripheral blood mononuclear cell (PBMC) fraction of fresh peripheral blood. PBMC were isolated using density gradient centrifugation with Ficoll-Paque PLUS (GE Healthcare Life Sciences, Pittsburg, PA). Monocytes were enriched from RM and human PBMC by positive selection using species-specific CD14 magnetic microbeads (Miltenyi Biotec) according to the manufacturer's recommended protocol.

Isolation of PMN From Human and RM Peripheral Blood

Red blood cells were lysed from fresh whole blood using Red Blood Cell Lysis Solution (Miltenyi Biotec, Bergisch Gladbach, Germany). A PMN-enriched cell population was isolated from red blood cell-depleted blood by positive selection of granulocytes using anti-CD66abce magnetic microbeads (Miltenyi Biotec) (30) according the manufacturer's recommended protocol.

Human and Rhesus-ized Monoclonal Antibody (mAb) Production

Human mAbs specific for the CD4bs site of HIV-1 Env, CH31 (31), and VRC01 (32), were expressed as human IgG1, IgG3 (IGHG3*01

allele), IgA1, IgA2, and RM IgG1 by transient cotransfection of heavy and light chain plasmids into Expi293-F cells with Expifectamine (Thermo Fisher Scientific, Waltham, MA). Secreted antibody was purified from cell culture supernatants by protein A or G resin columns as previously described (33, 34). The influenza specific CH65 mAb (35) produced as human IgG1, IgG3, IgA1, and IgA2 were used as negative controls for experiments with human antibodies. For experiments with RM IgG1, the V1V2-specific mAb HG107 (11) was produced as RM IgG1 (described below) and used as a negative control as this antibody does not bind to V1V2 of the subtype B Bal Env. The quality of all recombinant mAbs was evaluated using reduced and non-reduced SDS-PAGE followed by Coomassie stain or Western blot.

Rhesus-ization of antibodies was performed as previously described with some modifications (34). To generate VRC01 with a RM constant region, the human gamma constant region and kappa light chain constant region were exchanged for rhesus IgG1 constant regions (34). To produce rhesus-ized CH65 antibody the unmutated common ancestor antibody that gave rise to the human antibody lineage was first inferred using Cloanalyst (36). Using the inferred human germline antibody sequence, the macaque gene segments with the highest sequence homology were identified by searching the macaque library in Cloanalyst. All three affinity-matured complementarity-determining regions (CDRs) of the CH65 human heavy chain variable region (VH) or light chain variable region (VL) were grafted into the inferred macaque germline genes (**Supplemental Figure S1**). These variable regions were then attached to RM constant regions to form full-length immunoglobulin chains. The sequences were codon optimized using GeneOptimizer (GeneArt), synthesized *de novo* (GenScript, Piscataway, NJ), and expressed as described above.

RM IgG1 variants with extended hinges were designed with sequential repeats (0X, 1X, 2X, 3X and 4X) of the 18 amino acid (AA) RM hinge region between the CH1 and CH2 domains of RM IgG1. Antibody genes were synthesized (GenScript) similar to that previously described for human IgG1 and IgG3 (37). These antibodies were expressed and purified as described above.

Laboratory Methods

Monocyte Antibody-Dependent Phagocytosis (ADP) Assay

Monocyte ADP of fluorescently-labeled HIV-1 BaL virions (38–40) was measured as previously described (41). Briefly, 10 µL of fluorescent RFP-labeled HIV-1 BaL virions were mixed with 10 µL of recombinant human and RM monoclonal antibodies (mAbs) at a final concentration of 25 µg/mL for 2 hours at 37°C in round-bottom 96 well plates (Corning Life Sciences, Durham, NC) to permit formation of immune complexes. Monocytes isolated from human or RM peripheral blood were counted using a Muse Cell Analyzer (Milipore Sigma, Burlington, MA), and added to the immune-complex containing wells at 60,000 viable cells per well in 20 µL RPMI-1640 media supplemented with 10% FBS. Plates were sealed, shaken at 750 RPM, and centrifuged for 1 hour at 1200 x g in a 4°C centrifuge. After centrifugation, the plate seal was removed and the plate was incubated for 1 hour at 37°C in a 5% CO_2 atmosphere before being washed in 1% FBS PBS (wash buffer, WB), and fixed with a 4% formaldehyde PBS solution. Data acquisition and data analysis were performed as previously described (41), using a BD LSRFortessa flow cytometer and FlowJo Software (v9.9.6, BD Biosciences). The cytometer has been optimized and maintained using quality control procedures described by Perfetto and colleagues (42). ADP activity is presented as the phagocytosis score, calculated by percentage of cells positive × median fluorescence intensity (MFI), normalized by division with the corresponding result for the no-antibody control. An example of ADP assay data and calculation of scores is included as **Supplemental Figure S2**. Assays were performed in duplicate for each animal.

PMN Antibody-Dependent Phagocytosis (ADP) Assay

For PMN ADP of fluorescently-labeled HIV-1 subtype B BaL virions, immune complexes were formed as described as above. PMN isolated from human or RM peripheral blood were added to immune-complexes in 96-well plates at 60,000 viable cells per well in 200 µL RPMI-1640 media supplemented with 10% FBS and 1% HEPES. The plates were incubated at room temperature for 15 minutes, then centrifuged at room temperature for 1 minute at 300 x g, followed by a 1 hour incubation at 37°C in a 5% CO_2 atmosphere. Plates were then washed, fixed, acquired, and analyzed as described previously (41), and above.

Binding and Affinity to FcRs

The affinity of Fcγ receptors (FcγR) for our IgG mAbs was measured as previously described (25). Briefly, a Continuous Flow Microspotter (CFM, Carterra, Salt Lake City, UT) and carbodiimide chemistry was used to immobilize the antibodies on a medium density carboxymethyldextran sensorchip (Xantec Bioanalytics, Düsseldorf, DEU). An 8-point series of 1:3 dilution of the receptor beginning at 20 µM was then flowed over the sensor surface and the association and dissociation were measured for 5 minutes each using an imaging-based surface plasmon resonance (SPRi) instrument (MX96, IBIS Technologies, Pantheon 5, NLD). The results were analyzed in Scrubber 2 (BioLogic Software, Campbell Australia) using a steady state model to determine the equilibrium dissociation constants.

Quantification of FcRs on the Surface of Human and RM Monocytes and PMN

Frequencies of FcR-bearing effector cells and quantification of the amount of FcR on cell surfaces was determined by immunofluorescence staining of fresh whole blood. Briefly, 100 µL of human or RM peripheral blood was incubated at room temperature, protected from light, for 25 minutes with the following combination of fluorescently conjugated monoclonal antibodies: PE-CF594-CD3 (clone SP34-2, BD Biosciences); PE-

CF594-CD20 (clone 2H7, BD Biosciences); APC-Cy7-CD14 (clone MϕP9, BD Biosciences); PacificBlue-CD16 (clone 3G8, BD Biosciences); APC-CD32 (clone FL18.26, BD Biosciences); Alexa Fluor 700-CD64 (clone 10.1, BD Biosciences); PE-CD89 (clone A59, BD Biosciences); PerCP-Vio700-CD66 (clone TET2, Miltenyi Biotec); PE-Cy7-CD11b (clone ICRF44, Biolegend); FITC-CD62L (clone SK11, BD Biosciences); and PE-Cy5-CD49d (clone 9F10, BD Biosciences). After incubation, 2 mL of BD Pharm Lyse solution (BD Biosciences) was added to each tube, and incubated for 15 minutes at room temperature to lyse red blood cells. Leukocytes were subsequently pelleted by room temperature centrifugation for 5 minutes at 500 x g. The cell pellet was then washed with buffered saline and stained with a viability marker (Fixable Aqua Dead Cell Stain Kit, Thermo Fisher Scientific, Waltham, MA) for 20 minutes at room temperature. After two washes with 2 mL WB the cells were fixed in 1% paraformaldehyde buffer prior to data acquisition using our BD LSRFortessa flow cytometer. Quantum™ Simply Cellular® beads (Bangs Laboratories, Inc., Fishers, Indiana) were used to determine the antibody binding capacity (ABC) of FcR on the surface of cells according the manufacturers recommended procedure. Data analyses were performed using FlowJo software (v9.9.6, BD Biosciences).

FcR Sequence Analysis

FcR sequence analysis was performed using long-read RNA sequencing. RNA and genomic DNA were isolated from human and RM PBMC samples using the AllPrep DNA/RNA isolation kit (Qiagen, Germantown, MD). RNA was reverse transcribed using the Qiagen QuantiTect Reverse Transcription Kit (Qiagen) and FcγR gene-specific primers designed with PacBio barcodes (Pacific Biosciences, Menlo Park, CA). PCR products were purified using ZR-96 DNA clean and Concentrator™-5 (Zymo Research) following manufacturer's protocol. PacBio SMRTbell library preparation was performed in accordance with manufacturer's recommendations (Pacific Biosciences) and equal concentrations of ~30 amplicons were pooled and loaded onto a single SMRT cell as determined by Qubit quantification (ThermoFisher Scientific). Sequencing was performed on a PacBio Sequel II instrument using 2.1 or 3.0 chemistry (Pacific Biosciences). Datasets were loaded into PacBio SMRT Link 7.0.1 software package for demultiplexing of subreads and generating circular consensus sequences (CCS). And quality control was assessed by analyzing productivity and sequence read length before and after trimming. Data analysis was conducted using a pipeline similar to that previously described (43). Each unique CCS was aligned to GenBank deposited reference sequences using a long-read sequence alignment tool (44) and variants were identified using the GATK Haplotype Caller (45), and annotated with ANNOVAR (46).

Negative Stain Electron Microscopy

Antibody samples were diluted to 20 µg/ml with buffer containing 150 mM NaCl, 0.014 g/dL ruthenium red, and 20 mM HEPES buffer, pH 7.4, and incubated at room temperature for at least one hour. A 5-µl drop of diluted antibodies were applied to a glow-discharged carbon film covered 300 mesh copper EM grid and incubated 10 seconds, blotted with filter paper, rinsed with a 5 µl drop of buffer containing 7.5 mM NaCl and 1 mM HEPES, pH 7.4, for ~7 seconds, blotted and then stained with 0.6% uranyl formate for 1 minute. Excess stain was blotted and the grids were allowed to air dry. Grids were imaged in a Philips EM420 electron microscopy at 120 kV and 82,000x, and 60-80 images per sample with ~1000 particles per image were captured with a 2k x 2k CCD camera at a pixel size of 4.02 Å/pixel. Images were imported into the Relion software package and 2D class averages were calculated by standard methods (47).

SHIV-Infection of A66 Cells

SHIV.Bal(P4) virus stocks (48) grown in human PBMCs were titrated to determine the input required for optimal viral gene expression within 72 h post-infection of A66 cells as measured by intracellular p27 expression (WNPRC Immunology Services). A66 cells (provided by Dr. James Hoxie, University of Pennsylvania, Philadelphia, PA) are SupT1 cells (non-BC7 variant (49)) that have been stably transfected to express both rhesus CD4 and rhesus CCR5 receptors after knockout of endogenous human CXCR4 and CD4 (50). SHIV.BaL(P4) was used to infect 1×10^6 A66 cells by incubation with 24 ng/mL of p27 for 4 hours at 37°C and 5% CO_2 in the presence of DEAE-Dextran (10 µg/mL, Sigma Aldrich). The cells were subsequently resuspended at 0.33×10^6/mL and cultured for 3 days in complete medium containing 10 µg/mL DEAE-Dextran. On assay day, infection was monitored by measuring the frequency of cells expressing intracellular p27. The assays performed using the SHIV-infected target cells were considered reliable if the percentage of viable p27+ target cells on assay day was ≥10%. Assay data generated using infected cells was normalized to the frequency of live target cells positive for intracellular p27.

Infected Cell Antibody Binding Assay (ICABA)

ICABA was used to evaluate the ability of RM IgG hinge variant mAbs to bind Env on the surface of SHIV-infected cells. SHIV-infected A66 cells were obtained as described above. Cells incubated in the absence of virus (mock infected) were used as a negative control. Infected and mock infected cells were washed in PBS, dispensed into 96-well V-bottom plates at 2 x 10^5 cells/well and incubated with 1 µg/mL of indicated mAbs for 2 hours at 37°C. After two washes with 250 µL/well WB, the cells were stained with vital dye (Live/Dead Fixable Aqua Dead Cell Stain, Invitrogen) to exclude nonviable cells from subsequent analysis. Cells were washed with WB and stained with anti-CD4-PerCP-Cy5.5 (clone Leu-3; BD Biosciences) to a final dilution of 1:20 in the dark for 20 min at room temperature (RT). Cells were then washed again, and permeabilized using Cytofix/Cytoperm (BD Biosciences). Anti-p27 antibody (WNPRC Immunology Services, 1:500 dilution in 1x Cytoperm Solution, BD Biosciences) and a secondary PE-conjugated antibody (goat anti-human Ig Fc-PE, eBioscience, San Diego, CA., final

dilution of 1:400) were added to each well and incubated in the dark for 25 min at 4°C. Cells were washed three times with Cytoperm wash solution and resuspended in PBS-1% paraformaldehyde. The samples were acquired within 24 hours using a BD Fortessa cytometer. A minimum of 50,000 total events was acquired for each analysis. Gates were set to include singlet and live events. Data analysis was performed using FlowJo 9.6.6 software (BD Biosciences). Final data represents the PE MFI of binding of IgG mAbs to HIV Env, after normalization by subtraction of the PE MFI observed for cells stained with the secondary antibody alone. Assays were repeated twice and the average of the results is shown.

Antibody-Dependent Cell-Mediated Cytotoxicity (ADCC)

We used an infected cell elimination assay to measure ADCC activity of RM IgG hinge variant mAbs. SHIV-infected or mock-infected A66 cells were used as targets and NHP PBMCs rested overnight in R10 were used as a source of effector cells. On assay day, infected and uninfected target cells were washed in R10 and labelled with a fluorescent target-cell marker (TFL4; OncoImmunin) and a viability marker (NFL1; OncoImmunin) for 15 min at 37°C, as specified by manufacturer. Cells were washed in R10 and adjusted to a concentration of 0.2 x 10^6 cells/mL. PBMCs were then added to target cells at an effector/target ratio of 60:1 (12 x 10^6 cells/mL). The target/effector cell suspension was plated in V-bottom 96-well plates and co-cultured with each mAb at the starting concentration of 50 µg/mL with subsequent three dilutions at 1:10. Co-cultures were incubated for 6 hours at 37°C in 5% CO_2. After the incubation period, cells were washed and stained with anti-CD4-PerCP-Cy5.5 (BD Biosciences, clone Leu-3) at a final dilution of 1:20 in the dark for 20 min at RT. After washing with WB, cells were resuspended in 100 µL/well Cytofix/Cytoperm (BD Biosciences), incubated in the dark for 20 min at 4°C, washed in 1x Cytoperm wash solution (BD Biosciences) and co-incubated with anti-p27 antibody (WNPRC Immunology Services) to a final dilution of 1:500, and incubated in the dark for 25 min at 4°C. Three washes were performed with Cytoperm wash solution before resuspending the cells in 125 µL PBS-1% paraformaldehyde for acquisition. The samples were acquired within 24 h using a BD Fortessa cytometer. The appropriate compensation beads were used to compensate the spill over signal for the four fluorophores. Data analysis was performed using FlowJo 9.6.6 software (TreeStar). Mock-infected cells were used to appropriately position live cell p27+/- gates. Specific killing was determined by the reduction in % of p27+ cells in the presence of mAbs after taking into consideration non-specific killing according to the following formula: percent specific killing = [(Frequency of p27 positive cells in wells containing targets and effectors alone − Frequency of p27 positive cells in wells containing targets and effectors with antibodies)/Frequency of p27 positive cells in wells containing targets and effectors alone] ×100. CH65 (anti-influenza mAb) produced as human and RM IgG1 were used as negative controls. Assays were repeated twice and final data represents the mean and range of results.

Statistical Analysis

All statistical analysis was performed using SAS software (version 9.4; SAS Institute Inc., Cary, N.C.). Kruskal Wallis tests were used to compare response magnitudes between groups. In order to assess if two groups had different responses pairwise comparisons between groups were conducted using Wilcoxon rank sum tests. A p-value of less than 0.05 was considered to be statistically significant. Spearman's rank correlation coefficient was used to assess correlation between ADP activities of different antibody isotypes and the amount of cell-surface FcR.

RESULTS

HIV-1 Virion ADP Activity of Human and RM Monocytes and PMN From Peripheral Blood

Although associations between vaccine-elicited ADP responses and reduced infection risk have been observed in multiple preclinical vaccine studies conducted in RM (3, 4, 6, 8) and in the HVTN505 HIV-1 vaccine efficacy trial (16), it remains unknown how effectively ADP activity in the RM model can predict that of humans. To address this limitation, we compared the ADP activity of RM and human monocytes and PMNs using anti-HIV-1 CD4 binding site-specific mAbs CH31 and VRC01. Standard recombinant production techniques (33) were used to produce the mAbs as human IgG1, IgG3, IgA1, and IgA2. To test the function of the rhesus constant region, the human heavy and kappa light chain constant regions of VRC01 were exchanged for rhesus IgG1 constant regions (called RM VRC01 IgG1 hereafter) (34). We allowed the antibodies to interact with fluorescent HIV-1 BaL virions to form immune complexes, which were then incubated with monocytes or PMN isolated from peripheral blood of 23 RM or 23 healthy human donors. The anti-influenza mAb CH65 (35) and the HIV-1 V1V2 mAb HG107 (11) were used as negative controls as neither mAb was expected to specifically bind the HIV-1 subtype B BaL virions used in these experiments. ADP of fluorescent virions was detected by flow cytometry, and was reported as a score ratio (41). In virion ADP assays performed with peripheral blood monocytes (**Figure 1A**), we observed no significant differences (Wilcoxon $p>0.05$) in ADP activity of human and RM monocytes for phagocytosis mediated by any of the antibodies tested with the exception of CH31 IgA. CH31 IgA1 ADP with human monocytes was higher than that observed with RM monocytes (Wilcoxon $p<0.001$, **Figure 1A**). As shown in **Figure 1B**, we found that ADP activity of RM PMN was significantly higher (Wilcoxon $p<0.001$) than that observed for human PMN when mediated by CH31 and VRC01 IgG1, CH31 IgG3, and RM VRC01 IgG1. Despite these differences in the magnitudes of ADP activity, we observed a

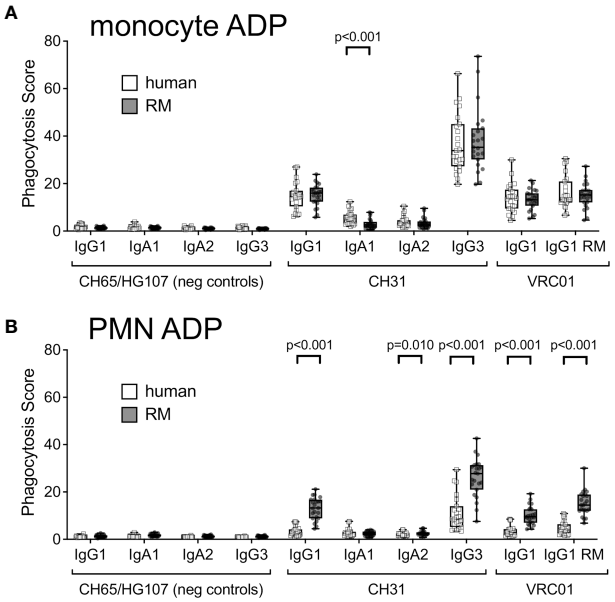

FIGURE 1 | ADP of immune complexes formed with fluorescent HIV-1 BaL virions and human or RM monoclonal antibodies, as indicated, in assays performed using **(A)** monocytes, and **(B)** PMN, isolated from peripheral blood of 23 humans (white boxes, square symbols) or 23 RM (gray boxes, round symbols), as sources of phagocytes. Box plots represent the interquartile ranges, horizontal lines indicate the medians, and error bars represent the range.

similar rank order of ADP activity for different antibody isotypes and subclasses, regardless of whether assays were performed with human or RM monocytes or PMN. For human and RM phagocytes, ADP activity was greatest when mediated by human CH31 IgG3, followed by RM VRC01 IgG1 and human CH31 or VRC01 IgG1 (Wilcoxon p<0.001 for human IgG3 versus RM or human IgG1); and was lowest when mediated by human CH31 IgA mAbs. These results demonstrate that although there are differences in the absolute magnitude of ADP activity when comparing human and RM phagocytes, there is functional homology across these two species for ADP activity irrespective of species mismatch between antibody and FcRs. Thus, we observed conservation of relative functional profiles between humans and RM for the types of antibodies tested.

Correlation of Human and RM ADP Activity Across Antibody Isotypes and Subclasses

As shown in **Figure 1**, we found that there was considerable variability in the magnitude of monocyte and PMN ADP activity across individual humans and RMs. We therefore used Spearman correlation testing to determine if ADP activity was correlated across antibody isotypes and subclasses to determine if phagocyte ADP activity was relatively high or low regardless of the composition of the immune complex involved. A representative scatter plot showing correlation of CH31 IgG1 and IgG3 ADP activities in assays performed with human monocytes is shown in **Figure 2A**. We found significant (Spearman p<0.05, r>0.5) positive correlations for ADP assays performed with human and RM monocytes (**Figures 2B, C**, respectively). Correlations were strongest when comparing subclasses within the IgG or IgA isotypes, and were weaker when comparing between IgG and IgA isotypes. We also observed significant (Spearman p<0.05, r>0.5) positive correlations for ADP assays performed with human and RM PMN (**Figures 2D, E**, respectively) across all ADP-mediating antibody isotypes and subclasses. Correlations were not evaluated for PMN ADP with CH31 IgA1 or IgA2 for humans (**Figure 2D**) and RM (**Figure 2E**) due to the majority of activities being similar to that observed with negative control IgA antibodies (**Figure 1B**). These analyses suggest that relative differences in ADP activity observed for individual humans and RM is related to the phagocytic propensity of the cells obtained from each blood donor, and is conserved across antibody isotype or subclass. Based on these results, we next sought to identify characteristics of RM and human peripheral blood phagocytes that contribute to differences in ADP activity across individuals.

Impact of *FCGR2A* Allelic Diversity on ADP Activity of Human and RM Peripheral Blood Monocytes and PMN

FcγRIIa has been previously implicated in IgG-mediated ADP of antibody responses against HIV-1 (16, 51–54). Single nucleotide polymorphisms (SNPs) in the human *FCGR2A* gene (which encodes FcγRIIa) affecting an amino acid within the IgG contact region result in FcγRIIa allelic variants with lower (R131) or higher (H131) relative affinities for IgG (26). To determine if these SNPs contributed to the differences in human monocyte (**Figure 3A**) and PMN (**Figure 3B**) ADP activity observed across individual human donors, we stratified the results of testing with CH31 IgG3 and IgG1 mAbs by homozygosity for the high affinity H131 allele (H/H, n=5 donors), homozygosity for the low affinity R131 allele (R/R, n=8 donors), and heterozygosity (H/R, n=10 donors). We found no significant differences (Wilcoxon p>0.05) in IgG3 or IgG1 ADP activity when comparing between donor groups separated by *FCGR2A* alleles. Thus, these data indicate that SNPs that have an effect on the affinity of human FcγRIIa did not significantly impact the *in vitro* ADP activity of human monocytes and PMN in these experiments and therefore do not explain the differences we observed for ADP activity across individual humans. We next performed a similar analysis for RM phagocytes. Due to limitations in available cells for genotyping, we were only able to define the *FCGR2A* alleles of 6 of the 23 RM included in our cohort. One SNP within the IgG contact region was identified within these RM. Three animals had a potential N-linked glycosylation site at position 128 (N128), and the other three did not (K128). We found no consistent trend that would

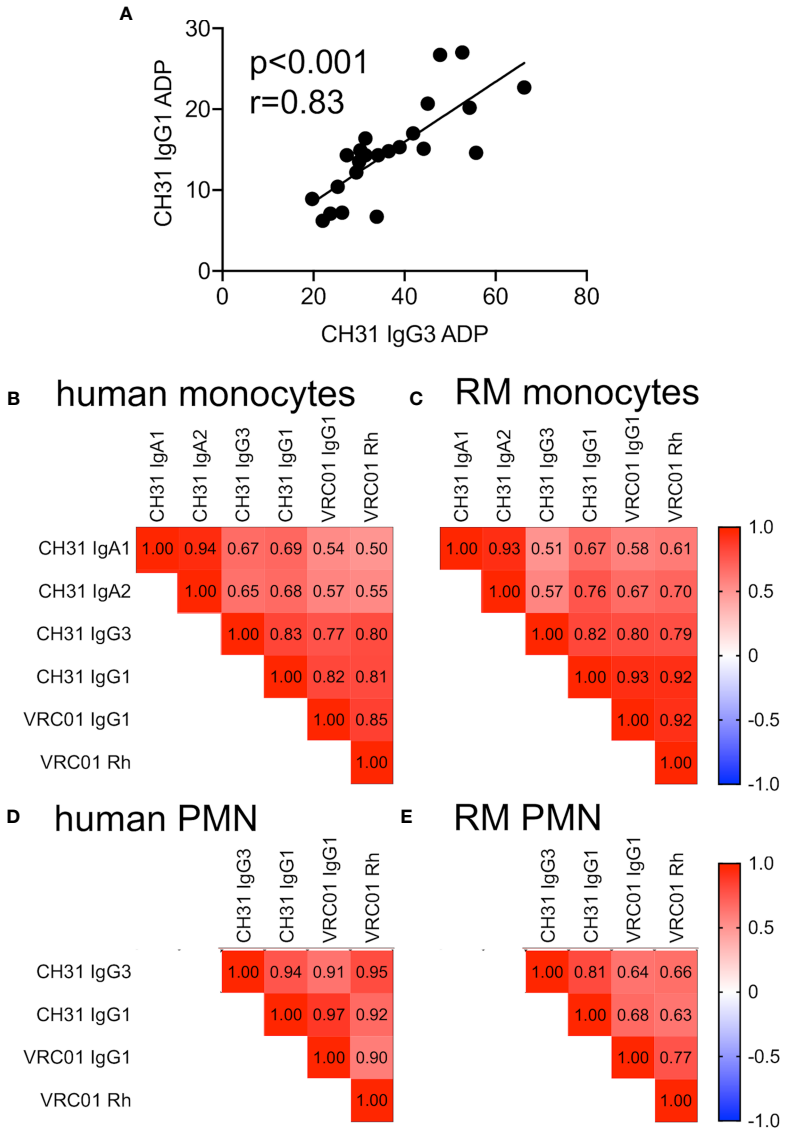

FIGURE 2 | **(A)** Correlation of CH31 IgG1 and IgG3 ADP activities in assays performed with human monocytes (n=23). (**B–E**) Heatmaps of Spearman correlation coefficients (r values) for ADP activities of indicated antibody isotypes in assays performed with **(B)** human monocytes, **(C)** RM monocytes, **(D)** human PMN, and **(E)** RM PMN. IgA correlations were omitted for neutrophil ADP due to the majority of responses being similar to negative controls. The p values for all Spearman correlations are all ≤0.01.

provide evidence of the amino acid composition at position 128 influencing stratification for IgG1 and IgG3 ADP activity of RM monocytes, but we did observe a trend for reduced ADP among RM PMN with N128 (**Figure 3C**).

Impact of Cell-Surface Abundance of FcRs on ADP Activity of Human and RM Peripheral Blood Monocytes and PMN

We next sought to determine if the amount of FcRs on the surface of human and RM monocytes and PMN correlate with ADP activity. We used flow cytometry phenotyping and fluorescent quantitation beads to detect and measure cell surface expression of FcRs. As shown in **Figure 4A**, human and RM monocytes express similar types of cell-surface FcRs; however, we observed significant differences in the levels of FcR expressed per cell. Levels of FcγRI and FcαR were lower on human monocytes when compared to RM monocytes (Wilcoxon p<0.001). Although human and RM blood contains similar frequencies of monocyte subsets when stratified by FcγRIII expression (55), we found higher levels of FcγRIII on human pan-monocytes compared to RM pan-monocytes (Wilcoxon p<0.001). Importantly, no differences were observed for cell-surface levels of FcγRII. We performed Spearman correlation

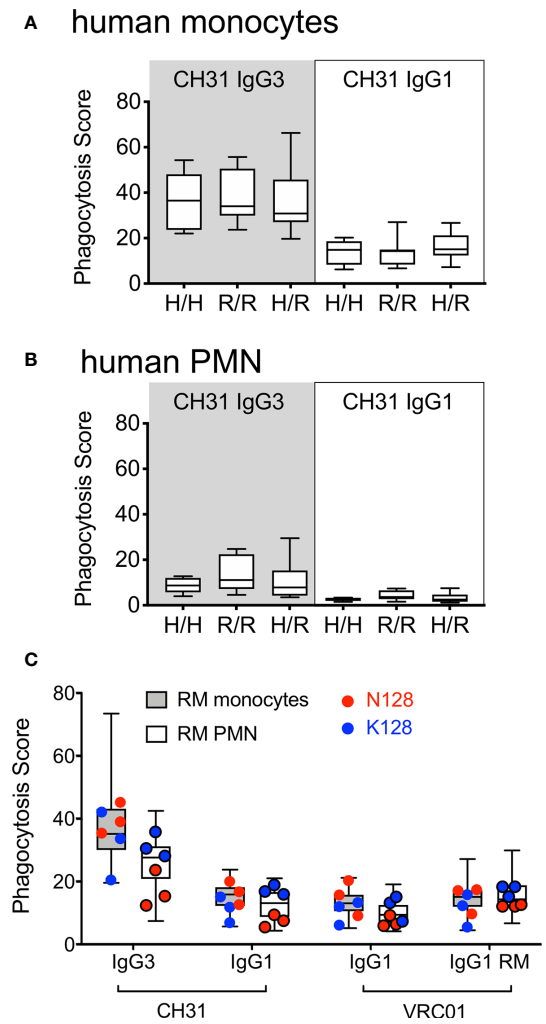

FIGURE 3 | ADP activity of IgG3 and IgG1 mAbs in assays performed with **(A)** human monocytes or **(B)** human PMN when stratified by presence of FcγRIIa SNPs known to impact affinity for IgG. 5 donors were homozygous for H131 (H/H), 8 were homozygous for R131 (R/R) and 10 were heterozygous (H/R). **(C)** ADP activity observed for RM monocyte or PMN ADP activity when evaluated with respect to SNPs within the RM FcγRIIa IgG contact region. Genotype data was only available for 6 of the 23 animals tested, which are represented by symbols overlaying the total data (box-whisker plots). RM with identified SNPs within the IgG contact region are represented by red (N128) and blue (K128) circles as indicated. For all plots, boxes extend to the interquartile ranges, horizontal lines indicate the medians, and error bars represent the range.

analysis to determine if there was a relationship between the level of cell-surface FcRs and ADP activity. We found no-significant correlations (Spearman $p>0.05$ and $r<0.5$) between IgG3 and IgG1 ADP activity and cell-surface levels of FcR for human monocytes (**Figure 4B**, upper panel). Similarly, ADP activity of RM monocytes was not correlated with cell-surface levels of FcR with the exception of ADP by human IgG1 antibodies, which surprisingly were weakly correlated with amount of FcαR on the cell surface (**Figure 4B**, lower panel). However, we found that levels of RM FcγRII were positively correlated with levels of FcαR (Spearman $r=0.60$, $p<0.005$) on RM monocytes as shown in **Supplemental Figure S3**. Thus, one possible explanation for the association of an IgG functional response with FcαR abundance is that monocyte IgG ADP activity is, at least in part, influenced by the levels of cell-surface FcγRII, which has a direct relationship with FcαR for expression on the surface of RM monocytes.

We found significant differences between PMN cell-surface expression of FcRs when comparing cells from humans and RM (**Figure 4C**). Human peripheral blood PMN expressed significantly less cell-surface FcγRI (Wilcoxon $p<0.001$), but more FcγRIII ($p<0.001$) and FcαR ($p<0.001$) when compared to RM. The presence of cell-surface FcγRI and absence of FcγRIII (specifically the FcγRIIIb isoform) on RM PMN is consistent with prior observations (27–29). As described above for monocyte ADP, we performed Spearman correlation analysis to identify relationships between cell surface FcRs and PMN ADP activity. For human PMN, we found weak (Spearman r between 0.42 and 0.58) but significant ($p<0.05$) positive correlations between the amount of cell surface FcγRII and ADP activity of human IgG1 antibodies. We also found weak negative correlations (Spearman $r < 0.6$) between IgG1 ADP and cell-surface levels of FcγRI, and between IgG ADP activity and FcαR levels (Spearman $r <0.7$, **Figure 4D**, upper panel). Consistent with this observation, we found that human PMN cell-surface levels of FcγRII were negatively correlated with levels of FcγRI (Spearman $r=-0.82$) and levels of FcαR (Spearman $r=-0.56$, **Supplemental Figure S3**). These findings suggest that cell-surface levels of FcγRII impact the IgG1 ADP activity of human PMN, and that the abundance of this receptor is inversely associated with the abundance of FcαR and FcγRI — which is normally absent or present in only low levels on the surface of canonical resting human PMNs (56). Interestingly, these relationships were not identified for RM PMN ADP. In contrast, we found significant, but weak ($r<0.5$), correlations between the levels of FcγRI and on the surface of RM PMN and CH31 IgG1 and IgG3 ADP activity (**Figure 4D**, lower panel). Moreover, no significant relationships between the cell-surface levels of different cell surface FcR were observed for RM PMN (**Supplemental Figure S3**). These observations suggest that RM PMN ADP may be more dependent on signaling through FcγRI instead of FcγRII. In light of this possibility, we explored whether there was *FCGR1A* allele-dependent stratification for IgG1 and IgG3 ADP activity of RM PMN. However, within our RM cohort we identified only one SNP in *FCGR1A* that changes an amino acid within the IgG contact region, and this SNP (H158) was only represented in one animal. It is therefore unlikely that *FCGR1A* allelic variation underlies the differences in PMN ADP activity we observed across individual RM donors.

Comparable Binding Affinities of Human IgG1 and IgG3 and RM IgG1 to Common Variants of Both Human and RM FcγRs

Although we identified differences in the magnitude of ADP across individuals, a consistent finding was that among all

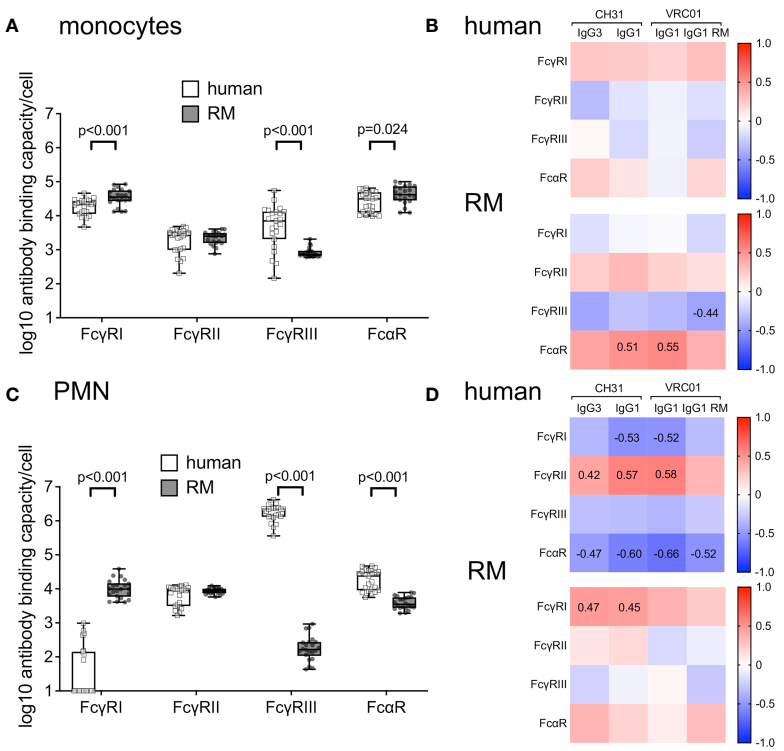

FIGURE 4 | **(A)** Number of cell-surface FcR measured as antibody binding capacity on the surface of human (n=23, white boxes with square symbols) and RM monocytes (n=21, gray boxes with round symbols). **(B)** There was no significant correlation (Spearman correlation p values all > 0.05 and r values < 0.5) between amount of cell-surface FcR and ADP activity of indicated mAbs in assays performed with human monocytes (top panels) or RM monocytes (bottom panels). **(C)** Number of cell-surface FcR measured as antibody binding capacity on the surface of human (n=23, white boxes with square symbols) and RM (n=22, gray boxes with round symbols) PMN. **(D)** Spearman correlations between amount of cell-surface FcR and ADP activity of human (top panels) or RM PMN (bottom panels). Numbers on heatmaps indicate Spearman r values of significant correlations (p<0.05).

humans and RM in our study cohort, the highest ADP activity was observed for immune complexes formed with IgG3. In fact, phagocytosis scores for CH31 IgG3 were approximately double those observed for CH31 IgG1 in assays using human and RM monocytes or PMN (**Figure 1**). This superior ADP activity of IgG3 has previously been demonstrated for assays performed using human phagocyte cell lines and primary human phagocytes (41, 57, 58). Importantly, the unique elongation of the hinge region in human IgG3 subclass, and not affinity for FcγRs, was shown to be responsible for the improved phagocytic potency of IgG3 when compared to IgG1 (37). We used multiplexed surface plasmon resonance (SPR) assays to evaluate the binding affinities of our panel of IgG1 and IgG3 antibodies to FcγRs. We identified only minor differences in binding affinities of the antibodies used in our study to common variants of both human (**Figure 5A**) and RM (**Figure 5B**) FcγRs. In **Figure 5**, human and RM variants of FcγRIIa and FcγRIIIa are identified by SNPs in the IgG contact region, and human FcγRIIIb variants are identified by canonical haplotype name (25, 59). An example sensogram for CH31 IgG1 binding to human FcRγIIa H131 at 200 nM print density is shown in **Figure 5C** and complete SPR sensor data are included as **Supplemental Figures S4–S5**. These results suggest that as previously described for interactions with human phagocytes, the potent RM phagocyte ADP activity we observed for virion immune complexes formed with human IgG3 antibodies is likely dependent on IgG3 hinge length.

Development of RM IgG1 With Elongated Hinge Regions

This functional homology for human IgG3 ADP across humans and RM is noteworthy because RM IgG3 is not structurally analogous to human IgG3. RM IgG3 lacks hinge region exon repetition, and is therefore not elongated when compared to other RM IgG subclasses (21). Therefore, to evaluate the role of antibody hinge length in determining ADP activity of RM phagocytes, we produced RM IgG1 antibodies with elongated hinge regions. To generate these reagents we used recombinant antibody production techniques to clone and express RM IgG1 with repetition of hinge region exons between the CH1 and CH2 regions. Comparison of RM and human IgG1 hinge exons are shown in **Figure 6A** and sequence alignments of the constructs used to produce RM IgG1 with elongated hinge regions are shown in **Figure 6B**. This strategy is similar to that previously used to define the contribution of hinge length to human IgG1 and IgG3 antibodies (37). We used the same nomenclature to describe these novel RM IgG1 variants —0X

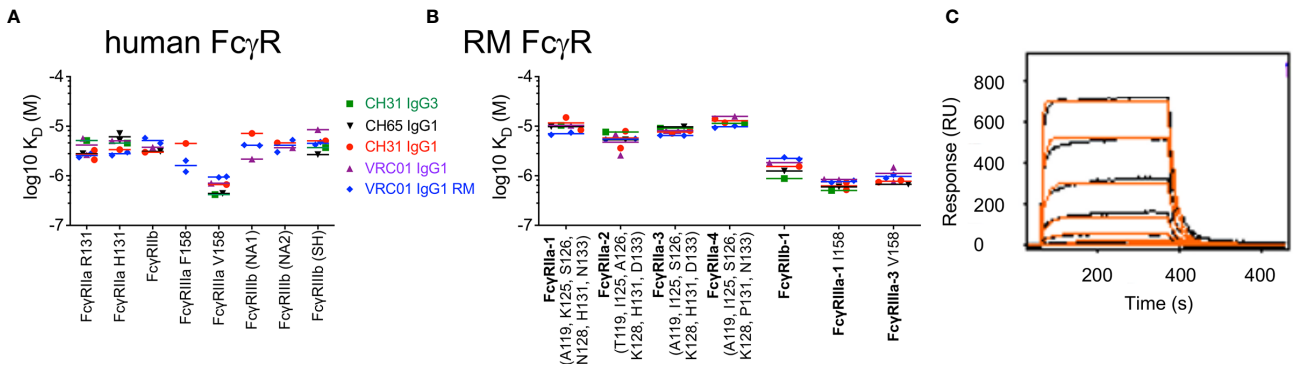

FIGURE 5 | Human IgG3, and human and RM IgG1 mAbs have similar binding affinities for common variants of **(A)** human or **(B)** RM FcγRs. Human and RM variants of FcγRIIa and FcγRIIIa are identified by SNPs in the IgG contact region, and human FcγRIIIb variants are identified by canonical haplotype name. Repeated symbols indicate results of technical replicates, and lines represent the means. Data for CH65 IgG1 binding to RM FcγRIIa-4 is not presented due to poor curve fit. **(C)** Example sensogram for CH31 IgG1 binding to human FcRγIIa H131 at 200 nM print density. Data represents testing of an 8 point series of 3-fold dilutions of CH31 IgG starting at 20 μM. The orange curve represents the kinetic fit; however, the reported values in A and B were calculated using the steady state signal at the end of the association phase.

represents the normal RM IgG1, with no repetition of the hinge exon. 1X includes 1 additional hinge region exon, 2X includes 2 additional hinge region exons, and so on. Therefore, the 3X RM IgG1 variant is expected to be the RM analog of the most common form of human IgG3 (22, 60). Hinge variant molecular weights were characterized by Coomassie-stained reduced SDS-PAGE, and all variants were found to be of the expected size (**Figures 6C**). We used negative stain electron microscopy to visualize the hinge region elongation. 2D class averages of RM IgG1 0X mAbs are shown in **Figure 6D**, and RM IgG1 1X mAbs are shown in **Figure 6E**. A selected example of each has been enlarged so that differences in the hinge region, located between the two Fab arms and the Fc region (indicated by white arrows), can be clearly seen. Variants with additional exon repeats (2X–4X) could not be clearly resolved by negative stain EM, likely due to flexibility conferred by the longer hinges. SPR analysis demonstrated that all hinge variants had similar binding affinities for RM FcγRs, and were similar to binding affinities of polyclonal IgG and purified IgG1 and IgG2 from RM sera (**Figure 6F**). Collectively, these data demonstrate the successful production of RM IgG1 mAbs with elongated hinge regions. We next used these novel reagents to determine if increased hinge length improves monocyte and PMN ADP activity of RM IgG1 mAbs.

Impact of Hinge Region Length on RM Antibody Functions

We used our previously described HIV-1 BaL virion ADP assay to compare phagocytic functionality of RM VRC01 IgG1 hinge variants. RM IgG1 hinge variants based on the anti-influenza mAb CH65 were used as negative controls. Monocytes and PMN were isolated from peripheral blood of two healthy male RM and used as sources of phagocytes. We found that RM VRC01 IgG1 ADP activity increased concomitant with increased antibody hinge length in assays performed with RM monocytes (**Figure 7A**) and RM PMN (**Figure 7B**). Monocyte and PMN ADP activity of all VRC01 hinge variants was significantly higher than that observed for the CH65 negative controls (Wilcoxon $p<0.05$). Notably, we observed that the 2X, 3X, and 4X IgG variants had significantly higher RM PMN ADP activity than the 0X variant which represents the hinge length present in normal RM IgG1 and IgG3. Moreover, monocyte and PMN ADP activities of the RM IgG1 3X variant, which is most structurally analogous to human IgG3, were similar to that observed in assays performed using human CH31 IgG3. These data demonstrate that increasing antibody hinge length can be used as a strategy to improve the ADP activity of RM monoclonal antibodies.

We next explored whether the ability of antibody to recognize infected cells and mediate antibody-dependent cellular cytotoxicity (ADCC) was impacted by elongation of the RM IgG1 hinge region. We found no impact of increased hinge length on the ability of RM IgG1 antibody to bind to the surface of a RM CD4-expressing T cell line infected with SHIV BaL virus (**Figure 8A**), or to mediate ADCC against these target cells in the presence of RM PBMC as a source of effector cells (**Figure 8B**).

Collectively, these data suggest that RM IgG1 elongated hinge variants improve ADP activity and do not negatively impact other non-neutralizing antibody functions including infected cell recognition and ADCC. Our use of endogenous rhesus sequences to extend the hinge region is likely to mitigate the potential for immunogenicity if administered to RM *in vivo*. Therefore, these novel reagents are expected to be useful surrogates for evaluating the protective or therapeutic potential of IgG3 antibodies of clinical interest in the preclinical RM model.

DISCUSSION

Improved prevention strategies, including the expanded use of antiretroviral drugs, have reduced HIV-1 transmission (61), yet there remains a need for additional approaches to limit HIV-1

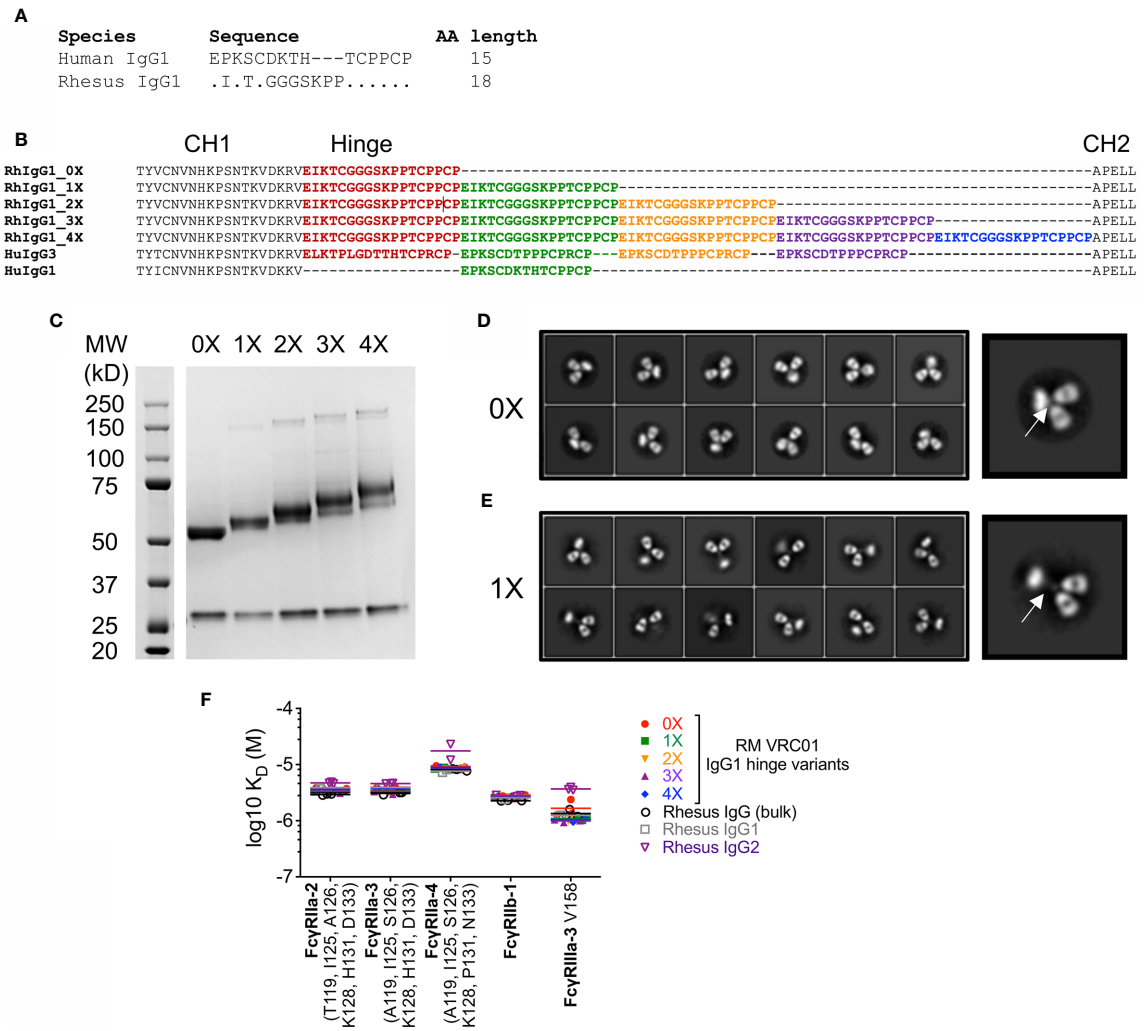

FIGURE 6 | **(A)** Alignment of amino acids that comprise human and RM IgG1 hinge regions. **(B)** Strategy for generation of RM IgG1 hinge variants by repetition of 18 amino acid RM hinge domains with comparison to human IgG1 and IgG3. **(C)** RM IgG1 hinge variants were produced by plasmid transfection of 293T cells and IgG1 molecular weight was characterized by Coomassie-stained reduced SDS-PAGE. **(D, E)** Negative stain electron microscopy 2D class averages of **(D)** RM 0X and **(E)** RM 1X IgG1 hinge variants. Selected images were enlarged to show detail. **(F)** RM IgG1 hinge variants mAbs have similar binding affinities for RM FcγRs. RM FcγR variants are identified by SNPs in the IgG contact region. Repeated symbols indicate results of technical replicates, and lines represent the means.

spread as part of an integrated program to end the global epidemic (62). Development of an effective vaccine against HIV-1 remains the foremost priority. Numerous vaccine candidates have been tested in RM models and humans, but vaccine studies performed in RMs (8, 63–67) have historically been inconsistent predictors of outcomes of human trials (68–71) —suggesting the need for a better understanding of comparative biology across these two species. Several vaccine studies performed in preclinical RM models and human clinical trials have identified associations between FcR-mediated antibody effector functions and reduced risk of infection (3–14). Among these FcR-mediated effector functions, vaccine elicited ADP activity has recently emerged as a common correlate of reduced infection risk in both species (3, 4, 6, 8, 16, 54). Of particular interest, it has recently been shown that ADP by monocytes and PMN can contribute to vaccine-mediated protection of RM (3). Ackerman and colleagues immunized RM with a DNA prime-Ad5 SIVmac239 Env-based vaccine regime *via* the intramuscular (IM) route, or intranasally in an aerosol (AE) formulation. Both regimens effectively reduced infection risk from smE660 intra-rectal challenge. ADP was identified as a correlate of this outcome in both the IM and AE vaccine groups. However, the phagocytes and antibody isotypes associated with this protective response differed by vaccine regimen. For animals vaccinated by the IM route, monocyte ADP and IgG were associated with reduced risk of infection, while ADP by neutrophils and IgA were associated with reduced risk of infection in animals vaccinated *via* the AE route. It is not yet known whether these intriguing observations would be recapitulated using similar vaccines in humans. Here, we

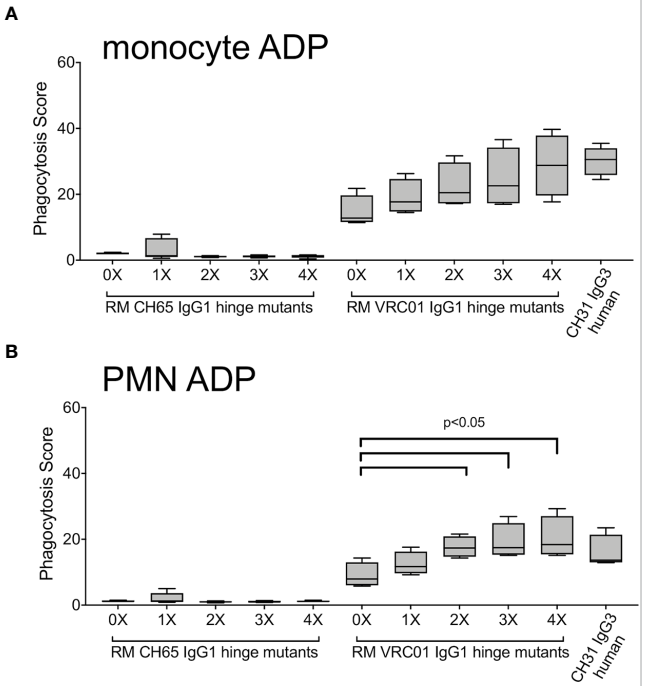

FIGURE 7 | ADP activity of immune complexes formed with fluorescent HIV-1 BaL virions and RM IgG1 hinge-variant mAbs in assays performed with **(A)** monocytes and **(B)** PMN isolated from 2 RM, evaluated in two independent experiments. Box plots represent the interquartile ranges, horizontal lines indicate the medians, and error bars extend to the 10th and 90th percentiles.

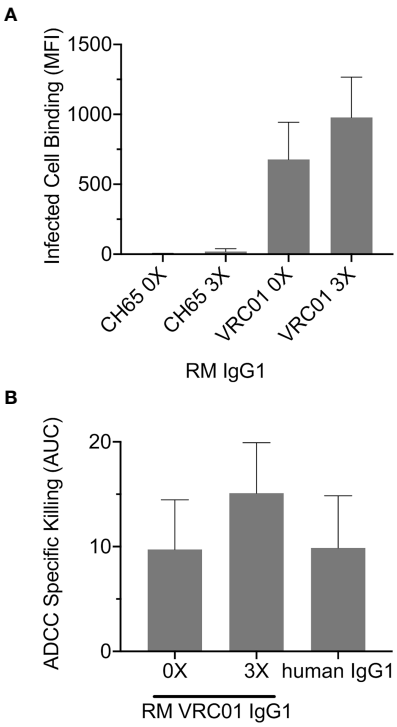

FIGURE 8 | **(A)** Infected cell binding and **(B)** ADCC activity of RM IgG1 are not significantly (Wilcoxon p>0.05) impacted by elongation of the RM IgG1 hinge region. Data represents results the mean and range from two independent experiments.

compared ADP activity of human and RM monocytes and PMN to bridge the gap in knowledge between RM and human ADP and to provide insight into how effectively this important FcR-mediated effector response in the RM model may predict that of humans.

We measured ADP activity with *in vitro* assays that used primary monocytes and PMN isolated from fresh whole blood of 23 humans and 23 RM as sources of phagocytes. Targets in these ADP assays were fluorescent HIV-1 BaL virions that had been incubated with CD4bs specific antibodies to form immune complexes. The antibodies were produced using recombinant techniques as human IgG1, IgG3, IgA1, IgA2, and RM IgG1. Although we observed some differences in the magnitude of ADP when comparing the responses observed in assays performed with human monocytes and PMN to those in assays performed with cells from RM, we observed a consistent ranking in activity by antibody isotype and subclass. Specifically, human and RM ADP activity was greatest when mediated by human CH31 IgG3, followed by RM VRC01 IgG1 and human CH31 or VRC01 IgG1. ADP activity was lowest when mediated by human IgA mAbs. These results demonstrate functional homology between CD4bs antibodies and FcRs from humans and RM for ADP activity, irrespective of species mismatch between antibody and FcRs. This finding suggests that ADP activity observed in preclinical RM models may be translatable to activity observed in human clinical studies.

We also discovered that there was substantial variability in ADP activity when comparing between individual humans or RMs. Strong correlations across all ADP-mediating antibody isotypes and subclasses provided evidence that differences in ADP activity observed for individual humans and RM is a result of intrinsic variability in the activity of phagocytes in each blood donor and is independent of characteristics of the antibody comprising the immune complex. We therefore investigated what factors may contribute to the observed differences in ADP activity of RM and human peripheral blood phagocytes. We first explored whether FcR allelic diversity impacted ADP activity. SNPs in human FcRs result in allelic variants with lower or higher relative affinities (1, 2, 26, 72, 73). Prior studies have described associations among specific FcR alleles and infection or progression of disease resulting from diverse types of viruses (51, 53, 74–78). Importantly, genetic polymorphisms of FcγRIIa, the receptor implicated in IgG-mediated ADP of HIV-1 (52, 79), have been shown to associate with disease progression (53) and with risk of infection in the setting of vertical transmission (51). Moreover, monocyte ADP was found to be a correlate of reduced infection risk in HVTN505 Phase 2b efficacy trial, and SNPs in the FcγRIIa gene (*FCGR2A*) modified this correlation (16, 54). We therefore hypothesized that genetic variation in *FCGR2A* contributed to the differential ADP activity we observed among phagocytes from different human and RM blood donors. Instead,

we found no evidence that human or RM ADP activity was impacted by *FCGR2A* genotype. We next used a quantitative flow cytometry approach to determine whether cell-surface abundance of FcγR contributed to the level of ADP activity observed in our *in vitro* assays. We found no significant correlations between levels of cell-surface FcγRII and ADP by human monocytes. Similarly, there was no consistent evidence of a relationship between RM monocyte ADP activity and FcγRII levels. In contrast, we observed that ADP activity of human IgG antibodies was positively correlated with the amount of FcγRII on the surface of human PMN and negatively correlated with cell-surface levels of FcγRI and FcαR. As we also demonstrated that the levels of FcγRII on the surface of human PMN were inversely related to the levels of FcγRI and FcαR, our findings are consistent with cell-surface levels of FcγRII having an impact on the IgG1 ADP activity of human PMN. Surprisingly, we did not find similar correlations between RM PMN FcγRII expression levels and ADP activity. Instead, we observed weak but significant correlations between the levels of FcγRI and on the surface of RM PMN and human IgG1 and IgG3 ADP activity. This result suggests that RM PMN ADP mediated by human IgG may be more dependent on signaling through FcγRI than FcγRII and warrants further exploration in future studies. Overall, our results indicate that abundance of FcR on the surface of human and RM phagocytes may contribute to a portion of the variability in ADP activity levels we observed *in vitro* for different blood donors, but it is likely that yet unknown characteristics of human and RM phagocytes are also involved. We believe that our results have important implications for design of passive or active immunization studies, especially in RM where the number of animals is typically small. RM studies intended to evaluate ADP as a correlate of protection should consider performing a screening assay to ensure that animals with low and high ADP activity are equally distributed in vaccine groups as our data demonstrated that accurate predictions of phagocyte ADP functionality cannot be made by genetic screening or by immunoprofiling phagocytes with flow cytometry.

Another principal result of our study was the demonstration that for human and RM monocytes and PMN, the highest ADP activity was consistently observed in assays performed with immune complexes formed with human IgG3. This finding is particularly relevant as accumulating evidence suggests that IgG3 responses likely contributed to reduced infection risk both in the RV144 (9, 80) and HVTN505 clinical trials (16, 54). And, although largely understudied, IgG3 is likely an important component of protective immunity against other pathogenic viruses, bacteria, and parasites (81). The superior ADP activity of human IgG3 when compared to other human IgG subclasses has been well-established in prior studies performed with human phagocyte cell lines and primary human phagocytes (41, 57, 58), and has been recently shown to be dependent on the unique elongation of the IgG3 hinge region and not due to a higher affinity for human FcγRs (37). RM IgG3 lacks hinge region exon repetition is therefore not structurally analogous to human IgG3 (21). This fundamental difference between human and rhesus IgG3 has implications for translation of preclinical studies aimed at defining antibody-mediated protection from infection or treatment of disease performed in the RM model. Specifically, passive immunization studies aimed at exploring the antiviral functionality of IgG3 using the RM model have been limited to the use of human IgG3, which like human IgG1 is expected to be immunogenic (34). To overcome this limitation, and to determine if antibody hinge length impacts ADP activity of RM phagocytes as previously demonstrated for human IgG and human phagocytes, we produced RM IgG1 antibodies with elongated hinge regions. We cloned repeats of the RM hinge region exon between the CH1 and CH2 domains of RM IgG1 to generate these novel antibodies. This approach is similar to that used to define the contribution of hinge length to ADP activity of human IgG1 and IgG3 (37). We found that elongation of RM IgG1 improved ADP activity in assays performed with RM monocytes and PMN. Similar to that described for human IgG1 and IgG3 hinge variants, elongation of the RM IgG1 hinge region had no impact on affinity to either human or RM FcγRs, and did not impact the ability of these antibodies to recognize Env-expressing cells and mediate ADCC. Our use of only native sequence already present in RM IgG1 is predicted to result in reduced immunogenicity in RM as previously shown for rhesus-ized IgG1 antibodies (34). Thus, we propose that these novel reagents should be used in future passive immunization studies aimed at defining the role of IgG3 and ADP in protection from virus challenge or control of disease in RM models.

The biophysical mechanism that promote improved ADP activity of antibodies with elongated hinges is not entirely clear. Elongated hinges confer flexibility to the antibody (82) that may facilitate increased access or interaction with FcγRs at the cell surface. Alternatively, there is also evidence that the hinge may impact epitope recognition. A recent study by Richardson and colleagues demonstrated that class-switching a V2-targeting broad neutralizing antibody from IgG1 to IgG3 improved Fc dependent effector functions including ADP and ADCC, as well as neutralization potency (83), suggesting that for some epitopes the hinge region may impact paratope-epitope interactions.

There are two main limitations to our work. The first is that our experiments were performed using antibodies specific for only one Env epitope region, the CD4bs. We were faced with restrictions on the volume of blood that could be obtained from the RM used for this study and were therefore limited in the number of mAbs that could be tested. We focused on the CD4bs antibodies CH31 and VRC01 as both of these antibodies have previously been shown to have potent ADP activity (37, 41). Additionally, VRC01 was previously used to define the contribution of hinge length to human ADP and is of high clinical relevance as a candidate for passive immunotherapy against HIV-1 (37, 84, 85). While the ability of hinge extension to enhance phagocytosis has been shown for antibodies targeting the CD4bs [current study and (37)], V3 loop (37), and V2 region (83), future work will be needed to compare ADP of antibodies specific for additional epitope regions using cells from RM and humans to determine if our findings are applicable to epitopes beyond the CD4bs. The second limitation is that we only had access to peripheral blood and could therefore only compare

ADP activity of human and RM circulating monocytes and PMN. Comparisons between phagocytes present in different anatomical and tissue compartments remain to be explored.

In summary, our work has several implications for translation of ADP response from studies performed in RM to humans. We demonstrated that there are major similarities between ADP activity of human and RM peripheral blood phagocytes, suggesting that RM may effectively predict responses in humans. However, our results also demonstrated substantial variability in ADP levels across individual RM and humans that could not be explained by FcR genotype or expression levels. This finding suggests that caution should be taken when assigning individuals to study groups, especially in RM studies that typically have highly restricted animal numbers as there is the potential to introduce unintentional biases. We also found that human IgG3 mediated the most robust ADP in both species. We therefore produced RM IgG1 with human IgG3-like hinge regions and demonstrated that ADP activity increased concomitant with the elongation of the hinge region. These novel reagents can be used in future passive immunization studies to investigate the protective or therapeutic potential of IgG3 antibodies of clinical interest in the preclinical RM model.

DATA AVAILABILITY STATEMENT

The raw data supporting the conclusions of this article will be made available by the authors, without undue reservation.

ETHICS STATEMENT

The studies involving human participants were reviewed and approved by Duke Health Institutional Review Board. The patients/participants provided their written informed consent to participate in this study. The animal study was reviewed and approved by Duke University Institutional Animal Care and Use Committee.

AUTHOR CONTRIBUTIONS

JP conceived the study, performed experiments, analyzed and interpreted data, and wrote the manuscript. MZT, RWE, DG, AC, RJE, DE, HC, TH, CJ, EM, MT, and ED performed experiments and analyzed data. SJ and RLS performed statistical analyses. TJH developed and characterized the fluorescent HIV-1 virions. KW and MH performed next generation sequencing analyses and interpretation. KS led the design, development, and production of the rhesus-ized monoclonal antibodies. MM, MA, GF, and GT interpreted data and contributed to design of the study. All authors contributed to the article and approved the submitted version.

FUNDING

This work was supported by NIH NIAID P01 grant AI120756, K01 grant OD024877, a fellowship from the Agency for Science, Technology and Research, Singapore, and the Duke University Center for AIDS Research (CFAR; NIH 5P30 AI064518).

ACKNOWLEDGMENTS

We thank Sarah Mudrak for project management support and Duke Department of Laboratory Animal Resources personnel for assistance with sample collection. We also thank Dr. James Hoxie for contributing the A66 cell line used in this study, and Dr. Sampa Santra for providing the SHIV.Bal(P4) virus stocks.

SUPPLEMENTARY MATERIAL

The Supplementary Material for this article can be found online at: https://www.frontiersin.org/articles/10.3389/fimmu.2021.678511/full#supplementary-material

REFERENCES

1. Nimmerjahn F, Ravetch JV. Fcgamma Receptors as Regulators of Immune Responses. *Nat Rev Immunol* (2008) 8(1):34–47. doi: 0.1038/nri2206
2. Ravetch JV, Kinet JP. Fc Receptors. *Annu Rev Immunol* (1991) 9:457–92. doi: 10.1146/annurev.iy.09.040191.002325
3. Ackerman ME, Das J, Pittala S, Broge T, Linde C, Suscovich TJ, et al. Route of Immunization Defines Multiple Mechanisms of Vaccine-Mediated Protection Against SIV. *Nat Med* (2018) 24(10):1590–8. doi: 10.1038/s41591-018-0161-0
4. Barouch DH, Alter G, Broge T, Linde C, Ackerman ME, Brown EP, et al. HIV-1 Vaccines. Protective Efficacy of Adenovirus/Protein Vaccines Against SIV Challenges in Rhesus Monkeys. *Science* (2015) 349(6245):320–4. doi: 10.1126/science.aab3886
5. Barouch DH, Liu J, Li H, Maxfield LF, Abbink P, Lynch DM, et al. Vaccine Protection Against Acquisition of Neutralization-Resistant SIV Challenges in Rhesus Monkeys. *Nature* (2012) 482(7383):89–93. doi: 10.1038/nature10766
6. Barouch DH, Stephenson KE, Borducchi EN, Smith K, Stanley K, McNally AG, et al. Protective Efficacy of a Global HIV-1 Mosaic Vaccine Against Heterologous SHIV Challenges in Rhesus Monkeys. *Cell* (2013) 155(3):531–9. doi: 10.1016/j.cell.2013.09.061
7. Barouch DH, Tomaka FL, Wegmann F, Stieh DJ, Alter G, Robb ML, et al. Evaluation of a Mosaic HIV-1 Vaccine in a Multicentre, Randomised, Double-Blind, Placebo-Controlled, Phase 1/2a Clinical Trial (APPROACH) and in Rhesus Monkeys (NHP 13-19). *Lancet* (2018) 392(10143):232–43. doi: 10.1016/S0140-6736(18)31364-3
8. Bradley T, Pollara J, Santra S, Vandergrift N, Pittala S, Bailey-Kellogg C, et al. Pentavalent HIV-1 Vaccine Protects Against Simian-Human Immunodeficiency Virus Challenge. *Nat Commun* (2017) 8:15711. doi: 10.1038/ncomms15711
9. Chung AW, Ghebremichael M, Robinson H, Brown E, Choi I, Lane S, et al. Polyfunctional Fc-effector Profiles Mediated by IgG Subclass Selection Distinguish RV144 and VAX003 Vaccines. *Sci Transl Med* (2014) 6 (228):228ra38. doi: 10.1126/scitranslmed.3007736
10. Haynes BF, Gilbert PB, McElrath MJ, Zolla-Pazner S, Tomaras GD, Alam SM, et al. Immune-Correlates Analysis of an HIV-1 Vaccine Efficacy Trial. *N Engl J Med* (2012) 366(14):1275–86. doi: 10.1056/NEJMoa1113425
11. Liao HX, Bonsignori M, Alam SM, McLellan JS, Tomaras GD, Moody MA, et al. Vaccine Induction of Antibodies Against a Structurally Heterogeneous Site of Immune Pressure Within HIV-1 Envelope Protein Variable Regions 1 and 2. *Immunity* (2013) 38(1):176–86. doi: 10.1016/j.immuni.2012.11.011

12. Florese RH, Demberg T, Xiao P, Kuller L, Larsen K, Summers LE, et al. Contribution of Nonneutralizing Vaccine-Elicited Antibody Activities to Improved Protective Efficacy in Rhesus Macaques Immunized With Tat/Env Compared With Multigenic Vaccines. *J Immunol* (2009) 182(6):3718–27. doi: 10.4049/jimmunol.0803115
13. Gomez-Roman VR, Patterson LJ, Venzon D, Liewehr D, Aldrich K, Florese R, et al. Vaccine-Elicited Antibodies Mediate Antibody-Dependent Cellular Cytotoxicity Correlated With Significantly Reduced Acute Viremia in Rhesus Macaques Challenged With Sivmac251. *J Immunol* (2005) 174 (4):2185–9. doi: 10.4049/jimmunol.174.4.2185
14. Vaccari M, Gordon SN, Fourati S, Schifanella L, Liyanage NP, Cameron M, et al. Adjuvant-Dependent Innate and Adaptive Immune Signatures of Risk of SIVmac251 Acquisition. *Nat Med* (2016) 22(7):762–70. doi: 10.1038/nm.4105
15. Om K, Paquin-Proulx D, Montero M, Peachman K, Shen X, Wieczorek L, et al. Adjuvanted HIV-1 Vaccine Promotes Antibody-Dependent Phagocytic Responses and Protects Against Heterologous SHIV Challenge. *PloS Pathog* (2020) 16(9):e1008764. doi: 10.1371/journal.ppat.1008764
16. Neidich SD, Fong Y, Li SS, Geraghty DE, Williamson BD, Young WC, et al. Antibody Fc Effector Functions and IgG3 Associate With Decreased HIV-1 Risk. *J Clin Invest* (2019) 129(11):4838–49. doi: 10.1172/JCI126391
17. Tay MZ, Wiehe K, Pollara J. Antibody-Dependent Cellular Phagocytosis in Antiviral Immune Responses. *Front Immunol* (2019) 10:332. doi: 10.3389/fimmu.2019.00332
18. Hayes JM, Cosgrave EF, Struwe WB, Wormald M, Davey GP, Jefferis R, et al. Glycosylation and Fc Receptors. *Curr Top Microbiol Immunol* (2014) 382:165–99. doi: 10.1007/978-3-319-07911-0_8
19. Jennewein MF, Alter G. The Immunoregulatory Roles of Antibody Glycosylation. *Trends Immunol* (2017) 38(5):358–72. doi: 10.1016/j.it.2017.02.004
20. Patel KR, Roberts JT, Barb AW. Multiple Variables At the Leukocyte Cell Surface Impact Fc Gamma Receptor-Dependent Mechanisms. *Front Immunol* (2019) 10:223. doi: 10.3389/fimmu.2019.00223
21. Scinicariello F, Engleman CN, Jayashankar L, McClure HM, Attanasio R. Rhesus Macaque Antibody Molecules: Sequences and Heterogeneity of Alpha and Gamma Constant Regions. *Immunology* (2004) 111(1):66–74. doi: 10.1111/j.1365-2567.2004.01767.x
22. Vidarsson G, Dekkers G, Rispens T. Igg Subclasses and Allotypes: From Structure to Effector Functions. *Front Immunol* (2014) 5:520. doi: 10.3389/fimmu.2014.00520
23. Crowley AR, Ackerman ME. Mind the Gap: How Interspecies Variability in IgG and Its Receptors May Complicate Comparisons of Human and Non-human Primate Effector Function. *Front Immunol* (2019) 10:697. doi: 10.3389/fimmu.2019.00697
24. Boesch AW, Osei-Owusu NY, Crowley AR, Chu TH, Chan YN, Weiner JA, et al. Biophysical and Functional Characterization of Rhesus Macaque IgG Subclasses. *Front Immunol* (2016) 7:589. doi: 10.3389/fimmu.2016.00589
25. Chan YN, Boesch AW, Osei-Owusu NY, Emileh A, Crowley AR, Cocklin SL, et al. Igg Binding Characteristics of Rhesus Macaque Fcγr. *J Immunol* (2016) 197(7):2936–47. doi: 10.4049/jimmunol.1502252
26. Bruhns P, Iannascoli B, England P, Mancardi DA, Fernandez N, Jorieux S, et al. Specificity and Affinity of Human Fcgamma Receptors and Their Polymorphic Variants for Human IgG Subclasses. *Blood* (2009) 113 (16):3716–25. doi: 10.1182/blood-2008-09-179754
27. Rogers KA, Scinicariello F, Attanasio R. Igg Fc Receptor III Homologues in Nonhuman Primate Species: Genetic Characterization and Ligand Interactions. *J Immunol* (2006) 177(6):3848–56. doi: 10.4049/jimmunol.177.6.3848
28. Musich T, Rahman MA, Mohanram V, Miller-Novak L, Demberg T, Venzon DJ, et al. Neutrophil Vaccination Dynamics and Their Capacity To Mediate B Cell Help in Rhesus Macaques. *J Immunol* (2018) 201(8):2287–302. doi: 10.4049/jimmunol.1800677
29. Weisgrau KL, Vosler LJ, Pomplun NL, Hayes JM, Simmons HA, Friedrichs KR, et al. Neutrophil Progenitor Populations of Rhesus Macaques. *J Leukoc Biol* (2019) 105(1):113–21. doi: 10.1002/JLB.1TA1117-431RR
30. Siemsen DW, Malachowa N, Schepetkin IA, Whitney AR, Kirpotina LN, Lei B, et al. Neutrophil Isolation From Nonhuman Species. *Methods Mol Biol* (2014) 1124:19–37. doi: 10.1007/978-1-62703-845-4_3
31. Bonsignori M, Montefiori DC, Wu X, Chen X, Hwang KK, Tsao CY, et al. Two Distinct Broadly Neutralizing Antibody Specificities of Different Clonal Lineages in a Single HIV-1-infected Donor: Implications for Vaccine Design. *J Virol* (2012) 86(8):4688–92. doi: 10.1128/JVI.07163-11
32. Wu X, Yang ZY, Li Y, Hogerkorp CM, Schief WR, Seaman MS, et al. Rational Design of Envelope Identifies Broadly Neutralizing Human Monoclonal Antibodies to HIV-1. *Science* (2010) 329(5993):856–61. doi: 10.1126/science.1187659
33. Liao HX, Levesque MC, Nagel A, Dixon A, Zhang R, Walter E, et al. High-Throughput Isolation of Immunoglobulin Genes From Single Human B Cells and Expression as Monoclonal Antibodies. *J Virol Methods* (2009) 158(1-2):171–9. doi: 10.1016/j.jviromet.2009.02.014
34. Saunders KO, Pegu A, Georgiev IS, Zeng M, Joyce MG, Yang ZY, et al. Sustained Delivery of a Broadly Neutralizing Antibody in Nonhuman Primates Confers Long-Term Protection Against Simian/Human Immunodeficiency Virus Infection. *J Virol* (2015) 89(11):5895–903. doi: 10.1128/JVI.00210-15
35. Whittle JR, Zhang R, Khurana S, King LR, Manischewitz J, Golding H, et al. Broadly Neutralizing Human Antibody That Recognizes the Receptor-Binding Pocket of Influenza Virus Hemagglutinin. *Proc Natl Acad Sci USA* (2011) 108(34):14216–21. doi: 10.1073/pnas.1111497108
36. Kepler TB. Reconstructing a B-cell Clonal Lineage. I. Statistical Inference of Unobserved Ancestors. *F1000Res* (2013) 2:103. doi: 10.12688/f1000research.2-103.v1
37. Chu TH, Crowley AR, Backes I, Chang C, Tay M, Broge T, et al. Hinge Length Contributes to the Phagocytic Activity of HIV-specific IgG1 and IgG3 Antibodies. *PloS Pathog* (2020) 16(2):e1008083. doi: 10.1371/journal.ppat.1008083
38. Campbell EM, Perez O, Melar M, Hope TJ. Labeling HIV-1 Virions With Two Fluorescent Proteins Allows Identification of Virions That Have Productively Entered the Target Cell. *Virology* (2007) 360(2):286–93. doi: 10.1016/j.virol.2006.10.025
39. Shukair SA, Allen SA, Cianci GC, Stieh DJ, Anderson MR, Baig SM, et al. Human Cervicovaginal Mucus Contains an Activity That Hinders HIV-1 Movement. *Mucosal Immunol* (2013) 6(2):427–34. doi: 10.1038/mi.2012.87
40. Edmonds TG, Ding H, Yuan X, Wei Q, Smith KS, Conway JA, et al. Replication Competent Molecular Clones of HIV-1 Expressing Renilla Luciferase Facilitate the Analysis of Antibody Inhibition in PBMC. *Virology* (2010) 408(1):1–13. doi: 10.1016/j.virol.2010.08.028
41. Tay MZ, Liu P, Williams LD, McRaven MD, Sawant S, Gurley TC, et al. Antibody-Mediated Internalization of Infectious Hiv-1 Virions Differs Among Antibody Isotypes and Subclasses. *PloS Pathog* (2016) 12(8):e1005817. doi: 10.1371/journal.ppat.1005817
42. Perfetto SP, Ambrozak D, Nguyen R, Chattopadhyay PK, Roederer M. Quality Assurance for Polychromatic Flow Cytometry Using a Suite of Calibration Beads. *Nat Protoc* (2012) 7(12):2067–79. doi: 10.1038/nprot.2012.126
43. Wenger AM, Peluso P, Rowell WJ, Chang PC, Hall RJ, Concepcion GT, et al. Accurate Circular Consensus Long-Read Sequencing Improves Variant Detection and Assembly of a Human Genome. *Nat Biotechnol* (2019) 37 (10):1155–62. doi: 10.1038/s41587-019-0217-9
44. Li H. Minimap2: Pairwise Alignment for Nucleotide Sequences. *Bioinformatics* (2018) 34(18):3094–100. doi: 10.1093/bioinformatics/bty191
45. DePristo MA, Banks E, Poplin R, Garimella KV, Maguire JR, Hartl C, et al. A Framework for Variation Discovery and Genotyping Using Next-Generation DNA Sequencing Data. *Nat Genet* (2011) 43(5):491–8. doi: 10.1038/ng.806
46. Wang K, Li M, Hakonarson H. ANNOVAR: Functional Annotation of Genetic Variants From High-Throughput Sequencing Data. *Nucleic Acids Res* (2010) 38(16):e164. doi: 10.1093/nar/gkq603
47. Scheres SH. Processing of Structurally Heterogeneous Cryo-EM Data in RELION. *Methods Enzymol* (2016) 579:125–57. doi: 10.1016/bs.mie.2016.04.012
48. Santra S, Tomaras GD, Warrier R, Nicely NI, Liao HX, Pollara J, et al. Human Non-neutralizing Hiv-1 Envelope Monoclonal Antibodies Limit the Number of Founder Viruses During SHIV Mucosal Infection in Rhesus Macaques. *PloS Pathog* (2015) 11(8):e1005042. doi: 10.1371/journal.ppat.1005042
49. Hoxie JA, LaBranche CC, Endres MJ, Turner JD, Berson JF, Doms RW, et al. CD4-Independent Utilization of the CXCR4 Chemokine Receptor by HIV-1 and HIV-2. *J Reprod Immunol* (1998) 41(1-2):197–211. doi: 10.1016/s0165-0378(98)00059-x
50. Schouest B, Leslie GJ, Hoxie JA, Maness NJ. Tetherin Downmodulation by SIVmac Nef Lost With the H196Q Escape Variant is Restored by an Upstream Variant. *PloS One* (2020) 15(8):e0225420. doi: 10.1371/journal.pone.0225420

51. Brouwer KC, Lal RB, Mirel LB, Yang C, van Eijk AM, Ayisi J, et al. Polymorphism of Fc Receptor IIa for IgG in Infants is Associated With Susceptibility to Perinatal HIV-1 Infection. *AIDS* (2004) 18(8):1187–94. doi: 10.1097/00002030-200405210-00012
52. Dugast AS, Tonelli A, Berger CT, Ackerman ME, Sciaranghella G, Liu Q, et al. Decreased Fc Receptor Expression on Innate Immune Cells is Associated With Impaired Antibody-Mediated Cellular Phagocytic Activity in Chronically HIV-1 Infected Individuals. *Virology* (2011) 415(2):160–7. doi: 10.1016/j.virol.2011.03.012
53. Forthal DN, Landucci G, Bream J, Jacobson LP, Phan TB, Montoya B. FcgammaRIIa Genotype Predicts Progression of HIV Infection. *J Immunol* (2007) 179(11):7916–23. doi: 10.4049/jimmunol.179.11.7916
54. Li SS, Gilbert PB, Carpp LN, Pyo CW, Janes H, Fong Y, et al. Fc Gamma Receptor Polymorphisms Modulated the Vaccine Effect on HIV-1 Risk in the HVTN 505 HIV Vaccine Trial. *J Virol* (2019) 93(21):e02041-18. doi: 10.1128/JVI.02041-18
55. Sugimoto C, Hasegawa A, Saito Y, Fukuyo Y, Chiu KB, Cai Y, et al. Differentiation Kinetics of Blood Monocytes and Dendritic Cells in Macaques: Insights to Understanding Human Myeloid Cell Development. *J Immunol* (2015) 195(4):1774–81. doi: 10.4049/jimmunol.1500522
56. Wang Y, Jonsson F. Expression, Role, and Regulation of Neutrophil Fcgamma Receptors. *Front Immunol* (2019) 10:1958. doi: 10.3389/fimmu.2019.01958
57. Boesch AW, Kappel JH, Mahan AE, Chu TH, Crowley AR, Osei-Owusu NY, et al. Enrichment of High Affinity Subclasses and Glycoforms From Serum-Derived IgG Using FcgammaRs as Affinity Ligands. *Biotechnol Bioeng* (2018) 115(5):1265–78. doi: 10.1002/bit.26545
58. Musich T, Li L, Liu L, Zolla-Pazner S, Robert-Guroff M, Gorny MK. Monoclonal Antibodies Specific for the V2, V3, CD4-binding Site, and gp41 of HIV-1 Mediate Phagocytosis in a Dose-Dependent Manner. *J Virol* (2017) 91(8):e02325–16. doi: 10.1128/JVI.02325-16
59. Nagelkerke SQ, Schmidt DE, de Haas M, Kuijpers TW. Genetic Variation in Low-To-Medium-Affinity Fcgamma Receptors: Functional Consequences, Disease Associations, and Opportunities for Personalized Medicine. *Front Immunol* (2019) 10:2237. doi: 10.3389/fimmu.2019.02237
60. Michaelsen TE, Frangione B, Franklin EC. Primary Structure of the "Hinge" Region of Human IgG3. Probable Quadruplication of a 15-Amino Acid Residue Basic Unit. *J Biol Chem* (1977) 252(3):883–9. doi: 10.1016/S0021-9258(19)75181-3
61. UNAIDS. *Unaids Data 2019*. JUNP. o. H. A., editor. Geneva, Switzerland: UNAIDS). UNAIDS Joint United Nations Programme on HIV/AIDS (2019).
62. Fauci AS, Folkers GK. Toward an AIDS-free Generation. *JAMA* (2012) 308 (4):343–4. doi: 10.1001/jama.2012.8142
63. Barouch DH, Yang ZY, Kong WP, Korioth-Schmitz B, Sumida SM, Truitt DM, et al. A Human T-cell Leukemia Virus Type 1 Regulatory Element Enhances the Immunogenicity of Human Immunodeficiency Virus Type 1 DNA Vaccines in Mice and Nonhuman Primates. *J Virol* (2005) 79(14):8828–34. doi: 10.1128/JVI.79.14.8828-8834.2005
64. Berman PW. Development of Bivalent rgp120 Vaccines to Prevent HIV Type 1 Infection. *AIDS Res Hum Retroviruses* (1998) 14 Suppl 3:S277–89.
65. Casimiro DR, Wang F, Schleif WA, Liang X, Zhang ZQ, Tobery TW, et al. Attenuation of Simian Immunodeficiency Virus SIVmac239 Infection by Prophylactic Immunization With Dna and Recombinant Adenoviral Vaccine Vectors Expressing Gag. *J Virol* (2005) 79(24):15547–55. doi: 10.1128/JVI.79.24.15547-15555.2005
66. Liang X, Casimiro DR, Schleif WA, Wang F, Davies ME, Zhang ZQ, et al. Vectored Gag and Env But Not Tat Show Efficacy Against Simian-Human Immunodeficiency Virus 89.6P Challenge in Mamu-A*01-negative Rhesus Monkeys. *J Virol* (2005) 79 (19):12321–31. doi: 10.1128/JVI.79.19.12321-12331.2005
67. Shiver JW, Fu TM, Chen L, Casimiro DR, Davies ME, Evans RK, et al. Replication-Incompetent Adenoviral Vaccine Vector Elicits Effective Anti-Immunodeficiency-Virus Immunity. *Nature* (2002) 415(6869):331–5. doi: 10.1038/415331a
68. Flynn NM, Forthal DN, Harro CD, Judson FN, Mayer KH, Para MF. Placebo-Controlled Phase 3 Trial of a Recombinant Glycoprotein 120 Vaccine to Prevent HIV-1 Infection. *J Infect Dis* (2005) 191(5):654–65. doi: 10.1086/428404
69. Hammer SM, Sobieszczyk ME, Janes H, Karuna ST, Mulligan MJ, Grove D, et al. Efficacy Trial of a DNA/rAd5 HIV-1 Preventive Vaccine. *N Engl J Med* (2013) 369(22):2083–92. doi: 10.1056/NEJMoa1310566
70. Pitisuttithum P, Gilbert P, Gurwith M, Heyward W, Martin M, van Griensven F, et al. Randomized, Double-Blind, Placebo-Controlled Efficacy Trial of a Bivalent Recombinant Glycoprotein 120 HIV-1 Vaccine Among Injection Drug Users in Bangkok, Thailand. *J Infect Dis* (2006) 194(12):1661–71. doi: 10.1086/508748
71. Sekaly RP. The Failed HIV Merck Vaccine Study: A Step Back or a Launching Point for Future Vaccine Development? *J Exp Med* (2008) 205(1):7–12. doi: 10.1084/jem.20072681
72. Bournazos S, Woof JM, Hart SP, Dransfield I. Functional and Clinical Consequences of Fc Receptor Polymorphic and Copy Number Variants. *Clin Exp Immunol* (2009) 157(2):244–54. doi: 10.1111/j.1365-2249.2009.03980.x
73. Shields RL, Namenuk AK, Hong K, Meng YG, Rae J, Briggs J, et al. High Resolution Mapping of the Binding Site on Human IgG1 for Fc Gamma RI, Fc Gamma RII, Fc Gamma RIII, and FcRn and Design of IgG1 Variants With Improved Binding to the Fc Gamma R. *J Biol Chem* (2001) 276(9):6591–604. doi: 10.1074/jbc.M009483200
74. Diamantopoulos PT, Kalotychou V, Polonyfi K, Sofotasiou M, Anastasopoulou A, Galanopoulos A, et al. Correlation of Fc-gamma RIIA Polymorphisms With Latent Epstein-Barr Virus Infection and Latent Membrane Protein 1 Expression in Patients With Low Grade B-cell Lymphomas. *Leuk Lymphoma* (2013) 54(9):2030–4. doi: 10.3109/10428194.2012.762512
75. Garcia G, Sierra B, Perez AB, Aguirre E, Rosado I, Gonzalez N, et al. Asymptomatic Dengue Infection in a Cuban Population Confirms the Protective Role of the RR Variant of the FcgammaRIIa Polymorphism. *Am J Trop Med Hyg* (2010) 82(6):1153–6. doi: 10.4269/ajtmh.2010.09-0353
76. Loke H, Bethell D, Phuong CX, Day N, White N, Farrar J, et al. Susceptibility to Dengue Hemorrhagic Fever in Vietnam: Evidence of an Association With Variation in the Vitamin D Receptor and Fc Gamma Receptor IIa Genes. *Am J Trop Med Hyg* (2002) 67(1):102–6. doi: 10.4269/ajtmh.2002.67.102
77. Yuan FF, Tanner J, Chan PK, Biffin S, Dyer WB, Geczy AF, et al. Influence of FcgammaRIIA and MBL Polymorphisms on Severe Acute Respiratory Syndrome. *Tissue Antigens* (2005) 66(4):291–6. doi: 10.1111/j.1399-0039.2005.00476.x
78. Zuniga J, Buendia-Roldan I, Zhao Y, Jimenez L, Torres D, Romo J, et al. Genetic Variants Associated With Severe Pneumonia in A/H1N1 Influenza Infection. *Eur Respir J* (2012) 39(3):604–10. doi: 10.1183/09031936.00020611
79. Ackerman ME, Dugast AS, McAndrew EG, Tsoukas S, Licht AF, Irvine DJ, et al. Enhanced Phagocytic Activity of HIV-specific Antibodies Correlates With Natural Production of Immunoglobulins With Skewed Affinity for FcgammaR2a and Fcgammar2b. *J Virol* (2013) 87(10):5468–76. doi: 10.1128/jvi.03403-12
80. Yates NL, Liao HX, Fong Y, deCamp A, Vandergrift NA, Williams WT, et al. Vaccine-Induced Env V1-V2 IgG3 Correlates With Lower HIV-1 Infection Risk and Declines Soon After Vaccination. *Sci Transl Med* (2014) 6 (228):228ra39. doi: 10.1126/scitranslmed.3007730
81. Damelang T, Rogerson SJ, Kent SJ, Chung AW. Role of IgG3 in Infectious Diseases. *Trends Immunol* (2019) 40(3):197–211. doi: 10.1016/j.it.2019.01.005
82. Roux KH, Strelets L, Michaelsen TE. Flexibility of Human IgG Subclasses. *J Immunol* (1997) 159(7):3372–82.
83. Richardson SI, Lambson BE, Crowley AR, Bashirova A, Scheepers C, Garrett N, et al. IgG3 Enhances Neutralization Potency and Fc Effector Function of an HIV V2-Specific Broadly Neutralizing Antibody. *PloS Pathog* (2019) 15(12): e1008064. doi: 10.1371/journal.ppat.1008064
84. Gruell H, Klein F. Antibody-Mediated Prevention and Treatment of HIV-1 Infection. *Retrovirology* (2018) 15(1):73. doi: 10.1186/s12977-018-0455-9
85. Corey L, Gilbert PB, Juraska M, Montefiori DC, Morris L, Karuna ST, et al. Two Randomized Trials of Neutralizing Antibodies to Prevent Hiv-1 Acquisition. *N Engl J Med* (2021) 384(11):1003–14. doi: 10.1056/NEJMoa2031738

Conflict of Interest: The authors declare that the research was conducted in the absence of any commercial or financial relationships that could be construed as a potential conflict of interest.

Citation: *Pollara J, Tay MZ, Edwards RW, Goodman D, Crowley AR, Edwards RJ, Easterhoff D, Conley HE, Hoxie T, Gurley T, Jones C, Machiele E, Tuyishime M, Donahue E, Jha S, Spreng RL, Hope TJ, Wiehe K, He MM, Moody MA, Saunders KO, Ackerman ME, Ferrari G and Tomaras GD (2021) Functional*

Homology for Antibody-Dependent Phagocytosis Across Humans and Rhesus Macaques. Front. Immunol. 12:678511. doi: 10.3389/fimmu.2021.678511

frontiers in Immunology

REVIEW
published: 08 June 2021
doi: 10.3389/fimmu.2021.683404

Beyond Binding: The Outcomes of Antibody-Dependent Complement Activation in Human Malaria

Dilini Rathnayake, Elizabeth H. Aitken and Stephen J. Rogerson *

Department of Infectious Diseases, Peter Doherty Institute for Infection and Immunity, University of Melbourne, Melbourne, VIC, Australia

Antibody immunity against malaria is effective but non-sterile. In addition to antibody-mediated inhibition, neutralisation or opsonisation of malaria parasites, antibody-mediated complement activation is also important in defense against infection. Antibodies form immune complexes with parasite-derived antigens that can activate the classical complement pathway. The complement system provides efficient surveillance for infection, and its activation leads to parasite lysis or parasite opsonisation for phagocytosis. The induction of complement-fixing antibodies contributes significantly to the development of protective immunity against clinical malaria. These complement-fixing antibodies can form immune complexes that are recognised by complement receptors on innate cells of the immune system. The efficient clearance of immune complexes is accompanied by complement receptor internalisation, abrogating the detrimental consequences of excess complement activation. Here, we review the mechanisms of activation of complement by alternative, classical, and lectin pathways in human malaria at different stages of the *Plasmodium* life cycle with special emphasis on how complement-fixing antibodies contribute to protective immunity. We briefly touch upon the action of anaphylatoxins, the assembly of membrane attack complex, and the possible reasons underlying the resistance of infected erythrocytes towards antibody-mediated complement lysis, relevant to their prolonged survival in the blood of the human host. We make suggestions for further research on effector functions of antibody-mediated complement activation that would guide future researchers in deploying complement-fixing antibodies in preventive or therapeutic strategies against malaria.

Keywords: malaria, immune complexes, classical complement pathway, infected erythrocytes, complement regulatory proteins, *Plasmodium falciparum* erythrocyte membrane protein 1

OPEN ACCESS

Edited by:
Guido Ferrari,
Duke University, United States

Reviewed by:
Matthew Parsons,
Emory University, United States
Stephanie Jost,
Beth Israel Deaconess Medical Center and Harvard Medical School, United States

***Correspondence:**
Stephen J. Rogerson
sroger@unimelb.edu.au

Specialty section:
This article was submitted to Comparative Immunology, a section of the journal Frontiers in Immunology

Received: *20 March 2021*
Accepted: *24 May 2021*
Published: *08 June 2021*

Citation:
Rathnayake D, Aitken EH and Rogerson SJ (2021) Beyond Binding: The Outcomes of Antibody-Dependent Complement Activation in Human Malaria. Front. Immunol. 12:683404. doi: 10.3389/fimmu.2021.683404

INTRODUCTION TO MALARIA

Malaria remains one of the major causes of severe morbidity and mortality globally. In 2019 alone, there were 229 million clinical episodes of malaria causing 0.4 million deaths. The most vulnerable groups include children under five years of age and pregnant women and the heaviest burden of disease is concentrated in sub-Saharan Africa (1). Clinical malaria presents as a febrile illness, that can progress to severe disease, causing death (2). Severe malaria often manifests as severe anaemia,

cerebral malaria or acute lung or kidney injury, Lung or kidney injury may lead to pulmonary oedema or renal failure, which is less common in children than adults [reviewed in (3)]. In pregnant women, infection in the placenta may cause adverse outcomes including abortion, stillbirth, intrauterine growth retardation, low infant birth weight, and neonatal death [reviewed in (4)]. Treatment strategies involve the use of artemisinin combination therapies, while vector control and effective surveillance are also important [reviewed in (5)].

In people living in malaria-endemic areas, immunity to malaria is gradually acquired following repeated exposure so that over time individuals become relatively protected from malaria and its complications [reviewed in (6)]. This naturally acquired immunity was demonstrated to be antibody-mediated, when antibodies transferred from apparently immune adults to young children with clinical malaria were able to reduce parasite densities (7).

The leading malaria vaccine candidate RTS,S induces antibodies to the circumsporozoite protein, and both naturally acquired and vaccine-induced antibodies fix complement and engage Fc receptors (8–10), discussed later.

The asexual replication of *Plasmodium* parasites within human erythrocytes is responsible for clinical symptoms of malaria. The parasite has a complex life cycle initiated by a *Plasmodium*-infected mosquito bite (see **Figure 1** for life cycle of *P. falciparum*).

We focus on the importance of understanding the roles of antibody-mediated complement activation in these different stages of the *Plasmodium* life cycle, together with the mechanisms that parasites adopt to evade complement attack to promote their survival. A deeper understanding of antibody-mediated complement activation across the *Plasmodium* life cycle will provide insights into harnessing complement activation in antibody-mediated protection in malaria.

COMPLEMENT ACTIVATION AND ITS ROLE IN MALARIA IMMUNITY

Introduction to the Complement System

The complement system is a first line of defense against invading pathogens. It consists of both soluble and membrane-bound proteins, of which many are proteases that are proteolytically cleaved in a sequential cascade during activation [reviewed in (11, 12)]. These proteins can be deposited on the surface of pathogens or on host cells to produce a membrane attack complex (MAC) *via* three pathways, namely the classical, alternative, and mannose-binding lectin (MBL) [reviewed in (11)]. In malaria, the complement system may be activated in response to whole parasites or parasite-derived proteins in the host circulation [reviewed in (13)] (**Figure 2**).

The activation of complement is tightly regulated by both soluble and membrane-bound complement regulatory proteins (CRPs) that act at definitive points of the cascade and that are essential to prevent autologous complement attack (**Figure 2**) [reviewed in (14)]. The membrane-bound CRPs are

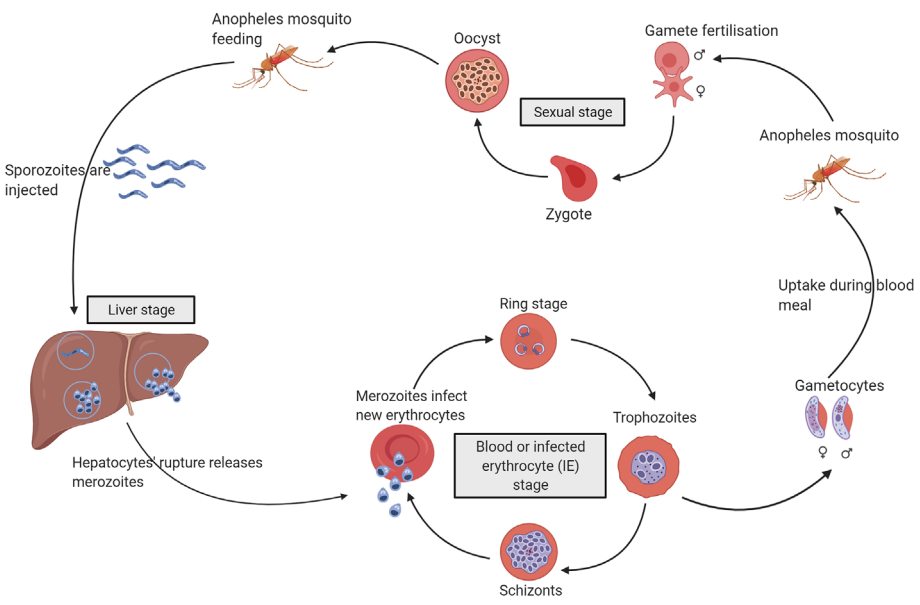

FIGURE 1 | The life cycle of *Plasmodium falciparum*. *P. falciparum* requires two hosts to complete its life cycle, the mosquito, and the human. Gametocytes are ingested by a female Anopheles mosquito during a blood meal. The gametocytes transform into gametes that fertilise to form zygotes and migrate through the mosquito gut wall to form oocysts. The oocysts rupture and release sporozoites that reach the salivary gland of the mosquito ready to be transmitted into another human host. The injected sporozoites reach the liver, and within hepatocytes, the parasites undergo division (liver stage) before rupture to release merozoites into the bloodstream. The merozoites infect new erythrocytes to form ring-stage parasites that mature into trophozoites and schizonts within the infected erythrocytes (IEs). The rupture of schizonts releases a new generation of merozoites to infect erythrocytes (blood stage). A small proportion of these parasites develop into gametocytes within the IEs, which are ingested by a female Anopheles mosquito for the continuation of the life cycle [reviewed in (3)].

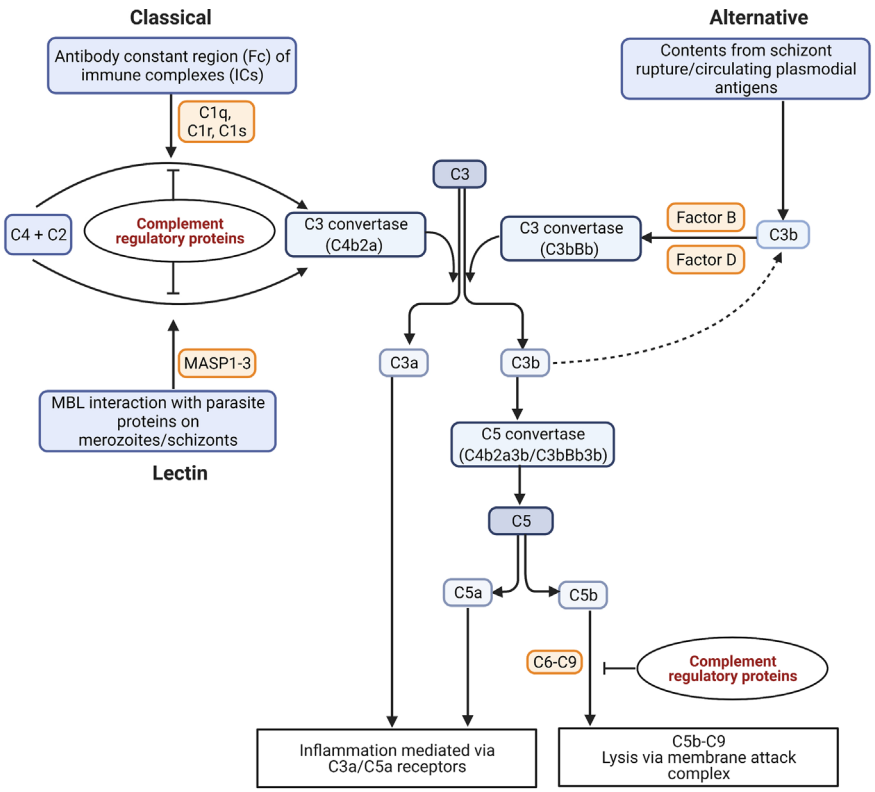

FIGURE 2 | Possible mechanisms of complement activation in malaria. The binding of C1q to antigen-antibody immune complexes (ICs) activates the classical pathway. The lectin pathway can be activated through the binding of mannose with the parasite proteins expressed on schizont surface. The serine proteases MASP1 and MASP2 (Mannan-binding lectin-associated serine proteases 1 and 2) bind to MBL in lectin pathway, and C1r and C1s bind to C1q to cleave two inactive proenzymes C4 and C2 in serum to produce C3 convertase (C4b2a). The alternative pathway is activated either by circulating plasmodial antigens, or products of schizont rupture like hematin. The spontaneous hydrolysis of C3 leads to the cleavage of factor B in serum by an active serum protease called factor D to form a distinct C3 convertase of the alternative pathway (C3bBb). The C3 convertases cleave C3 into C3a and C3b. The products of C3 and C5 cleavage, C3a and C5a, act as anaphylatoxins and interact with immune cell receptors (C3aR and C5aR) to drive inflammation. The assembly of C3b with the C3 convertases produces a C5 convertase (C4b2a3b/C3bBb3b) that can cleave C5 into C5a and C5b. The C5b recruits the factors C6, C7, C8, and C9 for the assembly of the membrane attack complex (MAC) (C5b-C9 or terminal complement complex) for cytolysis (14). [Figure adapted from (15)].

constitutively expressed on the surface of cells including erythrocytes and cells within organs like the kidney, while the fluid-phase CRPs circulate in the plasma and are recruited onto the cell surface upon requirement [reviewed in (16)].

Levels of Complement in Serum During Malaria

Alterations in the levels of complement in serum have been reported during malaria (17–22). The studies performed in a *P. lophurae* infected duck model showed decreased serum levels of initial complement proteins, C1, C2, and C4 during infection (23). Reduced levels of C4 in serum in simian malaria have been reported implicating classical complement activation (19). Rhesus monkeys infected with *P. coatneyi* showed decreased serum levels of initial complement proteins, C1, C2, and C4 during schizont rupture (24). Human studies showed reduced serum complement levels in patients with cerebral malaria compared to benign infection also indicating classical complement activation (17). Similarly, studies in malaria-infected pregnant women showed increased amounts of C1q, C3d, C4, and C9 in malaria-infected placentas compared to non-infected placentas (25), and deposition of IgG and C3 in some of the *P. falciparum*-infected placentas (26), although no association was shown between infection severity and the amount of complement deposited on the infected placentas. Genome-wide expression analyses showed an upregulation of C1q, C3, C5aR, and C3aR genes in the placentas of primigravid women with malaria compared to placentas of primigravid women without placental malaria (27), implying a role for classical complement activation in disease pathology.

Both the alternative and the classical complement pathways are activated in malaria, indicated by increased levels of alternative pathway derived components, Bb (a breakdown product of factor B) and classical pathway components like C4d (a split product of inactive C4b) as well as soluble C5b-C9 in natural *P. falciparum* infection (28). Complement activation is also regarded as one of the earliest immune responses against experimental *P. falciparum* infection and can be demonstrated when parasitaemia is still undetectable in peripheral blood (22). In studies performed in children with severe malarial anaemia and uncomplicated malaria,

the complement system is activated, but a higher level of complement consumption was observed in children with severe malarial anaemia compared to uncomplicated malaria (20).

The parasite components that directly activate complement in malaria include malarial antigens expressed on the surface of IEs (29), and the products of IE rupture like hematin (30). The antigens released by *P. falciparum* growing in culture including merozoites can activate all three pathways of complement, but they cause greatest activation of the alternative pathway (see **Figure 2**) (31).

The role of lectin complement pathway in malaria is not clearly demonstrated. MBL seems to recognise parasite proteins of *P. falciparum*-IEs (32, 33) and may activate lectin pathway.

Genetic studies also reveal a role of MBL protein in malaria. The concentration of MBL protein in serum is genetically determined and different haplotype variants of the MBL gene influence the circulating levels of MBL protein (34). In a study from Gabon, MBL gene polymorphisms were associated with reduced serum levels of MBL protein, and these mutations were present at a higher frequency in children with severe malaria compared to those with mild malaria, suggesting that low MBL levels might be a risk factor for severe malaria (35). This observation was further supported by another study from Ghana that showed low levels of MBL associated with the *mbl2* gene variant increased both susceptibility to *P. falciparum* infection and to severe malaria in young children (36).

By contrast, some studies were unable to show any associations between MBL polymorphisms with parasitaemia and severe disease. Multiple variant alleles of the *mbl2* gene that predicted low serum levels of MBL were not associated with infection or malaria severity in Ghanaian children (33), asymptomatic *P. falciparum* infection in Gabonese children (37), or clinical malaria in Gambian children (38). These discrepancies may be a result of the differences in study design as well as the disease manifestations, and age groups of children enrolled in each study. Taken together, all these studies highlight the possible importance of the lectin pathway in malaria severity, but further studies are needed to fully elucidate the role of MBL and its polymorphisms in malaria susceptibility.

Antibodies Activate the Classical Complement Pathway in Malaria

Antigen-antibody immune complexes (ICs) activate complement *via* the classical pathway in malaria [reviewed in (39)]. They are formed when antibodies bind malarial antigens circulating in plasma (**Figure 3A**) or expressed on the surface of sporozoites, merozoites, and IEs (**Figure 3B**). In individuals infected with malaria for the first time, ICs may first form approximately 10-14 days after infection, while in subsequent Plasmodium infections complement appears to be activated earlier (13).

The binding of globular head domains of the complement factor C1q with the antibody constant (Fc) domain regions of IgG hexamers or IgM binding antigen activates the classical complement pathway (40). The ability of IgG or IgM antibodies to activate the classical complement pathway depends on antibody isotype and subclass, with IgM-bound ICs having the highest ability to bind C1q and activate the classical pathway, while IgG4 has the lowest activity, and for the other IgG subclasses, the affinities for C1q are IgG3 > IgG1 > IgG2 [reviewed in (41)].

In the next section, we provide a brief overview of antibody-mediated complement fixation on different stages of *P. falciparum* within the human host. We discuss the mechanisms of clearance of the parasites *via* complement-mediated lysis that are brought about by activation of the classical complement pathway in the presence of ICs. We also review the influence of intrinsic and extrinsic properties of both host and parasite that could have a potential impact on complement-dependent lysis of different parasitic stages.

ANTIBODY-DEPENDENT COMPLEMENT FIXATION ON DIFFERENT PARASITIC STAGES

Sporozoites

After injection by the mosquito, *Plasmodium* spp. sporozoites enter the blood vessels and move through the circulation and

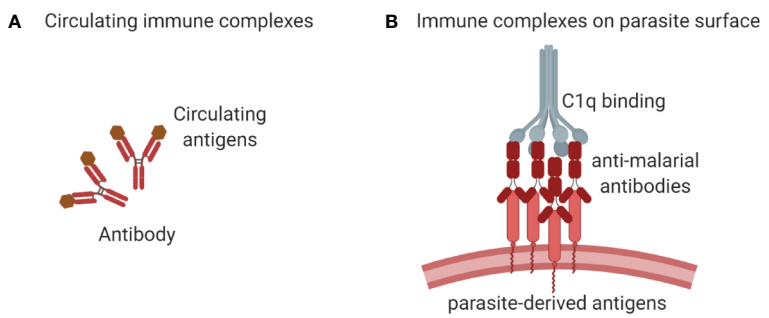

FIGURE 3 | The immune complexes (ICs) are formed when antigens and antibodies unite. They can be formed when the circulating plasmodial antigens cross-link with antibodies in the plasma **(A)** or antibodies can bind with the antigens expressed on the surface of sporozoites, merozoites, or IEs as shown in **(B)**. The circulating ICs (as in A) can also get deposited on the surface of the parasite or on other cells like uninfected erythrocytes, promoting complement deposition on host cell surfaces. These ICs recruit C1q when the globular head domains of C1q bind with the Fc constant region **(B)** of ICs to activate a cascade of downstream events of the classical complement pathway.

invade hepatocytes, where they divide to produce merozoites which are released to initiate blood-stage infection (**Figure 1**) [reviewed in (42)]. Targeting sporozoites is potentially an efficient way of preventing malaria as only a small number of sporozoites are injected by the female mosquito during a blood meal.

Studies in murine models have shown that the passive transfer of monoclonal antibodies against the sporozoites of *P. yoelii* inhibited liver infection and the progression to blood-stage infection (43, 44) while in humans, antibodies against *P. falciparum* sporozoites inhibited the movement of sporozoites into hepatocytes *in vitro* (9).

Recent *in vitro* studies conducted in humans showed that these naturally-acquired antibodies against sporozoites of *P. falciparum* can fix complement on the sporozoite surface and are predominantly of cytophilic subclasses, immunoglobulin 1 (IgG1) and IgG3 (9). The hepatocyte transversal inhibitory activity of the naturally acquired anti-sporozoite antibodies was substantially enhanced in the presence of complement, resulting in fixation of C1q on sporozoites and causing their death (9).

Studies show that immunisation with live-attenuated sporozoites of *P. falciparum* can induce sporozoite-specific IgG and IgM antibodies that can fix complement on the sporozoite surface. These antibodies can inhibit sporozoite traversal and invasion into hepatocytes and enhance sporozoite membrane permeability, resulting in sporozoite lysis (45, 46). Similarly, the RTS,S vaccine is based on the major circumsporozoite protein (CSP) on *P. falciparum* sporozoites, and anti-CSP antibodies are induced following RTS,S vaccination that are functional and fix complement factor C1q (47).

In summary, induction of complement-fixing antibodies against sporozoite antigens *via* natural exposure and vaccination can inhibit sporozoite transversal into liver hepatocytes leading to their lysis and death (9), and these antibodies are associated with protection from clinical malaria (9, 46).

Merozoites

Studies have identified merozoite surface proteins (MSP) such as $MSP1_{19}$, MSP3, and apical membrane antigen-1 [reviewed in (48)], as important targets of protective antibodies, particularly of type IgG (49). The antibodies targeting merozoites limit parasite replication and inhibit invasion of erythrocytes.

Both naturally acquired (50) and vaccine-induced (50, 51) human antibodies against merozoites promote C1q complement deposition on the merozoite surface and activation of the classical complement pathway, inhibiting merozoite invasion and lysing merozoites (50). A longitudinal cohort study performed in older children showed strong associations between complement-fixing antibodies against MSP1 and MSP2 with protection from clinical malaria and high parasitaemia (50). This observation is further supported by a similar study in malaria-exposed children (52) that showed that complement-fixing antibodies against merozoite antigens were a strong predictor of protection against malaria in children.

Gametocyte-Infected Erythrocytes

Gametocyte-IEs are the infective stages of the parasite that enable transmission of infection from human to mosquito [reviewed in (53)]. There is limited recognition of gametocyte-IEs by naturally acquired antibodies within the human host and this low level of recognition may facilitate the evasion of host immunity and transmission of infection to the mosquito (54).

When an Anopheles mosquito takes a blood meal, host serum components like complement proteins and antibodies are taken in along with the gametocyte-IEs (**Figure 1**) [reviewed in (53)]. In the mosquito midgut, the gametocytes emerge from the erythrocytes, and are exposed to complement proteins and antibodies [reviewed in (53)].

Most studies on immunity to *P. falciparum* sexual stages revolve around the major gametocyte surface antigen, Pfs230 [reviewed in (55)]. Previous studies showed that the transmission blocking activities of monoclonal antibodies against Pfs230 were complement dependent (56), and *in vitro* complement-mediated lysis of gametes by immune sera is associated with antibodies towards Pfs230 (57). But in membrane feeding assays, the transmission blocking activity of immune sera has yet to be shown to be complement dependent (58). Pfs230 is a leading candidate for transmission-blocking vaccines (59), and is likely a major antigenic target for complement-fixing antibodies.

Infected Erythrocytes

The clinical symptoms of malaria are attributable to blood-stage infection. Some of the major targets of acquired immunity to blood-stage infection are the surface antigens on *P. falciparum*-IEs (60).

Parasite antigens on the surface of IEs play a major role in the pathology of severe malaria *via* parasite sequestration leading to cytoadhesion of IEs to vascular endothelium [reviewed in (61)] or syncytiotrophoblast of the placenta (62). These surface antigens can undergo antigenic variations (63) and are known as variant surface antigens (VSA) (64). The dominant VSAs that are expressed on the surface of IEs are the *P. falciparum* erythrocyte membrane protein 1 (PfEMP1) family of proteins (65).

The surface of trophozoite-IE of *P. falciparum* is a target for antibody-dependent complement activation (29). In the presence of immune sera the classical complement pathway was activated as indicated by formation of complexes of C1s and C1 inhibitor, measured by ELISAs, although antibody-mediated lysis of IEs was not observed visually (29). Spectrometric quantification of the changes in optical absorbance induced by the release of haemoglobin serves as a better option (66).

Later, Weisner et al. showed that the complement cascade can be activated on the surface of IEs, detecting immunoglobulins, C3, C4, and C9 on the surface of IEs (but not uninfected erythrocytes) incubated with immune sera *via* western blot analyses (67). However, they failed to observe IE lysis by classical complement activation in the presence of immune sera suggesting that IEs are resistant to complement-mediated lysis, discussed in more detail in section 5.

Notwithstanding the resistance of antibody-opsonised IEs to complement-mediated lysis, IEs are susceptible to other mechanisms of antibody-mediated removal that are briefly discussed here. Previous studies have shown that antibody-opsonised IEs are cleared by monocytes (68, 69) and neutrophils (70) by cellular phagocytosis. Antibody-opsonised IEs can also activate NK cells, which resulted in lysis of IEs and inhibition of parasite growth (71).

Box 1 | Suggested future research on antibody and complement interactions in malaria.

- Clarify the cooperation between opsonins C3b and antibody in phagocytosis of merozoites, sporozoites, and IEs by phagocytic cells.
- Clarify the combined roles of both opsonins C3b and antibody in leukocyte activation by merozoites, sporozoites, and IEs.
- Quantify the contribution of C3b deposition on uninfected erythrocytes to anaemia during malaria.
- Investigate the association of complement in disease pathology of cerebral and placental malaria in human and consider whether temporary blockade of C5a generation by complement inhibitors such as the monoclonal anti-C5 antibody eculizumab or the C3 inhibitor compstatin could have a beneficial effect in treatment of cerebral or placental malaria.
- Define other antigenic targets on the surface of merozoites, sporozoites, IEs and gametocytes (if present) that would generate complement-fixing antibodies for protective immunity.
- Determine the association between antibody Fc region variations and antibody functionality for optimum complement activation by opsonised *Plasmodium* antigens.

COMPLEMENT ACTIVATION AND DISEASE OUTCOMES

Mechanisms of Immune Complex Clearance

Under normal physiological conditions, the ICs are efficiently cleared by a functional complement system preventing excess deposition of complement that brings detrimental effects to the host [reviewed in (11)]. The complement receptor 1 (CR1) on the surface of macrophages, B cells, neutrophils, dendritic cells, and erythrocytes in humans can recognise complement fragments C3b, iC3b, and C4b that are bound with ICs [reviewed in (11)]. CR1 binds, transports, and endocytoses C3b-bearing ICs to remove them from circulation [reviewed in (14)]. Additionally, the complement receptor 3 (CR3 or CD11b/CD18 complex) on the surface of leukocytes is involved in C3b-mediated opsonic phagocytosis by monocytes and neutrophils and plays a role in clearance of C3b-containing ICs [reviewed in (14)]. The Fc receptors of innate immune cells like neutrophils and monocytes can directly bind to the Fc domain of the ICs also promoting antibody-mediated opsonic phagocytosis (72).

Complement Activation in the Pathogenesis of Malaria

Mice infected with *P. yoelii* showed a downregulation of the level of expression of CR1 on monocytes or macrophages, a similar though less pronounced downregulation was reported in patients infected with *P. falciparum* and *P. vivax* compared to non-infected controls (73). Decreased CR1 expression on monocytes or macrophages in the mice was also associated with inhibited uptake of immune complexes and was also seen following exposure to lipopolysaccharide (73). Inflammation may contribute to decreased CR1 expression, which then leads to impaired ICs clearance in malaria, and possibly to disease as ICs are associated with increased disease severity (74). But the contribution of ICs to malaria pathogenesis is not fully known.

Both IgG and complement are shown to be deposited on the surface of uninfected erythrocytes in severe malarial anaemia (75, 76). Complement deposition promotes erythrophagocytosis of IC-deposited erythrocytes *via* CR1 on macrophage surface (77). In *Plasmodium* infection, erythrophagocytosis by macrophages seems complement-dependent (78), a possible mechanism for severe malarial anaemia not broadly discussed here (see **Box 1**).

Other than erythrophagocytosis, erythrocytes with C3b-containing ICs are taken up by splenic reticuloendothelial cells. This may lead to stripping off of the CR1 from the erythrocyte surface (76, 79, 80). CR1-deficient erythrocytes are recirculated and are susceptible to complement attack, implicating complement deposition as a driver of severe malarial anaemia. Among heavily malaria-exposed Gambian children, about half developed a positive direct antiglobulin (Coombs) test (81). IgG was eluted from the surface of their uninfected erythrocytes, and in many cases it was shown to recognise schizonts (82), although the antigen specificity of the antibodies bound to uninfected erythrocytes has not been studied in detail. More recent studies [reviewed in (83)] confirm the deposition of IgG and C3 on these cells. The antibodies are postulated to be immunologically unrelated to the uninfected erythrocytes (81).

Complement activation generates C5a *via* the cleavage of C5, by C5 convertase (see **Figure 2** for complement pathway). C5a is a potent inflammatory mediator (anaphylatoxin) that is readily cleared from plasma *via* receptor internalisation under normal physiological conditions [reviewed in (84)]. The ligation of C5 with C5a receptors (CD88 and C5L2) on innate immune cells promotes a cascade of conventional inflammatory events including increased leukocyte extravasation, neutrophil chemotaxis, degranulation, delayed apoptosis, phagocytosis, oxidative burst, and the activation of vascular endothelial cells to upregulate the expression of cell adhesion molecules [reviewed in (84)].

C5a is implicated in the pathogenesis of cerebral malaria (85) and placental malaria (86, 87). C5a is increased in women with placental malaria (87) and elevated C5a was associated with increased risk of birth of 'small-for-gestational-age' babies (86). Blocking C5a in a murine model of placental malaria resulted in improved placental and foetal development (86). Murine models have also highlighted a possible role for C5a in cerebral malaria as C5 deficient mice or those treated with antibodies blocking C5a and its receptor respectively did

not develop and could be rescued from cerebral malaria (85). Though there is some evidence for a role of the inflammatory complement C5a protein in disease, the anti-C5 monoclonal antibody eculizumab has not been studied in malaria (see **Box 1**).

The inflammatory effector functions mediated by the release of C5a in response to infection and the C3b-mediated opsonic phagocytosis of IEs (and/or other parasite stages, such as sporozoites, merozoites, and intraerythrocytic gametocytes) by innate immune cells are not discussed in detail in this review.

MECHANISMS OF EVASION OF COMPLEMENT-MEDIATED LYSIS BY *PLASMODIUM* IEs

Irrespective of the exposure of blood-stage parasites to serum complement over a relatively prolonged asexual blood-stage (**Figure 1**) (88), the IEs seem to be broadly resistant to complement-mediated lysis (67).

One reason why the IEs are resistant to complement-mediated lysis may be that the IEs may have low number of target sites for antibody-binding and complement activation. If this is below a certain threshold, even an excess of antigen-specific antibodies and serum complement may not activate the classical complement pathway (**Figure 4A**) (89).

Membrane-bound CRPs that act at different phases of the complement cascade tightly regulate complement activation [reviewed in (14)]. These include CD46 or membrane cofactor protein (MCP); CR1 which targets and cleaves C3 convertase; CD55 or decay accelerating factor (DAF) which accelerates the decay of both C3 and C5 convertase (90); and CD59 which acts on the terminal complement pathway (see **Figure 2**), targeting C5b-C9 to inhibit the assembly of MAC (90). Interestingly, the IEs appear to have high expression of CD59 that makes them resistant to complement mediated destruction (**Figure 4B**) (67). In addition to the membrane-bound CRPs, the *P. falciparum*-IEs also utilise soluble complement factors like factor I (FI) and factor H (FH) (**Figure 4B**) to evade complement mediated lysis. FH utilises factor I for recruiting FH-related protein FHL-1 onto the schizont surface to inactivate C3b and regulates alternative complement activation in response to the rupture of IEs (91–93).

In an *ex vivo* study of subjects with severe malaria anaemia, the levels of expression of CRPs were lower on uninfected erythrocytes than on IEs (94). This loss of CRPs on uninfected erythrocytes in severe malaria anaemia was not associated with changes in complement-fixing cytophilic antibodies or serum

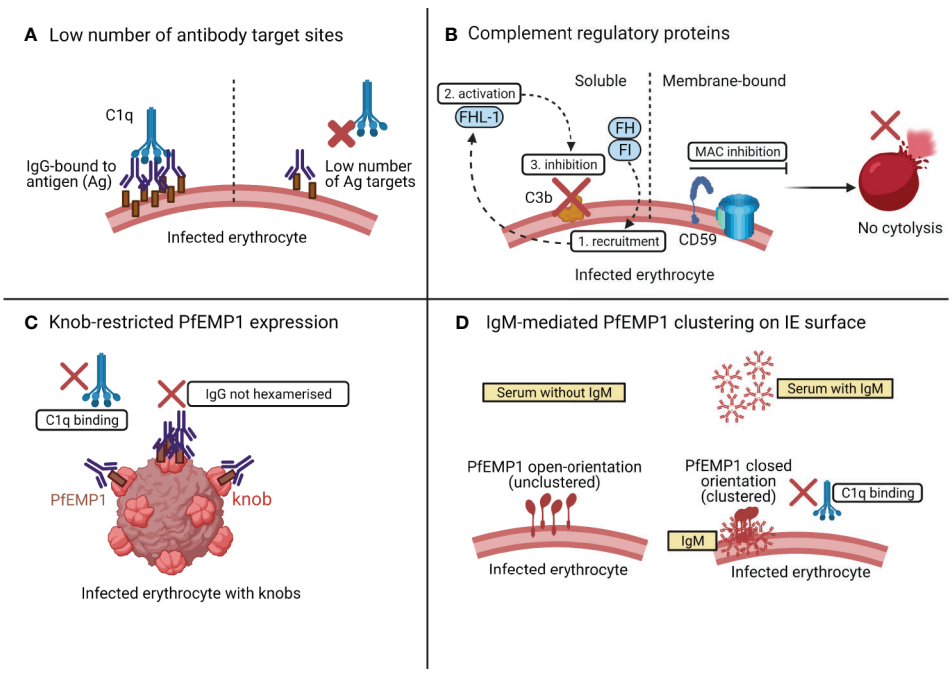

FIGURE 4 | Possible mechanisms of resistance of IEs to classical complement attack. As shown in **(A)**, if the number of PfEMP1 target sites on IEs are below a certain threshold level, complement is not activated even in the presence of an ample supply of antibody and complement. In **(B)**, the presence of complement regulatory proteins such as the membrane bound CD59, inhibits the MAC assembly, to prevent lysis of IEs. The soluble complement regulatory factors [factor I (FI) and factor H (FH)] are also recruited onto the schizont surface (1) and activate FH-like protein 1 (FHL-1) (2) to prevent C3b deposition (3) on the schizont surface, thus preventing complement activation. The knob-restricted expression of PfEMP1 on IEs in **(C)** provides an evolutionary advantage to the parasite to evade classical complement attack. In **(D)**, both PfEMP1 and C1q compete for the same binding site on IgM. Initial binding of IgM with PfEMP1 causes PfEMP1 clustering and prevents IgM-C1q interaction.

markers of complement activation (as measured by the serum levels of C3a and C5a) (94). High levels of CRPs on IEs may help protect parasites from complement-mediated damage even in the presence of complement-fixing antibodies (94) and even when the terminal complement complexes are deposited on the erythrocyte surface (67).

A recent study assessed the classical complement activation by PfEMP1-specific human IgG using recombinant PfEMP1 by ELISAs and native PfEMP1 on the surface of IEs by flow cytometry (89). The PfEMP1-specific antibodies were unable to activate classical complement pathway by binding to the native PfEMP1 expressed on the surface of IEs (89), but when they bound to recombinant PfEMP1, they activated the classical complement pathway as measured by the elevated levels of C1q, C3, and C4. The authors hypothesised that the knob-restricted expression of native PfEMP1 protein on the IE surface may provide an evolutionary advantage to the parasite to evade classical complement attack (89). The knobs are nanoscale protrusions of the erythrocyte membrane (95) and enable anchorage of PfEMP1 to the surface of IEs (61). The knob-restricted expression of PfEMP1 may hinder the interaction between PfEMP1 and IgG, which may restrict the formation of IgG hexamers for C1q recruitment (40) (**Figure 4C**).

Most of the studies discussed previously highlighted that complement fixing antibodies on IEs were of type IgG (29), especially the subclasses, IgG1 and IgG3 (67). A recent study assessed the complement activation by nonimmune IgM when bound to PfEMP1 on IEs (**Figure 4D**) (96). The binding of IgM to PfEMP1 did not result in complement-mediated lysis because C1q seemed to compete for the same binding pocket on IgM where PfEMP1 is already bound. The interaction between IgM and PfEMP1 prevents C1q deposition and changes the conformation of PfEMP1 to augment PfEMP1-mediated parasite interactions with host receptors for its sequestration and survival (96).

The above reasons seem to contribute to the lack of lysis of IEs by the classical pathway of complement.

FUTURE DIRECTIONS AND CONCLUDING REMARKS

Some evidence (9) suggests that ability to fix complement is an independent correlate of ability of sera to kill sporozoites. Passive transfer studies of a modified monoclonal antibody against PfRh5 (*P. falciparum* reticulocyte homologue 5) indicate that neutralising antibody alone requires high titres (97), indicating a role for Fc-mediated antibody function. This may not, however, be directly attributable to complement fixation as studies of vaccine-induced immunity suggested that NK cell and Fc receptor engagement rather than complement fixation were independent correlates of protection (10).

Despite such recent improvements in understanding of antibody-mediated complement interactions in protective immunity to malaria, the following gaps also should be addressed as priorities for future research (**Box 1**).

In this review, we summarise antibody-dependent complement activation by different stages of parasites during *P. falciparum* infection. Studies show that the inhibitory effect of antibodies directed against surface proteins of sporozoites (e.g., CSP), merozoites (e.g., $MSP1_{19}$), and sexual stages of *P. falciparum* (e.g., Pfs230) can be greatly augmented by the presence of complement. The binding of C1q to IgG-opsonised merozoites and sporozoites has shown to be associated with protective immunity in malaria. We also emphasise that IEs are resistant to complement mediated lysis in comparison to other parasitic stages. This may be due to some intrinsic properties of IEs, including the expression of complement regulatory proteins, an insufficient number of antigenic sites as targets for antibody binding, and the orientation of antigens on the parasite surface for restricted antibody binding for complement deposition. The attempts made to evaluate the underlying mechanisms of antibody-mediated complement activation during malaria will provide a deeper understanding of the processes that mediate complement-mediated protection and/or evasion.

AUTHOR CONTRIBUTIONS

DR gathered papers, organised, and drafted the review. Both EA and SR provided intellectual feedback, critically revised, and approved the final manuscript for submission. All authors contributed to the article and approved the submitted version.

FUNDING

DR is supported by the Melbourne Research Scholarship from the University of Melbourne and Miller Foundation Top-up Scholarship. The work of EA and SR is supported by grants from the National Health and Medical Research Council of Australia (GNT1092789 and GNT1143946), and by the Centre for Research Excellence in Malaria Elimination (GNT1134989).

ACKNOWLEDGMENTS

All the images were created with BioRender.com.

REFERENCES

1. World Health Organization. World Malaria Report 2020. In: *20 Years of Global Progress and Challenges*. Geneva: World Health Organization. (2020).
2. Langhorne J, Ndungu FM, Sponaas AM, Marsh K. Immunity to Malaria: More Questions Than Answers. *Nat Immunol* (2008) 9(7):725–32. doi: 10.1038/ni.f.205
3. Ashley EA, Pyae Phyo A, Woodrow CJ. Malaria. *Lancet* (2018) 391:1608–21. doi: 10.1016/S0140-6736(18)30324-6

4. Desai M, ter Kuile FO, Nosten F, McGready R, Asamoa K, Brabin B, et al. Epidemiology and Burden of Malaria in Pregnancy. *Lancet Infect Dis* (2007) 7 (2):93–104. doi: 10.1016/S1473-3099(07)70021-X
5. Basu S, Sahi PK. Malaria: An Update. *Indian J Pediatr* (2017) 84(7):521–8. doi: 10.1007/s12098-017-2332-2
6. Doolan DL, Dobaño C, Baird JK. Acquired Immunity to Malaria. *Clin Microbiol Rev* (2009) 22(1):13–36. doi: 10.1128/CMR.00025-08
7. Cohen S, McGregor IA, Carrington S. Gamma-Globulin and Acquired Immunity to Human Malaria. *Nature* (1961) 192:733–7. doi: 10.1038/192733a0
8. Kurtovic L, Atre T, Feng G, Wines BD, Chan J-A, Boyle MJ, et al. Multifunctional Antibodies Are Induced by the RTS,S Malaria Vaccine and Associated With Protection in a Phase 1/2a Trial. *J Infect Dis* (2020) jiaa144:1–11. doi: 10.1093/infdis/jiaa144
9. Kurtovic L, Behet MC, Feng G, Reiling L, Chelimo K, Dent AE, et al. Human Antibodies Activate Complement Against Plasmodium Falciparum Sporozoites, and are Associated With Protection Against Malaria in Children. *BMC Med* (2018) 16(1):1–17. doi: 10.1186/s12916-018-1054-2
10. Suscovich TJ, Fallon JK, Das J, Demas AR, Crain J, Linde CH, et al. Mapping Functional Humoral Correlates of Protection Against Malaria Challenge Following RTS,S/AS01 Vaccination. *Sci Transl Med* (2020) 12(553):1–14. doi: 10.1126/scitranslmed.abb4757
11. Ricklin D, Hajishengallis G, Yang K, Lambris JD. Complement: A Key System for Immune Surveillance and Homeostasis. *Nat Immunol* (2010) 11(9):785–97. doi: 10.1038/ni.1923
12. Wagner E, Frank MM. Therapeutic Potential of Complement Modulation. *Nat Rev Drug Discovery* (2010) 9(1):43–56. doi: 10.1038/nrd3011
13. Taylor RP, Stoute JA, Lindorfer MA. Mechanisms of Complement Activation in Malaria. In: JA Stoute, editor. *Complement Activation in Malaria Immunity and Pathogenesis*. United States: Springer (2018). p. 31–49.
14. Merle NS, Church SE, Fremeaux-Bacchi V, Roumenina LT. Complement System Part I - Molecular Mechanisms of Activation and Regulation. *Front Immunol* (2015) 6:1–30. doi: 10.3389/fimmu.2015.00262
15. Nauser CL, Farrar CA, Sacks SH. Complement Recognition Pathways in Renal Transplantation. *J Am Soc Nephrol* (2017) 28(9):2571–8. doi: 10.1681/ASN.2017010079
16. Noris M, Remuzzi G. Overview of Complement Activation and Regulation. *Semin Nephrol* (2013) 33(6):479–92. doi: 10.1016/j.semnephrol.2013.08.001
17. Adam C, Grniteau M, Gougerot-Pocidalo P, Verroust P, Lebras J, Gibert C, et al. Cryoglobulins, Circulating Immune Complexes, and Complement Activation in Cerebral Malaria. *Infect Immun* (1981) 31(2):530–5. doi: 10.1128/IAI.31.2.530-535.1981
18. Ade-Serrano MA, Ejezie GC, Kassim OO. Correlation of Plasmodium Falciparum Gametocytemia With Complement Component Titers in Rural Nigerian School Children. *J Clin Microbiol* (1981) 13(1):195–8. doi: 10.1128/JCM.13.1.195-198.1981
19. Glew RH, Atkinson JP, Frank MM, Collins WE, Neva FA. Serum Complement and Immunity in Experimental Simian Malaria. I. Cyclical Alterations in C4 Related to Schizont Rupture. *J Infect Dis* (1975) 131 (1):17–25. doi: 10.1093/infdis/131.1.17
20. Nyakoe NK, Taylor RP, Makumi JN, Waitumbi JN. Complement Consumption in Children With Plasmodium Falciparum Malaria. *Malar J* (2009) 8(1):7. doi: 10.1186/1475-2875-8-7
21. Neva FA, Howard WA, Glew RH, Krotoski WA, Gam AA, Collins WE, et al. Relationship of Serum Complement Levels to Events of the Malarial Paroxysm. *J Clin Invest* (1974) 54(2):451–60. doi: 10.1172/JCI107781
22. Roestenberg M, McCall M, Mollnes TE, van Deuren M, Sprong T, Klasen I, et al. Complement Activation in Experimental Human Malaria Infection. *Trans R Soc Trop Med Hyg* (2007) 101(7):643–9. doi: 10.1016/j.trstmh.2007.02.023
23. McGhee RB. The Effect of a Malaria Infection on the Titer of Complement and its Components in Ducks. *J Immunol* (1952) 68(4):421–7.
24. Atkinson JP, Glew RH, Neva FA, Frank MM. Serum Complement and Immunity in Experimental Simian Malaria. II. Preferential Activation of Early Components and Failure of Depletion of Late Components to Inhibit Protective Immunity. *J Infect Dis* (1975) 131(1):26–33. doi: 10.1093/infdis/131.1.26
25. Galbraith RM, Fox H, Hsi B, Galbraith GMP, Bray RS, Faulk WP. The Human Materno-Foetal Relationship in Malaria. II. Histological, Ultrastructural, and Immunopathologic Studies of the Placenta. *Trans R Soc Trop Med Hyg* (1980) 74(1):61–72. doi: 10.1016/0035-9203(80)90012-7
26. Yamada M, Steketee R, Abramowsky C, Kida M, Wirima J, Heymann D, et al. Plasmodium Falciparum Associated Placental Pathology: A Light and Electron Microscopic and Immunohistologic Study. *Am J Trop Med Hyg* (1989) 41(2):161–8. doi: 10.4269/ajtmh.1989.41.161
27. Muehlenbachs A, Fried M, Lachowitzer J, Mutabingwa TK, Duffy PE. Genome-Wide Expression Analysis of Placental Malaria Reveals Features of Lymphoid Neogenesis During Chronic Infection. *J Immunol* (2007) 179:557–65. doi: 10.4049/jimmunol.179.1.557
28. Wenisch C, Spitzauer S, Florris-Linau K, Rumpold H, Vannaphan S, Parschalk B, et al. Complement Activation in Severe Plasmodium Falciparum Malaria. *Clin Immunol Immunopathol* (1997) 85(2):166–71. doi: 10.1006/clin.1997.4417
29. Stanley HA, Mayes JT, Cooper NR, Reese RT. Complement Activation by the Surface of Plasmodium Falciparum Infected Erythrocytes. *Mol Immunol* (1984) 21(2):145–50. doi: 10.1016/0161-5890(84)90129-9
30. Pawluczkowycz AW, Lindorfer MA, Waitumbi JN, Taylor RP. Hematin Promotes Complement Alternative Pathway-Mediated Deposition of C3 Activation Fragments on Human Erythrocytes: Potential Implications for the Pathogenesis of Anemia in Malaria. *J Immunol* (2007) 179(8):5543–52. doi: 10.4049/jimmunol.179.8.5543
31. Korir JC, Nyakoe NK, Awinda G, Waitumbi JN. Complement Activation by Merozoite Antigens of Plasmodium Falciparum. *PloS One* (2014) 9(8):1–9. doi: 10.1371/journal.pone.0105093
32. Klabunde J, Uhlemann A-C, Tebo AE, Kimmel J, Schwarz RT, Kremsner PG, et al. Recognition of Plasmodium Falciparum Proteins by Mannan-Binding Lectin, A Component of the Human Innate Immune System. *Parasitol Res* (2002) 88(2):113–7. doi: 10.1007/s00436-001-0518-y
33. Garred P, Nielsen MA, Kurtzhals JAL, Malhotra R, Madsen HO, Goka BQ, et al. Mannose-Binding Lectin is a Disease Modifier in Clinical Malaria and May Function as Opsonin for Plasmodium Falciparum- Infected Erythrocytes. *Infect Immun* (2003) 71(9):5245–53. doi: 10.1128/IAI.71.9.5245-5253.2003
34. Lipscombe RJ, Sumiya M, Summerfield JA, Turner MW. Distinct Physicochemical Characteristics of Human Mannose Binding Protein Expressed by Individuals of Differing Genotype. *Immunology* (1995) 85:660–7.
35. Luty AJF, Kun JFJ, Kremsner PG. Mannose-Binding Lectin Plasma Levels and Gene Polymorphisms in Plasmodium Falciparum Malaria. *J Infect Dis* (1998) 178(4):1221–4. doi: 10.1086/515690
36. Holmberg V, Schuster F, Dietz E, Sagarriga JC, Anemana SD, Bienzle U, et al. Mannose-Binding Lectin Variant Associated With Severe Malaria in Young African Children. *Microbes Infect* (2008) 10:342–8. doi: 10.1016/j.micinf.2007.12.008
37. Mombo LE, Ntoumi F, Bisseye C, Ossari S, Lu CY, Nagel RL, et al. Human Genetic Polymorphisms and Asymptomatic Plasmodium Falciparum Malaria in Gabonese School Children. *Am J Trop Med Hyg* (2003) 68(2):186–90. doi: 10.4269/ajtmh.2003.68.186
38. Bellamy R, Ruwende C, Mcadam KPWJ, Thursz M, Sumiya M, Summerfield J, et al. Mannose Binding Protein Deficiency Is Not Associated With Malaria, Hepatitis B Carriage Nor Tuberculosis in Africans. *Q J Med* (1998) 91:13–8. doi: 10.1093/qjmed/91.1.13
39. Biryukov S, Stoute JA. Complement Activation in Malaria: Friend or Foe? *Trends Mol Med* (2014) 20(5):293–301. doi: 10.1016/j.molmed.2014.01.001
40. Diebolder CA, Beurskens FJ, Jong RND, Koning RI, Strumane K, Lindorfer MA, et al. Complement Is Activated by IgG Hexamers Assembled at the Cell Surface. *Science* (2014) 343(6176):1260–3. doi: 10.1126/science.1248943
41. Schroeder HW, Cavacini L. Structure and Function of Immunoglobulins. *J Allergy Clin Immunol* (2010) 125:237–49. doi: 10.1016/j.jaci.2009.09.046
42. Dundas K, Shears MJ, Photini S, Wright GJ. Important Extracellular Interactions Between Plasmodium Sporozoites and Host Cells Required for Infection. *Trends Parasitol* (2016) 35(2):1–18. doi: 10.1016/j.pt.2018.11.008
43. Sack BK, Miller JL, Vaughan AM, Douglass A, Kaushansky A, Mikolajczak S, et al. Model for In Vivo Assessment of Humoral Protection Against Malaria Sporozoite Challenge by Passive Transfer of Monoclonal Antibodies and Immune Serum. *Infect Immun* (2014) 82(2):808–17. doi: 10.1128/IAI.01249-13
44. Mellouk S, Berbiguier N, Druilhe P, Sedegah M, Galey B, Leef M, et al. Evaluation of an In Vitro Assay Aimed at Measuring Protective Antibodies Against Sporozoites. *Bull World Health Organ* (1990) 68:52–9.

45. Zenklusen I, Jongo S, Abdulla S, Ramadhani K, Lee Sim BK, Cardamone H, et al. Immunization of Malaria-Preexposed Volunteers With PfSPZ Vaccine Elicits Long-Lived IgM Invasion-Inhibitory and Complement-Fixing Antibodies. *J Infect Dis* (2018) 217(10):1569–78. doi: 10.1093/infdis/jiy080
46. Behet MC, Kurtovic L, van Gemert GJ, Haukes CM, Siebelink-Stoter R, Graumans W, et al. The Complement System Contributes to Functional Antibody-Mediated Responses Induced by Immunization With Plasmodium Falciparum Malaria Sporozoites. *Infect Immun* (2018) 86(7):1–15. doi: 10.1128/IAI.00920-17
47. Kurtovic L, Agius PA, Feng G, Drew DR, Ubillos I, Sacarlal J, et al. Induction and Decay of Functional Complement-Fixing Antibodies by the RTS,S Malaria Vaccine in Children, and a Negative Impact of Malaria Exposure. *BMC Med* (2019) 17(1):1–14. doi: 10.1186/s12916-019-1277-x
48. Cowman AF, Crabb BS. Invasion of Red Blood Cells by Malaria Parasites. *Cell* (2006) 124:755–66. doi: 10.1016/j.cell.2006.02.006
49. Stanisic DI, Richards JS, McCallum FJ, Michon P, King CL, Schoepflin S, et al. Immunoglobulin G Subclass-Specific Responses Against Plasmodium Falciparum Merozoite Antigens are Associated With Control of Parasitemia and Protection From Symptomatic Illness. *Infect Immun* (2009) 77(3):1165–74. doi: 10.1128/IAI.01129-08
50. Boyle MJ, Reiling L, Feng G, Langer C, Osier FH, Aspeling-Jones H, et al. Human Antibodies Fix Complement to Inhibit Plasmodium Falciparum Invasion of Erythrocytes and are Associated With Protection Against Malaria. *Immunity* (2015) 42(3):580–90. doi: 10.1016/j.immuni.2015.02.012
51. Feng G, Boyle MJ, Cross N, Chan JA, Reiling L, Osier F, et al. Human Immunization With a Polymorphic Malaria Vaccine Candidate Induced Antibodies to Conserved Epitopes That Promote Functional Antibodies to Multiple Parasite Strains. *J Infect Dis* (2018) 218(1):35–43. doi: 10.1093/infdis/jiy170
52. Reiling L, Boyle MJ, White MT, Wilson DW, Feng G, Weaver R, et al. Targets of Complement-Fixing Antibodies in Protective Immunity Against Malaria in Children. *Nat Commun* (2019) 10(1):610. doi: 10.1038/s41467-019-08528-z
53. Jong RM, Tebeje SK, Meerstein-Kessel L, Tadesse FG, Jore MM, Stone W, et al. Immunity Against Sexual Stage Plasmodium Falciparum and Plasmodium Vivax Parasites. *Immunol Rev* (2020) Jan 16293(1):190–215. doi: 10.1111/imr.12828
54. Chan JA, Drew DR, Reiling L, Lisboa-Pinto A, Dinko B, Sutherland CJ, et al. Low Levels of Human Antibodies to Gametocyte-Infected Erythrocytes Contrasts the PfEMP1-Dominant Response to Asexual Stages in P. Falciparum Malaria. *Front Immunol* (2019) 9:1–8. doi: 10.3389/fimmu.2018.03126
55. Williamson KC. Pfs230: From Malaria Transmission-Blocking Vaccine Candidate Toward Function. *Parasite Immunol* (2003) 25:351–9. doi: 10.1046/j.1365-3024.2003.00643.x
56. Read D, Lensen AH, Begarnie, Haley S, Raza A, Carter R. Transmission-Blocking Antibodies Against Multiple, Non-Variant Target Epitopes of the Plasmodium Falciparum Gamete Surface Antigen Pfs230 are All Complement-Fixing. *Parasite Immunol* (1994) 16:511–9. doi: 10.1111/j.1365-3024.1994.tb00305.x
57. Healer J, McGuinness D, Hopcroft P, Haley S, Carter R, Riley E. Complement-Mediated Lysis of Plasmodium Falciparum Gametes by Malaria- Immune Human Sera is Associated With Antibodies to the Gamete Surface Antigen Pfs230. *Infect Immun* (1997) 65(8):3017–23. doi: 10.1128/IAI.65.8.3017-3023.1997
58. Roeffen W, Beckers PJA, Teelen K, Lensen T, Sauerwein RW, Meuwissen JHET, et al. Plasmodium Falciparum: A Comparison of the Activity of Pfs230-Specific Antibodies in an Assay of Transmission-Blocking Immunity and Specific Competition Elisas. *Exp Parasitol* (1995) 80:15–26. doi: 10.1006/expr.1995.1003
59. Singh K, Burkhardt M, Nakuchima S, Herrera R, Muratova O, Gittis AG, et al. Structure and Function of a Malaria Transmission Blocking Vaccine Targeting Pfs230 and Pfs230-Pfs48/45 Proteins. *Commun Biol* (2020) 3 (1):1–12. doi: 10.1038/s42003-020-01123-9
60. Chan J-A, Stanisic DI, Duffy MF, Robinson LJ, Lin E, Kazura JW, et al. Patterns of Protective Associations Differ for Antibodies to P. Falciparum -Infected Erythrocytes and Merozoites in Immunity Against Malaria in Children. *Eur J Immunol* (2017) 47(12):2124–36. doi: 10.1002/eji.201747032
61. Smith JD, Rowe JA, Higgins MK, Lavstsen T. Malaria's Deadly Grip: Cytoadhesion of Plasmodium Falciparum Infected Erythrocytes. *Cell Microbiol* (2013) 15(12):1–7. doi: 10.1111/cmi.12183
62. Fried M, Duffy P. Adherence of Plasmodium Falciparum to Chondroitin Sulfate A in the Human Placenta. *Science* (1996) 272:2–5. doi: 10.1126/science.272.5267.1502
63. Roberts DJ, Craig AG, Berendt AR, Pinches R, Nash G, Marsh K, et al. Rapid Switching to Multiple Antigenic and Adhesive Phenotypes in Malaria. *Nature* (1992) 357(6380):689–92. doi: 10.1038/357689a0
64. Smith JD, Craig AG, Roberts DJ, Hudson-taylor DE, Peterson DS, Pinches R, et al. Switches in Expression of Plasmodium Falciparum Var Genes Correlate With Changes in Antigenic and Cytoadherent Phenotypes of Infected Erythrocytes. *Cell* (1995) 82(1):101–10. doi: 10.1016/0092-8674(95)90056-X
65. Chan JA, Howell KB, Reiling L, Ataide R, Mackintosh CL, Fowkes FJI, et al. Targets of Antibodies Against Plasmodium Falciparum-Infected Erythrocytes in Malaria Immunity. *J Clin Invest* (2012) 122(9):3227–38. doi: 10.1172/JCI62182
66. Meulenbroek EM, Wouters D, Zeerleder S. Methods for Quantitative Detection of Antibody-induced Complement Activation on Red Blood Cells. *J Vis Exp* (2014) 83:1–6. doi: 10.3791/51161
67. Wiesner J, Jomaa H, Wilhem M, Tony H, Kremsner PG, Horrocksl P, et al. Host Cell Factor CD59 Restricts Complement Lysis of Plasmodium Falciparum-Infected Erythrocytes. *Eur J Immunol* (1997) 27:2708–13. doi: 10.1002/eji.1830271034
68. Hommel M, Chan J, Umbers AJ, Langer C, Rogerson SJ, Smith JD, et al. Evaluating Antibody Functional Activity and Strain-Specificity of Vaccine Candidates for Malaria in Pregnancy Using In Vitro Phagocytosis Assays. *Parasit Vectors* (2018) 11(69):1–7. doi: 10.1186/s13071-018-2653-7
69. Zhou J, Feng G, Beeson J, Hogarth PM, Rogerson SJ, Yan Y, et al. Cd14hiCD16+ Monocytes Phagocytose Antibody-Opsonised Plasmodium Falciparum Infected Erythrocytes More Efficiently Than Other Monocyte Subsets, and Require CD16 and Complement to do So. *BMC Med* (2015) 13 (1):1–14. doi: 10.1186/s12916-015-0391-7
70. Celada A, Cruchaud A, Perrin LH. Phagocytosis of Plasmodium Falciparum-Parasitized Erythrocytes by Human Polymorphonuclear Leukocytes. *J Parasitol* (1983) 69(1):49–53. doi: 10.2307/3281273
71. Arora G, Hart GT, Manzella-lapeira J, Doritchamou JYA, Narum DL, Thomas LM, et al. NK Cells Inhibit Plasmodium Falciparum Growth in Red Blood Cells Via Antibody- Dependent Cellular Cytotoxicity. *Elife* (2018) 7:1–20. doi: 10.7554/eLife.36806
72. Nardin A, Lindorfer MA, Taylor RP. How are Immune Complexes Bound to the Primate Erythrocyte Complement Receptor Transferred to Acceptor Phagocytic Cells? *Mol Immunol* (1999) 36:827–35. doi: 10.1016/S0161-5890(99)00103-0
73. Fernandez-Arias C, Lopez JP, Nikolae J, Bautista-ojeda MD, Bautista-ojeda MD, Branch O, et al. Malaria Inhibits Surface Expression of Complement Receptor 1 in Monocytes/Macrophages, Causing Decreased Immune Complex Internalization. *J Immunol* (2013) 190:3363–72. doi: 10.4049/jimmunol.1103812
74. Thomas BN, Diallo DA, Noumsi GT, Moulds JM. Circulating Immune Complex Levels are Associated With Disease Severity and Seasonality in Children With Malaria From Mali. *Biomark Insights* (2012) 7:81–6. doi: 10.4137/BMI.S9624
75. Owuor BO, Odhiambo CO, Otieno WO, Adhiambo C, Makawiti DW, Stoute JA. Reduced Immune Complex Binding Capacity and Increased Complement Susceptibility of Red Cells From Children With Severe Malaria-Associated Anemia. *Mol Med* (2007) 14(3–4):89–97. doi: 10.2119/2007-00093.Owuor
76. Waitumbi JN, Opollo MO, Muga RO, Misore AO, Stoute A. Red Cell Surface Changes and Erythrophagocytosis in Children With Severe Plasmodium Falciparum Anemia. *Blood* (2000) 95(4):1481–7. doi: 10.1182/blood.V95.4.1481.004k15_1481_1486
77. Goka BQ, Kwarko H, Kurtzhals JAL, Gyan B, Ofori-Adjei E, Ohene SA, et al. Complement Binding to Erythrocytes Is Associated With Macrophage Activation and Reduced Haemoglobin in Plasmodium Falciparum Malaria. *Trans R Soc Trop Med Hyg* (2001) 95(5):545–9. doi: 10.1016/S0035-9203(01)90036-7
78. Dasari P, Fries A, Heber SD, Salama A, Blau I-W, Lingelbach K, et al. Malarial Anemia: Digestive Vacuole of Plasmodium Falciparum Mediates Complement Deposition on Bystander Cells to Provoke Hemophagocytosis. *Med Microbiol Immunol* (2014) 203:383–93. doi: 10.1007/s00430-014-0347-0
79. Waitumbi JN, Donvito B, Kisserli A, Cohen JHM, Stoute JA. Age-Related Changes in Red Blood Cell Complement Regulatory Proteins and

Susceptibility to Severe Malaria. *J Infect Dis* (2004) 190(6):1183–91. doi: 10.1086/423140
80. Stoute JA, Odindo AO, Owuor BO, Mibei EK, Opollo MO, Waitumbi JN. Loss of Red Blood Cell–Complement Regulatory Proteins and Increased Levels of Circulating Immune Complexes are Associated With Severe Malarial Anemia. *J Infect Dis* (2003) 187(3):522–5. doi: 10.1086/367712
81. Facer CA, Bray RS, Brown J. Direct Coombs Antiglobulin Reactions in Gambian Children With Plasmodium Falciparum Malaria I. *Incidence Class Specificity Clin Exp Immunol* (1979) 35:119–27.
82. Facer CA. Direct Coombs Antiglobulin Reactions in Gambian Children With Plasmodium Falciparum Malaria II. *Specificity Erythrocyte-Bound IgG Clin Exp Immunol* (1980) 39:279–88.
83. Stoute JA. Complement Receptor 1 and Malaria. *Cell Microbiol* (2011) 13 (10):1441–50. doi: 10.1111/j.1462-5822.2011.01648.x
84. Wood AJT, Vassallo A, Summers C, Chilvers ER, Conway-Morris A. C5a Anaphylatoxin and its Role in Critical Illness-Induced Organ Dysfunction. *Eur J Clin Invest* (2018) 48(12):e13028. doi: 10.1111/eci.13028
85. Patel SN, Berghout J, Lovegrove FE, Ayi K, Conroy A, Serghides L, et al. C5 Deficiency and C5a or C5aR Blockade Protects Against Cerebral Malaria. *J Exp Med* (2008) 205(5):1133–43. doi: 10.1084/jem.20072248
86. Conroy AL, Silver KL, Zhong K, Rennie M, Ward P, Sarma JV, et al. Complement Activation and the Resulting Placental Vascular Insufficiency Drives Fetal Growth Restriction Associated With Placental Malaria. *Cell Host Microbe* (2013) 13(2):215–26. doi: 10.1016/j.chom.2013.01.010
87. Conroy A, Serghides L, Finney C, Owino SO, Kumar S, Gowda DC, et al. C5a Enhances Dysregulated Inflammatory and Angiogenic Responses to Malaria in Vitro: Potential Implications for Placental Malaria. *PloS One* (2009) 4(3): e4953. doi: 10.1371/journal.pone.0004953
88. David PH, Hommel M, Miller LH, Udeinya IJ, Oligino LD. Parasite Sequestration in Plasmodium Falciparum Malaria: Spleen and Antibody Modulation of Cytoadherence of Infected Erythrocytes. *Proc Natl Acad Sci* (1983) 80(16):5075–9. doi: 10.1073/pnas.80.16.5075
89. Larsen MD, Quintana M del P, Ditlev SB, Bayarri-Olmos R, Ofori MF, Hviid L, et al. Evasion of Classical Complement Pathway Activation on Plasmodium Falciparum-Infected Erythrocytes Opsonized by PfEMP1-Specific Igg. *Front Immunol* (2019) 9(Jan):1–10. doi: 10.3389/fimmu.2018.03088
90. Sarma JV, Ward PA. The Complement System. *Cell Tissue Res* (2011) 343 (1):227–35. doi: 10.1007/s00441-010-1034-0
91. Rosa TFA, Flammersfeld A, Ngwa CJ, Kiesow M, Fischer R, Zipfel PF, et al. The Plasmodium Falciparum Blood Stages Acquire Factor H Family Proteins to Evade Destruction by Human Complement. *Cell Microbiol* (2016) 18 (4):573–90. doi: 10.1111/cmi.12535
92. Reiss T, Rosa TF de A, Blaesius K, Bobbert RP, Zipfel PF, Skerka C, et al. Cutting Edge: Fhr-1 Binding Impairs Factor H–Mediated Complement Evasion by the Malaria Parasite Plasmodium Falciparum. *J Immunol* (2018) 201(12):3497–502. doi: 10.4049/jimmunol.1800662
93. Kennedy AT, Schmidt CQ, Thompson JK, Weiss GE, Taechalertpaisarn T, Gilson PR, et al. Recruitment of Factor H as a Novel Complement Evasion Strategy for Blood-Stage Plasmodium Falciparum Infection. *J Immunol* (2016) 196(3):1239–48. doi: 10.4049/jimmunol.1501581
94. Oyong DA, Kenangalem E, Poespoprodjo JR, Beeson JG, Anstey NM, Price RN, et al. Loss of Complement Regulatory Proteins on Uninfected Erythrocytes in Vivax and Falciparum Malaria Anemia. *JCI Insight* (2018) 3 (22):1–11. doi: 10.1172/jci.insight.124854
95. Nagao E, Kaneko O, Dvorak JA. Plasmodium Falciparum-Infected Erythrocytes: Qualitative and Quantitative Analyses of Parasite-Induced Knobs by Atomic Force Microscopy. *J Struct Biol* (2000) 130:34–44. doi: 10.1006/jsbi.2000.4236
96. Akhouri RR, Goel S, Furusho H, Skoglund U, Wahlgren M. Architecture of Human Igm in Complex With P. *Falciparum Erythrocyte Membrane Protein 1 Cell Rep* (2016) Feb14(4):723–36. doi: 10.1016/j.celrep.2015.12.067
97. Douglas AD, Baldeviano GC, Jin J, Miura K, Diouf A, Zenonos ZA, et al. A Defined Mechanistic Correlate of Protection Against Plasmodium Falciparum Malaria in non-Human Primates. *Nat Commun* (2019) 10(1953):1–8. doi: 10.1038/s41467-019-09894-4

Conflict of Interest: The authors declare that the research was conducted in the absence of any commercial or financial relationships that could be construed as a potential conflict of interest.

frontiers in Immunology

ORIGINAL RESEARCH
published: 29 November 2021
doi: 10.3389/fimmu.2021.766272

Bruton's Tyrosine Kinase Inhibitors Impair FcγRIIA-Driven Platelet Responses to Bacteria in Chronic Lymphocytic Leukemia

*Leigh Naylor-Adamson[1], Anisha R. Chacko[1], Zoe Booth[1], Stefano Caserta[2], Jenna Jarvis[2], Sujoy Khan[3], Simon P. Hart[4], Francisco Rivero[1], David J. Allsup[1,5] and Mònica Arman[1]**

[1] Centre for Atherothrombosis and Metabolic Disease, Hull York Medical School, Faculty of Health Sciences, University of Hull, Hull, United Kingdom, [2] Department of Biomedical Sciences, Faculty of Health Sciences, University of Hull, Hull, United Kingdom, [3] Department of Immunology & Allergy, Queens Centre, Castle Hill Hospital, Hull University Teaching Hospitals NHS Trust, Cottingham, United Kingdom, [4] Respiratory Research Group, Hull York Medical School, Faculty of Health Sciences, University of Hull, Hull, United Kingdom, [5] Department of Haematology, Queens Centre for Oncology and Haematology, Castle Hill Hospital, Hull University Teaching Hospitals NHS Trust, Cottingham, United Kingdom

OPEN ACCESS

Edited by:
Gabriella Scarlatti, San Raffaele Hospital (IRCCS), Italy

Reviewed by:
Norma Maugeri, San Raffaele Scientific Institute (IRCCS), Italy
Jochen Mattner, University Hospital Erlangen, Germany

***Correspondence:**
Mònica Arman
Monica.Arman@hyms.ac.uk

Specialty section:
This article was submitted to Microbial Immunology, a section of the journal Frontiers in Immunology

Received: *28 August 2021*
Accepted: *25 October 2021*
Published: *29 November 2021*

Citation:
Naylor-Adamson L, Chacko AR, Booth Z, Caserta S, Jarvis J, Khan S, Hart SP, Rivero F, Allsup DJ and Arman M (2021) Bruton's Tyrosine Kinase Inhibitors Impair FcγRIIA-Driven Platelet Responses to Bacteria in Chronic Lymphocytic Leukemia. Front. Immunol. 12:766272. doi: 10.3389/fimmu.2021.766272

Bacterial infections are a major cause of morbidity and mortality in chronic lymphocytic leukemia (CLL), and infection risk increases in patients treated with the Bruton's tyrosine kinase (Btk) inhibitor, ibrutinib. Btk and related kinases (like Tec) are expressed in non-leukemic hematopoietic cells and can be targeted by ibrutinib. In platelets, ibrutinib therapy is associated with bleeding complications mostly due to off-target effects. But the ability of platelets to respond to bacteria in CLL, and the potential impact of ibrutinib on platelet innate immune functions remain unknown. FcγRIIA is a tyrosine kinase-dependent receptor critical for platelet activation in response to IgG-coated pathogens. Crosslinking of this receptor with monoclonal antibodies causes downstream activation of Btk and Tec in platelets, however, this has not been investigated in response to bacteria. We asked whether ibrutinib impacts on FcγRIIA-mediated activation of platelets derived from CLL patients and healthy donors after exposure to *Staphylococcus aureus* Newman and *Escherichia coli* RS218. Platelet aggregation, α-granule secretion and integrin αIIbβ3-dependent scavenging of bacteria were detected in CLL platelets but impaired in platelets from ibrutinib-treated patients and in healthy donor-derived platelets exposed to ibrutinib *in vitro*. While levels of surface FcγRIIA remained unaffected, CLL platelets had reduced expression of integrin αIIbβ3 and GPVI compared to controls regardless of therapy. In respect of intracellular signaling, bacteria induced Btk and Tec phosphorylation in both CLL and control platelets that was inhibited by ibrutinib. To address if Btk is essential for platelet activation in response to bacteria, platelets derived from X-linked agammaglobulinemia patients (lacking functional Btk) were exposed to *S. aureus* Newman and *E. coli* RS218, and FcγRIIA-dependent aggregation was observed. Our data suggest that ibrutinib impairment of FcγRIIA-mediated platelet activation by bacteria results from a combination of Btk and Tec inhibition, although off-target effects on

additional kinases cannot be discarded. This is potentially relevant to control infection-risk in CLL patients and, thus, future studies should carefully evaluate the effects of CLL therapies, including Btk inhibitors with higher specificity for Btk, on platelet-mediated immune functions.

Keywords: platelet, FcγRIIA, *Staphylococcus aureus*, *Escherichia coli*, Bruton's tyrosine kinase inhibitor, ibrutinib, chronic lymphocytic leukemia (CLL)

INTRODUCTION

Chronic lymphocytic leukemia (CLL) is the most common form of leukemia in the Western World, with approximately 3750 new cases diagnosed annually in the United Kingdom (1). Infectious complications are a major cause of morbidity and mortality in CLL patients (2, 3). The increased risk of infection is due to multiple factors including inherent disease-related immune dysfunction due to secondary hypogammaglobulinemia and T-lymphocyte dysfunction; patient-related factors like age, frailty and co-morbidities; and therapy-related immunosuppression (4).

Bruton's tyrosine kinase (Btk) is a member of the Tec family of cytoplasmic tyrosine kinases, with a primary role in CLL pathogenesis through signaling downstream of the B cell receptor (BCR) (5). The first-generation inhibitor of Btk (iBtk), ibrutinib, is an effective therapeutic strategy for CLL but has significant toxicity, particularly related to infections and hemorrhagic complications (5–8), due to inhibition of Btk expressed in other (non-B lymphocyte) hematopoietic cells and off-target effects on other kinases (9–11). Bleeding complications are linked to ibrutinib inhibition of platelet responses to multiple agonists that specifically signal through tyrosine kinase-linked receptors, including GPVI, GPIb-IX-V, CLEC-2, and integrins αIIbβ3 and α2β1 (12–16). Healthy individuals and CLL patients can be classified in two groups characterized by low or high platelet sensitivity to ibrutinib based on collagen-induced platelet aggregation *in vitro*, which is related to drug efflux pumps (17). However, a recent study suggests that ibrutinib-dependent bleeding in CLL patients also involves underlying disease-related changes in platelets including decreased platelet count and impaired platelet response to ADP (18).

Platelets play important immune functions during infection like scavenging and containment of bacteria, secretion of antimicrobial substances and interaction with leukocytes (19–24). In CLL, alterations in the innate immune system have been reported, including impaired function of neutrophils, natural killer cells and monocyte/macrophages (4, 25, 26), however, platelet immune functions remain uncharacterized. Moreover, the potential effect of iBtk therapy on platelet responses to infection has not been addressed. *Streptococcus pneumoniae* and *Haemophilus influenzae* are predominant pathogens in CLL, however, ibrutinib treatment has also been associated with serious infections by *Staphylococcus aureus* and *Escherichia coli* (3, 6, 27, 28). Importantly, most of these bacterial species are known to cause platelet activation (29–32). When platelets encounter bacteria, contact among them usually involves multiple bacterial strain-specific interactions with different platelet receptors [e.g., FcγRIIA (also known as CD32a), αIIbβ3, GPIb, complement receptor gC1q-R, and Toll-like receptor 2] (33, 34). Although each one of these molecular interactions can contribute to the adhesion and/or platelet activation steps, FcγRIIA has a central role in triggering final platelet activation in response to a wide range of bacteria (29–31).

FcγRIIA recognizes IgG-opsonized pathogens and signals *via* its cytoplasmic immunoreceptor tyrosine-based activation motif domain (30). Ligation of FcγRIIA by antibody crosslinking causes phosphorylation of Btk and Tec in healthy donor platelets (35) and leads to platelet activation that can be inhibited by iBtks (36). However, activation of FcγRIIA by bacteria is different from crosslinking the receptor with antibodies (29–31). Distinct features of the former include the presence of a lag phase between stimulation and onset of aggregation, and the fact that FcγRIIA phosphorylation and platelet secretion depend on integrin αIIbβ3 engagement (29, 31). Therefore, it is necessary to study the effect of iBtks on platelet FcγRIIA activation following exposure to pathophysiological stimuli including bacteria.

In this study, we analyze if platelets from CLL patients can respond to bacteria in an FcγRIIA-dependent manner and investigate the hypothesis that ibrutinib impairs such responses potentially contributing to the increased risk of infection reported in CLL patients treated with this drug.

MATERIAL AND METHODS

Reagents

See **Supplementary Information** for details.

Bacterial Culture and Preparation

S. aureus Newman (a gift from Prof Steve Kerrigan, RCSI, Ireland) and *E. coli* RS218 (a gift from Prof Ian Henderson, University of Queensland, Australia) were cultured and prepared as described (29, 31) (**Supplementary Information**).

Human Samples and Ethical Considerations

This study was performed in accordance with relevant ethics committees: Hull York Medical School (reference number 1501) and UK National Health Service Research Ethics (08/H1304/35). Informed consent was obtained from all participants.

Peripheral blood from CLL and X-linked agammaglobulinemia (XLA) patients was taken at the Departments of Haematology and

Immunology & Allergy, respectively, at Castle Hill Hospital (Cottingham, UK). Blood was drawn using sodium citrate or acid-citrate-dextrose (ACD) vacutainers (see below), and shipped to the University of Hull within 4 hours of venepuncture for immediate testing. Ibrutinib-treated CLL patients were taking a daily dose of 420 mg, except for two patients who were taking 140 mg. Blood from healthy donors was collected at the University of Hull in syringes containing sodium citrate or ACD from volunteers over 18 years of age not treated with concurrent anti-platelet agents.

Platelet-rich plasma (PRP) and platelet-poor plasma (PPP) were obtained from sodium citrated blood, while washed platelets (WP) were prepared from blood in ACD, as detailed in **Supplementary Information**.

Platelet Aggregation

Platelet aggregation in PRP or WP was done under stirring conditions (1000 rpm) at 37°C using light transmission aggregometry with a CHRONO-LOG 490 aggregometer (CHRONO-LOG, Havertown, PA, USA). WP reactions were supplemented with 1 mg/ml human fibrinogen and 0.2 mg/ml human IgGs before experimentation. Platelets were stimulated with bacteria and other agonists, including crosslinked collagen-related peptide (CRP-xl), thrombin receptor activator peptide 6 amide (TRAP-6) and ADP. To crosslink FcγRIIA, platelets were incubated with anti-FcγRIIA monoclonal antibody (mAb) (4 µg/ml, clone IV.3) for 2 minutes, followed by the addition of crosslinking $F(ab')_2$ rabbit anti-mouse IgG (30 µg/ml), altogether designated as IV.3-xl hereafter.

Platelet Factor 4 Secretion

Supernatants from light transmission aggregometry reactions were collected and analyzed for human platelet factor 4 (PF4) by enzyme-linked immunosorbent assay (ELISA) (R&D Systems), as described in **Supplementary Information** (29).

Platelet Scavenging and Spreading

PRP samples diluted to $2x10^7$ platelets/ml including 15% autologous plasma were incubated for 1 hour with *S. aureus* Newman or fibrinogen immobilized on glass coverslips. Cells were stained with Hoechst 33342 (to visualize bacteria) and TRITC phalloidin (to visualize platelets) and imaged using a Zeiss Axio Observer fluorescence microscope equipped with ApoTome structured illumination and an AxioCam 506 camera (Zeiss, UK). See **Supplementary Information** for details.

Flow Cytometry

Flow cytometry was performed in PRP samples using a BD LSR Fortessa cell analyzer (BD Biosciences) as described in **Supplementary Information**. Data were analyzed using the FlowJO software (BD Biosciences).

Phospho-Tec ELISA

WP ($10x10^8$/ml) supplemented with 1 mg/ml fibrinogen plus 0.2 mg/ml hIgGs were stimulated as required in aggregation conditions. Samples were lysed 3 minutes after the start of aggregation, or at a parallel time point in the case of samples where inhibitors blocked aggregation, by adding an equal volume of 2x lysis buffer (29) and analyzed using a RayBio human phosphotyrosine Tec ELISA kit (RayBiotech. Georgia, USA) following the manufacturer's instructions.

Western Blot

Protein detection in whole platelet lysates was done by SDS-PAGE and near-Infrared Western Blot Detection (LI-COR Biosciences) using lysates collected from PRP samples in the absence of αIIbβ3 inhibitors, as previously described (29) with minor modifications (see **Supplementary Information** for details).

Statistical Analysis

GraphPad Prism was used to perform the statistical analysis, including normality Kolmogorov-Smirnov and Shapiro-Wilk tests. Data are presented as the mean ± SD. In case of comparisons between two groups, means were evaluated using Student t-test or Mann-Whitney U test, for parametric and non-parametric data, respectively. If more than two groups were considered, one-factor or two-factor analysis of variance (ANOVA) or Kruskal-Wallis test (for parametric and non-parametric data, respectively) followed by multiple comparison tests were performed. For categorical variables, p values were calculated using the chi-square test or Fisher's exact test. $P \leq 0.05$ was considered significant.

RESULTS

CLL Patients' Characteristics

A total of 34 untreated and 32 ibrutinib-treated CLL patients were enrolled with their characteristics summarized in **Table 1**. The median age was 72 years, and most patients received concurrent medications for co-morbidities (**Supplementary Table 1**). The median number of drugs excluding ibrutinib was four for ibrutinib-treated, and three for untreated patients (**Supplementary Table 2**). Antiplatelet and anticoagulants were present in 6% of ibrutinib-treated (e.g., aspirin) and 18% of untreated (e.g., aspirin, clopidogrel, warfarin) CLL patients (**Supplementary Table 1**). Notably, 59% of ibrutinib-treated patients were taking prophylactic antibiotics, and 13% were on combined chemotherapy (venetoclax).

CLL Patients Taking Ibrutinib Have Impaired Platelet Activation in Response to FcγRIIA Crosslinking and Bacteria

Bacteria interact with plasma proteins (including IgGs) and platelet receptors in a bacterial strain-specific manner (34). *S. aureus* Newman and *E. coli* RS218 are known to cause IgG-dependent FcγRIIA-mediated aggregation and granule secretion in platelets derived from healthy donors (29, 31). Therefore, we asked whether platelets from CLL patients would be similarly responsive to bacteria and, if so, whether ibrutinib treatment would interfere with platelet immune functions. We tested platelet activation induced by clustering of FcγRIIA *via* IV.3-xl,

TABLE 1 | Characteristics of chronic lymphocytic leukemia patients enrolled in the study.

	Overall (n=66)		Ibrutinib-untreated CLL (n=34)		Ibrutinib-treated CLL (n=32)		P value*
Sex:							
Male	43	(65%)	21	(62%)	22	(69%)	0.61
Female	23	(35%)	13	(38%)	10	(31%)	
Age (years)	72	(45-86)	72.5	(45-86)	71	(55-82)	0.93
17p deletion							
Positive	5	(8%)	0	(0%)	5	(16%)	0.02
Negative	61	(92%)	34	(100%)	27	(84%)	
Trisomy 12							
Positive	0	(0%)	0	(0%)	0	(0%)	>0.99
Negative	66	(100%)	34	(100%)	32	(100%)	
11q deletion							
Positive	7	(11%)	1	(3%)	6	(19%)	0.05**
Negative	59	(89%)	33	(97%)	26	(81%)	
13q deletion							
Positive	14	(21%)	0	(0%)	14	(44%)	<0.001 **
Negative	52	(79%)	34	(100%)	18	(56%)	
β2 microglobulin	2.45	(1.4-6.5)	2.3	(1.4-6.5)	2.5	(1.5-6.3)	0.27
IgG at Diagnosis (g/L)	8.9	(3.1-22)	9.15	(3.1-21.5)	8.8	(5.2-22)	0.97
CD38							
Positive	20	(30%)	9	(26%)	11	(34%)	0.59
Negative	46	(70%)	25	(74%)	21	(66%)	
Binet stage[#]							
A	49	(74%)	23	(68%)	26	(81%)	0.12
B	4	(6%)	4	(12%)	0	(0%)	
C	11	(17%)	6	(18%)	5	(16%	
Time from Diagnosis (years)	4	(0.1-23.4)	1.95	(0.1-13.9)	8.1	(1-23.4)	<0.001 **
Time on Ibrutinib (years)	-		-		1.35	(0.1-3.4)	-
Number of Medications excluding ibrutinib	4	(0-9)	3	(0-9)	4	(1-8)	–
Hb (g/L)	133	(88-163)	129	(87-152)	139.5	(95-163)	0.57
WCC (x10^9/L)	20	(2-379)	38	(3-379)	11.65	(2-319)	0.009 **
Lymphocyte (x10^9/L)[##]	16	(0.6-372)	40	(1.9-372)	3	(0.6-279)	<0.001 **
Platelet Count (x10^9/L)	152	(39-378)	166	(39-378)	147	(75-253)	0.05**

*Hb, hemoglobin; WCC, white blood cell count. [#]For Binet staging, untreated patients are n=33, and treated patients are n = 31. [##]For lymphocyte counts, untreated patients were n = 13, and treated patients were n = 16. *Significant difference (p ≤ 0.05).*

Data is shown as number (%) or median (range) as appropriate. Cytogenetic tests, CD38 positivity test, and IgG and β2 microglobulin levels are at time of diagnosis; the rest of measurements are at time of blood sample collection. All p values are for comparisons between ibrutinib-untreated and ibrutinib-treated CLL groups. P values for continuous variables were evaluated using Student t-test or Mann-Whitney test, for parametric and non-parametric data, respectively. For categorical variables, p values were calculated using the chi-square test or Fisher's exact test. P ≤ 0.05 was considered significant. See Supplementary Information for normal hematological and serum immunoglobulin reference ranges, and ***Supplementary Tables 1***, ***2*** *for information on patients' concurrent medications.*

bacteria, and GPVI-specific agonist, CRP-xl, in the presence of plasma. We also stimulated platelets with TRAP-6 and ADP, which are agonists for G-protein coupled receptors that are not affected by ibrutinib (12–14).

Platelets derived from untreated CLL patients responded to FcγRIIA crosslinking (IV.3-xl) and CRP-xl at levels comparable to controls (**Figure 1A**). *S. aureus* Newman and *E. coli* RS218 induced full or nearly full aggregation in 8 and 9 out of 13 samples respectively, similarly to TRAP-6 and ADP, with aggregation to *S. aureus* Newman and TRAP-6 being significantly lower than in controls (**Figure 1A**). The antiplatelet agent, clopidogrel, was taken by two CLL patients, but their platelets aggregated fully to bacteria; however, two aspirin-treated CLL patients showed a reduction in aggregation to bacteria, especially *S. aureus* Newman (**Supplementary Figure 1**).

Platelet aggregation to *S. aureus* Newman and *E. coli* RS218 is characterized by a lag time between bacterial stimulation and start of aggregation that contrasts with the immediate onset of aggregation caused by IV.3-xl (29, 31). Ibrutinib-untreated CLL platelets in which aggregation in response to bacteria was detected (**Figure 1A**) showed a statistically significant decrease in lag times compared to controls (**Figure 1C**). Overall, our data indicates that platelets from ibrutinib-free CLL patients aggregate to bacteria in the presence of autologous plasma, although a trend to decreased aggregation compared to FcγRIIA crosslinking is seen.

In contrast, platelets from ibrutinib-treated CLL patients showed strong inhibition of IV.3-xl-induced aggregation, and a significant decrease in aggregation to bacteria (**Figure 1A**). As opposed to IV.3-xl, heterogeneity in platelet aggregation to CRP-xl was observed in our ibrutinib-treated platelet group (**Figure 1A**). In previous studies, defects in collagen-induced platelet aggregation were detected in only a subset of ibrutinib-treated patients (12, 13); and the presence of ibrutinib low and high sensitivity groups of both healthy individuals and CLL patients regarding platelet responses to collagen has been reported (17). As published (12, 13), responses to TRAP-6 and ADP (which signal through G-protein coupled receptors) were mostly unaffected in our ibrutinib-treated group (**Figure 1A**). Differences in aggregation among the three clinical groups were

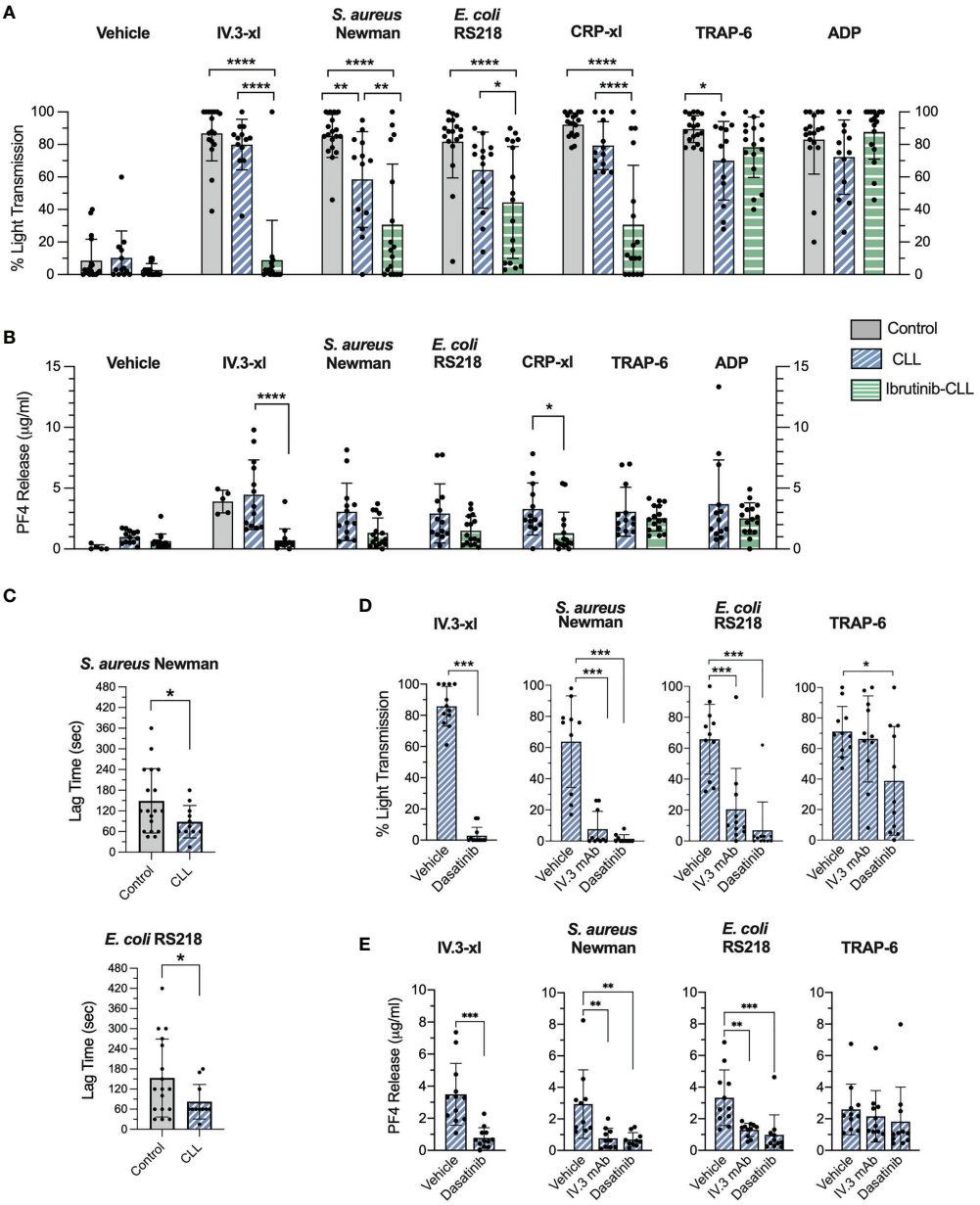

FIGURE 1 | CLL platelet aggregation and secretion in response to bacteria and IV.3 mAb mediated FcγRIIA crosslinking are impaired in CLL patients taking ibrutinib. **(A)** Characterization of platelet aggregation responses in healthy controls (n=17-18), untreated (n=13) and ibrutinib-treated (n=16-17) CLL patients. PRP samples were stimulated with crosslinked IV.3 mAb (IV.3-xl; 4 μg/ml mAb IV.3 followed by 30 μg/ml F(ab')2 rabbit anti-mouse IgG), *S. aureus* Newman, *E. coli* RS218, 3 μg/ml CRP-xl, 3 μM TRAP-6, or 10 μM ADP. Aggregation was recorded by light transmission aggregometry. Reactions were run for 20 minutes from onset of aggregation for IV.3-xl and bacteria, and 10 minutes for the rest of agonists, and maximum aggregation was calculated. **(B)** Characterization of α-granule secretion in ibrutinib-untreated (n=13) and treated (n=15-16) CLL patients. Supernatants from PRP aggregation reactions were collected at 20 minutes of onset of aggregation for IV.3-xl and bacteria, and 10 minutes in the case of other agonists. Levels of PF4 as a marker of α-granule secretion were measured by PF4 ELISA. **(C)** Lag time for onset of platelet aggregation in response to bacteria. For healthy donor and ibrutinib-untreated platelet samples, the lag time for onset of aggregation (e.g., time between bacteria injection and start of platelet aggregation) was calculated in those cases in which aggregation took place in response to *S. aureus* Newman (healthy controls, n=18; CLL, n=11) and *E. coli* RS218 (healthy controls, n=17; CLL, n=11). **(D)** Effect of FcγRIIA and Src inhibition on ibrutinib-untreated CLL platelet aggregation. PRP samples (n=10-12) were incubated with 4 μM dasatinib (Src inhibitor) for 2 min, 20 μg/ml IV.3 mAb (FcγRIIA inhibitor) for 10 minutes, or vehicle before being stimulated with agonists and monitored by light transmission aggregometry. **(E)** Effect of FcγRIIA and Src inhibition on ibrutinib-untreated CLL platelet α-granule secretion. Supernatants from aggregation reactions above were collected at 20 minutes of onset of aggregation for IV.3-xl and bacteria, and 10 minutes in the case of other agonists. PF4 release was measured by ELISA. Data is shown as mean ± SD. Statistical significance was calculated using two-way ANOVA for **(A, B)**, or one-way ANOVA for **(D, E)**, followed by Tukey's or Sidak's multiple comparison correction. An unpaired t-test was performed for **(C)** (*$p \leq 0.05$, **$p \leq 0.01$, ***$p \leq 0.001$, ****$p \leq 0.0001$).

not due to varying platelet concentrations in PRP samples (**Supplementary Figure 2**).

We next measured release of PF4, a chemokine that can interact with bacteria directly (29, 37), as a marker of α-granule secretion. PF4 was secreted by ibrutinib-untreated CLL platelets upon IV.3-xl and bacteria stimulation (**Figure 1B**) to similar levels as healthy controls (**Figures 1B** and **4C**) (29). In contrast, ibrutinib-treated CLL patients showed an inhibitory trend of PF4 secretion in response to bacteria, IV.3-xl and CRP-xl, with the latter two being significantly reduced compared to untreated CLL platelets (**Figure 1B**). PF4 release in response to TRAP-6 and ADP was not affected by ibrutinib treatment (**Figure 1B**).

To investigate if the CLL platelet responses observed above were mediated by FcγRIIA, aggregation and secretion were measured after incubating PRP with IV.3 mAb, which without the crosslinking $F(ab')_2$ inhibits FcγRIIA activation. Consistent with previous observations in healthy donor platelets (29, 31), CLL platelet aggregation and PF4 secretion to *S. aureus* Newman and *E. coli* RS218 were inhibited by IV.3 mAb and by the Src inhibitor, dasatinib (**Figures 1D, E**).

Thus, our results support that platelet immune recognition of bacteria *via* FcγRIIA is impaired in CLL patients treated with ibrutinib.

The Ability of Platelets to Scavenge *S. aureus* Newman Is Impaired by Ibrutinib Treatment in CLL Patients

As innate immune effectors, platelets scan the vasculature and collect bacteria (21). Therefore, we next investigated if CLL platelets retain the capacity to scavenge bacteria and whether this is impaired by ibrutinib. Platelets from healthy controls and CLL patients were found to scavenge *S. aureus* Newman in the presence of autologous plasma with an average (± SD) of 15 ± 8.5 and 13 ± 11.5 bacteria per platelet (bacteria clusters), respectively (**Figures 2A, B**). Pre-treatment of PRP samples with the integrin αIIbβ3 inhibitor, eptifibatide, abolished scavenging of bacteria by both control and CLL platelets (**Figures 2A, B**), pointing out to a key role for the integrin in this response. Scavenging was also dependent upon FcγRIIA (**Supplementary Figure 3**). Remarkably, platelets from CLL patients taking ibrutinib could bind to *S. aureus* Newman, but showed no morphological changes indicative of activation as compared to controls and were not able to scavenge bacteria (**Figures 2A, B**).

The same platelet samples were tested for spreading on immobilized fibrinogen. During spreading, the actin cytoskeleton rearranges causing cellular protrusions including finger-like filopodia and laterally extended lamellipodia; the latter being characteristic of later stages of spreading (38). A statistically significant decrease in total number of CLL platelets binding to fibrinogen was detected compared to healthy controls (**Figures 2A, C**), however, both groups showed similar percentages of platelets with lamellipodia. In contrast, platelets from CLL patients taking ibrutinib bound to fibrinogen to similar levels as controls, but did not spread (**Figures 2A, C**), consistent with published studies performed with washed platelets (14, 39). These data show decreased efficiency in platelet bacteria-scavenging ability and spreading in CLL patients treated with ibrutinib.

Changes in CLL Platelet Granularity and Membrane Expression of αIIbβ3 and GPVI, but not FcγRIIA, Are Differentially Dependent on Ibrutinib Treatment

The reduction in platelet responses to bacteria observed in ibrutinib-treated CLL patients could be due to heterogeneity in surface expression of important receptors like FcγRIIA and αIIbβ3 (40). Therefore, we performed flow cytometry analyses of platelets derived from our three clinical groups to measure membrane protein levels of αIIbβ3, FcγRIIA and GPVI in PRP samples (**Supplementary Figure 4**). This analysis revealed no change in cell size, but a significant decrease in granularity/complexity in untreated CLL platelets (**Figure 3A**). We also observed significant reductions of αIIbβ3 (as detected by two different mAb clones against CD41, the αIIb subunit) and GPVI, but not FcγRIIA (CD32), in CLL platelets independently of ibrutinib treatment when compared to healthy control platelets (**Figure 3B**). This suggests that decreased levels of αIIbβ3 in blood circulating platelets are unlikely to be the major or only cause of inhibition of ibrutinib-treated CLL platelet responses to bacteria.

Ibrutinib and Acalabrutinib Inhibit Healthy Donor Platelet Activation in Response to Antibody-Mediated FcγRIIA Crosslinking and Bacteria

To investigate the direct effect of ibrutinib on platelet response to bacteria, we performed light transmission aggregometry with healthy control PRP stimulated *in vitro* with different concentrations of ibrutinib (**Figure 4A** and **Supplementary Figure 5A**). Pre-incubation with 5μM ibrutinib for 5 minutes significantly inhibited platelet aggregation to *S. aureus* Newman and *E. coli* RS218, but did not cause a significant reduction of aggregation in response to CRP-xl or TRAP-6. A lower dose of ibrutinib (2 μM) was able to abolish aggregation to FcγRIIA crosslinking (IV.3-xl) (**Figure 4A**). Longer pre-incubation times with ibrutinib (20 and 40 minutes) did not significantly reduce the concentration of drug needed to inhibit aggregation to bacteria (data not shown). As internal controls, IV.3 mAb alone (FcγRIIA inhibitor) and dasatinib (Src inhibitor) were used in PRP, and both inhibited aggregation to *S. aureus* Newman and *E. coli* RS218, but not TRAP-6 (**Supplementary Figure 5C**), as previously reported (29, 31). The integrin αIIbβ3 inhibitor eptifibatide, as expected, blocked aggregation in response to all agonists including TRAP-6 (**Supplementary Figure 5C**) (29, 31).

The high concentrations of ibrutinib needed to inhibit aggregation in PRP contrasted with previous studies done in washed platelets (12, 14, 16), thus we wondered if binding of ibrutinib to plasma proteins (41) may explain the difference. As seen in **Supplementary Figure 6A**, washed platelet aggregation in response to *S. aureus* Newman was inhibited by 0.5 μM ibrutinib, while 0.1 μM ibrutinib was sufficient to inhibit the

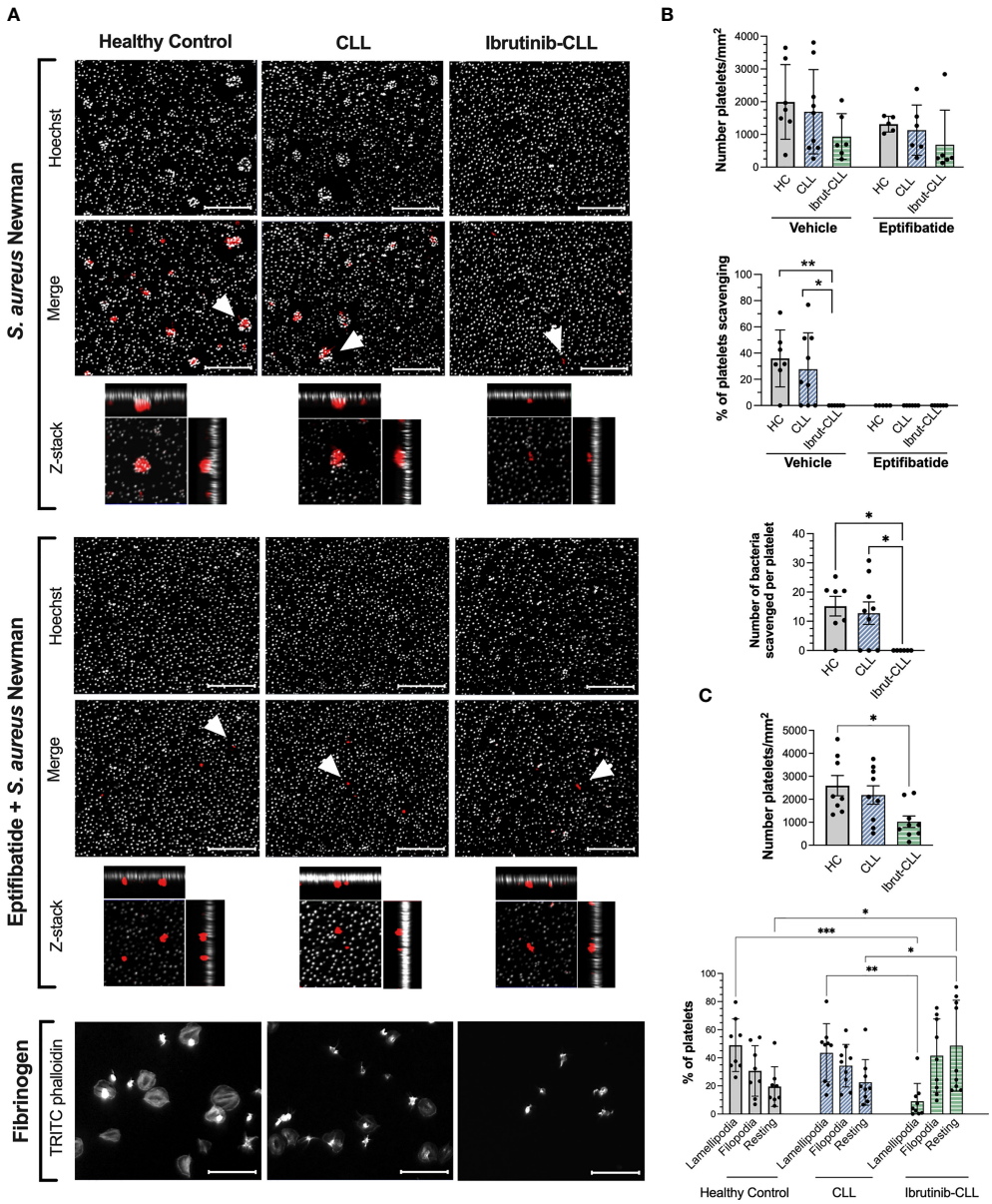

FIGURE 2 | *S. aureus* Newman can be scavenged by platelets from ibrutinib-untreated but not ibrutinib-treated CLL patients. PRP samples from healthy controls, ibrutinib-untreated CLL and ibrutinib-treated CLL were adjusted to 2 x10^7 platelets/ml and 15% autologous plasma. Samples were incubated with eptifibatide (9 μM) to inhibit integrin αIIbβ3 or vehicle for 2 minutes and incubated for 1 hour with *S. aureus* Newman or fibrinogen immobilized on glass coverslips. Coverslips were then washed, fixed, permeabilized, and stained with Hoechst 33342 (grey color, bacteria staining) and TRITC phalloidin (red color, platelet staining). Coverslips were mounted and visualized by fluorescence microscopy. **(A)** Representative images are presented, with scale bars showing 20 μm. For *S. aureus* Newman, arrowheads indicate examples of clusters of bacteria scavenged by platelets, and maximum projections of Z-stack images of individual platelets are included. **(B)** Platelet interactions with *S. aureus* Newman. Graphs show number of platelets per surface area (top panel), the percentage of platelets scavenging bacteria (middle panel) and the number of bacteria per cluster (bottom panel). Number of samples per clinical group were as follows: healthy controls, n=7 vehicle and n=5 eptifibatide; CLL, n=9 vehicle and n=6 eptifibatide; ibrutinib-treated CLL, n=6 for both vehicle and eptifibatide. **(C)** Platelet spreading on immobilized fibrinogen. Graphs show number of platelets per surface area and percentage of platelets with filopodia (finger-like cellular protrusions) and lamellipodia (laterally extended protrusions characteristic of later stages of spreading). Healthy controls, n=8; CLL, n=9, ibrutinib-CLL, n=9. All data is shown as mean ± SD. Statistical significance was calculated using one-way or two-way ANOVA followed by Tukey's multiple comparison correction (*p ≤ 0.05, **p ≤ 0.01, ***p ≤ 0.001).

response to *E. coli* RS218 and FcγRIIA crosslinking (IV.3-xl). A higher dose of ibrutinib (1 μM) was necessary to inhibit washed platelet aggregation stimulated with CRP-xl. None of the ibrutinib concentrations tested in PRP and washed platelets caused inhibition of TRAP-6 induced aggregation (**Figure 4A** and **Supplementary Figures 5A, 6A**).

The second generation iBtk, acalabrutinib, was also assessed for its ability to inhibit platelet responses to bacteria. Like

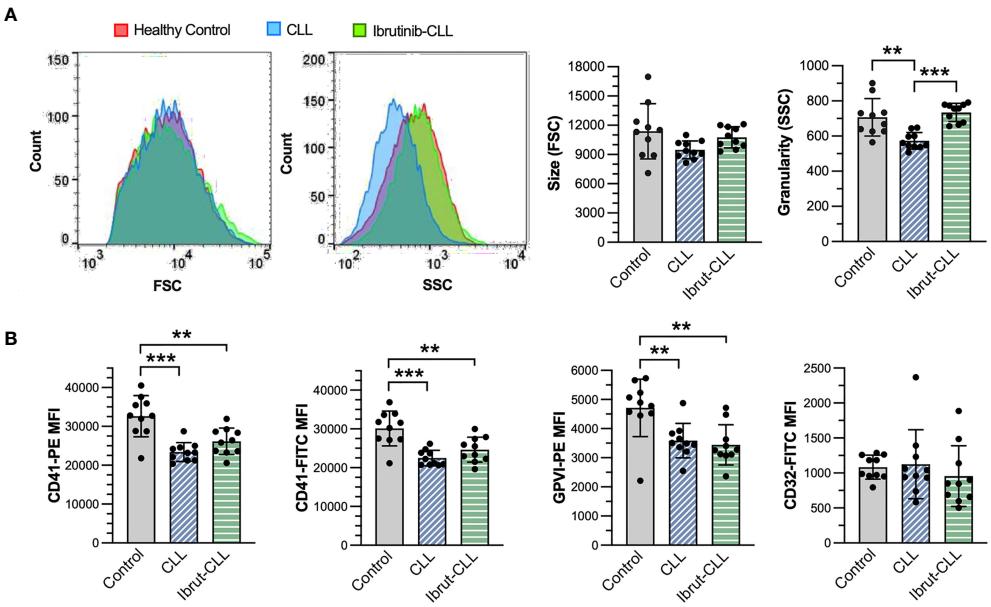

FIGURE 3 | Although different in granularity, platelets from ibrutinib-treated and untreated CLL patients similarly reduce membrane expression of αIIbβ3 and GPVI, but not FcγRIIA. PRP samples from healthy donors (n=10), CLL (n=10) and ibrutinib-treated CLL (n=10) patients were diluted to 1 x10^7 platelets/ml and incubated with monoclonal antibodies against human integrin αIIb (CD41), GPVI and FcγRIIA (CD32) before being analyzed by flow cytometry. **(A)** Left histograms show size and granularity in gated platelets, respectively as forward (FSC) and side (SSC) scatter, in representative samples. The bar graphs (right) show the distribution of platelet size and granularity across the three experimental groups. **(B)** Bar graphs show the mean fluorescence intensity (MFI) of CD41, GPVI, and CD32 in gated platelets, across the three experimental groups. For CD41, technical replicates with two different antibody clones (PE-conjugated clone 5B12, FITC-conjugated clone P2) are shown (left panels). Statistical significance was evaluated in ANOVA analyses, followed by Tukey's multiple comparison correction. Data is presented as mean ± SD. (**p ≤ 0.01, ***p ≤ 0.001).

ibrutinib, acalabrutinib binds irreversibly to Btk at C481 and is highly bound to plasma proteins (42, 43). In PRP, 10-15 μM acalabrutinib impaired aggregation after IV.3-xl and bacteria exposure, but not in response to CRP-xl and TRAP-6 (**Figure 4B** and **Supplementary Figure 5B**). In washed platelets, the inhibitory effects of acalabrutinib were more prominent. Aggregation to IV.3-xl was inhibited by 5-10 μM acalabrutinib, while for bacteria, 1μM and 10 μM inhibited aggregation upon exposure to *E. coli* RS218 and *S. aureus* Newman respectively (**Supplementary Figure 6B**). Washed platelet aggregation after stimulation with TRAP-6 and CRP-xl was unaffected or only partially inhibited (10 μM) by acalabrutinib respectively (**Supplementary Figure 6B**), as previously described (17, 44).

Ibrutinib and acalabrutinib also inhibited platelet α-granule secretion (PF4) in response to IV.3-xl and bacteria, but not to TRAP-6 (**Figure 4C**). As previously reported (29, 31), eptifibatide blocked PF4 release in response to bacteria, but not to IV.3-xl (**Figure 4C**). Moreover, PF4 release in response to bacteria (but not TRAP-6) was inhibited by blocking FcγRIIA with IV.3 mAb alone (**Figure 4C**). This confirms previous observations of the interplay between FcγRIIA and αIIbβ3 in mediating platelet activation, including secretion, to bacteria.

Hence, in keeping with the above results from our clinical cohort of ibrutinib-treated CLL patients, iBtks strongly and directly inhibit immune function even in platelets derived from healthy donors.

Bacteria Induce FcγRIIA- and αIIbβ3-Dependent Btk Activation That Is Inhibited by iBtks

We showed that ibrutinib can inhibit platelet immune recognition of bacteria, mediated by FcγRIIA, whilst not impacting on the surface levels of this receptor, thus we sought to investigate downstream intracellular signaling events. The binding of ibrutinib and acalabrutinib to Btk C481 blocks Btk autophosphorylation in Y223 that is critical for its activation (5). FcγRIIA crosslinking with non-physiological agonists induces Btk Y223 phosphorylation (35), yet it remains unknown if this is also critical downstream of bacteria recognition. In healthy donors, phosphorylation of Btk Y223 was detected in PRP after IV.3-xl and bacteria exposure, although at lower levels than those induced by CRP-xl (**Figure 5A**). For *S. aureus* Newman and *E. coli* RS218, inhibition of FcγRIIA (with IV.3 mAb alone) and αIIbβ3 (with eptifibatide) reduced Btk phospho-Y223 signal to basal levels (**Figures 5B.1, B.4** and **B.5**), which indicates that both receptors control Btk activation in response to bacteria, as opposed to CRP-xl (**Figures 5B.1, B.2**) and TRAP-6 (**Figure 5B.6**). For all agonists tested, Btk phospho-Y223 was inhibited below basal levels by ibrutinib and acalabrutinib as expected (**Figures 5A, B**).

We wondered whether signaling through FcγRIIA, rather than GPVI, would be more reliant on Btk activity, and hence sensitive to ibrutinib inhibition. Therefore, we analyzed if there

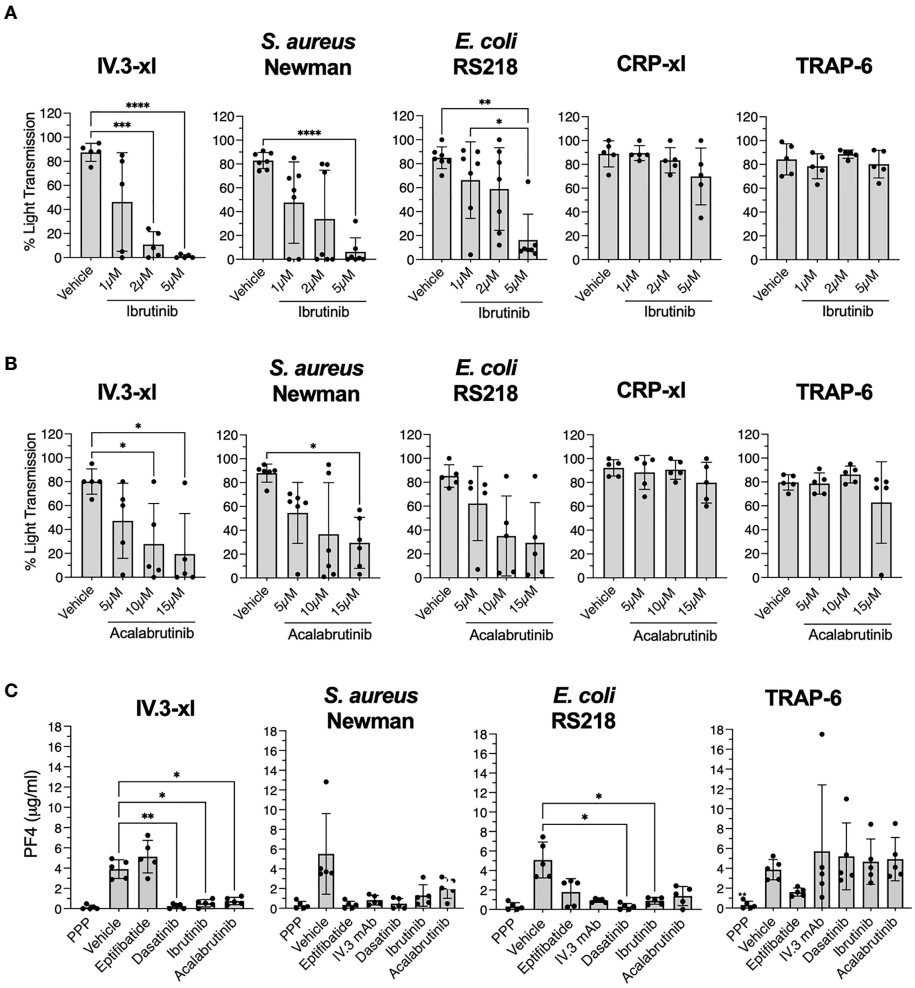

FIGURE 4 | Ibrutinib and acalabrutinib inhibit healthy control platelet activation by bacteria and IV.3 mAb mediated FcγRIIA crosslinking in the presence of plasma. **(A)** Characterization of the effect of ibrutinib on platelet aggregation. PRP from healthy controls was incubated *in vitro* with different doses of ibrutinib for 5 minutes before stimulation with the following agonists: crosslinked IV.3 mAb (IV.3-xl; 4 μg/ml IV.3 mAb followed by 30 μg/ml F(ab')2 rabbit anti-mouse IgG; n=5), *S. aureus* Newman (n=7), *E. coli* RS218 (n=7), 3 μg/ml CRP-xl (n=5) and 3 μM TRAP-6 (n=5). Aggregation was measured by light transmission aggregometry. Reactions were run for 20 minutes from onset of aggregation for IV.3-xl and bacteria, and 10 minutes for the rest of agonists, and maximum aggregation was calculated. **(B)** Characterization of the effect of acalabrutinib on platelet aggregation. PRP from healthy controls was incubated *in vitro* with different doses of acalabrutinib for 5 min before stimulating with agonists: IV.3-xl (n=5), *S. aureus* Newman (n=6), *E. coli* RS218 (n=5), 3 μg/ml CRP-xl (n=5) and 3 μM TRAP-6 (n=5). Aggregation was measured by light transmission aggregometry as above. **(C)** PRP from healthy controls (n=5) was incubated with vehicle or inhibitors, 9 μM eptifibatide (αIIbβ3 inhibitor), 20 μg/ml IV.3 mAb (to inhibit FcγRIIA), 4 μM dasatinib (Src inhibitor), or iBtks, 5 μM ibrutinib and 15 μM acalabrutinib. Samples were then stimulated with stated agonists. Supernatants from aggregation reactions were collected at 20 minutes of onset of aggregation for IV.3-xl and bacteria, and 10 minutes for TRAP-6. Levels of PF4 as a marker of α-granule secretion were measured by PF4 ELISA. Data is shown as mean ± SD. Statistical significance was calculated using one-way ANOVA followed by Tukey's multiple comparison correction (*$p \leq 0.05$, **$p \leq 0.01$, ***$p \leq 0.001$, ****$p \leq 0.0001$).

was a correlation between the ibrutinib concentration found to inhibit Btk Y223 phosphorylation and that needed to inhibit aggregation. Upon IV.3-xl, concentrations of ibrutinib that reduced Btk phospho-Y223 to basal levels (1 μM) or below (2 μM) were also able to partially decrease aggregation (**Figure 5C**), with total inhibition of aggregation requiring higher concentrations of ibrutinib (5 μM). In contrast, inhibition of Btk Y223 phosphorylation did not correlate with suppression of CRP-xl induced aggregation (**Figure 5C**), as previously reported (16). Thus, phosphorylation of Btk Y223 downstream of bacteria recognition uses both FcγRIIA and integrin pathways, with FcγRIIA potentially being more sensitive to ibrutinib treatment than GPVI, in healthy donor-derived platelets.

We next sought to investigate CLL samples and found that CLL platelets activated Btk in response to IV.3-xl, bacteria, CRP-xl and TRAP-6 to a similar degree as healthy controls (compare **Figures 5A, D**). This contrasted with ibrutinib-treated CLL platelets in which no phosphorylation of Btk Y223 was detected in response to IV.3-xl, CRP-xl and TRAP-6 (**Figure 5D**).

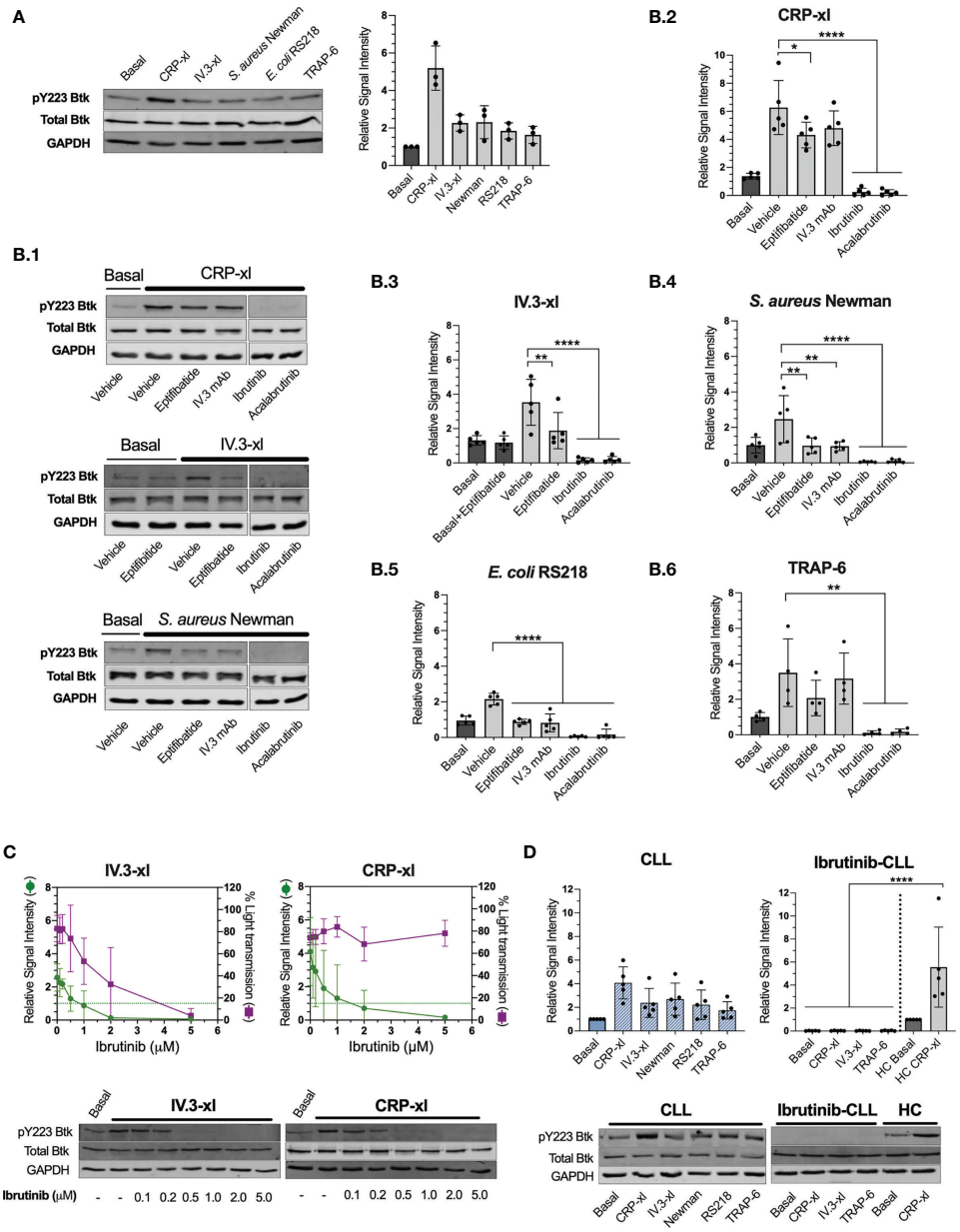

FIGURE 5 | Platelet stimulation by bacteria or crosslinked IV.3 mAb causes Btk activation in healthy donors and CLL patients that is inhibited by ibrutinib and acalabrutinib. Phosphorylation of Btk at Y223 was measured by immunoblotting in whole cell lysates collected from healthy control or CLL PRP aggregation reactions using the following agonists: 3 μg/ml CRP-xl, crosslinked IV.3 (IV.3-xl; 4 μg/ml mAb IV.3 followed by 30 μg/ml F(ab')2 rabbit anti-mouse IgG), *S. aureus* Newman, *E. coli* RS218, and 3 μM TRAP-6. In some cases, platelet inhibitors were used as indicated below. All lysates were collected at 3 minutes after the start of aggregation, or a parallel time point in samples in which aggregation was inhibited. Lysates were adjusted to an equivalent of 5 x10^8 platelets/ml as explained in Materials and Methods. **(A)** Btk pY223 phosphorylation in healthy donor platelets stimulated with assorted agonists. Pooled data from three independent experiments done with different donors is shown on the right-hand side graph as mean ± SD. Data was normalized to GAPDH. On the left, one representative experiment is presented. **(B)** Effect of platelet inhibitors on Btk pY223 phosphorylation in healthy control platelets. Before adding agonists, PRP was pre-incubated with either vehicle, 9μM eptifibatide (αIIbβ3 inhibitor, 2 minutes), 20 μg/ml IV.3 mAb (to inhibit FcγRIIA, 10 minutes), or iBtks (5 minutes), 5μM ibrutinib and 15μM acalabrutinib. B.1. Representative images of five independent experiments for CRP-xl, IV.3-xl and *S. aureus* Newman. B.2 to B.6. Pooled data shown as mean ± SD. Five independent experiments were done for all agonists except for TRAP-6 that was tested four times. Data was normalized to GAPDH. Statistical significance was calculated using one-way ANOVA followed by Tukey's multiple comparison correction. **(C)** Ibrutinib dose-response curve for inhibition of Btk Y223 phosphorylation (green) and aggregation (purple) in response to IV.3-xl (n=5) and CRP-xl (n=4). Representative results are shown below the graphs. **(D)** Btk Y223 phosphorylation in PRP from ibrutinib-untreated (n=5) and treated (n=5) CLL patients stimulated with assorted agonists. Healthy control (HC) samples were included as positive controls. Statistical significance was calculated using one-way or two-way ANOVA followed by Tukey's multiple comparison correction (*p ≤ 0.05, **p ≤ 0.01, ****p ≤ 0.0001).

Bacteria Induce Platelet Tec Kinase Activation That Is Inhibited by Ibrutinib

Platelets express two members of the Tec family of tyrosine kinases, Btk and Tec. Although Btk has an approximate 8 to 10-fold greater level of expression in human platelets (45), studies suggest that ibrutinib-mediated inhibition of Tec has important consequences in platelet function (14, 16). Thus, we aimed to decipher if Tec activation takes place downstream of FcγRIIA-mediated platelet response to bacteria as seen for IV.3-xl (35). Due to the lack of phospho-specific antibodies to detect Tec autophosphorylation site Y206 (46), total levels of Tec tyrosine phosphorylation were measured by ELISA.

In healthy donor-derived platelets, Tec phosphorylation increased upon exposure to *S. aureus* Newman and *E. coli* RS218, and was inhibited by pre-treatment with ibrutinib (**Figure 6**). Moreover, when CLL platelets were stimulated with *S. aureus* Newman, Tec phosphorylation reached similar levels as those observed in healthy controls (**Figure 6**). We used CRP-xl to compare Tec phosphorylation across our three clinical groups. As seen in **Figure 6**, healthy donor and untreated CLL platelets stimulated with CRP-xl showed an increase in phospho-Tec that was significantly decreased in platelets from ibrutinib-treated patients. Overall, these data suggest that ibrutinib, both at concentrations used *in vitro* and at therapeutic doses, affects platelet Tec activation.

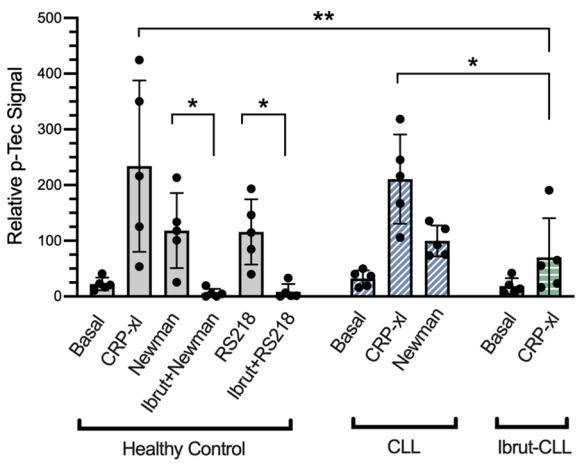

FIGURE 6 | Platelet responses to bacteria involve Tec kinase activation. Characterisation of platelet Tec phosphorylation in healthy controls (n=5), ibrutinib-untreated CLL (n=5) and ibrutinib-treated CLL (n=5) patients. Washed platelets from the three clinical groups were supplemented with fibrinogen and human IgG (commercially available IgGs pooled from healthy donors). Healthy control platelets were incubated *in vitro* with 5 μM ibrutinib, 15 μM acalabrutinib or vehicle for 5 minutes before adding agonists. Platelet samples were stimulated with either 3 μg/ml CRP-xl, *S. aureus* Newman or *E. coli* RS218. Relative phosphorylation of Tec was measured by a phospho-Tec ELISA. Data is shown as mean ± SD. Two-way ANOVA and Sidak's multiple comparison test were used to compare CRP-xl responses across the three clinical groups. For the effect of ibrutinib on bacteria-induced phospho-Tec in healthy controls, one way ANOVA followed by Tukey's multiple comparison correction was done. (*$p \leq 0.05$, **$p \leq 0.01$).

XLA-Derived Platelets Respond to Bacteria in an FcγRIIA-Dependent Manner

Mutations in the *Btk* gene resulting in lack of Btk expression or function cause XLA, a condition characterized by markedly reduced or absent B cells and profound hypogammaglobulinemia (47). To investigate if Btk function is essential for FcγRIIA-mediated platelet responses to bacteria, we obtained PRP from two XLA patients receiving periodic intravenous immunoglobulin treatment. Platelets from both patients aggregated to *S. aureus* Newman and *E. coli* RS218 although with varying lag times (**Figure 7A**). Upon crosslinking of FcγRIIA (IV.3-xl), no or less aggregation was observed in patients 2 and 1 respectively (**Figure 7A**), suggesting that this pathway is more strongly affected by Btk deficiency than bacteria-induced activation. Importantly, XLA platelet responses to bacteria were still dependent on FcγRIIA, as aggregation was blocked by pre-incubating PRP with inhibitory IV.3 mAb alone (**Figure 7B**). Conversely, we detected normal XLA platelet aggregation in response to CRP-xl and TRAP-6 (**Figure 7A**), which was independent of FcγRIIA (**Figure 7B**). These results suggest that while Btk has an active role in FcγRIIA-mediated platelet function, this is not essential for FcγRIIA-mediated responses to bacteria.

DISCUSSION

This study has focused on platelet immune responses in CLL in the context of bacterial infection and ibrutinib therapy. Infectious complications are a major burden in CLL, and the increased risk of infection is multifactorial, including immunosuppression inherent to disease, patients' age and co-morbidities, and therapy toxicity (3, 4, 6, 27, 28). In CLL, alterations can be found in both the adaptive and innate immune systems, namely T lymphocyte dysfunction, hypogammaglobulinemia, complement defects, and impairment in antimicrobial activity of neutrophils and monocytes (4, 25, 26). Because it is possible that CLL platelets had immune function abnormalities that could be exacerbated by ibrutinib, the first part of our study had two aims: to characterize platelet responses to bacteria in CLL (e.g., in the absence of CLL-targeted treatment) and to investigate the effect of ibrutinib therapy on these responses.

Overall, ibrutinib-untreated CLL platelets responded to *S. aureus* and *E. coli* in an FcγRIIA-dependent manner in the presence of autologous plasma, as seen by platelet aggregation, secretion and scavenging of bacteria. We found that platelet scavenging of *S. aureus* Newman was both FcγRIIA and αIIbβ3-dependent. However, more investigations are needed to further characterize the molecular mechanisms underlying platelet scavenging of pathogens, including potential bacterial-strain specific processes. Previous studies suggest that alternative mechanisms could take place. Gaertner et al. (21) have shown that platelets can scavenge fibrin-bound *E. coli* and *S. aureus*, both *in vitro* and *in vivo*, boosting the phagocytic activity of neutrophils; while Palankar et al. (22) described a mechanism by which PF4 binding to *E. coli* promotes antibody opsonization

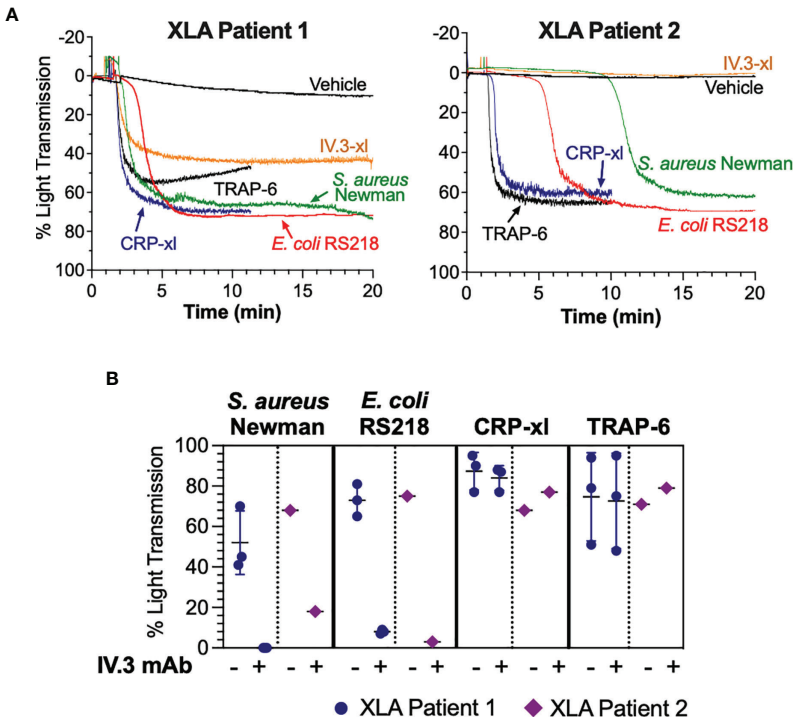

FIGURE 7 | Platelet responses to bacteria can take place in the absence of functional Btk. **(A)** Characterization of bacteria-induced aggregation of platelets from X-linked agammaglobulinemia patients. PRP samples from two XLA patients were stimulated with crosslinked IV.3 mAb (IV.3-xl; 4 μg/ml IV.3 mAb followed by 30μg/ml F(ab')$_2$ rabbit anti-mouse IgG), *S. aureus* Newman, *E. coli* RS218, 3 μg/ml CRP-xl, and 3 μM TRAP-6. Aggregation was measured by light transmission aggregometry. **(B)** PRP from XLA patients was incubated with 20 μg/ml IV.3 mAb (to inhibit FcγRIIA) or vehicle, before stimulation with either *S. aureus* Newman, *E. coli* RS218, 3 μg/ml CRP-xl or 3 μM TRAP-6. Aggregation was measured by light transmission aggregometry. Patient 1 (n=3, in different days) had a missense mutation in codon 28 affecting the Btk pleckstrin homology domain, which causes lack of Btk function. Patient 2 (n=1) had a mutation in exon 3 resulting in absence of Btk expression.

and FcγRIIA-mediated platelet spreading that covers the opsonized bacteria leading to bacterial killing (22). Platelets have also been shown to kill *S. aureus* Newman, but not *S. pneumoniae*, in a process that was FcγRIIA independent (23). Moreover, the releasate derived from platelet aggregation can directly kill *S. aureus* and enhance the antimicrobial function of macrophages (23, 48).

Despite the overall response to bacteria, some variation was observed in ibrutinib-untreated CLL platelets, with some samples not reaching full activation. Differences in bacteria-induced aggregation in healthy donor platelets are not uncommon (49, 50), however, variation in CLL could be due to additional factors like co-morbidities and related medications (51). Indeed, most of our CLL patients were taking multiple medications reflecting a typical population of CLL patients often with multiple comorbidities. The increased bleeding risk found in ibrutinib-treated patients is exacerbated by concurrent intake of antiplatelet or anticoagulant therapy (7), and *in vitro* studies show that ibrutinib amplifies the effect of cangrelor and indomethacin on platelets (14, 17). However, in our study a minority of patients were taking antiplatelet medications, and thus, future research should be done to investigate the effect of different drug combinations, including iBtk combinations with antiplatelet drugs, on platelet immune functions. Other factors that might explain why platelets from some CLL patients did not activate fully to bacteria are plasma immunoglobulin concentrations (52) and polymorphic variants of FcγRIIA (53, 54). Notably, some of these factors might also account for variable platelet responses to bacteria within healthy individuals (49, 50). Although variations in the expression of FcγRIIA (55) could also affect platelet activation by microorganisms, no significant changes in FcγRIIA levels were detected among our clinical groups.

Three observations suggested alterations in circulating CLL platelets: a decrease in platelet granularity/complexity, an ibrutinib-independent decrease in membrane levels of αIIbβ3 and GPVI compared to controls, and a reduction in lag time for onset of platelet aggregation in response to bacteria; although the latter could also be due to changes in plasma composition in CLL. Our flow cytometry results differ from others in which αIIbβ3 surface expression in CLL platelets was similar to healthy donors (40, 56) but decreased upon ibrutinib treatment (40). Moreover, reduced GPVI levels in CLL platelets were found in one study (56), but not another (40). Platelet alterations could originate during megakaryopoiesis as CLL is characterized by bone marrow dysfunction (57); however, they could also reflect

interactions with unknown-disease-related factors once platelets are released into the circulation (57). The modulation of membrane receptor levels can affect platelet reactivity to external stimuli as well as platelet senescence and lifespan (58); and changes in platelet granularity might reflect some degree of activation (with granule centralization) (19). Therefore, future studies are needed to characterize CLL platelet proteomic and structural changes and their potential consequences in platelet function in the presence and absence of iBtks.

A key finding of this investigation is that therapeutic doses of ibrutinib impair platelet responses to *S. aureus* Newman and *E. coli* RS218. While it is still possible that an underlying CLL platelet immune dysfunction is significantly worsened by iBtks, the fact that ibrutinib and acalabrutinib also inhibited platelets derived from healthy donors points out to the ability of iBtks to directly interfere with platelet immune functions (independently of additional CLL-specific changes). Despite some conflicting reports regarding the increased risk of infection during ibrutinib therapy in B-cell malignancies, Ball et al. have recently published a systematic review and meta-analysis of randomized controlled trials, including more than 2000 patients, in which a significantly higher risk of infections associated with ibrutinib treatment has been found (6). Ibrutinib inhibition of platelet immune functions might contribute to infection by interfering with the ability of platelets to contain and kill pathogens and crosstalk with other immune cells (19–24, 48, 59); however, this hypothesis will need further evaluation in view of the complex multifactorial nature of infection complications in CLL. For example, ibrutinib affects neutrophil, monocyte and macrophage responses to fungi (10, 11), and these effects might also have important consequences in responses to bacteria. Furthermore, infections cannot be explained by Btk inhibition alone, as seen by the decline in the risk of infection and neutropenia rate over time on ibrutinib therapy presumably due to gradual immune reconstitution (60–62). Notably, in our study some platelet samples from ibrutinib-treated patients aggregated to bacteria, mainly *E. coli* RS218, suggesting the presence of Btk-independent mechanisms of activation. It is important to point out that immune responses in CLL, including those ones in which platelets might be involved, are likely microorganism dependent. Thus, frequent pathogens like *S. pneumoniae*, *H. influenzae*, but also fungi (63) should be examined in this context.

To clarify if newer iBtks with improved selectivity for Btk over other kinases (5, 42, 64) might be beneficial to treat B-cell malignancies, it is important to understand how Btk and structurally related kinases like Tec work in non-malignant cells, including platelets. For this reason, the second part of our study investigated the role of Btk in platelet immunity. Previous studies on healthy donor platelets reported a role for Btk and Tec in FcγRIIA-mediated platelet activation in response to artificial antibody crosslinking and sera from heparin-induced thrombocytopenia patients (35, 36). Here, we studied Btk and Tec activation downstream of bacteria-stimulated platelets from healthy donors and CLL patients. Bacteria and FcγRIIA crosslinking with IV.3 mAb caused Btk activation, and platelet aggregation that was more sensitive to ibrutinib than CRP-xl stimulation, suggesting that Btk has a role downstream of FcγRIIA, as supported by investigations by Goldmann et al. (36). Although the peak plasma concentration of ibrutinib is only 0.3-0.4 μM (65), Btk activation was abolished in platelets derived from ibrutinib-treated patients, which confirmed that therapeutic doses of ibrutinib target platelet Btk. Nonetheless, bacteria also caused platelet Tec phosphorylation that was inhibited by ibrutinib.

Because platelets are anucleated, intracellular signaling studies often rely on animal models. For GPVI, the relative contribution of Btk and Tec in GPVI-mediated platelet activation was studied using platelets from knockout mice, and only those from double Btk and Tec knockout animals were insensitive to CRP-xl (66). However, this strategy is not feasible in the context of our study because murine platelets do not express FcγRIIA, and platelets from FcγRIIA-transgenic mice do not respond to many bacterial strains that are known to activate human platelets, even when supplemented with human IgGs (29). This should be taken as a warning of the limitations of using animal models that lack FcγRIIA to address platelet immune functions that depend on IgGs, thus linking innate and acquired immune responses. Instead, we tested platelets from two XLA patients, which lack functional Btk, and found that they responded to bacteria in an FcγRIIA-dependent manner, although we detected some impairment in aggregation to FcγRIIA crosslinking (IV.3-xl) that will require further investigation. Most commonly, XLA patients suffer from respiratory infections caused by *S. pneumoniae* and *H. influenza*. Although *S. aureus* infections are also reported (67, 68), generally they are not considered significant problems in patients who receive regular immunoglobulin replacement therapy (47), which further suggests that Btk is not essential for the immune system to control infection by specific bacterial species in the presence of normal IgGs. Altogether, and as found for GPVI (15, 35, 66, 69), our results suggest that either Btk is dispensable for platelet aggregation to *S. aureus* and *E. coli*, or there is enough Btk/Tec kinase functional redundancy to rescue the activating signaling when Btk is absent. It is also possible that other tyrosine kinases can compensate for the loss of Btk, but still be off-targeted by ibrutinib in CLL patients. Platelet-bacteria interactions are complex and can involve multiple receptor-ligand combinations that are bacterial-strain specific (70), therefore, it is also possible that crosstalk between FcγRIIA/αIIbβ3 and other receptors (e.g., GPIb, complement receptor gC1q-R, and Toll-like receptor 2) (33, 34) and signaling pathways can overcome the absence of Btk.

In summary, this study shows that CLL platelets can respond to *S. aureus* and *E. coli* bacteria in an FcγRIIA-dependent manner and provides evidence that ibrutinib impairs such responses. Mechanistically, while FcγRIIA expression was not altered by the treatment, our data demonstrates that ibrutinib inhibits both Btk and Tec kinases downstream of FcγRIIA/αIIbβ3 activation in response to bacteria stimulation. This points out to the importance of evaluating the effect of iBtks used to treat CLL and other hematological malignancies on platelet immune functions.

DATA AVAILABILITY STATEMENT

The raw data supporting the conclusions of this article will be made available by the authors, without undue reservation.

ETHICS STATEMENT

The studies involving human participants were reviewed and approved by Hull York Medical School Ethics Committee (Ethics reference number 1501) and UK National Health Service Research Ethics Committee (Ethics reference number 08/H1304/35). The patients/participants provided their written informed consent to participate in this study.

AUTHOR CONTRIBUTIONS

LN-A designed research, performed most experiments, analyzed data, and wrote the manuscript. AC designed, performed, and analyzed scavenging experiments. ZB and JJ performed experiments. SC designed and supervised flow cytometry research and analyzed data. SK provided access to XLA patients. SH provided key reagents and intellectual input. FR designed and performed platelet scavenging research and analyzed data. DA provided and coordinated access to CLL patients and designed and supervised the study. MA designed and directed research, performed experiments, analyzed data and wrote the manuscript. All authors contributed to the article and approved the submitted version.

FUNDING

This work was supported by the University of Hull and Hull University Teaching Hospital Trust. LN-A and ARC were recipients of University of Hull PhD scholarships.

ACKNOWLEDGMENTS

The authors would like to thank Prof. Steven Kerrigan (RCSI, Ireland) and Prof. Ian Henderson (University of Queensland, Australia) for kindly providing *S. aureus* Newman and *E. coli* RS218, respectively. We also thank all the patients, healthy donors and staff who participated in the study, and the J. Andrew Grant Fund for Cardiovascular Research for support.

SUPPLEMENTARY MATERIAL

The Supplementary Material for this article can be found online at: https://www.frontiersin.org/articles/10.3389/fimmu.2021.766272/full#supplementary-material

REFERENCES

1. *HMRN. Haematological Malignancy Research Network* (2018). Available at: https://www.hmrn.org/.
2. Nosari A. Infectious Complications in Chronic Lymphocytic Leukemia. *Mediterr J Hematol Infect Dis* (2012) 4:2012070. doi: 10.4084/mjhid.2012.070
3. Korona-Glowniak I, Grywalska E, Grzegorczyk A, Roliński J, Glowniak A, Malm A. Bacterial Colonization in Patients With Chronic Lymphocytic Leukemia and Factors Associated With Infections and Colonization. *J Clin Med* (2019) 8:861. doi: 10.3390/jcm8060861
4. Teh BW, Tam CS, Handunnetti S, Worth LJ, Slavin MA. Infections in Patients With Chronic Lymphocytic Leukaemia: Mitigating Risk in the Era of Targeted Therapies. *Blood Rev* (2018) 32:499–507. doi: 10.1016/j.blre.2018.04.007
5. Wen T, Wang J, Shi Y, Qian H, Liu P. Inhibitors Targeting Bruton's Tyrosine Kinase in Cancers: Drug Development Advances. *Leukemia* (2021) 35:312–32. doi: 10.1038/s41375-020-01072-6
6. Ball S, Das A, Vutthikraivit W, Edwards PJ, Hardwicke F, Short NJ, et al. Risk of Infection Associated With Ibrutinib in Patients With B-Cell Malignancies: A Systematic Review and Meta-Analysis of Randomized Controlled Trials. *Clin Lymphoma Myeloma Leukemia* (2020) 20:87–97.e5. doi: 10.1016/j.clml.2019.10.004
7. Lipsky AH, Farooqui MZH, Tian X, Martyr S, Cullinane AM, Nghiem K, et al. Incidence and Risk Factors of Bleeding-Related Adverse Events in Patients With Chronic Lymphocytic Leukemia Treated With Ibrutinib. *Haematologica* (2015) 100:1571–8. doi: 10.3324/haematol.2015.126672
8. Munir T, Brown JR, O'Brien S, Barrientos JC, Barr PM, Reddy NM, et al. Final Analysis From RESONATE: Up to Six Years of Follow-Up on Ibrutinib in Patients With Previously Treated Chronic Lymphocytic Leukemia or Small Lymphocytic Lymphoma. *Am J Hematol* (2019) 94:1353–63. doi: 10.1002/ajh.25638
9. Honigberg LA, Smith AM, Sirisawad M, Verner E, Loury D, Chang B, et al. The Bruton Tyrosine Kinase Inhibitor PCI-32765 Blocks B-Cell Activation and is Efficacious in Models of Autoimmune Disease and B-Cell Malignancy. *Proc Natl Acad Sci* (2010) 107:13075–80. doi: 10.1073/pnas.1004594107
10. Fiorcari S, Maffei R, Vallerini D, Scarfò L, Barozzi P, Maccaferri M, et al. BTK Inhibition Impairs the Innate Response Against Fungal Infection in Patients With Chronic Lymphocytic Leukemia. *Front Immunol* (2020) 11:2158. doi: 10.3389/fimmu.2020.02158
11. Blez D, Blaize M, Soussain C, Boissonnas A, Meghraoui-Kheddar A, Menezes N, et al. Ibrutinib Induces Multiple Functional Defects in the Neutrophil Response Against Aspergillus Fumigatus. *Haematologica* (2019) 105(2):478–89. doi: 10.3324/haematol.2019.219220
12. Levade M, David E, Garcia C, Laurent P-A, Cadot S, Michallet A-S, et al. Ibrutinib Treatment Affects Collagen and Von Willebrand Factor-Dependent Platelet Functions. *Blood* (2014) 124:3991–5. doi: 10.1182/blood-2014-06-583294
13. Kamel S, Horton L, Ysebaert L, Levade M, Burbury K, Tan S, et al. Ibrutinib Inhibits Collagen-Mediated But Not ADP-Mediated Platelet Aggregation. *Leukemia* (2015) 29:783–7. doi: 10.1038/leu.2014.247
14. Bye AP, Unsworth AJ, Vaiyapuri S, Stainer AR, Fry MJ, Gibbins JM. Ibrutinib Inhibits Platelet Integrin αiibβ3 Outside-In Signaling and Thrombus Stability But Not Adhesion to Collagen. *Arterioscler Thromb Vasc Biol* (2015) 35:2326–35. doi: 10.1161/atvbaha.115.306130
15. Nicolson PLR, Nock SH, Hinds J, Garcia-Quintanilla L, Smith CW, Campos J, et al. Low Dose Btk Inhibitors Selectively Block Platelet Activation by CLEC-2. *Haematologica* (2021) 106(1):208–19. doi: 10.3324/haematol.2019.218545
16. Nicolson PLR, Hughes CE, Watson S, Nock SH, Hardy AT, Watson CN, et al. Inhibition of Btk by Btk-Specific Concentrations of Ibrutinib and Acalabrutinib Delays But Does Not Block Platelet Aggregation to GPVI. *Haematologica* (2018) 103(12):2097–108. doi: 10.3324/haematol.2018.193391
17. Series J, Garcia C, Levade M, Viaud J, Sié P, Ysebaert L, et al. Differences and Similarities in Ibrutinib and Acalabrutinib Effects on Platelet Functions. *Haematologica* (2019) 104(11):2292–9 doi: 10.3324/haematol.2018.207183
18. Dmitrieva EA, Nikitin EA, Ignatova AA, Vorobyev VI, Poletaev AV, Seregina EA, et al. Platelet Function and Bleeding in Chronic Lymphocytic Leukemia

and Mantle Cell Lymphoma Patients on Ibrutinib. *J Thromb Haemost* (2020) 18:2672–84. doi: 10.1111/jth.14943
19. Koupenova M, Clancy L, Corkrey HA, Freedman JE. Circulating Platelets as Mediators of Immunity, Inflammation, and Thrombosis. *Circ Res* (2018) 122:337–51. doi: 10.1161/circresaha.117.310795
20. Ali RA, Wuescher LM, Worth RG. Platelets: Essential Components of the Immune System. *Curr Trends Immunol* (2015) 16:65–78.
21. Gaertner F, Ahmad Z, Rosenberger G, Fan S, Nicolai L, Busch B, et al. Migrating Platelets Are Mechano-Scavengers That Collect and Bundle Bacteria. *Cell* (2017) 171:1368–82.e23. doi: 10.1016/j.cell.2017.11.001
22. Palankar R, Kohler TP, Krauel K, Wesche J, Hammerschmidt S, Greinacher A. Platelets Kill Bacteria by Bridging Innate and Adaptive Immunity *via* Platelet Factor 4 and Fcγriia. *J Thromb Haemost* (2018) 16:1187–97. doi: 10.1111/jth.13955
23. Wolff M, Handtke S, Palankar R, Wesche J, Kohler TP, Kohler C, et al. Activated Platelets Kill Staphylococcus Aureus, But Not Streptococcus Pneumoniae—The Role of Fcγriia and Platelet Factor 4/Heparinantibodies. *J Thromb Haemost* (2020) 18:1459–68. doi: 10.1111/jth.14814
24. Kraemer BF, Campbell RA, Schwertz H, Cody MJ, Franks Z, Tolley ND, et al. Novel Anti-Bacterial Activities of β-Defensin 1 in Human Platelets: Suppression of Pathogen Growth and Signaling of Neutrophil Extracellular Trap Formation. *PloS Pathog* (2011) 7:e1002355. doi: 10.1371/journal.ppat.1002355
25. Dearden C. Disease-Specific Complications of Chronic Lymphocytic Leukemia. *Hematology* (2008) 2008:450–6. doi: 10.1182/asheducation-2008.1.450
26. Haseeb M, Anwar MA, Choi S. Molecular Interactions Between Innate and Adaptive Immune Cells in Chronic Lymphocytic Leukemia and Their Therapeutic Implications. *Front Immunol* (2018) 9:2720. doi: 10.3389/fimmu.2018.02720
27. Tillman BF, Pauff JM, Satyanarayana G, Talbott M, Warner JL. Systematic Review of Infectious Events With the Bruton Tyrosine Kinase Inhibitor Ibrutinib in the Treatment of Hematologic Malignancies. *Eur J Haematol* (2018) 100:325–34. doi: 10.1111/ejh.13020
28. Varughese T, Taur Y, Cohen N, Palomba ML, Seo SK, Hohl TM, et al. Serious Infections in Patients Receiving Ibrutinib for Treatment of Lymphoid Cancer. *Clin Infect Dis* (2018) 67:687–92. doi: 10.1093/cid/ciy175
29. Arman M, Krauel K, Tilley DO, Weber C, Cox D, Greinacher A, et al. Amplification of Bacteria-Induced Platelet Activation Is Triggered by Fcγriia, Integrin αiibβ3, and Platelet Factor 4. *Blood* (2014) 123:3166–74. doi: 10.1182/blood-2013-11-540526
30. Arman M, Krauel K. Human Platelet IgG Fc Receptor Fcγriia in Immunity and Thrombosis. *J Thromb Haemost* (2015) 13:893–908. doi: 10.1111/jth.12905
31. Watson CN, Kerrigan SW, Cox D, Henderson IR, Watson SP, Arman M. Human Platelet Activation by Escherichia Coli: Roles for Fcγriia and Integrin αiibβ3. *Platelets* (2016) 27:1–6. doi: 10.3109/09537104.2016.1148129
32. Moriarty RD, Cox A, McCall M, Smith SGJ, Cox D. Escherichia Coli Induces Platelet Aggregation in an Fcγriia-Dependent Manner. *J Thromb Haemost* (2016) 14:797–806. doi: 10.1111/jth.13226
33. Hamzeh-Cognasse H, Damien P, Chabert A, Pozzetto B, Cognasse F, Garraud O. Platelets and Infections – Complex Interactions With Bacteria. *Front Immunol* (2015) 6:82. doi: 10.3389/fimmu.2015.00082
34. Kerrigan SW, Poole A. Focusing on the Role of Platelets in Immune Defence Against Invading Pathogens. *Platelets* (2015) 26:285–5. doi: 10.3109/09537104.2015.1038230
35. Oda A, Ikeda Y, Ochs HD, Druker BJ, Ozaki K, Handa M, et al. Rapid Tyrosine Phosphorylation and Activation of Bruton's Tyrosine/Tec Kinases in Platelets Induced by Collagen Binding or CD32 Cross-Linking. *Blood* (2000) 95:1663–70.
36. Goldmann L, Duan R, Kragh T, Wittmann G, Weber C, Lorenz R, et al. Oral Bruton Tyrosine Kinase Inhibitors Block Activation of the Platelet Fc Receptor CD32a (Fcγriia): A New Option in HIT? *Blood Adv* (2019) 3:4021–33. doi: 10.1182/bloodadvances.2019000617
37. Krauel K, Pötschke C, Weber C, Kessler W, Fürll B, Ittermann T, et al. Platelet Factor 4 Binds to Bacteria, Inducing Antibodies Cross-Reacting With the Major Antigen in Heparin-Induced Thrombocytopenia. *Blood* (2011) 117:1370–8. doi: 10.1182/blood-2010-08-301424
38. Allen RD, Zacharski LR, Widirstky ST, Rosenstein R, Zaitlin LM, Burgess DR. Transformation and Motility of Human Platelets: Details of the Shape Change and Release Reaction Observed by Optical and Electron Microscopy. *J Cell Biol* (1979) 83:126–42. doi: 10.1083/jcb.83.1.126
39. Rigg RA, Aslan JE, Healy LD, Wallisch M, Thierheimer MLD, Loren CP, et al. Oral Administration of Bruton's Tyrosine Kinase Inhibitors Impairs GPVI-Mediated Platelet Function. *Am J Physiol-Cell Ph* (2016) 310:C373–80. doi: 10.1152/ajpcell.00325.2015
40. Dobie G, Kuriri FA, Omar MMA, Alanazi F, Gazwani AM, Tang CPS, et al. Ibrutinib, But Not Zanubrutinib, Induces Platelet Receptor Shedding of GPIb-IX-V Complex and Integrin αiibβ3 in Mice and Humans. *Blood Adv* (2019) 3:4298–311. doi: 10.1182/bloodadvances.2019000640
41. Bose P, Gandhi VV, Keating MJ. Pharmacokinetic and Pharmacodynamic Evaluation of Ibrutinib for the Treatment of Chronic Lymphocytic Leukemia: Rationale for Lower Doses. *Expert Opin Drug Met* (2016) 12:1381–92. doi: 10.1080/17425255.2016.1239717
42. Byrd JC, Harrington B, O'Brien S, Jones JA, Schuh A, Devereux S, et al. Acalabrutinib (ACP-196) in Relapsed Chronic Lymphocytic Leukemia. *N Engl J Med* (2016) 374:323–32. doi: 10.1056/nejmoa1509981
43. Podoll T, Pearson PG, Evarts J, Ingallinera T, Bibikova E, Sun H, et al. Bioavailability, Biotransformation, and Excretion of the Covalent BTK Inhibitor Acalabrutinib in Rats, Dogs, and Humans. *Drug Metab Dispos* (2018) 47(2):145–54. doi: 10.1124/dmd.118.084459
44. Bye AP, Unsworth AJ, Desborough MJ, Hildyard CAT, Appleby N, Bruce D, et al. Severe Platelet Dysfunction in NHL Patients Receiving Ibrutinib Is Absent in Patients Receiving Acalabrutinib. *Blood Adv* (2017) 1:2610–23. doi: 10.1182/bloodadvances.2017011999
45. Burkhart JM, Vaudel M, Gambaryan S, Radau S, Walter U, Martens L, et al. The First Comprehensive and Quantitative Analysis of Human Platelet Protein Composition Allows the Comparative Analysis of Structural and Functional Pathways. *Blood* (2012) 120:e73–82. doi: 10.1182/blood-2012-04-416594
46. Nore BF, Mattsson PT, Antonsson P, Bäckesjö C-M, Westlund A, Lennartsson J, et al. Identification of Phosphorylation Sites Within the SH3 Domains of Tec Family Tyrosine Kinases. *Biochim Et Biophys Acta Bba - Proteins Proteom* (2003) 1645:123–32. doi: 10.1016/s1570-9639(02)00524-1
47. Conley ME, Dobbs AK, Farmer DM, Kilic S, Paris K, Grigoriadou S, et al. Primary B Cell Immunodeficiencies: Comparisons and Contrasts. *Annu Rev Immunol* (2009) 27:199–227. doi: 10.1146/annurev.immunol.021908.132649
48. Ali RA, Wuescher LM, Dona KR, Worth RG. Platelets Mediate Host Defense Against Staphylococcus Aureus Through Direct Bactericidal Activity and by Enhancing Macrophage Activities. *J Immunol* (2017) 198:344–51. doi: 10.4049/jimmunol.1601178
49. Ford I, Douglas CWI, Cox D, Rees DGC, Heath J, Preston FE. The Role of Immunoglobulin G and Fibrinogen in Platelet Aggregation by Streptococcus Sanguis. *Brit J Haematol* (1997) 97:737–7446. doi: 10.1046/j.1365-2141.1997.1342950.x
50. McNicol A, Zhu R, Pesun R, Pampolina C, Jackson E, Bowden G, et al. A Role for Immunoglobulin G in Donor-Specific Streptococcus Sanguis-Induced Platelet Aggregation. *Thromb Haemostasis* (2006) 95:288–93. doi: 10.1160/th05-07-0491
51. Harrison P, Mackie I, Mumford A, Briggs C, Liesner R, Winter M, et al. Haematology BC for S in. Guidelines for the Laboratory Investigation of Heritable Disorders of Platelet Function. *Brit J Haematol* (2011) 155:30–44. doi: 10.1111/j.1365-2141.2011.08793.x
52. Ishdorj G, Streu E, Lambert P, Dhaliwal HS, Mahmud SM, Gibson SB, et al. IgA Levels at Diagnosis Predict for Infections, Time to Treatment, and Survival in Chronic Lymphocytic Leukemia. *Blood Adv* (2019) 3:2188–98. doi: 10.1182/bloodadvances.2018026591
53. Warmerdam PA, van de Winkel JG, Vlug A, Westerdaal NA, Capel PJ. A Single Amino Acid in the Second Ig-Like Domain of the Human Fc Gamma Receptor II Is Critical for Human IgG2 Binding. *J Immunol Baltim Md 1950* (1991) 147:1338–43.
54. Tomiyama Y, Kunicki TJ, Zipf TF, Ford SB, Aster RH. Response of Human Platelets to Activating Monoclonal Antibodies: Importance of Fc Gamma RII (CD32) Phenotype and Level of Expression. *Blood* (1992) 80:2261–8. doi: 10.1182/blood.V80.9.2261.2261

55. Rosenfeld SI, Ryan DH, Looney RJ, Anderson CL, Abraham GN, Leddy JP. Human Fc Gamma Receptors: Stable Inter-Donor Variation in Quantitative Expression on Platelets Correlates With Functional Responses. *J Immunol Baltim Md 1950* (1987) 138:2869–73.
56. Qiao J, Schoenwaelder SM, Mason KD, Tran H, Davis AK, Kaplan ZS, et al. Low Adhesion Receptor Levels on Circulating Platelets in Patients With Lymphoproliferative Diseases Before Receiving Navitoclax (ABT-263). *Blood* (2013) 121:1479–81. doi: 10.1182/blood-2012-12-467415
57. Luu S, Gardiner EE, Andrews RK. Bone Marrow Defects and Platelet Function: A Focus on MDS and CLL. *Cancers* (2018) 10:147. doi: 10.3390/cancers10050147
58. Au AE, Josefsson EC. Regulation of Platelet Membrane Protein Shedding in Health and Disease. *Platelets* (2016) 28:1–12. doi: 10.1080/09537104.2016.1203401
59. Krijgsveld J, Zaat SAJ, Meeldijk J, van Veelen PA, Fang G, Poolman B, et al. Thrombocidins, Microbicidal Proteins From Human Blood Platelets, Are C-Terminal Deletion Products of CXC Chemokines. *J Biol Chem* (2000) 275:20374–81. doi: 10.1074/jbc.275.27.20374
60. Coutre SE, Byrd JC, Hillmen P, Barrientos JC, Barr PM, Devereux S, et al. Long-Term Safety of Single-Agent Ibrutinib in Patients With Chronic Lymphocytic Leukemia in 3 Pivotal Studies. *Blood Adv* (2019) 3:1799–807. doi: 10.1182/bloodadvances.2018028761
61. Sun C, Tian X, Lee YS, Gunti S, Lipsky A, Herman SEM, et al. Partial Reconstitution of Humoral Immunity and Fewer Infections in Patients With Chronic Lymphocytic Leukemia Treated With Ibrutinib. *Blood* (2015) 126:2213–9. doi: 10.1182/blood-2015-04-639203
62. Byrd JC, Hillmen P, O'Brien S, Barrientos JC, Reddy NM, Coutre S, et al. Long-Term Follow-Up of the RESONATE Phase 3 Trial of Ibrutinib vs Ofatumumab. *Blood* (2019) 133:2031–42. doi: 10.1182/blood-2018-08-870238
63. Maffei R, Maccaferri M, Arletti L, Fiorcari S, Benatti S, Potenza L, et al. Immunomodulatory Effect of Ibrutinib: Reducing the Barrier Against Fungal Infections. *Blood Rev* (2019) 40:100635. doi: 10.1016/j.blre.2019.100635
64. Hopper M, Gururaja T, Kinoshita T, Dean JP, Hill RJ, Mongan A. Relative Selectivity of Covalent Inhibitors Requires Assessment of Inactivation Kinetics and Cellular Occupancy: A Case Study of Ibrutinib and Acalabrutinib. *J Pharmacol Exp Ther* (2019) 372:331–8. doi: 10.1124/jpet.119.262063. jpet.119.262063.
65. Advani RH, Buggy JJ, Sharman JP, Smith SM, Boyd TE, Grant B, et al. Bruton Tyrosine Kinase Inhibitor Ibrutinib (PCI-32765) Has Significant Activity in Patients With Relapsed/Refractory B-Cell Malignancies. *J Clin Oncol* (2012) 31:88–94. doi: 10.1200/jco.2012.42.7906
66. Atkinson BT, Ellmeier W, Watson SP. Tec Regulates Platelet Activation by GPVI in the Absence of Btk. *Blood* (2003) 102:3592–9. doi: 10.1182/blood-2003-04-1142
67. Rawat A, Jindal AK, Suri D, Vignesh P, Gupta A, Saikia B, et al. Clinical and Genetic Profile of X-Linked Agammaglobulinemia: A Multicenter Experience From India. *Front Immunol* (2021) 11:612323. doi: 10.3389/fimmu.2020.612323
68. Duraisingham SS, Manson A, Grigoriadou S, Buckland M, Tong CYW, Longhurst HJ. Immune Deficiency: Changing Spectrum of Pathogens. *Clin Exp Immunol* (2015) 181:267–74. doi: 10.1111/cei.12600
69. Quek LS, Bolen J, Watson SP. A Role for Bruton's Tyrosine Kinase (Btk) in Platelet Activation by Collagen. *Curr Biol* (1998) 8:1137–S1. doi: 10.1016/s0960-9822(98)70471-3
70. Kerrigan SW. The Expanding Field of Platelet–Bacterial Interconnections. *Platelets* (2015) 26:293–301. doi: 10.3109/09537104.2014.997690

Conflict of Interest: DA has received honoraria for speaking from Gilead Pharmaceuticals, funding for conference attendance from Bayer and CSL Behring and research funding from Roche.

The remaining authors declare that the research was conducted in the absence of any commercial or financial relationships that could be construed as a potential conflict of interest.

Publisher's Note: All claims expressed in this article are solely those of the authors and do not necessarily represent those of their affiliated organizations, or those of the publisher, the editors and the reviewers. Any product that may be evaluated in this article, or claim that may be made by its manufacturer, is not guaranteed or endorsed by the publisher.

frontiers in Immunology

ORIGINAL RESEARCH
published: 30 November 2021
doi: 10.3389/fimmu.2021.760571

An HIV Vaccine Protective Allele in *FCGR2C* Associates With Increased Odds of Perinatal HIV Acquisition

*Joy Ebonwu[1,2], Ria Lassaunière[3], Maria Paximadis[2,4], Mark Goosen[2,4], Renate Strehlau[5,6], Glenda E. Gray[7,8], Louise Kuhn[9,10] and Caroline T. Tiemessen[2,4]**

[1] Division of Public Health Surveillance and Response, National Institute for Communicable Diseases, Johannesburg, South Africa, [2] Faculty of Health Sciences, University of the Witwatersrand, Johannesburg, South Africa, [3] Virus Research and Development Laboratory, Department of Virus and Microbiological Special Diagnostics, Statens Serum Institut, Copenhagen, Denmark, [4] Centre for HIV & STIs, National Institute for Communicable Diseases, Johannesburg, South Africa, [5] Empilweni Services and Research Unit, Rahima Moosa Mother and Child Hospital, Johannesburg, South Africa, [6] Department of Paediatrics and Child Health, Faculty of Health Sciences, University of the Witwatersrand, Johannesburg, South Africa, [7] Perinatal HIV Research Unit, Faculty of Health Sciences, University of the Witwatersrand, Johannesburg, South Africa, [8] South African Medical Research Council, Cape Town, South Africa, [9] Gertrude H. Sergievsky Centre, College of Physicians and Surgeons, Columbia University, New York, NY, United States, [10] Department of Epidemiology, Mailman School of Public Health, Columbia University, New York, NY, United States

OPEN ACCESS

Edited by:
Amy W Chung, The University of Melbourne, Australia

Reviewed by:
Bronwyn Gunn, Washington State University, United States
Justin Pollara, Duke University, United States

***Correspondence:**
Caroline T. Tiemessen
carolinet@nicd.ac.za

Specialty section:
This article was submitted to Viral Immunology, a section of the journal Frontiers in Immunology

Received: *18 August 2021*
Accepted: *11 November 2021*
Published: *30 November 2021*

Citation:
Ebonwu J, Lassaunière R, Paximadis M, Goosen M, Strehlau R, Gray GE, Kuhn L and Tiemessen CT (2021) An HIV Vaccine Protective Allele in FCGR2C Associates With Increased Odds of Perinatal HIV Acquisition. Front. Immunol. 12:760571. doi: 10.3389/fimmu.2021.760571

In the Thai RV144 HIV-1 vaccine trial, a three-variant haplotype within the Fc gamma receptor 2C gene (*FCGR2C*) reduced the risk of HIV-1 acquisition. A follow-on trial, HVTN702, of a similar vaccine candidate found no efficacy in South Africa, where the predominant population is polymorphic for only a single variant in the haplotype, c.134-96C>T (rs114945036). To investigate a role for this variant in HIV-1 acquisition in South Africans, we used the model of maternal-infant HIV-1 transmission. A nested case-control study was conducted of infants born to mothers living with HIV-1, comparing children with perinatally-acquired HIV-1 (cases, n = 176) to HIV-1-exposed uninfected children (controls, n = 349). All had received nevirapine for prevention of mother-to-child transmission. The *FCGR2C* copy number and expression variants (c.–386G>C, c.–120A>T c.169T>C, and c.798+1A>G) were determined using a multiplex ligation-dependent probe amplification assay and the c.134-96C>T genotype with Sanger sequencing. The copy number, genotype and allele carriage were compared between groups using univariate and multivariate logistic regression. The *FCGR2C* c.134-96C>T genotype distribution and copy number differed significantly between HIV-1 cases and exposed-uninfected controls (P = 0.002, P_{Bonf} = 0.032 and P = 0.010, P_{Bonf} = > 0.05, respectively). The *FCGR2C* c.134-96T allele was overrepresented in the cases compared to the controls (58% *vs* 42%; P = 0.001, P_{Bonf} = 0.016). Adjusting for birthweight and *FCGR2C* copy number, perinatal HIV-1 acquisition was associated with the c.134-96C>T (AOR = 1.89; 95% CI 1.25-2.87; P = 0.003, P_{Bonf} = 0.048) and c.169C>T (AOR = 2.39; 95% CI 1.45-3.95; P = 0.001, P_{Bonf} = 0.016) minor alleles but not the promoter variant at position c.–386G>C. The c.134-96C>T variant was in strong linkage disequilibrium with the c.169C>T variant, but remained significantly associated with perinatal acquisition when adjusted for c.169C>T in multivariate analysis. In contrast to the protective effect

observed in the Thai RV144 trial, we found the *FCGR2C* variant c.134-96T-allele associated with increased odds of perinatal HIV-1 acquisition in South African children. These findings, taken together with a similar deleterious association found with HIV-1 disease progression in South African adults, highlight the importance of elucidating the functional relevance of this variant in different populations and vaccination/ disease contexts.

Keywords: Fc gamma receptor, FCGR2C, genetic variant, polymorphism, gene copy number, perinatal HIV-1 acquisition, genetic association study, South Africa

INTRODUCTION

The crystallisable fragment (Fc) region of immunoglobulin G (IgG) antibodies interacts with Fc gamma receptors (FcγRs) expressed on the surface of hematopoietic cells to mediate effector functions. In humans, FcγRs are divided into three classes (FcγRI, FcγRII, and FcγRIII) based on structural domain organization, differences in affinity and specificity for IgG subclasses, and whether their binding triggers activating or inhibitory signals. The low affinity FcγRs are encoded by five genes on chromosome 1q23, namely *FCGR2A, FCGR2B, FCGR2C*, *FCGR3A* and *FCGR3B* (1) and play different roles in regulating immune responses (2). Functionally significant genetic variants occur for all low affinity FcγRs. These affect FcγRs by altering receptor cell surface density, binding affinities to IgGs, glycosylation patterns, cellular distribution, or subcellular localization (3, 4). Apart from single nucleotide polymorphisms (SNPs), copy number variation (CNV) has been demonstrated for *FCGR2C*, *FCGR3A and FCGR3B* (5, 6), and has been correlated with protein expression levels (7). Genes are duplicated or deleted at the *FCGR2/3* locus within well-defined copy number variable regions (CNRs), namely CNR1, CNR2, CNR3 (8, 9) and CNR4 (9). The most common are CNR1, which comprises genes of *FCGR2C*, *HSPA7* and *FCGR3B* and CNR2 that includes the distal part of *FCGR2A* (exon 8 and 3'-untranslated region [3'UTR]), *HSPA6, FCGR3A* and proximal part of *FCGR2C* (excluding exon 8 and 3'UTR) (9).

The *FCGR2C* gene, encoding FcγRIIc, is described as a pseudogene and is the product of an unequal crossover event between the 5' part of *FCGR2B* genes and 3' part of *FCGR2A* (10). Expression of the membrane-bound FcγRIIc protein depends on a combination of three minor alleles that include the c.169T>C variant in exon 3, which substitutes a premature stop codon with a glutamine at amino acid 57, and two splice variants in intron 7 - c.798+1A>G and c.799-1G>C (6, 11). Due to significant variation of the minor allele frequencies in different populations (12), FcγRIIc protein expression is subject to ethnic variation. The splice variant c.798+1A>G minor allele rarely occurs in black Africans and East Asians, thus, few individuals in this population express FcγRIIc compared to approximately 33% of Caucasians (12). An additional *FCGR2C* c.134-96C>T variant (also known as *FCGR2C* 126C>T) has been identified as clinically significant (13). Overall, genetic variation of *FCGR2C* has been associated with rheumatoid arthritis (14) idiopathic thrombocytopenic purpura (15), HIV-tuberculosis co-infection (16), antibody responses to vaccinations (11, 13, 17) and HIV disease progression (18).

In the RV144 vaccine trial, where the vaccine regimen was designed against HIV-1 clade B and E, a three-variant haplotype within *FCGR2C* [c.353C>T (rs138747765); c.391+111G>A (rs78603008) and c.134-96C>T (rs114945036)] reduced the risk of HIV-1 acquisition in Thai adults. The vaccine test subjects carrying at least one minor allele of the c.134-96C>T tag variant had an estimated vaccine efficacy of 91% against the CRF01_AE 169K HIV-1 strain and 64% against any HIV-1 strain, while those with wild type allele exhibited a vaccine efficacy of 15% and 11%, respectively (13). Conversely, two variants within the haplotype were associated with increased risk of HIV-1 acquisition in the HIV Vaccine Trials Network (HVTN) 505 vaccine trial (17). A follow-on trial of a similar vaccine regime to RV144 (HVTN 702 vaccine trial) tested in South Africa showed no efficacy (19). The cause underlying the different vaccine trial outcomes remains undetermined. However, differences in vaccine regimen, population, demographics and environment should be considered (17). A role for population genetics warrants consideration, since black South Africans do not possess the complete Thai *FCGR2C* haplotype and are only polymorphic for c.134-96C>T (rs114945036) (12).

The c.134-96C>T *FCGR2C* variant has been implicated in HIV-1 disease progression in a black South African cohort (18). However, unlike the protective effect observed for Thai vaccinees, the minor allele was associated with increased odds of HIV-1 disease progression in those already infected. It is unknown whether the alternate protective and deleterious roles of the *FCGR2C* c.134-96C>T variant in the Thai vaccinees and HIV-1 infected South Africans is due to different mechanisms involved before and after HIV-1 infection or whether the genetic differences associated with the haplotype alters its role in the two populations. Establishing the role of the c.134-96C>T variant in HIV-1 protective immunity in other models of persistent HIV-1 exposure, such as infants born to HIV-1 infected mothers, will be informative.

Mother-to-child transmission (MTCT) is an attractive model in which to study immune correlates of protection since both members of the transmitting dyad are known, timing of transmission can be ascertained with reasonable precision, and it affords the opportunity to assess factors contributing to both the infectiousness of the transmitter (mother) and susceptibility of the recipient (infant) (20, 21). Limitations of this model are that

transmission occurs between genetically similar individuals, exposure to HIV-1 occurs at a time of early immune development, and immune circumstances during pregnancy are associated with tolerance of the fetal allograft (22). Nevertheless, it provides a unique opportunity to investigate the role of FcγR-mediated effector functions, since the individual (fetus/infant) at risk is passively immunized with HIV-1-specific antibodies through trans-placental transfer of IgG from the HIV-1 infected mother and the model is not confounded by interspecies differences as observed for non-human primate studies (23). In this study, we investigate the association between the *FCGR2C* c.134-96C>T variant and HIV-1 acquisition in black South African children born to women living with HIV.

MATERIALS AND METHODS

Study Design and Population

A nested case-control study was undertaken to investigate the association between the *FCGR2C* variants and HIV-1 perinatal acquisition in children, combining data from past studies of five perinatal cohorts at two hospitals in Johannesburg, South Africa (24–27). One of the five cohorts consists of 546 HIV-infected children who were recruited as part of two sequential randomized clinical trials (NEVEREST 2 and 3) (24–26). The remaining four cohorts comprised of 849 HIV-1 infected mothers and their infants who were recruited and followed prospectively, of whom 83 (10%) infants acquired HIV (27). In the present study, only samples that were found and with sufficient volume were genotyped. *FCGR2C* genotypic data from 99 out of 546 and 77 of 83 HIV-1-infected children (cases) from the NEVEREST and mother-infant cohorts, respectively (n = 176) were compared with 349 of the HIV-exposed uninfected children (controls).

Mode of transmission was defined according to the presence or absence of detectable HIV-1 deoxyribonucleic acid (DNA) in the infant at birth and six weeks of age. Infants that tested HIV-1 positive at six weeks of age, but who were negative at birth, were considered to be infected intrapartum (during labor and delivery) (n = 31), while infants that tested HIV-1 positive at birth were considered infected *in utero* (n = 19). Infants who were HIV-1 positive at six weeks, but had no birth sample, were categorized as 'undetermined' (n = 28). In the 'undetermined' category, 25/28 (89.2%) mothers received single-dose nevirapine or triple-drug combination therapy (two nucleoside reverse transcriptase inhibitors with either a protease inhibitor or non-nucleoside reverse transcriptase inhibitor) known to reduce intrapartum transmission (27–29). Genotyping generated a result for all the *FCGR2C* variants assessed in this study in 27 out of the 28 samples. It was thus concluded that the majority (n = 27) of infants were likely infected *in utero* and were combined with the *in utero* group to form an *in utero*-enriched group. For the NEVEREST cohort, there were no birth samples as the children were recruited from six weeks of life. They were therefore classified as mixed transmission since a few were breastfeeding infections and *in utero* infections could not be distinguished from intrapartum infections (n = 99). All study participants were black South Africans and received nevirapine for prevention of MTCT. Maternal antiretroviral therapy was not routinely used at the time.

Ethics

Ethics approval for the study was obtained from the University of the Witwatersrand Human Research Ethics Committee (Reference numbers: M170585; M180575).

Genotyping

FCGR2C copy number and SNPs that affect gene expression – c.169T>C (p.X57Q), c.798+1A>G, and the *FCGR2B/C* promoter variant at position c.–386G>C and c.–120A>T – were determined using the *FCGR*-specific multiplex ligation-dependent probe amplification assay (MRC Holland, Amsterdam, The Netherlands) according to manufacturer's instructions. Amplicons were separated by capillary electrophoresis on an ABI Genetic Analyser 3130 (Life Technologies, Applied Bio systems, Foster City, CA, USA) and fragments analyzed with the Coffalyzer.NET software (MRC Holland) using peak height as a measure of gene/allele copy number. We did not utilize gene-specific polymerase chain reactions (PCR) to distinguish *FCGR2B* and *FCGR2C* promoter sequences since earlier findings indicate that African individuals do not possess the promoter variant in *FCGR2B*, and thus any detected c.–386G>C minor alleles were in *FCGR2C* (12).

The *FCGR2C* c.134-96C>T (rs114945036) variant was genotyped through conventional PCR and Sanger nucleotide sequencing. In brief, a 6,374 base pair fragment was amplified with the Expand Long Template PCR System (Roche, Mannheim, Germany) using the *FCGR2B/C* sense primer (5'-ATGTATGGGGTGTCTGTGTGTC-3') and *FCGR2C*-specific antisense primer (5'-CTCAAATTGGGCAGCCTTCAC-3') (15). The PCR reaction consisted of ~20 ng genomic DNA as template, 3.75 U Expand Long Template enzyme mix, 5 µl 10× PCR buffer 3 (2.75 mM $MgCl_2$), 500 µM of each deoxynucleotide, 0.3 µM of each oligonucleotide primer, and molecular grade water to a final volume of 50 µl. The PCR conditions were initial denaturation at 94°C for 2 minutes, followed by 10 cycles of 94°C for 10 seconds (denaturation), 60°C for 15 seconds (annealing) and 68°C for 7 minutes (elongation). Thereafter, 25 cycles repeat process of denaturation, annealing and elongation respectively at 94°C for 15 seconds, 60°C for 15 seconds and 68°C for 7 minutes plus 20 seconds cycle elongation for each successive cycle; and a final elongation cycle at 72°C for 7 minutes. The internal antisense primer (5'-CCTCCACTGACCAGAAAGCAC-3') was used in standard BigDye Terminator v3.1 Cycle Sequencing reactions. Sequences were analyzed in Sequencer version 4.5 (Gene Codes Corporation, Ann Arbor, MI) and area under the curve of the electropherogram used to determine allele count for individuals bearing more than two *FCGR2C* gene copies.

Nomenclature

The SNP nomenclature used in this manuscript refers to the amino acid positions in the full protein, in accordance with the Human Genome Variation Society (HGVS) guidelines (30).

The numbering of nucleotides is according to the Genome Reference Consortium Human Reference 38 [GRCh38 (hg38)].

Statistical Analysis

Categorical data were summarized as proportions and the Fisher's Exact test was used for comparisons. For numerical data, the t-test was used for comparison of means. Univariate and multivariate analyses were conducted to determine factors associated with perinatal HIV acquisition. Adjustment for multiple comparisons was performed using the Bonferroni correction, which considered 16 independent tests — four unrelated clinical subgroups each tested for four variants (gene copy number, c.134-96C>T, c.169T<C, and c.–386G>C). Both unadjusted and adjusted P values are reported. Analysis of an association between *FCGR2C* variants and HIV-1 acquisition was limited to variants whose allele frequencies were ≥ 5%. Due to the low frequencies of minor allele homozygotes, their effect was tested using dominant model approach, where participants were divided into two genotype groups: homozygous genotype of the major allele and the two genotypes containing at least one minor allele. All analyses were performed in STATA version 15.1 (StataCorp LP, Texas, USA).

Linkage disequilibrium between *FCGR2C* functional variants and CNRs was computed using the Haploview software package (31) and expressed as D prime (D′) and square of the correlation coefficient (r^2). The closer D′ is to 1 the stronger the LD between two loci. Hardy-Weinberg equilibrium was considered for individuals with two gene copies and the statistics abstracted from the Haploview analysis output. For the analysis, genotypic data with multiple gene copies were considered homozygous if all copies carried the same allele or heterozygous when both alleles were present.

RESULTS

Cohort

This nested case-control study investigated *FCGR2C* genotypic data from 525 children to determine the role of *FCGR2C* variants and HIV-1 acquisition in South African children born to women living with HIV-1. The cohort includes 176 HIV-1 infected (cases) and 349 HIV-exposed-uninfected (controls) children. The HIV-1 infected children comprised four transmission mode groups: *in utero* (n = 19), *in utero*-enriched (n = 46), intrapartum (n = 31) and mixed (n = 99). Overall, there was no significant difference in sex, gestation and breastfeeding status between the HIV-1 infected and HIV-1 uninfected cohort. However, the total HIV-1 infected and HIV-1 exposed-uninfected groups differed significantly in birth weight at delivery. Specifically, a higher proportion of HIV-infected children had a birth weight below 2500 g (22% *vs.* 11%; $P = 0.001$, $P_{Bonf} = 0.016$) (**Table 1**).

FCGR2C Copy Number Distribution and HIV-1 Acquisition

The *FCGR2C* gene, highly homologous to *FCGR2B* in the first six exons and *FCGR2A* in the last two exons, is subject to CNV within previously described distinct regions (**Figure 1**). We did not observe any individual with a complete absence of the *FCGR2C* gene. Overall, *FCGR2C* CNV occurred in 166/525 (32%) children, with the frequency of duplications (n = 114) 2.2-fold higher than deletions (n = 52) (69% *vs.* 31%). The copy number distribution was significantly different between the HIV-1 infected and HIV-1 exposed-uninfected groups but not after Bonferroni correction ($P = 0.010$, $P_{Bonf} > 0.05$) (**Table 2**). Variation in copy number among the whole study cohort was observed more frequently in CNR1, which encompasses a complete *FCGR2C* copy, *HSPA7* and *FCGR3B* (28%; n = 147) than CNR2, with an incomplete *FCGR2C* copy, *HSPA6* and *FCGR3A* (2.7%; n = 14). In six instances (1.1%), we observed CNV for only *FCGR2C* in the absence of duplicated/deleted flanking genes, as previously described among the South African black population (12). A duplication in both CNR1 and CNR2 was observed in one individual. Given the differences between the CNRs, their copy number variability was determined separately.

TABLE 1 | Demographic and clinical characteristics of perinatal HIV-1 acquisition groups.

Variables	HIV-1-exposed uninfected	Total HIV-1 infected		*In utero* infected		*In utero*-enriched infected		Mixed infected		Intrapartum infected	
	n = 349	n = 176	*P* value	n = 19	*P* value	n = 46	*P* value	n = 99	*P* value	n = 31	*P* value
Sex	(n = 346)	(n = 176)	1.000		0.487		0.875		0.569		0. 260
Male	160 (46)	80 (45)		7 (37)		20 (43)		42 (42)		18 (58)	
Female	189 (54)	96 (55)		12 (63)		26 (57)		57 (58)		13 (42)	
Gestation	(n = 327)	(n = 164)	0.355	(n = 18)	0.105	(n = 44)	0.788	(n = 95)	1.000	(n = 25)	**0.013**
Term	295 (90)	143 (87)		14 (78)		39 (89)		86 (91)		18 (72)	(P_{Bonf} =
Preterm (<37 weeks)	32 (10)	21 (13)		4 (22)		5 (11)		9 (9)		7 (28)	0.208)
Birth weight (g)	(n = 344)	(n = 168)	**0.001**		0.251		**0.003**	(n = 92)	**0.001**	(n = 30)	0.898
≥2500	307 (89)	131 (78)	**(P_{Bonf} =**	15 (79)		34 (74)	**(P_{Bonf} =**	70 (76)	**(P_{Bonf} =**	27 (90)	
<2500	37 (11)	37 (22)	**0.016)**	4 (21)		12 (26)	**0.048)**	22 (24)	**0.016)**	3 (10)	
Breastfed	(n = 346)	(n = 170)	1.000	(n = 18)	0.384	(n = 45)	0.117	(n = 95)	0.780	(n = 30)	0.359
No	271 (78)	134 (79)		16 (89)		40 (89)		73 (77)		21 (70)	
Yes	75 (22)	36 (21)		2 (11)		5 (11)		22 (23)		9 (30)	

Data are n (%) unless otherwise specified.

The P values refer to comparisons between the HIV-1-exposed uninfected (control) group and each of the HIV-1 infected (case) groups.

Bold indicates statistical significance of P < 0.05; P_{Bonf}, Bonferroni corrected P value.

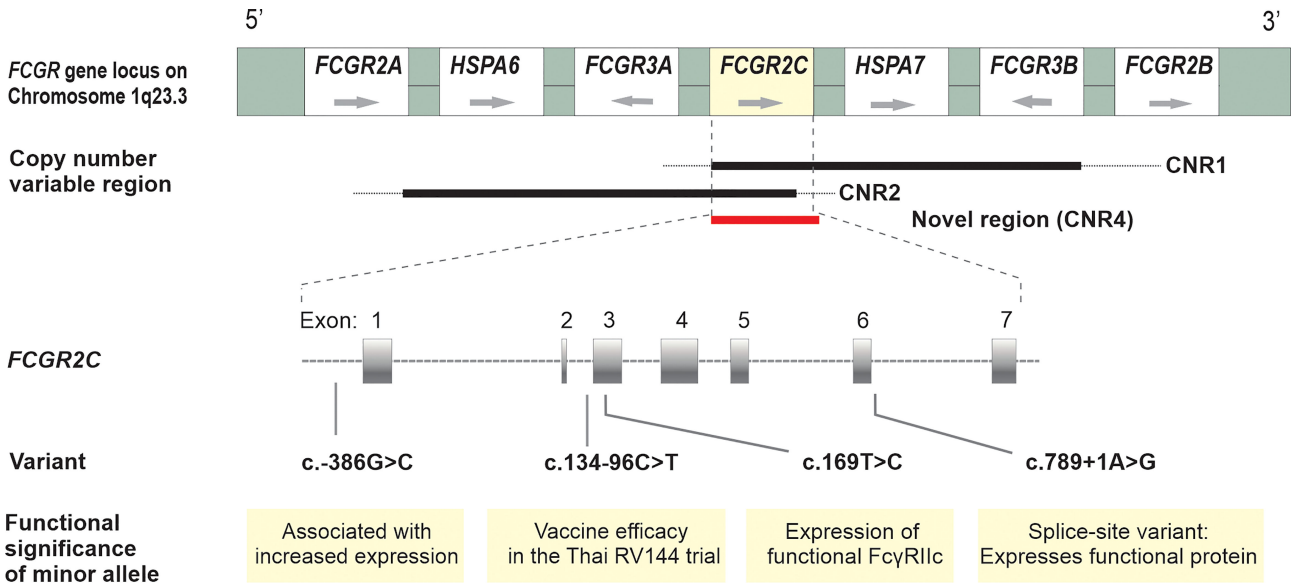

FIGURE 1 | Schematic diagram of the *FCGR* gene locus on chromosome 1q23 with their orientation; CNV of *FCGR2C* within distinct copy number variable regions – previously designated CNR1, CNR2 (8,9) and a novel region (CNR4) where only *FCGR2C* duplicated/deleted, as described among South African black population (12); Functional and clinically significant *FCGR2C* variants and their positions on the gene.

Within CNR1, CNV was significantly different between the HIV-1 infected and HIV-1 exposed-uninfected groups (P = 0.009, P_{Bonf} > 0.05). This difference was primarily determined by gene deletions. There were a higher number of HIV-1 exposed-uninfected children with a single gene copy compared to HIV-1 infected children (36% *vs.* 14%) (**Table 2**). Using two *FCGR2C* gene copies as reference, the possession of a single gene copy was independently associated with reduced odds of HIV-1 acquisition (OR = 0.29; 95% CI 0.12-0.71; P = 0.007, P_{Bonf} > 0.05) and retained significance after controlling for birthweight and *FCGR2C* genotypes (AOR = 0.37; 95% CI 0.15-0.90; P = 0.029, P_{Bonf} > 0.05) (**Table 3**). The CNR2 and the novel CNR4 variability were excluded from further association analysis due to low frequencies (< 5%).

FCGR2C Variants That Determine the Expression of Surface FcγRIIc

We further genotyped functional *FCGR2C* variants that determine the expression of FcγRIIc (c.−386G>C, c.169T>C and c.798+1A>G) and the c.134-96C>T variant that associated with risk of HIV-1 acquisition in the Thai RV144 HIV-1 vaccine trial (**Figure 1**). To assess the role of the *FCGR2C* genotypes and allele distribution in perinatal HIV-1 acquisition, children with a single *FCGR2C* gene copy were considered homozygous; those with more than one *FCGR2C* gene copy were considered homozygous if all the alleles were the same or heterozygous if both alleles were present. With MLPA, we obtained genotypic data from 166 out of the 176 HIV-1 infected for c.169T>C and c.−386G>C variants.

A SNP in exon 3 (c.169T>C) that results in an open reading frame (ORF) or a stop codon determines the expression of FcγRIIc when present with the minor allele of two splice variants in intron 7 (c.798+1A>G and c.799-1G>C). While 129/515 (25%) of individuals carried at least one *FCGR2C*-ORF (c.169C allele), only 4/129 (3%) individuals possessed the c.798 +1G minor allele that represents the classic *FCGR2C*-ORF and predicts FcγRIIc expression (6, 32). Of the four individuals with the c.798+1G minor allele, three were HIV-1-exposed uninfected and one HIV-1 infected. Conversely, the c.169C allele co-occurred with the c.798+1A allele in 97% (n = 125) of the participants, representing the non-classic *FCGR2C*-ORF that does not yield surface expression of FcγRIIc. The c.799-1G>C splice cite variant was not genotyped, since it has been shown that the c.169C and c.798+1A alleles are syntenic with the c.799-1G allele in South African population (12).

While the c.169T>C variant alone does not result in surface expression of FcγRIIc, it may have other unknown functional consequences and was therefore investigated for a possible association with HIV-1 perinatal transmission. The c.169T>C genotype distribution was significantly different between HIV-1 infected and HIV-1 exposed-uninfected children (P = 0.002, P_{Bonf} = 0.032) (**Figure 2**i). In a dominant model, the c.169C was overrepresented in the HIV-1 infected compared to the uninfected children (32% *vs.* 22%) and significantly associated with increased odds of HIV acquisition (OR = 1.68; 95% CI 1.11-2.55; P = 0.013, P_{Bonf} > 0.05). The strength of association increased after adjusting for birthweight and CNR1 copy number (AOR = 2.39; 95% CI 1.45-3.95; P = 0.001, P_{Bonf} = 0.016). For the *FCGR2B/C* promoter variant at position −386G>C, which modulates gene expression levels, no significant difference in genotype frequency was observed between the HIV-1 infected and HIV-1 uninfected cohort

TABLE 2 | *FCGR2C* copy number distribution in HIV-1-exposed infected and uninfected infants.

Variables	Total study cohort	HIV-1-exposed uninfected	TotalHIV-1 infected		*In utero* infected		*In utero*-enriched infected		Mixed infected		Intrapartum infected	
	n = 525	n = 349	n = 176	*P* value	n = 19	*P* value	n = 46	*P* value	n = 99	*P* value	n = 31	*P* value
FcγRIIc copy number				**0.010** (P_{Bonf} = 0.16)		0.672		0.142		0.095		**0.028** (P_{Bonf} = 0.448)
1 copy	52 (10)	44 (12)	8 (4)		1 (5.3)		3 (6)		5 (5)		0 (0)	
2 copies	359 (68)	233 (67)	126 (72)		13 (68.4)		28 (61)		71 (72)		27 (87)	
≥3 copies	114 (22)	72 (21)	42 (24)		5 (26.3)		15 (33)		23 (23)		4 (13)	
CNR1	(n = 147)	(n = 105)	(n = 42)	**0.009** (P_{Bonf} = 0.144)	(n = 5)	0.162	(n = 15)	**0.035** (P_{Bonf} = 0.56)	(n = 23)	0.228	(n = 4)	0.296
deletion	44 (30)	38 (36)	6 (14)		0 (0)		1 (7)		5 (22)		0 (0)	
duplication	103 (70)	67 (64)	36 (86)		5 (100)		14 (93)		18 (78)		4 (100)	
CNR2	(n = 14)	(n = 8)	(n = 6)	0.767	(n = 1)	0.444	(n = 2)	0.444	(n = 4)	0.180	(n = 0)	
deletion	5 (36)	3 (37.5)	2 (33)		1(100)		2 (100)		0		0	
duplication	9 (64)	5 (62.5)	4 (67)		0 (0)		0		4 (100)		0	
CNR4	(n = 6)	(n = 3)	(n = 3)	0.100	(n = 0)		(n = 1)	0.250	(n = 2)	0.100	(n = 0)	
deletion	3 (50)	3 (100)	0		0		0		0)		0	
duplication	3 (50)	0	3 (100)		0		1 (100)		2(100)		0	

Data are n (%) unless otherwise specified.
The P values refer to comparisons between the HIV-1-exposed uninfected (control) group and each of the HIV-1 infected (case) groups.
Bold indicates statistical significance of P < 0.05; P_{Bonf}, Bonferroni corrected P value.

($P = 0.288$) (**Figure 2**ii). The homozygous −386 CC genotype was not observed in any individual. Due to the low frequency of the splice site variant c.798+1A>G minor allele, an association analysis was not conducted.

The Thai *FCGR2C* Haplotype Tag Variant c.134-96C>T Associates With Increased Odds of Perinatal HIV-1 Transmission

The *FCGR2C* c.134-96C>T genotype distribution was significantly different between the children who acquired HIV-1 and those who did not ($P = 0.002$, $P_{Bonf} = 0.032$) (**Figure 2**iii). In particular, the c.134-96T-allele was overrepresented in the HIV-1-infected children compared to the exposed-uninfected children (58% *vs.* 42%; $P = 0.001$, $P_{Bonf} = 0.016$). The overrepresentation was primarily driven by the *in utero*-enriched (63% *vs.* 42%; $P = 0.011$, $P_{Bonf} > 0.05$) and mixed (59% *vs.* 42%; $P = 0.004$, $P_{Bonf} > 0.05$) infected groups (**Figure 2**iii). We combined the *in utero*-enriched and mixed transmission groups into a larger *in utero*-enriched group, excluding the 27 HIV-1 infected and 75 HIV-1 exposed uninfected breastfed individuals, and still observed overrepresentation of the minor allele in the HIV-1 infected children (60% *vs.* 43%; $P = 0.002$, $P_{Bonf} = 0.048$) (data not shown).

The association between *FCGR2C* c.134-96C>T variant and HIV acquisition was assessed in a univariate model and a multivariate model that controlled for birthweight and CNR1 copy number, which were statistically significant at univariate analysis (**Table 4**). In a dominant model, the c.134-96C>T minor allele was associated with increased odds of perinatal HIV-1 transmission at univariate (OR = 1.89; 95% CI 1.31-2.73; $P = 0.001$, $P_{Bonf} = 0.016$) and multivariate analysis (AOR = 1.89; 95% CI 1.25-2.87; $P = 0.003$, $P_{Bonf} = 0.048$). The association was specific to the *in utero*-enriched (OR = 2.34; 95% CI 1.24-4.42; $P = 0.009$, $P_{Bonf} > 0.05$) and the mixed transmission groups (OR = 1.94; 95% CI 1.24-3.06; $P = 0.004$, $P_{Bonf} > 0.05$) but not the *in utero* (OR = 1.24; 95% CI 0.49-3.12; $P = 0.653$) and intrapartum groups (OR = 1.29; 95% CI 0.62-2.69; $P = 0.500$). Statistical significance was retained in both *in utero*-enriched (AOR = 2.49; 95% CI 1.31-4.76; $P = 0.006$, $P_{Bonf} > 0.05$) and mixed transmission groups (AOR = 2.06; 95% CI 1.28-3.30; $P = 0.003$, $P_{Bonf} = 0.048$) after adjusting for birthweight.

TABLE 3 | Effect of *FCGR2C* CNR1 copy number distribution on perinatal HIV-1 acquisition, adjusting for birthweight and *FCGR2C* genotypes.

FcγRIIc copy number (Total group)	Univariate		Multivariate	
	OR (95% CI)	P-value	Adjusted OR	P-value
1 copy	0.29 (0.12-0.71)	**0.007** (P_{Bonf} = 0.112)	0.37 (0.15-0.90)	**0.029** (P_{Bonf} = 0.464)
2 copies	Ref		Ref	
≥3 copies	0.99 (0.63-1.57)	0.978	0.74 (0.43-1.27)	0.275

OR, Odds Ratio; CI, Confidence Interval; P_{Bonf}, Bonferroni corrected P value.
Bold indicates statistical significance of P < 0.05.

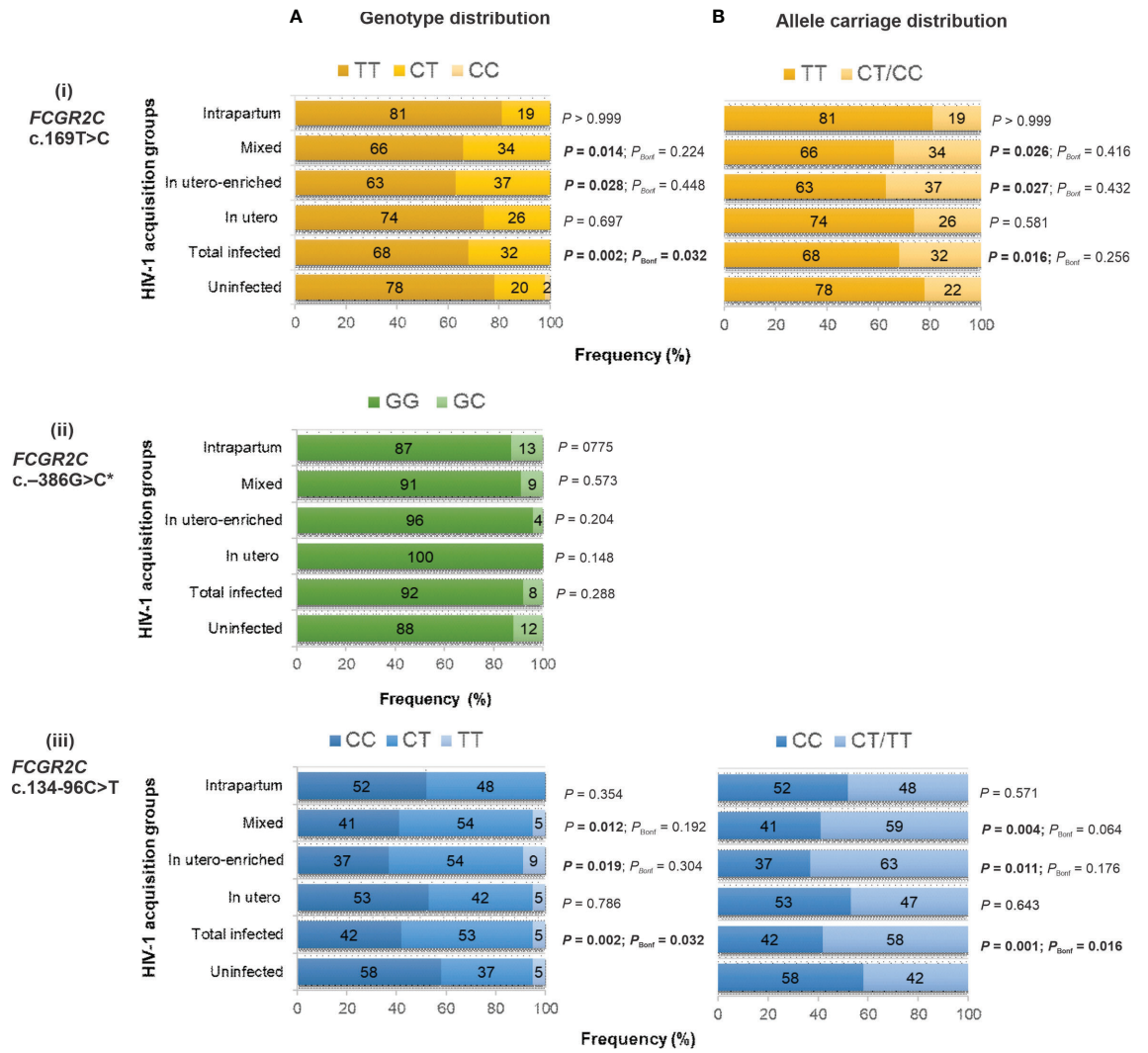

FIGURE 2 | Genotype **(A)** and allele carriage **(B)** distribution of functional *FCGR2C* variants and their association with perinatal HIV-1 acquisition in black South Africans [HIV-1-exposed uninfected (n = 349), total infected (n = 176 for c.134-96C>T; n = 166 for c.169T>C and c.–386G>C), *in utero* infected (n = 19), *in utero*-enriched infected (n = 46), mixed infected (n = 99 for c.134-96C>T; n = 89 for c.169T>C and c.–386G>C) and intrapartum infected (n = 31)]. * No individual with homozygous –386 CC genotype.

The *FCGR2C* c.134-96C>T and c.169T>C Are in High Linkage Disequilibrium

The observed genotype frequencies for *FCGR2C* c.–386G>C, c.134-96C>T, c.169T>C were in Hardy-Weinberg equilibrium ($P > 0.05$). We also observed that 71% (39/55) of children carrying a c.169C were heterozygous for the *FCGR2B/C* promoter variant (data not shown). We analyzed linkage disequilibrium between the *FCGR2C* variants and CNRs, with and without considering the CNV. It was important to determine whether the observed variants associated with HIV-1 acquisition act independently or linkage disequilibrium plays a part. Our result demonstrated high linkage disequilibrium between c.134-96C>T and c.169T>C both without considering CNV ($D' = 0.867$; $r^2 = 0.319$) and when only those with two gene copies were included ($D' = 0.908$ and $r^2 = 0.213$) (**Figure 3**). Both c.134-96C>T and c.169T>C independently associated with increased odds of HIV-1 acquisition, but in multivariate analysis, c.134-96C>T retained significance (AOR = 1.91; 95% CI 1.23-2.96; $P = 0.004$, $P_{Bonf} > 0.05$) while c.169T>C did not (AOR = 1.14; 95% CI 0.70-1.86; $P = 0.590$).

Effect of *FCGR2C* c.134-96C>T and Maternal Viral Load on Perinatal Acquisition of HIV-1

Maternal viral load is a key determinant of MTCT of HIV-1 infection. For the NEVEREST cohorts, the maternal viral load was not recorded. However, in the birth cohort with the defined modes of transmission, information on maternal HIV-1 viral

TABLE 4 | Univariate and multivariate analysis of the effect of *FCGR2C* c.134-96C>T on perinatal acquisition of HIV-1.

Genotype	Univariate		Multivariate	
	OR (95% CI)	*P* value	Adjusted OR (95% CI)	*P* value
*Total infected**				
CC	Ref		Ref	
CT/TT	1.89 (1.31-2.73)	**0.001 (P_{Bonf} = 0.016)**	1.89 (1.25-2.87)	**0.003 (P_{Bonf} = 0.048)**
In utero-enriched#				
CC	Ref		Ref	
CT/TT	2.34 (1.24-4.42)	**0.009** (P_{Bonf} = 0.144)	2.49 (1.31-4.76)	**0.006** (P_{Bonf} = 0.064)
Mixed#				
CC	Ref		Ref	
CT/TT	1.94 (1.24-3.06)	**0.004** (P_{Bonf} = 0.064)	2.06 (1.28-3.30)	**0.003 (P_{Bonf} = 0.048)**
In utero				
CC	Ref			
CT/TT	1.24 (0.49-3.12)	0.653		
Intrapartum				
CC	Ref			
CT/TT	1.29 (0.62-2.69)	0.500		

OR, Odds Ratio; CI, Confidence Interval; P_{Bonf}, Bonferroni corrected P value.
Bold indicates statistical significance of P < 0.05.
**adjusted for birthweight and CNR1 copy number.*
#adjusted for birthweight.

load was available for 279 mothers of whom 70 transmitted HIV to their infants and 209 did not. The mean HIV-1 viral load was significantly higher in transmitting mothers than non-transmitting mothers (4.53 vs. 3.95 $\log_{10}$ copies/ml; $P < 0.0001$). The maternal *FCGR2C* c.134-96C>T variant independently associated with HIV-1 transmission (OR = 1.98; 95% CI 1.16-3.37; $P = 0.012$, $P_{Bonf} = 0.192$) and when controlled for maternal viral load and birthweight (AOR = 2.03; 95% CI 1.14-3.62; $P = 0.016$, $P_{Bonf} = 0.256$). In this small subset, the infant *FCGR2C* c.134-96C>T variant was independently

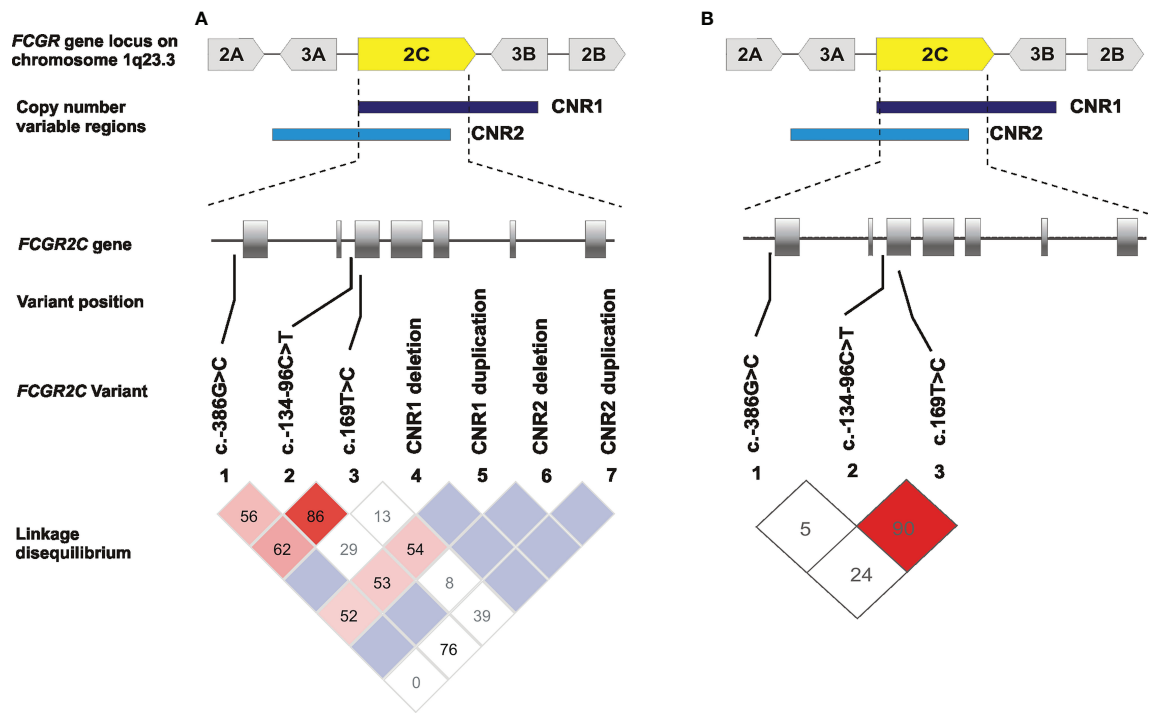

FIGURE 3 | Linkage disequilibrium of the single nucleotide polymorphisms (SNPs) and copy number regions (CNRs) in *FCGR2C* gene in South African children born to women living with HIV-1. **(A)** LD plots for SNPs without considering CNV and **(B)** when only those with two gene copies were included. Values reflect D′ measures of LD and color in the squares given by standard D′/LOD (log of the odds of there being LD between two loci) color scheme, with bright red color used to display very strong LD.

associated with HIV-1 acquisition (OR = 1.92; 95% CI 1.14-3.23; P = 0.014, P_{Bonf} = 0.224). The significant association remained when adjusted for maternal viral load (AOR = 2.10; 95% CI 1.13-3.87; P = 0.018, P_{Bonf} = 0.288), specifically in the *in utero*-enriched transmission group (AOR = 2.67; 95% CI 1.33-5.37; P = 0.006, P_{Bonf} = 0.064) (**Table 5**).

Mother-Child *FCGR2C* c.134-96C>T Genetic Similarity and HIV-1 Acquisition

We next evaluated mother-child *FCGR2C* c.134-96C>T genotype concordance and association with HIV-1 acquisition. Concordance was defined as mother and infant each bearing at least one T allele (mother-child: CT/TT-CT/TT) or both were homozygous for the C allele (CC). Discordance was defined as one individual within the dyad possessing a CC genotype and the other bearing a T allele (CT/TT). Possession of a T allele in both mother and infant was overrepresented in the HIV-1-infected children compared to the exposed-uninfected children (45% *vs.* 28%; P = 0.012, P_{Bonf} = 0.192). Independently, MTCT was more likely among the mother-child concordant CT/TT group compared to the concordant CC group (OR = 2.58; 95% CI 1.36-4.88; P = 0.004, P_{Bonf} = 0.064) and retained significance after adjusting for maternal viral load, birthweight and infant CNR1 copy number (AOR = 2.87; 95% CI 1.36-6.06; P = 0.006, P_{Bonf} = 0.096) (**Table 6**).

DISCUSSION

Previous studies have reported both functional and clinical relevance of *FCGR2C* genetic variability, including single nucleotide polymorphisms and copy number variations. Expression of the membrane-bound FcγRIIc protein in individuals bearing the *FCG2C* c.169T>C minor allele (*FCGR2C*-ORF) has been associated with susceptibility to idiopathic thrombocytopenic purpura (15), Kawasaki disease (32), systemic lupus erythematosus and increased antibody responses to vaccinations (11). Furthermore, the *FCGR2C* c.134-96C>T tag variant associated with reduced risk of HIV-1 infection in the Thai phase 3 RV144 HIV-1 vaccine trial (13) and increased risk of HIV-1 disease progression in black South Africans (18). In addition, increased risk of HIV-1 acquisition in the HVTN 505 vaccine trial was associated with two variants within the Thai *FCGR2C* haplotype but not the c.134-96C>T tag variant (17).

In this study, we report further associations between *FCGR2C* variants and perinatal HIV-1 acquisition in South African children. Deletion of CNRI was significantly protective of perinatal HIV-1 acquisition compared to two gene copies, but the significance was not retained after Bonferroni correction. However, the observed association between CNR1 and perinatal HIV-1 acquisition might not be due to *FCGR2C* copy number variability because *FCGR3B* and *HSPA7* genes are also deleted with CNR1. The associations appear to be unrelated to surface expression of membrane-bound FcγRIIc. While some children carried the c.169C open reading frame allele, the co-occurrence of the splice-site variant c.798+1A allele predicted the absence of FcγRIIc expression in the majority of children. The latter allele gives rise to alternative mRNA splicing and a premature stop codon with associated loss of surface expression (6, 32). Only four children carried both the c.169C open reading frame allele and the splice-site variant c.798+1G allele required for functional expression of FcγRIIc. This finding correlates with previous studies that suggested rare to absent expression of FcγRIIc in the black African population (12, 32) and raises questions around the functional relevance of the c.169T>C variant.

The *FCGR2C* c.134-96T-minor allele was associated with increased odds of perinatally acquired HIV-1 acquisition in South African children. Specifically, a significant association was observed in the *in utero*-enriched and mixed transmission groups but not in the *in utero* and intrapartum transmission groups. The *in utero*-enriched and mixed transmission groups are very similar in terms of drug treatment, as all were exposed to nevirapine for prevention of MTCT. Due to the nevirapine, fewer infants in the mixed group would have had intrapartum transmission and therefore were likely *in-utero* enriched. After adjusting for multiple comparisons using Bonferroni correction, the overall c.134-96C>T association retained significance, primarily driven by the mixed transmission group. The non-significance in the *in utero*-enriched group may potentially be due to small sample size. We postulate that the role of c.134-96C>T in HIV-1 acquisition is more pronounced during the course of pregnancy and at the maternal-fetal interface (3). In a subset of our study cohort, the observed association with

TABLE 5 | Effect of *FCGR2C* c.134-96C>T on perinatal acquisition of HIV-1 in study cohort with information on maternal viral load.

Genotype	Univariate		Multivariate	
	OR (95% CI)	*P* value	Adjusted OR (95% CI)	*P* value
*Total infected**				
CC	Ref		Ref	
CT/TT	1.92 (1.14-3.23)	**0.014** (P_{Bonf} = 0.224)	2.10 (1.13-3.87)	**0.018** (P_{Bonf} = 0.288)
In utero-enriched#				
CC	Ref		Ref	
CT/TT	2.34 (1.24-4.42)	**0.009** (P_{Bonf} = 0.144)	2.67 (1.33-5.37)	**0.006** (P_{Bonf} = 0.064)

OR, Odds Ratio; CI, Confidence Interval; P_{Bonf}, Bonferroni corrected P value.
Bold indicates statistical significance of P < 0.05.
**adjusted for maternal viral load, birthweight and CNR1 copy number.*
#adjusted for maternal viral load and birthweight.

TABLE 6 | Mother-child *FCGR2C* c.134-96C>T genetic similarity and HIV-1 acquisition[a].

Genotype (mother-child pair)	HIV-1-exposed uninfected n = 222	HIV-1 infected n = 76	Univariate		Multivariate*	
			OR (95% CI)	*P* value	OR (95% CI)	*P* value
Concordant CC	94 (42)	20 (26)	Ref		Ref	
Concordant CT/TT	62 (28)	34 (45)	2.58 (1.36-4.88)	**0.004** (P_{Bonf} = 0.064)	2.87 (1.36-6.06)	**0.006** (P_{Bonf} = 0.096)
Discordant	66 (30)	22 (29)	1.57 (0.79-3.10)	0.197	1.50 (0.68-3.29)	0.308

OR, Odds Ratio; CI, Confidence Interval; P_{Bonf}, Bonferroni corrected P value.

Bold indicates statistical significance of P < 0.05.

**adjusted for maternal viral load, birthweight and CNR1 copy number.*

[a]*"Concordant" denotes mother-child pairs with same FCGR2C c.134-96C>T genotype. "Discordant" denotes mother-child pairs with different genotypes.*

FCGR2C c.134-96C>T variant remained when adjusted for maternal viral load, a key determinant of MTCT of HIV-1 infection. In both mother and child, the *FCGR2C* c.134-96C>T variant was associated with HIV-1 transmission and acquisition, respectively. Concordance in mother-child possession of the c.134-96T-allele further associated with a greater risk of MTCT compared to homozygosity for the C-allele in both mother and infant.

Assessing the role of the *FCGR2C* c.134-96C>T tag variant in both HIV-1 acquisition and disease progression has produced contrasting results of both protective and deleterious effects. The Thai phase 3 RV144 HIV vaccine trial provided the first clinical evidence of vaccine-induced protection, where the *FCGR2C* c.134-96C>T tag variant reduced the risk of HIV acquisition (13). Subsequently, two variants within the Thai *FCGR2C* haplotype were associated with increased risk of HIV-1 acquisition in vaccine recipients in the HVTN 505 trial but the c.134-96C>T tag variant was not. The population in this trial was predominantly Caucasian men who have sex with men (17). The *FCGR2C* c.134-96C>T tag variant was also associated with HIV-1 disease progression in South African adults (18). In this mother-child transmission model study, we establish its role in increased predisposition to HIV-1 acquisition. Whether the contrasting associations bear any functional significance is currently not clear and the modulating risk factors may not necessarily overlap (18). The differing results may be attributable to a variety of factors, including genetic differences between populations. It has been shown that two of the three variants within the Thai *FCGR2C* haplotype are absent in the African population, including black South Africans (12).

These findings may be of consequence to efforts aimed at elucidating the different outcomes of the two very similar HIV-1 vaccine efficacy trials, RV144 in Thailand and HVTN702 in South Africa. In addition to population genetic differences, the vaccine regimen evaluated in the RV144 and HVTN702 vaccine efficacy trials were also different. The RV144 vaccine candidate was specific for HIV-1 clades B and E with alum as adjuvant. This vaccine candidate elicited robust cross-clade immune responses in South Africans (33). However, in subsequent clinical trials the RV144 vaccine regimen was modified to increase immunogenicity and improve the duration of vaccine-induced immune responses (34). The vaccine regimen was HIV-1 clade C-specific, the predominant clade in South Africa, and was adjuvanted with MF59 (34, 35). The adapted ALVAC-HIV and Bivalent Subtype C gp120–MF59 vaccine regimen evaluated in HVTN 702 trial showed no efficacy among South African adults, despite previous evidence of immunogenicity (19). The differential vaccine efficacy between the RV144 and HVTN 702 trials might be due to differences in some components of the vaccine regimen and host genetics. In vaccine design, it is important to consider host genetic variation that can modulate vaccine efficacy (36). We previously established that black South Africans do not possess the complete Thai *FCGR2C* haplotype and are only polymorphic for c.134-96C>T (rs114945036) (12).

The functional mechanisms underlying the association of the variants within the Thai *FCGR2C* haplotype with HIV-1 acquisition, disease progression and vaccine efficacy is largely undefined. It raises many biological questions as to how expression of the membrane-bound FcγRIIc protein or the variants could modulate HIV-1 infection. The proposed impact of the *FCGR2C* variant haplotypes on immunity against HIV is unknown, one can only speculate. It is increasingly evident that it does not involve expression of the surface FcγRIIc receptor, since a limited number of individuals in the available genetic association studies bear the minor alleles that predict expression of the surface molecule. It is unknown whether a truncated soluble form of the FcγRIIc protein is produced in individuals with the premature stop codon or alternative splicing variants that prevent surface expression of FcγRIIc. Results from a study suggest that variants within the Thai *FCGR2C* haplotype either directly associate with the expression of *FCGR2C* in human B cells or in correlation with other causal variants that affect expression levels (36). The correlation with *FCGR2A* was observed across different populations and was specific to the c.134-96C>T variant (36, 37). We have proposed that the variants modulate transcription factor binding that may alter mRNA expression (18). This may in turn affect processes regulated by mRNA from the *FCGR2C* gene.

In conclusion, the *FCGR2C* variant c.134-96T-allele, which was associated with protection in the Thai RV144 trial, was associated with increased odds of perinatal HIV-1 acquisition in black South African children. This adds to other deleterious associations found for *FCGR2C* variants in the context of HIV-1 (17, 18) and warrants investigation of these variants in South African adults actively immunized in the HVTN 702 trial (19) and individuals passively immunized with the broadly neutralizing VRC01 antibody in the Antibody Mediated Prevention (AMP) trials (38). Collectively, these intriguing results highlight the need for further mechanistic studies to

establish the functional relevance of *FCGR2C* variation in different populations and more broadly in contexts of vaccination and disease.

DATA AVAILABILITY STATEMENT

The raw data supporting the conclusions of this article will be made available by the authors, without undue reservation.

ETHICS STATEMENT

Ethics approval for the study was obtained from the University of the Witwatersrand Human Research Ethics Committee (Reference numbers: M170585; M180575). Written informed consent to participate in this study was provided by the participants' legal guardian/next of kin.

AUTHOR CONTRIBUTIONS

RS, GG, and LK recruited study participants and acquired clinical data. MG extracted DNA from blood samples. JE and MP genotyped individuals. JE managed and analyzed the data. JE and RL wrote the first draft of the manuscript. CT and RL designed the study and supervised the research. All co-authors critically revised the manuscript for intellectual content. All authors contributed to the article and approved the submitted version.

FUNDING

This study is supported in part by grants from the National Institutes of Child Health and Human Development (HD 42402, HD 47177, HD 57784, HD 073977 and HD 073952), Secure the Future Foundation, the South African Medical Research Council, and the South African Research Chairs Initiative of the Department of Science and Innovation and National Research Foundation (84177).

ACKNOWLEDGMENTS

The authors wish to acknowledge Johanna Ledwaba, Brent Oosthuysen and Monalisa Kalimashe for their kind assistance with the genetic analyser. Thanks also to all clinical staff and laboratory staff who contributed towards recruitment of the study subjects and sample processing and storage, respectively.

SUPPLEMENTARY MATERIAL

The Supplementary Material for this article can be found online at: https://www.frontiersin.org/articles/10.3389/fimmu.2021.760571/full#supplementary-material

REFERENCES

1. Li X, Ptacek TS, Brown EE, Edberg JC. Fcγ Receptors: Structure, Function and Role as Genetic Risk Factors in SLE. *Genes Immun* (2009) 10(5):380–9. doi: 10.1038/gene.2009.35
2. Nimmerjahn F, Ravetch JV. Fcgamma Receptors as Regulators of Immune Responses. *Nat Rev Immunol* (2008) 8(1):34–47. doi: 10.1038/nri2206
3. Lassaunière R, Musekiwa A, Gray GE, Kuhn L, Tiemessen CT. Perinatal HIV-1 Transmission: Fc Gamma Receptor Variability Associates With Maternal Infectiousness and Infant Susceptibility. *Retrovirology* (2016) 13(1):40. doi: 10.1186/s12977-016-0272-y
4. Boesch AW, Brown E, Ackerman ME. The Role of Fc Receptors in HIV Prevention and Therapy. *Immunol Rev* (2015) 268(1):296–310. doi: 10.1111/imr.12339
5. Breunis WB, van Mirre E, Geissler J, Laddach N, Wolbink G, van der Schoot E, et al. Copy Number Variation at the FCGR Locus Includes FCGR3A, FCGR2C and FCGR3B But Not FCGR2A and FCGR2B. *Hum Mutat* (2009) 30(5):E640–650. doi: 10.1002/humu.20997
6. van der Heijden J, Breunis WB, Geissler J, de Boer M, van den Berg TK, Kuijpers TW. Phenotypic Variation in IgG Receptors by Nonclassical FCGR2C Alleles. *J Immunol Baltim Md* (2012) 188(3):1318–24 doi: 10.4049/jimmunol.1003945.
7. Stranger BE, Forrest MS, Dunning M, Ingle CE, Beazley C, Thorne N, et al. Relative Impact of Nucleotide and Copy Number Variation on Gene Expression Phenotypes. *Science* (2007) 315(5813):848–53. doi: 10.1126/science.1136678
8. Niederer HA, Willcocks LC, Rayner TF, Yang W, Lau YL, Williams TN, et al. Copy Number, Linkage Disequilibrium and Disease Association in the FCGR Locus. *Hum Mol Genet* (2010) 19(16):3282–94. doi: 10.1093/hmg/ddq216
9. Nagelkerke SQ, Tacke CE, Breunis WB, Geissler J, Sins JWR, Appelhof B, et al. Nonallelic Homologous Recombination of the FCGR2/3 Locus Results in Copy Number Variation and Novel Chimeric FCGR2 Genes With Aberrant Functional Expression. *Genes Immun* (2015) 16(6):422–9. doi: 10.1038/gene.2015.25
10. Warmerdam PA, Nabben NM, van de Graaf SA, van de Winkel JG, Capel PJ. The Human Low Affinity Immunoglobulin G Fc Receptor IIC Gene is a Result of an Unequal Crossover Event. *J Biol Chem* (1993) 268(10):7346–9. doi: 10.1016/S0021-9258(18)53181-1
11. Li X, Wu J, Ptacek T, Redden DT, Brown EE, Alarcón GS, et al. Allelic-Dependent Expression of an Activating Fc Receptor on B Cells Enhances Humoral Immune Responses. *Sci Transl Med* (2013) 5(216):216ra175. doi: 10.1126/scitranslmed.3007097
12. Lassaunière R, Tiemessen CT. Variability at the FCGR Locus: Characterization in Black South Africans and Evidence for Ethnic Variation in and Out of Africa. *Genes Immun* (2016) 17(2):93–104. doi: 10.1038/gene.2015.60
13. Li SS, Gilbert PB, Tomaras GD, Kijak G, Ferrari G, Thomas R, et al. FCGR2C Polymorphisms Associate With HIV-1 Vaccine Protection in RV144 Trial. *J Clin Invest* (2014) 124(9):3879–90. doi: 10.1172/JCI75539
14. Stewart-Akers AM, Cunningham A, Wasko MC, Morel PA. Fc Gamma R Expression on NK Cells Influences Disease Severity in Rheumatoid Arthritis. *Genes Immun* (2004) 5(7):521–9. doi: 10.1038/sj.gene.6364121
15. Breunis WB, van Mirre E, Bruin M, Geissler J, de Boer M, Peters M, et al. Copy Number Variation of the Activating FCGR2C Gene Predisposes to Idiopathic Thrombocytopenic Purpura. *Blood* (2008) 111(3):1029–38. doi: 10.1182/blood-2007-03-079913
16. Machado LR, Bowdrey J, Ngaimisi E, Habtewold A, Minzi O, Makonnen E, et al. Copy Number Variation of Fc Gamma Receptor Genes in HIV-Infected

and HIV-Tuberculosis Co-Infected Individuals in Sub-Saharan Africa. *PloS One* (2013) 8(11):e78165. doi: 10.1371/journal.pone.0078165
17. Li SS, Gilbert PB, Carpp LN, Pyo C-W, Janes H, Fong Y, et al. Fc Gamma Receptor Polymorphisms Modulated the Vaccine Effect on HIV-1 Risk in the HVTN 505 HIV Vaccine Trial. *J Virol* (2019) 93(21):e02041–18. doi: 10.1128/JVI.02041-18
18. Lassaunière R, Paximadis M, Ebrahim O, Chaisson RE, Martinson NA, Tiemessen CT. The FCGR2C Allele That Modulated the Risk of HIV-1 Infection in the Thai RV144 Vaccine Trial is Implicated in HIV-1 Disease Progression. *Genes Immun* (2019) 20(8):651–9. doi: 10.1038/s41435-018-0053-9
19. Gray GE, Bekker L-G, Laher F, Malahleha M, Allen M, Moodie Z, et al. Vaccine Efficacy of ALVAC-HIV and Bivalent Subtype C Gp120-MF59 in Adults. *N Engl J Med* (2021) 384(12):1089–100. doi: 10.1056/NEJMoa2031499
20. Aldrovandi GM, Kuhn L. What Babies and Breasts can Teach Us About Natural Protection From HIV Infection. *J Infect Dis* (2010) 202(S3):S366–70. doi: 10.1086/655972
21. Braibant M, Barin F. The Role of Neutralizing Antibodies in Prevention of HIV-1 Infection: What can We Learn From the Mother-to-Child Transmission Context? *Retrovirology* (2013) 10:103. doi: 10.1186/1742-4690-10-103
22. Tiemessen CT, Kuhn L. Immune Pathogenesis of Pediatric HIV-1 Infection. *Curr HIV/AIDS Rep* (2006) 3(1):13–9. doi: 10.1007/s11904-006-0003-4
23. Trist HM, Tan PS, Wines BD, Ramsland PA, Orlowski E, Stubbs J, et al. Polymorphisms and Interspecies Differences of the Activating and Inhibitory Fcγrii of Macaca Nemestrina Influence the Binding of Human IgG Subclasses. *J Immunol* (2014) 192(2):792–803. doi: 10.4049/jimmunol.1301554
24. Reitz C, Coovadia A, Ko S, Meyers T, Strehlau R, Sherman G, et al. Initial Response to Protease-Inhibitor-Based Antiretroviral Therapy Among Children Less Than 2 Years of Age in South Africa: Effect of Cotreatment for Tuberculosis. *J Infect Dis* (2010) 201(8):1121–31. doi: 10.1086/651454
25. Coovadia A, Abrams EJ, Stehlau R, Meyers T, Martens L, Sherman G, et al. Reuse of Nevirapine in Exposed HIV-Infected Children After Protease Inhibitor-Based Viral Suppression: A Randomized Controlled Trial. *JAMA* (2010) 304(10):1082–90. doi: 10.1001/jama.2010.1278
26. Coovadia A, Abrams EJ, Strehlau R, Shiau S, Pinillos F, Martens L, et al. Efavirenz-Based Antiretroviral Therapy Among Nevirapine-Exposed HIV-Infected Children in South Africa: A Randomized Clinical Trial. *JAMA* (2015) 314(17):1808–17. doi: 10.1001/jama.2015.13631
27. Kuhn L, Schramm DB, Donninger S, Meddows-Taylor S, Coovadia AH, Sherman GG, et al. African Infants' CCL3 Gene Copies Influence Perinatal HIV Transmission in the Absence of Maternal Nevirapine. *AIDS Lond Engl* (2007) 21(13):1753–61. doi: 10.1097/QAD.0b013e3282ba553a
28. Forbes JC, Alimenti AM, Singer J, Brophy JC, Bitnun A, Samson LM, et al. A National Review of Vertical HIV Transmission. *AIDS* (2012) 26(6):757–63. doi: 10.1097/QAD.0b013e328350995c
29. Townsend CL, Cortina-Borja M, Peckham CS, de Ruiter A, Lyall H, Tookey PA. Low Rates of Mother-to-Child Transmission of HIV Following Effective Pregnancy Interventions in the United Kingdom and Ireland, 2000-2006. *AIDS Lond Engl* (2008) 22(8):973–81. doi: 10.1097/QAD.0b013e3282f9b67a
30. den Dunnen JT, Dalgleish R, Maglott DR, Hart RK, Greenblatt MS, McGowan-Jordan J, et al. HGVS Recommendations for the Description of Sequence Variants: 2016 Update. *Hum Mutat* (2016) 37(6):564–9. doi: 10.1002/humu.22981
31. Barrett JC, Fry B, Maller J, Daly MJ. Haploview: Analysis and Visualization of LD and Haplotype Maps. *Bioinforma Oxf Engl* (2005) 21(2):263–5. doi: 10.1093/bioinformatics/bth457
32. Nagelkerke SQ, Tacke CE, Breunis WB, Tanck MWT, Geissler J, Png E, et al. Extensive Ethnic Variation and Linkage Disequilibrium at the FCGR2/3 Locus: Different Genetic Associations Revealed in Kawasaki Disease. *Front Immunol* (2019) 10:185. doi: 10.3389/fimmu.2019.00185
33. Gray GE, Huang Y, Grunenberg N, Laher F, Roux S, Andersen-Nissen E, et al. Immune Correlates of the Thai RV144 HIV Vaccine Regimen in South Africa. *Sci Transl Med* (2019) 11(510):eaax1880. doi: 10.1126/scitranslmed.aax1880
34. Bekker L-G, Moodie Z, Grunenberg N, Laher F, Tomaras GD, Cohen KW, et al. Subtype C ALVAC-HIV and Bivalent Subtype C Gp120/MF59 HIV-1 Vaccine in Low-Risk, HIV-Uninfected, South African Adults: A Phase 1/2 Trial. *Lancet HIV* (2018) 5(7):e366–78. doi: 10.1016/S2352-3018(18)30071-7
35. Laher F, Moodie Z, Cohen KW, Grunenberg N, Bekker L-G, Allen M, et al. Safety and Immune Responses After a 12-Month Booster in Healthy HIV-Uninfected Adults in HVTN 100 in South Africa: A Randomized Double-Blind Placebo-Controlled Trial of ALVAC-HIV (Vcp2438) and Bivalent Subtype C Gp120/MF59 Vaccines. *PloS Med* (2020) 17(2):e1003038. doi: 10.1371/journal.pmed.1003038
36. Peng X, Li SS, Gilbert PB, Geraghty DE, Katze MG. FCGR2C Polymorphisms Associated With HIV-1 Vaccine Protection Are Linked to Altered Gene Expression of Fc-γ Receptors in Human B Cells. *PloS One* (2016) 11(3):e0152425. doi: 10.1371/journal.pone.0152425
37. Geraghty DE, Thorball CW, Fellay J, Thomas R. Effect of Fc Receptor Genetic Diversity on HIV-1 Disease Pathogenesis. *Front Immunol* (2019) 10. doi: 10.3389/fimmu.2019.00970
38. Corey L, Gilbert PB, Juraska M, Montefiori DC, Morris L, Karuna ST, et al. Two Randomized Trials of Neutralizing Antibodies to Prevent HIV-1 Acquisition. *N Engl J Med* (2021) 384(11):1003–14. doi: 10.1056/NEJMoa2031738

Conflict of Interest: The authors declare that the research was conducted in the absence of any commercial or financial relationships that could be construed as a potential conflict of interest.

Publisher's Note: All claims expressed in this article are solely those of the authors and do not necessarily represent those of their affiliated organizations, or those of the publisher, the editors and the reviewers. Any product that may be evaluated in this article, or claim that may be made by its manufacturer, is not guaranteed or endorsed by the publisher.

frontiers in Immunology

PERSPECTIVE
published: 15 December 2021
doi: 10.3389/fimmu.2021.788203

FcγR Genetic Variation and HIV-1 Vaccine Efficacy: Context And Considerations

Ria Lassaunière[1*] *and Caroline T. Tiemessen*[2,3*]

[1] Virus and Microbiological Special Diagnostics, Statens Serum Institut, Copenhagen, Denmark, [2] Centre for HIV and STI's, National Institute for Communicable Diseases, Johannesburg, South Africa, [3] Faculty of Health Sciences, University of the Witwatersrand, Johannesburg, South Africa

Receptors for the crystallisable fragment (Fc) of immunoglobulin (Ig) G, Fcγ receptors (FcγRs), link the humoral and cellular arms of the immune response, providing a diverse armamentarium of antimicrobial effector functions. Findings from HIV-1 vaccine efficacy trials highlight the need for further study of Fc-FcR interactions in understanding what may constitute vaccine-induced protective immunity. These include host genetic correlates identified within the low affinity Fcγ-receptor locus in three HIV-1 efficacy trials – VAX004, RV144, and HVTN 505. This perspective summarizes our present knowledge of FcγR genetics in the context of findings from HIV-1 efficacy trials, and draws on genetic variation described in other contexts, such as mother-to-child HIV-1 transmission and HIV-1 disease progression, to explore the potential contribution of *FcγR* variability in modulating different HIV-1 vaccine efficacy outcomes. Appreciating the complexity and the importance of the collective contribution of variation within the *FCGR* gene locus is important for understanding the role of FcγRs in protection against HIV-1 acquisition.

Keywords: FCGR genes, Fc gamma receptor (FcγR), variant, polymorphism, copy number, HIV - human immunodeficiency virus, vaccine, disease progression

OPEN ACCESS

Edited by:
Gabriella Scarlatti,
San Raffaele Hospital (IRCCS), Italy

Reviewed by:
Bin Su,
Capital Medical University, China
Christiane Moog,
Institut National de la Santé et de la Recherche Médicale (INSERM), France

***Correspondence:**
Caroline T. Tiemessen
carolinet@nicd.ac.za
Ria Lassaunière
mlas@ssi.dk

Specialty section:
This article was submitted to Viral Immunology, a section of the journal Frontiers in Immunology

Received: *01 October 2021*
Accepted: *29 November 2021*
Published: *15 December 2021*

Citation:
Lassaunière R and Tiemessen CT (2021) FcγR Genetic Variation and HIV-1 Vaccine Efficacy: Context And Considerations. Front. Immunol. 12:788203. doi: 10.3389/fimmu.2021.788203

INTRODUCTION

Despite enormous research efforts over 30 years, a highly efficacious preventative HIV vaccine remains elusive. Nonetheless, each vaccine efficacy trial provided new insight. Only one HIV-1 vaccine trial has shown some level of protection against HIV-1 acquisition. The RV144 vaccine trial (1), conducted in Thailand, achieved modest vaccine efficacy at 31.2%, while 6 other efficacy trials – VAX003 (2), VAX004 (3), HVTN502 (the Step trial) (4), HVTN503 (the Phambili trial) (5), HVTN505 (6), and HVTN702 (the RV144 follow-on trial) (7) – failed to prevent HIV-1 acquisition in vaccinees, and even increased risk in some individuals (4, 8). Many differences could account for the efficacy outcomes, including the vaccine regimen (design, virus subtype, and adjuvant), diversity of circulating virus strains, sex, modes of transmission, different risk populations, geography, and host genetics.

The initial immune correlate analysis from RV144 (9) provided the impetus for more detailed study of immune correlates to better understand vaccine-induced immune protection against

HIV-1. These subsequent studies and analyses have revealed the inordinately complex nature of immunological mechanisms that collectively act to provide protection against acquisition of HIV-1 [reviewed in (10)]. In particular, they have highlighted many HIV-specific antibody parameters as correlates of HIV-1 acquisition risk (9, 11–14), many of which bind FcγRs to mediate their functions. Indeed, FcγR-mediated effector functions associate with vaccine protection (9, 15). Host genetic correlates further implicating a role for FcγRs have been identified in three efficacy trials, VAX004 (16), RV144 (17), and HVTN505 (18); each conducted in different population groups with distinct allelic variability across FcγRs (19).

Here we summarize our present knowledge of FcγR genetics in the context of findings from HIV-1 efficacy trials, and include studies of mother-to-child HIV-1 transmission and HIV-1 disease progression. We highlight the complexity of the *FCGR* locus, the importance of using validated methods to aid interpretation, the inclusion of *FCGR* gene copy number determination, and population genetic differences, among other considerations outlined.

THE LOW AFFINITY FcγRs AND HOST GENETIC VARIABILITY

IgG, elicited through active immunization (infection or vaccination) or transferred passively (intravenous infusion or transplacental), modulates an antiviral response through several mechanisms. The antigen binding fragment (Fab) may neutralize virus infection by binding viral surface proteins and preventing attachment to host receptors, while the antibody Fc domain direct immune mechanisms through the engagement of FcγRs. Cross-linking of FcγRs on the cell surface through multivalent interactions, initiates responses that include antibody-dependent cellular cytotoxicity (ADCC), antibody-dependent cellular phagocytosis (ADCP), oxidative burst, release of inflammatory mediators, and regulation of antibody production (**Figure 1A**) (21–24).

FcγRs are a complex family of activating and inhibitory receptors, comprising three classes of molecules and different isoforms: FcγRIa, FcγRIIa/b/c, and FcγRIIIa/b (**Figure 1B**). All FcγRs are glycoproteins belonging to the Ig superfamily and consist of a ligand-binding α-chain with two (FcγRII and FcγRIII) or three (FcγRI) extracellular Ig-like domains, a transmembrane domain, and intracytoplasmic domain. The activating or inhibitory signaling motifs are located either within the α-chain (FcγRII) or associated signaling subunits (FcγRI and FcγRIIIa) (25). Unique to the FcγR family, FcγRIIIb attaches to the cell membrane with a glycosylphosphatidylinositol anchor. Despite lacking intrinsic cytoplasmic signaling domains, FcγRIIIb induces several cell responses (26–28). Each FcγR is expressed on specific cell types, either constitutively or induced, and has particular affinities for IgG and its subtypes (IgG1-4). The genes that encode FcγRs – *FCGR1A*, *FCGR2A/B/C*, and *FCGR3A/B* – are further subject to considerable allelic variation, resulting from segmental genomic duplications/deletions or single nucleotide polymorphisms.

FCGR2C, *FCGR3A*, and *FCGR3B* occur at different gene copies due to the gain or loss of defined copy number regions (CNR1-5, **Figure 1C**). The number of *FCGR* genes per diploid genome directly correlate with FcγR surface density and function (29, 30). In addition to this gene dosage effect, duplications/deletions create chimeric *FCGRs* that alter the cellular distribution, expression, and function of FcγRs. A deletion of CNR1, present in 7.4-18.1% of individuals depending on ethnicity, juxtaposes the 5'-regulatory sequences of *FCGR2C* with the coding sequence of *FCGR2B*, creating the chimeric *FCGR2B'* and expression of FcγRIIb on cytotoxic NK cells where it inhibits cell activation and ADCC (31, 32). A CNR2 deletion, present in <1.5% of individuals, leads to an *FCGR2A/2C* chimera that result in reduced FcγRIIa surface levels and oxidative burst response (32, 33). Conversely, a CNR2 duplication, present in 1.6-4.5% of individuals, leads to an *FCGR2C/2A* chimeric gene that increases FcγRIIc expression levels.

Allelic variation for FcγRI is low. In contrast, several single nucleotide variants with a known phenotypic or functional consequence exist for FcγRIIa/b/c and FcγRIIIa/b (34). Distinct amino acid changes in the membrane proximal Ig-like domain of FcγRIIa and FcγRIIIa alter their affinity for IgG subtypes and associated effector functions, including FcγRIIa-p.H166R (alias H131R, rs1801274) and FcγRIIIa-p.F176V (alias F158V, rs396991) (35–38). Conversely, in the transmembrane domain of FcγRIIb, the p.I232T variant (rs1050501) alters its inclusion in lipid rafts and inhibitory signaling (39). In FcγRIIIb, a combination of six amino acid changes determine the human neutrophil antigens (HNA) 1a/b/c – molecules that are antigenically distinct and modulate neutrophil phagocytosis and oxidative burst (40). Unlike other *FCGR*s, *FCGR2C* occurs predominantly as a pseudogene, where a combination of *FCGR2C* minor alleles – p.X57Q (alias X13Q) and c.798+1A>G (rs76277413) – determine its surface expression (20, 41). Other co-inherited single nucleotide variants (haplotypes) within the promotor region of *FCGR2B/C* and spanning *FCGR3A* modulate surface expression levels of FcγRIIb/c and FcγRIIIa, respectively (42–44).

Over the past few years, research identified several new *FCGR* variants of clinical relevance in the context of HIV-1 (described below). Although, linkage disequilibrium (co-occurring variants) in the *FCGR* locus has impeded identification of potential causal variants (19, 45, 46). Studying *FCGR* variants in different population groups in the same and/or different context may help define a role for specific variants, since linkage disequilibrium is inconsistent between geographical populations (19). Of note, describing new *FCGR* variants and assigning them to specific FcγRs warrants caution, since high nucleotide sequence homology between *FCGR*s could lead to inaccurate assignment of variants to specific genes (34); thus, highlighting the need for validated genotyping methods. In general, for the description of new and conventional *FCGR* variants, we encourage the use of a single international genotypic variation nomenclature as described by the Human Genome Variation Society (HGVS) to enable cross-referencing of *FCGR* variants between studies (34, 47). We include here the HGVS name for all variants.

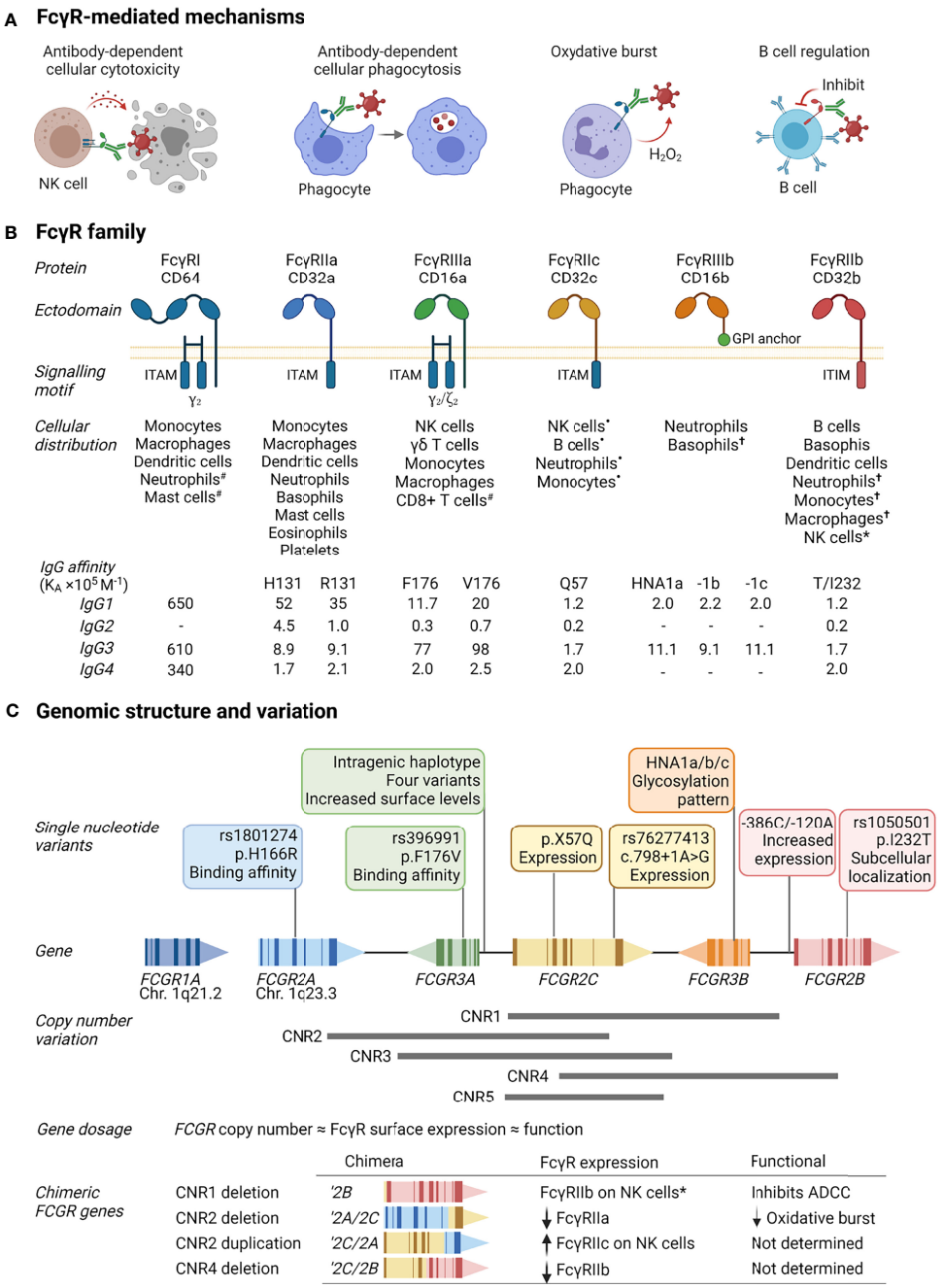

FIGURE 1 | FcγR function, structure and variability. **(A)** FcγRs activate or inhibit immune mechanisms that include killing of infected cells through antibody-dependent cellular cytotoxicity, clearance of immune complexes through phagocytosis, release of reactive oxygen species [superoxide anion (O^-_2) and hydrogen peroxide (H_2O_2)], and regulation of B cell activation through co-engaging the B cell receptor and inhibitory FcγRIIb by immune complexes. **(B)** FcγRs comprise a family of receptors: FcγRI, FcγRIIa, FcγRIIb, FcγRIIc, FcγRIIIa, FcγRIIIb; also known by their cluster of differentiation (CD) markers CD64, CD32a, CD32b, CD32c, CD16a, and CD16b, respectively. The FcγRs IgG binding chain activates or regulates immune responses depending on its association with or inclusion of an immunoreceptor tyrosine activation motif (ITAM) or inhibitory motif (ITIM). Unique among FcγRs, FcγRIIIb attaches to the cell membrane with a glycosylphosphatidylinositol (GPI) anchor. Each receptor has a specific cell expression profile and affinity for IgG and its subtypes (IgG1-4), shown as affinity constants (K_A×10^5 M^{-1}); -, no binding. Expression patterns: #inducible expression; •in individuals bearing the *FCGR2C* expression variants (20); †very low expression or expressed by rare subsets; *expressed in individuals bearing a *FCGR2C-FCGR3B* gene deletion. **(C)** The cluster of *FCGR2A/B/C* and *FCGR3A/B* genes on chromosome 1q23.3 that encode FcγRIIa/b/c and FcγRIIIa/b are polymorphic. Variants include nonsynonymous single nucleotide polymorphisms that alter the receptor's binding affinity for certain IgG subtypes, determine expression of an otherwise pseudogene, increase surface expression, glycosylation, and subcellular localization. Large segmental duplications and deletions in the *FCGR* cluster further modify FcγR expression levels and create chimeric genes that yield FcγRs with altered cellular distribution and/or function. Created with BioRender.com.

FcγR GENE VARIANTS AND HIV VACCINE EFFICACY TRIALS

In HIV-1 vaccine efficacy trials, studies have shown clear associations between FcγR-mediated effector functions and risk of HIV-1 acquisition following vaccination (9, 15, 16, 48). To dissect further, three vaccine efficacy studies to date have investigated FcγR variation as a modifier of antibody Fc-mediated effector functions and HIV-1 acquisition risk (**Figure 2A**).

The VAX004 trial evaluated a recombinant envelope protein (AIDSVAX B/B) prime-boost regimen in predominantly Caucasian men who have sex with men (3). Vaccine recipients who remained uninfected had higher antibody-dependent cell-mediated virus inhibition (ADCVI) responses, which encompass ADCC, ADCP and the induction of soluble antiviral factors, than

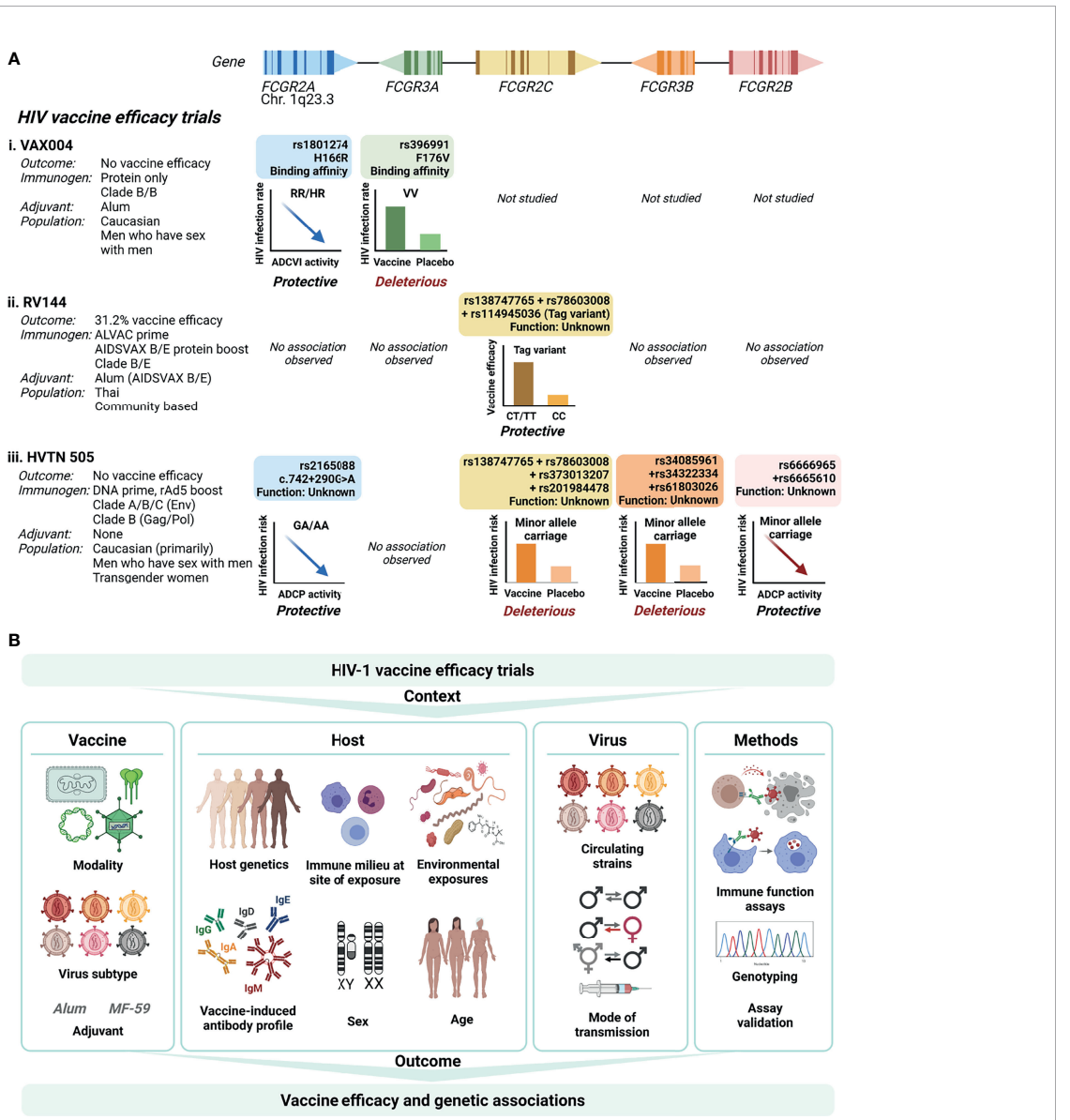

FIGURE 2 | *FCGR* variant associations with HIV-1 vaccine efficacy trial outcomes. **(A)** To date, three HIV-1 vaccine efficacy trials investigated the association between *FCGR* variants and HIV-1 acquisition risk: VAX004, RV144 and HVTN505. The trials differed with regard to vaccine modalities, target HIV-1 subtypes, study populations, mode of HIV-1 transmission, and host ethnicities. In VAX004 and HVTN505 vaccinees bearing minor alleles within *FCGR2A* and *FCGR2B*, enhanced Fc-mediated effector functions [antibody-dependent cellular viral inhibition (ADCVI) and antibody-dependent cellular phagocytosis (ADCP), respectively] associated with reduced risk of HIV-1 acquisition. In VAX004, enhanced HIV-1 acquisition occurred in vaccinees homozygous for the FcγRIIIa-176V allele. Co-inherited intragenic minor alleles in *FCGR2C* enhanced vaccine efficacy in RV144, but increased HIV-1 acquisition risk in HVTN505. Similarly, co-inherited minor alleles in the 5' untranslated region of *FCGR3B* associated with HIV-1 acquisition risk in HVTN505. **(B)** Defining *FCGR* genetic associations with HIV-1 vaccine efficacy is affected by several factors relating to the vaccine, the host, the virus and methodology used. Created with BioRender.com.

those who became infected (48). The magnitude of ADCVI responses inversely correlated with the HIV-1 acquisition rate, but only in individuals bearing low affinity alleles for FcγRIIa-p.H166R (HR/RR genotypes) and FcγRIIIa-p.F176V (FF genotype) (48) (**Figure 2Ai**). When adjusted for linkage disequilibrium between the two variants, an independent association with FcγRIIa-p.H166R remained. However, the FcγRIIa-p.H166R variant itself did not predict acquisition rate (16). Conversely, in the low risk behavioral group, vaccinees homozygous for the p.176V allele were at greater rate of acquiring HIV-1 compared to those who received the placebo (hazard ratio 4.51), suggesting enhanced infection from the use of AIDSVAX B/B in this genotype group (16).

The RV144 trial, which evaluated a heterologous ALVAC-HIV (vCP1521) canary pox vector prime and AIDSVAX B/E protein boost regimen, demonstrated modest vaccine efficacy (31.2%) in Thai individuals (1). The primary determinants of vaccine efficacy were binding IgG to the variable loops 1 and 2 (V1V2) region of gp120 and binding of plasma IgA to envelope (9). In a secondary analysis, the combination of high levels of ADCC and low plasma anti-HIV-1 envelope IgA antibodies inversely correlated with HIV-1 acquisition risk (9). Variants within FcγRIIIa, the major FcγR involved in NK cell-mediated ADCC, did not associate with HIV-1 acquisition risk (17) (**Figure 2Aii**). Conversely, three single nucleotide variants within *FCGR2C* significantly modified vaccine efficacy that include *FCGR2C* 126C>T (HVGS name: c.134-96C>T, rs114945036), c.353C>T (p. T118I, rs138747765), and c.391+111G>A (rs78603008) (17). All variants were in complete linkage disequilibrium in Thai RV144 trial participants, forming a haplotype. Possession of the haplotype associated with an estimated vaccine efficacy of 91% against CRF01_AE 169K HIV-1 and 64% against any HIV-1 strain, compared to 15% and 11% in the absence of the haplotype, respectively. The functional significance of the variant is unrelated to FcγRIIc surface expression, since only one study participant carried an FcγRIIc-p.57Q allele that predicts expression (17). Alternatively, the haplotype locates within a weak transcriptional enhancer (49). The minor alleles likely abrogate binding of repressor proteins within the regulatory motif and increase mRNA expression. Indeed, in Epstein-Barr virus transformed lymphoblastoid B-cell lines from European Caucasians, the minor allele haplotype associated with increased expression of *FCGR2A* and/or *FCGR2C* exon 7 (50). Other *FCGR2C* variants in complete linkage disequilibrium with the haplotype include c.113-1058T>C (rs2169052/rs115953596) and c.113-684C>T (rs111828362) (49) were not genotyped in RV144 participants and warrant further investigation. Of significance, two components of the haplotype, p.T118I (rs138747765) and c.391+111G>A (rs78603008), are rarely polymorphic in Africans (19), where the RV144 follow-up trial HVTN 702 failed to protect against HIV-1 infection (7).

The HVTN 505 trial that evaluated another heterologous prime-boost regimen – a multigene, multiclade DNA prime and recombinant adenovirus 5 (rAd5) boost – did not show any efficacy in a cohort of predominantly Caucasian men who have sex with men (6). However, ADCP responses and binding of immune complexes to recombinant FcγRIIa-p.166H inversely correlated with HIV-1 acquisition risk (15) (**Figure 2Aiii**). The associations increased for individuals without HIV-1 envelope IgA. Intriguingly, in a phase IIa clinical trial of the same DNA/rAd5 regimen (HVTN 204) (51), a different group did not detect ADCP responses (52). The cause of the distinct observations is unclear; both groups used the same assay albeit a different antibody source (isolated IgG vs. serum) and antigen (vaccine clade-specific gp120 vs. Con S gp140) (52). In the HVTN 505 trial participants, targeted sequencing of regions encoding the extracellular domains of FcγRs identified several variants that associated with HIV-1 acquisition risk or Fc-mediated effector functions. An *FCGR2A* intronic variant modified HIV-1 acquisition risk, *FCGR2A*-intron13-645-G/A (HGVS name: c.742+290G>A, rs2165088) (15). In vaccine recipients bearing the minor allele of c.742+290G>A, the magnitude of ADCP responses and FcγRIIa-p.166H binding to antibody-rgp140 complexes associated with reduced risk of HIV-1 acquisition (15). The functional consequence of *FCGR2A* c.742+290G>A is unknown and it does not appear to be in complete or high linkage disequilibrium with other variants in, or flanking, *FCGR2A*. Inverse correlations between ADCP with HIV-1 acquisition risk similarly occurred for participants bearing minor alleles of two *FCGR2B* variants (synonymous *FCGR2B*-exon5-523-G/A; HGVS name: c.336G>A, rs6665610 and *FCGR2B*-intron14-352-T/G; HGVS name: c.760+26T>G, rs6666965) (18). c.336G>A is in high linkage disequilibrium with seven other *FCGR2B* variants and associated with decreased expression of *FCGR2A* (18).

Furthermore, in HVTN 505 participants, a four-variant *FCGR2C* haplotype and three-variant *FCGR3B* haplotype associated with increased HIV-1 acquisition risk (hazard ratio 9.79 and 2.78, respectively) (18) (**Figure 2Aiii**). The *FCGR2C* haplotype comprise two of the three *FCGR2C* variants identified as protective in the RV144 vaccine trial (p.T118I, rs138747765; and c.391+111G>A, rs78603008). The lack of association with the third *FCGR2C* variant (c.134-96C>T, rs114945036) is likely due to incomplete linkage disequilibrium of the three *FCGR2C* variants in Caucasians (49), the predominant ethnicity of HVTN 505 participants. Additional *FCGR2C* variants were in complete linkage disequilibrium in HVTN 505 participants, *FCGR2C*-intron15-403-C/T (HGVS name: c.760+81C>T, rs373013207] and *FCGR2C*-intron15-433-G/A (HGVS name: c.760+111G>A, rs201984478). The functional consequences of these variants remains to be determined. The haplotype within *FCGR3B* that also associated with increased HIV-1 acquisition comprise three variants in the 5' untranslated region of *FCGR3B*, 111 to 126 nucleotides upstream of the transcription start site and potentially in the gene promoter region. These include *FCGR3B*-5'utr222-G/A (HGVS name: c.-111G>T; rs34085961), *FCGR3B*-5'utr44-T/A (HGVS name: c.-181T>A, rs34322334), and *FCGR3B*-5'utr99-C/G (HGVS name: c.-126C>G, rs61803026). In individuals with the *FCGR3B* haplotype, vaccination was less likely to induce potentially protective envelope-specific IgG and/or CD8+ T-cell responses than for individuals without the *FCGR3B* haplotype.

FcγR VARIANTS IN OTHER HIV INFECTION AND DISEASE CONTEXTS

Mother-to-child-transmission. Investigations of *FCGR* variants and mother-to-child-transmission risk are limited to two Kenyan cohorts and one South African cohort (53–55). In a Kenyan cohort of grouped perinatal HIV-1 transmission routes (*in utero*, intrapartum, and breastfeeding), infants with the FcγRIIa-p.166HH genotype were at increased risk of acquiring HIV-1 compared with infants bearing the p.166HR genotype (53). Studies of a Kenyan cohort with a large representation of breastfeeding HIV-1 transmission and our South African cohort with predominantly *in utero* and intrapartum HIV-1 transmission, did not replicate these findings (55, 56). In the latter two cohorts, the maternal FcγRIIIa-F176V variant associated with HIV-1 transmission, although with contrasting findings. In the Kenyan cohort of predominantly breastfeeding women, heterozygous mothers (FV) had an increased risk of transmitting HIV-1 compared to homozygous mothers (combined FF/VV); however, carriage of the 176V allele did not predict HIV-1 transmission (56). If adjustment for multiple comparisons were applied in the study, the association would not have been statistically significant. In contrast, our South African cohort revealed a protective role for the 176V allele in *in utero* transmission, where the association remained significant after adjustment for multiple comparisons (55). A recent study of *FCGR2C* variability in South African children revealed a protective role for a single gene copy of *FCGR2C/3B* per diploid genome (57). In contrast, children bearing the minor allele of the *FCGR2C* variant c.134-96C>T (rs114945036) – identified as protective in Thai RV144 vaccine recipients (17) – were more likely to acquire HIV-1 compared to children homozygous for the c.134-96C allele (57).

Disease progression. The FcγRIIa low affinity genotype, p.166RR, predicted a faster CD4 decline compared to p.166RH/HH in the Multicenter AIDS Cohort Study (MACS) of predominantly Caucasian men who have sex with men (58). A similar analysis in Kenyan women – a different host genetic background, sex and route of transmission – showed no effect (59). In addition, the variant did not modify natural control of HIV-1 infection in African Americans (60, 61). Despite convincing evidence for a role for ADCC in natural HIV-1 control [reviewed in (62)], the FcγRIIIa-p.F176V variant does not appear to modify HIV-1 disease course in Caucasians (58) or African Americans (60) (after adjusting for multiple comparisons). Neither FcγRIIa-p.H166R, FcγRIIIa-p.F176V, nor FcγRIIb-p.I232T associated with HIV-1 control in the French multicentric CODEX cohort (63). Of note, the potential for FcγR variants to modify HIV-1 control may only become apparent when considering variability within the ligand, such as IgG γ chain phenotypes (GM allotypes). For example, in individuals bearing the FcγRIIa p.166HH or FcγRIIIa p.176FV/VV genotypes, HIV-1 viraemic control was more likely in the absence of the IgG GM21 allotype (61). Beyond the protein-coding region, a variant located 3.1 kilobases upstream of *FCGR2A*, g.1954 A>G (rs10800309), modified HIV-1 disease progression in a cohort of predominantly Caucasian men and women (63). In particular, homozygosity for g.1954A allele, which associates with increased FcγRIIa surface expression on myeloid cells, predicted natural control of HIV-1 independent of HLA-B57 and HLA-B27 (63). Another non-coding variant, the *FCGR2C* variant c.134-96C>T (rs114945036), predicted HIV-1 disease progression in South Africans (49), the same population where the RV144 follow-on trial, HVTN702, failed to show efficacy (7). However, in the French multicentric CODEX cohort of predominantly Caucasian individuals, the same *FCGR2C* variant did not associate with disease progression (63). It is unclear whether the different outcomes of RV144 and HVTN702 result from diverse population genetics, that include *FCGR2C*, or vaccine-associated factors that include differences in HIV-1 subtype envelopes, mismatched circulating strains, adjuvant or additional booster vaccination. Regardless, the collective findings further emphasize the importance of the *FCGR2C* locus, and additional study in different contexts will help elucidate the underlying protective/deleterious mechanisms.

DISCUSSION

Many factors affect the host immunological response to immunization and to the pathogen (HIV) encountered. These include i) the route of inoculation and of HIV-1 acquisition, ii) immunogen/virus variability, iii) vaccine regimen (modality, dose, timing, adjuvant), iv) other prior exposures (related or unrelated), comorbidities and pre-existing infections, v) age, vi) sex, vii) geography (population genetics), and viii) genetic variation of the host (**Figure 2B**). The immune milieu present at antigen encounter is affected by all these factors, which collectively define what could be called "an immunological founder effect" – a measure of an individual's immune capability that dictates the likelihood of producing a protective response to vaccination or infection. As context matters, the antibody Fc-FcγR axis, implicated in protection from acquisition of HIV-1 in vaccine recipients, would be expected to be modulated by these factors.

Investigations of FcγRs and their variants warrant several considerations. i) There are no association studies of *FCGR* copy number variation and HIV vaccine outcome. In RV144, ADCC was a correlate of protection. It is therefore plausible that a CNR1 deletion, which results in the expression of the inhibitory FcγRIIb on NK cells and subsequent inhibition of ADCC, may have an effect on vaccine efficacy. ii) Investigations of single nucleotide variants need to adjust for *FCGR* gene copy number. Certain minor alleles are more prevalent in individuals with more than two gene copies and may confound quantitative trait loci studies of *FCGR* variants (49). iii) Investigations of Fc-mediated effector functions should consider the autologous FcγR variants since they modulate binding of the receptor to antibodies, surface expression levels of the receptor, and/or cell activation/inhibition (64). iv) *FCGR* genes are highly homologous. Assigning single nucleotide variants to specific *FCGR*s requires validated

methods. v) Considerable linkage disequilibrium between single nucleotide variants exist across the *FCGR* gene region (19, 45, 46), complicating identification of potential causal variants. vi) Increasing evidence suggest a clinical significance for non-coding *FCGR* variants highlighting potential complex cis- or transgene regulation that warrants characterization and investigation in other contexts. vii) FcγRs often co-occur on the same cell type. Elucidating the role of a single variant requires adjusting for allelic variants in co-expressed FcγRs, since the collective function of all co-expressed FcγRs will determine the effector response. Furthermore, phenotypic and functional analyses of *FCGR* genotype combinations are highly relevant, as demonstrated by an association of the *FCGR2A* rs1801274: rs10800309 diplotype with cell-type specific FcγRII expression (65) and FcγRIIa: FcγRIIIb haplotypes with neutrophil function (66). viii) *FCGR* variation – gene copy number variation, single nucleotide variants, and linkage disequilibrium – differ significantly between population groups and genetic association cannot necessarily be extrapolated between groups. ix) Phenotypic and functional consequences of allelic variants should be studied in the disease context and immune milieu of the condition under study, since disease may alter allelic function (67).

In summary, *FCGR* genetic variants have been associated with protective or deleterious infection and disease outcomes. Much insight can be gained into the potential functional significance of these variants by testing samples from other efficacy trials. For example, HVTN 702, which was non-efficacious in South Africans immunized with subtype C envelope ALVAC-HIV (vCP2438) prime and an MF59-adjuvanted subtype C bivalent envelope protein boost (7). Similarly, individuals passively immunized with broadly neutralizing antibody (VRC01) in the Antibody Mediated Prevention (AMP) trials (68) provide another informative study model. Harnessing host genetic variation between populations, and studying the collective contribution of *FCGR* variants in different infection/disease contexts, will provide much needed insights into what constitutes protective immunity to HIV-1. Importantly, the considerations discussed here extend beyond the context of HIV, bearing relevance to other infections and vaccination strategies that encompass endemic [e.g. malaria (69)], epidemic [e.g. influenza and respiratory syncytial virus (70–72)], pandemic [e.g. severe acute respiratory syndrome coronavirus 2 (SARS-CoV-2) (73)], and emerging/re-emerging infectious diseases [e.g. Ebola (74, 75)].

DATA AVAILABILITY STATEMENT

The original contributions presented in the study are included in the article/supplementary material. Further inquiries can be directed to the corresponding author.

AUTHOR CONTRIBUTIONS

RL and CT conceptualized and wrote the article. Figures were generated by RL. All authors contributed to the article and approved the submitted version.

FUNDING

CT receives funding as part of the South African Research Chairs Initiative of the Department of Science and Innovation and National Research Foundation (84177).

REFERENCES

1. Rerks-Ngarm S, Pitisuttithum P, Nitayaphan S, Kaewkungwal J, Chiu J, Paris R, et al. Vaccination With ALVAC and AIDSVAX to Prevent HIV-1 Infection in Thailand. *N Engl J Med* (2009) 361:2209–20. doi: 10.1056/NEJMoa0908492
2. Pitisuttithum P, Gilbert P, Gurwith M, Heyward W, Martin M, Van Griensven F, et al. Randomized, Double-Blind, Placebo-Controlled Efficacy Trial of a Bivalent Recombinant Glycoprotein 120 HIV-1 Vaccine Among Injection Drug Users in Bangkok, Thailand. *J Infect Dis* (2006) 194:1661–71. doi: 10.1086/508748
3. Flynn NM, Forthal DN, Harro CD, Judson FN, Mayer KH, Para MF, et al. Placebo-Controlled Phase 3 Trial of a Recombinant Glycoprotein 120 Vaccine to Prevent HIV-1 Infection. *J Infect Dis* (2005) 191:654–65. doi: 10.1086/428404
4. Buchbinder SP, Mehrotra DV, Duerr A, Fitzgerald DW, Mogg R, Li D, et al. Efficacy Assessment of a Cell-Mediated Immunity HIV-1 Vaccine (the STEP Study): A Double-Blind, Randomised, Placebo-Controlled, Test-Of-Concept Trial. *Lancet* (2008) 372:1881–93. doi: 10.1016/S0140-6736(08)61591-3
5. Gray GE, Allen M, Moodie Z, Churchyard G, Bekker LG, Nchabeleng M, et al. Safety and Efficacy of the HVTN 503/Phambili Study of a Clade-B-Based HIV-1 Vaccine in South Africa: A Double-Blind, Randomised, Placebo-Controlled Test-Of-Concept Phase 2b Study. *Lancet Infect Dis* (2011) 11:507–15. doi: 10.1016/S1473-3099(11)70098-6
6. Hammer SM, Sobieszczyk ME, Janes H, Karuna ST, Mulligan MJ, Grove D, et al. Efficacy Trial of a DNA/rAd5 HIV-1 Preventive Vaccine. *N Engl J Med* (2013) 369:2083–92. doi: 10.1056/NEJMoa1310566
7. Gray GE, Bekker LG, Laher F, Malahleha M, Allen M, Moodie Z, et al. Vaccine Efficacy of ALVAC-HIV and Bivalent Subtype C Gp120-MF59 in Adults. *N Engl J Med* (2021) 384:1089–100. doi: 10.1056/NEJMoa2031499
8. Gray GE, Moodie Z, Metch B, Gilbert PB, Bekker LG, Churchyard G, et al. Recombinant Adenovirus Type 5 HIV Gag/Pol/Nef Vaccine in South Africa: Unblinded, Long-Term Follow-Up of the Phase 2b HVTN 503/Phambili Study. *Lancet Infect Dis* (2014) 14:388–96. doi: 10.1016/S1473-3099(14)70020-9
9. Haynes BF, Gilbert PB, McElrath MJ, Zolla-Pazner S, Tomaras GD, Alam SM, et al. Immune-Correlates Analysis of an HIV-1 Vaccine Efficacy Trial. *N Engl J Med* (2012) 366:1275–86. doi: 10.1056/NEJMoa1113425
10. Tomaras GD, Plotkin SA. Complex Immune Correlates of Protection in HIV-1 Vaccine Efficacy Trials. *Immunol Rev* (2017) 275:245–61. doi: 10.1111/imr.12514
11. Gottardo R, Bailer RT, Korber BT, Gnanakaran S, Phillips J, Shen X, et al. Plasma IgG to Linear Epitopes in the V2 and V3 Regions of HIV-1 Gp120 Correlate With a Reduced Risk of Infection in the RV144 Vaccine Efficacy Trial. *PloS One* (2013) 8:e75665. doi: 10.1371/journal.pone.0075665
12. Zolla-Pazner S, Decamp A, Gilbert PB, Williams C, Yates NL, Williams WT, et al. Vaccine-Induced IgG Antibodies to V1V2 Regions of Multiple HIV-1 Subtypes Correlate With Decreased Risk of HIV-1 Infection. *PloS One* (2014) 9:e87572. doi: 10.1371/journal.pone.0087572
13. Yates NL, Liao HX, Fong Y, Decamp A, Vandergrift NA, Williams WT, et al. Vaccine-Induced Env V1-V2 IgG3 Correlates With Lower HIV-1 Infection Risk and Declines Soon After Vaccination. *Sci Transl Med* (2014) 6:228ra239. doi: 10.1126/scitranslmed.3007730
14. Tomaras GD, Ferrari G, Shen X, Alam SM, Liao HX, Pollara J, et al. Vaccine-Induced Plasma Iga Specific for the C1 Region of the HIV-1 Envelope Blocks Binding and Effector Function of IgG. *Proc Natl Acad Sci USA* (2013) 110:9019–24. https://doi.org/10.1073/pnas.1301456110

15. Neidich SD, Fong Y, Li SS, Geraghty DE, Williamson BD, Young WC, et al. Antibody Fc Effector Functions and IgG3 Associate With Decreased HIV-1 Risk. *J Clin Invest* (2019) 129:4838–49. doi: 10.1172/JCI126391
16. Forthal DN, Gabriel EE, Wang A, Landucci G, Phan TB. Association of Fcgamma Receptor IIIa Genotype With the Rate of HIV Infection After Gp120 Vaccination. *Blood* (2012) 120:2836–42. doi: 10.1182/blood-2012-05-431361
17. Li SS, Gilbert PB, Tomaras GD, Kijak G, Ferrari G, Thomas R, et al. FCGR2C Polymorphisms Associate With HIV-1 Vaccine Protection in RV144 Trial. *J Clin Invest* (2014) 124:3879–90. doi: 10.1172/JCI75539
18. Li SS, Gilbert PB, Carpp LN, Pyo CW, Janes H, Fong Y, et al. Fc Gamma Receptor Polymorphisms Modulated the Vaccine Effect on HIV-1 Risk in the HVTN 505 HIV Vaccine Trial. *J Virol* (2019) 93(21):e02041–18. doi: 10.1128/JVI.02041-18
19. Lassauniere R, Tiemessen CT. Variability at the FCGR Locus: Characterization in Black South Africans and Evidence for Ethnic Variation in and Out of Africa. *Genes Immun* (2016) 17:93–104. doi: 10.1038/gene.2015.60
20. Van Der Heijden J, Breunis WB, Geissler J, De Boer M, Van Den Berg TK, Kuijpers TW. Phenotypic Variation in IgG Receptors by NonclassicalFCGR2C Alleles. *J Immunol* (2012) 188:1318–24. doi: 10.4049/jimmunol.1003945
21. Hogarth PM. Fc Receptors Are Major Mediators of Antibody Based Inflammation in Autoimmunity. *Curr Opin Immunol* (2002) 14:798–802. doi: 10.1016/S0952-7915(02)00409-0
22. Amigorena S, Bonnerot C, Drake JR, Choquet D, Hunziker W, Guillet JG, et al. Cytoplasmic Domain Heterogeneity and Functions of IgG Fc Receptors in B Lymphocytes. *Science* (1992) 256:1808–12. doi: 10.1126/science.1535455
23. Muta T, Kurosaki T, Misulovin Z, Sanchez M, Nussenzweig MC, Ravetch JV. A 13-Amino-Acid Motif in the Cytoplasmic Domain of Fc Gamma RIIb Modulates B-Cell Receptor Signalling. *Nature* (1994) 368:70–3. doi: 10.1038/368070a0
24. Tzeng SJ, Bolland S, Inabe K, Kurosaki T, Pierce SK. The B Cell Inhibitory Fc Receptor TrIgGers Apoptosis by a Novel C-Abl Family Kinase-Dependent Pathway. *J Biol Chem* (2005) 280:35247–54. doi: 10.1074/jbc.M505308200
25. Lanier LL, Yu G, Phillips JH. Analysis of Fc Gamma RIII (CD16) Membrane Expression and Association With CD3 Zeta and Fc Epsilon RI-Gamma by Site-Directed Mutation. *J Immunol* (1991) 146:1571–6. https://www.jimmunol.org/content/146/5/1571
26. Rosales C, Brown EJ. Signal Transduction by Neutrophil Immunoglobulin G Fc Receptors. Dissociation of Intracytoplasmic Calcium Concentration Rise From Inositol 1,4,5-Trisphosphate. *J Biol Chem* (1992) 267:5265–71. doi: 10.1016/S0021-9258(18)42761-5
27. Salmon JE, Brogle NL, Edberg JC, Kimberly RP. Fc Gamma Receptor III Induces Actin Polymerization in Human Neutrophils and Primes Phagocytosis Mediated by Fc Gamma Receptor Ii. *J Immunol* (1991) 146:997–1004. https://www.jimmunol.org/content/146/3/997
28. Garcia-Garcia E, Nieto-Castaneda G, Ruiz-Saldana M, Mora N, Rosales C. FcgammarIIa and FcgammarIIIb Mediate Nuclear Factor Activation Through Separate Signaling Pathways in Human Neutrophils. *J Immunol* (2009) 182:4547–56. doi: 10.4049/jimmunol.0801468
29. Willcocks LC, Lyons PA, Clatworthy MR, Robinson JI, Yang W, Newland SA, et al. Copy Number of FCGR3B, Which Is Associated With Systemic Lupus Erythematosus, Correlates With Protein Expression and Immune Complex Uptake. *J Exp Med* (2008) 205:1573–82. doi: 10.1084/jem.20072413
30. Breunis WB, Van Mirre E, Geissler J, Laddach N, Wolbink G, van der Schoot E, et al. Copy Number Variation at the FCGR Locus Includes FCGR3A, FCGR2C and FCGR3B But Not FCGR2A and FCGR2B. *Hum Mutat* (2009) 30:E640–650. doi: 10.1002/humu.20997
31. Mueller M, Barros P, Witherden AS, Roberts AL, Zhang Z, Schaschl H, et al. Genomic Pathology of Sle-Associated Copy-Number Variation at the FCGR2C/FCGR3B/FCGR2B Locus. *Am J Hum Genet* (2013) 92:28–40. doi: 10.1016/j.ajhg.2012.11.013
32. Niederer HA, Willcocks LC, Rayner TF, Yang W, Lau YL, Williams TN, et al. Copy Number, Linkage Disequilibrium and Disease Association in the FCGR Locus. *Hum Mol Genet* (2010) 19:3282–94. doi: 10.1093/hmg/ddq216
33. Nagelkerke SQ, Tacke CE, Breunis WB, Geissler J, Sins JW, Appelhof B, et al. Nonallelic Homologous Recombination of the FCGR2/3 Locus Results in Copy Number Variation and Novel Chimeric FCGR2 Genes With Aberrant Functional Expression. *Genes Immun* (2015) 16:422–9. doi: 10.1038/gene.2015.25
34. Nagelkerke SQ, Schmidt DE, De Haas M, Kuijpers TW. Genetic Variation in Low-To-Medium-Affinity Fcgamma Receptors: Functional Consequences, Disease Associations, and Opportunities for Personalized Medicine. *Front Immunol* (2019) 10:2237. doi: 10.3389/fimmu.2019.02237
35. Bruhns P, Iannascoli B, England P, Mancardi DA, Fernandez N, Jorieux S, et al. Specificity and Affinity of Human Fcγ Receptors and Their Polymorphic Variants for Human IgG Subclasses. *Blood* (2009) 113:3716–25. doi: 10.1182/blood-2008-09-179754
36. Sanders LA, Feldman RG, Voorhorst-Ogink MM, De Haas M, Rijkers GT, Capel PJ, et al. Human Immunoglobulin G (IgG) Fc Receptor Iia (Cd32) Polymorphism and IgG2-Mediated Bacterial Phagocytosis by Neutrophils. *Infection Immun* (1995) 63:73–81. doi: 10.1128/iai.63.1.73-81.1995
37. Warmerdam PA, Van De Winkel JG, Vlug A, Westerdaal NA, Capel PJ. A Single Amino Acid in the Second Ig-Like Domain of the Human Fc Gamma Receptor II Is Critical for Human IgG2 Binding. *J Immunol* (1991) 147:1338–43. https://www.jimmunol.org/content/147/4/1338.long
38. Wu J, Edberg JC, Redecha PB, Bansal V, Guyre PM, Coleman K, et al. A Novel Polymorphism of Fcgammariiia (Cd16) Alters Receptor Function and Predisposes to Autoimmune Disease. *J Clin Invest* (1997) 100:1059–70. doi: 10.1172/JCI119616
39. Floto RA, Clatworthy MR, Heilbronn KR, Rosner DR, Macary PA, Rankin A, et al. Loss of Function of a Lupus-Associated Fcγriib Polymorphism Through Exclusion From Lipid Rafts. *Nat Med* (2005) 11:1056–8. doi: 10.1038/nm1288
40. Salmon JE, Edberg JC, Kimberly RP. Fc Gamma Receptor III on Human Neutrophils. Allelic Variants Have Functionally Distinct Capacities. *J Clin Invest* (1990) 85:1287–95. doi: 10.1172/JCI114566
41. Li X, Wu J, Ptacek T, Redden David T, Brown Elizabeth E, Alarcón Graciela S, et al. Allelic-Dependent Expression of an Activating Fc Receptor on B Cells Enhances Humoral Immune Responses. *Sci Transl Med* (2013) 5:216ra175–216ra175. doi: 10.1126/scitranslmed.3007097
42. Su K, Wu J, Edberg JC, Li X, Ferguson P, Cooper GS, et al. A Promoter Haplotype of the Immunoreceptor Tyrosine-Based Inhibitory Motif-Bearing Fcγriib Alters Receptor Expression and Associates With Autoimmunity. I. Regulatory FCGR2B Polymorphisms and Their Association With Systemic Lupus Erythematosus. *J Immunol* (2004) 172:7186–91. doi: 10.4049/jimmunol.172.11.7186
43. Su K, Li X, Edberg JC, Wu J, Ferguson P, Kimberly RP. A Promoter Haplotype of the Immunoreceptor Tyrosine-Based Inhibitory Motif-Bearing Fcγriib Alters Receptor Expression and Associates With Autoimmunity. Ii. Differential Binding of Gata4 and Yin-Yang1 Transcription Factors and Correlated Receptor Expression and Function. *J Immunol* (2004) 172:7192–9. doi: 10.4049/jimmunol.172.11.7192
44. Lassaunière R, Shalekoff S, Tiemessen CT. A Novel FCGR3A Intragenic Haplotype Is Associated With Increased Fcγriiia/CD16a Cell Surface Density and Population Differences. *Hum Immunol* (2013) 74:627–34. doi: 10.1016/j.humimm.2013.01.020
45. Van Der Pol WL, Jansen MD, Sluiter WJ, Van De Sluis B, Leppers-Van De Straat FG, Kobayashi T, et al. Evidence for Non-Random Distribution of Fcgamma Receptor Genotype Combinations. *Immunogenetics* (2003) 55:240–6. doi: 10.1007/s00251-003-0574-9
46. Lejeune J, Piegu B, Gouilleux-Gruart V, Ohresser M, Watier H, Thibault G. FCGR2c Genotyping by Pyrosequencing Reveals Linkage Disequilibrium With FCGR3A V158F and FCGR2A H131R Polymorphisms in a Caucasian Population. *MAbs* (2012) 4:784–7. doi: 10.4161/mabs.22287
47. Den Dunnen JT, Antonarakis SE. Mutation Nomenclature Extensions and Suggestions to Describe Complex Mutations: A Discussion. *Hum Mutat* (2000) 15:7–12. doi: 10.1002/(SICI)1098-1004(200001)15:1<7::AID-HUMU4>3.0.CO;2-N
48. Forthal DN, Gilbert PB, Landucci G, Phan T. Recombinant Gp120 Vaccine-Induced Antibodies Inhibit Clinical Strains of HIV-1 in the Presence of Fc Receptor-Bearing Effector Cells and Correlate Inversely With HIV Infection Rate. *J Immunol* (2007) 178:6596–603. doi: 10.4049/jimmunol.178.10.6596
49. Lassauniere R, Paximadis M, Ebrahim O, Chaisson RE, Martinson NA, Tiemessen CT. The FCGR2C Allele That Modulated the Risk of HIV-1 Infection in the Thai Rv144 Vaccine Trial Is Implicated in HIV-1 Disease Progression. *Genes Immun* (2019) 20:651–9. doi: 10.1038/s41435-018-0053-9

50. Peng X, Li SS, Gilbert PB, Geraghty DE, Katze MG. FCGR2C Polymorphisms Associated With HIV-1 Vaccine Protection Are Linked to Altered Gene Expression of Fc-Gamma Receptors in Human B Cells. *PloS One* (2016) 11: e0152425. https://doi.org/10.1371/journal.pone.0152425
51. Churchyard GJ, Morgan C, Adams E, Hural J, Graham BS, Moodie Z, et al. A Phase IIa Randomized Clinical Trial of a Multiclade HIV-1 DNA Prime Followed by a Multiclade Rad5 HIV-1 Vaccine Boost in Healthy Adults (Hvtn204). *PloS One* (2011) 6:e21225. doi: 10.1371/journal.pone.0021225
52. Chung AW, Kumar MP, Arnold KB, Yu WH, Schoen MK, Dunphy LJ, et al. Dissecting Polyclonal Vaccine-Induced Humoral Immunity Against HIV Using Systems Serology. *Cell* (2015) 163:988–98. doi: 10.1016/j.cell.2015.10.027
53. Brouwer KC, Lal RB, Mirel LB, Yang C, Van Eijk AM, Ayisi J, et al. Polymorphism of Fc Receptor IIa for IgG in Infants Is Associated With Susceptibility to Perinatal HIV-1 Infection. *AIDS* (2004) 18:1187–94. doi: 10.1097/00002030-200405210-00012
54. Milligan C, Overbaugh J. The Role of Cell-Associated Virus in Mother-To-Child HIV Transmission. *J Infect Dis* (2014) 210(Suppl 3):S631–640. doi: 10.1093/infdis/jiu344
55. Lassauniere R, Musekiwa A, Gray GE, Kuhn L, Tiemessen CT. Perinatal HIV-1 Transmission: Fc Gamma Receptor Variability Associates With Maternal Infectiousness and Infant Susceptibility. *Retrovirology* (2016) 13:40. doi: 10.1186/s12977-016-0272-y
56. Milligan C, Richardson BA, John-Stewart G, Nduati R, Overbaugh J. FCGR2A and FCGR3A Genotypes in Human Immunodeficiency Virus Mother-To-Child Transmission. *Open Forum Infect Dis* (2015) 2:ofv149. doi: 10.1093/ofid/ofv149
57. Ebonwu J, Lassaunière R, Paximadis M, Goosen M, Strehlau R, Gray GE, et al. An HIV Vaccine Protective Allele in FCGR2C Associates With Increased Odds of Perinatal HIV Acquisition. *Front Immunol* (2021) 12:760571. doi: 10.3389/fimmu.2021.760571
58. Forthal DN, Landucci G, Bream J, Jacobson LP, Phan TB, Montoya B. FcgammaRIIa Genotype Predicts Progression of HIV Infection. *J Immunol* (2007) 179:7916–23. doi: 10.4049/jimmunol.179.11.7916
59. Weis JF, Mcclelland RS, Jaoko W, Mandaliya KN, Overbaugh J, Graham SM. Short Communication: Fc Gamma Receptors IIa and IIIa Genetic Polymorphisms Do Not Predict HIV-1 Disease Progression in Kenyan Women. *AIDS Res Hum Retroviruses* (2015) 31:288–92. doi: 10.1089/aid.2014.0209
60. Poonia B, Kijak GH, Pauza CD. High Affinity Allele for the Gene of FCGR3a Is Risk Factor for HIV Infection and Progression. *PloS One* (2010) 5:e15562. doi: 10.1371/journal.pone.0015562
61. Deepe RN, Kistner-Griffin E, Martin JN, Deeks SG, Pandey JP. Epistatic Interactions Between Fc (GM) and Fcγr Genes and the Host Control of Human Immunodeficiency Virus Replication. *Hum Immunol* (2012) 73:263–6. doi: 10.1016/j.humimm.2011.12.008
62. Lewis GK. Role of Fc-Mediated Antibody Function in Protective Immunity Against HIV-1. *Immunology* (2014) 142:46–57. doi: 10.1111/imm.12232
63. Carapito R, Mayr L, Molitor A, Verniquet M, Schmidt S , Tahar O, et al. A FcγRIIa Polymorphism Has a HLA-B57 and HLA-B27 Independent Effect on HIV Disease Outcome. *Genes Immun* (2020) 21:263–8. doi: 10.1038/s41435-020-0106-8
64. Su B, Dispinseri S, Iannone V, Zhang T, Wu H, Carapito R, et al. Update on Fc-Mediated Antibody Functions Against HIV-1 Beyond Neutralization. *Front Immunol* (2019) 10.2968 doi: 10.3389/fimmu.2019.02968
65. Roederer M, Quaye L, Mangino M, Beddall Margaret h, Mahnke Y, Chattopadhyay P, et al. The Genetic Architecture of the Human Immune System: A Bioresource for Autoimmunity and Disease Pathogenesis. *Cell* (2015) 161:387–403. doi: 10.1016/j.cell.2015.02.046
66. Van Der Heijden J, Nagelkerke S, Zhao X, Geissler J, Rispens T, Van Den Berg TK, et al. Haplotypes of Fcγriia and Fcγriiib Polymorphic Variants Influence IgG-Mediated Responses in Neutrophils. *J Immunol* (2014) 192:2715–21. doi: 10.4049/jimmunol.1203570
67. Phaahla NG, Lassauniere R, Da Costa Dias B, Waja Z, Martinson NA, Tiemessen CT. Chronic HIV-1 Infection Alters the Cellular Distribution of FcgammaRIIIa and the Functional Consequence of the FcgammaRIIIa-F158V Variant. *Front Immunol* (2019) 10:735. doi: 10.3389/fimmu.2019.00735
68. Corey L, Gilbert PB, Juraska M, Montefiori DC, Morris L, Karuna ST, et al. Two Randomized Trials of Neutralizing Antibodies to Prevent HIV-1 Acquisition. *N Engl J Med* (2021) 384:1003–14. doi: 10.1056/NEJMoa2031738
69. Teo A, Feng G, Brown GV, Beeson JG, Rogerson SJ. Functional Antibodies and Protection Against Blood-Stage Malaria. *Trends Parasitol* (2016) 32:887–98. doi: 10.1016/j.pt.2016.07.003
70. Boudreau CM, Alter G. Extra-Neutralizing FcR-Mediated Antibody Functions for a Universal Influenza Vaccine. *Front Immunol* (2019) 10:440. doi: 10.3389/fimmu.2019.00440
71. Vanderven HA, Kent SJ. The Protective Potential of Fc-Mediated Antibody Functions Against Influenza Virus and Other Viral Pathogens. *Immunol Cell Biol* (2020) 98:253–63. doi: 10.1111/imcb.12312
72. Van Erp EA, Luytjes W, Ferwerda G, Van Kasteren PB. Fc-Mediated Antibody Effector Functions During Respiratory Syncytial Virus Infection and Disease. *Front Immunol* (2019) 10:548. doi: 10.3389/fimmu.2019.00548
73. Natarajan H, Crowley AR, Butler SE, Xu S, Weiner JA, Bloch EM, et al. Markers of Polyfunctional SARS-CoV-2 Antibodies in Convalescent Plasma. *mBio* (2021) 12:e00765–00721. doi: 10.1128/mBio.00765-21
74. Liu Q, Fan C, Li Q, Zhou S, Huang W, Wang L, et al. Antibody-Dependent-Cellular-Cytotoxicity-Inducing Antibodies Significantly Affect the Post-Exposure Treatment of Ebola Virus Infection. *Sci Rep* (2017) 7:45552. doi: 10.1038/srep45552
75. Paquin-Proulx D, Gunn BM, Alrubayyi A, Clark DV, Creegan M, Kim D, et al. Associations Between Antibody Fc-Mediated Effector Functions and Long-Term Sequelae in Ebola Virus Survivors. *Front Immunol* (2021) 12:682120. doi: 10.3389/fimmu.2021.682120

Conflict of Interest: The authors declare that the research was conducted in the absence of any commercial or financial relationships that could be construed as a potential conflict of interest.

Publisher's Note: All claims expressed in this article are solely those of the authors and do not necessarily represent those of their affiliated organizations, or those of the publisher, the editors and the reviewers. Any product that may be evaluated in this article, or claim that may be made by its manufacturer, is not guaranteed or endorsed by the publisher.

frontiers in Immunology

ORIGINAL RESEARCH
published: 20 December 2021
doi: 10.3389/fimmu.2021.759688

Detection of Antibody Responses Against SARS-CoV-2 in Plasma and Saliva From Vaccinated and Infected Individuals

*Jéromine Klingler[1,2], Gregory S. Lambert[1], Vincenza Itri[1], Sean Liu[1], Juan C. Bandres[1,3], Gospel Enyindah-Asonye[1], Xiaomei Liu[1,2], Viviana Simon[1,4,5,6], Charles R. Gleason[4], Giulio Kleiner[4], Hsin-Ping Chiu[4], Chuan-Tien Hung[4], Shreyas Kowdle[4], Fatima Amanat[4,7], Benhur Lee[4], Susan Zolla-Pazner[1,4], Chitra Upadhyay[1] and Catarina E. Hioe[1,4,8]**

[1] Division of Infectious Diseases, Department of Medicine, Icahn School of Medicine at Mount Sinai, New York, NY, United States, [2] James J. Peters VA Medical Center, Bronx, NY, United States, [3] Infectious Diseases Section, James J. Peters VA Medical Center, Bronx, NY, United States, [4] Department of Microbiology, Icahn School of Medicine at Mount Sinai, New York, NY, United States, [5] Department of Pathology, Molecular and Cell Based Medicine Icahn School of Medicine at Mount Sinai, New York, NY, United States, [6] Global Health and Emerging Pathogen Institute, Icahn School of Medicine at Mount Sinai, New York, NY, United States, [7] Graduate School of Biomedical Sciences, Icahn School of Medicine at Mount Sinai, New York, NY, United States, [8] Research & Development Service, James J. Peters VA Medical Center, Bronx, NY, United States

OPEN ACCESS

Edited by:
Masakazu Kamata,
University of Alabama at Birmingham, United States

Reviewed by:
Bhrugu J. Yagnik,
Emory University, United States
Narayanaiah Cheedarla,
Emory University, United States

***Correspondence:**
Catarina E. Hioe
catarina.hioe@mssm.edu;
catarina.hioe@va.gov

Specialty section:
This article was submitted to Viral Immunology, a section of the journal Frontiers in Immunology

Received: 16 August 2021
Accepted: 29 November 2021
Published: 20 December 2021

Citation:
Klingler J, Lambert GS, Itri V, Liu S, Bandres JC, Enyindah-Asonye G, Liu X, Simon V, Gleason CR, Kleiner G, Chiu H-P, Hung C-T, Kowdle S, Amanat F, Lee B, Zolla-Pazner S, Upadhyay C and Hioe CE (2021) Detection of Antibody Responses Against SARS-CoV-2 in Plasma and Saliva From Vaccinated and Infected Individuals. Front. Immunol. 12:759688. doi: 10.3389/fimmu.2021.759688

Antibodies (Abs) are essential for the host immune response against SARS-CoV-2, and all the vaccines developed so far have been designed to induce Abs targeting the SARS-CoV-2 spike. Many studies have examined Ab responses in the blood from vaccinated and infected individuals. However, since SARS-CoV-2 is a respiratory virus, it is also critical to understand the mucosal Ab responses at the sites of initial virus exposure. Here, we examined plasma versus saliva Ab responses in vaccinated and convalescent patients. Although saliva levels were significantly lower, a strong correlation was observed between plasma and saliva total Ig levels against all SARS-CoV-2 antigens tested. Virus-specific IgG1 responses predominated in both saliva and plasma, while a lower prevalence of IgM and IgA1 Abs was observed in saliva. Antiviral activities of plasma Abs were also studied. Neutralization titers against the initial WA1 (D614G), B.1.1.7 (alpha) and B.1.617.2 (delta) strains were similar but lower against the B.1.351 (beta) strain. Spike-specific antibody-dependent cellular phagocytosis (ADCP) activities were also detected and the levels correlated with spike-binding Ig titers. Interestingly, while neutralization and ADCP potencies of vaccinated and convalescent groups were comparable, enhanced complement deposition to spike-specific Abs was noted in vaccinated versus convalescent groups and corresponded with higher levels of IgG1 plus IgG3 among the vaccinated individuals. Altogether, this study demonstrates the detection of Ab responses after vaccination or infection in plasma and saliva that correlate significantly, although Ig isotypic differences were noted. The induced plasma Abs

displayed Fab-mediated and Fc-dependent functions with comparable neutralization and ADCP potencies, but a greater capacity to activate complement was elicited upon vaccination.

Keywords: SARS-CoV-2, COVID-19, vaccination, antibody isotypes, neutralization, ADCP, complement fixation, saliva

INTRODUCTION

Antibodies (Abs) are an essential component of the immune responses against coronavirus disease-2019 (COVID-19). In the USA, three COVID-19 vaccines have received an authorization for emergency use from the FDA: two messenger RNA (mRNA) vaccines from Pfizer-BioNTech (BNT162b2) and Moderna (mRNA-1273), and one adenovirus-vectored vaccine from Johnson & Johnson/Janssen (Ad26.CoV2.S). All three vaccines are designed to induce Abs targeting SARS-CoV-2 spike (1, 2), a membrane-anchored protein on the viral surface that contains the receptor-binding domain (RBD) necessary for binding and entry into the host cells (3–5). Other vaccines utilized in other countries also function to generate Abs against SARS-CoV-2 spike protein (6). In addition, several monoclonal Abs targeting spike protein are under development (7), and three have been authorized for emergency use by the FDA for the treatment of mild to moderate non-hospitalized COVID-19 patients: REGEN-COV (Casirivimab with Imdevimab), Eli Lilly (Bamlanivimab and Etesevimab) and Vir Biotechnology/ GlaxoSmithKline (Sotrovimab).

Many studies have evaluated Ab responses against SARS-CoV-2 elicited by infection or vaccination, but most examined Abs in the blood. Considering that SARS-CoV-2 is a respiratory virus, Abs in the mucosal sites would serve as the frontline defense against this virus; however, limited data are currently available. Similarities and differences have been noted in the distribution of Ig isotypes in the blood and mucosal tissues. The primary Abs found in the blood are IgG, representing ~75% of serum Ig. Among the four IgG subtypes, IgG1 and IgG2 comprise 66% and 23% of IgG, whereas IgG3 and IgG4 are minor components (<10% each). IgM and IgA are also abundant in blood and constitute 10% to 15% of serum Ig. IgA is the major Ab isotype of the mucosal immune system and exists as IgA1 and IgA2 (8). Of these two subtypes, IgA1 Abs predominate in both serum and secretions, but IgA2 percentages are higher in secretions than in serum. Consistent with this information, our previous study demonstrated that anti-spike Ab responses in convalescent plasma collected 1-2 months post-infection, were dominated by IgG1, although the levels varied tremendously among subjects (9). Variable levels of IgM and IgA1 were also detected and constituted the prominent Ig isotypes in some individuals. Other studies have shown that SARS-CoV-2-specific IgG, IgM and IgA responses could be detected in serum and saliva from COVID-19 patients, even though IgM and IgA declined more rapidly (10–12). However, the isotypes of vaccine-elicited Ab responses in mucosa have not been studied so far.

While the primary antiviral function of Abs is to neutralize virions, Abs also have non-neutralizing effector functions mediated *via* their Fc fragments. Virus-neutralizing activity was detected in IgG, IgM, and IgA fractions from COVID-19 convalescent plasma (9). COVID-19 vaccines also demonstrate the capacity to elicit potent neutralizing Ab responses (13–17). However, the full properties of Abs elicited by vaccination or infection are not yet known. In particular, limited data exists for Fc-mediated activities induced by vaccination which could play a role in vaccine efficacy (18). The binding of anti-spike Abs to virions, infected cells, or soluble spike proteins creates immune complexes capable of engaging Fc receptors (FcRs) or complement *via* the Abs' Fc fragments (19, 20). These interactions are determined by the Ig isotypes, as each isotype engages distinct FcRs and activates the complement system with varying potency (19, 21). The FcR engagement triggers a cascade of intracellular signals critical for Fc-mediated activities, including Ab-dependent cellular phagocytosis (ADCP) and Ab-dependent cellular cytotoxicity (ADCC). Binding of C1q, the first component in the classical complement pathway, to Fc fragments on immune complexes activates the downstream complement cascade, resulting in the deposition of C3 and C4 degradation products. Depositions initiates the generation of C5 convertase and the assembly of the membrane-attack complex which is responsible for complement-mediated lysis. Complement-opsonized immune complexes also interact with complement receptors on leukocytes to trigger effector functions, including complement-dependent cell-mediated phagocytosis and cytotoxicity (22, 23).

In this study, we assessed Ab responses elicited against different SARS-CoV-2 antigens from plasma and saliva samples collected from both vaccinated and convalescent donors using a multiplex bead assay that was developed in our previous study (9, 24). Saliva was used as a model for oral and upper respiratory mucosal secretions, and both saliva and blood specimens from each donor were obtained simultaneously. We further compared spike- and RBD-specific Ig isotypes in the same pairs of plasma and saliva samples. Additionally, vaccine- and infection-induced plasma Abs were examined for virus neutralization and Fc-dependent functions that included ADCP, C1q binding and C3d deposition. This study provides evidence for distinct SARS-CoV-2-specific Ig isotypes in plasma compared to saliva and differences in complement binding activities associated with Ig isotype profiles.

METHODS

Recombinant Proteins

SARS-CoV-2 spike and RBD proteins were produced as described (25, 26). S1, S2, and nucleoprotein antigens were

purchased from ProSci Inc, CA (#97-087, #97-079 and #97-085, respectively).

Human Specimens

Plasma and saliva specimens were obtained from volunteers enrolled in IRB-approved protocols at the Icahn School of Medicine at Mount Sinai (IRB#17-00060, IRB#19-01243) and the James J. Peter Veterans Affairs Medical Center (IRB#BAN-1604): RN#1, RN#4 and RV#1-5 after immunization; RP#2-5, 7, 12, 13 after infection; and four contemporaneous non-vaccinated COVID-19-negative subjects. Thirteen additional convalescent plasma samples (CVAP samples) were obtained from 134-229 days after symptom onset under the JJPVAMC Quality Improvement project "Evaluation of the clinical significance of two COVID-19 serologic assays". Post-immunization plasma were also collected from 20 participants in the longitudinal observational PARIS (Protection Associated with Rapid Immunity to SARS-CoV-2, IRB#20-03374) study. The clinical data are summarized in **Supplemental Tables 1** and **2**. All participants signed written consent forms prior to sample and data collection. All participants provided permission for sample banking and sharing. All samples were heat-inactivated before use.

Multiplex Bead Ab Binding Assay

Measurement of total Ig and Ig isotypes to SARS-CoV-2 antigen-coupled beads was performed as described (9). The quantification was based on MFI values at the designated sample dilutions. For total Ig responses, specimens were diluted 4-fold from 1:100 to 1:6,400 or 102,400 (plasma) or 2-fold from 1:2 to 1:16 (saliva), reacted with antigen-coated beads, and treated sequentially with biotinylated anti-human total Ig antibodies and PE-streptavidin. Titration curves were plotted for all antigens tested and the end-point titers were determined. The isotyping assays were performed at one dilution (1:200 for plasma, 1:4 for saliva) using human Ig isotype or subclass-specific secondary antibodies and the MFI values were shown. Complement deposition onto plasma Abs reactive with spike and RBD were measured according to (27) with modifications. For the C1q assay, beads with spike-Ab or RBD-Ab complexes were incubated with C1q Component from Human Serum (10 μg/mL, Sigma, #C1740) for 1 hour at room temperature, followed by an anti-C1q-PE antibody (Santa Cruz, #sc-53544 PE). For the C3d assay, Complement Sera Human (33.3%, Sigma, #S1764) was added to the beads for 1 hour at 37°C, followed by a biotinylated monoclonal anti-C3d antibody (Quidel, #A702). The relative levels of C1q and C3d deposition were obtained as MFI, from which titration curves were plotted and areas-under the curves (AUC) were calculated.

Virus Neutralization

Recombinant SARS-CoV-2 viruses encoding GFP and bearing SARS-CoV-2 spike proteins of the initial WA1 strain (D614G, designated WT), B.1.1.7 (alpha), B.1.351 (beta) or B.1.617.2 (delta) variants were used in neutralization assays as described (9, 28, 29). Virus infection in 293T-hACE2-TMPRSS2 cells initially seeded on collagen-coated 96-well plates was detected by GFP^+ cells. At 18-22 hours post infection, GFP counts were acquired by the Celigo imaging cytometer (Nexcelom Biosciences, version 4.1.3.0). Each condition was tested in duplicate.

ADCP

ADCP assays were performed using a reported protocol (30) with some modifications. FluoSpheres carboxylate-modified microspheres (Thermo Fisher, #F8823) were coupled with SARS-CoV-2 spike protein using the xMAP Antibody Coupling Kit (5 μg protein/~$36.4x10^9$ beads, Luminex #40-50016). Spike-conjugated microspheres were incubated with diluted plasma for 2 hours at 37°C in the dark. After washing and centrifugation (2,000 g, 10 minutes), the beads (~$3x10^8$ beads, 10 μL/well) were incubated with THP-1 cells ($0.25x10^5$ cells, 200 μL/well) for 16 hours. The samples were analyzed on an Attune NxT flow cytometer (Thermo Fisher, #A24858). Data analysis was performed using FCS Express 7 Research Edition (*De Novo* Software).

Statistical Analysis

Statistical analyses were performed as designated in the figure legends using GraphPad Prism 8 (GraphPad Software, San Diego, CA).

RESULTS

Detection of Plasma and Saliva Ab Responses to SARS-CoV-2 Antigens After Vaccination and Infection

Paired plasma and saliva specimens were collected from seven healthy recipients of COVID-19 mRNA vaccines and seven convalescent COVID-19 patients. Among vaccinees, two individuals received the Pfizer-BioNTech vaccine and five received the Moderna vaccine. Samples were collected 15-37 days after the second vaccine dose (**Supplemental Table 1A**). Convalescent patients presented with varying disease severity and donated samples 189-256 days post symptom onset (**Supplemental Table 1B**). In addition, samples from four COVID-19-negative non-vaccinated donors were tested in parallel and used to establish cut-off values.

Plasma and saliva samples were titrated for total Ig against SARS-CoV-2 spike, RBD, S1, S2, and nucleoprotein antigens. Bovine serum albumin (BSA) served as a negative control. Titration curves were plotted (**Supplemental Figure 1**), and the end-point titers were calculated (**Figure 1A**). All plasma specimens from vaccinated subjects exhibited titrating amounts of Ig against spike, RBD, S1 and S2 above the cut-off levels, although S2 reactivity was notably lower. As expected, reactivity was not observed against nucleoprotein, apart from one sample that showed weak reactivity slightly above the cut-off value. On the other hand, convalescent plasma samples displayed titrating Ig against spike, RBD, S1, S2 as well as nucleoprotein, and S2 reactivity was again the weakest. The presence of nucleoprotein-specific Abs differentiated convalescent from vaccinated subjects;

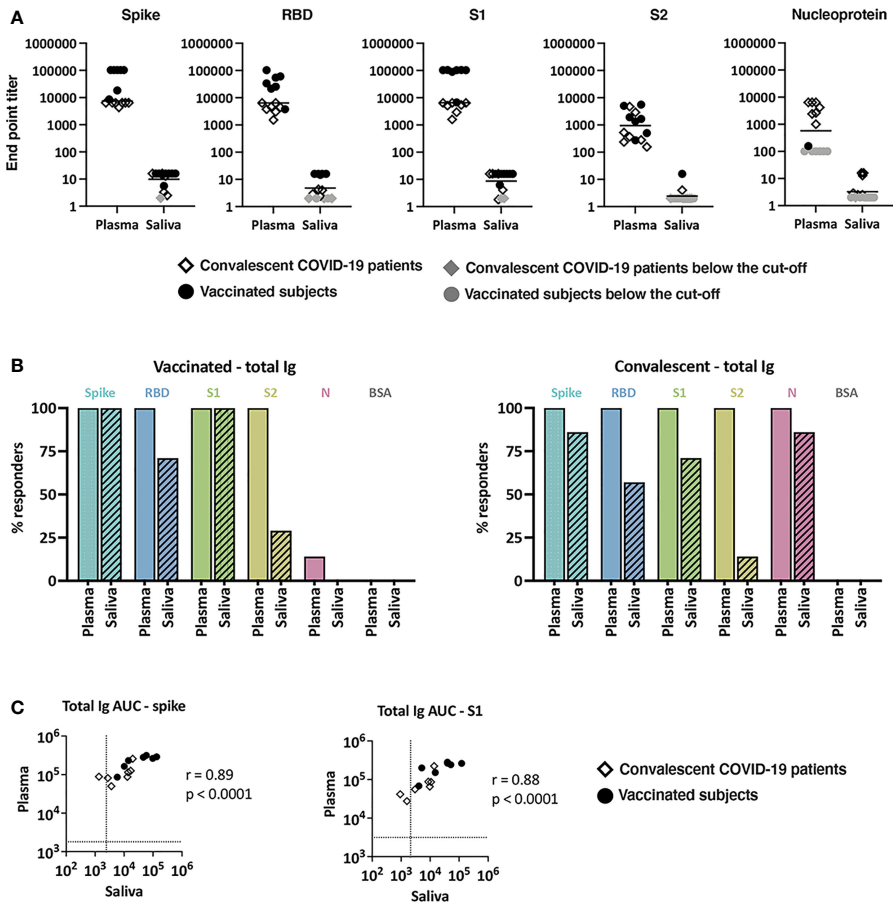

FIGURE 1 | Levels of SARS-CoV-2-specific total Ig in plasma and saliva. **(A)** Titers of antigen-specific total Ig in plasma versus saliva specimens from vaccinated donors and convalescent COVID-19 patients. End-point titers were calculated from reciprocal dilutions that reached the cut-off values (mean + 3SD of negative controls at the lowest dilution). Data points below the cut-off are shown at the lowest reciprocal dilutions (100 for plasma, 2 for saliva) as gray circles (vaccinated) or gray diamonds (convalescent). **(B)** The percentages of responders above cut-off for each antigen based on plasma versus saliva total Ig from seven vaccinated subjects (left panel) and seven convalescent COVID-19 patients (right panel). **(C)** Spearman correlation of spike- and S1-specific total Ig levels in plasma versus saliva from vaccinated and convalescent subjects. Areas under the curves (AUC) were calculated from the titration curves in **Supplemental Figure 1**. The dotted line indicates the cut-off value.

these antibodies were present in plasma from convalescent but not vaccinated subjects (**Figure 1A** and **Supplemental Figure 1**). Correlation analyses further indicated that the levels of Abs against spike and each of spike fragments (RBD, S1, S2) correlated well in both groups but no correlation was found between spike and nucleoprotein Ab levels (**Supplemental Figure 2**). A similar pattern of reactivity and correlation was seen with saliva samples (**Supplemental Figures 1**, **2**), albeit saliva titers were about 3 log lower compared to plasma titers (**Figure 1A**).

We then calculated the number of responders (i.e. number of individuals reaching levels above cut-offs) and found that 100% of vaccinated and convalescent subjects showed plasma Ig reactivity to spike, RBD, S1, and S2, and all convalescent subjects displayed plasma reactivity to nucleoprotein (**Figure 1B**). By contrast, only some vaccinated and convalescent subjects had positive saliva Ig reactivity. Five of the 7 saliva specimens from the vaccinated group exhibited Ig reactivity against RBD and 2 of the 7 against S2. Depending on the antigens, saliva Ig reactivity was also detected in one to six of the seven convalescent individuals. Nonetheless, the levels of total Ig in plasma and saliva correlated significantly for spike, S1, and other tested antigens (**Figure 1C** and data not shown).

Similarities and Differences in Ig Isotypes Against SARS-CoV-2 Spike and RBD Present in Plasma Versus Saliva From Vaccinated and Convalescent Subjects

The plasma and saliva specimens were subsequently evaluated for total Ig, IgM, IgG1-4, IgA1 and IgA2 against spike (**Figure 2A**) and RBD (**Supplemental Figure 3A**). Based on the titration data for total Ig (**Supplemental Figure 1**), plasma was tested at 1:200 dilution, while saliva was tested at 1:4 dilution. The percentage of responders for each isotype was determined using cut-off values, which were calculated as mean+3 standard deviations (SD) of the four negative specimens (**Figure 2B**).

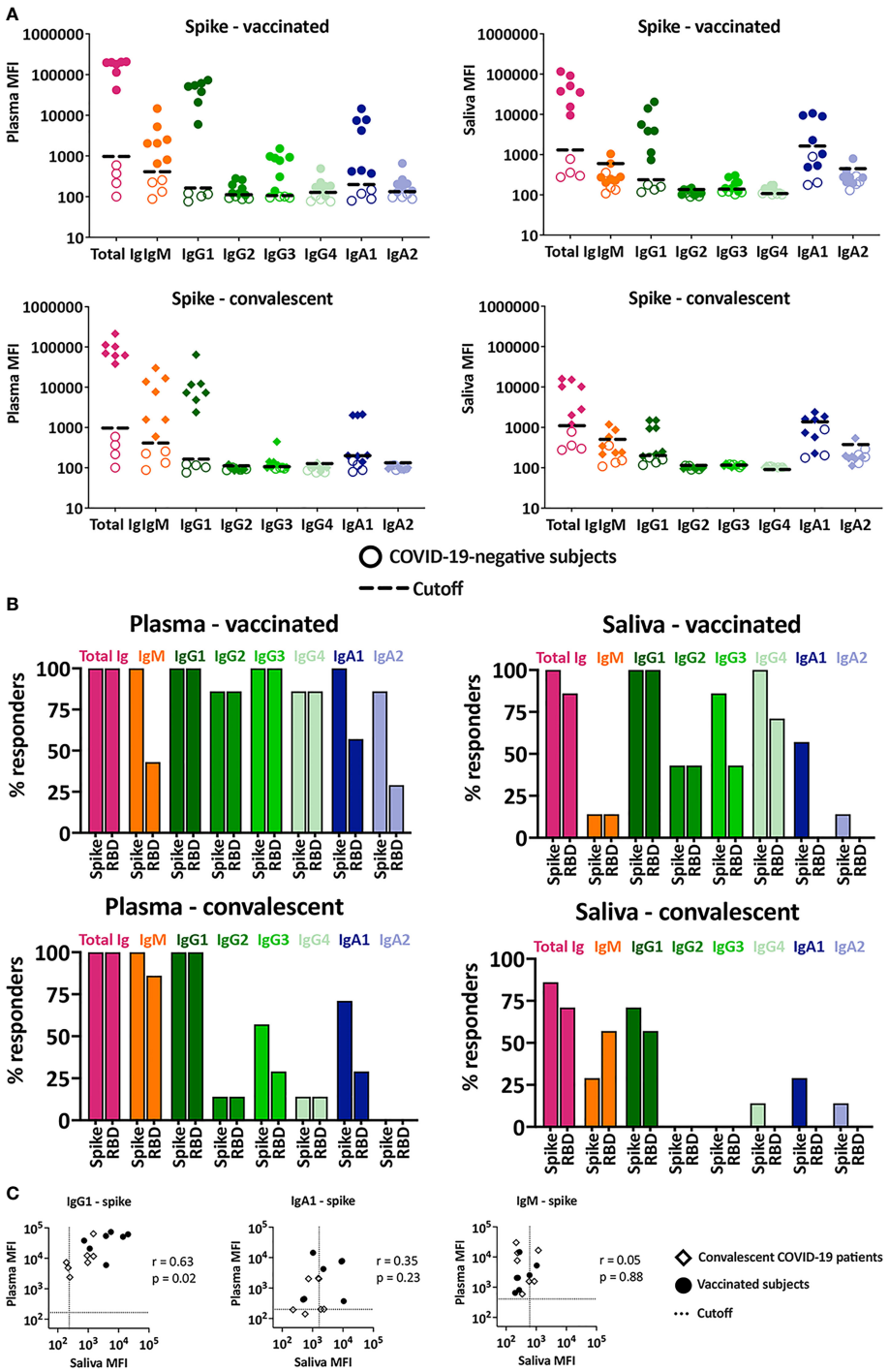

FIGURE 2 | Ig isotypes against SARS-CoV-2 spike and RBD in plasma versus saliva after vaccination and infection. **(A)** Total Ig, IgM, IgG1, IgG2, IgG3, IgG4, IgA1 and IgA2 levels against spike were measured in plasma (left) and saliva (right) specimens from vaccinated (top panels) and convalescent COVID-19 patients (lower panels). For controls, samples from four COVID-19-negative individuals (open symbols) were tested in parallel. The dotted line represents the cut-off calculated as mean of the four control specimens + 3SD for each isotype. **(B)** The percentages of responders among vaccinated (top panels) and convalescent subjects (lower panels) for each spike- or RBD-specific Ig isotype on the basis of plasma (left) and saliva (right) reactivity. **(C)** Spearman correlation between spike- and RBD-specific IgG1, IgA1 and IgM levels in plasma versus saliva from vaccinated and convalescent subjects.

All vaccinated and convalescent plasma specimens had detectable levels of total Ig, IgM, and IgG1 against spike (**Figures 2A, B**). Similar results were observed for RBD-specific total Ig and IgG1 (**Figure 2B** and **Supplemental Figure 3A**), while RBD-specific plasma IgM was detected in fewer samples due to high background (**Figure 2B** and **Supplemental Figure 3A**), in agreement with our previous findings (9). Saliva total Ig and IgG1 against spike and RBD were also detected in most vaccinated and convalescent subjects. Interestingly, although anti-spike IgM was present in plasma from all vaccine recipients and convalescent patients, saliva IgM was detected in only a few individuals and at low levels approaching background (**Figures 2A, B**), providing evidence for the discordance in IgM responses in saliva versus plasma.

A significant proportion (>86%) of plasma specimens from vaccinated subjects displayed IgG2, IgG3, and IgG4 Abs against spike and RBD (**Figure 2B**, top panels), albeit at relatively low levels compared to IgG1 (**Figure 2A**, top panels and **Supplemental Figure 3**). Low levels of these minor IgG subtypes were also detected in saliva from some vaccinees (>43%). In the convalescent group, the percentages of IgG2-4 responders were much lower (**Figure 2B**, bottom panels) and the levels were near the cut-offs in plasma and saliva (**Figure 2A**, bottom panels).

Of IgA subtypes, IgA1 predominated over IgA2 in both plasma and saliva samples. Among vaccinees, 100% had plasma IgA1 Abs against spike and 86% exhibited spike-specific IgA2, although IgA2 MFI values were near the cutoff (**Figures 2A, B**). Similar results were seen for RBD-specific IgA1 and IgA2, albeit with lower percent responders and higher cut-off values (**Figures 2A, B** and **Supplemental Figure 3A**). A comparable pattern was observed in convalescent plasma (**Figures 2A, B** bottom panels). The percentage of responders with specific IgA1 and IgA2 in saliva were surprisingly low. Saliva IgA1 against spike was detected in only 50% of vaccinees and 25% of convalescent patients. RBD-specific IgA1 and IgA2 against spike- and RBD were barely detected in saliva from vaccinated and convalescent subjects.

Correlation analysis of Ig isotypes in plasma versus saliva further revealed that IgG1 levels against both spike and RBD correlated strongly (**Figure 2C**). In contrast, no correlation was seen with IgM and IgA1, congruent with the differences noted in the percent IgM and IgA1 responders (**Figure 2B**). The correlation was sporadically observed for the other isotypes, but their MFI levels were near or below background (**Supplemental Figures 3B, C**).

In summary, Ab responses against spike, RBD, S1, and S2 were detected in plasma and saliva from both vaccinated and convalescent individuals, while Ab responses to nucleoprotein were detected in plasma and saliva of the convalescent group only. The dominant spike- and RBD-specific Ab isotype in saliva and plasma of both vaccinated and convalescent groups was IgG1, albeit the levels varied among individuals. IgM responses were prevalent in plasma of both vaccinated and convalescent groups but were not observed in most saliva samples. Induction of IgA1 predominated over IgA2 following vaccination and infection and was more prevalent in plasma than saliva.

Plasma Neutralizing Activities Against Wild Type Versus B.1.351, B.1.1.7 and B.1.617.2 Variants

Neutralizing activities by vaccine- and infection-induced plasma Abs were examined against WT and variant SARS-CoV-2 strains. Serially titrated specimens from seven vaccinated individuals, seven convalescent COVID-19, and three non-vaccinated COVID-19-negative controls were tested. Neutralization assays were performed using recombinant VSV (rVSV) expressing WT, B.1.1.7 (alpha), B.1.351 (beta), or B.1.617.2 (delta) spike proteins (29). The rVSV neutralization correlated strongly with live SARS-CoV-2 virus neutralization, demonstrating Spearman's r >0.9 across multiple studies (29). Control samples showed background neutralization below or near 50% against all four viruses. All samples from vaccinated and convalescent groups attained >50% neutralization against WT (**Figure 3A**). In fact, all achieved near or above 90% neutralization. Similar results were observed for neutralization against B.1.1.7 and B.1.617.2. In contrast, 2 vaccinee samples and 1 convalescent specimen did not reach 50% neutralization against the B.1.351 variant. The IC_{50} titers against B.1.351 were also lower than the titers against WT (6-fold change in median) (**Figure 3B**), while the titers against B.1.1.7, B.1.617.2 and WT were not similar (**Figure 3C**). Of note, no difference was apparent in IC_{50} titers of vaccinated versus convalescent subjects against all four strains.

Detection of Spike-Specific ADCP Activities in Plasma of All Vaccinated and Convalescent Donors

Because Ig isotypes are key determinants of Fc functions, we examined the Fc-mediated Ab activities in plasma specimens for both vaccinated and convalescent donors. Two Fc-dependent functions were evaluated: 1) spike-specific ADCP using THP-1 phagocytes and spike-coated fluorescent beads and 2) complement activation based on C1q and C3d deposition on spike-Ab and RBD-Ab complexes.

Spike-specific ADCP was detected above control in each of the specimens from all vaccinated and convalescent subjects (**Figures 4A, B**) and the levels corresponded with the spike-specific total Ig levels (**Figure 4C**). To assess the ADCP capacity and account for Ig level differences among samples, we calculated the AUC ratios of spike-specific ADCP over spike-binding total Ig. No difference between vaccinated and convalescent subjects was observed (**Figure 4D**). Of note, ADCP assays were performed with saliva samples, but no activity was detectable above background. When saliva was concentrated, ADCP was measurable in few specimens (data not shown), but the volumes of most samples were inadequate, precluding their assessment in this and other functional assays.

C1q and C3d Deposition on Spike- and RBD-Specific Abs in Plasma From Vaccinated and Convalescent Subjects

C1q and C3d deposition on antigen-Ab complexes was measured utilizing antigen-coupled bead assays. The data show variability

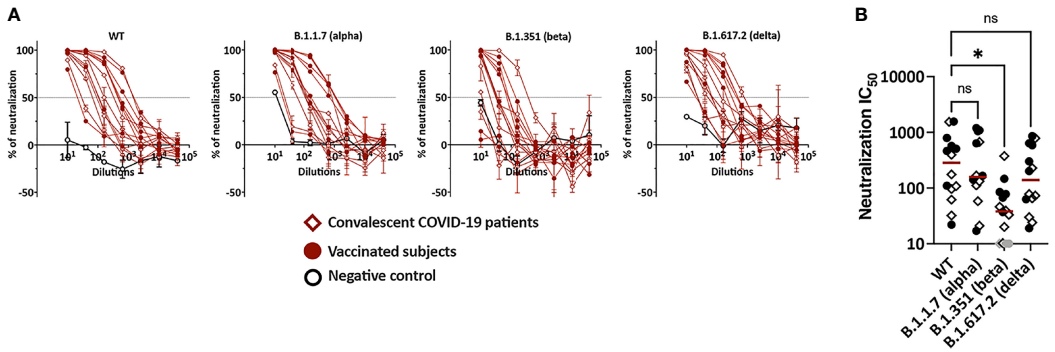

FIGURE 3 | Plasma neutralization activities against WT versus variants. **(A)** Neutralization of recombinant VSV viruses bearing the spike proteins of SARS-CoV-2 WT, B.1.531, B.1.1.7 or B.1.617.2 by plasma specimens from vaccinated and convalescent COVID-19 donors. Plasma samples from three COVID-19-negative individuals were tested in parallel; these negative control data are shown as mean + SD of replicates from all three samples. The dotted line indicates 50% neutralization. **(B)** Comparison of neutralization IC50 titers against WT versus B.1.351, B.1.1.7 and B.1.617.2. The specimens that did not reach 50% neutralization were shown as gray symbols at the lowest reciprocal dilution. Statistical analysis was performed using a Kruskal-Wallis test. *p <0.05; ns, non-significant. Red line: median.

in C1q and C3d binding to spike-bound plasma Abs from both vaccinated and convalescent groups (**Figures 5A, B**). C1q and C3d binding levels correlated strongly (**Figure 5C**). Interestingly, C1q and C3d deposition was detected only in one convalescent plasma sample and at low levels (**Figures 5A, B**). In the vaccinated group, one sample did not show any C1q or C3d binding to spike, and the remaining six exhibited a range of C1q and C3d binding levels above the control. Similar results were observed with C1q and C3d binding to RBD-specific plasma Abs (**Supplemental Figure 4**). The calculated ratios of C1q or C3d AUC to total Ig AUC further indicate higher capacity of vaccine-induced Abs to bind and activate complement (**Figure 5D**). These findings were supported by data from additional 20 vaccinated and 13 convalescent donors from separate cohorts, in which the greater capacity of vaccine-induced Abs to bind C1q and C3d was even more pronounced (**Figure 5E** and **Supplemental Figures 5** and **6**).

The differential complement binding activity is likely related to the relative levels of IgG subtypes generated by vaccination compared to infection. The IgG1 and IgG3 subtypes in particular have greater potency to activate the classical complement cascade (9). Indeed, the relative levels of IgG1+IgG3 over IgG2+IgG4 were higher in plasma from the vaccine group than the convalescent group (**Figure 2**). The low IgG3 levels were also observed with the larger cohort of convalescent plasma previously reported (9). To support this data, regression analyses were performed and showed that among the spike- and RBD-binding Ig isotypes tested, IgG1 and IgG3 Abs contributed most significantly to the complement binding activities (r^2 = 0.74-0.95, p <0.0001).

The functional properties of plasma Abs induced after vaccination versus natural infection are summarized in **Figure 6**. The heatmap clearly shows more potent complement activation in plasma from vaccinated versus convalescent groups, even though neutralization and ADCP potencies were indistinguishable.

DISCUSSION

This study provides evidence that plasma and saliva levels of Abs elicited after vaccination or infection correlate strongly. The data bolster previous findings showing that Abs against spike and nucleoprotein were similarly detected in plasma and saliva following SARS-CoV-2 infection (31). The total levels of Abs in saliva, however, were about 100-fold lower than in plasma. Consequently, lower percentages of responders were observed for saliva versus plasma Abs, with more notable differences for S2 which induces the lowest Ab titers among the five antigens tested. Nonetheless, saliva Abs against spike, RBD, and S1 were readily detected in the majority of vaccinated and convalescent groups, and saliva Abs against nucleoprotein were detectable in all convalescent individuals tested. While these data indicate the potential use of saliva for monitoring of anti-spike Ab responses in vaccinated and convalescent individuals, lower positive responses were detected, indicating the lower sensitivity of Ab detection in saliva. Differential Ig isotypes were also seen in saliva versus plasma, although the functional implications are unclear as the antiviral activities of saliva Abs have not been investigated.

Our isotyping analysis demonstrated that IgG1 is the dominant isotype in both plasma and saliva from all vaccinated individuals and convalescent patients. However, the IgM and IgA levels were lower in saliva versus plasma. This contrasts to recent findings in milk from convalescent mothers where the dominant spike-specific Ab responses were IgA and this response was not necessarily associated with induction of IgG or IgM Abs (32). However, after vaccination milk Ab responses were dominated by IgG (33). Our data further show that compared to natural infection, vaccination induces a higher prevalence for IgG2-4 Abs both in plasma and saliva, albeit at relatively low levels. Of note, 100% of plasma from vaccinated subjects had detectable spike and RBD-specific IgG3 Abs, while only 57% and 29% responders were observed for convalescent

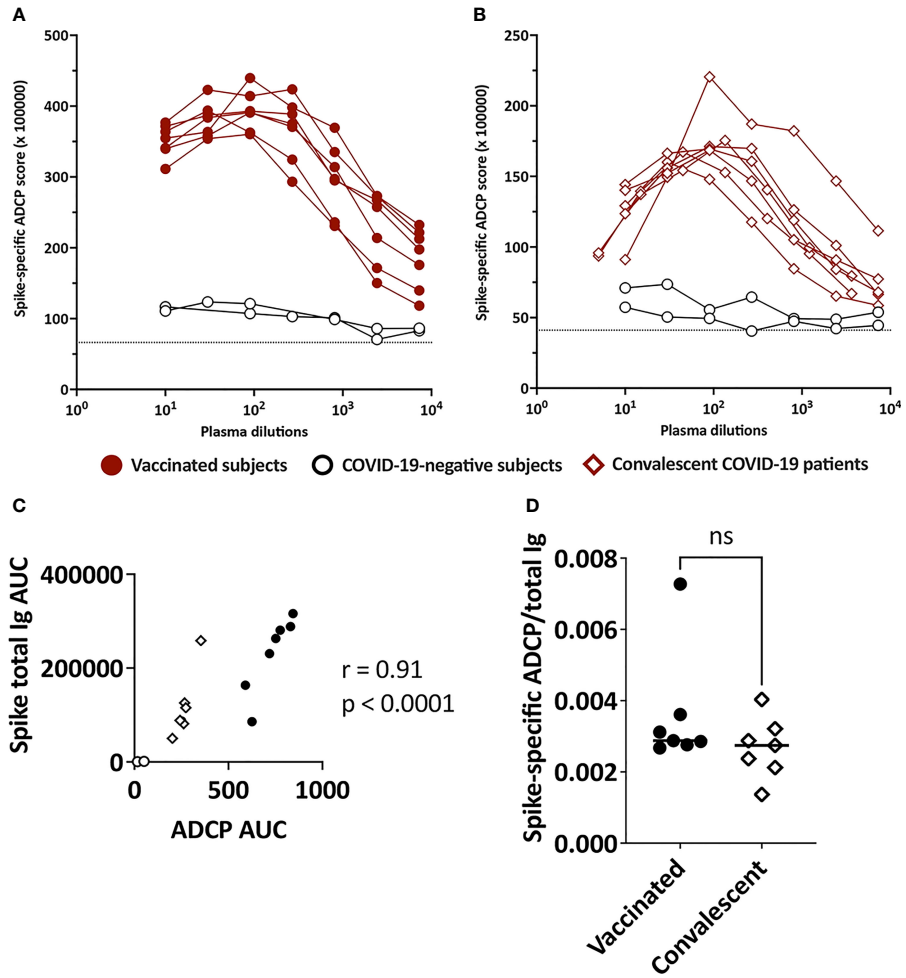

FIGURE 4 | ADCP activities in plasma of vaccinated and convalescent individuals. Spike-specific ADCP activities in plasma specimens from **(A)** vaccinated and **(B)** convalescent donors were tested along with two control plasma samples from COVID-19-negative individuals. ADCP was measured by flow cytometry after incubation of plasma-treated spike-coated fluorescent beads with THP-1 phagocytes. ADCP scores were calculated as % bead$^+$ cells × MFI of bead$^+$ cells. The dotted line indicates the background. **(C)** Correlation between spike-specific ADCP AUC and spike-specific total Ig AUC from the seven vaccinated individuals, seven convalescent patients and two negative controls. **(D)** Ratio of spike-specific ADCP AUC to spike-specific total Ig AUC from the seven vaccinated individuals and seven convalescent patients. ns, not significant ($p > 0.05$).

plasma, respectively. The samples tested in this study were obtained >189 days post symptom onset, but the pattern was similar to that seen in convalescent plasma collected earlier (<8 weeks post symptom onset, 7-17% responders for spike- and RBD-specific IgG3 Abs) (9), indicating that this IgG subtype profile is maintained throughout the observation period.

We examined the potential plasma neutralization against the initial Seattle WA1 strain (WT) and SARS-CoV-2 variants of concern (B.1.1.7, B.1.351, B.1.617.2), and observed potent neutralization activity against WT in each of the studied samples. In agreement with published reports (34, 35), weaker neutralization activities were seen against B.1.351 (beta), while neutralization of B1.1.7 (alpha) and B.1.617.2 (delta) was comparable to that of WT (36–39). No difference was seen in the IC_{50} titers against each of these four viruses between vaccine and convalescent groups. The neutralization titers against WT after vaccination were also similar to those of convalescent samples collected at earlier time points (<8 weeks after symptom onset) (9). The effects of these mutations on the non-neutralizing Fc-dependent functions are yet to be determined. Similar to neutralization, spike-specific ADCP activities were detected in plasma from all vaccinated and convalescent individuals. However, no correlation was observed between neutralization and ADCP activities (data not shown). Moreover, complement binding activities were distinct from neutralization and ADCP, suggesting that these functions may be mediated by distinct Ig populations or by Abs targeting different epitopes. The ability to thwart neutralization may offer an advantage to the transmissibility of these and other emerging variants, but the significance of Fc-mediated antiviral activities remains unclear.

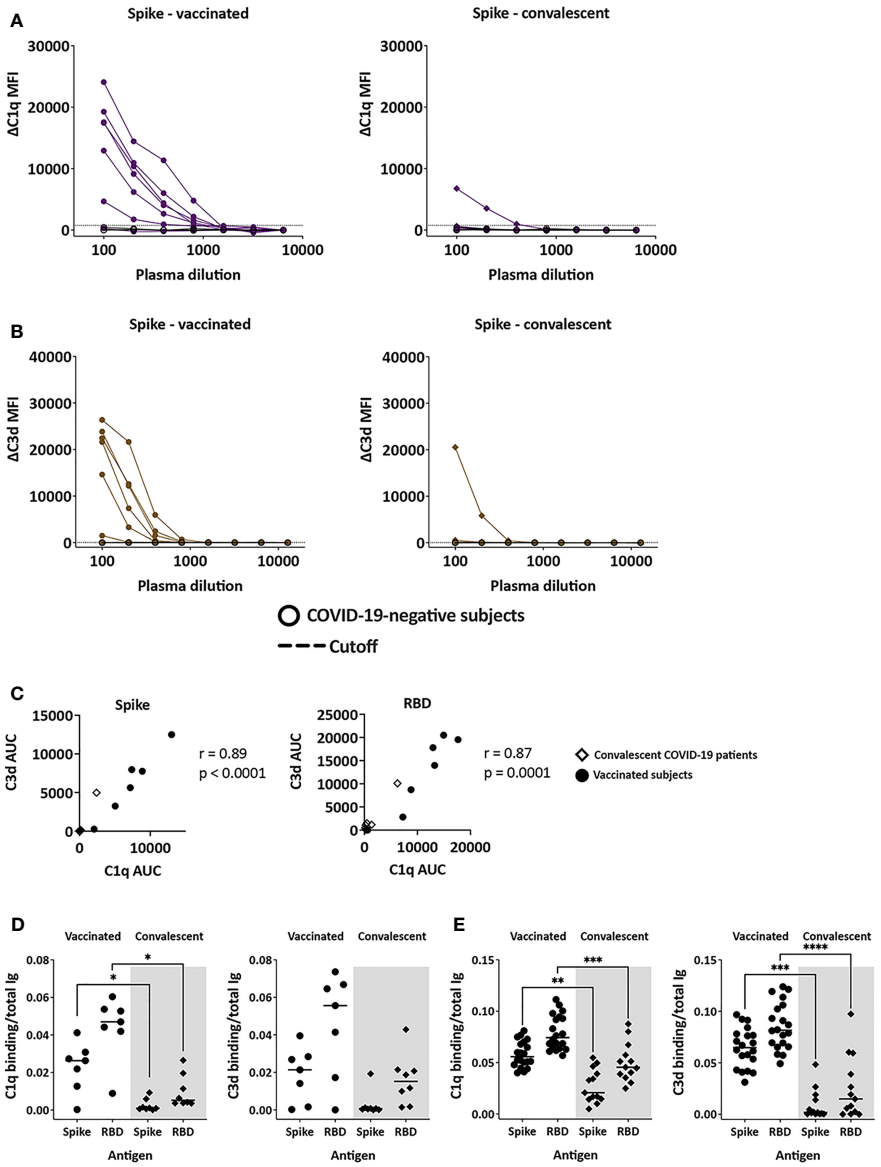

FIGURE 5 | Complement-binding activities in the plasma of vaccinated and convalescent individuals. **(A, B)** The binding of C1q **(A)** and C3d **(B)** to spike-specific Abs in plasma specimens from vaccinated (left) and convalescent (right) donors was assessed together with four COVID-19-negative controls in multiplex bead assays. Specimens were diluted 2-fold from 1:100 to 1:6,400 or 12,800. The dotted line represents the 100x dilution cut-off values calculated as mean + 3SD of the four control specimens. ΔC1q and ΔC3d MFI values were calculated by subtracting background MFI from each assay. **(C)** Spearman correlation between C1q AUC and C3d AUC values for spike- or RBD-specific Abs in plasma specimens from vaccinated and convalescent donors. **(D, E)** Ratio of C1q and C3d binding AUC to total Ig AUC of specimens from 7 vaccinated and 7 convalescent donors **(D)** and from additional 20 recipients of Pfizer or Moderna mRNA vaccines and 13 convalescent donors **(E)**. Statistical significance was assessed using a Kruskal-Wallis test (*p < 0.05, **p < 0.01, ***p < 0.001, ****p < 0.0001).

While neutralization and ADCP capacity induced by vaccination and infection were indistinguishable, vaccine-induced plasma Abs displayed a more robust ability to mediate complement binding and activation as compared to infection-induced counterparts. The differential potencies were apparent when Ab levels were considered and when comparison was made with infection-induced Abs from earlier or later time points (data not shown). Evaluation of more plasma samples independently collected from separate cohorts of vaccinated and convalescent donors revealed a consistent pattern with significantly greater capacities of vaccine-induced Abs to bind and activate complement. The mRNA vaccine-induced Ab responses were also reported in recent work with >8000 finger stick blood specimens to have higher seroconversion rates and greater cross-reactivity with SARS-CoV-1 and Middle Eastern respiratory syndrome (MERS)-CoV RBDs (40), implying the

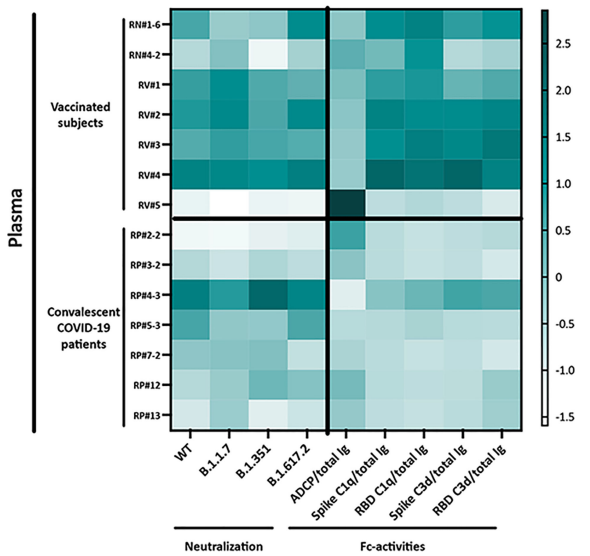

FIGURE 6 | Heatmap to show the relative levels of neutralization (IC_{50}) and Fc-mediated activities (ratios to total Ig) in plasma specimens from vaccinated and convalescent donors. Z-scores calculated for each Ab activity were used to generate the heatmap.

superior quality of vaccine-induced Ab responses. Greater complement deposition activity was associated with higher levels of IgG1 and IgG3, the two IgG subtypes with the highest potency for complement fixation. Nonetheless, our study was limited by its relatively small sample sizes that are also restricted to mRNA vaccine recipients and sample collection at only one time point, precluding us from evaluating Abs elicited by other types of vaccines and from assessing changes of vaccine-induced responses over time. Analysis of longitudinally collected specimens with a larger sample size from recipients of different COVID-19 vaccines are warranted to reach definitive conclusions.

In addition to Ig isotypes, a parameter known to influence complement binding is Fc glycosylation, as the removal of terminal galactose from IgG Fc glycans has been shown to decrease C1q binding and downstream classical complement activation without affecting FcγR-mediated functions (41, 42). Similarly, the sialylation of IgG Fc domains has been demonstrated to impair complement-dependent cytotoxicity (43). The Fc glycan compositions of vaccine- and infection-induced Abs are yet unknown. The importance of complement binding/activation for protection against SARS-CoV-2 also requires further investigation. It should be noted, however, that human neutralizing monoclonal Abs against SARS-CoV-2 requires a functional Fc region capable of binding complement and engaging FcγR for ADCP and ADCC, for optimal protection therapy (44).

In conclusion, this study demonstrated that saliva and plasma Ab responses against SARS-CoV-2 antigens were elicited following vaccination or infection. Ab responses in plasma and saliva correlated significantly, although Ig isotypic differences were noted between the vaccinated and convalescent individuals. Moreover, vaccination- and infection-induced plasma Abs exhibited Fab-mediated and Fc-dependent functions that included neutralization against WT and variants, phagocytosis, and complement activation. This study provide initial evidence for a superior potency of vaccine-induced Abs against spike to activate complement *via* the classical pathway, although the clinical significance of this function remains unclear and requires further investigation.

DATA AVAILABILITY STATEMENT

The raw data supporting the conclusions of this article will be made available by the authors, without undue reservation.

ETHICS STATEMENT

The studies involving human participants were reviewed and approved by IRB and review committees at the Icahn School of Medicine at Mount Sinai and the James J. Peter Veterans Affairs Medical Center. The patients/participants provided their written informed consent to participate in this study.

AUTHOR CONTRIBUTIONS

JK and CH wrote the manuscript. JK, GL, SZ-P, CU, and CH designed the experiments. JK, GL, VI, and XL performed the experiments and collected the data. JK, GL, BL, SZ-P, CU, and CH analyzed the data. H-PC, C-TH, SK, FA, and BL provided protocols, antigens, cells and virus stocks. GE-A, JB, and SL obtained specimens. VS, CG, and GK provided specimens. All authors read and approved the final manuscript.

FUNDING

This work was supported in part by the Department of Medicine of the Icahn School of Medicine at Mount Sinai Department of Medicine (to SZ-P and CH); the Department of Microbiology and the Ward-Coleman estate for endowing the Ward-Coleman Chairs at the Icahn School of Medicine at Mount Sinai (to BL), the Department of Veterans Affairs [Merit Review Grant I01BX003860] (to CH) and [Research Career Scientist Award 1IK6BX004607] (to CH); the National Institutes of Health [grant AI139290] to CH, [grants R01 AI123449, R21 AI1498033] to BL, [grant R01 AI140909] to CU; the NIAID Collaborative Influenza Vaccine Innovation Centers (CIVIC) [contract 75N93019C00051], NIAID Center of Excellence for Influenza Research and Surveillance (CEIRS) [contracts HHSN272201400008C and HHSN272201400006C], NIAID [grants U01AI141990 and U01AI150747], the generous support of the JPB Foundation and the Open Philanthropy Project [research grant 2020-215611[5384]] and anonymous donors to VS. The funders were not involved in the study design, collection, analysis, interpretation of data, the writing of this article or the decision to submit it for publication.

ACKNOWLEDGMENTS

We thank Dr. Florian Krammer for providing spike and RBD antigens, and all the donors for their contribution to the research. We would like to thank the expertise and assistance of Dr. Christopher Bare and the Dean's Flow Cytometry CORE at Mount Sinai. We would like to thank Rozita Emami-Gorizi and Jameel Z. Iqbal (James J. Peters VA Medical Center), the PARIS study team (Hala Alshammary, Angela A Amoako, Dalles Andre, Mahmoud H Awawda, Katherine F Beach, Maria C Bermúdez-González, Juan Manuel Carreno, Gianna Cai, Rachel L Chernet, Christian Cognigni, Karine David, Lily Q Eaker, Emily D Ferreri, Daniel L Floda, Hisaaki Kawabata, Florian Krammer, Giulio Kleiner, Neko Lyttle, Wanni A Mendez, Lubbertus C F Mulder, Ismail Nabeel, Annika Oostenink, Ariel Raskin, Aria Rooker, Kayla T Russo, Ashley Beathrese T Salimbangon, Miti Saksena, Amber S Shin, Gagandeep Singh, Viviana Simon, Levy A Sominsky, Komal Srivastava, Johnston Tcheou, Ania Wajnberg) and the Personalized Virology Initiative team at the Simon lab at Mount Sinai for the participants recruitment and sample processing.

SUPPLEMENTARY MATERIAL

The Supplementary Material for this article can be found online at: https://www.frontiersin.org/articles/10.3389/fimmu.2021.759688/full#supplementary-material

REFERENCES

1. Amanat F, Krammer F. SARS-CoV-2 Vaccines: Status Report. *Immunity* (2020) 52(4):583–9. doi: 10.1016/j.immuni.2020.03.007
2. Le TT, Andreadakis Z, Kumar A, Román RG, Tollefsen S, Saville M, et al. The COVID-19 Vaccine Development Landscape. *Nat Rev Drug Discov* (2020) 19:305–6. doi: 10.1038/d41573-020-00073-5
3. Yan R, Zhang Y, Li Y, Xia L, Guo Y, Zhou Q. Structural Basis for the Recognition of SARS-CoV-2 by Full-Length Human ACE2. *Science* (2020) 367:1444–8. doi: 10.1126/science.abb2762
4. Hoffmann M, Kleine-Weber H, Schroeder S, Krüger N, Herrler T, Erichsen S, et al. SARS-CoV-2 Cell Entry Depends on ACE2 and TMPRSS2 and Is Blocked by a Clinically Proven Protease Inhibitor. *Cell* (2020) 181:271–80.e8. doi: 10.1016/j.cell.2020.02.052
5. Walls AC, Park Y-J, Tortorici MA, Wall A, McGuire AT, Veesler D. Structure, Function, and Antigenicity of the SARS-CoV-2 Spike Glycoprotein. *Cell* (2020) 181:281–92.e6. doi: 10.1016/j.cell.2020.02.058
6. García-Montero C, Fraile-Martínez O, Bravo C, Torres-Carranza D, Sanchez-Trujillo L, Gómez-Lahoz AM, et al. An Updated Review of SARS-CoV-2 Vaccines and the Importance of Effective Vaccination Programs in Pandemic Times. *Vaccines* (2021) 9:433. doi: 10.3390/vaccines9050433
7. Marovich M, Mascola JR, Cohen MS. Monoclonal Antibodies for Prevention and Treatment of COVID-19. *JAMA* (2020) 324:131–2. doi: 10.1001/jama.2020.10245
8. Charles A Janeway J, Travers P, Walport M, Shlomchik MJ. The Mucosal Immune System, in: *Immunobiol Immune Syst Health Dis* (2001). Available at: https://www.ncbi.nlm.nih.gov/books/NBK27169/ (Accessed August 11, 2021).
9. Klingler J, Weiss S, Itri V, Liu X, Oguntuyo KY, Stevens C, et al. Role of IgM and IgA Antibodies in the Neutralization of SARS-CoV-2. *J Infect Dis* (2020) 223(6):957–70. doi: 10.1093/infdis/jiaa784
10. Isho B, Abe KT, Zuo M, Jamal AJ, Rathod B, Wang JH, et al. Persistence of Serum and Saliva Antibody Responses to SARS-CoV-2 Spike Antigens in COVID-19 Patients. *Sci Immunol* (2020) 5(52):eabe5511. doi: 10.1126/sciimmunol.abe5511
11. Sterlin D, Mathian A, Miyara M, Mohr A, Anna F, Claër L, et al. IgA Dominates the Early Neutralizing Antibody Response to SARS-CoV-2. *Sci Transl Med* (2021) 13:eabd2223. doi: 10.1126/scitranslmed.abd2223
12. Cervia C, Nilsson J, Zurbuchen Y, Valaperti A, Schreiner J, Wolfensberger A, et al. Systemic and Mucosal Antibody Responses Specific to SARS-CoV-2 During Mild Versus Severe COVID-19. *J Allergy Clin Immunol* (2021) 147:545–57.e9. doi: 10.1016/j.jaci.2020.10.040
13. Rogliani P, Chetta A, Cazzola M, Calzetta L. SARS-CoV-2 Neutralizing Antibodies: A Network Meta-Analysis Across Vaccines. *Vaccines* (2021) 9 (3):227. doi: 10.3390/vaccines9030227
14. Polack FP, Thomas SJ, Kitchin N, Absalon J, Gurtman A, Lockhart S, et al. Safety and Efficacy of the BNT162b2 mRNA Covid-19 Vaccine. *N Engl J Med* (2020) 383:2603–15. doi: 10.1056/NEJMoa2034577
15. Walsh EE, Frenck RW, Falsey AR, Kitchin N, Absalon J, Gurtman A, et al. Safety and Immunogenicity of Two RNA-Based Covid-19 Vaccine Candidates. *N Engl J Med* (2020) 383:2439–50. doi: 10.1056/NEJMoa2027906
16. Sahin U, Muik A, Derhovanessian E, Vogler I, Kranz LM, Vormehr M, et al. COVID-19 Vaccine BNT162b1 Elicits Human Antibody and TH1 T Cell Responses. *Nature* (2020) 586:594–9. doi: 10.1038/s41586-020-2814-7
17. Jackson LA, Anderson EJ, Rouphael NG, Roberts PC, Makhene M, Coler RN, et al. An mRNA Vaccine Against SARS-CoV-2 — Preliminary Report. *N Engl J Med* (2020) 0:null. doi: 10.1056/NEJMoa2022483
18. Tauzin A, Nayrac M, Benlarbi M, Gong SY, Gasser R, Beaudoin-Bussières G, et al. A Single Dose of the SARS-CoV-2 Vaccine BNT162b2 Elicits Fc-Mediated Antibody Effector Functions and T Cell Responses. *Cell Host Microbe* (2021) 29:1137–50.e6. doi: 10.1016/j.chom.2021.06.001
19. Bournazos S, Ravetch JV. Diversification of IgG Effector Functions. *Int Immunol* (2017) 29:303–10. doi: 10.1093/intimm/dxx025
20. Goldberg BS, Ackerman ME. Antibody-Mediated Complement Activation in Pathology and Protection. *Immunol Cell Biol* (2020) 98:305–17. doi: 10.1111/imcb.12324
21. Pincetic A, Bournazos S, DiLillo DJ, Maamary J, Wang TT, Dahan R, et al. Type I and Type II Fc Receptors Regulate Innate and Adaptive Immunity. *Nat Immunol* (2014) 15:707–16. doi: 10.1038/ni.2939
22. Kellner C, Otte A, Cappuzzello E, Klausz K, Peipp M. Modulating Cytotoxic Effector Functions by Fc Engineering to Improve Cancer Therapy. *Transfus Med Hemother Off Organ Dtsch Ges Transfusionsmed Immunhamatol* (2017) 44:327–36. doi: 10.1159/000479980
23. Lee C-H, Romain G, Yan W, Watanabe M, Charab W, Todorova B, et al. IgG Fc Domains That Bind C1q But Not Effector Fcγ Receptors Delineate the Importance of Complement-Mediated Effector Functions. *Nat Immunol* (2017) 18:889–98. doi: 10.1038/ni.3770
24. Weiss S, Klingler J, Hioe C, Amanat F, Baine I, Arinsburg S, et al. A High Through-Put Assay For Circulating Antibodies Directed Against The S Protein Of Severe Acute Respiratory Syndrome Coronavirus 2 (Sars-Cov-2). *J Infect Dis* (2020) 222(10):1629–34. doi: 10.1093/infdis/jiaa531
25. Amanat F, Stadlbauer D, Strohmeier S, Nguyen THO, Chromikova V, McMahon M, et al. A Serological Assay to Detect SARS-CoV-2 Seroconversion in Humans. *Nat Med* (2020) 26(7):1033–6. doi: 10.1038/s41591-020-0913-5
26. Stadlbauer D, Amanat F, Chromikova V, Jiang K, Strohmeier S, Arunkumar GA, et al. SARS-CoV-2 Seroconversion in Humans: A Detailed Protocol for a Serological Assay, Antigen Production, and Test Setup. *Curr Protoc Microbiol* (2020) 57:e100. doi: 10.1002/cpmc.100
27. Perez LG, Martinez DR, deCamp AC, Pinter A, Berman PW, Francis D, et al. V1V2-Specific Complement Activating Serum IgG as a Correlate of Reduced HIV-1 Infection Risk in RV144. *PloS One* (2017) 12:e0180720. doi: 10.1371/journal.pone.0180720
28. Oguntuyo KY, Stevens CS, Hung C-T, Ikegame S, Acklin JA, Kowdle SS, et al. Quantifying Absolute Neutralization Titers Against SARS-CoV-2 by a Standardized Virus Neutralization Assay Allows for Cross-Cohort Comparisons of COVID-19 Sera. *medRxiv* (2020) 12(1):e02492–20. doi: 10.1101/2020.08.13.20157222

29. Ikegame S, Siddiquey MNA, Hung C-T, Haas G, Brambilla L, Oguntuyo KY, et al. Neutralizing Activity of Sputnik V Vaccine Sera Against SARS-CoV-2 Variants. *Nat Commun* (2021) 12:4598. doi: 10.1038/s41467-021-24909-9
30. Balasubramanian P, Williams C, Shapiro MB, Sinangil F, Higgins K, Nádas A, et al. Functional Antibody Response Against V1V2 and V3 of HIV Gp120 in the VAX003 and VAX004 Vaccine Trials. *Sci Rep* (2018) 8:542. doi: 10.1038/s41598-017-18863-0
31. Pisanic N, Randad PR, Kruczynski K, Manabe YC, Thomas DL, Pekosz A, et al. COVID-19 Serology at Population Scale: SARS-CoV-2-Specific Antibody Responses in Saliva. *J Clin Microbiol* (2020) 59(1):e02204–20. doi: 10.1128/JCM.02204-20
32. Fox A, Marino J, Amanat F, Krammer F, Hahn-Holbrook J, Zolla-Pazner S, et al. Robust and Specific Secretory IgA Against SARS-CoV-2 Detected in Human Milk. *iScience* (2020) 23:101735. doi: 10.1016/j.isci.2020.101735
33. Fox A, Norris C, Amanat F, Zolla-Pazner S, Powell RL. The Vaccine-Elicited Immunoglobulin Profile in Milk After COVID-19 mRNA-Based Vaccination Is IgG-Dominant and Lacks Secretory Antibodies. *medRxiv* (2021) 2021.03.22.21253831. doi: 10.1101/2021.03.22.21253831
34. Trombetta CM, Marchi S, Viviani S, Manenti A, Benincasa L, Ruello A, et al. Serum Neutralizing Activity Against B.1.1.7, B.1.351 and P.1 SARS-CoV-2 Variants of Concern in Hospitalized COVID-19 Patients. *Viruses* (2021) 13:1347. doi: 10.3390/v13071347
35. Jangra S, Ye C, Rathnasinghe R, Stadlbauer D, Krammer F, Simon V, et al. SARS-CoV-2 Spike E484K Mutation Reduces Antibody Neutralisation. *Lancet Microbe* (2021) 2:e283–4. doi: 10.1016/S2666-5247(21)00068-9
36. Bian L, Gao F, Zhang J, He Q, Mao Q, Xu M, et al. Effects of SARS-CoV-2 Variants on Vaccine Efficacy and Response Strategies. *Expert Rev Vaccines* (2021) 20(4):1–9. doi: 10.1080/14760584.2021.1903879
37. Bates TA, Leier HC, Lyski ZL, McBride SK, Coulter FJ, Weinstein JB, et al. Neutralization of SARS-CoV-2 Variants by Convalescent and Vaccinated Serum. *medRxiv* (2021) 12(1):135. doi: 10.1101/2021.04.04.21254881
38. Carreño JM, Alshammary H, Singh G, Raskin A, Amanat F, Amoako A, et al. Evidence for Retained Spike-Binding and Neutralizing Activity Against Emerging SARS-CoV-2 Variants in Serum of COVID-19 mRNA Vaccine Recipients. *EBioMedicine* (2021) 73:103626. doi: 10.1016/j.ebiom.2021.103626
39. Dupont L, Snell LB, Graham C, Seow J, Merrick B, Lechmere T, et al. Neutralizing Antibody Activity in Convalescent Sera From Infection in Humans With SARS-CoV-2 and Variants of Concern. *Nat Microbiol* (2021) 6(11):1433–42. doi: 10.1038/s41564-021-00974-0
40. Assis R, Jain A, Nakajima R, Jasinskas A, Kahn S, Palma A, et al. Substantial Differences in SARS-CoV-2 Antibody Responses Elicited by Natural Infection and mRNA Vaccination. *bioRxiv* (2021) 6(1):132. doi: 10.1101/2021.04.15.440089
41. Hodoniczky J, Zheng YZ, James DC. Control of Recombinant Monoclonal Antibody Effector Functions by Fc N-Glycan Remodeling *In Vitro*. *Biotechnol Prog* (2005) 21:1644–52. doi: 10.1021/bp050228w
42. Boyd PN, Lines AC, Patel AK. The Effect of the Removal of Sialic Acid, Galactose and Total Carbohydrate on the Functional Activity of Campath-1h. *Mol Immunol* (1995) 32:1311–8. doi: 10.1016/0161-5890(95)00118-2
43. Quast I, Keller CW, Maurer MA, Giddens JP, Tackenberg B, Wang L-X, et al. Sialylation of IgG Fc Domain Impairs Complement-Dependent Cytotoxicity. *J Clin Invest* (2015) 125:4160–70. doi: 10.1172/JCI82695
44. Winkler ES, Gilchuk P, Yu J, Bailey AL, Chen RE, Chong Z, et al. Human Neutralizing Antibodies Against SARS-CoV-2 Require Intact Fc Effector Functions for Optimal Therapeutic Protection. *Cell* (2021) 184:1804–1820.e16. doi: 10.1016/j.cell.2021.02.026

Conflict of Interest: The Icahn School of Medicine at Mount Sinai has filed patent applications relating to SARS-CoV-2 serological assays and listed VS as co-inventor. Mount Sinai has spun out a company, Kantaro, to market serological tests for SARS-CoV-2.

The remaining authors declare that the research was conducted in the absence of any commercial or financial relationships that could be construed as a potential conflict of interest.

Publisher's Note: All claims expressed in this article are solely those of the authors and do not necessarily represent those of their affiliated organizations, or those of the publisher, the editors and the reviewers. Any product that may be evaluated in this article, or claim that may be made by its manufacturer, is not guaranteed or endorsed by the publisher.

frontiers in Immunology

ORIGINAL RESEARCH
published: 06 January 2022
doi: 10.3389/fimmu.2021.787603

Structure and Fc-Effector Function of Rhesusized Variants of Human Anti-HIV-1 IgG1s

*William D. Tolbert[1], Dung N. Nguyen[1], Marina Tuyishime[2,3,4], Andrew R. Crowley[5], Yaozong Chen[1], Shalini Jha[2,3], Derrick Goodman[2,3,4], Valerie Bekker[2,3,4], Sarah V. Mudrak[2,3,4], Anthony L. DeVico[6], George K. Lewis[6], James F. Theis[7], Abraham Pinter[7], M. Anthony Moody[3,8], David Easterhoff[3], Kevin Wiehe[3,9], Justin Pollara[2,3,4], Kevin O. Saunders[2,3], Georgia D. Tomaras[2,3,4], Margaret Ackerman[5], Guido Ferrari[2,3,4] and Marzena Pazgier[1]**

[1] Infectious Disease Division, Department of Medicine of Uniformed Services University of the Health Sciences, Bethesda, MD, United States, [2] Department of Surgery, Duke University School of Medicine, Durham, NC, United States, [3] Human Vaccine Institute, Duke University School of Medicine, Durham, NC, United States, [4] Center for Human Systems Immunology, Duke University School of Medicine, Durham, NC, United States, [5] Thayer School of Engineering, Dartmouth College, Hanover, NH, United States, [6] Division of Vaccine Research, Institute of Human Virology, University of Maryland School of Medicine, Baltimore, MD, United States, [7] Public Health Research Institute, New Jersey Medical School, Rutgers University, Newark, NJ, United States, [8] Department of Pediatrics, Duke University School of Medicine, Durham, NC, United States, [9] Department of Medicine, Duke University School of Medicine, Durham, NC, United States*

OPEN ACCESS

Edited by:
Constantinos Petrovas, Centre Hospitalier Universitaire Vaudois (CHUV), Switzerland

Reviewed by:
Morgane Bomsel, Centre National de la Recherche Scientifique (CNRS), France
Bruce David Wines, Burnet Institute, Australia

***Correspondence:**
Marzena Pazgier
marzena.pazgier@usuhs.edu

Specialty section:
This article was submitted to Viral Immunology, a section of the journal Frontiers in Immunology

Received: *01 October 2021*
Accepted: *09 December 2021*
Published: *06 January 2022*

Citation:
Tolbert WD, Nguyen DN, Tuyishime M, Crowley AR, Chen Y, Jha S, Goodman D, Bekker V, Mudrak SV, DeVico AL, Lewis GK, Theis JF, Pinter A, Moody MA, Easterhoff D, Wiehe K, Pollara J, Saunders KO, Tomaras GD, Ackerman M, Ferrari G and Pazgier M (2022) Structure and Fc-Effector Function of Rhesusized Variants of Human Anti-HIV-1 IgG1s. Front. Immunol. 12:787603. doi: 10.3389/fimmu.2021.787603

Passive transfer of monoclonal antibodies (mAbs) of human origin into Non-Human Primates (NHPs), especially those which function predominantly by a Fc-effector mechanism, requires an *a priori* preparation step, in which the human mAb is reengineered to an equivalent NHP IgG subclass. This can be achieved by changing both the Fc and Fab sequence while simultaneously maintaining the epitope specificity of the parent antibody. This Ab reengineering process, referred to as rhesusization, can be challenging because the simple grafting of the complementarity determining regions (CDRs) into an NHP IgG subclass may impact the functionality of the mAb. Here we describe the successful rhesusization of a set of human mAbs targeting HIV-1 envelope (Env) epitopes involved in potent Fc-effector function against the virus. This set includes a mAb targeting a linear gp120 V1V2 epitope isolated from a RV144 vaccinee, a gp120 conformational epitope within the Cluster A region isolated from a RV305 vaccinated individual, and a linear gp41 epitope within the immunodominant Cys-loop region commonly targeted by most HIV-1 infected individuals. Structural analyses confirm that the rhesusized variants bind their respective Env antigens with almost identical specificity preserving epitope footprints and most antigen-Fab atomic contacts with constant regions folded as in control RM IgG1s. In addition, functional analyses confirm preservation of the Fc effector function of the rhesusized mAbs including the ability to mediate Antibody Dependent Cell-mediated Cytotoxicity (ADCC) and antibody dependent cellular phagocytosis

by monocytes (ADCP) and neutrophils (ADNP) with potencies comparable to native macaque antibodies of similar specificity. While the antibodies chosen here are relevant for the examination of the correlates of protection in HIV-1 vaccine trials, the methods used are generally applicable to antibodies for other purposes.

Keywords: antibody engineering, rhesusization, Fc-effector function, non-human primates, HIV

INTRODUCTION

The only vaccine to show efficacy although limited against HIV-1 infection has been the RV144 vaccine trial in Thailand consisting of a canarypox ALVAC-HIV DNA prime and AIDSVAX B/E protein boost which showed an overall efficacy of 31.2% against HIV-1 acquisition (1). Secondary analyses of correlates of reduced risk of infection revealed the role played by antibody-dependent cellular-cytotoxicity (ADCC) and Fc effector functions against HIV-1 Env in the absence of high levels of Env-specific serum IgA (2–5). Breakthrough infections showed vaccine pressure on the V2 loop region of Env which could be seen by sequence changes in V2 (6–9). Many attempts to reproduce this protective effect with the same or similar vaccine regimens have succeeded in non-human primates (NHP) (10–18), but a study in humans did not show efficacy, potentially due to differences in adjuvant (MF59 vs. alum), and subtype and sequences of the immunogens (subtype C vs AE) (19, 20). While still under investigation, additional reasons for this discordance may include differences in the circulating strains in human populations versus those in NHP challenge stocks and most importantly, human-NHP interspecies differences in host genetics that may contribute to the type, magnitude, functionality and duration of the induced immune response. However, the HVTN 505 HIV-1 clinical efficacy trial consisting of a DNA and Adenovirus 5 vaccine regimen, despite lacking overall efficacy, did show a correlation between anti-Env serum IgG3, antibody dependent cellular phagocytosis (ADCP) and *in vitro* FcγRIIa engagement and a reduced risk of HIV-1 infection as well as a correlation between FcγRIIa engagement and a decreased viral load setpoint in breakthrough vaccinees (21), indicating that strategies to induce more potent antibody Fc effector functions in a greater proportion of vaccinees are needed.

Rhesus macaque (RM), *Macaca mulatta*, the most often used primate in NHP studies, shares approximately 93% genome identity with humans, but that high degree of similarity breaks down in immune system genes. There are significant differences in immunoglobulin (IgG) subclasses, Fc receptor diversity and Fcγ receptor (FcγR) expression patterns between human and RM that complicate the translation of experimental results in RM to humans (22–24). RM IgG subclasses are in general more similar to each other than are their human counterparts; both macaques and humans have four IgG subclasses, but macaques lack highly divergent subclasses such as human IgG3 with its long repetitive hinge region. Macaques also lack an FcγRIIIb gene which was the result of a gene duplication event that occurred after the divergence of macaques from other higher primates (25); humans have a FcγRIIIa and a FcγRIIIb receptor while macaques only have a FcγRIIIa receptor. Both have FcγRIIa (activating) and FcγRIIb (inhibitory) receptors. Although human IgGs can bind macaque FcγRs, these and other differences change the Fc/FcγR functional landscape between the two species.

Given the difficulty in reproducing RV144 vaccine limited efficacy results in other vaccine trials, it is important to be able to define mechanistic aspects of the correlates of protection conferred by the human vaccine in NHP. This is typically done for antibodies cloned from HIV-1 infected or vaccinated individuals by passive transfer of the monoclonal antibody (mAb) or mAb mix into NHP followed by a viral challenge to test its ability to protect against infection or to provide post-infection control. Many NHP passive transfer trials have been used to successfully test antibodies that function predominately by neutralization, where an Fc effector mismatch is less of an issue (26–28). In these studies, a mAb of human origin is directly transferred into NHP without reengineering to the equivalent RM IgG subclass. Although convenient, such approaches potentially suffer from anti-drug antibody (ADA) responses that can quickly remove species mismatched antibodies from circulation, thereby abrogating any functional effect. The longer the duration of the trial, the higher the probability of inducing such responses becomes (29). Furthermore, passive transfer testing of mAbs that function predominately by Fc-effector mechanisms, such as those from the RV144 trial, require both a minimization of the ADA response and a match of the Fc of the infused antibody to that of the host to more accurately mirror what is happening in macaque immunization trials. For human mAbs to be tested in RM this means rhesusization of both the Fc and Fab while simultaneously maintaining epitope specificity.

Here we describe a successful attempt to rhesusize a set of human mAbs targeting HIV-1 Env epitopes involved in potent Fc-effector mechanisms. This set includes a mAb targeting the linear gp120 V1V2 epitope isolated from a RV144 vaccinee (30), a gp120 conformational epitope within the Cluster A region isolated from a RV305 vaccinated individual, a RV144 vaccinee who had further boosts with RV144 immunogens in the RV305 vaccine trial that was designed to test if correlates of protection in RV144 could be boosted in RV144 vaccinees (31), and a linear gp41 epitope within the immunodominant Cys-loop region commonly targeted by most HIV-1 infected individuals (32). Antibodies binding to these three regions have been implicated in protection from infection from HIV-1, but not in neutralization of the virus. Structural analyses confirm that the rhesusized variants bind their respective Env antigens with almost identical specificity as their human counterparts—preserving epitope footprints and most antigen-Fab atomic

contacts with constant regions folded as in control RM IgG1. Functional analyses confirm their Fc effector functionality, including the ability to mediate Antibody Dependent Cell-mediated Cytotoxicity (ADCC), Antibody Dependent Cellular Phagocytosis by monocytes (ADCP), and Antibody Dependent Cellular Phagocytosis by neutrophils (ADNP) with potencies comparable to native macaque antibodies of similar specificity. This will facilitate the testing of their impact on the virus in the future in an animal model. While the antibodies chosen here are relevant for examining the correlates of protection in HIV-1 trials the methods used are generally applicable to antibodies for other purposes.

MATERIAL AND METHODS

Rhesusization of Antibodies

Human variable regions were rhesusized as previously described with minor modifications (33). For each human antibody sequence of interest, we used the immunogenetics sequence analysis software Cloanalyst (https://www.bu.edu/computationalimmunology/research/software) to infer an unmutated common ancestor (UCA) sequence using only rhesus germline immunoglobulin gene segments. In this approach, Cloanalyst aligns the human antibody sequence to the closest rhesus V, D, and J gene segments using Cloanalyst's rhesus Ig gene segment library which is based on a draft version of genome sequencing of the rhesus Ig loci (34). The resulting rhesus UCA is thus comprised of the rhesus V, D, and J gene segments with the highest identity to the human antibody sequence. Amino acids with high uncertainty in the inference of the rhesus UCA were changed to match the human amino acid at that position. The rhesus UCA amino acid sequence and the human amino acid sequence were then aligned, and CDR1, 2, and 3 of the rhesus UCA were replaced with the corresponding CDR1, 2, and 3 of the human amino acid sequence producing the rhesusized antibody sequence. The rhesusized v-regions for the heavy and light chain were attached to macaque constant regions (AF045537, AF050635, FJ795843).

Antibody Expression and Purification

IgGs were prepared by co-transfection of heavy and light chain plasmids into HEK expi293F cells (Thermo Fisher Scientific) grown in expi293F expression medium in 8% CO_2. Seven days post-transfection cells were pelleted by centrifugation and the medium filtered. IgGs were purified by passage of the medium over a HiTrap protein A column (GE Healthcare) equilibrated in PBS. IgGs were eluted with 0.1 M glycine pH 3.0 and the pH of the eluted protein immediately raised to neutral pH by addition of 1 M Tris-HCl pH 8.5. Fabs were generated by papain digest. IgGs were first incubated with immobilized papain (Thermo Fisher Scientific) at 37°C for 3-4 hours in 20 mM sodium phosphate pH 7.2 supplemented with 3.5 mg/ml cysteine. Immobilized papain agarose was removed by centrifugation and the supernatant filtered. Fabs were separated from undigested IgG and Fc by passage over a HiTrap protein A column. Fabs were then further purified by size exclusion chromatography over a Superdex 200 gel filtration column (GE Healthcare) equilibrated in 20 mM Tris-HCl pH 7.2 and 100 mM ammonium acetate.

Preparation of Protein Complexes

Clade A/E 93TH057gp120 $core_e$ with a His^{375} to Ser mutation was prepared by transfection of GnT1$^-$ HEK 293F Freestyle cells (Thermo Fisher Scientific) with 0.5 mg of plasmid/liter of culture. Cells were grown in Freestyle 293 medium (Thermo Fisher Scientific) supplemented with 2.5% Ultra Low IgG Fetal Bovine Serum (FBS) (Gibco) in 8% CO_2 for 7 days. Cells were pelleted, the medium filtered, and gp120 was purified from medium by passage over a 17b affinity column which consisted of the anti-gp120 antibody 17b covalently linked to protein A agarose. gp120 was eluted from the column with 0.1 M glycine pH 3.0 and the pH raised after elution by addition of 1 M Tris-HCl pH 8.5. The protein was concentrated and the buffer exchanged for 50 mM sodium acetate pH 6.0 and 300 mM sodium chloride. Glycans were then truncated by addition of Endo H_f (New England Biolabs) and incubation at 37°C overnight. Endo H_f, endoglycosidase H linked to maltose binding protein, was removed by passage over an amylose column (New England Biolabs) equilibrated in 25 mM Tris-HCl pH 7.2 and 200 mM sodium chloride. The flow through fractions containing gp120 were further purified by size exclusion chromatography over a Superdex 200 gel filtration column (GE Healthcare) equilibrated in 20 mM Tris-HCl pH 7.2 and 100 mM ammonium acetate prior to use in complex formation with RhDH677.3 Fab. A V2 peptide corresponding to the clade A/E 92TH023 gp120 V2 loop sequence (Asp^{167}-Lys-Lys-Gln-Lys-Val-His-Ala-Leu-Phe-Tyr-Lys-Leu-Asp-Ile-Val-Pro-Ile^{184}) was synthesized by Genescript (www.genescript.com) without modifications for use in complex formation with RhDH827 Fab.

The C1C2 Cluster A region RhDH677.3 complex was made by mixing RhDH677.3 Fab with purified clade A/E 93TH057gp120 $core_e$ and the CD4 mimetic M48U1 in a molar ration of 1.2:1.2:1 of Fab:M48U1:gp120. The complex was allowed to incubate on ice for 30 minutes before purification by size exclusion chromatography over a Superdex 200 gel filtration column equilibrated in 20 mM Tris-HCl pH 7.2 and 100 mM ammonium acetate. The V1V2 region RhDH827 complex was made by mixing RhDH827 Fab with V2 peptide resuspended in water in a molar ratio of 1.2:1 peptide:Fab. The complex was incubated on ice for 30 minutes and purified by size exclusion chromatography over a Superdex 200 column equilibrated in 20 mM Tris-HCl pH 7.2 and 100 mM ammonium acetate. In both cases elution fractions corresponding to the complex molecular weight were combined and concentrated to approximately 10 mg/ml for use in crystallization trials.

Surface Plasmon Resonance Affinity Measurements of IgGs to Antigens

All surface plasma resonance (SPR) assays of IgGs to antigens were performed on a Biacore 3000 (GE Healthcare) with a

running buffer of 10 mM HEPES pH 7.5 and 150 mM NaCl supplemented with 0.05% Tween 20 at 25° C. Kinetic measurements were done by immobilizing IgG on a protein A chip (Cytiva) and passage of serial dilutions of antigen in running buffer over the chip for 200 seconds. Complexes were then allowed to dissociate for 400 seconds by passage of running buffer at the same flow rate. IgG was removed from chip using regeneration buffer, 100 mM glycine pH 2.5, and fresh IgG reapplied between cycles. The antigen for C1C2 Cluster A region RM JR4, DH677.3, and RhDH677.3 was monomeric full length single chain (FLSC), a covalent dimer of $gp120_{BaL}$ and CD4 that specifically exposes CD4i epitopes (35), in a concentration range of 6.25 to 200 nM and IgGs were immobilized on the protein A chip to a response unit (RU) of ~60-120. The antigen for gp41 region 7B2 and Rh7B2 was a synthetic gp41 peptide (residues 596-606) with C-terminal amidation (GenScript) in a concentration range of 6.4-25.6 μM and IgGs were immobilized to a RU of ~400-500. The antigen for V1V2 region DH827, RhDH827, and RM DH614.2 was a synthetic V2 peptide (gp120 residues 167-184) in a concentration range of 12.5-50 μM and IgGs were immobilized to a RU of ~600. Sensorgrams were corrected by subtraction of the corresponding blank channel and buffer background and normalized to a Rmax of 100 RU for curve fitting purposes. Kinetic constants were determined using a 1:1 Langmuir binding model with the BIAevaluation software (GE Healthcare). Goodness of fit of the curves were evaluated by the Chi^2 of the fit with a value below 3 considered as being acceptable (based upon use of a Rmax = 100 RU).

Crystallization, Data Collection and Structure Solution

Crystals were initially grown from commercial crystallization screens (Molecular Dimensions Proplex Eco and Rigaku precipitant synergy) and later optimized to produce crystals suitable for data collection by the hanging drop vapor diffusion method. C1C2 Cluster A region RhDH677.3 complex crystals were grown from 20% PEG 4000 and 0.1 M sodium citrate pH 4.5 and V1V2 region RhDH827 complex crystals were grown from 16.75% PEG 3350, 10.05% isopropanol, and 0.2 M ammonium citrate/citric acid pH 4.5. Crystals were briefly soaked in crystallization buffer supplemented with 20% MPD (2-Methyl-2,4-pentanediol) and flash frozen in liquid nitrogen prior to data collection.

Diffraction data for the RhDH677.3 complex were collected at the Stanford Synchrotron Radiation Light Source (SSRL) beamline 12-2 on a Dectris Pilatus 6M area detector and diffraction data for the RhDH827 complex were collected at the National Synchrotron Light Source II (NSLS-II) beamline 17-ID-2 on a Dectris Eiger 16M area detector. All data were processed and reduced with HKL2000 (36) or imosflm and scala from the CCP4 suite (37). Structures were solved by molecular replacement with PHASER from the CCP4 suite (37) based on the coordinates of the human DH677.3 complex for the RhDH677.3 complex (PDB ID 6MFP) and the macaque Fab structure of RM JR4 for the RhDH827 complex (PDB ID 4RFE). Refinement was carried out with Refmac (37) and/or Phenix (38) and model building was done with COOT (37). Data collection and refinement statistics are shown in **Table 1**.

Structure Validation and Analysis

Ramachandran statistics were calculated with MolProbity and illustrations were prepared with Pymol Molecular graphics (http://pymol.org). The processed data and final model for the RhDH677.3 complex are deposited in the PDB with accession number 7N8Q and those for the RhDH827 complex are deposited with accession number 7N0X.

Surface Plasmon Resonance Affinity Measurements of FcγR Binding

The affinity of IgG variants for RM and human Fcγ receptors (FcγRs) were measured as previously described (23). Briefly, the antibodies were immobilized on a medium density carboxymethyldextran sensor (Xantec Bioanalytics, CMD200M) using a Continuous Flow Microspotter (Carterra) and carbodiimide chemistry. The soluble analyte consisted of dilutions of receptor beginning at 20 μM and diluted by 1:3 over an 8-point series. Association and dissociation were measured for 5 minutes each on an imaging-based surface plasmon resonance (SPRi) instrument (IBIS Technologies, MX96). The results were analyzed in Scrubber 2 (BioLogic Software) using a first-order kinetic model to determine the equilibrium dissociation constant.

HIV-1 IMC-Infection of $CEM.NKR_{CCR5}$ Cells

The infection of cells was performed as previously reported (43). Briefly, R5 tropic HIV-1 IMC virus stocks (1086.C, CH505, SF162) were titrated to determine the input required for optimal viral gene expression within 72 h post-infection of $CEM.NKR_{CCR5}$ cells as measured by intra-cellular p24 expression. Stocks were used to infect 2×10^6 cells with each IMC by incubation with the appropriate dose for 30 min at 37°C and 5% CO_2 in the presence of DEAE-Dextran (7.5 μg/mL). The cells were subsequently resuspended at 0.5×10^6/mL and cultured for 2 days in complete medium containing 7.5 μg/mL DEAE-Dextran. On assay day, the infection was monitored by measuring the frequency of cells expressing intracellular p24. The assays performed using the IMC-infected target cells were considered reliable if the percentage of viable p24+ target cells on assay day was ≥20%. Assay data generated using infected cells was normalized to the % of target cells positive for intracellular p24.

SHIV-Infection of A66 Cells

The infection of A66 cells [SupT1 cells (non-BC7 variant variant (44) that have been stably transfected to express both rhesus CD4 and rhesus CCR5 receptors after knockout of endogenous human CXCR4 and CD4 (45), provided by James Hoxie, University of Pennsylvania, Philadelphia, PA] was conducted as described previously (46). Briefly, R5 tropic SHIV virus stocks SF162.P3 (32) grown in human PBMCs, or CH505.375H (47) and 1157(QNE)Y173H (48) grown in

TABLE 1 | Data collection and refinement statistics.

	RhDH677.3 Fab-M48U1-gp120$_{93TH057}$ core$_e$	RhDH827 Fab-V2 peptide
Data collection		
Wavelength, Å	0.979	0.979
Space group	$P2_1$	C2
Cell parameters		
a, b, c, Å	99.2, 82.7, 111.9	81.6, 71.9, 87.7
α, β, γ, °	90, 112.0, 90	90, 111.5, 90
Complexes/a.u.	2	1
Resolution, (Å)	50-2.9 (2.95-2.9)	50-2.0 (2.1-2.0)
# of reflections		
Total	77,728	126,613
Unique	31,091 (1,645)	31,034 (4,384)
R_{merge}[a], %	10.6 (62.7)	9.5 (47.4)
R_{pim}[b], %	7.8 (46.7)	5.3 (26.5)
$CC_{1/2}$[c]	0.98 (0.71)	0.99 (0.81)
Wilson B_{factor} (1/Å^2)[d]	64	27.6
I/σ	9.6 (1.1)	5.3 (1.5)
Completeness, %	82.7 (86.0)	99.5 (98.2)
Redundancy	2.5 (2.5)	4.0 (4.0)
Refinement Statistics		
Resolution, Å	50.0 - 2.9	50.0 - 2.0
R[e], %	25.5	18.1
R_{free}[f], %	29.6	20.9
# of atoms		
Protein	11,758	3,361
Water	15	273
Ligand/Ion	284	7
Overall B value (Å)^2		
Protein	71	37
Water	42	43
Ligand/Ion	69	61
Root mean square deviation		
Bond lengths, Å	0.007	0.007
Bond angles, °	1.6	0.9
Ramachandran[g]		
favored, %	80.2	96.1
allowed, %	13.9	3.0
outliers, %	5.9	0.9
PDB ID	7N8Q	7N0X

Values in parentheses are for highest-resolution shell.

[a]R_{merge} = Σ|I - <I>|/ΣI, where I is the observed intensity and <I> is the average intensity obtained from multiple observations of symmetry-related reflections after rejections.

[b]R_{pim} = as defined in (39).

[c]$CC_{1/2}$ = as defined by Karplus and Diederichs (40).

[d]Wilson B_{factor} as calculated in (41).

[e]$R = \Sigma||F_o|-|F_c||/\Sigma|F_o|$, where F_o and F_c are the observed and calculated structure factors, respectively.

[f]R_{free} = as defined by Brünger (42).

[g]Calculated with MolProbity.

Rhesus PBMCs were titrated to determine the input required for optimal viral gene expression within 72 h post-infection of A66 cells as measured by intracellular p27 expression. A66 cells (1×10^6 cells per infection) were incubated for 4 hours at 37°C and 5% CO_2 in the presence of DEAE-Dextran (10 µg/mL, Sigma Aldrich). The cells were subsequently resuspended at 0.33×10^6/mL and cultured for 3 days in complete medium containing 10 µg/mL DEAE-Dextran. On assay day, infection was monitored by measuring the frequency of cells expressing intracellular p27. The assays performed using the SHIV-infected target cells were considered reliable if the percentage of viable p27+ target cells on assay day was ≥10%. Assay data generated using infected cells was normalized to the frequency of live target cells positive for intracellular p27.

Infected Cell Antibody Binding Assay (ICABA)

ICABA was used to evaluate the ability of mAbs to bind Env on the surface of HIV- or SHIV-infected cells. HIV-infected CEM.NKR.CCR5 cells and SHIV-infected A66 cells were obtained as described above. Cells incubated in the absence of virus (mock infected) were used as a negative control. Infected and mock infected cells were washed in PBS, dispensed into 96-well V-bottom plates at 2 x 10^5 cells/well and incubated with 1 µg/mL of indicated mAbs for 2 hours at 37 °C. After two washes with 250 µL/well WB, the cells were stained with vital dye (Live/Dead Fixable Aqua Dead Cell Stain, Invitrogen) to exclude nonviable cells from subsequent analysis. Cells were washed with wash buffer (5%FBS in PBS) and stained with anti-CD4-PerCP-Cy5.5 (clone OKT-4 for CEM.NKR.CCR5 cells or clone Leu-3 for A66 cells; BD Biosciences) to a final dilution of 1:20 in the dark for 20 min at room temperature (RT). Cells were then washed again, and permeabilized using Cytofix/Cytoperm (BD Biosciences). Anti-p24 antibody (clone KC57-RD1; Beckman Coulter, 1:100 dilution in 1x Cytoperm Solution, BD Biosciences) and a secondary FITC-conjugated antibody (goat anti-human IgG(H+L)-FITC, KPL, final dilution of 1:100 or Goat Anti Rh IgG(H+L)-FITC, Southern Biotech, final dilution of 1:200) for CEM.NKR.CCR5 cells; anti-p27 antibody (WNPRC Immunology Services, 1:500 dilution in 1x Cytoperm Solution, BD Biosciences) and a secondary PE-conjugated antibody (goat anti-human Ig Fc-PE, eBioscience, San Diego, CA., final dilution of 1:400 or Goat Anti-Rh IgG(H+L)-PE, Southern Biotech, final dilution of 1:200) were added to each well and incubated in the dark for 25 min at 4°C. Cells were washed three times with Cytoperm wash solution and resuspended in PBS-1% paraformaldehyde. The samples were acquired within 24 hours using a BD Fortessa cytometer. A minimum of 50,000 total events was acquired for each analysis. Gates were set to include singlet and live events. Data analysis was performed using FlowJo 9.6.6 software (BD Biosciences). Final data represents the frequency of infected cells (Ab+p24+ or Ab+p27+) and FITC MFI or PE MFI of binding of IgG mAbs to HIV Env, after normalization by subtraction of the frequency or MFI observed for cells stained with the secondary antibody alone.

Renilla Luciferase-Based ADCC Assay

The LucR-based ADCC assay was conducted as described by Pollara et al. (49). The day prior to the ADCC assay, cryopreserved PBMCs to be used as effectors in the assay were thawed in R10 [RPMI medium supplemented with 10% Fetal Bovine Serum (FBS)], counted and assessed for viability and resuspended in R10 overnight. On the day of the assay, infected $CEM.NKR_{CCR5}$ cells were counted, assessed for viability (viability was ≥ 80% to be used in the assay) and the concentration was adjusted to 2 x 10^5 viable cells/mL (5 x 10^3

cells/well). PBMCs were then counted, assessed for viability, pelleted and resuspended in the infected CEM.NKR_{CCR5} cells at a concentration of 6 x 10^6 PBMCs/mL (1.5 x 10^5 PBMCs/well) (effector: target cell ratio of 30:1). The mAbs starting at 50 μg/mL were serially diluted 1:5. The effector/target cell mix and antibody dilutions were plated in opaque 96-well half-area plates, centrifuged at 300 x g for 1 min after 30 min incubation at room temperature, and then incubated for 5.5 hrs at 37°C, 5.5% CO_2 to allow ADCC-mediated cell lysis to proceed. After 5.5 hrs, ViviRen substrate (Promega) was diluted 1:500 in R10 and added 1:1 to the assay wells. The substrate generates luminescence only in live, infected cells; not in dead or lysed cells. The final readout was the luminescence intensity generated by the presence of residual intact target cells that have not been lysed by the effector population in the presence of ADCC-mediating antibodies. The percentage of specific killing was calculated using the formula

$$\% \text{ specific killing} = \frac{\text{RLU of target + effector well} - \text{RLU of test well}}{\text{RLU of target + effector well}} \times 100$$

In the analysis, the RLU of the target + effector wells represent lysis by effector cells in the absence of any source of antibody. Synagis, a human mAb specific for respiratory syncytial virus (50), and DSP_Rh, a macaque mAb specific for desipramine (DSPR1) from the nonhuman primate reagent resource (www.nhpreagents.org), were used as negative controls.

ADCC-GranToxiLuc Assay

ADCC activity was detected according to the previously described ADCC-GranToxiLux (GTL) procedure using recombinant SHIV.1157QNE(Y173H) gp120 coated CEM.NKR_{CCR5} as target cells and cryopreserved PBMC from a HIV-seronegative donor as effector cells (51) with E:T ratio of 30:1 The mAbs starting at 50 μg/mL were serially diluted 1:5. The results of the GTL assay were considered positive if % Granzyme B activity after background subtraction was ≥8% for the infected target cells.

ADCC AUC

The specific killing activities in the ADCC assay were summarized for each subject and antigen by computing the area under the dilution curve (AUC) which was calculated from dilution curves using non-linear trapezoidal rule. Non-specific killing activities mediated by negative control mAbs, Synagis or DSP_Rh, were subtracted from the corresponding human or rhesus mAbs prior to AUC calculation.

Antibody Dependent Cellular Phagocytosis (ADCP) and Antibody Dependent Neutrophil Phagocytosis (ADNP)

ADCP was performed as previously described (52, 53). Briefly, ADCP was quantified by covalently binding biotinylated SHIV 1157(QNE)Y173H gp120 Env glycoprotein (1μg gp120/μL of bead) to 9x10^5 neutravidin fluorescent beads (ThermoFisher, F8776). Beads were then incubated with monoclonal antibodies for 2 hours to form immune complexes. THP-1 cells (ATCC, TIB-202) pre-treated with anti-CD4 (Biolegend, 344602) were then added to the immune complexes (25,000 cells/well) and spinoculated at 4°C. Following spinoculation, the cells were incubated at 37°C for 1 hour and fixed with 2% paraformaldehyde. The fluorescence of the cells was detected using flow cytometry (BD LSRFortessa). To calculate phagocytosis scores a cutoff was first assigned based on the 95th percentile of the no-antibody control (PBS only). The magnitude of the ADCP immune response (ADCP score) was calculated by multiplying the mean fluorescence intensity (MFI) and frequency of phagocytosis-positive cells and dividing by the MFI and frequency of the bead-positive cells in an antibody-negative (PBS) control well. Control antibodies were selected based positive binding to SHIV 1157(QNE) gp120 antigen. CH31_IgG3 mAb (Catalent), and CH235_12_IgA (54) (kindly provided by Huaxin Liao, Mattia Bonsignori, and Bart Haynes, Duke University) HIV specific, CD4bs broadly neutralizing antibodies (55), were included as positive controls and the non–HIV-specific CH65 IgG1 mAb (Catalent) (56) was included as a negative control. ADNP was performed as described for ADCP with the following modification: HL-60 cells (ATCC, CCL-240) pre-treated with DMSO for 5 days (57) were used as effector cells. The IgA antibody positive control was utilized to confirm that differentiation of the HL-60 cells to be neutrophil-like with expression of FcR alpha engagement. Positivity cutoff was 2.2 calculated from the mean + 3 standard deviations of the negative control.

Infectious Virion Capture Assay (IVCA) (Column)

Infectious virion capture assay (IVCA) was measured as previously described (53, 58–60). Briefly, the IVCA method utilizes a Protein G column based capture of Ig-virion immune complexes allowing for the analysis of infectious virions (TZM-bl infectivity assay). Briefly, antibodies were mixed with SHIV1157 (QNE)Y173H (kindly provided by Abraham Pinter, Rutgers New Jersey Medical School) at final concentration of 25 μg/ml (200 μl volume) to form Ab-virion immune complexes (IC), which were passed through a protein G column. The infectivity of the flow-through was measured by a TZM-bl infection assay. The percentage of captured infectious virions (iVirion) were calculated as follows: iVirion = [(100- flow-through infectivity)/(virus no-Ab infectivity)] x 100. HIVIG polyclonal human sera (NIH HIV Reagent Program) was included as a positive controls and the non–HIV-specific CH65 IgG1 mAb (Catalent) (61) was included as a negative control. Positivity cutoff was 15.6% calculated from the mean + 3 standard deviations of the negative control.

RESULTS

Engineering Rhesusized Variants of Human mAbs

Three HIV-1 specific human antibodies, DH677.3, DH827, and 7B2, were converted to macaque versions, i.e. rhesusized, with the aid of both the macaque genome and structural information

about each antibody's epitope (30–33). For clarity rhesusized versions of antibodies will begin with an Rh in the name and native macaque antibodies will have an RM designation; human antibodies will have no designation to be consistent with the names assigned to them by the literature. Sequence changes were kept to a minimum to maintain specificity and reduce immunogenicity. The schematic of how theses rhesusized variants were made is shown in **Figure 1**. First, the inferred macaque germline gene closest in sequence to the human antibody was identified. At positions where the equivalent position in the macaque germline sequence could not be determined the corresponding amino acid from the human sequence was used. Complementary determining regions (CDRs) were then changed to that of the human antibody. When structural information about the epitope in human showed that residues outside of the CDRs were involved in binding antigen, those human contact residues were introduced into the macaque germline sequence. The rhesusized antibody therefore consists of macaque framework sequences modified to be human only at positions that are part of the paratope and human CDR sequences with fully macaque constant regions (the resulting rhesusized sequences are shown in **Figure S1**). Altogether, generation of Rh7B2 V_H and V_L required 18 changes in sequence for heavy chain framework residues and 17 changes in framework residues for the light chain relative to the human 7B2; one additional heavy chain change relative to the macaque sequence was required due to a framework epitope contact and one light chain change due to a missing macaque residue at position 65 in the germline sequence. Generation of RhDH677.3 V_H and V_L required 9 heavy chain and 7 light chain changes in sequence relative to the human DH677.3 as well as one heavy chain change at position 6 due to a missing residue in the macaque germline sequence. Generation of RhDH827 V_H and V_L required 11 heavy and 7 light chain framework changes in sequence. The heavy chain C_H (C_H1) and Fc (C_H2 and C_H3) of all the antibodies were fully macaque with 27 changes and 3 inserted glycine residues relative to the human IgG1 (91% overall identity). C_L differences varied for each antibody depending on whether the light chain was kappa, RhDH677.3 and Rh7B2, or lambda, RhDH827. RhDH677.3 and Rh7B2 had 17 changes in their C_L kappa light chains relative to their human counterparts (84.1% identity) and RhDH827 had 12 changes in its C_L relative to its lambda equivalent (88.6% identity). Therefore, excluding CDRs, the Rh7B2 Fab was 78.4% identical in sequence to the 7B2 Fab and 98.8% identical in sequence to the inferred macaque germline gene, the RhDH677.3 Fab was 90.4% identical in sequence to the DH677.3 Fab and 99.4% identical to its macaque germline sequence, and the RhDH827 Fab was 88% identical to the DH827 Fab and 100% identical to its macaque germline sequence.

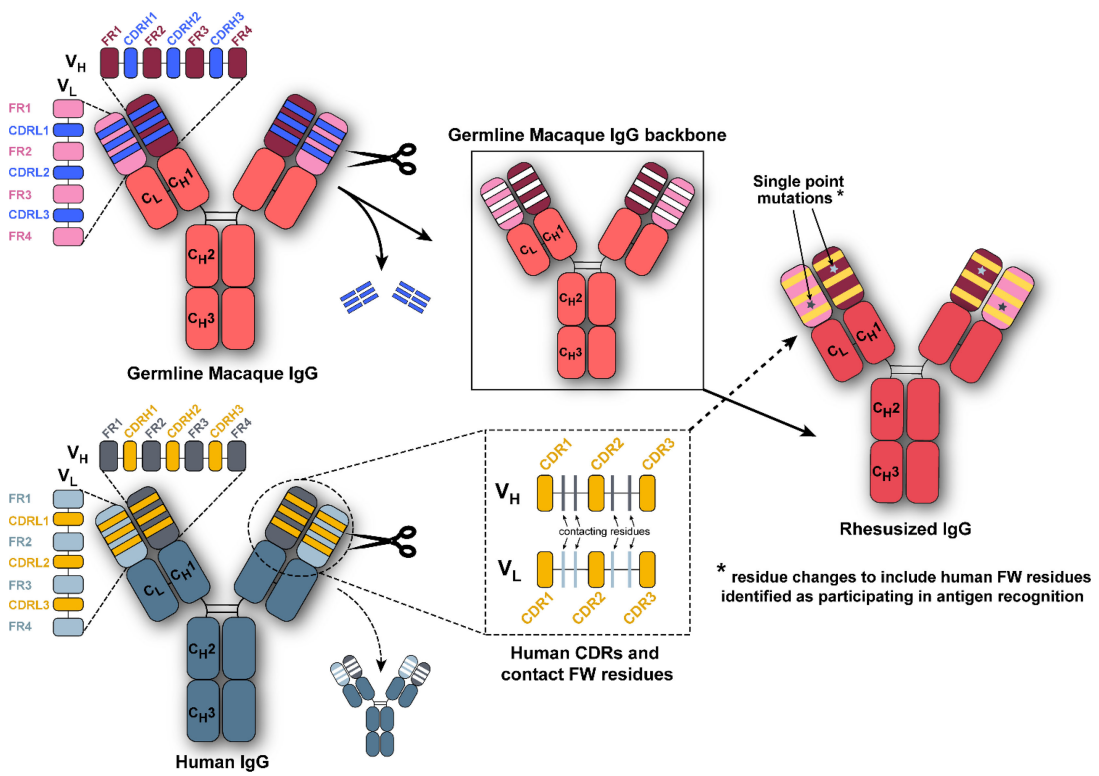

FIGURE 1 | Composition scheme for rhesusized antibody engineering. We grafted the human complementary-determining regions (CDRs) and any framework (FW) residues contributing to antigen binding when structural data was available of the parental human monoclonal antibody (bottom left panel) onto the macaque germline framework and antibody backbone (top left panel) to generate the rhesusized antibody (right panel).

Rhesusized mAb Variants Bind to RM and Human Fcγ Receptors With Similar Binding Affinities to Those of RM Origin

Proper rhesusization should result in an antibody variant that preserves its structural integrity and both the binding properties mediated by the Fc of the equivalent RM IgG subclass and those mediated by the Fab (i.e. epitope specificity and binding interface) of the parent human mAb. Accordingly, rhesusized mAb variants were generated in a RM IgG1 backbone to match the original parent human IgG1 backbone (**Figures 1** and **S1**). To validate this design we tested the Fc binding properties of our rhesusized variants to receptors expressed on effector cells involved in Fc-effector functions to see if they were comparable to mAb IgG1s of RM origin. We show in **Figure 2**, **Table S1** and **Figure S2** the SPR binding kinetics of RhDH677.3, Rh7B2 and RhDH827 to both rhesus and human low affinity FcγRs measured with IgG immobilized on a sensor chip and FcγR in solution. Two antibody specificities were used as controls of RM origin. The antibody used as a control for an epitope from the C1C2 Cluster A region was RM JR4, a mAb derived from the peripheral blood B cells of a rhesus macaque infected with the simian-human immunodeficiency virus (SHIV) KB9 mutant that contains gp41 glycosylation site deletions (62). Antibodies used as a control for an epitope in the V1V2 region were clonal variants of RM DH614 (RM DH614.1, RM DH614.2 and RM DH614.3), mAbs isolated from a RM vaccinated with the vaccine regimen used in RV144 (63). Among the receptors tested were polymorphic variants 1, 2 and 4 of RM FcγRIIa (e.g. RM FcγRIIa-1,-2 and -4), RM FcγRIIb-1 and RM FcγRIIIa-1 and 3 as described in (23). Human receptors tested included high and low affinity variants of FcγRIIa and FcγRIIIa and a low affinity inhibitory receptor FcγRIIb. Interestingly, binding affinities of the rhesusized IgG variants to all low affinity RM receptors tested were in the range of binding affinities detected for IgG variants that were cloned directly from an RM host with no statistical difference between the groups. The only statistical difference between the rhesusized and RM antibody groups was seen in an unpaired T-test for the low affinity allelic variant of human FcγRIIa(R131) with P value = 0.0173. No significant differences in affinities to the other human Fcγ receptors were detected This indicates that the engineered rhesus Fc backbone is properly folded and the variants fully preserve the Fc-binding properties of an IgG1 of RM origin to all RM Fcγ receptors

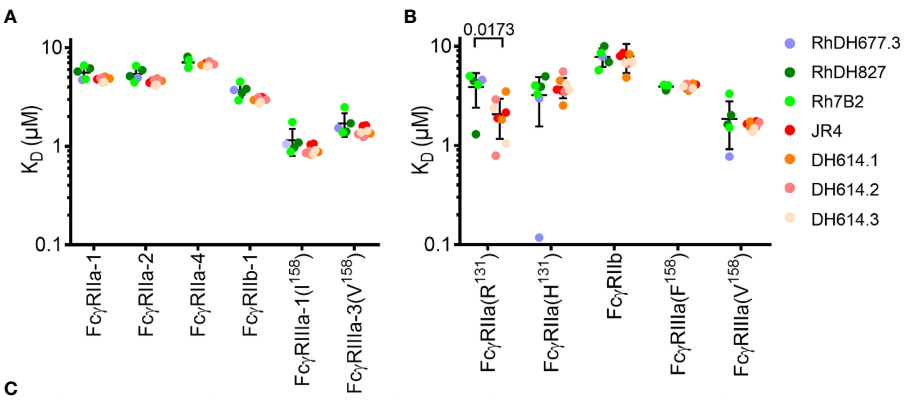

C

IgG		Antigen	k_{on} (M^{-1} s^{-1})	k_{off} (s^{-1})	K_D (nM)	Fitting mode	Chi^2
C1C2 specific	RhDH677.3	FLSC*	7.42×10^4	1.89×10^{-4}	2.54	1:1	0.289
	DH677.3	FLSC*	1.39×10^5	4.05×10^{-5}	0.29	1:1	0.596
V2-peptide specific	RhDH827	$gp120_{92TH023}$ V2-peptide(167-184)	1.78×10^2	4.86×10^{-4}	2.73×10^3	1:1	2.44
	DH827	$gp120_{92TH023}$ V2-peptide(167-184)	1.82×10^2	6.90×10^{-3}	3.80×10^3	1:1	4.12
gp41-peptide specific	Rh7B2	$gp41_{BaL}$ peptide (596-606)	9.15×10^2	5.34×10^{-4}	583	1:1	3.86
	7B2	$gp41_{BaL}$ peptide (596-606)	1.03×10^3	6.54×10^{-4}	634	1:1	4.33
C1C2 specific	RM JR4	FLSC*	1.30×10^5	1.30×10^{-4}	0.85	1:1	0.869
V2-peptide specific	RM DH614.2	$gp120_{92TH023}$ V2-peptide (167-184)	1.70×10^2	3.84×10^{-4}	2.26×10^3	1:1	5.69

FIGURE 2 | Affinity of rhesusized variants for low affinity receptors. Binding affinities of **(A)** rhesus and **(B)** human FcγRs. Equilibrium binding constants (K_D) measured by SPR for common rhesus and human FcγR allotypes. Data show individual replicates, and error bars denote the standard deviation. Data are representative of 2 independent experiments. RhDH677.3, RhDH827, and Rh7B2 are rhesusized mAbs. RM JR4 (62), RM DH614.1, RM DH614.2, and RM DH614.3 (63) are mAbs originally isolated from a RM vaccinated with the vaccine regime used in RV144. The P-value for an unpaired T-test for rhesusized and RM mAbs is shown above the compared pair. **(C)** SPR binding kinetics for rhesusized (RhDH677.3, RhDH827, and Rh7B2) and human [DH677.3 (30), DH827 (31) and 7B2 (32)] mAb pairs. RM JR4 (62) and RM DH614.2 (63), mAbs originally isolated from RM, were used as controls. FLSC, a covalent dimer of $gp120_{BaL}$ and domain 1 and 2 of CD4 (35) was used as antigen for C1C2 Cluster A specific mAbs RhDH677.3, DH677.3 and control JR4, $gp120_{92TH023}$ V2 peptide (residues 167-184) was used as antigen for V1V2 region mAbs RhDH827, DH827 and control RM DH614.2, and $gp41_{BaL}$ peptide (residues 596-606) was used as antigen for gp41 region specific mAbs Rh7B2 and 7B2.

involved in Fc-effector mechanisms and all but one human low affinity Fcγ receptors. The rhesusized mAb variants therefore preserve the RM IgG1 structure with variable regions (V) and antigen-binding characteristics of the parent human mAb. Rhesusized mAb variants bind to RM and human Fcγ receptors with similar binding affinities to those of RM origin.

Rhesusized mAb Variants Bind to Antigen With Similar Binding Affinities to Those of Human Origin

We also examined the integrity and binding properties of the Fab to see if the recognition of HIV-1 Env was preserved in the variants as compared to their human counterparts. First, we used surface plasmon resonance analyses (SPR) to test the biding properties of human and rhesusized antibody pairs to appropriate antigens. For CD4 inducible (CD4i) antibodies (e.g. RM JR4 and DH677.3) we used full length single chain (FLSC), a covalent dimer of $gp120_{BaL}$ and CD4 that specifically exposes CD4i epitopes (35). For antibodies specific for linear epitopes within the V2 loop (e.g. DH827 and D614 lineage) or gp41 (e.g. 7B2) we used the peptides that were used in co-crystallization studies (30, 32). As shown in **Figure 2B** and **Figure S3** all pairs tested with the exception of DH677.3 had identical or highly similar binding kinetics; RhDH677.3 had an approximately 8-fold lower K_D than human DH677.3 mainly due to an increase in the off-rate. This difference in affinity could be result of slight differences in the paratope, discussed in more detail below, or the result of removal of a glycan attached to Asn^{72} of the heavy chain sequence (Asp^{72} in RhDH677.3); this glycan sits outside of the paratope but could affect the affinity by interacting with the gp120 N-terminus.

Next, to more carefully examine the molecular details of the antibody-antigen interface and to assess if mAb epitopes were fully preserved in the rhesusized variants we solved crystal structures of both the RhDH677.3 and RhDH827 Fabs in complex with their respective cognate Env antigens (**Table 1**). Shown in **Figure 3** is the structure of RhDH677.3 Fab in complex with $gp120_{93TH057}core_e$ and the CD4 peptide mimetic M48U1. The parent of RhDH677.3, DH677.3, is a Cluster A specific antibody isolated from a RV305 vaccinee, a follow up study of a subset of RV144 vaccinees with delayed boosting using RV144 immunogens (31, 64) with a similar epitope footprint to RV144 mAbs (65). The RhDH677.3 Fab-$gp120_{93TH057}$ $core_e$-M48U1 complex (**Figure 3A**) crystallized in space group $P2_1$ with two complexes in the asymmetric unit and diffracted to 2.9 Å resolution (**Table 1**). The CD4 mimetic M48U1 was only found bound to one of the two complexes in the asymmetric unit due to clashes with neighboring complexes in the crystal. The gp120 in the second complex was therefore more disordered and less like the typical CD4-bound gp120 conformation present in the first complex of the asymmetric unit. However, within the region corresponding to the antibody-gp120 interface both copies of the complex were still highly similar with nearly identical conformations (**Figure S4**). Since the RV305 mAb DH677.3 also crystallized with two complexes in the asymmetric unit but with M48U1 bound for both copies (31), we only used the first complex (with M48U1 bound) from the RhDH677.3 Fab-$gp120_{93TH057}$ $core_e$-M48U1 complex crystal structure for comparison (**Table S2**). Values from the DH677.3 structure on the other hand, represent an average of those from both copies.

RhDH677.3, similar to its progenitor DH677.3, binds at the base of the 7-stranded β-sandwich of the gp120 inner domain with contributions from the inner domain mobile layers 1 and 2 (**Figure 3**). The total buried surface area (BSA) for the RhDH677.3-gp120 interface in the complex is 1800 $Å^2$ which is very similar to the BSA for the interface contributed by its human counterpart, DH677.3, 1894 $Å^2$ (**Table S2**). RhDH677.3 antibody-gp120 contacts involve residues in layer 1 (residues 53, 71-80 and 82), layer 2 (residues 219-222), and the 7-stranded β-sandwich (residues 84, 223-224, 244-246, and 491-492) (**Figure 3C**) almost entirely mimicking the antigen footprint of DH677.3. The only noticeable difference with its human counterpart is that the RhDH677.3 Fab-gp120 interface lacks two additional gp120 residues buried in the DH677.3 Fab-gp120 interface, i.e. Ala^{60} and Glu^{87}. Overall, the lower total BSA for the macaque RhDH677.3 complex is mostly a result of slightly lower BSA values in most gp120 regions (**Figures 3B–D**, **Table S2**). The macaque complex buries 530 $Å^2$ of the gp120 inner domain layer 1, 120 $Å^2$ of layer 2, and 226 $Å^2$ of the 7-stranded β-sandwich, while the human structure buries an average of 540 $Å^2$ of layer 1, 133 $Å^2$ of layer 2, and 261 $Å^2$ of the 7-stranded β-sandwich. The added surface area for the human complex comes in part from additional contributions from light chain framework contacts near the N-terminus, slightly higher BSA values for CDRs H3 and L3, and framework residue differences between the human and macaque antibodies (**Figure 4** and **Figure S2**). The framework residue changes include light chain framework region 1 which contains an alanine, Ala^1, in the macaque germline sequence and an aspartic acid, Asp^1, in the human sequence. Ala^1 in the macaque sequence does not contact gp120 at all, while Asp^1 *via* its side chain makes main chain contacts to gp120 residues Thr^{71}, Cys^{74}, Val^{75}, and Pro^{76} and side chain contacts with Pro^{76} (**Figure 3C**),. This one residue difference largely accounts for the 31 $Å^2$ increase in BSA for this region (**Figure 4C, D**). The second is in the heavy chain framework region 3 which contains an aspartic acid, Asp^{72}, in the macaque germline sequence that is not glycosylated but an asparagine, Asn^{72}, in the human structure that is. This glycan sits outside of the antibody paratope on the edge of the β-sandwich and is not directly involved in binding in the 7-stranded β-sandwich gp120 complex but could potentially make contact to the eighth strand in an 8-stranded β-sandwich complex. One additional framework residue difference seems to have an indirect effect on the interface. In the macaque structure Ser^{31} in CDR H1 does not contribute to the interface, but in human structure Ala^{30} instead of Thr^{30} in framework region 1 allows Ser^{31} to contribute to the interface and the total BSA. In total these sequence differences help explain the 58 $Å^2$ greater gp120 BSA and the 36 $Å^2$ greater Fab BSA for the human complex as compared to the macaque complex. Despite the differences in the BSA values, the gp120 antigen complexes

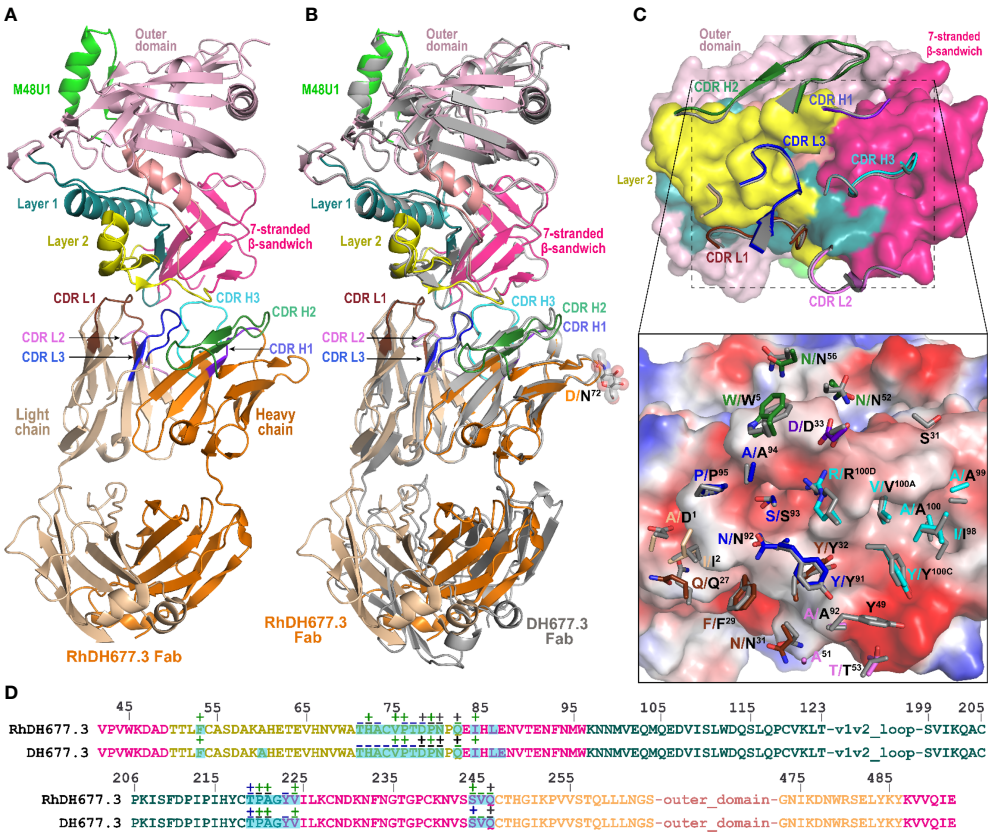

FIGURE 3 | Crystal structure of RhDH677.3 Fab-gp120$_{93TH057}$ core$_e$-M48U1 complex. **(A)** The overall structure of the complex is shown as a ribbon diagram. The light chain (LC) and heavy chain (HC) of the RhDH677.3 Fab are colored in wheat and orange, respectively. The complementary-determining regions (CDRs) of RhDH677.3 Fab are colored as following: CDR H1 is purple blue, CDR H2 is dark green, CDR H3 is cyan, CDR L1 is dark brown, CDR L2 is purple, and CDR L3 is blue. Outer domain of gp120 is light pink. Layers 1, 2 and the 7-stranded -sandwich of the inner domain are colored as green, yellow and magenta, respectively. **(B)** Structural comparison of RhDH677.3 Fab-gp120$_{93TH057}$ core$_e$ and DH677.3 Fab-gp120$_{93TH057}$ core$_e$ complexes. The RhDH677.3 Fab-gp120$_{93TH057}$ core$_e$ complex is colored as indicated in panel A and the DH677.3 Fab-gp120$_{93TH057}$ core$_e$ complex is colored in gray. The complexes are superimposed based upon gp120 and the heavy and light chain variable (V_H and V_L) domains. The carbohydrate at position Asn^{72} of the DH677.3 Fab is shown as sticks. **(C)** The RhDH677.3 Fab-gp120$_{93TH057}$ core$_e$ interface. gp120 is shown as a molecular surface and colored as described in A (top panel) and by electrostatic potential (bottom panel) with red, blue and white representing negative, positive and neutral electrostatic potential, respectively. CDRs of RhDH677.3 Fab are shown as ribbons (top panel) and side chains of binding residues are shown as sticks (bottom panel). Binding residues of RhDH677.3 Fab are colored as in panel A and binding residues of DH677.3 Fab are colored in dark gray. **(D)** Contact residues of gp120 are mapped onto the gp120$_{93TH057}$core sequence. Contact residues are defined by a 5 Å cutoff and marked above the sequence with (+) for side chain and (-) for main chain to indicate the type of contact. Contact types are colored as following: hydrophilic (green), hydrophobic (blue) and both (black). Buried surface residues are as determined by PISA and are shaded green.

formed by both antibodies are highly similar with root mean square deviations (RMSD) between main chain atoms of the variable domains of the Fab and the variable domains of the Fab-gp120 core interface of 0.72 and 1.03 Å^2, respectively (**Figure 5**). Altogether the structural analysis confirms the close similarity between RhDH677.3 and DH677.3 with regard to their recognition of gp120, although sequence differences within framework regions do modulate the binding interface even when they only make minor contributions, either directly like Ala^1 in the macaque light chain or indirectly like Thr^{30} in the macaque heavy chain.

The second rhesusized mAb included for structural characterization was DH827, an antibody from the RV144 vaccine trial (30). In contrast to DH677.3 which is specific for a discontinuous, conformational epitope, DH827 recognizes a linear epitope within the V2 loop region. Interestingly, V2 loop specific antibodies fall into four main categories depending upon the V2 loop conformation and epitope region (66). V2qt and V2q antibodies bind the V2 loop in the quaternary trimeric form of the envelope structure (V2qt) such as PGT145 or (V2q) such as PG9 and PG16. V2i antibodies, e.g. 830A, directly overlap the $\alpha_4\beta_7$ integrin binding site on the V2 loop, and V2p antibodies bind the V2 loop in peptide-like conformation that only partially overlaps the integrin binding site, e.g. RV144 mAbs CH58, CH59, and DH827 (67–69). A sieve analysis of breakthrough HIV-1 infections in RV144 identified Lys^{169} as a site of antibody induced pressure on the virus (7). V2p antibodies from RV144 vaccinees (including DH827) often contain a Glu-Asp motif in

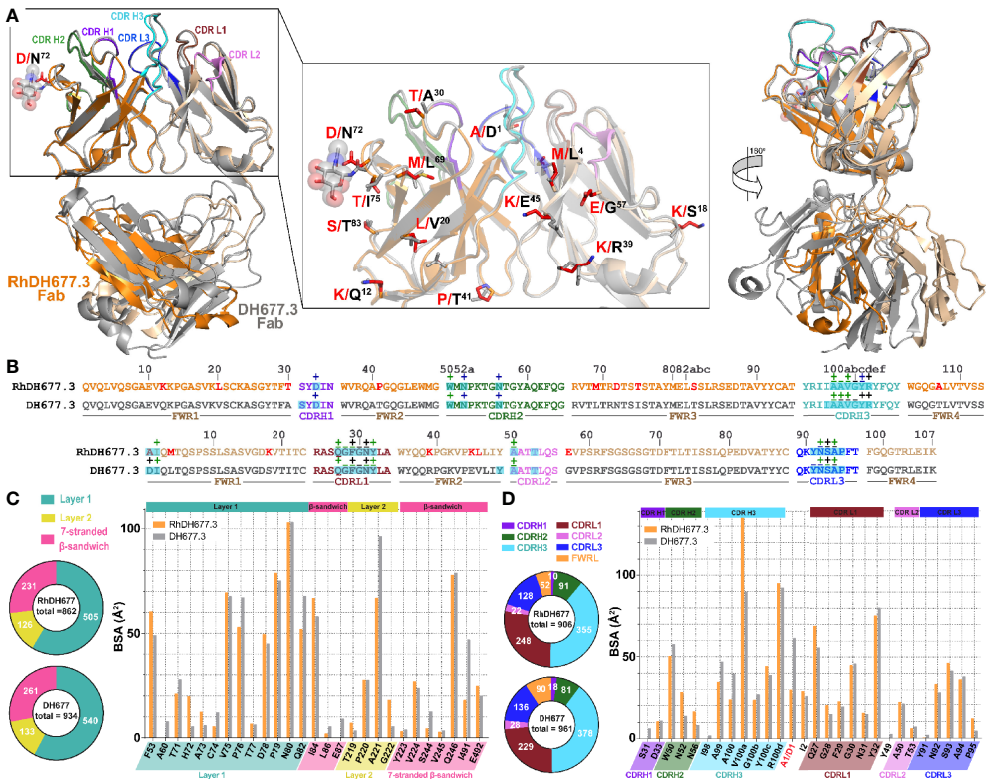

FIGURE 4 | Structural comparison of RhDH677.3 and DH677.3 Fab antigen complexes. **(A)** The RhDH677.3 Fab and its CDRs are colored as indicated in **Figure 3** and the DH677.3 Fab is colored in gray. The complexes are superimposed based on the variable domains of light and heavy chains. Residues that differ between the two Fab are shown in stick and highlighted in red for RhDH677.3 Fab and in black for DH677.3 Fab (middle panel). A 180° view reveals the structural difference of the constant domains in RhDh677.3 and DH677.3 Fabs (right panel) **(B)** Contact residues of RhDH677.3 and DH677.3 Fabs with gp120 are mapped onto the Fab sequences and colored as described for panel **(A)** Contact residues are defined by a 5 Å cutoff and marked above the sequence with (+) for side chain and (-) for main chain to indicate the type of contact. Contact types are colored as following: hydrophilic (green), hydrophobic (blue) and both (black). Residues that differ between RhDH677.3 and DH677.3 are highlighted in red. Buried surface residues are determined by PISA and are shaded green. **(C)** Pie charts showing the buried surface binding (BSA) contributions of gp120 to binding and are colored as in **Figure 3** . The BSA contributions to binding of gp120 residues are shown as calculated by PISA. BSA contributions for gp120 contact residues to RhDH677.3/DH677.3 binding are shown in orange and gray, respectively. **(D)** Pie charts showing the buried surface binding (BSA) contributions to gp120 binding for RhDH677.3/DH677.3 Fabs and are colored as in panel **(A)** The BSA contributions to binding for RhDH677.3 CDR residues are colored in orange and BSA contributions to binding for DH677.3 CDR residues are shown in gray.

their CDR L2 and depend on Lys^{169} in binding the V2 loop (70). DH827 differs from many other V2p Abs in that it is less dependent upon Lys^{169}.

In order to confirm that the rhesusized RhDH827 mAb maintains the V2p specificity of its parent mAb, we crystallized RhDH827 in complex with a clade A/E 93TH057gp120 V2 sequence peptide (**Table 1**, **Figure 6**). The crystals belonged to space group C2, diffracted to 2.0 Å resolution, and contained one RhDH827 Fab heavy and light chain bound to one V2 peptide in the asymmetric unit. RhDH827 binds the V2 peptide in a more helical conformation than many of the other RV144 Abs, e.g. CH58 and CH59, which allows it to make hydrophobic contacts with Val^{172}, Leu^{175}, Phe^{176}, and Leu^{179}. A discontinuation of the helix at the C-terminus allows it to extend its contacts to Ile^{181}, Val^{182}, and Pro^{183} (**Figures 6B, C**). Sixty-seven (67)% of the total 852 Å^2 peptide BSA comes from these hydrophobic residues as opposed to 21.4% from Lys^{168} and Lys^{169} (**Figures 6D, E**). Outward facing residues of the helix contribute little if anything to the peptide BSA, i.e. Gln^{170}, Lys^{171}, Ala^{174}, Tyr^{177}, and Lys^{179}. Likewise, RhDH827 is also less dependent upon Lys^{169}. It focuses instead upon Lys^{168} and downstream hydrophobic residues in the V2 sequence; Lys^{169} accounts for 8.7% of the total peptide BSA while Lys^{168} accounts for 12.7% (**Figures 6C–E**). RhDH827 binds the V2 peptide mainly with CDRs H2, H3, L1 and L3. Glu^{50} and Asp^{51} of the Glu-Asp motif in CDR L2 make salt bridges with Lys^{169} and Lys^{168} of the peptide respectively, but account for almost all of CDR L2's contribution to binding (**Figure 6F**). CDRs L1 and L3 provide much of the remaining contact surface for the N-terminus of the peptide, while CDRs H2 and H3 primarily interact with the C-terminus. The total light chain BSA contribution to the interface is 293 Å^2, 124 Å^2 from CDR L1, 37 Å^2 from CDR L2, and 130 Å^2 from CDR L3, and the total heavy chain BSA contribution 492 Å^2, 51 Å^2 from CDR H1, 184 Å^2 from CDR H2, and 257 Å^2 from

A

	V domain (V_H+V_L)	C domain (C_L+C_H1)	V domain (V_H+V_L)-gp120 core/V2 peptide	Fab(V+C domain)-gp120 core/V2 peptide
RhDH677.3 versus DH677.3	0.72	1.66	1.03	2.98
RhDH827 versus DH827	0.95	1.16	1.02	2.13

B

C domain (C_L+C_H1), Kappa light chain

	RhDH677.3	6U6M	6U6O	6VOR	6VOS	6VSR
RhDH677.3		2.84	2.91	1.80	1.86	2.00
6U6M	2.84		0.79	2.77	2.79	2.87
6U6O	2.91	0.79		2.77	2.81	2.83
6VOR	1.80	2.77	2.77		0.54	0.74
6VOS	1.86	2.79	2.81	0.54		1.04
6VSR	2.00	2.87	2.83	0.74	1.04	

C domain (C_L+C_H1), Lambda light chain

	RhDH827	4RFE	3Q6G	4Q2Z	5T4Z	5UKN	5UKO	5UKP
RhDH827		0.89	0.72	0.96	0.90	0.96	0.98	0.62
4RFE	0.89		0.97	0.98	0.89	1.19	1.21	0.97
3Q6G	0.72	0.97		1.21	0.84	1.27	1.39	0.59
4Q2Z	0.96	0.98	1.21		1.07	1.05	1.15	0.86
5T4Z	0.90	0.89	0.84	1.07		1.18	1.26	0.90
5UKN	0.96	1.19	1.27	1.05	1.18		0.33	0.67
5UKO	0.98	1.21	1.39	1.15	1.26	0.33		0.73
5UKP	0.62	0.97	0.59	0.86	0.90	0.67	0.73	

FIGURE 5 | Comparison of overall structures of Rhesusized mAb variants to human and RM counterparts. **(A)** RMSD values for main chain atoms for pairwise comparisons of Fab V or C domains and Fab V or Fab-gp120 core complex between rhesusized and human variants. **(B)** RMSD values for main chain atoms for pairwise comparisons of Fab C domains of RhDH677.3 and RhDH827 to RM mAb Fabs available in the PDB with kappa and lambda light chains, respectively.

CDR H3 (**Table S2**). Aside from the two salt bridges from CDR L2 (Glu^{50} and Asp^{51} to Lys^{169} and Lys^{168} respectively) and three hydrogen bonds from the heavy chain (one from CDR H3 Ser^{100} to His^{173} and two from CDR H2 tyrosine residues to the main chain carbonyls of Leu^{179} and Ile^{181}) most of the interface is hydrophobic in nature which may help it tolerate mutations that disrupt the salt bridges to Lys^{168} or Lys^{169} and changes to Ile^{181}, the hydrophobic residue with the single largest contribution to the BSA; changes in Lys^{169} and Ile^{181} were identified in RV144 breakthrough viruses implicating this region in the protective effect of the vaccine (7).

RhDH827 was crystalized with the same V2 peptide as used previously for its human counterpart DH827 (30) however, the complex structure of RhDH827 was solved at higher resolution (2.0 versus 2.9 Å for DH827). In addition, there is a one amino acid insertion in the light chain CDR L3 at position 95A of RhDH827 that is absent in DH827 due to a difference in sequence between the clone of DH827 used to generate RhDH827 (30). These differences slightly complicate the direct comparison of the two structures. Although the RMSD value for the comparison of the main chain atoms of the antibody variable domains and the bound peptide is very low, 1 Å (**Figure 5A**), there are some differences in specific contacts at the antibody-peptide interface. For example, in the RhDH827-V2 complex, Lys^{168} and Lys^{169} of peptide account for approximately 18% of the total peptide BSA with 8.9 $Å^2$ and 9.1 $Å^2$ contributed for Lys^{168} and Lys^{169}, respectively. Furthermore, in the RhDH827 complex, the N-terminus of the peptide fold into an amphipathic helical conformation with hydrophobic residues from that region Val^{172}, Leu^{175}, Phe^{176}, and Leu^{179} together with those from the C-terminus after a break in the helix e.g. Ile^{181}, Val^{182}, and Pro^{183}, making up approximately 65% of the peptide BSA. This is comparable to the 67% seen for the corresponding residues in the DH827 complex, but the total peptide BSA is significantly lower for the human antibody, 817 $Å^2$ versus 852 $Å^2$. The lower resolution of the human complex could potentially explain this difference; density for the peptide is weaker at both the N and C termini in the human structure which makes the side chain positions for these residues less certain.

Interestingly, contributions from the heavy and light chain CDRs are roughly comparable between the two structures with the exception of one major difference in CDR L3. RhDH827 has an extra histidine, His^{95A}, relative to the human DH827, due to a difference in the DH827 clone used to make RhDH827 (**Figure 6C** and **Figure S2**). This changes the conformation of the CDR L3 loop. As a consequence, CDR L3 Ile^{94} makes the same contacts to the peptide in the human complex that CDR L3 Thr^{94} makes to the peptide in the rhesusized complex. His^{95A} itself adds little to the interface. The slightly shorter CDR L3 in the human structure also changes the conformation of the C-t2erminus of the peptide, mainly in the area near the end of the peptide helix. This conformational difference may explain the slightly higher BSAs for CDR H3 Pro^{99} and CDR L1 Tyr^{32} in the human structure. Outside of these regions the structures are largely identical with similar BSA values for both the heavy and light chain residues as can be seen in the bar chart of BSA by residue (**Figure 6F**).

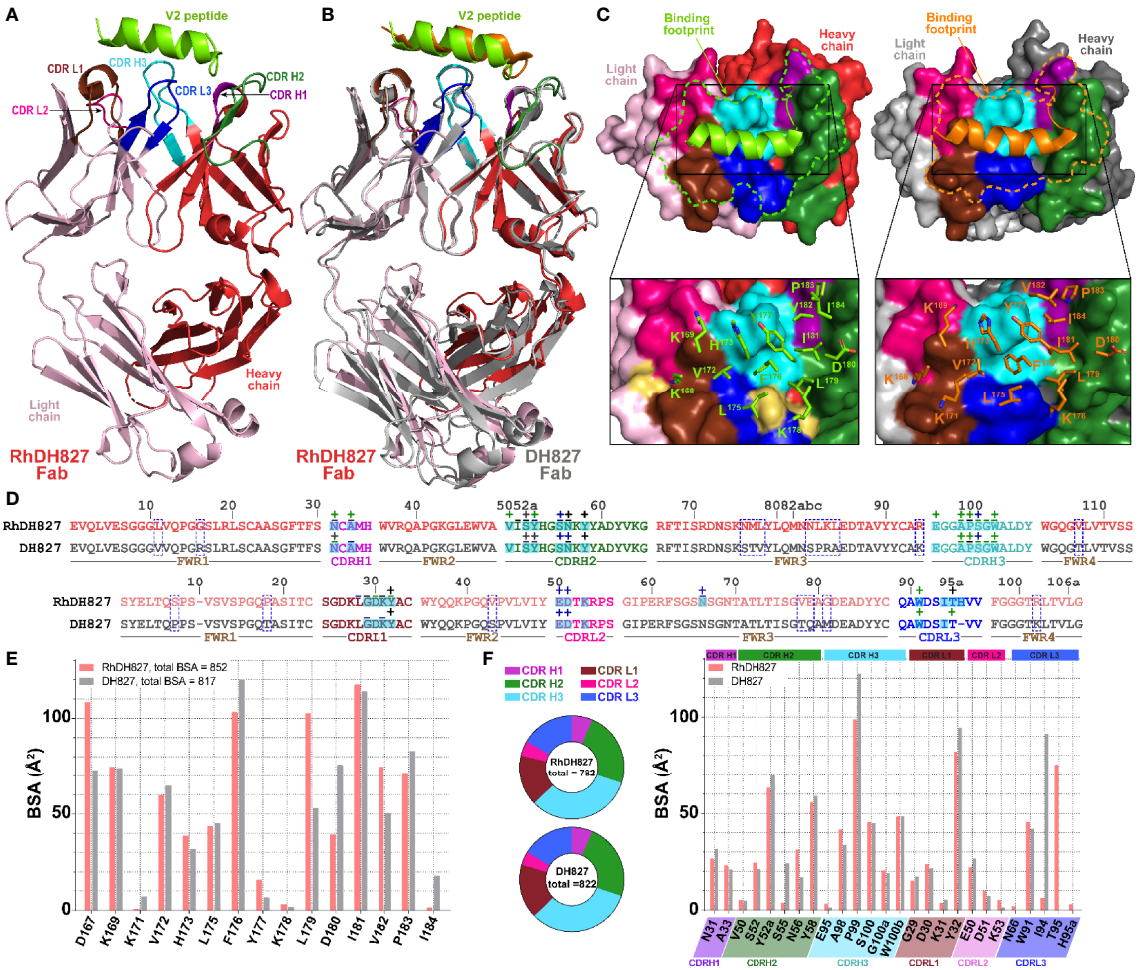

FIGURE 6 | Crystal structure ofRhDH827 Fab-V2 peptide complex. **(A)** The overall structure of the complex is shown as a ribbon diagram. The V2 peptide is green and the light chain (LC) and heavy chain (HC) of RhDH827 Fab are colored in light pink and red, respectively. The CDRs of RhDH827 Fab are colored as following colors: CDR L1 (brown), CDR L2 (pink), CDR L3 (blue), CDR H1 (purple), CDR H2 (dark green), and CDR H3 (cyan). **(B)** Structural comparison of RhDH827 Fab-V2 peptide and DH827 Fab-V2 peptide complexes. The RhDH827 Fab-V2 peptide complex is colored as indicated in panel A and the DH677.3 Fab-V2 peptide complex is colored in gray with V2 peptide colored in orange. The complexes are superimposed based on the variable heavy (V_H) domain. **(C)** RhDH827 andDH827 Fabs are shown as a molecular surface and the CDRs of both Fabs surface are colored as in panel **(A)** The light chain (LC) and heavy chain (HC) of DH827 Fab are colored in light and dark gray, respectively. Binding footprints for V2 peptide on RhDH827 and DH827 Fabs are outlined in green and orange, respectively (top panel). Residues contributing to the binding are shown as sticks (bottom panel). Extra binding residues on RhDH827 are colored in yellow. **(D)** Contact residues of RhDH827 and DH827 Fabs with V2 peptide are mapped onto the Fab sequences and colored as described for panel **(A)** Contact residues are defined by a 5 Å cutoff and marked above the sequence with (+) for side chain and **(-)** for main chain to indicate the type of contact. Contact types are colored as following: hydrophilic (green), hydrophobic (blue) and both (black). Residues that differ between RhDH827 and DH827 are highlighted in blue dashed-line box. Buried surface residues are determined by PISA and are shaded green. **(E)** The buried surface area (BSA) contributions of V2 peptide to binding of RhDH827/DH827 Fabs are shown in red and gray, respectively. The BSA contributions to binding of V2 residues as calculated by PISA. **(F)** Pie charts showing the BSA of RhDH827/DH827 Fabs buried at the complex interface and are colored as in panel **(A)** The BSA contributions to binding for RhDH827 CDR residues are colored in red and BSA contributions to binding for DH677.3 CDR residues are shown in gray.

Constant (C) Regions of Rhesusized mAb Variants Show Close Structural Similarity to C Domains of RM IgG1

Analysis of the structures of Fab-antigen complexes of rhesusized and human IgG pairs confirm close similarity of their V domain structures and good preservation of the contacts at the antigen-Fab interface. While in the rhesusized IgG1 variants the V domains are of mixed sequence, assembled from the closest RM germline framework mAb sequence and CDRs engrafted from human counterpart, the C domains (C_L+C_H1) are unchanged and formed from fully RM IgG1 sequences (**Figure 1**). Of note RhDH677.3 and RhDH827 represent kappa and lambda light chains, respectively. In order to check if sequence changes in the V domains contribute to changes in overall architecture of the rhesusized variant C domains we compared the structures of the C domains of RhDH677.3 and

RhDH827 to C domain structures from RM IgG1 Fabs available in Protein Data Bank (**Figure 5B**). We used entries from PDB of antibodies of different specificities (including antibodies unrelated to HIV-1) but matched RhDH677.3 with antibodies with kappa light chains and RhDH827 with antibodies with lambda light chains. Overall the RMSD values for the C domains of RhDH677.3 as compared to the other kappa light chain containing antibodies fell within a range of 1.8-2.91 Å which is slightly higher than the highest RMSD value for kappa light chain antibody comparisons in the absence of RhDH677.3 (RMSD range of 0.54-2.87 Å). In contrast, the RMSDs for the C domains of RhDH827 as compared to the other lambda light chain containing antibodies fell within a range of 0.62-0.98 Å which is lower than the RMSD range for all other lambda antibodies in the absence of RhDH827 (0.33-1.39 Å). This indicates that there is a poorer agreement among the kappa light chain C domain structures in general and with RhDH677.3 in particular although this could be in part due to the lower resolution from the RhDH677.3 complex structure. The better agreement among the C domain structures with lambda light chains may be a reflection of the higher resolution of the RhDH827 structure but it could also be in part due to the fewer number of changes relative to the human sequence for the lambda light chain, 12, versus the kappa light chain, 17, since human lambda and kappa C domains were initially used as models for the generation of both structures.

Rhesusized mAb Variants Mediate Antibody Fc Effector Functions (i.e. Recognition of SHIV-1 Infected Cells, ADCC, ADCP, ADNP, and Virion Capture) Comparable to Their Human Counterparts

Structural and SPR analyses indicate that the rhesusized mAb variants preserve the antigen binding properties of their human counterparts, and SPR binding confirms that their binding affinities to the low affinity RM and human FcγRs are comparable to mAbs of RM origin. To see if these features translate into 'proper' functional activity, we assessed their binding to HIV-infected CEM.NKR.CCR5 cells and SHIV-infected A66 cells using the gating strategy demonstrated in **Figure 7A**. We observed similar percentages of HIV-infected cells bound by each pair of human and rhesusized mAb (%Ab +p24/p27+) to each HIV-1 Infectious Molecular Clone (IMC) and SHIV tested here (**Figure 7B**). The percentage of infected cells bound by the combination of three mAbs, DH677.3 (C1C2), DH827 (V2) and 7B2 (gp41) was also similar between human and macaque. The human version of DH677.3 demonstrated a difference in binding to SHIV.CH505.375H- and SHIV.1157QNE(Y173H)-infected cells as compared to its rhesus counterpart. A similar increase in binding was observed with the V2-targeting RhDH827 Ab as compared to its human version to SHIV.SF162.P3-infected cells. Overall, there was similar binding of rhesusized mAbs to HIV-infected cells as compared to their human counterparts.

The ADCC activity of the rhesusized variants to their human counterparts was also compared using HIV-infected CEM.NKR.CCR5 cells as targets in a luciferase-based ADCC assay (49). Peripheral blood mononuclear cells (PBMCs) isolated from an HIV-1-seronegative individual were used as effector cells and subtype B HIV-1 SF162-, subtype C HIV-1 CH505- or 1086-infected cells were used as targets in the presence of serial dilutions of mAbs. We observed similar area under the curve (AUC) values for human and rhesus mAb pairs against the three IMCs tested here (**Figure 7C).** The analysis of ADCC activity for mAbs in the ADCC-GTL assay (51) also revealed similar magnitudes in AUC values for each individual mAb pair and for macaque and human mAb combinations (**Figure S5**).

The capacity of the C1-C2 and V2 specific rhesusized variants to mediate phagocytosis by monocytes (ADCP) and neutrophils (ADNP) was assessed using the THP-1 and HL-60 cell lines with SHIV 1157(QNE)Y173H gp120 protein coated microspheres, respectively (**Figure 8A**). Overall, the rhesusized Abs had similar levels of phagocytosis to their human counterparts. The V2 Abs had modestly higher phagocytosis scores compared to the C1C2 specific antibodies, likely due to improved epitope exposure on Env protein. To assess recognition of virus particles as one of the first steps in antibody effector function, we also assessed the capacity of all 3 antibody specificities to bind infectious SHIV 1157(QNE)Y173H virions (**Figure 8B**). As expected, the C1C2 antibody specificities did not bind and capture virus. However, the V1V2 and gp41 specific antibodies did capture infectious virions.

Taken together these data indicate that rhesusized mAb binding and ADCC to *in vitro* infected cells are comparable antibody Fc effector functions for human mAb counterparts as well as anti-HIV-1 antibodies of human or rhesus origin.

DISCUSSION

The number of antibodies and antibody-based therapeutics used clinically continues to grow (71, 72). Since many of these products are derived from antibodies from a nonhuman origin they need to be adapted to the human immune system, or 'humanized', before they can be used clinically. Simple grafting of an antibody's complementary determining regions (CDRs) to a human antibody backbone sequence often leads to reduced antigen affinity either by omission of paratope residues outside of the CDRs or by subtle structural changes due to differences in the sequence of framework residues. Conversely, grafting of the entire heavy and light chain variable domain, V_H and V_L, onto constant heavy and light chain backbones to make a chimera, while maintaining paratope structure introduces a greater number changes and potentially increases immunogenicity. This has typically made humanization of antibodies a multistep process in which the initial incarnation of a humanized antibody is subsequently modified to increase its affinity for antigen in order to match that of the parent mAb. The sequencing of the human genome has aided this process by making it possible to identify the closest germline sequence to minimize the number of needed residue changes and potentially decrease immunogenicity.

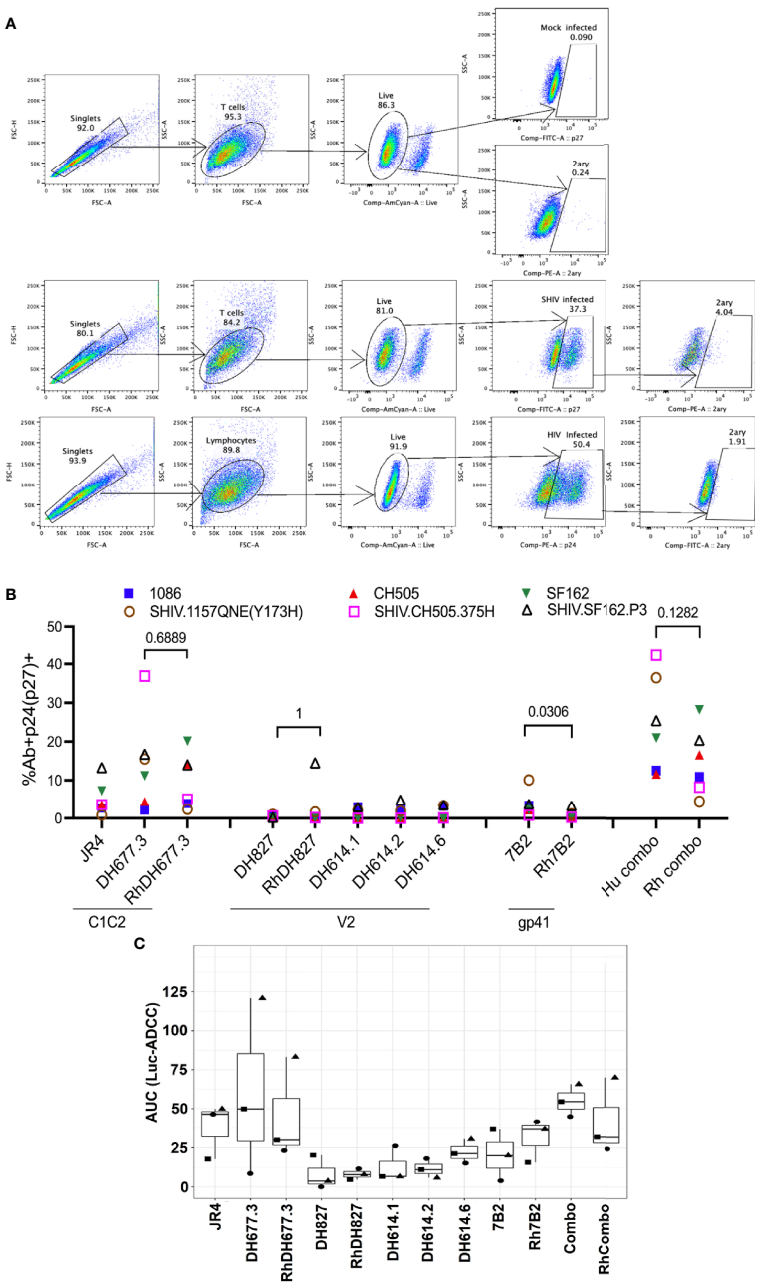

FIGURE 7 | ADCC activities of rhesusized mAb variants. **(A)** The gating strategy for the binding of mAbs to HIV.IMC-infected CEM.NKR cells and SHIV-infected A66 cells. The binding of mAbs to mock-infected cells (top), SHIV-infected A66 cells (middle) and HIV-infected CEM.NKR cells and (bottom). Cells were first gated for singlets (FSC-H vs. FSC-A) and T cells (SSC-A vs. FSC-A). The T cells were further analyzed for their uptake of the Live/Dead Aqua stain to determine live versus dead cells. Live cells were analyzed for the intracellular expression of p24 or p27. Each well was stained either with anti-p24 (CEM.NKR cells that were infected with HIV) or anti-p27 antibody (A66 cells infected with SHIV). Infected cells, p24+ (infected with HIV.IMCs) or p27+ (infected with SHIVs), were analyzed for binding of the tested mAb by staining with a secondary mAb (2ary). The far-right panel indicate 2ary Ab only (these are the well that lack primary Ab of interest) which shows that in presence of secondary antibody alone we did not detect any binding to either mock or infected cells. Mock-infected cells were used to properly set the gate for the infected cell population and the 2ary mAb. FSC, forward scatter; SSC, side scatter. **(B)** The percentage of infected cells bound by the tested mAb. The antibodies listed on the x-axis are grouped by the epitope specificity: C1C2 (RM JR4, DH677.3), V2 (DH827, RM DH614.1, RM DH614.2, RM DH614.6), gp41 immunodominant (gp41), and the combination (DH677.3, DH827, 7B2). Each color represents a different HIV-1 Infectious Molecular Clone (IMC) or SHIV. Each Ab/virus combination was tested once using a single well. **(C)** ADCC activities are shown as area under the curve (AUC) for each mAb calculated from dilution curves (starting concentration 50 μg/mL with 1:5 serial dilutions) against HIV.IMC-infected cells determined by a Renilla Luciferase-based ADCC assay (Luc-ADCC) with PBMCs from an HIV-1-seronegative individual as effectors at an E:T ratio of 30:1. Each symbol represents a different IMC. Each experiment in panel C was performed once with two biological replicates. Wilcoxon rank sum test was used to assess statistical significance; p-values less than 0.05 were considered significant.

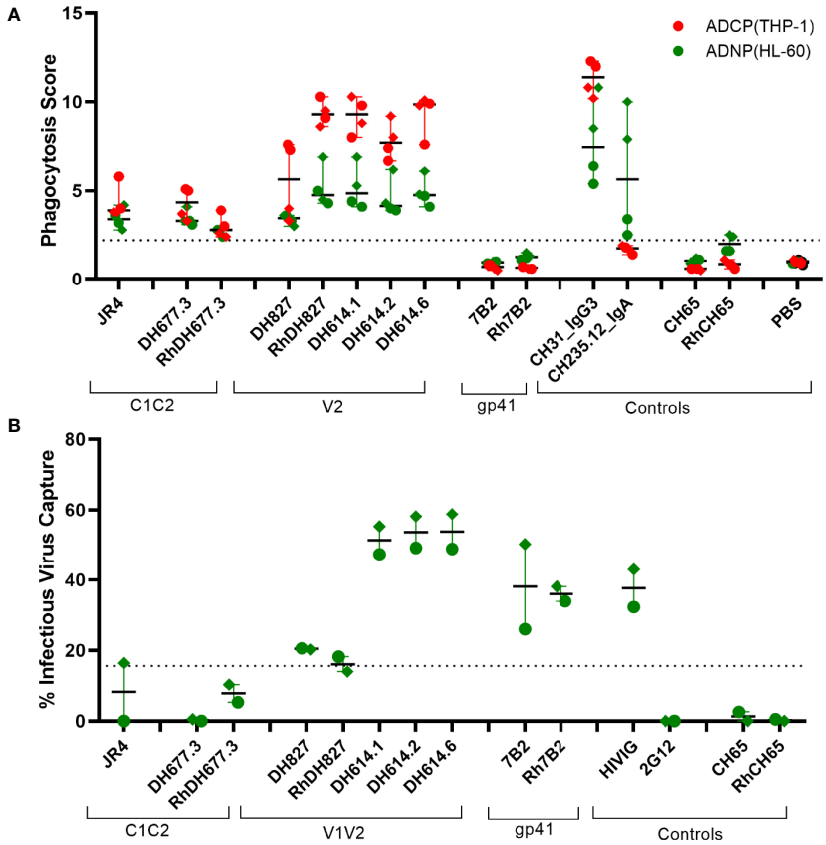

FIGURE 8 | Virion binding and phagocytic activities of Rhesusized mAb **(A)** Antibody-dependent phagocytosis of monocytes using monocytic THP1 cell line and neutrophils using HL60 cell line with SHIV 1157(QNE)Y173H gp120-coated beads. **(B)** Binding of antibody variants to infectious SHIV1157(QNE)Y173H. Dotted lines represent positivity cutoffs of 15.6% and 2.2 for virus capture and ADCP/ADNP, respectively. The data represent an average of two independent experiments with two replicates for each experiment for ADCP/ADNP and one replicate for virion binding. Rhesus macaque antibody versions are marked with Rh. Positive controls (CH31 IgG3, CH235.12 IgA) and negative controls (7B2, Rh7B2, Ch65, RhCH65 and PBS) are shown.

The close phylogenetic relationship between humans and nonhuman primates (NHPs), including Rhesus macaque (RM), *Macaca mulatta*, makes them an important animal model in the testing of new vaccines, antibodies or antibody based therapeutics. For human antibodies to be tested in RM this requires the reverse of humanization, i.e. rhesusization. The latter is essential to enable proper interaction with host immune system. Ideally this is done with the fewest number of sequence changes both to preserve the paratope structure of the parent mAb and to minimize immunogenicity. Here we have applied the rhesusization process to three human anti-HIV-1 antibodies recognizing Env which impact the virus predominantly by a Fc-effector mechanism (DH677.3, DH827, and 7B2) to facilitate their use in future NHP challenge studies.

We were able to obtain crystal structures of antigen complexes for two of our rhesusized variants in conditions similar to those used to obtain the structures of their human counterparts. This allowed us to perform a detailed analysis of the complex interface and to detect any changes introduced in the rhresusization process. Some slight differences were seen in the RhDH677.3 complex in contacts made by the Fab outside of the CDRs. Framework residues from the human mAb contributed slightly more to the interface than the corresponding residues from the rhesusized version. Interestingly, these differences could largely be attributed to positions that differed between the human and macaque germline sequences and are reflected in the total interface BSA, 1800 $Å^2$ for RhDH677.3 and 1984 $Å^2$ for DH677.3, and in the approximately 8-fold reduction in affinity for RhDH677.3 to antigen. Thus, for antibodies that involve framework residues in antigen engagement, rhesusization within framework areas should to be done carefully to avoid losses that can potentially lead to a decrease of affinity to antigen. Similar conclusions could be drawn from the comparison of the human and macaque versions of DH827 although a one residue difference in sequence in the light chain and different resolutions for the two structures made the comparison more difficult.

Importantly, the Fc-functionality of the rhesusized mAbs were fully preserved. SPR results confirmed that the rhesusized mAbs had affinities to both macaque and human FcγRs similar to mAbs originally isolated from RM. Rhesusized mAbs also bound

to HIV-1 infected cells at levels comparable to those of their human counterpart. They also displayed ADCC, ADCP and ADNP activities in the same range as macaque mAbs of similar specificity.

In conclusion, reducing immunogenicity potentially comes at the cost of reduced affinity to antigen. Even highly somatically mutated species matched antibodies can elicit immune reactions that remove them from circulation. This has been the case in macaques with the introduction of anti-SIV mAbs (73) and in humans with the introduction of broadly neutralizing antibodies against HIV-1, PG9 in clinicaltrials.gov NCT01937455 (74) and VRC07 in VRC 603, clinicaltrials.gov NCT03374202 (75). Rhesusization can potentially minimize the impact of such off-target reactions and extend their half-life in sera when they are evaluated in NHP models (33), but anti-idiotype immune responses are still possible (76). Rhesusization also places the antibody specificity within the context of the host immune response affording a more direct comparison to vaccine elicited antibodies of similar specificity. This may enable use of the RM model to more accurately test antibody correlates of protection from HIV-1 infection identified in human vaccine trials and more generally antibodies and antibody based therapeutics that utilize Fc mediated effector functions as part of their mechanism of action.

DATA AVAILABILITY STATEMENT

The datasets generated and/or analyzed during the current study are available in the Protein Data Bank (PDB) http://www.rcsb.org under admission codes: 6OZ2 and 6OZ4.

AUTHOR CONTRIBUTIONS

WT, DN, GT, GF, and MP designed, performed research, and analyzed the data, MT, SJ, and GF designed, performed, and analyzed cell binding and ADCC data. AC, YC, and MA designed, performed, and analyzed SPR binding data. KW helped with rhesus germline gene inference. GT, KS, and JP designed and produced RM IgG variants. DG and GT designed and analyzed phagocytosis experiments. AD, GL, DE, MM, VB, and SM helped design the mAb selections and experiments. JT and AP provided the SHIV QNE and helped with experimental design. WT, DN, and MP wrote the manuscript and all authors provided comments or revisions. All authors contributed to the article and approved the submitted version.

FUNDING

Funding for this study was provided by the National Institute of Health grants: P01 AI120756 to GT, R01 AI116274 to MP, R01 AI129769 to MP, with support from the Duke Center for AIDS Research P30 AI064518. The funders had no role in study design, data collection and analysis, decision to publish, or preparation of the manuscript and the contents of this publication are solely the responsibility of the authors.

ACKNOWLEDGMENTS

We thank Sheetal Sawant, Duke University for statistical advice. Use of the Stanford Synchrotron Radiation Lightsource, SLAC National Accelerator Laboratory, is supported by the U.S. Department of Energy, Office of Science, Office of Basic Energy Sciences under Contract No. DE-AC02-76SF00515. The SSRL Structural Molecular Biology Program is supported by the DOE Office of Biological and Environmental Research, and by the National Institutes of Health, National Institute of General Medical Sciences.

SUPPLEMENTARY MATERIAL

The Supplementary Material for this article can be found online at: https://www.frontiersin.org/articles/10.3389/fimmu.2021.787603/full#supplementary-material

REFERENCES

1. Rerks-Ngarm S, Pitisuttithum P, Nitayaphan S, Kaewkungwal J, Chiu J, Paris R, et al. Vaccination With ALVAC and AIDSVAX to Prevent HIV-1 Infection in Thailand. *N Engl J Med* (2009) 361(23):2209–20. doi: 10.1056/NEJMoa0908492
2. Bonsignori M, Pollara J, Moody MA, Alpert MD, Chen X, Hwang KK, et al. Antibody-Dependent Cellular Cytotoxicity-Mediating Antibodies From an HIV-1 Vaccine Efficacy Trial Target Multiple Epitopes and Preferentially Use the VH1 Gene Family. *J Virol* (2012) 86(21):11521–32. doi: 10.1128/JVI.01023-12
3. Haynes BF, Gilbert PB, McElrath MJ, Zolla-Pazner S, Tomaras GD, Alam SM, et al. Immune-Correlates Analysis of an HIV-1 Vaccine Efficacy Trial. *N Engl J Med* (2012) 366(14):1275–86. doi: 10.1056/NEJMoa1113425
4. Tomaras GD, Ferrari G, Shen X, Alam SM, Liao HX, Pollara J, et al. Vaccine-Induced Plasma IgA Specific for the C1 Region of the HIV-1 Envelope Blocks Binding and Effector Function of IgG. *Proc Natl Acad Sci USA* (2013) 110):9019–24. doi: 10.1073/pnas.1301456110
5. Li SS, Gilbert PB, Tomaras GD, Kijak G, Ferrari G, Thomas R, et al. FCGR2C Polymorphisms Associate With HIV-1 Vaccine Protection in RV144 Trial. *J Clin Invest* (2014) 124(9):3879–90. doi: 10.1172/JCI75539
6. Karasavvas N, Billings E, Rao M, Williams C, Zolla-Pazner S, Bailer RT, et al. The Thai Phase III HIV Type 1 Vaccine Trial (RV144) Regimen Induces Antibodies That Target Conserved Regions Within the V2 Loop of Gp120. *AIDS Res Hum Retroviruses* (2012) 28(11):1444–57. doi: 10.1089/aid.2012.0103
7. Rolland M, Edlefsen PT, Larsen BB, Tovanabutra S, Sanders-Buell E, Hertz T, et al. Increased HIV-1 Vaccine Efficacy Against Viruses With Genetic Signatures in Env V2. *Nature* (2012) 490(7420):417–20. doi: 10.1038/nature11519
8. Gottardo R, Bailer RT, Korber BT, Gnanakaran S, Phillips J, Shen X, et al. Plasma IgG to Linear Epitopes in the V2 and V3 Regions of HIV-1 Gp120

Correlate With a Reduced Risk of Infection in the RV144 Vaccine Efficacy Trial. *PloS One* (2013) 8(9):e75665. doi: 10.1371/journal.pone.0075665
9. Zolla-Pazner S, deCamp AC, Cardozo T, Karasavvas N, Gottardo R, Williams C, et al. Analysis of V2 Antibody Responses Induced in Vaccinees in the ALVAC/AIDSVAX HIV-1 Vaccine Efficacy Trial. *PloS One* (2013) 8(1): e53629. doi: 10.1371/journal.pone.0053629
10. Barouch DH, Liu J, Li H, Maxfield LF, Abbink P, Lynch DM, et al. Vaccine Protection Against Acquisition of Neutralization-Resistant SIV Challenges in Rhesus Monkeys. *Nature* (2012) 482(7383):89–93. doi: 10.1038/nature10766
11. Pegu P, Vaccari M, Gordon S, Keele BF, Doster M, Guan Y, et al. Antibodies With High Avidity to the Gp120 Envelope Protein in Protection From Simian Immunodeficiency Virus SIV(mac251) Acquisition in an Immunization Regimen That Mimics the RV-144 Thai Trial. *J Virol* (2013) 87(3):1708–19. doi: 10.1128/JVI.02544-12
12. Gordon SN, Doster MN, Kines RC, Keele BF, Brocca-Cofano E, Guan Y, et al. Antibody to the Gp120 V1/V2 Loops and CD4+ and CD8+ T Cell Responses in Protection From SIVmac251 Vaginal Acquisition and Persistent Viremia. *J Immunol* (2014) 193(12):6172–83. doi: 10.4049/jimmunol.1401504
13. Roederer M, Keele BF, Schmidt SD, Mason RD, Welles HC, Fischer W, et al. Immunological and Virological Mechanisms of Vaccine-Mediated Protection Against SIV and HIV. *Nature* (2014) 505(7484):502–8. doi: 10.1038/nature12893
14. Gordon SN, Liyanage NP, Doster MN, Vaccari M, Vargas-Inchaustegui DA, Pegu P, et al. Boosting of ALVAC-SIV Vaccine-Primed Macaques With the CD4-SIVgp120 Fusion Protein Elicits Antibodies to V2 Associated With a Decreased Risk of SIVmac251 Acquisition. *J Immunol* (2016) 197(7):2726–37. doi: 10.4049/jimmunol.1600674
15. Vaccari M, Gordon SN, Fourati S, Schifanella L, Liyanage NP, Cameron M, et al. Adjuvant-Dependent Innate and Adaptive Immune Signatures of Risk of SIVmac251 Acquisition. *Nat Med* (2016) 22(7):762–70. doi: 10.1038/nm.4105
16. Malherbe DC, Mendy J, Vang L, Barnette PT, Reed J, Lakhashe SK, et al. Combination Adenovirus and Protein Vaccines Prevent Infection or Reduce Viral Burden After Heterologous Clade C Simian-Human Immunodeficiency Virus Mucosal Challenge. *J Virol* (2018) 92(2):e01092–17. doi: 10.1128/JVI.01092-17
17. Singh S, Ramirez-Salazar EG, Doueiri R, Valentin A, Rosati M, Hu X, et al. Control of Heterologous Simian Immunodeficiency Virus SIVsmE660 Infection by DNA and Protein Coimmunization Regimens Combined With Different Toll-Like-Receptor-4-Based Adjuvants in Macaques. *J Virol* (2018) 92(15):e00281–18. doi: 10.1128/JVI.00281-18
18. Felber BK, Lu Z, Hu X, Valentin A, Rosati M, Remmel CAL, et al. Co-Immunization of DNA and Protein in the Same Anatomical Sites Induces Superior Protective Immune Responses Against SHIV Challenge. *Cell Rep* (2020) 31(6):107624. doi: 10.1016/j.celrep.2020.107624
19. Gray GE, Bekker LG, Laher F, Malahleha M, Allen M, Moodie Z, et al. Vaccine Efficacy of ALVAC-HIV and Bivalent Subtype C Gp120-MF59 in Adults. *N Engl J Med* (2021) 384(12):1089–100. doi: 10.1056/NEJMoa2031499
20. Shen X, Laher F, Moodie Z, McMillan AS, Spreng RL, Gilbert PB, et al. HIV-1 Vaccine Sequences Impact V1V2 Antibody Responses: A Comparison of Two Poxvirus Prime Gp120 Boost Vaccine Regimens. *Sci Rep* (2020) 10(1):2093. doi: 10.1038/s41598-020-57491-z
21. Neidich SD, Fong Y, Li SS, Geraghty DE, Williamson BD, Young WC, et al. Antibody Fc Effector Functions and IgG3 Associate With Decreased HIV-1 Risk. *J Clin Invest* (2019) 129(11):4838–49. doi: 10.1172/JCI126391
22. Boesch AW, Osei-Owusu NY, Crowley AR, Chu TH, Chan YN, Weiner JA, et al. Biophysical and Functional Characterization of Rhesus Macaque IgG Subclasses. *Front Immunol* (2016) 7:589. doi: 10.3389/fimmu.2016.00589
23. Chan YN, Boesch AW, Osei-Owusu NY, Emileh A, Crowley AR, Cocklin SL, et al. IgG Binding Characteristics of Rhesus Macaque FcgammaR. *J Immunol* (2016) 197(7):2936–47. doi: 10.4049/jimmunol.1502252
24. Tolbert WD, Subedi GP, Gohain N, Lewis GK, Patel KR, Barb AW, et al. From Rhesus Macaque to Human: Structural Evolutionary Pathways for Immunoglobulin G Subclasses. *MAbs* (2019) 11(4):709–24. doi: 10.1080/19420862.2019.1589852
25. Lejeune J, Brachet G, Watier H. Evolutionary Story of the Low/Medium-Affinity IgG Fc Receptor Gene Cluster. *Front Immunol* (2019) 10:1297. doi: 10.3389/fimmu.2019.01297
26. Mascola JR, Lewis MG, Stiegler G, Harris D, VanCott TC, Hayes D, et al. Protection of Macaques Against Pathogenic Simian/Human Immunodeficiency Virus 89.6PD by Passive Transfer of Neutralizing Antibodies. *J Virol* (1999) 73(5):4009–18. doi: 10.1128/JVI.73.5.4009-4018.199
27. Burton DR, Hessell AJ, Keele BF, Klasse PJ, Ketas TA, Moldt B, et al. Limited or No Protection by Weakly or Nonneutralizing Antibodies Against Vaginal SHIV Challenge of Macaques Compared With a Strongly Neutralizing Antibody. *Proc Natl Acad Sci USA* (2011) 108:11181–6. doi: 10.1073/pnas.1103012108
28. Shingai M, Donau OK, Plishka RJ, Buckler-White A, Mascola JR, Nabel GJ, et al. Passive Transfer of Modest Titers of Potent and Broadly Neutralizing Anti-HIV Monoclonal Antibodies Block SHIV Infection in Macaques. *J Exp Med* (2014) 211(10):2061–74. doi: 10.1084/jem.20132494
29. Martinez-Navio JM, Fuchs SP, Pedreno-Lopez S, Rakasz EG, Gao G, Desrosiers RC. Host Anti-Antibody Responses Following Adeno-Associated Virus-Mediated Delivery of Antibodies Against HIV and SIV in Rhesus Monkeys. *Mol Ther* (2016) 24(1):76–86. doi: 10.1038/mt.2015.191
30. Easterhoff D, Pollara J, Luo K, Janus B, Gohain N, Williams LD, et al. HIV Vaccine Delayed Boosting Increases Env Variable Region 2-Specific Antibody Effector Functions. *JCI Insight* (2020) 5(2):e131437. doi: 10.1172/jci.insight.131437
31. Easterhoff D, Pollara J, Luo K, Tolbert WD, Young B, Mielke D, et al. Boosting With AIDSVAX B/E Enhances Env Constant Region 1 and 2 Antibody-Dependent Cellular Cytotoxicity Breadth and Potency. *J Virol* (2020) 94(4): e01120–19. doi: 10.1128/JVI.01120-19
32. Santra S, Tomaras GD, Warrier R, Nicely NI, Liao HX, Pollara J, et al. Human Non-Neutralizing HIV-1 Envelope Monoclonal Antibodies Limit the Number of Founder Viruses During SHIV Mucosal Infection in Rhesus Macaques. *PloS Pathog* (2015) 11(8):e1005042. doi: 10.1371/journal.ppat.1005042
33. Saunders KO, Pegu A, Georgiev IS, Zeng M, Joyce MG, Yang ZY, et al. Sustained Delivery of a Broadly Neutralizing Antibody in Nonhuman Primates Confers Long-Term Protection Against Simian/Human Immunodeficiency Virus Infection. *J Virol* (2015) 89(11):5895–903. doi: 10.1128/JVI.00210-15
34. Ramesh A, Darko S, Hua A, Overman G, Ransier A, Francica JR, et al. Structure and Diversity of the Rhesus Macaque Immunoglobulin Loci Through Multiple *De Novo* Genome Assemblies. *Front Immunol* (2017) 8:1407. doi: 10.3389/fimmu.2017.01407
35. Fouts TR, Tuskan R, Godfrey K, Reitz M, Hone D, Lewis GK, et al. Expression and Characterization of a Single-Chain Polypeptide Analogue of the Human Immunodeficiency Virus Type 1 Gp120-CD4 Receptor Complex. *J Virol* (2000) 74(24):11427–36. doi: 10.1128/JVI.74.24.11427-11436.2000
36. Otwinowski Z, Minor W, Charles W. "Processing of X-Ray Diffraction Data Collected in Oscillation Mode,". In: *Meth Enzymol*. Academic Press (1997). p. 307–26.
37. Collaborative Computational Project N. The CCP4 Suite: Programs for Protein Crystallography. *Acta Crystallogr D Biol Crystallogr* (1994) 50(Pt 5):760–3. doi: 10.1107/S0907444994003112
38. Adams PD, Afonine PV, Bunkoczi G, Chen VB, Davis IW, Echols N, et al. PHENIX: A Comprehensive Python-Based System for Macromolecular Structure Solution. *Acta Crystallogr D Biol Crystallogr* (2010) D66:213–21. doi: 10.1107/S0907444909052925
39. Weiss MS. GlobalIndicators of X-Ray Data Quality. *J Appl Cryst* 34 (2001):130–5. doi: 10.1107/S0021889800018227
40. Karplus PA, Diederichs K. Linking Crystallographic Model and Data Quality. *Science* (2012) 336:1030–3. doi: 10.1126/science.1218231
41. Popov AN, Bourenkov GP. Choice of Data-Collection Parameters Based on Statistic Modelling. *Acta Crystallogr D Biol Crystallogr* (2003) 59:1145–53. doi: 10.1107/S0907444903008163
42. Brunger AT. Free R Value: Cross-Validation in Crystallography. In: *Methods in Enzymology*. Academic Press (1997). p. 366–96.
43. Mielke D, Bandawe G, Pollara J, Abrahams MR, Nyanhete T, Moore PL, et al. Antibody-Dependent Cellular Cytotoxicity (ADCC)-Mediating Antibodies Constrain Neutralizing Antibody Escape Pathway. *Front Immunol* (2019) 10:2875. doi: 10.3389/fimmu.2019.02875
44. Hoxie JA, LaBranche CC, Endres MJ, Turner JD, Berson JF, Doms RW, et al. CD4-Independent Utilization of the CXCR4 Chemokine Receptor by HIV-1 and HIV-2. *J Reprod Immunol* (1998) 41(1-2):197–211. doi: 10.1016/s0165-0378(98)00059-x

45. Schouest B, Leslie GJ, Hoxie JA, Maness NJ. Tetherin Downmodulation by SIVmac Nef Lost With the H196Q Escape Variant is Restored by an Upstream Variant. *PloS One* (2020) 15(8):e0225420. doi: 10.1371/journal.pone.0225420
46. Pollara J, Tay MZ, Edwards RW, Goodman D, Crowley AR, Edwards RJ, et al. Functional Homology for Antibody-Dependent Phagocytosis Across Humans and Rhesus Macaques. *Front Immunol* (2021) 12:678511. doi: 10.3389/fimmu.2021.678511
47. Li H, Wang S, Kong R, Ding W, Lee FH, Parker Z, et al. Envelope Residue 375 Substitutions in Simian-Human Immunodeficiency Viruses Enhance CD4 Binding and Replication in Rhesus Macaques. *Proc Natl Acad Sci USA* (2016) 113(24):E3413–22. doi: 10.1073/pnas.1606636113
48. Song RJ, Chenine AL, Rasmussen RA, Ruprecht CR, Mirshahidi S, Grisson RD, et al. Molecularly Cloned SHIV-1157ipd3n4: A Highly Replication-Competent, Mucosally Transmissible R5 Simian-Human Immunodeficiency Virus Encoding HIV Clade C Env. *J Virol* (2006) 80(17):8729–38. doi: 10.1128/JVI.00558-06
49. Pollara J, Bonsignori M, Moody MA, Liu P, Alam SM, Hwang KK, et al. HIV-1 Vaccine-Induced C1 and V2 Env-Specific Antibodies Synergize for Increased Antiviral Activities. *J Virol* (2014) 88(14):7715–26. doi: 10.1128/JVI.00156-14
50. Johnson S, Oliver C, Prince GA, Hemming VG, Pfarr DS, Wang SC, et al. Development of a Humanized Monoclonal Antibody (MEDI-493) With Potent *In Vitro* and *In Vivo* Activity Against Respiratory Syncytial Virus. *J Infect Dis* (1997) 176(5):1215–24. doi: 10.1086/514115
51. Pollara J, Hart L, Brewer F, Pickeral J, Packard BZ, Hoxie JA, et al. High-Throughput Quantitative Analysis of HIV-1 and SIV-Specific ADCC-Mediating Antibody Responses. *Cytometry A* (2011) 79(8):603–12. doi: 10.1002/cyto.a.21084
52. Ackerman ME, Moldt B, Wyatt RT, Dugast AS, McAndrew E, Tsoukas S, et al. A Robust, High-Throughput Assay to Determine the Phagocytic Activity of Clinical Antibody Samples. *J Immunol Methods* (2011) 366(1-2):8–19. doi: 10.1016/j.jim.2010.12.016
53. Tay MZ, Liu P, Williams LD, McRaven MD, Sawant S, Gurley TC, et al. Antibody-Mediated Internalization of Infectious HIV-1 Virions Differs Among Antibody Isotypes and Subclasses. *PloS Pathog* (2016) 12(8):e1005817. doi: 10.1371/journal.ppat.1005817
54. Bonsignori M, Zhou T, Sheng Z, Chen L, Gao F, Joyce MG, et al. Maturation Pathway From Germline to Broad HIV-1 Neutralizer of a CD4-Mimic Antibody. *Cell* (2016) 165(2):449–63. doi: 10.1016/j.cell.2016.02.022
55. Bonsignori M, Montefiori DC, Wu X, Chen X, Hwang KK, Tsao CY, et al. Two Distinct Broadly Neutralizing Antibody Specificities of Different Clonal Lineages in a Single HIV-1-Infected Donor: Implications for Vaccine Design. *J Virol* (2012) 86(8):4688–92. doi: 10.1128/JVI.07163-11
56. Whittle JR, Zhang R, Khurana S, King LR, Manischewitz J, Golding H, et al. Broadly Neutralizing Human Antibody That Recognizes the Receptor-Binding Pocket of Influenza Virus Hemagglutinin. *Proc Natl Acad Sci USA* (2011) 108(34):14216–21. doi: 10.1073/pnas.1111497108
57. Worley MJ, Fei K, Lopez-Denman AJ, Kelleher AD, Kent SJ, Chung AW. Neutrophils Mediate HIV-Specific Antibody-Dependent Phagocytosis and ADCC. *J Immunol Methods* (2018) 457:41–52. doi: 10.1016/j.jim.2018.03.007
58. Liu P, Yates NL, Shen X, Bonsignori M, Moody MA, Liao HX, et al. Infectious Virion Capture by HIV-1 Gp120-Specific IgG From RV144 Vaccinees. *J Virol* (2013) 87(14):7828–36. doi: 10.1128/JVI.02737-12
59. Liu P, Williams LD, Shen X, Bonsignori M, Vandergrift NA, Overman RG, et al. Capacity for Infectious HIV-1 Virion Capture Differs by Envelope Antibody Specificity. *J Virol* (2014) 88(9):5165–70. doi: 10.1128/JVI.03765-13
60. Mayer KH, Seaton KE, Huang Y, Grunenberg N, Isaacs A, Allen M, et al. Safety, Pharmacokinetics, and Immunological Activities of Multiple Intravenous or Subcutaneous Doses of an Anti-HIV Monoclonal Antibody, VRC01, Administered to HIV-Uninfected Adults: Results of a Phase 1 Randomized Trial. *PloS Med* (2017) 14(11):e1002435. doi: 10.1371/journal.pmed.1002435
61. Buchacher A, Predl R, Strutzenberger K, Steinfellner W, Trkola A, Purtscher M, et al. Generation of Human Monoclonal Antibodies Against HIV-1 Proteins; Electrofusion and Epstein-Barr Virus Transformation for Peripheral Blood Lymphocyte Immortalization. *AIDS Res Hum Retroviruses* (1994) 10(4):359–69. doi: 10.1089/aid.1994.10.359
62. Gohain N, Tolbert WD, Acharya P, Yu L, Liu T, Zhao P, et al. Co-Crystal Structures of Antibody N60-I3 and Antibody JR4 in Complex With Gp120 Define More Cluster A Epitopes Involved in Effective Antibody-Dependent Effector Function Against HIV-1. *J Virol* (2015) 89(17):8840–54. doi: 10.1128/JVI.01232-15
63. Luo K, Liao HX, Zhang R, Easterhoff D, Wiehe K, Gurley TC, et al. Tissue Memory B Cell Repertoire Analysis After ALVAC/AIDSVAX B/E Gp120 Immunization of Rhesus Macaques. *JCI Insight* (2016) 1(20):e88522. doi: 10.1172/jci.insight.88522
64. Rerks-Ngarm S, Pitisuttithum P, Excler JL, Nitayaphan S, Kaewkungwal J, Premsri N, et al. Randomized, Double-Blind Evaluation of Late Boost Strategies for HIV-Uninfected Vaccine Recipients in the RV144 HIV Vaccine Efficacy Trial. *J Infect Dis* (2017) 215(8):1255–63. doi: 10.1093/infdis/jix099
65. Tolbert WD, Van V, Sherburn R, Tuyishime M, Yan F, Nguyen DN, et al. Recognition Patterns of the C1/C2 Epitopes Involved in Fc-Mediated Response in HIV-1 Natural Infection and the RV114 Vaccine Trial. *mBio* (2020) 11(3):e00208–20. doi: 10.1128/mBio.00208-20
66. Zolla-Pazner S, Alvarez R, Kong XP, Weiss S. Vaccine-Induced V1V2-Specific Antibodies Control and or Protect Against Infection With HIV, SIV and SHIV. *Curr Opin HIV AIDS* (2019) 14(4):309–17. doi: 10.1097/COH.0000000000000551
67. Arthos J, Cicala C, Martinelli E, Macleod K, Van Ryk D, Wei D, et al. HIV-1 Envelope Protein Binds to and Signals Through Integrin Alpha4beta7, the Gut Mucosal Homing Receptor for Peripheral T Cells. *Nat Immunol* (2008) 9(3):301–9. doi: 10.1038/ni1566
68. Tassaneetrithep B, Tivon D, Swetnam J, Karasavvas N, Michael NL, Kim JH, et al. Cryptic Determinant of Alpha4beta7 Binding in the V2 Loop of HIV-1 Gp120. *PloS One* (2014) 9(9):e108446. doi: 10.1371/journal.pone.0108446
69. Peachman KK, Karasavvas N, Chenine AL, McLinden R, Rerks-Ngarm S, Jaranit K, et al. Identification of New Regions in HIV-1 Gp120 Variable 2 and 3 Loops That Bind to Alpha4beta7 Integrin Receptor. *PloS One* (2015) 10(12):e0143895. doi: 10.1371/journal.pone.0143895
70. Wiehe K, Easterhoff D, Luo K, Nicely NI, Bradley T, Jaeger FH, et al. Antibody Light-Chain-Restricted Recognition of the Site of Immune Pressure in the RV144 HIV-1 Vaccine Trial is Phylogenetically Conserved. *Immunity* (2014) 41(6):909–18. doi: 10.1016/j.immuni.2014.11.014
71. Almagro JC, Daniels-Wells TR, Perez-Tapia SM, Penichet ML. Progress and Challenges in the Design and Clinical Development of Antibodies for Cancer Therapy. *Front Immunol* (2017) 8:1751. doi: 10.3389/fimmu.2017.01751
72. Lu RM, Hwang YC, Liu IJ, Lee CC, Tsai HZ, Li HJ, et al. Development of Therapeutic Antibodies for the Treatment of Diseases. *J BioMed Sci* (2020) 27:1. doi: 10.1186/s12929-019-0592-z
73. Fuchs SP, Martinez-Navio JM, Piatak M Jr, Lifson JD, Gao G, Desrosiers RC. AAV-Delivered Antibody Mediates Significant Protective Effects Against SIVmac239 Challenge in the Absence of Neutralizing Activity. *PloS Pathog* (2015) 11(8):e1005090. doi: 10.1371/journal.ppat.1005090
74. Priddy FH, Lewis DJM, Gelderblom HC, Hassanin H, Streatfield C, LaBranche C, et al. Adeno-Associated Virus Vectored Immunoprophylaxis to Prevent HIV in Healthy Adults: A Phase 1 Randomised Controlled Trial. *Lancet HIV* (2019) 6(4):e230–9. doi: 10.1016/S2352-3018(19)30003-7
75. Casazza JP, Cale EM, Narpala S, Novik L, Yamshchikov GV, Lin BC, et al. "Durable HIV-1 Antibody Production in Humans After AAV8-Mediated Gene Transfer". In: *Conference on Retroviruses and Opportunistic Infections* (2021). (virtual).
76. Harding FA, Stickler MM, Razo J, DuBridge R. The Immunogenicity of Humanized and Fully Human Antibodies: Residual Immunogenicity Resides in the CDR Regions. *MAbs* (2010) 2(3):256–65. doi: 10.4161/mabs.2.3.11641

Author Disclaimer: The views expressed in this presentation are those of the authors and do not reflect the official policy or position of the Uniformed Services University, US Army, the Department of Defense, or the US Government.

Conflict of Interest: The authors declare that the research was conducted in the absence of any commercial or financial relationships that could be construed as a potential conflict of interest.

Publisher's Note: All claims expressed in this article are solely those of the authors and do not necessarily represent those of their affiliated organizations, or those of the publisher, the editors and the reviewers. Any product that may be evaluated in

this article, or claim that may be made by its manufacturer, is not guaranteed or endorsed by the publisher.

frontiers in Immunology

ORIGINAL RESEARCH
published: 22 February 2022
doi: 10.3389/fimmu.2022.820148

A Quantitative Approach to Unravel the Role of Host Genetics in IgG-FcγR Complex Formation After Vaccination

Melissa M. Lemke[1], Robert M. Theisen[1], Emily R. Bozich[1], Milla R. McLean[2], Christina Y. Lee[1], Ester Lopez[2], Supachai Rerks-Ngarm[3], Punnee Pitisuttithum[4], Sorachai Nitayaphan[5], Sven Kratochvil[6], Bruce D. Wines[7,8,9], P. Mark Hogarth[7,8,9], Stephen J. Kent[2,10,11], Amy W. Chung[2†] and Kelly B. Arnold[1*†]*

[1] Department of Biomedical Engineering, University of Michigan, Ann Arbor, MI, United States, [2] Department of Microbiology and Immunology, The University of Melbourne, at the Peter Doherty Institute for Infection and Immunity, Melbourne, VIC, Australia, [3] Department of Disease Control, Ministry of Public Health, Bangkok, Thailand, [4] Vaccine Trial Centre, Faculty of Tropical Medicine, Mahidol University, Bangkok, Thailand, [5] Armed Forces Research Institute of Medical Sciences, Bangkok, Thailand, [6] The Ragon Institute of Massachusetts General Hospital, Massachusetts Institute of Technology and Harvard University, Cambridge, MA, United States, [7] Immune Therapies Group, Burnet Institute, Melbourne, VIC, Australia, [8] Department of Immunology and Pathology, Monash University, Melbourne, VIC, Australia, [9] Department of Clinical Pathology, The University of Melbourne, Melbourne, VIC, Australia, [10] ARC Centre of Excellence in Convergent Bio-Nano Science and Technology, The University of Melbourne, Melbourne, VIC, Australia, [11] Melbourne Sexual Health Centre, Alfred Hospital, Monash University Central Clinical School, Melbourne, VIC, Australia

OPEN ACCESS

Edited by:
Justin Pollara,
Duke University, United States

Reviewed by:
Ria Lassauniere,
Statens Serum Institut (SSI), Denmark
Simone Richardson,
National Institute of Communicable Diseases (NICD), South Africa

***Correspondence:**
Kelly B. Arnold
kbarnold@umich.edu
Amy W. Chung
awchung@unimelb.edu.au

†These authors have contributed equally to this work and share senior authorship

Specialty section:
This article was submitted to Viral Immunology, a section of the journal Frontiers in Immunology

Received: *22 November 2021*
Accepted: *25 January 2022*
Published: *22 February 2022*

Citation:
Lemke MM, Theisen RM, Bozich ER, McLean MR, Lee CY, Lopez E, Rerks-Ngarm S, Pitisuttithum P, Nitayaphan S, Kratochvil S, Wines BD, Hogarth PM, Kent SJ, Chung AW and Arnold KB (2022) A Quantitative Approach to Unravel the Role of Host Genetics in IgG-FcγR Complex Formation After Vaccination. Front. Immunol. 13:820148. doi: 10.3389/fimmu.2022.820148

Fc-mediated immune functions have been correlated with protection in the RV144 HIV vaccine trial and are important for immunity to a range of pathogens. IgG antibodies (Abs) that form complexes with Fc receptors (FcRs) on innate immune cells can activate Fc-mediated immune functions. Genetic variation in both IgGs and FcRs have the capacity to alter IgG-FcR complex formation *via* changes in binding affinity and concentration. A growing challenge lies in unraveling the importance of multiple variations, especially in the context of vaccine trials that are conducted in homogenous genetic populations. Here we use an ordinary differential equation model to quantitatively assess how IgG1 allotypes and FcγR polymorphisms influence IgG-FcγRIIIa complex formation in vaccine-relevant settings. Using data from the RV144 HIV vaccine trial, we map the landscape of IgG-FcγRIIIa complex formation predicted post-vaccination for three different IgG1 allotypes and two different FcγRIIIa polymorphisms. Overall, the model illustrates how specific vaccine interventions could be applied to maximize IgG-FcγRIIIa complex formation in different genetic backgrounds. Individuals with the G1m1,17 and G1m1,3 allotypes were predicted to be more responsive to vaccine adjuvant strategies that increase antibody FcγRIIIa affinity (e.g. glycosylation modifications), compared to the G1m-1,3 allotype which was predicted to be more responsive to vaccine boosting regimens that increase IgG1 antibody titers (concentration). Finally, simulations in mixed-allotype populations suggest that the benefit of boosting IgG1 concentration versus IgG1 affinity may be dependent upon the presence of the G1m-1,3 allotype. Overall this work provides a

quantitative tool for rationally improving Fc-mediated functions after vaccination that may be important for assessing vaccine trial results in the context of under-represented genetic populations.

Keywords: systems serology, Fc receptor, IgG1 allotype, Fc receptor polymorphism, HIV, RV144, ADCC, vaccine boosting

INTRODUCTION

Antibodies (Abs) are a vital component of the protective immune response elicited by vaccination. Immunoglobulin G (IgG) Abs that activate Fc effector functions are important for protection against a number of pathogens (1–5) and have been correlated with protection in HIV vaccine trials (6, 7). Antigen bound IgG immune complexes can trigger Fc effector functions by the crosslinking of IgG Fc portions with Fc receptors on the surface of innate immune cells. Fc functional capacity is directly correlated to the number of immune complexes formed that activate Fc receptors (8), which is regulated by numerous factors including IgG subclass concentrations, availability of FcRs and their respective binding properties (9). These properties vary in individuals and several studies have demonstrated that they are influenced by genetic factors including IgG1 allotypes and FcR polymorphisms (10–12).

Currently, four human IgG1allotypes (G1m1 [or G1m(a)], G1m2 [or G1m(x)], G1m3 [or G1m(f)], G1m17 [or G1m(z)]) have been identified (13). These allotypic determinants are inherited in a Mendelian pattern, i.e. sets of G1m haplotypes are inherited. G1m3 and G1m17 allotypes are mutually exclusive and refer to different amino acid changes at the same position (14). G1m17 allotypes are almost always linked with G1m1 (written together as G1m1,17 but hereafter referred to as G1m1 in this text), whereas G1m3 can exist with or without G1m1 (e.g. G1m1,3 or G1m-1,3 respectively). Interestingly, common allotypes are shared within ethnic or genetic populations. People with African ancestory have an enriched prevalence of G1m1 allotypes, those with a European ancestory have enriched G1m1 and G1m-1,3 allotypes while those with Asian ancestory have enriched G1m1 and G1m1,3 allotypes (15, 16). Recent research suggests that IgG1 allotypic variation is linked with all four IgG subclass concentrations, potentially due to allotype-linked variation in expression and degradation (12). Importantly these allotype-linked differences in IgG subclass concentrations are also observed in an antigen-specific manner upon vaccination. For example a recent phase I HIV vaccine trial (17) observed that G1m1 vaccinees (G1m1 & G1m1,3) reported to have higher HIV-specific IgG1:IgG2 ratios compared to the G1m-1,3 allotype, mainly driven by elevated HIV-specific IgG1 titers in G1m1 individuals (10).

In parallel, a range of FcγR polymorphisms have been identified in humans, some of which have greater Fc binding affinity and hence are associated with enhanced Fc functional capacity (11, 18–20). Individuals carrying the high affinity FcγRIIa H^{131} polymorphism, most commonly associated with enhanced ADCP, have positive outcomes in both cancer (21) and infectious diseases, including HIV (22, 23). The FcγRIIIa V^{158} polymorphism, with higher affinity than FcγRIIIa F^{158}, has been associated with enhanced ADCC functionality and linked to better outcomes within the mAb cancer field (24, 25). Conversely, this same polymorphism has been associated with HIV disease progression (26) and the lack of protection in the HIV VAX004 vaccine trial (27). The distribution of these polymorphisms can also vary between different populations (28). Though FcR polymorphisms clearly dictate affinity for IgG subclasses, their overall role in FcγR activation is more ambiguous, especially in the context of variability in IgG subclass concentrations.

To date, few studies have explored the relative roles of IgG1 allotypes and FcR polymorphisms in FcR activation after vaccination, as their distributions are not measured in vaccine trials. In addition, it is difficult to unravel the parallel influences of both subclass concentrations and binding affinities that arise from differences in IgG1 allotype and FcγR polymorphism combinations. Recently, we computationally assessed the mechanistic underpinnings of IgG-FcγR complex formation after vaccination and demonstrated that synergistic relationships can occur between antibody parameters that regulate FcγR activation, that would not be apparent from studying each in isolation (21). Therefore, it is plausible that multiple immunogenetic changes may also have synergistic influences upon FcγR activation, which are greater than those that would be expected from simply summing changes evaluated in isolation. These are often too complex to be captured experimentally when parameters are examined individually.

Here we use data from the HIV RV144 vaccine trial and a mechanistic computational model to assess the relative roles of IgG1 allotypes and FcγR polymorphisms in IgG-FcγRIIIa immune complex formation after HIV vaccination. We demonstrate how genetic background may influence an individual's Fc functional response upon vaccination and suggest specific interventions that would most effectively improve IgG-FcγRIIIa immune complex formation in each allotype/polymorphism combination.

MATERIALS AND METHODS

We applied an ordinary differential equation (ODE) model as previously published and validated with RV144 plasma samples (**Figure 1**) (29). The model predicts IgG-FcγR dimer complex formation (Ag : IgG:IgG : FcγR:FcγR) at steady state as a function of IgG subclass, antigen, and FcR dimer concentrations. In the model, two IgG antibodies bind each antigen before forming a complex with dimeric FcR. We obtained parameters for the model from literature and with measurements made previously (29) where median fluorescent intensity (MFI) of HIV env

glycoprotein 120 (gp120) strain A244 (env) specific IgG1, IgG2, IgG3, and IgG4 was measured in the plasma of 105 RV144 vaccinees (8). We converted MFI measurements into a relative concentration measurement based on a reference concentration (17) of HIV-specific IgG in a similar vaccine trial. Though this reference concentration does not directly represent our plasma samples, we do not have the ability to directly measure concentration through the use of a standard curve, so the concentrations predicted throughout by the model are thus not to be used as absolute measures, but as relative measures.

Evaluating Combined IgG1 Concentration and Affinity Parameter Changes

In order to evaluate the relative and combined roles of IgG1 allotype (i.e. IgG subclass changes) and FcR affinity (i.e. FcR polymorphisms), IgG1 affinity for FcγRIIIA-V^{158} or IgG1 concentration were held constant at its baseline value (listed in the parameter table in **Figure 1C**), while the other parameter was varied over 50 values spanning 1.7-256 nM or 2e-6-8e-4 $nm^{-1}s^{-1}$. Model outputs from all simulations were subtracted by the baseline complex formation to calculate the difference in complex formation for each condition. We simulated 2,500 different combinations of IgG1 concentration and IgG1 affinity for FcγRIIIA-V^{158} spanning 1.7-256 nM or 2e-6-8e-4 $nm^{-1}s^{-1}$ respectively while holding all other model parameters at baseline. We then subtracted each of these values by the model output with both IgG1 affinity and concentration at baseline. To identify regions where synergy between IgG1 concentration and IgG1 affinity for FcγR occurred, we used element-wise subtraction of the additive simulations (parameters were altered in isolation and added together) from simulations where parameters altered together in the model. The range of possible IgG1 concentration values was calculated by multiplying the maximum and minimum calculated IgG1 concentrations in the RV144 plasma samples (29) by each allotype conversion factor and taking the minimum and maximum results across all possible allotypes (23). Maximum and minimum IgG1 affinity values were selected as the highest and lowest affinity glycosylation forms of IgG1 across all FcgRIIIA polymorphisms (30).

Evaluating Boosting of IgG1 Concentrations in Individuals With Different FcγRIIIa Polymorphisms

In order to model how changes in IgG subclass concentrations (that may occur upon vaccine boosting) can influence IgG-FcγR complex formation in individuals with different FcγRIIIa polymorphisms, we used the model to predict complex formation for each polymorphism by altering initial IgG1 and IgG3 concentrations from 0.004X to 20X baseline (post-vaccination measurements) in 2,500 different combinations. Affinity values for each FcγRIIIa polymorphism to each IgG subclass were used from previously published literature (11). We used IgG1 and IgG3 titers measured in RV144 vaccinees post-vaccination and after a simulated 170% IgG1 boost. This boosting value was chosen by using the highest fold change in HIV-specific Ab titers recorded in the RV306 follow up trial from 26 weeks (our initial post-vaccination timepoint) and after boosting in group 4b with AIDSVAX B/E and ALVAC-HIV at 18.5 months (31). A Wilcoxon matched pairs signed rank test was used to evaluate the difference in predicted complex formation for each individual across the two polymorphisms, both before and after boosting. All parameters besides initial IgG1 and IgG3 remained at their baseline value listed in the parameter table (**Figure 1C**) for all the above-described simulations. Specific IgG1 and IgG3 values were chosen using MATLAB's log spacing

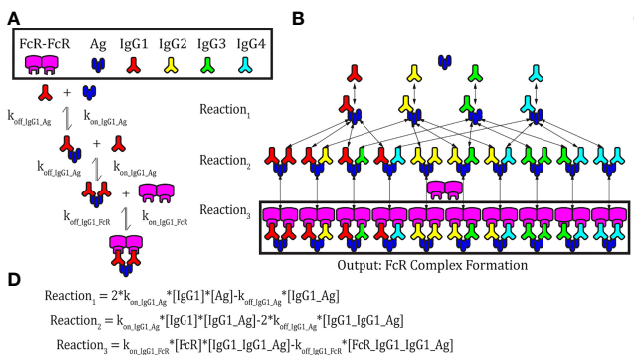

C

Parameter	Baseline Value	Units
K_{eq}-IgGx -env $^{\alpha}$	5,000	$\times 10^5 nM^{-1}$
K_{eq}-IgG1 -FcR $^{\beta}$	200	$\times 10^5 nM^{-1}$
K_{eq}-IgG2 -FcR $^{\beta}$	7	$\times 10^5 nM^{-1}$
K_{eq}-IgG3 -FcR $^{\beta}$	980	$\times 10^5 nM^{-1}$
K_{eq}-IgG4 -FcR $^{\beta}$	25	$\times 10^5 nM^{-1}$
IgG1 initial concentration $^{\gamma}$	85.4	nM
IgG2 initial concentration $^{\gamma}$	0.133	nM
IgG3 initial concentration $^{\gamma}$	3.07	nM
IgG4 initial concentration $^{\gamma}$	0.102	nM
env initial concentration $^{\delta}$	25	nM
FcR initial concentration $^{\delta}$	20	nM

FIGURE 1 | Model schematic. **(A)** An example set of reversible reactions describing the sequential binding of IgG1 to antigen (Ag) and dimeric FcγR with the respective forward (k_{on}) and reverse (k_{off}) reaction rates. **(B)** Ordinary differential equations were used to predict total HIV Ag-IgG-FcγR complexes formed as a function of concentration and binding affinity of Ag, IgG subclasses, and FcγR. The model assumes a single FcγR type. Reversible reactions are represented by double ended arrows. Model output was the sum of all dimeric FcγR complexes formed (boxed in black) at steady state. **(C)** The baseline parameters for FcγRIIIA-V^{158} complex formation with the following sources: $^{\alpha}$SPR measurement from pooled purified IgG from HIV infected individuals binding to monomeric gp120. All IgG subtypes share one affinity value to the antigen of focus, gp120 env (unpublished data). $^{\beta}K_{eq}$ measured in Bruhns et al. (11). $^{\gamma}$The average estimated IgG concentrations from individuals 1-30 in the RV144 data in this manuscript (see methods for notes on conversion from MFI to mM unit). $^{\delta}$Concentrations used in multiplex experimental protocol. **(D)** Equations describing the example reactions in panel **(A)** Reactions follow mass action kinetics and consist of a forward reaction (on rate, k_{on}, multiplied by the concentrations of substrates) and a reverse reaction (off rate, k_{off}, multiplied by the concentration of the product of the forward reaction). Differential equations for change in each complex over time were generated for each complex.

function, logspace(), to give 50 values between 0.004X and 20X baseline.

Simulating IgG1 Allotypes and Glycosylation

Baseline IgG subclass initial concentrations from all 105 RV144 vaccinees were assumed to be the G1m1,3 (15) IgG1 allotype. These were then converted into G1m1 and G1m1,3 for simulations based on conversion factors for initial IgG1, IgG2, IgG3 and IgG4 concentration as previously published (21), which were estimated using allotyped human plasma samples from previous a Phase I HIV vaccine trial (17). To predict affinity changes resulting from glycosylation, we estimated those that would be expected from afucosylation of IgG1 by taking the highest fold change for affinity of IgG1 to FcγRIIIa-V^{158} (31X; $62*10^{-3}$ $nM^{-1}s^{-1}$) reported in the literature (30). This high affinity glycosylation (afuscosylation with hyper-galactosylation and bisection) was compared to a baseline affinity ($2*10^{-3}$ $nM^{-1}s^{-1}$).

In order to evaluate affinity changes resulting from glycosylation, projected upon all vaccinees for each of the three allotypes, the IgG-FcR immune complex formation was simulated at baseline, and the difference between each individual's complex formation at baseline and with glycosylation for each allotyped population and compared them with a Friedman test with Dunn's multiple comparisons in GraphPad Prism.

Allotype projections were performed as previously published (29), by first calculating the conversion factor. Under the assumption that the original RV144 data was G1m1,3 (15), the conversion factor was calculated to generate the corresponding IgG subclass concentrations for the G1m-1,3 and G1m1 allotypes. To calculate this value, we found the mean concentration for each IgG within each allotype from human plasma samples analyzed in Kratochvil et al. (17). Then, these values were divided by the corresponding mean IgG concentration for samples with the G1m1,3 allotype.

$$cf_{G1mj}^{IgGi} = \textit{conversion factor for IgGi to allotype G1mj}$$

$$m_{G1mj}^{IgGi} = \textit{mean concentration of IgGi in allotype G1mj}$$

$$cf_{G1mj}^{IgGi} = m_{G1mj}^{IgGi} / m_{G1m1,3}^{IgGi}$$

Each vaccinee's initial IgG concentrations and baseline initial IgG concentrations were converted using the respective conversion factors as follows:

$$IgGi_{G1mj}^{x} = \textit{Initial IgGi concentration for vaccinee x in allotype G1mj}$$

$$IgGi_{G1mj}^{x} = cf_{G1mj}^{IgGi} * IgGi_{G1m1,3}^{x}$$

Determining Preferred Boosting Method in IgG1 Allotypes

Simulations as above, projecting all 105 RV144 vaccinees as the three IgG1 allotypes and two FcRIIIA polymorphisms (FcγRIIIa-V^{158} and FcγRIIIa-F^{158}) were calculated, providing predictions for six different genetic combinations (**Figure 5A**). In each of these six genotypes we then simulated a boost in either IgG1 initial concentration or k_{on} IgG1-FcR (ie IgG1 affinity to FcR) by 10%, 25%, 50%, 75%, 100%, 250%, 500%, 750%, or 1000% above their personal baseline. The six genotypes were compared at baseline using a Friedman test with Dunn's multiple comparisons in GraphPad Prism 9.

To modify the original parameter to include the boost, a new concentration or affinity was calculated using the following formula, where the original parameter is specific to the individual and genotype:

$$\textit{New parameter} = \textit{original parameter} + (\textit{original parameter} * \textit{boost})$$

Evaluating Mixed Allotype Populations

To determine the importance of affinity and concentration-based interventions within 10 mixed allotype populations, simulations were run as described above projecting all 105 RV144 vaccinees into different allotypes. Within this analysis, 10 mixed allotype populations were simulated with varying proportions of individuals assigned to each allotype. Each allotype is represented in each population at 100%, 66%, 33%, 17%, or 0% (see **Figure 6** for specific breakdowns). Each vaccinee (n = 105) was randomly assigned an allotype to fulfill the population breakdown. In populations where vaccinees couldn't be evenly split into the population's allotypes, remaining vaccinees were again randomly assigned an allotype (i.e. 70 vaccinees assigned to G1m1, 18 assigned to G1m1,3 and 17 to G1m-1,3 in Population F). We performed this randomized vaccinee allotype assignment 25 times for each population to create a more robust and representative population n = 2,625 for each population. All simulations were run with FcγRIIIa-V^{158} affinity values.

RESULTS

Synergism Between IgG1 Concentration and IgG1 Affinity

Genetic background has the potential to influence both IgG1 concentration (via IgG1 allotypes) and IgG1 binding affinity for FcR (via FcR polymorphisms). In order to better understand the relationship between these two parameters and how they influence FcγRIIIa activation, we applied an ODE model to predict Antigen-IgG-FcR immune complex formation as both parameters were altered simultaneously over a physiological range of 2500 unique parameter combinations (**Figure 2A**). The resulting landscape illustrated the interdependence of these two parameters, and how simultaneous changes have the potential for a synergistic influence on complex formation. Specifically, IgG1 affinity was only effective for increasing complex formation, upon IgG1 titers surpassing specific concentration thresholds (around ~10-230 nM depending on the affinity value). Likewise, increasing IgG1 concentration had a limited effect, which was determined by IgG1 affinity. Furthermore, in situations where both IgG1 concentration and

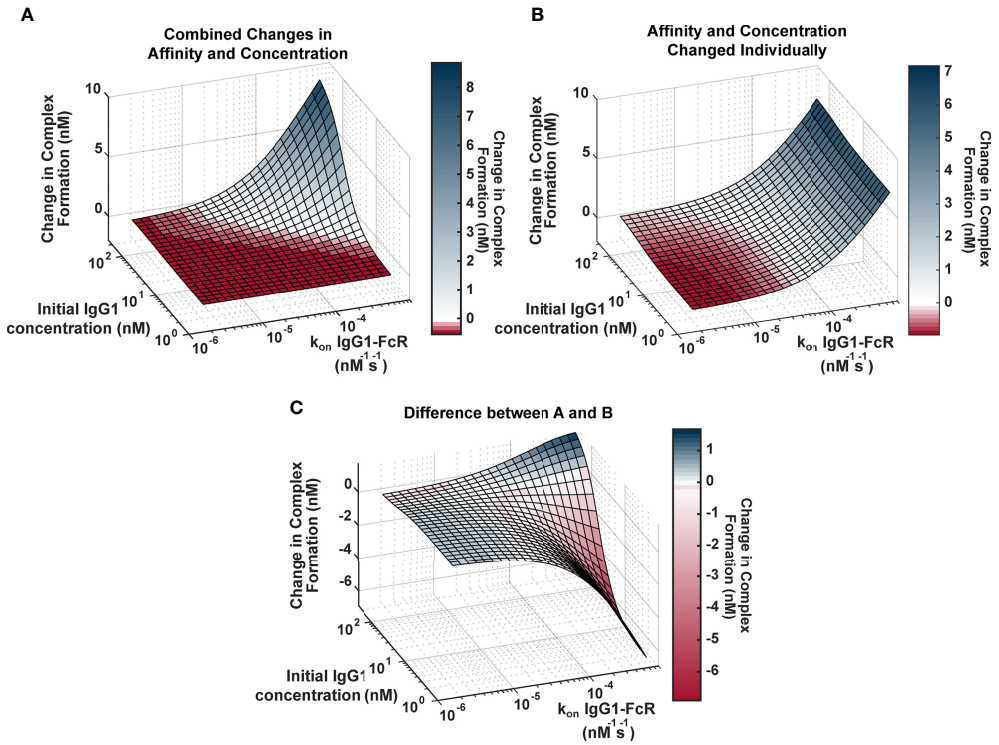

FIGURE 2 | Landscape illustrating the relationships between IgG1 concentration and IgG1- FcγR affinity across the physiological landscape of parameters (2500 unique parameter combinations). **(A)** Model predictions for the change in complex formation from baseline when IgG1 initial concentration (x axis) and k_{on} IgG1- FcγR (y axis) were altered individually and the resulting change in complex formation is added together (z axis). Color indicates predicted change in complex formation from baseline. **(B)** Model predictions for the change in complex formation from baseline when both parameters are altered simultaneously in the model. Color indicates predicted change in complex formation from baseline. **(C)** The difference between **(A, B)**, illustrating parameter combinations where synergy occurs. Blue indicates positive synergy, where the combined parameter changes **(B)** result in greater complex formation compared to was predicted by separate changes added together **(A)**, white indicates no synergy, and red indicates anergy; where the combined parameter changes **(B)** result in lower complex formation compared to was predicted by separate changes added together **(A)**.

IgG1 affinity were high (~200 nM and ~7e-4 $nM^{-1}s^{-1}$, respectively), the model predicted non-linear increases in complex formation, beyond what would be predicted from adding the changes resulting from both parameters individually.

To illustrate the synergistic result of modulating multiple parameters more clearly, we created a second surface that predicted complex formation, if IgG1 concentration and IgG1 affinity were altered separately in the model and resulting changes were added together (**Figure 2B**). The surface represents what would be expected if changes in IgG1 concentration and affinity were considered separately in isolation, and notable features include: 1) the ability of each parameter to influence complex formation without the other; and 2) absence of the potential for very high complex formation when both parameters are high.

To identify specific parameter ranges where synergisms or anergisms occur (combined changes are greater than or less than what would be expected from separate parameter changes added together), we next subtracted "additive" (parameters changed separately; **Figure 2B**) surface from the "combined" surface (parameters changed simultaneously; **Figure 2A**) to create **Figure 2C**. Positive regions of this surface (blue) indicate regions where combined parameters changes are much greater than what would be expected from adding separate changes, whereas the negative regions (red) represent parameter combinations where actual changes would be much less than what would be expected from adding individual changes. This landscape indicates the potential for synergistic complex formation (blue) when both concentration and affinity are high (102-230 nM, and 2.9e-5-7e-4 $nM^{-1}s^{-1}$). Interestingly it also illustrates the potential to overestimate complex formation when IgG1 affinity is high, but IgG1 concentration is low (1.7-102 nM, and 2.9e-5-7e-4 $nM^{-1}s^{-1}$). Altogether these results have important implications for how genetic background (which has the capacity to alter both IgG1 concentration and IgG1 affinity for FcγR) may influence FcγR activation after vaccination and may allow for more rational design of vaccine interventions.

FcR Polymorphism Influences FcγR Activation After Boosting

One interesting result of the previous simulations in **Figure 2** was that there is a limit in the effects of increasing IgG1

concentration alone, and at higher IgG1 concentrations, IgG1 affinity determines the limit. This result has implications for vaccine boosting in individuals with different FcR polymorphisms. We hypothesized that the effect of boosting (large changes in IgG1 concentration) would be limited in individuals with the low affinity FcγRIIIa-F^{158} polymorphism, whereas it would be much higher in individuals with the higher affinity FcγRIIIa-V^{158} polymorphism. Therefore we hypothesized that the differences in immune complex formation between the two polymorphisms would become even greater after boosting (compared to first vaccination).

To test this idea, we ran simulations for the high and low affinity FcγRIIIa polymorphisms by changing the affinity for all IgGs to FcγRIIIa according to published values (11) (FcγRIIIa-V^{158} light pink, and FcγRIIIa-F^{158} dark pink, respectively; **Figure 3A**) at 2,500 different initial IgG1 and IgG3 concentration combinations with all other parameters maintained using baseline values (FcγRIIIa-V^{158} light pink, and FcγRIIIa-F^{158} dark pink; **Figure 3B**). IgG1 and IgG3 have previously been identified as the significant IgG subtypes of importance (29) due to IgG1's high initial concentration and IgG3's high affinity to FcR (**Figures 1C**, **3A**). The resulting profile of both polymorphism surfaces revealed that changes in IgG1 concentration were predicted to increase complex formation up to a certain point, illustrated by a plateau around 300 nM, after which no additional changes in complex formation would be predicted regardless of IgG1 increases. Comparing results for the two polymorphisms (light pink vs. dark pink surface) revealed that the biggest differences between polymorphisms occur in the plateaus regions, when IgG1 concentration is high; specifically, the FcγRIIIa-V^{158} polymorphism plateau is 66% higher than the FcγRIIIa-F^{158} plateau.

Based on individual IgG1 and IgG3 initial concentrations measured in the RV144 plasma samples (n=105) we plotted each individual on both surfaces at baseline (light orange), and after a simulated boost (31) in IgG1 concentration (dark orange; **Figure 3B**). After first vaccination, many vaccinees were predicted to be in an IgG1 sensitive region, regardless of FcR polymorphism. However, an increase in antigen-specific IgG1 (similar to the boost applied in RV306) moves many vaccinees from the IgG1 sensitive region (30-300 nM) onto or nearing the plateau region, where complex formation is highly dependent on FcR polymorphism. Indeed, the difference in complex formation between the polymorphisms after boosting was significantly greater than it was at baseline (after first vaccination) (Wilcoxon matched-pair rank test, $p < 0.0001$; **Figure 3C**).

The G1m-1,3 IgG1 Allotype Is Not Predicted to be Sensitive to IgG1 Fc Glycosylation Modifications

Model results in **Figure 2** revealed the potential for unexpected interactions between IgG1 concentration and IgG1 affinity. In a setting with low IgG1 concentration, there is the potential that large increases in IgG1 affinity to FcγR will have little to no effect on IgG-FcγR complex formation. Conversely, at high IgG1 concentrations, results revealed the potential for non-linear increases in complex formation. Based on these observations, we used the model to assess how IgG1 concentration differences in IgG1 allotypes may influence sensitivity to FcR affinity modifications (e.g. glycosylation).

Previous studies suggest that IgG1 allotype alters all four IgG subclass concentrations, hence we used these measurements to estimate the median IgG1, IgG2, IgG3 and IgG4 concentrations for each allotype (**Figure 4A**) (17). As the G1m1,3 allotype is expected to be prevalent in the original RV144 (Thai) population, we assumed all original RV144 vaccinees (n=105) were of the G1m1,3 (**Figure 4A**, white bar) allotype (25), which is expected to have higher IgG1 and IgG3 concentrations, compared to G1m1 (gray bar) and G1m-1,3 (black bar) which have higher IgG4.

Using results in **Figure 2**, we plotted each IgG1 allotype on the surface based on expected median IgG1 concentration (**Figures 4B, C**). Using this same principle, we also added lines showing where

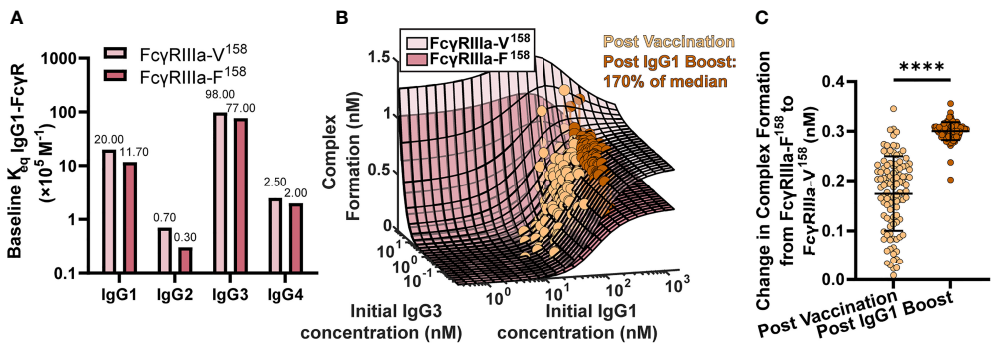

FIGURE 3 | FcγR polymorphisms have a greater influence on complex formation after IgG1 boosting. **(A)** Baseline K_{eq} of each IgG subtype to the high affinity FcγRIIIa-V^{158} polymorphism (light pink) and the low affinity FcγRIIIa-F^{158} polymorphism (dark pink) as reported by Bruhns et al. (11). **(B)** Complex formation (z axis) predicted by the model for 2500 combinations of initial IgG1 and IgG3 concentration (x and y axes) for FcγRIIIa-V^{158} (light pink) and FcγRIIIa-F^{158} (dark pink). Each dot represents an RV144 plasma sample (n=105) with respective initial IgG1 and IgG3 concentrations plotted post-vaccination (baseline-light orange), and after a simulated 170% (145 nm) boost of IgG1 (dark orange). The simulated boost magnitude was estimated based on the highest fold change seen in RV306 between 26 weeks and peak HIV specific IgG titer (2.64X in arm 4b) (31). **(C)** The difference in complex formation predicted between the FcγRIIIa-F^{158} and FcγRIIIa-V^{158} polymorphisms post-vaccination (light orange) and post-IgG1 boost (dark orange; Wilcoxon matched-pairs signed rank test; ****p-value < 0.0001).

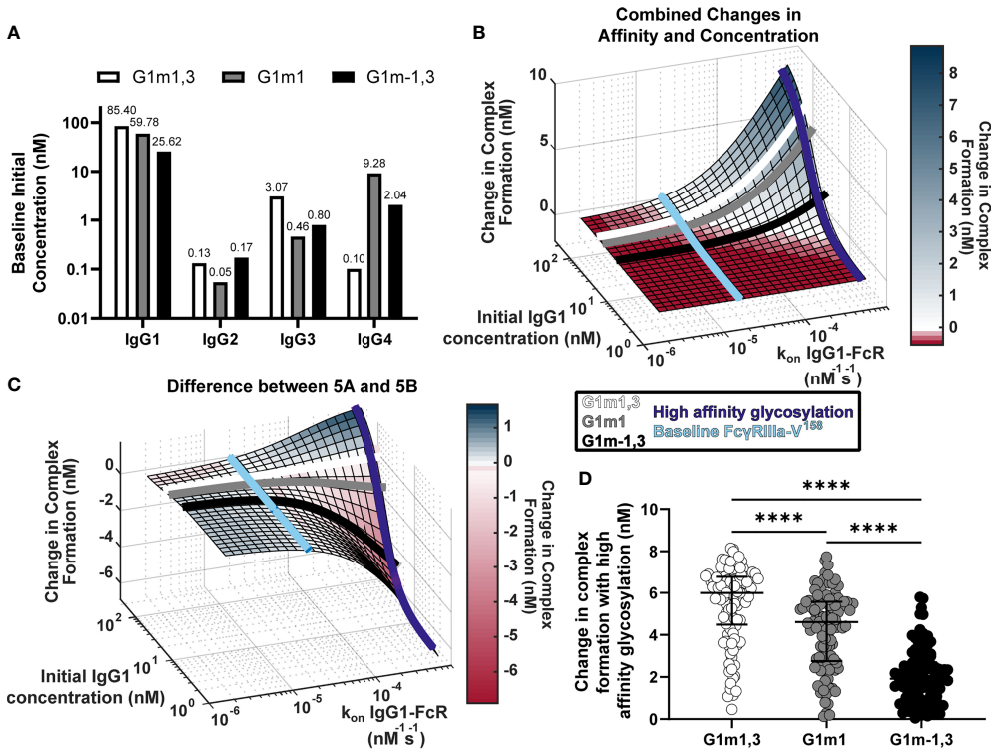

FIGURE 4 | Glycosylation differentially impacts IgG1 allotypes. **(A)** Expected IgG1, IgG2, IgG3, and IgG4 concentrations for G1m1,3 (white), G1m1 (gray), and G1m-1,3 (black) allotypes based on previously published work (17, 29). **(B)** Model predictions for complex formation as IgG1 concentration and k_{on} IgG1- FcγR are altered over physiological ranges (**Figure 2B**). Lines indicate IgG1 concentrations for three different IgG1 allotypes (G1m1,3 (white), G1m1 (gray), G1m-1,3 (black)), and the affinity change expected from an afucosylation glycosylation modification (purple) compared to baseline (light blue). **(C)** The difference (**Figure 2C**) between the combined parameter change surface (**Figure 2A**) and the additive surface (**Figure 2B**). Lines indicate IgG1 concentrations for three different IgG1 allotypes (G1m1,3 (white), G1m1 (gray), G1m-1,3 (black)), and the affinity change expected from an afucosylation glycosylation modification (dark blue) compared to baseline FcgRIIIaV158 (light blue). **(D)** Change in complex formation from baseline affinity to an afucosylated affinity in each allotype, G1m1,3 (white), G1m1 (gray), and G1m-1,3 (black) (Friedman test with Dunn's multiple comparisons test; ****p-value < 0.001).

the baseline affinity measurement is for FcγRIIIa-V^{158} (light blue, 2e-5 $nM^{-1}s^{-1}$) as well as potential maximal increases in affinity similar to what would be expected with an IgG1 Fc afucosylation modification (purple, 62e-5 $nM^{-1}s^{-1}$) based on values in the published literature (30). Results indicate that G1m1,3 and G1m1 allotypes are expected to follow similar trajectories, where increases in affinity would considerably increase complex formation after ~3e-5 $nM^{-1}s^{-1}$ reaching complex formation levels of 6.5 nM and 5.2 nM respectively. Conversely for the G1m-1,3 allotype (lower IgG1 concentration) the model illustrates how similar glycosylation modification would result in much lower complex formation [only ~1.8 nM complex formation after a high affinity glycosylation modification (**Figure 4B**)].

Plotting the same lines representing IgG1 allotypes and FcRs onto a second surface illustrating the differences between combined changes in concentration and affinity and the individually changed analysis, we see that at baseline FcγRIIIa-V^{158} affinity values (**Figure 4C**, light blue) the predicted combined effects of IgG concentration changes are not much different between an individual and additive method. In contrast, after afucosylation, the additive method would overestimate complex formation in G1m-1,3 by 4.3 nM, while it is only slightly different in G1m1 (1.1 nM) and G1m1,3 (0.08 nM) (**Figure 4C**). Using the same conversion factors as above, we projected every RV144 vaccinee from G1m1,3 into G1m1 and G1m-1,3, and simulated each individual's complex formation after RV144 first vaccination and with the afucosylation change in affinity. Unsurprisingly, the change in complex formation with afucosylation was significantly different in each allotype following the trend of median IgG1 concentration (Median change in complex formation: G1m1,3, 6.0 nM; G1m1 4.6 nM; G1m-1,3 1.9 nM; Friedman test with Dunn's multiple comparisons, all p<0.0001) (**Figure 4D**).

IgG1 Allotype Determines Whether Vaccine Boosts That Increase IgG1 Concentration vs. Boosts That Increase IgG1 Affinity Would Be More Effective for Improving FcR Activation

Our model results suggest that the effect of changes in IgG1 concentration varies depending on a given IgG1 affinity to FcR. One intriguing implication of this result is that individuals with

different IgG1 allotypes (different baseline IgG1 concentration) could be differentially sensitive to vaccines that increase antibody titers (IgG1 concentration) vs. adjuvants that modify IgG1 affinity *via* glycosylation. To explore this idea quantitatively, we simulated 6 different genotypes (FcγRIIIa-F^{158} and FcγRIIIa-V^{158} polymorphisms in the G1m1,3, G1m1 and G1m-1,3 allotypes). As expected we found significant differences in complex formation across all 6 genotypes (**Figure 5A**).

We then simulated nine different boosts, 10%-1000% above values after first vaccination for either IgG1 concentration (**Figure 5B**) or IgG1 affinity (**Figure 5C**) in all vaccinees. We used the median change in complex formation for each genetic background and boosting level to create heatmaps that illustrate the expected resulting change in complex formation. Intriguingly, results illustrated how concentration boosting (increasing antibody titers) has a larger effect on the allotypes with lower initial IgG1 concentration (**Figure 5B**) and that affinity boosts have a larger effect on the allotypes with higher initial IgG1 concentration (**Figure 5C**).

In order to definitively show which type of boosting is optimal for each boosting level and genetic background, we calculated the ratio of change in complex formation with a boost in IgG1 concentration over change in complex formation with a boost in IgG1 affinity to FcγRIIIa (**Figure 5D**). The resulting heat maps illustrates how concentration boosting is predicted to be more beneficial than affinity boosting for the G1m-1,3 allotype until 750% (purple). The lower starting concentration of IgG1 in G1m-1,3 (median IgG1 25.62 nM) prevents affinity changes from improving complex formation until it reaches at least 1e-4 $nM^{-1}s^{-1}$. Conversely, model results indicated that the G1m1,3 and G1m1 allotypes (with higher starting IgG1 concentrations) would be most responsive to changes in affinity (**Figure 5D**). Overall, these results suggest specific vaccine interventions that may be differentially effective for inducing improved Fc effector functions for individuals with different IgG1 allotypes. A separate analysis of FcγRIIa resulted in a similar outcome (**Figure S1**).

Amount of G1m-1,3 Allotype in a Population Determines Whether Boosting IgG1 Antibody Titers Will Be Effective

Given that the model predicts that IgG1 allotype drives the preferred boosting type and that many populations worldwide have different allotype distributions, we next simulated boosting in mixed allotype populations with FcγRIIIa-V^{158}. These populations were simulated by randomly assigning vaccinees to an allotype based on the given ratio of allotypes for the indicated population (Populations A-J; **Figure 6**). Each individual was then projected into their assigned allotype. To be robust in these assignments, this was repeated 25 times for each population and the data was pooled (n = 2,625 for each population).

We performed both IgG1 concentration and IgG1 affinity boosting as described above (**Figure 6**). Overall, we found that the populations with majority G1m-1,3 (populations A-D) benefit more from concentration boosts, and populations higher in G1m1,3 benefit more from FcR affinity boosts (populations G, H, and J) (**Figures 6A, B**). Interestingly, population C, which was 50% G1m1,3, and 50% G1m-1,3, only gained minimal benefits from affinity boosts compared to populations G, H and J, (**Figure 6B**). When we evaluated the ratio of change in complex formation from a concentration boost over change with an affinity boost, we found IgG1 concentration boosting to be beneficial for almost all populations at the lowest boosting level (10-25%), but only remained beneficial at higher boosting levels in populations with a higher prevalence of G1m-1,3 allotypes (**Figure 6C**). Notably the level at which affinity boosting becomes more beneficial than concentration boosting seems to closely follow the level of G1m-1,3 within the population and this holds true for FcγRIIIa-V^{158}, FcγRIIIa-H^{131}, and FcγRIIIa-R^{131} (**Figures S2–S4**). Altogether this suggests specific guidelines for rational vaccine design to improve FcγRIIIa activation in future trials with mixed allotype populations.

DISCUSSION

Here we identify specific mechanisms by which heterogeneity in FcγR activation after vaccination may be linked to IgG1 allotypes and FcγR polymorphisms. Importantly, we found that vaccine boosting regimens which increase IgG1 antibody titers may have limited utility in some allotypes (G1m1,3 and G1m1) and may be more effective in others (G1m-1,3). Instead, for G1m1,3 and G1m1 allotypes, vaccine boosting strategies that modulate IgG1 affinity to FcγR (e.g. *via* adjuvants that modify glycosylation) may be required to improve FcγR activation. The model also illustrates how the influence of FcγRIIIa affinity from different FcR polymorphisms is predicted to have limited influence upon FcR activation until higher IgG1 antibody titers are reached, such as those expected after vaccine boosting. These differences arise from synergistic relationships between IgG1 concentration and affinity for FcγR that could not have been predicted without a computational model.

The computational model also demonstrates how concurrent changes in antigen specific IgG1 antibody titers and IgG1 affinity for FcγR may have more (synergistic), or less (anergistic) of an effect on FcγR activation than previously appreciated. These results suggest that focusing vaccine design on either concentration or affinity alone may not have the expected result. The model identified specific values for IgG1 affinity to FcγR (~10^{-4} $nM^{-1}s^{-1}$ at baseline IgG1 concentration), that would need to be reached before changes IgG1 concentration will have a great effect (**Figure 2**). This can be visualized in **Figure 2C** where predictions of the additive effects of changes in affinity and concentration in isolation were often overestimated than the actual effects when both were changed in combination.

Perhaps one of the most important outcomes reported here is the potential for differential sensitivity of IgG1 allotypes to boosting regimens that increase antibody titers vs. vaccine adjuvants that may influence glycosylation profiles (i.e. FcR affinity). The model predicts that 2 of the 3 allotypes we evaluated would not be sensitive to boosting regimens that increased IgG1 concentration. This has implications for RV144 and associated follow-up trials, where different allotype distributions would be expected depending on geographic location. Though IgG1 allotype was not measured directly in RV144, the Thai population would likely have a greater

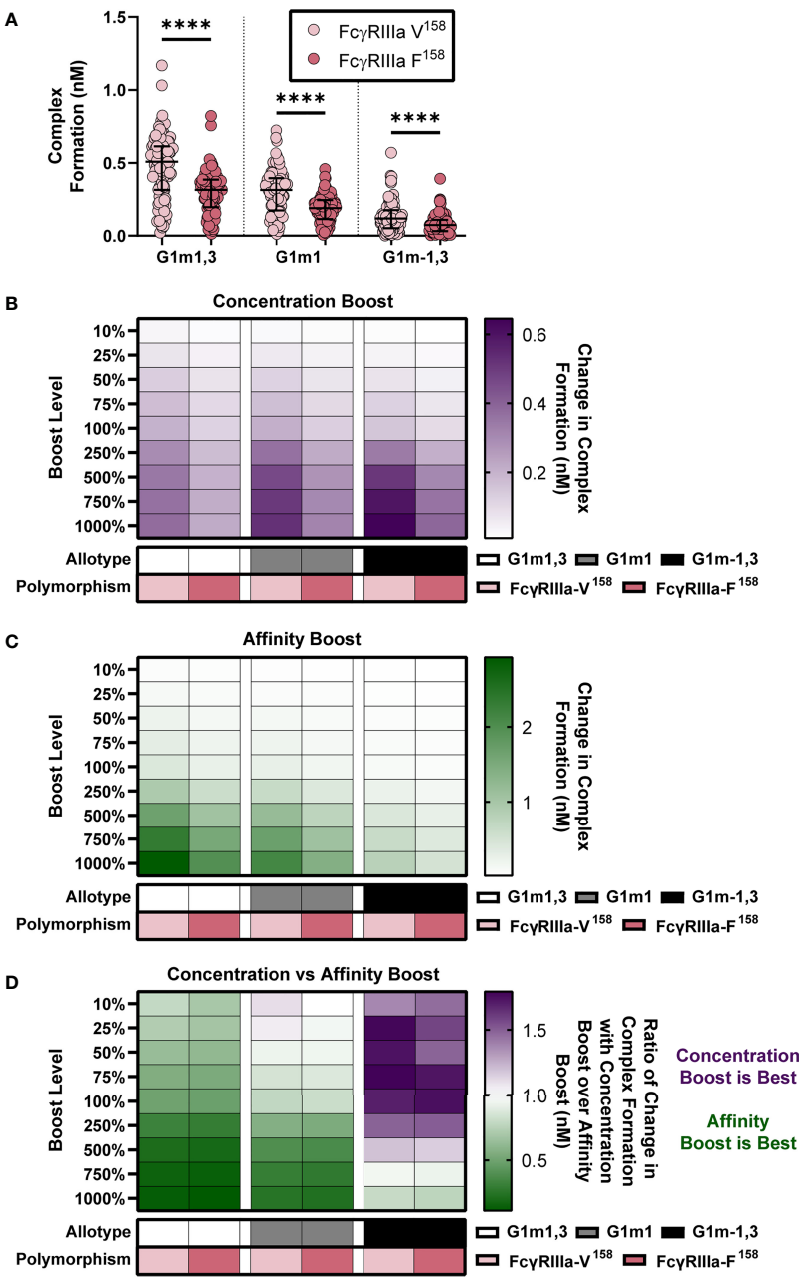

FIGURE 5 | IgG1 allotype determines whether boosting IgG1 concentration or boosting IgG1 affinity (k_{on} IgG1- FcγR) would be most effective for increasing complex formation. **(A)** Model predictions for complex formation of RV144 vaccinees (n=105) in two FcγRIIIa polymorphisms, FcγRIIIa-V^{158} (light pink) and FcγRIIIa-F^{158} (dark pink), and three IgG1 allotypes, G1m1,3 (original RV144 data), G1m1 and G1m-1,3. Polymorphisms were simulated by altering the binding affinities of each IgG subtype to FcγR as previously published (11) and indicated in **Figure 3A**. Allotypes are simulated by multiplying each vaccinee's IgG1, IgG2, IgG3 and IgG4 initial concentration by its respective conversion factor as previously published (29) and indicated in **Figure 4A** (Friedman test with Dunn's multiple comparisons test comparing the two polymorphisms within each allotype; ****p-value < 0.001). **(B)** Simulated IgG1 concentration boosting in each allotype (G1m1,3, white; G1m1, gray; G1m-1,3 black) and polymorphism (FcγRIIIa-V^{158}, light pink; FcγRIIIa-F^{158}, dark pink) combination. Boosts were calculated by multiplying the individual's baseline initial IgG1 concentration value by the boost levels and then this was added on top of each individual's baseline. **(B)** Color indicates median change in complex formation for each genetic background. **(C)** Simulated boosting of k_{on} IgG1- FcγR in each allotype (G1m1,3, white; G1m1, gray; G1m-1,3 black) and polymorphism (FcγRIIIa-V^{158}, light pink; FcγRIIIa-F^{158}, dark pink) combination. Boosts were calculated by multiplying the individual's baseline k_{on} IgG1- FcγR value by the boost levels and then this was added on top of each individual's baseline. Color indicates median change in complex formation for each genetic background and boost as indicated. **(D)** The ratio of median change in complex formation with a boost in IgG1 concentration over median change in complex formation with a boost in k_{on} IgG1-FcγR (affinity) at each boosting level. This ratio shows which type of boost is most effective for increasing complex formation (IgG1 concentration, purple; k_{on} IgG1-FcγR, green) and when both are equally beneficial (white).

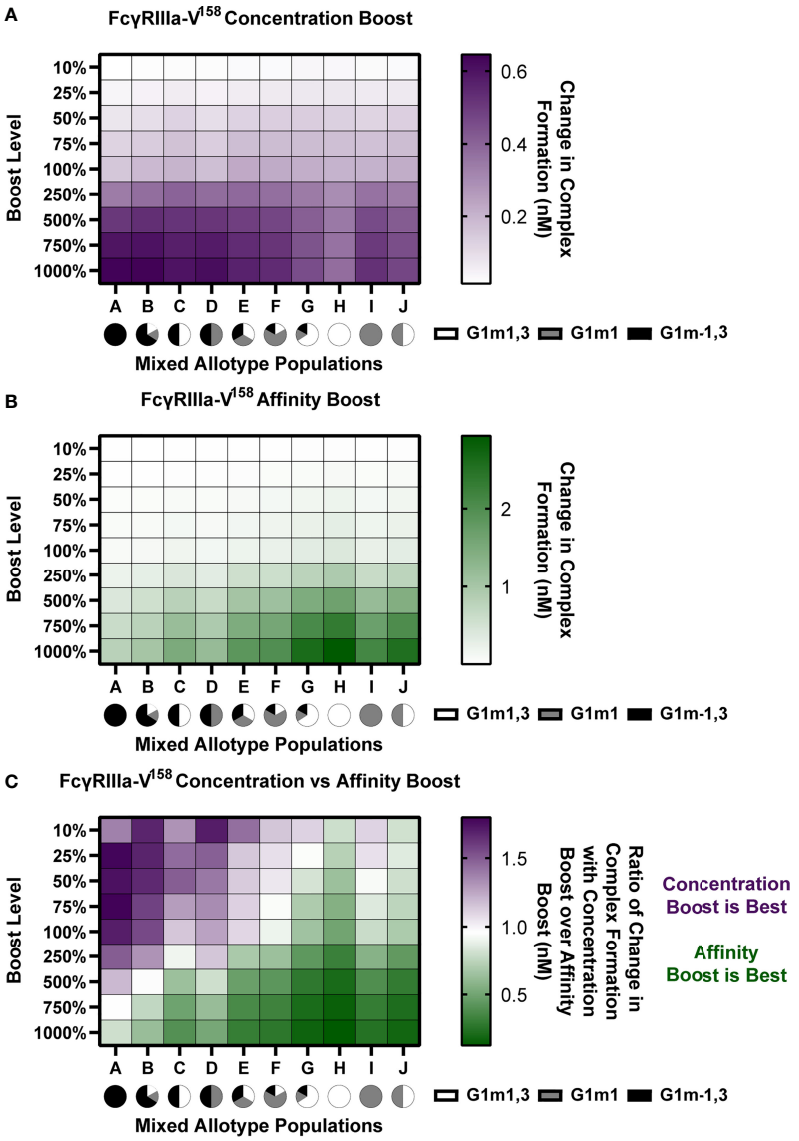

FIGURE 6 | In mixed allotype populations, the benefit of boosting IgG1 concentration vs. IgG1 affinity is dependent on the presence of the G1m-1,3 allotype. **(A)** Boosting of initial IgG1 concentration in mixed allotype populations (G1m1,3, white; G1m1, gray; G1m-1,3 black) for FcγRIIIa-V^{158}. Color indicates predicted change in complex formation **(B)** Boosting of k_{on} IgG1- FcγR in mixed allotype populations (G1m1,3, white; G1m1, gray; G1m-1,3 black). Color indicates predicted change in complex formation **(C)** The ratio of median change in complex formation with a boost in IgG1 over median change in complex formation with a boost in k_{on} IgG1-FcγR at each boosting level. This ratio indicates which type of boost is predicted to be most effective for increasing complex formation (IgG1 concentration, purple; k_{on} IgG1-FcγR, green).

prevalence of the G1m1,3 allotype compared to other trials conducted in South Africa, which have previously been reported to have greater prevalence of G1m1 and G1m-1,3 (32). Model results suggest that while an initial vaccination would be most effective in G1m1,3 (due to high baseline IgG1 titers), boosting regimens to increase IgG1 concentration may not improve Fc-mediated functions. Indeed RV305 (33) and RV306 (34) conducted in Thai populations did increase HIV-specific IgG titers, but to our knowledge the resulting changes in FcγR activation have not yet been evaluated. While the model suggests that FcγR polymorphism is not essential in determining which boosting type and boosting level will be most beneficial (**Figure 6**), it would still make an impact in individuals with relatively high HIV specific IgG1 titers (G1m1,3 and G1m1).

A key limitation is the study is the evaluation of only one FcγR type (FcγRIIIa) and one binding site on one antigen, though we would expect similar results for different FcγRs and antigen binding sites (29). Future models could be expanded to examine multiple FcRs simultaneously in the case of individuals heterozygous for FcR polymorphism or to investigate FcR type competition.

Furthermore, this study is based only upon assumed IgG1 allotypic distributions. Though IgG1 allotype measurements would be ideal for validating model findings, they were not available for the samples used in this analysis. Future experimental vaccine studies using samples with known allotype and FcR polymorphism information will be needed to be conducted to confirm this study.

Overall, this study illustrates several different scenarios where host genetics is predicted to influence Fc effector responses upon vaccine boosting and that different vaccine boosting regimens are likely to have varied benefits depending on host genotypes. Specifically the model could use genetic background to guide the focus of vaccine regimens towards concentration boosting or adjuvant adjustments that affect affinity values. Given that Fc effector functions have been demonstrated to be important for the control and protection of numerous other infectious diseases including COVID-19 and influenza where vaccine boosting regimens are currently being implemented (1, 35–37), future studies that explore the influence of antibody allotypes and FcR polymorphism upon these vaccine boosting strategies could provide valuable insight.

DATA AVAILABILITY STATEMENT

The original contributions presented in this study are included in the article/**Supplementary Material**. The code for this study can be found on GitHub at https://github.com/melissalemke/FcR-ODE-Genetics. Further inquiries can be directed to the corresponding authors.

ETHICS STATEMENT

Experimental measurements used here were part of previously published study that was reviewed and approved by the Institutional Review Board at the University of Melbourne. All data provided for this study was de-identified of demographics (including gender and age). The study was reviewed by the Institutional Review Board at the University of Michigan and determined to be "Not Regulated" (HUM00191689).

AUTHOR CONTRIBUTIONS

ML designed the study, performed computational analysis, created figures, and wrote the manuscript. RT and EB performed computational analysis and edited the manuscript. MM and EL performed experimental measurements and edited the manuscript. SJK provided information used to calculate conversion factors for IgG1 allotypes and edited the manuscript. SR-N, PP, and SN conducted the RV144 Vaccine trial. BW and PH provided rsFcγR dimers and edited the manuscript. SJK arranged institutional ethics and edited the manuscript. AC designed the study, wrote the manuscript, and oversaw experimental analysis. KA designed the study, wrote the manuscript, and oversaw computational analysis. All authors contributed to the article and approved the submitted version.

FUNDING

This work was supported by the Australia National Health & Medical Research Center (NHMRC) (APP1125164 to AC and GNT1145303 to PMH and BW) and the American Foundation for AIDS Research (amfAR) Mathilde Krim Fellowship (109499-61-RKVA) to AC, and by start-up funds from the University of Michigan to KA. SJK and AC are supported by NHMRC fellowships.

ACKNOWLEDGMENTS

The data necessary to calculate allotype conversion was generously shared by Robin J. Shattock and Paul F. McKay (Imperial College London). The authors would like to thank participants in the RV144 trial.

SUPPLEMENTARY MATERIAL

The Supplementary Material for this article can be found online at: https://www.frontiersin.org/articles/10.3389/fimmu.2022.820148/full#supplementary-material

REFERENCES

1. Selva KJ, van de Sandt CE, Lemke MM, Lee CY, Shoffner SK, Chua BY, et al. Systems Serology Detects Functionally Distinct Coronavirus Antibody Features in Children and Elderly. *Nat Commun* (2021) 12:1–14. doi: 10.1038/s41467-021-22236-7. 2021 12:1.
2. Adeniji OS, Giron LB, Purwar M, Zilberstein NF, Kulkarni AJ, Shaikh MW, et al. Covid-19 Severity is Associated With Differential Antibody Fc-Mediated Innate Immune Functions. *mBio* (2021) 12:2037. doi: 10.1128/MBIO.00281-21
3. DiLillo DJ, Tan GS, Palese P, Ravetch J V. Broadly Neutralizing Hemagglutinin Stalk–Specific Antibodies Require Fcγr Interactions for Protection Against Influenza Virus In Vivo. *Nat Med* (2014) 20:143–51. doi: 10.1038/nm.3443. 2014 20:2.
4. Aitken EH, Damelang T, Ortega-Pajares A, Alemu A, Hasang W, Dini S, et al. Developing a Multivariate Prediction Model of Antibody Features Associated With Protection of Malaria-Infected Pregnant Women From Placental Malaria. *eLife* (2021) 10:e65776. doi: 10.7554/ELIFE.65776
5. Lu LL, Chung AW, Rosebrock TR, Ghebremichael M, Yu WH, Grace PS, et al. A Functional Role for Antibodies in Tuberculosis. *Cell* (2016) 167:433–443.e14. doi: 10.1016/J.CELL.2016.08.072
6. Chung AW, Kumar MP, Arnold KB, Yu WH, Schoen MK, Dunphy LJ, et al. Dissecting Polyclonal Vaccine-Induced Humoral Immunity Against HIV Using Systems Serology. *Cell* (2015) 163:988–98. doi: 10.1016/J.CELL.2015.10.027
7. Haynes BF, Gilbert PB, McElrath MJ, Zolla-Pazner S, Tomaras GD, Alam SM, et al. Immune-Correlates Analysis of an HIV-1 Vaccine Efficacy Trial. *New Engl J Med* (2012) 366:1275–86. doi: 10.1056/NEJMoa1113425
8. McLean MR, Madhavi V, Wines BD, Hogarth PM, Chung AW, Kent SJ. Dimeric Fcγ Receptor Enzyme-Linked Immunosorbent Assay To Study HIV-Specific Antibodies: A New Look Into Breadth of Fcγ Receptor Antibodies Induced by the RV144 Vaccine Trial. *J Immunol* (2017) 199:816–26. doi: 10.4049/JIMMUNOL.1602161
9. Arnold KB, Chung AW. Prospects From Systems Serology Research. *Immunology* (2018) 153:279–89. doi: 10.1111/IMM.12861

10. Kratochvil S, McKay PF, Chung AW, Kent SJ, Gilmour J, Shattock RJ. Immunoglobulin G1 Allotype Influences Antibody Subclass Distribution in Response to HIV Gp140 Vaccination. *Front Immunol* (2017) 8:1883. doi: 10.3389/fimmu.2017.01883
11. Bruhns P, Iannascoli B, England P, Mancardi DA, Fernandez N, Jorieux S, et al. Specificity and Affinity of Human Fcγ Receptors and Their Polymorphic Variants for Human IgG Subclasses. *Blood* (2009) 113:3716–25. doi: 10.1182/BLOOD-2008-09-179754
12. Pandey JP, French MAH. GM Phenotypes Influence the Concentrations of the Four Subclasses of Immunoglobulin G in Normal Human Serum. *Hum Immunol* (1996) 51:99–102. doi: 10.1016/S0198-8859(96)00205-4
13. Vidarsson G, Dekkers G, Rispens T. IgG Subclasses and Allotypes: From Structure to Effector Functions. *Front Immunol* (2014) 0:520. doi: 10.3389/FIMMU.2014.00520
14. Webster CI, Bryson CJ, Cloake EA, Jones TD, Austin MJ, Karle AC, et al. A Comparison of the Ability of the Human IgG1 Allotypes G1m3 and G1m1,17 to Stimulate T-Cell Responses From Allotype Matched and Mismatched Donors. *mAbs* (2016) 8:253–63. doi: 10.1080/19420862.2015.1128605/SUPPL_FILE/KMAB_A_1128605_SM4718.PDF
15. Johnson WE, Kohn PH, Steinberg AG. Population Genetics of the Human Allotypes Gm, Inv, and A2m: An Analytical Review. *Clin Immunol Immunopathol* (1977) 7:97–113. doi: 10.1016/0090-1229(77)90034-4
16. Jefferis R, Lefranc M-P. Human Immunoglobulin Allotypes. *mAbs* (2009) 1:332–8. doi: 10.4161/MABS.1.4.9122.
17. Kratochvil S, McKay PF, Kopycinski JT, Bishop C, Hayes PJ, Muir L, et al. A Phase 1 Human Immunodeficiency Virus Vaccine Trial for Cross-Profiling the Kinetics of Serum and Mucosal Antibody Responses to CN54gp140 Modulated by Two Homologous Prime-Boost Vaccine Regimens. *Front Immunol* (2017) 8:595. doi: 10.3389/fimmu.2017.00595
18. Hogarth PM, Pietersz GA. Fc Receptor-Targeted Therapies for the Treatment of Inflammation, Cancer and Beyond. *Nat Rev Drug Discov* (2012) 11:311–31. doi: 10.1038/nrd2909. 2012 11:4.
19. Hirvinen M, Heiskanen R, Oksanen M, Pesonen S, Liikanen I, Joensuu T, et al. Fc-Gamma Receptor Polymorphisms as Predictive and Prognostic Factors in Patients Receiving Oncolytic Adenovirus Treatment. *J Trans Med* (2013) 11:1–12. doi: 10.1186/1479-5876-11-193. 2013 11:1.
20. Hussain K, Hargreaves CE, Rowley TF, Sopp JM, Latham K V, Bhatta P, et al. Impact of Human Fcγr Gene Polymorphisms on IgG-Triggered Cytokine Release: Critical Importance of Cell Assay Format. *Front Immunol* (2019) 0:390. doi: 10.3389/FIMMU.2019.00390
21. Tamura K, Shimizu C, Hojo T, Akashi-Tanaka S, Kinoshita T, Yonemori K, et al. Fcγr2a and 3A Polymorphisms Predict Clinical Outcome of Trastuzumab in Both Neoadjuvant and Metastatic Settings in Patients With HER2-Positive Breast Cancer. *Ann Oncol* (2011) 22:1302–7. doi: 10.1093/ANNONC/MDQ585
22. Sanders LAM, Feldman RG, Voorhorst-Ogink MM, de Haas M, Rijkers GT, Capel PJA, et al. Human Immunoglobulin G (IgG) Fc Receptor IIA (CD32) Polymorphism and IgG2- Mediated Bacterial Phagocytosis by Neutrophils. *Infect Immun* (1995) 63:73–81. doi: 10.1128/IAI.63.1.73-81.1995
23. Forthal DN, Landucci G, Bream J, Jacobson LP, Phan TB, Montoya B. Fcγriia Genotype Predicts Progression of HIV Infection. *J Immunol* (2007) 179:7916–23. doi: 10.4049/JIMMUNOL.179.11.7916
24. Wang W, Erbe AK, Hank JA, Morris ZS, Sondel PM. NK Cell-Mediated Antibody-Dependent Cellular Cytotoxicity in Cancer Immunotherapy. *Front Immunol* (2015) 0:368. doi: 10.3389/FIMMU.2015.00368
25. Cartron G, Dacheux L, Salles G, Solal-Celigny P, Bardos P, Colombat P, et al. Therapeutic Activity of Humanized Anti-CD20 Monoclonal Antibody and Polymorphism in IgG Fc Receptor Fcγriiia Gene. *Blood* (2002) 99:754–8. doi: 10.1182/BLOOD.V99.3.754
26. Poonia B, Kijak GH, Pauza CD. High Affinity Allele for the Gene of FCGR3A Is Risk Factor for HIV Infection and Progression. *PloS One* (2010) 5(12): e15562. doi: 10.1371/JOURNAL.PONE.0015562
27. Forthal DN, Gabriel EE, Wang A, Landucci G, Phan TB. Association of Fcγ Receptor IIIa Genotype With the Rate of HIV Infection After Gp120 Vaccination. *Blood* (2012) 120:2836–42. doi: 10.1182/BLOOD-2012-05-431361
28. van Schie RCAA, Wilson ME. Evaluation of Human Fcγriia (CD32) and Fcγriiib (CD16) Polymorphisms in Caucasians and African-Americans Using Salivary DNA. *Clin Diagn Lab Immunol* (2000) 7:676–81. doi: 10.1128/CDLI.7.4.676-681.2000/ASSET/19718AC9-8A64-424B-A84E-6ED7DC399024/ASSETS/GRAPHIC/CD0400250001.JPEG
29. Lemke MM, McLean MR, Lee CY, Lopez E, Bozich ER, Rerks-Ngarm S, et al. A Systems Approach to Elucidate Personalized Mechanistic Complexities of Antibody-Fc Receptor Activation Post-Vaccination. *Cell Rep Med* (2021) 2 (9):100386. doi: 10.1016/J.XCRM.2021.100386
30. Dekkers G, Treffers L, Plomp R, Bentlage AEH, de, Koeleman CAM BM, Lissenberg-Thunnissen SN, et al. Decoding the Human Immunoglobulin G-Glycan Repertoire Reveals a Spectrum of Fc-Receptor- and Complement-Mediated-Effector Activities. *Front Immunol* (2017) 8:877. doi: 10.3389/fimmu.2017.00877
31. Pitisuttithum P, Kaewkungwal J, Dhitavat J, Nitayaphan S, Phd A, Karasavvas N, et al. Late Boosting of the RV144 Regimen With AIDSVAX B/E and ALVAC-HIV in HIV-Uninfected Thai Volunteers: A Double-Blind, Randomised Controlled Trial. *Articles Lancet HIV* (2020) 7:238–86. doi: 10.1016/S2352-3018(19)30406-0
32. Jefferis R, Lefranc MP. Human Immunoglobulin Allotypes: Possible Implications for Immunogenicity. *mAbs* (2009) 1:332–8. doi: 10.4161/MABS.1.4.9122
33. Pitisuttithum P, Nitayaphan S, Chariyalertsak S, Kaewkungwal J, Dawson P, Dhitavat J, et al. Late Boosting of the RV144 Regimen With AIDSVAX B/E and ALVAC-HIV in HIV-Uninfected Thai Volunteers, a Randomised Controlled Trial. *Lancet HIV* (2020) 7:e238. doi: 10.1016/S2352-3018(19)30406-0
34. Rerks-Ngarm S, Pitisuttithum P, Excler J-L, Nitayaphan S, Kaewkungwal J, Premsri N, et al. Randomized, Double-Blind Evaluation of Late Boost Strategies for HIV-Uninfected Vaccine Recipients in the RV144 HIV Vaccine Efficacy Trial. *J Infect Dis* (2017) 215:1255–63. doi: 10.1093/INFDIS/JIX099
35. Lee WS, Selva KJ, Davis SK, Wines BD, Reynaldi A, Esterbauer R, et al. Decay of Fc-Dependent Antibody Functions After Mild to Moderate COVID-19. *Cell Rep Med* (2021) 2(6):100296. doi: 10.1016/J.XCRM.2021.100296
36. Pozzetto B, Legros V, Djebali S, Barateau V, Guibert N, Villard M, et al. Immunogenicity and Efficacy of Heterologous ChadOx1/BNT162b2 Vaccination. *Nature* (2021) 600:701–6. doi: 10.1038/s41586-021-04120-y. 2021.
37. Vanderven HA, Jegaskanda S, Wines BD, Hogarth PM, Carmuglia S, Rockman S, et al. Antibody-Dependent Cellular Cytotoxicity Responses to Seasonal Influenza Vaccination in Older Adults. *J Infect Dis* (2018) 217:12–23. doi: 10.1093/INFDIS/JIX554

Conflict of Interest: The authors declare that the research was conducted in the absence of any commercial or financial relationships that could be construed as a potential conflict of interest.

Publisher's Note: All claims expressed in this article are solely those of the authors and do not necessarily represent those of their affiliated organizations, or those of the publisher, the editors and the reviewers. Any product that may be evaluated in this article, or claim that may be made by its manufacturer, is not guaranteed or endorsed by the publisher.

frontiers in Immunology

ORIGINAL RESEARCH
published: 24 February 2022
doi: 10.3389/fimmu.2022.841859

Examination of IgG Fc Receptor CD16A and CD64 Expression by Canine Leukocytes and Their ADCC Activity in Engineered NK Cells

Robert Hullsiek[1], Yunfang Li[1], Kristin M. Snyder[1,2], Sam Wang[1], Da Di[1], Antonella Borgatti[2,3,4,5,6], Chae Lee[1], Peter F. Moore[7], Cong Zhu[1], Chiara Fattori[3,4], Jaime F. Modiano[2,3,4,5,8,9,10], Jianming Wu[1,2,4] and Bruce Walcheck[1,2,4,5,8*]*

[1] Department of Veterinary and Biomedical Sciences, University of Minnesota, St. Paul, MN, United States, [2] Animal Cancer Care and Research Program, University of Minnesota, St. Paul, MN, United States, [3] Department of Veterinary Clinical Sciences, College of Veterinary Medicine, University of Minnesota, St. Paul, MN, United States, [4] Masonic Cancer Center, University of Minnesota, Minneapolis, MN, United States, [5] Center for Immunology, University of Minnesota, Minneapolis, MN, United States, [6] Clinical Investigation Center, University of Minnesota, St. Paul, MN, United States, [7] Department of Pathology, Microbiology, Immunology, School of Veterinary Medicine, University of California, Davis, CA, United States, [8] Stem Cell Institute, University of Minnesota, Minneapolis, MN, United States, [9] Institute for Engineering in Medicine, University of Minnesota, Minneapolis, MN, United States, [10] Department of Laboratory Medicine and Pathology, School of Medicine, University of Minnesota, Minneapolis, MN, United States

OPEN ACCESS

Edited by:
R. Keith Reeves, Duke University, United States

Reviewed by:
Marina Tuyishime, Duke University, United States
Justin Pollara, Duke University, United States
Hans Klingemann, NantKwest, Inc., United States

***Correspondence:**
Bruce Walcheck
walch003@umn.edu
Jianming Wu
jmwu@umn.edu

Specialty section:
This article was submitted to Comparative Immunology, a section of the journal Frontiers in Immunology

Received: *22 December 2021*
Accepted: *31 January 2022*
Published: *24 February 2022*

Citation:
Hullsiek R, Li Y, Snyder KM, Wang S, Di D, Borgatti A, Lee C, Moore PF, Zhu C, Fattori C, Modiano JF, Wu J and Walcheck B (2022) Examination of IgG Fc Receptor CD16A and CD64 Expression by Canine Leukocytes and Their ADCC Activity in Engineered NK Cells. Front. Immunol. 13:841859. doi: 10.3389/fimmu.2022.841859

Human natural killer (NK) cells can target tumor cells in an antigen-specific manner by the recognition of cell bound antibodies. This process induces antibody-dependent cell-mediated cytotoxicity (ADCC) and is exclusively mediated by the low affinity IgG Fc receptor CD16A (FcγRIIIA). Exploiting ADCC by NK cells is a major area of emphasis for advancing cancer immunotherapies. CD64 (FcγRI) is the only high affinity IgG FcR and it binds to the same IgG isotypes as CD16A, but it is not expressed by human NK cells. We have generated engineered human NK cells expressing recombinant CD64 with the goal of increasing their ADCC potency. Preclinical testing of this approach is essential for establishing efficacy and safety of the engineered NK cells. The dog provides particular advantages as a model, which includes spontaneous development of cancer in the setting of an intact and outbred immune system. To advance this immunotherapy model, we cloned canine CD16A and CD64 and generated specific mAbs. We report here for the first time the expression patterns of these FcγRs on dog peripheral blood leukocytes. CD64 was expressed by neutrophils and monocytes, but not lymphocytes, while canine CD16A was expressed at high levels by a subset of monocytes and lymphocytes. These expression patterns are similar to that of human leukocytes. Based on phenotypic characteristics, the CD16A$^+$ lymphocytes consisted of T cells (CD3$^+$ CD8$^+$ CD5^{dim} α/β TCR$^+$) and NK cells (CD3$^-$ CD5$^-$ CD94$^+$), but not B cells. Interestingly, the majority of canine CD16A$^+$ lymphocytes were from the T cell population. Like human CD16A, canine CD16A was downregulated by a disintegrin and metalloproteinase 17 (ADAM17) upon leukocyte activation, revealing a conserved means of regulation. We also directly

demonstrate that both canine CD16A and CD64 can induce ADCC when expressed in the NK cell line NK-92. These findings pave the way to engineering canine NK cells or T cells with high affinity recombinant canine CD64 to maximize ADCC and to test their safety and efficacy to benefit both humans and dogs.

Keywords: natural killer cells (NK cells), Fc receptor, IgG, canine (dog), antibody-dependent cell-mediated cytotoxicity (ADCC)

INTRODUCTION

NK cells are innate cytotoxic lymphocytes that interrogate cells in the body to identify those that are stressed, infected, or neoplastic (1). NK cells are rapidly activated and release cytolytic factors as well as cytokines and chemokines that stimulate other components of the immune system. NK cell activation is mediated by various ligands and by antibodies attached to target cells (1). The latter process induces an effector function referred to as antibody-dependent cell-mediated cytotoxicity (ADCC) and it is exclusively mediated by the IgG Fc receptor CD16A (FcγRIIIA) on human NK cells (2, 3).

Anti-tumor mAbs provide a rapidly expanding repertoire of antigen-specific targeting elements for NK cells (4). However, their clinical performance is limited by certain attributes of CD16A. It is well described that CD16A undergoes rapid ectodomain shedding by a disintegrin and metalloproteinase 17 (ADAM17) upon NK cell activation with diverse stimuli (3). Preventing this process in human NK cells by engineering a noncleavable CD16A or blocking ADAM17 enhanced their release of IFNγ and target cell killing in the presence of mAb therapies (5–7). CD16A is also a low affinity FcγR that stably binds to cell-bound IgG, but not soluble monomeric IgG. In humans, two CD16A allelic variants with either a phenylalanine (F) or a valine (V) at amino acid position 158 have been described (8). CD16A-158V has ≈ 2-fold higher affinity for IgG1 as compared to CD16A-158F (9, 10). Studies have shown that cancer patients homozygous for CD16A-158V responded significantly better to tumor targeting mAbs (11–13), indicating that increased binding affinity between CD16A and tumor-targeting mAbs will enhance NK cell anti-tumor effector functions. A strategy to increase both the binding affinity and avidity between NK cells and antibody-opsonized tumor cells has involved modifying the FcγR on NK cells (3, 14, 15). Human CD64 (FcγRI), the only high affinity IgG Fc receptor, binds to the same IgG isotypes as CD16A but with > 30-fold higher affinity than CD16A-158V (10, 16). CD64, however, is expressed by myeloid leukocyte populations but not lymphocytes, including NK cells (10). Therefore, we have engineered human NK cells to express recombinant versions of CD64 to increase their attachment efficiency to antibody-coated tumor cells to kill these cells (17, 18). Moreover, due to its high affinity state, NK cells expressing recombinant CD64 can be "armed" with anti-tumor mAbs, which can be switched for universal tumor antigen targeting (14, 17, 18).

The clinical translation of engineered NK cell immunotherapies into successful cancer therapies has been slow, due in part to the use of animal models with critical species differences in their immune cell effector functions. For instance, the study of ADCC in mice is confounded by the considerable divergence in human and mouse FcγR expression profiles and function. Mature human NK cells uniformly express high levels of CD16A under steady state conditions. Mouse leukocytes express two versions of CD16 (10). Mouse CD16 (FcγRIII) is expressed at low levels by NK cells and is actually more closely related to human CD32A (FcγRIIA), which is not expressed by human NK cells (10, 19). CD16-2 (FcγRIV) is the mouse orthologue of CD16A, but it is not expressed by resting NK cells (20). In addition, CD16-2 has been reported to bind IgE and promote IgE-mediated inflammation (21, 22). Both versions of mouse CD16 are also not shed by ADAM17 (23), demonstrating differences in their regulation compared to human CD16A. An ideal animal model for understanding the mechanisms that underlie success and failure of human immunotherapies should incorporate heterogeneous spontaneous disease and an intact immune system that is similar to humans. A comparable incidence of human and certain canine malignancies, combined with their shared biologic and pathologic characteristics, and similar response to therapy indicate that dogs can provide a clinically relevant disease model (24–26).

Based on morphology, canine NK cells are medium to large lymphocytes with electron-dense intracytoplasmic granules that contain granzyme B and perforin. These cells express at the mRNA level several genes associated with NK cells, such as NK1.1, NKG2D, CD94, CD96, NKp30, NKp44, NKp46, NKG2D, CD16A, DNAM-1, perforin, and granzyme B (26, 27), and based on transcriptome analysis, canine NK cells are globally more similar to human NK cells than to mouse NK cells (26). Canine NK cells also mediate natural cytotoxicity and ADCC (27–32). However, a lack of available species-specific antibodies has hindered efforts to study FcγRs on canine leukocytes. The focus of our study was to characterize canine CD16A and CD64 leukocyte expression patterns and their capacity to induce ADCC.

MATERIALS AND METHODS

Cells

Peripheral blood was collected from healthy pet dogs with consent from owners. The dogs consisted of various breeds and mixed breeds. All animals had received routine veterinary care, vaccinations, parasite control, and were considered to be in overall good health. Blood collection was carried out in strict accordance with the recommendations in the Guide for the Care

and Use of Laboratory Animals of the National Institutes of Health. The protocol was approved by the Institutional Animal Care and Use Committee of the University of Minnesota (Protocol Numbers: 1304-30546A and 1903–36913A). Blood was collected in K2-EDTA blood collection tubes (BD Biosciences, Franklin Lakes, NJ). Total leukocytes and PBMCs were isolated as we have previously described (33). Leukocytes with ≥ 95% viability, as assessed by trypan blue staining, were used in the described assays. Cell lines used were NK-92MI cells, an IL-2 independent version of NK-92 cells (34), SKOV-3 cells, and 293T, which were obtained from ATCC (Manassas, VA). FreeStyle 293-F cells were obtained from Thermo Fisher Scientific (Waltham, MA). All cells were cultured per the manufacturer's directions, as we have previously described (17, 18). For cell activation, leukocytes were stimulated with phorbol-12-myristate-13-acetate (PMA) (MilliporeSigma, Burlington, MA), as previously described (33). Some cells were pre-incubated for 30 min on ice with the function-blocking anti-ADAM17 mAb MEDI3622 (5 μg/ml) prior to activation.

Antibodies

To produce mAbs to canine CD16A and CD64, BALB/c mice were immunized intraperitoneally with purified soluble protein of each FcγR and hybridomas generated based on previous methods (35, 36). The anti-ADAM17 mAb MEDI3622 has been previously described (5, 33, 37). The anti-canine α/β TCR and γ/δ TCR mAbs (CA15.8G7 and CA20.8H1, respectively) have been previously described (30, 38, 39). Isotype-matched negative control mAbs were purchased from BioLegend (San Diego, CA) and BD Biosciences (Franklin Lakes, NJ). Affinity purified canine serum IgG was purchased from Southern Biotech (Birmingham, AL). Fluorophore or biotin-conjugated $F(ab')_2$ goat anti-mouse secondary antibodies and fluorophore-conjugated streptavidin were purchased from Jackson ImmunoResearch Laboratories (West Grove, PA) and BioLegend. Zombie Violet™ Fixable Viability Kit was purchased from Biolegend. All commercially available mAbs are listed in **Table 1**.

Flow Cytometry

For cell staining, nonspecific antibody binding sites were blocked for 30 min using 25% canine serum and 25% FBS in PBS buffer (without Ca^{+2} and Mg^{+2}) (Lonza, Walkersville, MD) prior to their staining with antibodies. All cell staining was analyzed on a FACSCelesta instruments (BD Biosciences), as previously described (33). Briefly, for controls, fluorescence minus one was used as well as appropriate isotype-matched antibodies. An FSC-A/SSC-A plot was used to set an electronic gate on leukocyte populations and an FSC-A/FSC-H plot was used to set an electronic gate on single cells. Fixable viability dyes eFluor 506 (Thermo Fisher Scientific) or Zombie Violet (BioLegend, San Diego, CA) were used to assess live vs. dead cells, as per the manufacturer's instructions. Canine leukocyte subsets were identified based on their forward and side light-scattering characteristics and various phenotypic markers, as described. In some cases, we attempted to enhance the staining by particular mAbs to better distinguish leukocyte subsets, as was the case for the anti-CD94 mAb HP-3D9. This was done by staining dog cells leukocytes with an unconjugated mAb, biotin-conjugated $F(ab')_2$ goat anti-mouse secondary antibodies, then fluorophore-conjugated streptavidin. Cell washes were performed between all steps. If the cells were to be stained with additional mouse-derived mAbs, the cells were first treated for 15 min with 5% mouse serum in PBS buffer. This served to occupy any free arms of cell-attached anti-mouse secondary antibodies, preventing them from binding subsequently added mouse-derived mAbs, which would result in artifactual staining.

Canine IgG adsorption to NK-92 cells was performed as previously described (17, 18), with some modifications. Briefly, cells were incubated with the indicated concentrations of canine IgG previously biotinylated using an EZ-Link™ Sulfo-NHS-LC-Biotin Kit (Thermo Fisher Scientific) per the manufacturer's instructions, for 2 h at 37°C in MEM-α basal media supplemented with HEPES (10 mM), and 2-mercaptoethanol (0.1 mM). Binding levels of biotinylated canine IgG was determined by staining the cells with allophycocyanin-streptavidin (Jackson ImmunoResearch).

Western Blotting

Protein concentrations were quantified using a bicinchoninic acid assay (BCA) (Pierce Biotechnology, Waltham, MA). Five micrograms of protein [1X Laemmli sample buffer (Bio-Rad Laboratories), 0.1M DTT] was resolved by SDS-PAGE and transferred to a nitrocellulose membrane. Blots were blocked in Intercept TBS blocking buffer (LI-COR Biosciences, Lincoln, NE) for 1 h at room temperature and incubated with primary antibodies and Quick Western IRDye 680RD detection reagent

TABLE 1 | Commercially available mAbs.

Antigen	Clone	Species	Company
Influenza Hemagglutinin A-Tag	12CA5	Mouse	Santa Cruz Biotechnology, Dallas, TX
canine CD4	YKIX302.9	Rat	Bio-Rad Laboratories, Hercules, CA
canine CD3	CA17.2A12	Mouse	Bio-Rad Laboratories
canine CD5	YKIX322.3	Rat	Bio-Rad Laboratories
human CD14	TÜK4	Mouse	Bio-Rad Laboratories
canine CD20	6C12	Caninized	Invivogen, San Diego, CA
canine CD20	6C12	Mouse	Invivogen
canine NKp46	48A	Mouse	MilliporeSigma, Burlington, MA
human CD94	HP-3D9	Mouse	BD Biosciences, Franklin Lakes, NJ

(LI-COR Biosciences) overnight at 4°C. Blots were visualized using an Odyssey imager (LI-COR Biosciences). Primary antibodies used were anti-canine CD64 clone 10 and anti-canine-CD16A clone 4A5 at 5μg/ml each.

Cytotoxicity Assays

ADCC assays were conducted using a DELFIA EuTDA cytotoxicity according to the manufacturer's instructions (PerkinElmer, Waltham, MA) and as we have previously described (17, 18). Briefly, SKOV-3-canine CD20 target cells were labeled with Bis(acetoxymethyl)-2-2:6,2 terpyridine 6,6 dicarboxylate (BATDA) for 30 min in their culture medium, washed in culture medium, and pipetted into a 96-well non-tissue culture-treated U-bottom plates at a density of 8×10^3 cells/well. Caninized anti-canine CD20 mAb was either adsorbed to NK-92 cells at 5 μg/ml in MEM-α basal media supplemented with HEPES (10 mM) then washed with MEM-α basal media or the mAb was added directly to the SKOV-3 cells at 5 μg/ml and NK-92 cells were added at the indicated E:T ratios. The plates were centrifuged at 400 × g for 1 min and then incubated for 2 h in a humidified 5% CO_2 atmosphere at 37°C. At the end of the incubation, the plates were centrifuged at 500 × g for 5 min and supernatants were transferred to a 96 well DELFIA Yellow Plate (PerkinElmer) and combined with europium. Fluorescence was measured by time-resolved fluorometry using a BMG Labtech CLARIOstar plate reader (Cary, NC). BATDA-labeled target cells alone with or without therapeutic antibodies were cultured in parallel to assess spontaneous lysis and in the presence of 1% Triton-X to measure maximum lysis. ADCC for each sample is represented as % specific release and was calculated using the following formula: Percent Specific Release = (Experimental release – Spontaneous release)/(Maximal release – Spontaneous release)*100. For each experiment, assays were conducted in triplicate that were measured using two or three replicate assay wells.

Cloning of Canine CD16A, CD64, and CD20, Generation of Expression Constructs, and Cell Line Transduction

Total RNA was isolated from canine peripheral blood leukocytes using TRIzol total RNA isolation reagent (Thermo Fisher Scientific). Peripheral blood cDNA was synthesized with the SuperScript First-Strand Synthesis (Thermo Fisher Scientific) and used in RT-PCR for expression construct generation. Full-length canine CD16A cDNA corresponding to two extracellular domains, transmembrane segment, and cytoplasmic region was amplified using the forward primer 5'-CTC TAG ACT GCC GGA TCC GCA GTG ACT TGC TGA CCC TAA TGT G-3' and the reverse primer 5'-TCG AAT TTA AAT GGA TCC AGA GAG GTC CAG AGG GGT TGC TTT -3'. The underlined nucleotides indicate *Bam* HI restriction sites. To generate N-terminus hemagglutinin A (HA)-tagged canine CD16A, we amplified a cDNA fragment using the forward primer (5'-GCC CAG CCG GCC AGA TCT ACA CAA GCT GCA GAT GTC CCA-3') and the reverse primer (5'- GCG GAT CCC GGG AGA TCT AGA GAG GTC CAG AGG GGT TGC TTT -3'). The underlined nucleotides indicate *Bgl* II restriction sites. An In-Fusion HD Cloning Kit (Takara Bio USA, San Jose, CA) was used to clone the canine CD16A cDNA fragment into a pDisplay vector (Thermo Fisher Scientific) linearized with *Bgl* II (New England Biolabs, Ipswich, MA). The expression cassette consisting of Igκ signal peptide, N-terminal HA tag, and canine CD16A was amplified using the forward primer (5'-TCT AGA CTG CCG GAT CCA CTA GTA ACG GCC GCC AGT GT-3') and the reverse primer (5'- TCG AAT TTA AAT GGA TCC AGA GAG GTC CAG AGG GGT TGC TTT-3'). The underlined nucleotides indicate *Bam* HI restriction sites. Canine CD16A or HA-tagged CD16A were then cloned into the retrovirus expression vector pBMN-I-GFP (Addgene, Watertown, MA) linearized by *Bam* HI (New England Biolabs) using the In-Fusion HD Cloning Kit.

Full-length canine CD64 cDNA corresponding to three extracellular domains, transmembrane segment, and cytoplasmic region was amplified using the forward primer (5'-TCT AGA CTG CCG GAT CCG GAG ATA ACA TGT GGC TCT TGA CAG TTC TA -3') and the reverse primer (5'- TCG AAT TTA AAT GGA TCC AAA AAG AAG TGG GAG GCA CCA TC-3'). The underlined nucleotides indicate *Bam* HI restriction sites. HA-tagged canine CD64 was amplified using the forward primer (5'-GCC CAG CCG GCC AGA TCT CAA ACA GAC CCC GTA AAG GCA -3') and the reverse primer (5'-GCG GAT CCC GGG AGA TCT AAA AAG AAG TGG GAG GCA CCA TC -3'). The underlined nucleotides indicate *Bgl* II restriction sites. Their cloning into pDisplay and/or pBMN-I-GFP were carried out as described above.

Full-length canine CD20 cDNA was amplified using the forward primer (5'-TCT AGA CTG CCG GAT CCA GAG GGT GAG ATG ACA ACA CCC AGA-3') and the reverse primer (5'-TCG AAT TTA AAT GGA TCC TTA AGG GAT GCT GTC GTT TTC TAT-3'). The underlined nucleotides indicate *Bam* HI restriction sites. The cloning of canine CD20 into pBMN-I-GFP was carried out as described above. The expression of all constructs in pBMN-I-GFP were confirmed using the sequencing primers 5'-TAG CTG GAA GAA CAC GCC CGT A-3' and 5'-GCA GAA GTA GGA GCC ATT GTG T-3'. Pseudo retrovirus particles were generated as previously described (40), and were subsequently used for NK-92 or SKOV-3 cell transduction. Cells were sorted through FACSAria II cell sorting on GFP expression (BD Biosciences).

Cloning of Soluble Canine CD16A and CD64, Generation of Expression Constructs, and Cell Line Transduction

Canine CD16A cDNA corresponding to amino acids 1-205 with a 6×histidine-tag at the carboxyl terminus was amplified using the forward primer 5'-GAA GAC ACC GAC TCT AGA GCA GTG ACT TGC TGA CCC TAA TGT GA -3' (the underlined nucleotides indicate an *Xba* I restriction site) and the reverse primer 5'-GTA GTC AGC CCG GGA TCC TTA ATG ATG ATG ATG ATG ATG GGG CCA GTG TGA AAG GAG TA-3' (the underlined nucleotides indicate a *Bam* HI restriction site). Canine CD64 cDNA corresponding to amino acids 1-280 with a

6×histidine-tag at the carboxyl terminus was amplified using the forward primer 5'-GAC TCT AGA GGA GAT AAC ATG TGG CTC TTG ACA GTT CTA -3' (the underlined nucleotides indicate an Xba I restriction sites and the reverse primer 5'-CCG GGA TCC TTA ATG ATG ATG ATG ATG ATG CAC TTG AAG CTC CAA CTC AGG G-3' (the underlined nucleotides indicate a Bam HI restriction sites). Amplified cDNA was digested by *Xba* I and *Bam* HI then and cloned into a pLenti-3F vector (a gift from Dr. Fang Li's lab, University of Minnesota, St Paul, MN) digested with the same restriction enzymes. The expression of all constructs in pLenti-3F were confirmed using the sequencing primers 5'-CAT GGG AAA GCA TCG CTA CGA A-3' and 5'-TCA GAT TGA CCA CAT GCC CCT C-3'. Pseudo-lentiviral particles containing soluble canine CD16A or CD64 were generated using 293T cells and packaging vectors pMD2.G and pCMV-dR8.74psPAX2 (Addgene). Pseudo-lentiviral particles were transduced into the FreeStyle 293-F cells. The 293-F cell line was established under puromycin selection. The 293-F cells stably expressing soluble canine CD16A or CD64 were cultured in the FreeStyle™ 293 Expression Medium (Thermo Fisher Scientific) and cell culture supernatants were harvested when cell density reached 2.5×10^6/ml. Soluble canine CD16A or CD64 were purified from cell culture supernatants using a two-step purification procedure. First step, Ni-affinity chromatography. His-tagged proteins in cell culture supernatants were purified on a HisTrap HP His tag protein purification column (Cytiva, Marlborough, MA) according to the manufacture's protocol. Second step, Fast protein liquid chromatography. Soluble canine CD16A and CD64 from the first step purification were injected into a Superdex 200 Increase 10/300 GL column (Millipore-Sigma) on an AKTA pure protein purification system (Cytiva). The purity of proteins was >95% as determined by SDS-PAGE.

Statistical Analyses

Comparison between two groups was done using Student t test. Comparison between three or more groups was done using one-way ANOVA followed by Tukey honest significance *post hoc* test. Results are depicted as mean ± SD. The symbols used to represent the p values were as follows; **, $P \leq 0.01$; ***, $P \leq 0.001$; ****, $P \leq 0.0001$.

RESULTS

Generation of Anti-cCD16A and cCD64 mAbs

In humans, CD16 consists of two isoforms, CD16A and CD16B, encoded by two highly homologous genes (41). CD16A is a transmembrane protein expressed by lymphocytes and some monocytes, whereas CD16B is linked to the plasma membrane *via* a GPI anchor and primarily expressed by neutrophils (42, 43). Canine CD16 is a transmembrane protein and therefore we refer to it here as CD16A (16). The CD16B isoform does not exist in the canine genome or cDNA (16, 19). Currently, there are no commercially available mAbs specific to canine CD16A or CD64 or any that are cross-reactive that we are aware of. For canine CD16A, this may be due to its relatively low levels of amino acid sequence identity and similarity with human CD16A (57.1% and 71.7%, respectively) (**Supplementary Figure 1A**). The amino acid sequence identity and similarity between canine CD64 and human CD64 are higher, 71.3% and 80.7%, respectively (**Supplementary Figure 1B**). Reactivity by the anti-human CD16 mAb clone LNK16 with dog peripheral blood monocytes has been reported (44), though others demonstrated a lack of specific activity by the same mAb with dog PBMCs (45). We also observed no specific reactivity by LNK16 and several other anti-human CD16 or CD64 mAbs with dog leukocytes (data not shown). Therefore, we expressed soluble forms of canine CD16A and CD64 to immunize mice and for initial hybridoma screening by ELISA. The anti-CD16A mAb clone 4A5 and the anti-CD64 mAb clone 10 were used in all analyses described below. Due to the lack of commercially available canine NK cell lines, we used the human NK cell line NK-92 for stable expression of intact versions of canine CD16A or CD64. An advantage of these cells is that they lack expression of endogenous FcγRs (46). The canine CD16A and CD64 expression constructs were engineered with an N-terminus HA-tag for detection, as illustrated in **Figure 1A**. The retroviral vector used for transduction also expressed eGFP as a separate protein for an additional marker (**Figure 1B**). As shown in **Figure 1C**, the anti-CD16A mAb clone 4A5 (IgG1) demonstrated selective reactivity with NK-92 canine CD16A cells and the anti-CD64 mAb clone 10 (IgG1) demonstrated selective reactivity with NK-92 canine CD64 cells. Neither mAb stained NK-92 control cells (**Figure 1C**). We also observed similar reactivity by 4A5 and 10 with recombinant soluble canine CD16A and CD64, respectively, by Western blotting (**Figure 1D**).

Expression of CD16A and CD64 by Canine Leukocytes

We used flow cytometry to examine the expression patterns of CD16A and CD64 by dog peripheral blood leukocytes. The general leukocyte populations of polymorphonuclear cells (PMNs), monocytes, and lymphocytes were identified based on their characteristic forward and side light-scattering and by their expression of well characterized markers, including CD4 (neutrophils and lymphocyte), CD14 (monocytes), and CD5 (T cells) (**Figure 2A**). The anti-canine CD16A clone 4A5 stained a subset of monocytes and lymphocytes, and for some dogs it marginally stained PMNs and/or a small subset of cells in this population (**Figure 2A**). This staining pattern was consistent for all the anti-canine CD16 mAbs generated, which had distinct complementarity-determining region nucleotide sequences from 4A5 (data not shown). In contrast to the expression pattern of CD16A, the anti-canine CD64 clone 10 stained essentially all PMNs and monocytes (**Figure 2A**). With some dogs, we noted a small subset of unstained cells in the PMN population (**Figure 2A**). Taken together, the expression patterns of CD16A and CD64 on dog peripheral blood leukocytes were very similar to that of their human orthologues on peripheral blood leukocytes (47).

We next examined dog peripheral blood lymphocytes to determine which subsets expressed CD16A based on available phenotypic markers. To assess its expression on T cells, we used

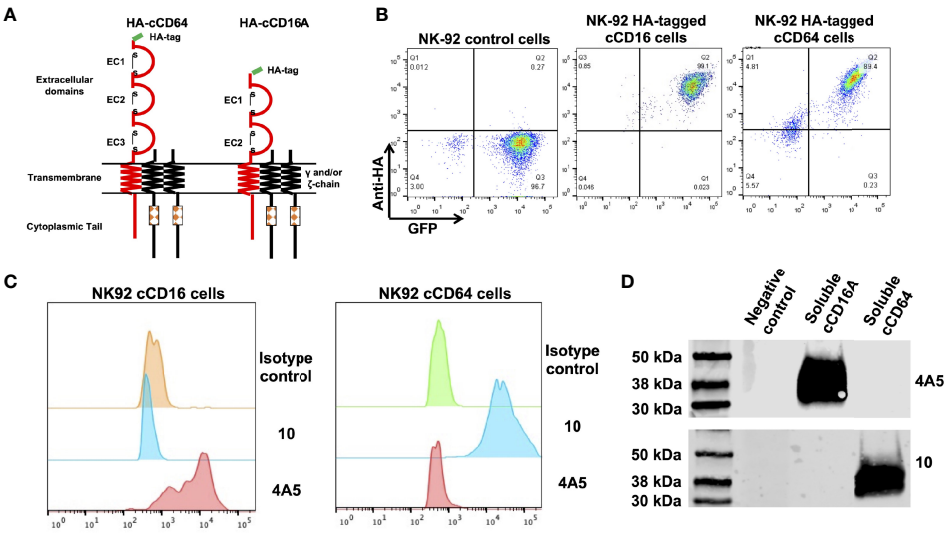

FIGURE 1 | Characterization of anti-canine CD16A and CD64 mAbs. **(A)** Schematic representation of recombinant intact canine CD16A and CD64 with an N-terminus HA-tag. The signaling adaptors FcRγ and/or CD3ζ (γ and/or ζ chain) non-covalently associate with human CD16A and CD64 as a homo or heterodimer. **(B)** Flow cytometric analyses of NK-92 cells transduced with an empty vector (control cells), NK-92 canine CD16A (cCD16A) cells, and NK-92 canine CD64 (cCD64) cells stained with an anti-HA mAb. **(C)** Flow cytometric analyses of NK-92 cCD16A cells and NK-92 cCD64 cells stained with an isotype-matched negative control mAb, the anti-canine CD16A mAb 4A5, or the anti-canine CD64 mAb 10. **(D)** Western blot analysis of recombinant soluble canine CD16A, recombinant soluble canine CD64, or soluble human CD177 (negative control) using the mAbs 4A5 or 10. Equal protein loading was confirmed by BCA. All data are representative of three independent experiments.

mAbs to canine α/β TCR, γ/δ TCR, CD8, CD4, and CD3. We found that canine CD16A was expressed on T cells, and that $CD3^+$ $CD16A^+$ T cells (**Figure 2B**, panel 1) represented 3.08% (± 1.94% SD) of the peripheral blood lymphocytes in the group of dogs that were examined (n = 12). Moreover, $CD16A^+$ lymphocytes primarily expressed an α/β TCR versus γ/δ TCR (**Figure 2B**, panels 2 and 3) and CD8 versus CD4 (**Figure 2B**, panels 4 and 5). CD16A expression was also observed on $CD3^-$ lymphocytes (**Figure 2B**, panel 1) as well as α/β TCR^- lymphocytes (**Figure 2B**, panel 2), which usually was a smaller subset than $CD3^+$ $CD16A^+$ T cells and consisted of 1.23% ± 0.97% SD, n = 12) of the peripheral blood lymphocytes. B cells were identified by their expression of CD20 and CD22 (data not shown), and essentially none of these cells expressed CD16A (**Figure 2B**, panel 6).

In dogs, CD5 is typically classified as a canine T cell marker and is expressed at varying densities, referred to as $CD5^{dim}$ and $CD5^{bright}$ (24). We detected CD16A expression on $CD5^-$ and $CD5^{dim}$ lymphocytes, but not on $CD5^{bright}$ lymphocytes (**Figure 2B**, panel 7). In most dogs we observed that $CD5^{dim}$ $CD16A^+$ lymphocytes were the predominant population, but in some dogs $CD5^-$ $CD16A^+$ lymphocytes were an equivalent or the predominant population (**Figure 2C**). Within the $CD16A^+$ lymphocyte population, CD5 expression corresponded with CD3 expression. That is, $CD16A^+$ lymphocytes were either $CD3^+$ $CD5^+$ or $CD3^-$ $CD5^-$ (**Figure 2C**). In humans, the non-B cell, $CD3^-$ $CD5^-$ $CD16A^+$ lymphocyte population represents NK cells (48). CD56 and CD94 are broad markers of human NK cells (49, 50). CD56 is not an NK cell marker in dogs (51, 52), whereas CD94 has been reported to be expressed by dog NK and NK T cells (53). Using a commercially available anti-human CD94 mAb that cross-reacts with canine CD94 (53), we found it stained a portion of $CD3^-$ $CD16A^+$ and $CD3^+$ $CD16A^+$ lymphocytes, which varied between dogs (**Figure 2D**). The above findings thus indicate that $CD16^+$ lymphocytes in the dog consist of NK cells and T cells (e.g., NK T cells), and that the latter is the predominant population, which contrasts with humans (48, 54, 55).

Ectodomain Shedding of Canine CD16A

Human CD16A undergoes a rapid downregulation in expression by a proteolytic process mediated by a disintegrin and metalloproteinase-17 (ADAM17) upon cell activation with various stimuli (23, 40, 56, 57). For instance, the treatment of human leukocytes with the phorbol ester PMA induces efficient CD16A downregulation by ADAM17 (40). We found that this also occurred upon the activation of canine leukocytes with PMA. For instance, in **Figure 3**, CD16A levels on $CD5^{dim}$ lymphocytes are shown before and after PMA activation. We have previously reported on ADAM17 activity in dog neutrophils and that it can be blocked by an ADAM17 mAb (33). This mAb also blocked the downregulation of CD16A on activated canine lymphocytes (**Figure 3**). Taken together, our findings reveal a similar regulation of human and canine CD16A by ADAM17, a process that does not occur for mouse CD16 (23).

Induction of ADCC by Canine CD16A and CD64

Human CD16A is a potent activating receptor that induces ADCC upon engaging antibodies attached to target cells (1).

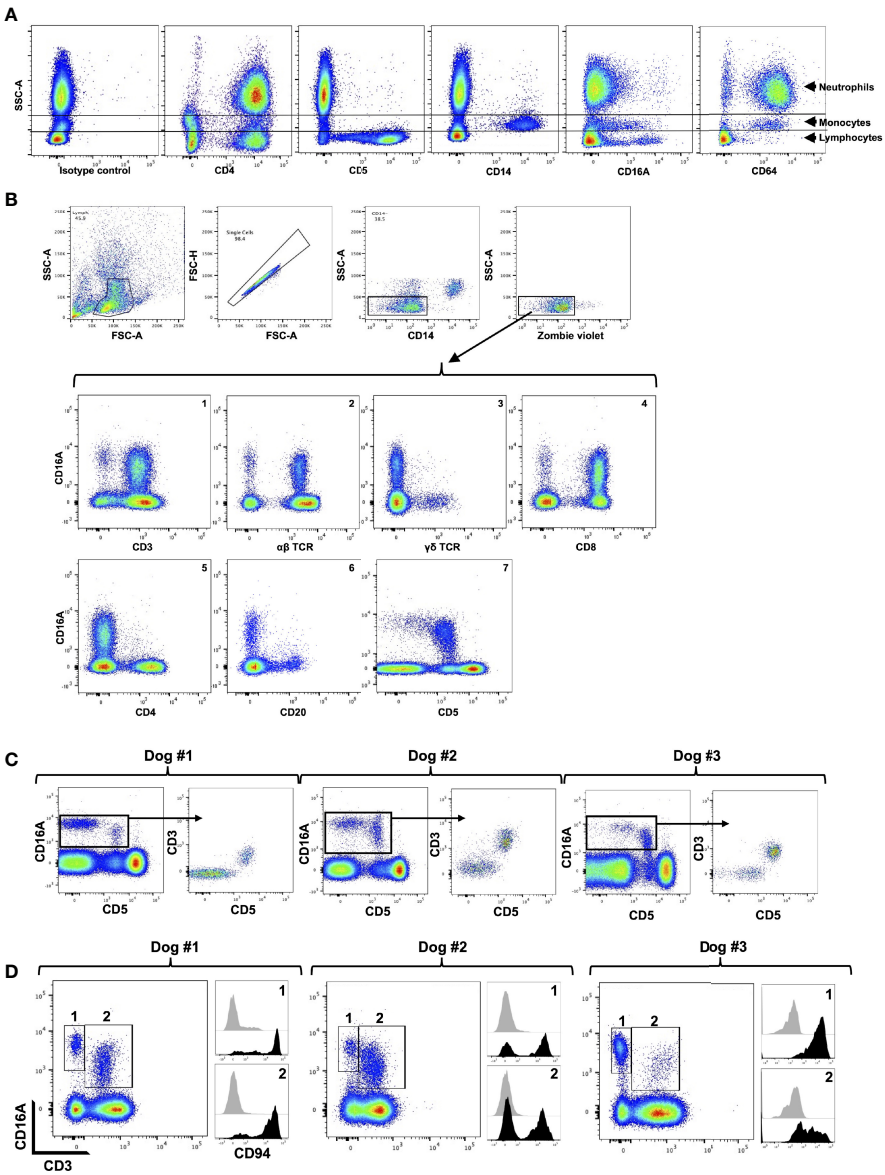

FIGURE 2 | CD16A and CD64 expression by canine leukocyte subsets. **(A)** Canine peripheral blood leukocytes were stained for the indicated markers and examined by flow cytometry. The y-axis = light side scatter area (SSC-A) and the x-axis = Log 10 fluorescence. Data are representative of multiple independent experiments using leukocytes from separate canine donors. **(B)** CD16A is expressed by T cells and non-B cell, non-T cell lymphocytes. The top panels show the gating strategy on peripheral blood mononuclear cells to examine single cell, viable, lymphocytes. The gating strategy was used in B-C. The bottom panels show the expression of CD16A on various lymphocyte populations using the indicated markers. All data are representative of multiple independent experiments using leukocytes from separate canine donors. **(C)** CD16A expression on $CD5^-$ and $CD5^+$ lymphocytes. For each dog examined, CD16A versus CD5 staining of lymphocytes was determined (left panel). From this plot, $CD16^+$ cells were gated and their expression of CD3 versus CD5 determined. **(D)** Expression of CD94 by $CD3^-$ $CD16^+$ and $CD3^+$ $CD16^+$ lymphocytes. These populations were gated on for each dog examined (left panel) and their staining levels of CD94 were determined (right panel), as indicated by the corresponding numbers. The black filled histograms represent CD94 staining, and the grey filled histograms represent isotype-matched negative control staining. For panels **(C, D)** different dogs were examined.

We directly tested whether canine CD16A could induce ADCC. For this experiment, NK-92 cells were transduced with intact canine CD16A that lacked an HA-tag due to the potential it might interfere with IgG binding. Canine CD16A expression was verified using the anti-canine CD16A mAb 4A5 (data not shown). To avoid a xenogeneic response between NK-92 cells and canine target cells, as has been reported by others (58), we used the human ovarian cancer cell line SKOV-3 as target cells that we transduced to express canine CD20 (**Figure 4A**). Like human IgGs, canine IgGs consist of four subclasses (IgG 1, 2, 3, and 4 also referred to as A, B, C, and D) (16, 59). Canine IgG2 (IgGB) is the functional analog of human IgG1 and it binds to

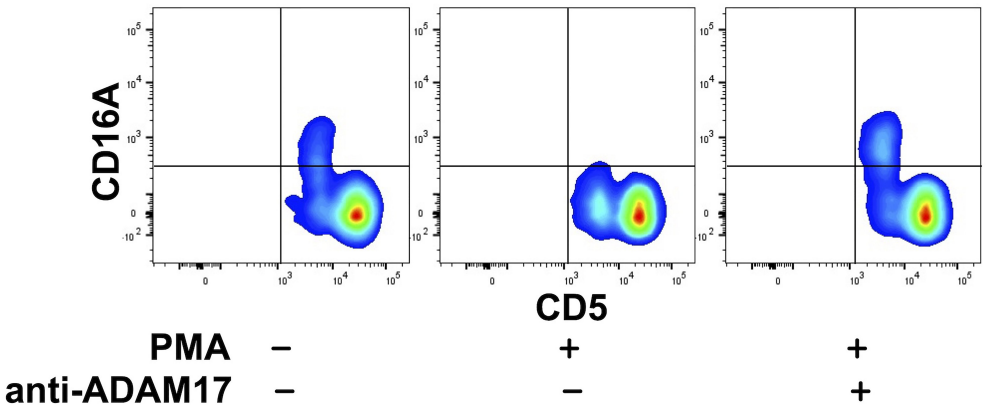

FIGURE 3 | Canine CD16A is downregulated by ADAM17 upon lymphocyte activation. Canine peripheral blood mononuclear cells were treated with or without PMA in the presence or absence of an ADAM17 function blocking mAb. Relative cell-staining levels of CD16A on $CD5^{dim}$ or $CD5^{bright}$ cells were determined by flow cytometry. All density plots show representative data of three independent experiments using leukocytes from separate canine donors.

canine CD16A and canine CD64 (16). To target canine CD20, we used a commercially available "caninized" mAb containing a canine IgG2 Fc region (**Figure 4B**). We observed that NK-92 cells expressing canine CD16A mediated significantly higher levels of cytolysis in the presence of the anti-CD20 mAb when compared to cells in the absence of the mAb at various effector: target (E:T) ratios (**Figure 4C**).

Human and canine CD16A binds to IgG with low affinity as well as reduced avidity when downregulated in expression by ADAM17 upon NK cell activation. These may serve as checkpoint processes for maintaining immune homeostasis, but they also reduce the efficacy of anti-tumor therapeutic mAbs (3). To address this, we have engineered human NK cells with recombinant versions of CD64 (14, 17, 18), the only high affinity FcγR (10, 60). Human CD64 binds to the same IgG isotypes as CD16A (10), as is also the case for canine CD64 (16), and it signals the same as CD16A by noncovalent association with FcRγ and/or CD3ζ (18). Moreover, CD64 is not cleaved by ADAM17 (17). **Figure 5A** shows that NK-92 cells expressing canine CD64 also effectively mediated ADCC of SKOV-3 canine CD20 cells in the presence of a caninized anti-CD20 mAb. Due to the high affinity state of CD64, we found that engineered NK-92 cells expressing human CD64 could be armed with tumor-targeting mAbs and mediate ADCC (17, 18). NK-92 cells expressing canine CD64 also bound soluble monomeric canine IgG and at higher levels than NK-92 cells expressing canine CD16A (**Figure 5B**). Additionally, NK-92 cells expressing canine CD64 could be armed with a caninized anti-CD20 mAb and mediate ADCC of SKOV-3-cCD20 cells (**Figure 5C**). Collectively, our data demonstrate that canine CD16 and CD64 can induce ADCC by NK-92 cells, similar to their human orthologues.

DISCUSSION

Human CD64 and CD16A play a critical role in the effector activities of anti-tumor therapeutic mAbs (15). Both FcγRs have been cloned from dog leukocytes and their IgG binding characteristics examined (16). However, their cell surface expression patterns on dog leukocytes have not been previously determined. We generated mAbs to canine CD64 and CD16A and show their expression on myeloid and lymphoid leukocyte subsets in the dog, which in general was similar to humans (47). A closer look at canine lymphocytes revealed CD16A expression on $CD3^+$ T cells and $CD3^-$ lymphocytes, but not on B cells. Interesting is that canine $CD16A^+$ lymphocytes were predominantly in the $CD3^+$ fraction, and expressed an α/β TCR and CD8, whereas in humans, $CD16A^+$ lymphocytes primarily occur in the $CD3^-$ fraction (48). Though, it has been reported that the proportion of α/β TCR^+ $CD8^+$ $CD16A^+$ T cells in humans can increase during certain viral infections, and that these cells demonstrated NK cell properties (55). Huang et al., reported that the $CD5^{dim}$ canine lymphocyte population was primarily α/β TCR^+ and $CD8^+$ with NK cell-like effector functions (38). We speculate that canine NK T cells include $CD3^+$ $CD5^{dim}$ α/β TCR^+ $CD8^+$ $CD94^+$ $CD16A^+$ cells, and it will be interesting to examine their effector functions in future studies.

Canine NK cells are phenotypically distinguished based on their lack of B cell markers, CD3, CD4, and TCRs (24, 25). $CD5^{bright}$ lymphocytes in the dog have been classified as T cell (24); however, there are conflicting views on CD5 expression by canine NK cells, which have been reported as $CD5^{+/-}$ and $CD5^{dim}$ (27, 30, 38). Both populations have been shown to mediate natural cytotoxicity and ADCC (27, 28, 30, 31, 38). We observed that CD5 expression levels on $CD16A^+$ lymphocytes ranged from negative to dim, and this directly corresponded with their CD3 expression. Thus, canine $CD16A^+$ lymphocytes appear to consist of $CD3^+$ $CD5^{dim}$ T cells, as discussed above, and $CD3^-$ $CD5^-$ $CD20^-$ (or $CD22^-$) lymphocytes. The phenotypic characterization of canine NK cells is at this point is a work in progress. NK cell markers detected by antibodies consist of CD94 and NKp46 (24). We show that CD94 expression varied on $CD3^-$ $CD16A^+$ lymphocytes, as well $CD3^+$ $CD16A^+$ lymphocytes. NKp46 expression has been reported to also vary on dog peripheral blood NK cells, and its

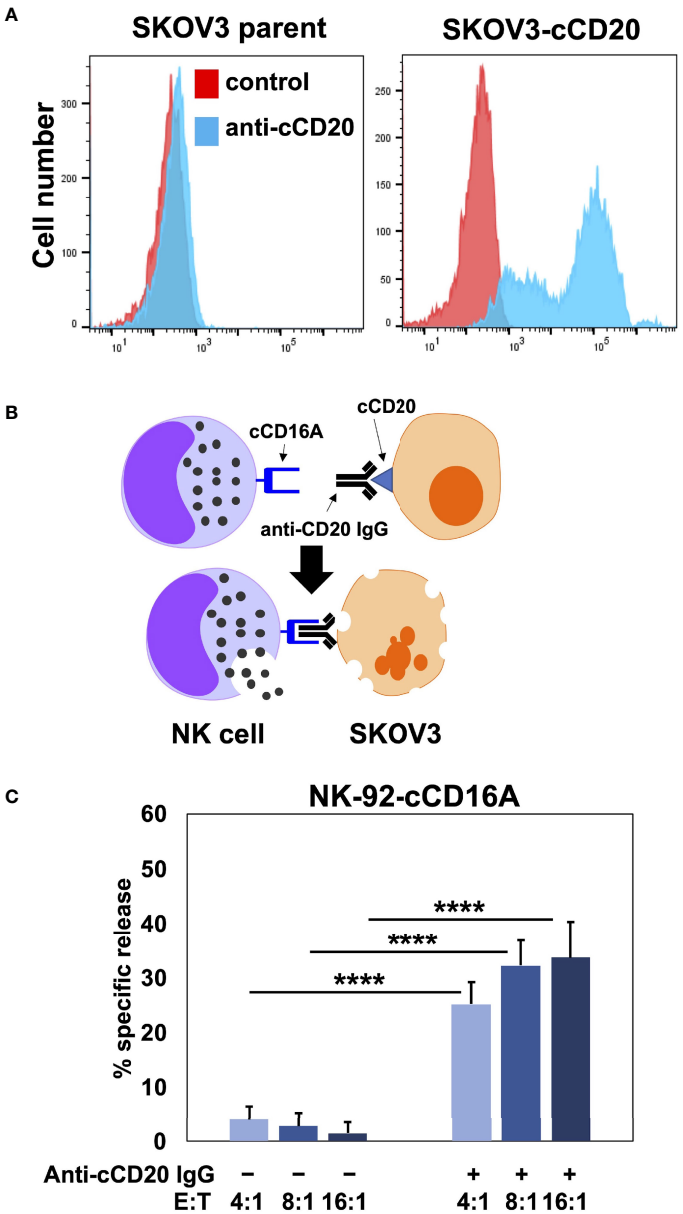

FIGURE 4 | NK-92 cells expressing canine CD16A mediate ADCC. **(A)** SKOV-3 parental cells and SKOV-3-canine CD20 (cCD20) cells were stained with an anti-canine CD20 mAb or an isotype-matched negative control mAb (control) and examined by flow cytometry. **(B)** Schematic representation of ADCC. SKOV-3-canine CD20 cells treated with a caninized anti-canine CD20 mAb in the presence of NK-92 canine CD16A (cCD16A) cells. **(C)** NK-92 canine CD16A cells were incubated with SKOV-3 canine CD20 cells at the indicated E:T ratios in the presence or absence of a caninized anti-canine CD20 mAb for 2 h at 37 °C. Data are represented as % specific release and the mean ± SD of 3 independent experiments is shown. Statistical significance is indicated as ****$p < 0.0001$.

expression appears to indicate recent activation and expansion (27, 29, 31, 61, 62). Using the only commercially available anti-canine NKp46 mAb, we observed inconsistent staining of dog peripheral blood lymphocytes, which at times did not stain above an isotype-matched negative control mAb (data not shown). As is the case in humans (1), CD16A may represent a pan-marker of mature NK cells in the peripheral blood of dogs.

Our study shows that the clone 4A5 mAb recognizes canine CD16A and not CD64. CD32B is the only other expressed canine FcγR (16). We did not directly demonstrate that 4A5 does not recognize canine CD32B; however, we feel this is unlikely considering that full-length canine CD16A and CD32B have only ~30% amino acid identity (data not shown). In addition, CD32B is expressed by human and mouse B cells and functions as an inhibitory receptor that blocks antibody production (10). We did not observe 4A5 staining of canine B cells.

Mouse leukocytes express in addition to classic CD16, CD16-2 (FcγRIV), an orthologue of human CD16A (10, 60). A review article

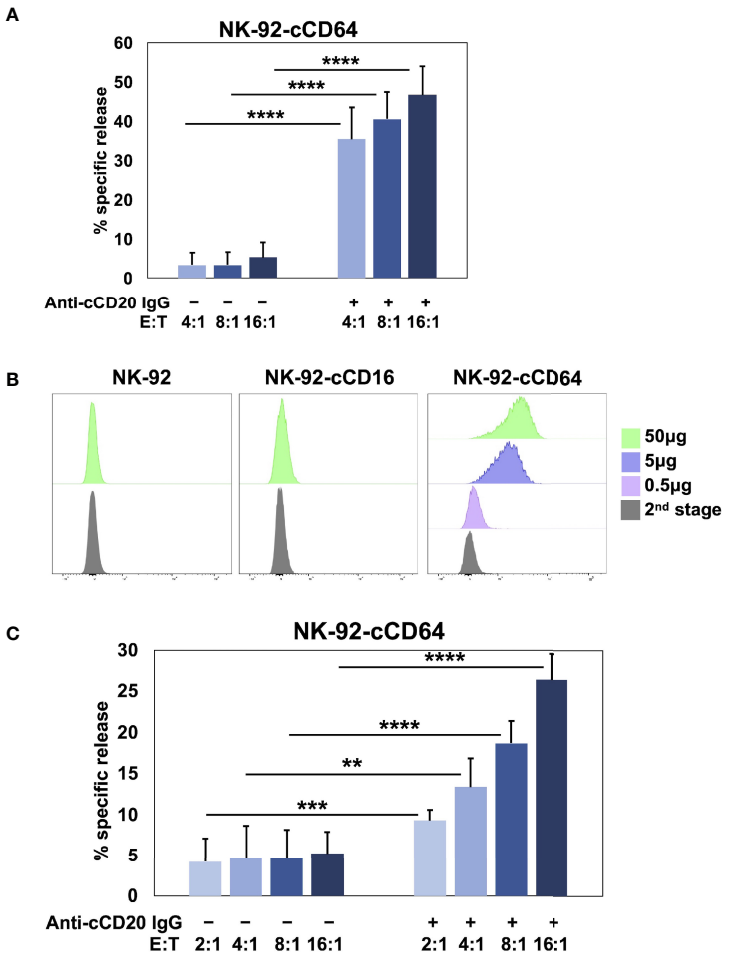

FIGURE 5 | NK-92 cells expressing canine CD64 mediate ADCC when armed with a tumor-targeting mAb. **(A)** NK-92 canine CD64 (cCD64) cells were incubated with SKOV-3 canine CD20 cells at the indicated E:T ratios in the presence or absence of a caninized anti-canine CD20 mAb for 2 h at 37°C. Data are represented as % specific release and the mean ± SD of 3 independent experiments is shown. Statistical significance is indicated as ****$p < 0.0001$. **(B)** NK-92-cCD16A and NK-92-cCD64 cells were incubated with or without biotinylated canine IgG at various concentrations for 1 h at 37°C, washed, stained with fluorophore-conjugated streptavidin, and analyzed by flow cytometry. Data are representative of at least 3 independent experiments. **(C)** NK-92 canine CD64 cells were incubated in the presence or absence of caninized anti-canine CD20 mAb (5µg/ml), washed, and exposed to SKOV-3 canine CD20 cells at the indicated E:T ratios for 2 h at 37°C. Data are represented as % specific release and the mean ± SD of 3 independent experiments is shown. Statistical significance is indicated as **$p < 0.01$, ***$p < 0.001$, ****$p < 0.0001$.

by Nimmerjahn et al. in 2006 reported on the presence of an *FCGR4* gene on chromosome 38 in the dog (19). This was based on an early rough draft of the dog genome sequence from 16 years ago. According to the most updated *Canis lupus familiaris* assembly ROS_Cfam_1.0 (RefSeq: GCF_014441545.1), chromosome 38 of C. lupus (updated on December 23, 2021, Chr 38_21,137,358.21, 146,800, Length: 9,443 nucleotides) contains the *FCGR3A* gene (also known as LOC478984), which encodes for the low affinity IgG Fc receptor CD16A, and lacks the *FCGR4* gene. Humans also lack this gene (10, 60).

We directly show that canine CD16A when expressed in the human NK cell line NK-92 can induce ADCC. Others have reported that NK-92 cells expressing a canine CD16A fusion protein consisting of the extracellular region of canine CD16A and the transmembrane and intracellular regions of canine FcRγ also mediated ADCC (58). Human CD16A signaling is normally mediated by a non-covalent association with the signaling adapters FcRγ and/or CD3ζ (1, 63, 64). NK-92 cells express FcRγ and CD3ζ (65), and therefore canine CD16A likely associated with these signaling adaptors to induce ADCC. Indeed, seven amino acids in the transmembrane region of human CD16A have been shown to be critical for FcRγ and CD3ζ association (65), and all seven amino acids are conserved in the transmembrane region of canine CD16A (**Supplementary Figure 1A**).

A critical effector function of several clinically successful mAbs targeting tumors is ADCC (66); however, CD16A undergoes rapid shedding from the cell surface of NK cells by ADAM17 following its signaling or by various other stimuli (23, 40, 56, 57). This appears to

reduce the efficacy of tumor mAb therapies, and perhaps especially so in the tumor microenvironment (3). Indeed, CD16A downregulation has been reported to occur by NK cells in the tumor microenvironment of ovarian cancer (67). ADAM17 activity has been demonstrated in canine leukocytes (33), and we show in this study that blocking the metalloprotease prevented CD16A downregulation upon canine lymphocyte activation. Further studies will be required to determine if canine CD16A is cleaved at the same location as human CD16A and the functional effects of blocking this process. Human NK cells expressing a non-cleavable version of CD16A or upon blocking ADAM17 activity demonstrated increased killing of tumor cells by ADCC and production of IFNγ (5–7), and thus this may be an approach to enhance ADCC by $CD16A^+$ canine lymphocytes.

Another property of CD16A that appears to decrease the efficacy of mAb therapies is that it is a low affinity member of the FcγR family. Indeed, clinical studies in humans have shown that increasing the affinity by which NK cells engage anti-tumor mAbs significantly improved patient outcome (11, 12, 68, 69). This is an active area of research that includes approaches such as modifying the Fc region of anti-tumor antibodies or the FcγR on NK cells (14, 15, 66). For the latter, we have engineered human NK cells to express recombinant versions of human CD64 (17, 18), the only high affinity IgG Fc receptor in humans and dogs (10, 16). Human CD64 is normally expressed by myeloid cells and not NK cells (10). We observed the same CD64 expression pattern in dogs. Similar to canine CD16A, canine CD64 expression in NK-92 cells induced ADCC, and due to its high affinity state, monomeric canine IgG could be adsorbed to these cells. Additionally, NK-92 canine CD64 cells armed with a caninized anti-canine CD20 mAb effectively killed target cells expressing canine CD20. NK-92 canine CD64 cells appeared to have higher ADCC activity when anti-canine CD20 mAb was added to the assay compared to NK-92 canine CD64 cells armed with anti-canine CD20 mAb; however, we did not perform a direct comparison. Nevertheless, it is possible that some of the adsorbed mAb internalized (especially if antibody aggregates were present) or dissociated from CD64, leading to lower ADCC activity by the armed NK-92 canine CD64 cells. It will be interesting to determine in future studies if primary dog NK cells or T cells can be engineered to express canine CD64 and if this enhances their ADCC potency. NK cells, due to their lack of graft-vs-host response, expressing canine CD64 could provide an off-the-shelf adoptive cell therapy option used in combination with assorted anti-tumor targeting mAbs. This would provide broad tumor antigen targeting to reduce tumor antigen escape and for treating various malignancies. The development of mAbs that target tumor antigens in dogs and induce ADCC has been minimal at this time (70). However, as tools and our understanding about canine immune cells rapidly increase, it is likely a surge in immunotherapies for dogs will follow.

Dogs also offer a key animal model for the translation of immunotherapies. The study of ADCC in rodent syngeneic tumor models is limited by species differences in immune cell effector functions, including significant differences in human and mouse CD16 expression and function (see Introduction). The dog spontaneous cancer model incorporates heterogeneous disease and an intact immune system with many similarities to humans to help determine the mechanisms that underlie success and failure of immunotherapies (24–26). We have extended the current understanding of the dog immune system by demonstrating phenotypic and functional characteristics of canine CD16A and CD64 to advance utilizing these FcγRs for therapeutic approaches.

DATA AVAILABILITY STATEMENT

The raw data supporting the conclusions of this article will be made available by the authors, without undue reservation.

ETHICS STATEMENT

The animal study was reviewed and approved by Institutional Animal Care and Use Committee of the University of Minnesota. Written informed consent was obtained from the owners for the participation of their animals in this study.

AUTHOR CONTRIBUTIONS

RH, YL, KS, SW, CL, CZ, and CF designed the experiments, collected, assembled, analyzed, and interpreted the data. JW and BW designed the experiments, interpreted the data, and wrote the manuscript. PM contributed vital reagents. JM and AB interpreted the data. All authors contributed to the manuscript preparation as well as read and approved the submitted version.

FUNDING

This work was supported by University of Minnesota College of Veterinary Medicine Comparative Medicine Signature Program Grant (to BW, JW, AB); University of Minnesota Animal Cancer Care and Research Program Canine Cancer Charitable Grant and GreyLong Gift (to BW); Howard Hughes Medical Institute and Burroughs Wellcome Fund Medical Research Fellowship (to KS); NIH UL1TR002494 supporting the University of Minnesota Clinical and Translational Science Institute K-R01 Scholar Award (to AB), and NIH P30 CA77598 supporting the University of Minnesota, Masonic Cancer Center, Flow Cytometry resource.

ACKNOWLEDGMENTS

We would like to thank Kathy Stuebner and Amber Winter from the University of Minnesota, College of Veterinary Medicine, Clinical Investigation Center for assistance in acquiring canine peripheral blood samples, and Taylor DePauw with flow cytometry assistance.

SUPPLEMENTARY MATERIAL

The Supplementary Material for this article can be found online at: https://www.frontiersin.org/articles/10.3389/fimmu.2022.841859/full#supplementary-material

Supplementary Figure 1 | Amino acid alignment of human and canine CD16A or canine CD64. The amino acid sequences of human and canine CD16A and CD64

are from the NCBI reference sequences (human CD16: X52645.1; canine CD16A: XM_022415348; human CD64: X14356.1; canine CD64: NM_001002976). The amino acid sequence of the human CD16A and CD64 transmembrane regions (underlined) is based on a previous study (71). **(A)** Alignment of human and canine CD16A. The red boxed letters represent amino acids critical for association with the signaling adaptors FcRγ and CD3ζ (65). **(B)** Alignment of human and canine CD64.

REFERENCES

1. Miller JS, Lanier LL. Natural Killer Cells in Cancer Immunotherapy. *Annu Rev Cancer Biol* (2019) 3:77–103. doi: 10.1146/annurev-cancerbio-030518-055653
2. Alderson KL, Sondel PM. Clinical Cancer Therapy by NK Cells *via* Antibody-Dependent Cell-Mediated Cytotoxicity. *J BioMed Biotechnol* (2011) 2011:379123. doi: 10.1155/2011/379123
3. Wu J, Mishra HK, Walcheck B. Role of ADAM17 as a Regulatory Checkpoint of CD16A in NK Cells and as a Potential Target for Cancer Immunotherapy. *J Leukoc Biol* (2019) 105(6):1297–303. doi: 10.1002/JLB.2MR1218-501R
4. Zahavi D, Weiner L. Monoclonal Antibodies in Cancer Therapy. *Antibodies (Basel)* (2020) 9(3):1–20. doi: 10.3390/antib9030034
5. Mishra HK, Pore N, Michelotti EF, Walcheck B. Anti-ADAM17 Monoclonal Antibody MEDI3622 Increases IFNgamma Production by Human NK Cells in the Presence of Antibody-Bound Tumor Cells. *Cancer Immunol Immunother* (2018) 67(9):1407–16. doi: 10.1007/s00262-018-2193-1
6. Pomeroy EJ, Hunzeker JT, Kluesner MG, Lahr WS, Smeester BA, Crosby MR, et al. A Genetically Engineered Primary Human Natural Killer Cell Platform for Cancer Immunotherapy. *Mol Ther* (2020) 28(1):52–63. doi: 10.1016/j.ymthe.2019.10.009
7. Zhu H, Blum RH, Bjordahl R, Gaidarova S, Rogers P, Lee TT, et al. Pluripotent Stem Cell-Derived NK Cells With High-Affinity Noncleavable CD16a Mediate Improved Antitumor Activity. *Blood* (2020) 135(6):399–410. doi: 10.1182/blood.2019000621
8. Wu J, Edberg JC, Redecha PB, Bansal V, Guyre PM, Coleman K, et al. A Novel Polymorphism of FcgammaRIIIa (CD16) Alters Receptor Function and Predisposes to Autoimmune Disease. *J Clin Invest* (1997) 100(5):1059–70. doi: 10.1172/JCI119616
9. Koene HR, Kleijer M, Algra J, Roos D, von dem Borne AE, de Haas M. Fc gammaRIIIa-158v/F Polymorphism Influences the Binding of IgG by Natural Killer Cell Fc gammaRIIIa, Independently of the Fc gammaRIIIa-48l/R/H Phenotype. *Blood* (1997) 90(3):1109–14. doi: 10.1182/blood.V90.3.1109
10. Bruhns P. Properties of Mouse and Human IgG Receptors and Their Contribution to Disease Models. *Blood* (2012) 119(24):5640–9. doi: 10.1182/blood-2012-01-380121
11. Cartron G, Dacheux L, Salles G, Solal-Celigny P, Bardos P, Colombat P, et al. Therapeutic Activity of Humanized Anti-CD20 Monoclonal Antibody and Polymorphism in IgG Fc Receptor FcgammaRIIIa Gene. *Blood* (2002) 99 (3):754–8. doi: 10.1182/blood.v99.3.754
12. Musolino A, Naldi N, Bortesi B, Pezzuolo D, Capelletti M, Missale G, et al. Immunoglobulin G Fragment C Receptor Polymorphisms and Clinical Efficacy of Trastuzumab-Based Therapy in Patients With HER-2/Neu-Positive Metastatic Breast Cancer. *J Clin Oncol* (2008) 26(11):1789–96. doi: 10.1200/JCO.2007.14.8957
13. Bibeau F, Lopez-Crapez E, Di Fiore F, Thezenas S, Ychou M, Blanchard F, et al. Impact of Fc{gamma}RIIa-Fc{gamma}RIIIa Polymorphisms and KRAS Mutations on the Clinical Outcome of Patients With Metastatic Colorectal Cancer Treated With Cetuximab Plus Irinotecan. *J Clin Oncol* (2009) 27 (7):1122–9. doi: 10.1200/JCO.2008.18.0463
14. Walcheck B, Wu J. iNK-CD64/16A Cells: A Promising Approach for ADCC? *Expert Opin Biol Ther* (2019) 19(12):12290–32. doi: 10.1080/14712598.2019.1667974
15. Dixon KJ, Wu J, Walcheck B. Engineering Anti-Tumor Monoclonal Antibodies and Fc Receptors to Enhance ADCC by Human NK Cells. *Cancers (Basel)* (2021) 13(2):1–13. doi: 10.3390/cancers13020312
16. Bergeron LM, McCandless EE, Dunham S, Dunkle B, Zhu Y, Shelly J, et al. Comparative Functional Characterization of Canine IgG Subclasses. *Vet Immunol Immunopathol* (2014) 157(1-2):31–41. doi: 10.1016/j.vetimm.2013.10.018
17. Snyder KM, Hullsiek R, Mishra HK, Mendez DC, Li Y, Rogich A, et al. Expression of a Recombinant High Affinity IgG Fc Receptor by Engineered NK Cells as a Docking Platform for Therapeutic Mabs to Target Cancer Cells. *Front Immunol* (2018) 9:2873. doi: 10.3389/fimmu.2018.02873
18. Hintz HM, Snyder KM, Wu J, Hullsiek R, Dahlvang JD, Hart GT, et al. Simultaneous Engagement of Tumor and Stroma Targeting Antibodies by Engineered NK-92 Cells Expressing CD64 Controls Prostate Cancer Growth. *Cancer Immunol Res* (2021) 9(11):1270–82. doi: 10.1158/2326-6066.CIR-21-0178
19. Nimmerjahn F, Ravetch JV. Fcgamma Receptors: Old Friends and New Family Members. *Immunity* (2006) 24(1):19–28. doi: 10.1016/j.immuni.2005.11.010
20. Nimmerjahn F, Bruhns P, Horiuchi K, Ravetch JV. FcgammaRIV: A Novel FcR With Distinct IgG Subclass Specificity. *Immunity* (2005) 23(1):41–51. doi: 10.1016/j.immuni.2005.05.010
21. Hirano M, Davis RS, Fine WD, Nakamura S, Shimizu K, Yagi H, et al. IgEb Immune Complexes Activate Macrophages Through FcgammaRIV Binding. *Nat Immunol* (2007) 8(7):762–71. doi: 10.1038/ni1477
22. Mancardi DA, Iannascoli B, Hoos S, England P, Daeron M, Bruhns P. FcgammaRIV Is a Mouse IgE Receptor That Resembles Macrophage FcepsilonRI in Humans and Promotes IgE-Induced Lung Inflammation. *J Clin Invest* (2008) 118(11):3738–50. doi: 10.1172/JCI36452
23. Wang Y, Wu J, Newton R, Bahaie NS, Long C, Walcheck B. ADAM17 Cleaves CD16b (FcgammaRIIIb) in Human Neutrophils. *Biochim Biophys Acta* (2013) 1833(3):680–5. doi: 10.1016/j.bbamcr.2012.11.027
24. Gingrich AA, Modiano JF, Canter RJ. Characterization and Potential Applications of Dog Natural Killer Cells in Cancer Immunotherapy. *J Clin Med* (2019) 8(11):1–18. doi: 10.3390/jcm8111802
25. Kisseberth WC, Lee DA. Adoptive Natural Killer Cell Immunotherapy for Canine Osteosarcoma. *Front Vet Sci* (2021) 8:672361. doi: 10.3389/fvets.2021.672361
26. Gingrich AA, Reiter TE, Judge SJ, York D, Yanagisawa M, Razmara A, et al. Comparative Immunogenomics of Canine Natural Killer Cells as Immunotherapy Target. *Front Immunol* (2021) 12:670309. doi: 10.3389/fimmu.2021.670309
27. Foltz JA, Somanchi SS, Yang Y, Aquino-Lopez A, Bishop EE, Lee DA. NCR1 Expression Identifies Canine Natural Killer Cell Subsets With Phenotypic Similarity to Human Natural Killer Cells. *Front Immunol* (2016) 7:521. doi: 10.3389/fimmu.2016.00521
28. Park JY, Shin DJ, Lee SH, Lee JJ, Suh GH, Cho D, et al. The Anti-Canine Distemper Virus Activities of Ex Vivo-Expanded Canine Natural Killer Cells. *Vet Microbiol* (2015) 176(3-4):239–49. doi: 10.1016/j.vetmic.2015.01.021
29. Canter RJ, Grossenbacher SK, Foltz JA, Sturgill IR, Park JS, Luna JI, et al. Radiotherapy Enhances Natural Killer Cell Cytotoxicity and Localization in Pre-Clinical Canine Sarcomas and First-in-Dog Clinical Trial. *J Immunother Cancer* (2017) 5(1):98. doi: 10.1186/s40425-017-0305-7
30. Lee SH, Shin DJ, Kim Y, Kim CJ, Lee JJ, Yoon MS, et al. Comparison of Phenotypic and Functional Characteristics Between Canine Non-B, Non-T Natural Killer Lymphocytes and CD3(+)CD5(dim)CD21(-) Cytotoxic Large Granular Lymphocytes. *Front Immunol* (2018) 9:841. doi: 10.3389/fimmu.2018.00841
31. Kim Y, Lee SH, Kim CJ, Lee JJ, Yu D, Ahn S, et al. Canine Non-B, Non-T NK Lymphocytes Have a Potential Antibody-Dependent Cellular Cytotoxicity Function Against Antibody-Coated Tumor Cells. *BMC Vet Res* (2019) 15 (1):339. doi: 10.1186/s12917-019-2068-5
32. Mizuno T, Kato Y, Kaneko MK, Sakai Y, Shiga T, Kato M, et al. Generation of a Canine Anti-Canine CD20 Antibody for Canine Lymphoma Treatment. *Sci Rep* (2020) 10(1):11476. doi: 10.1038/s41598-020-68470-9
33. Snyder KM, McAloney CA, Montel JS, Modiano JF, Walcheck B. Ectodomain Shedding by ADAM17 (a Disintegrin and Metalloproteinase 17) in Canine Neutrophils. *Vet Immunol Immunopathol* (2021) 231:110162. doi: 10.1016/j.vetimm.2020.110162
34. Tam YK, Maki G, Miyagawa B, Hennemann B, Tonn T, Klingemann HG. Characterization of Genetically Altered, Interleukin 2-Independent Natural

Killer Cell Lines Suitable for Adoptive Cellular Immunotherapy. *Hum Gene Ther* (1999) 10(8):1359–73. doi: 10.1089/10430349950018030
35. Jones WM, Walcheck B, Jutila MA. Generation of a New Gamma Delta T Cell-Specific Monoclonal Antibody (GD3.5). Biochemical Comparisons of GD3.5 Antigen With the Previously Described Workshop Cluster 1 (WC1) Family. *J Immunol* (1996) 156(10):3772–9.
36. Walcheck B, Leppanen A, Cummings RD, Knibbs RN, Stoolman LM, Alexander SR, et al. The Monoclonal Antibody CHO-131 Binds to a Core 2 O-Glycan Terminated With Sialyl-Lewis X, Which Is a Functional Glycan Ligand for P-Selectin. *Blood* (2002) 99(11):4063–9. doi: 10.1182/blood-2001-12-0265
37. Mishra HK, Ma J, Mendez D, Hullsiek R, Pore N, Walcheck B. Blocking ADAM17 Function With a Monoclonal Antibody Improves Sepsis Survival in a Murine Model of Polymicrobial Sepsis. *Int J Mol Sci* (2020) 21(18):1–20. doi: 10.3390/ijms21186688
38. Huang YC, Hung SW, Jan TR, Liao KW, Cheng CH, Wang YS, et al. CD5-Low Expression Lymphocytes in Canine Peripheral Blood Show Characteristics of Natural Killer Cells. *J Leukoc Biol* (2008) 84(6):1501–10. doi: 10.1189/jlb.0408255
39. Moore PF, Affolter VK, Olivry T, Schrenzel MD. The Use of Immunological Reagents in Defining the Pathogenesis of Canine Skin Diseases Involving Proliferation of Leukocytes. In: KW Kwochka, T Willemse, C von Tscharner, editors. *Advances in Veterinary Dermatology*. Oxford, UK: Butterworth Heinemann (1998).
40. Jing Y, Ni Z, Wu J, Higgins L, Markowski TW, Kaufman DS, et al. Identification of an ADAM17 Cleavage Region in Human CD16 (FcgammaRIII) and the Engineering of a Non-Cleavable Version of the Receptor in NK Cells. *PloS One* (2015) 10(3):e0121788. doi: 10.1371/journal.pone.0121788
41. Ravetch JV, Perussia B. Alternative Membrane Forms of Fc Gamma RIII (CD16) on Human Natural Killer Cells and Neutrophils. Cell Type-Specific Expression of Two Genes That Differ in Single Nucleotide Substitutions. *J Exp Med* (1989) 170(2):481–97. doi: 10.1084/jem.170.2.481
42. Selvaraj P, Rosse WF, Silber R, Springer TA. The Major Fc Receptor in Blood has a Phosphatidylinositol Anchor and Is Deficient in Paroxysmal Noctural Hemoglobinuria. *Nature* (1988) 333:565–7. doi: 10.1038/333565a0
43. Huizinga TW, Kerst M, Nuyens JH, Vlug A, von dem Borne AE, Roos D, et al. Binding Characteristics of Dimeric IgG Subclass Complexes to Human Neutrophils. *J Immunol* (1989) 142(7):2359–64.
44. Tuohy JL, Lascelles BD, Griffith EH, Fogle JE. Association of Canine Osteosarcoma and Monocyte Phenotype and Chemotactic Function. *J Vet Intern Med* (2016) 30(4):1167–78. doi: 10.1111/jvim.13983
45. Gibbons N, Goulart MR, Chang YM, Efstathiou K, Purcell R, Wu Y, et al. Phenotypic Heterogeneity of Peripheral Monocytes in Healthy Dogs. *Vet Immunol Immunopathol* (2017) 190:26–30. doi: 10.1016/j.vetimm.2017.06.007
46. Binyamin L, Alpaugh RK, Hughes TL, Lutz CT, Campbell KS, Weiner LM. Blocking NK Cell Inhibitory Self-Recognition Promotes Antibody-Dependent Cellular Cytotoxicity in a Model of Anti-Lymphoma Therapy. *J Immunol* (2008) 180(9):6392–401. doi: 10.4049/jimmunol.180.9.6392
47. Patel KR, Roberts JT, Barb AW. Multiple Variables at the Leukocyte Cell Surface Impact Fc Gamma Receptor-Dependent Mechanisms. *Front Immunol* (2019) 10:223. doi: 10.3389/fimmu.2019.00223
48. Lanier LL, Kipps TJ, Phillips JH. Functional Properties of a Unique Subset of Cytotoxic CD3+ T Lymphocytes That Express Fc Receptors for IgG (CD16/Leu-11 Antigen). *J Exp Med* (1985) 162(6):2089–106. doi: 10.1084/jem.162.6.2089
49. Lanier LL, Testi R, Bindl J, Phillips JH. Identity of Leu-19 (CD56) Leukocyte Differentiation Antigen and Neural Cell Adhesion Molecule. *J Exp Med* (1989) 169(6):2233–8. doi: 10.1084/jem.169.6.2233
50. Lanier LL, Chang C, Phillips JH. Human NKR-P1A. A Disulfide-Linked Homodimer of the C-Type Lectin Superfamily Expressed by a Subset of NK and T Lymphocytes. *J Immunol* (1994) 153(6):2417–28.
51. Otani I, Niwa T, Tajima M, Ishikawa A, Watanabe T, Tsumagari S, et al. CD56 Is Expressed Exclusively on CD3+ T Lymphocytes in Canine Peripheral Blood. *J Vet Med Sci* (2002) 64(5):441–4. doi: 10.1292/jvms.64.441
52. Grondahl-Rosado C, Bonsdorff TB, Brun-Hansen HC, Storset AK. NCR1+ Cells in Dogs Show Phenotypic Characteristics of Natural Killer Cells. *Vet Res Commun* (2015) 39(1):19–30. doi: 10.1007/s11259-014-9624-z
53. Graves SS, Gyurkocza B, Stone DM, Parker MH, Abrams K, Jochum C, et al. Development and Characterization of a Canine-Specific Anti-CD94 (KLRD-1) Monoclonal Antibody. *Vet Immunol Immunopathol* (2019) 211:10–8. doi: 10.1016/j.vetimm.2019.03.005
54. Groh V, Porcelli S, Fabbi M, Lanier LL, Picker LJ, Anderson T, et al. Human Lymphocytes Bearing T Cell Receptor Gamma/Delta Are Phenotypically Diverse and Evenly Distributed Throughout the Lymphoid System. *J Exp Med* (1989) 169(4):1277–94. doi: 10.1084/jem.169.4.1277
55. Bjorkstrom NK, Gonzalez VD, Malmberg KJ, Falconer K, Alaeus A, Nowak G, et al. Elevated Numbers of Fc Gamma RIIIA+ (CD16+) Effector CD8 T Cells With NK Cell-Like Function in Chronic Hepatitis C Virus Infection. *J Immunol* (2008) 181(6):4219–28. doi: 10.4049/jimmunol.181.6.4219
56. Romee R, Foley B, Lenvik T, Wang Y, Zhang B, Ankarlo D, et al. NK Cell CD16 Surface Expression and Function Is Regulated by a Disintegrin and Metalloprotease-17 (ADAM17). *Blood* (2013) 121(18):3599–608. doi: 10.1182/blood-2012-04-425397
57. Lajoie L, Congy-Jolivet N, Bolzec A, Gouilleux-Gruart V, Sicard E, Sung HC, et al. ADAM17-Mediated Shedding of FcgammaRIIIA on Human NK Cells: Identification of the Cleavage Site and Relationship With Activation. *J Immunol* (2014) 192(2):741–51. doi: 10.4049/jimmunol.1301024
58. Mizuno T, Takeda Y, Tsukui T, Igase M. Development of a Cell Line-Based Assay to Measure the Antibody-Dependent Cellular Cytotoxicity of a Canine Therapeutic Antibody. *Vet Immunol Immunopathol* (2021) 240:110315. doi: 10.1016/j.vetimm.2021.110315
59. Donaghy D, Moore AR. Identification of Canine IgG and Its Subclasses, IgG1, IgG2, IgG3 and IgG4, by Immunofixation and Commercially Available Antisera. *Vet Immunol Immunopathol* (2020) 221:110014. doi: 10.1016/j.vetimm.2020.110014
60. Nimmerjahn F, Ravetch JV. Fcgamma Receptors as Regulators of Immune Responses. *Nat Rev Immunol* (2008) 8(1):34–47. doi: 10.1038/nri2206
61. Grondahl-Rosado C, Boysen P, Johansen GM, Brun-Hansen H, Storset AK. NCR1 Is an Activating Receptor Expressed on a Subset of Canine NK Cells. *Vet Immunol Immunopathol* (2016) 177:7–15. doi: 10.1016/j.vetimm.2016.05.001
62. Judge SJ, Yanagisawa M, Sturgill IR, Bateni SB, Gingrich AA, Foltz JA, et al. Blood and Tissue Biomarker Analysis in Dogs With Osteosarcoma Treated With Palliative Radiation and Intra-Tumoral Autologous Natural Killer Cell Transfer. *PloS One* (2020) 15(2):e0224775. doi: 10.1371/journal.pone.0224775
63. Lanier LL, Yu G, Phillips JH. Co-Association of CD3 Zeta With a Receptor (CD16) for IgG Fc on Human Natural Killer Cells. *Nature* (1989) 342(6251):803–5. doi: 10.1038/342803a0
64. Letourneur O, Kennedy IC, Brini AT, Ortaldo JR, O'Shea JJ, Kinet JP. Characterization of the Family of Dimers Associated With Fc Receptors (Fc Epsilon RI and Fc Gamma RIII). *J Immunol* (1991) 147(8):2652–6.
65. Blazquez-Moreno A, Park S, Im W, Call MJ, Call ME, Reyburn HT. Transmembrane Features Governing Fc Receptor CD16A Assembly With CD16A Signaling Adaptor Molecules. *Proc Natl Acad Sci USA* (2017) 114(28):E5645–54. doi: 10.1073/pnas.1706483114
66. Gauthier M, Laroye C, Bensoussan D, Boura C, Decot V. Natural Killer Cells and Monoclonal Antibodies: Two Partners for Successful Antibody Dependent Cytotoxicity Against Tumor Cells. *Crit Rev Oncol Hematol* (2021) 160:103261. doi: 10.1016/j.critrevonc.2021.103261
67. Felices M, Chu S, Kodal B, Bendzick L, Ryan C, Lenvik AJ, et al. IL-15 Super-Agonist (ALT-803) Enhances Natural Killer (NK) Cell Function Against Ovarian Cancer. *Gynecol Oncol* (2017) 145(3):453–61. doi: 10.1016/j.ygyno.2017.02.028
68. Vitale M, Cantoni C, Pietra G, Mingari MC, Moretta L. Effect of Tumor Cells and Tumor Microenvironment on NK-Cell Function. *Eur J Immunol* (2014) 44(6):1582–92. doi: 10.1002/eji.201344272
69. Zahavi D, AlDeghaither D, O'Connell A, Weiner LM. Enhancing Antibody-Dependent Cell-Mediated Cytotoxicity: A Strategy for Improving Antibody-Based Immunotherapy. *Antibody Ther* (2018) 1(1):7–12. doi: 10.1093/abt/tby002
70. Klingemann H. Immunotherapy for Dogs: Still Running Behind Humans. *Front Immunol* (2021) 12:665784. doi: 10.3389/fimmu.2021.665784

71. Zidovetzki R, Rost B, Armstrong DL, Pecht I. Transmembrane Domains in the Functions of Fc Receptors. *Biophys Chem* (2003) 100(1-3):555–75. doi: 10.1016/s0301-4622(02)00306-x

Conflict of Interest: The authors declare that the research was conducted in the absence of any commercial or financial relationships that could be construed as a potential conflict of interest.

Publisher's Note: All claims expressed in this article are solely those of the authors and do not necessarily represent those of their affiliated organizations, or those of the publisher, the editors and the reviewers. Any product that may be evaluated in this article, or claim that may be made by its manufacturer, is not guaranteed or endorsed by the publisher.

frontiers in Immunology

REVIEW
published: 17 March 2022
doi: 10.3389/fimmu.2022.830482

Leveraging Antibody, B Cell and Fc Receptor Interactions to Understand Heterogeneous Immune Responses in Tuberculosis

Stephen M. Carpenter[1,2] *and Lenette L. Lu*[3,4,5]*

[1] Division of Infectious Disease and HIV Medicine, Department of Medicine, Case Western Reserve University, Cleveland, OH, United States, [2] Cleveland Medical Center, University Hospitals Cleveland Medical Center, Cleveland, OH, United States, [3] Division of Geographic Medicine and Infectious Diseases, Department of Internal Medicine, UT Southwestern Medical Center, Dallas, TX, United States, [4] Department of Immunology, UT Southwestern Medical Center, Dallas, TX, United States, [5] Parkland Health and Hospital System, Dallas, TX, United States

Despite over a century of research, *Mycobacterium tuberculosis (Mtb)*, the causative agent of tuberculosis (TB), continues to kill 1.5 million people annually. Though less than 10% of infected individuals develop active disease, the specific host immune responses that lead to *Mtb* transmission and death, as well as those that are protective, are not yet fully defined. Recent immune correlative studies demonstrate that the spectrum of infection and disease is more heterogenous than has been classically defined. Moreover, emerging translational and animal model data attribute a diverse immune repertoire to TB outcomes. Thus, protective and detrimental immune responses to *Mtb* likely encompass a framework that is broader than T helper type 1 (Th1) immunity. Antibodies, Fc receptor interactions and B cells are underexplored host responses to *Mtb*. Poised at the interface of initial bacterial host interactions and in granulomatous lesions, antibodies and Fc receptors expressed on macrophages, neutrophils, dendritic cells, natural killer cells, T and B cells have the potential to influence local and systemic adaptive immune responses. Broadening the paradigm of protective immunity will offer new paths to improve diagnostics and vaccines to reduce the morbidity and mortality of TB.

Keywords: antibody, Fc receptor, B cell, tuberculosis, Fc effector function, iBALT, antigen presentation, T cell

OPEN ACCESS

Edited by:
R. Keith Reeves,
Duke University, United States

Reviewed by:
Frank Verreck,
Biomedical Primate Research Centre (BPRC), Netherlands
Amanda Jezek Martinot,
Tufts University, United States

***Correspondence:**
Lenette L. Lu
lenette.lu@utsouthwestern.edu

Specialty section:
This article was submitted to Comparative Immunology, a section of the journal Frontiers in Immunology

Received: *07 December 2021*
Accepted: *07 February 2022*
Published: *17 March 2022*

Citation:
Carpenter SM and Lu LL (2022) Leveraging Antibody, B Cell and Fc Receptor Interactions to Understand Heterogeneous Immune Responses in Tuberculosis. Front. Immunol. 13:830482. doi: 10.3389/fimmu.2022.830482

THE CHALLENGE OF HETEROGENEITY IN CLINICAL TUBERCULOSIS

Every six seconds, an individual is diagnosed with tuberculosis (TB); every twenty seconds an individual dies from active disease (1). This level of morbidity and mortality persists today despite shorter antimicrobial treatment regimens and more sensitive, specific and widely distributed diagnostics. Strategies that prevent active disease are necessary to complement advances in detection and cure. However, defining the targets of prevention is challenged by the heterogeneity of manifestations and outcomes in clinical TB.

Improvements in microbiologic, immunologic and radiographic tools to identify and characterize humans infected with *Mycobacterium tuberculosis* (*Mtb*) have expanded the

phenotypic spectrum appreciated within and beyond the classical states of latent infection and active disease (**Figure 1**). Over 90% of human TB is thought to exist as latent infection. This state is defined by the presence of IFNγ secreting T cell response to *Mtb* antigens after exposure to the bacteria and the absence of signs and symptoms of active disease. The host response is historically captured by the tuberculin skin test (TST), a cell mediated response to intradermal injection of a mixture of *Mtb* proteins prepared from culture called purified protein derivative (PPD). To overcome false positive responses to non-tuberculous mycobacteria (NTM), including the vaccine strain, *Mycobacterium bovis* Bacille Calmette-Guérin (BCG), IFNγ release assays (IGRA) were developed as blood tests that measure responses to the *Mtb* proteins ESAT6, CFP10 and TB7.7. Yet despite enhanced specificity, the rates of false negatives have limited the use of these T cell-based tests in the diagnosis of the remaining 5-10% of TB which is active disease. Instead, active TB disease is defined by the presence of clinical signs and symptoms, radiographic evidence of disease and microbiological evidence of bacteria (detectable by culture, cell wall stain or nucleic acid amplification). Thus, only latent but not active TB is routinely diagnosed using markers of the host immune response. Specific patterns of human immune reactivity that are sterilizing have not yet been discovered but has significant implications for understanding protection from *Mtb* infection and disease (2).

Beyond latent and active TB, immunological and imaging modalities point towards states of infection after *Mtb* exposure that do not fall into the latent versus active TB dichotomy (**Figure 1**). Waxing and waning T cell and antibody responses to *Mtb* antigens in a subset of individuals with "latent TB" suggest the existence of states after *Mtb* exposure outside of the traditional definition but are also not active disease (3). Detection of *Mtb* RNA and DNA from individuals who meet the definitions of clinical and microbiological cure show bacterial persistence, highlighting the difficulty of conventional immune and microbiological assays to identify the presence of bacteria (4, 5). Finally, highly sensitive computed tomography (CT) and positron emission tomography (PET) imaging has demonstrated different lesions concomitantly regressing and progressing within the same individual, indicating immune response heterogeneity between granulomatous lesions that may underlie clinical outcomes (6–9). These findings advance our understanding of the spectrum of clinical TB, demanding similar innovation in models of disease to expand beyond the current T helper type 1 (Th1)-centric immunological paradigm to capture the diverse spectrum of *Mtb* infection and disease (10–12).

THE POTENTIAL OF ANTIBODIES AND B CELLS TO INFLUENCE TUBERCULOSIS

As a major arm of adaptive immunity, B cells and antibodies have the potential to modulate immune responses to *Mtb*. In contrast to the dominant roles uncovered in responses to viral and other bacterial infections, antibodies and B cells fill a minor part of the literature on the host response to *Mtb*. Yet even in this limited evaluation, there is data to suggest that humoral immunity is a complex and promising path towards understanding TB immunology.

Divergent interpretations of antibody and B cell data reflect limitations in contemporary experimental systems. Ablation of B cell (13) and antibody Fc effector functions (14) in mice and non-human primate models (15) impact local bacterial burden and pathology, and antibody Fc features correlate with different human disease states (16–18). Yet, passive transfer of antibodies into mice do not consistently confer protection (19), human deficiencies in immunoglobulins or B cells do not incur increased risk of TB (20, 21) and antibody titers alone are unable to define infection and disease (22). For animal studies, one of

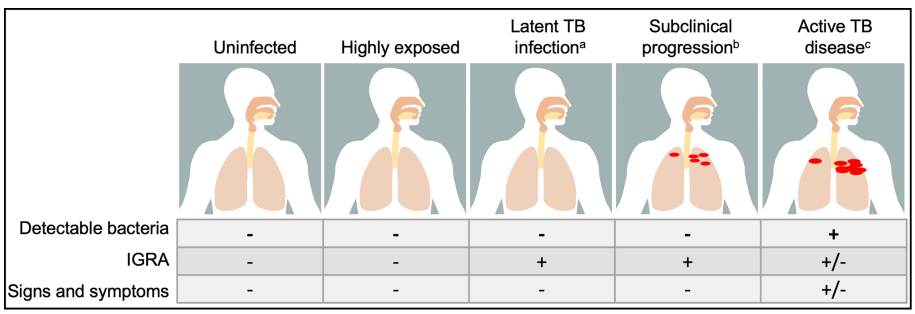

FIGURE 1 | The spectrum of outcomes in human tuberculosis (TB) is heterogenous. Classical clinical states are defines by the presence of detectable bacteria and host response to *Mycobacterium tuberculosis* antigens by interferon γ release assay (IGRA), with uninfected having neither, latent TB infection having a positive IGRA but no detectable bacteria and active TB disease diagnosed by the capture of *Mtb* by growth in culture, nucleic acid amplification or cell wall stain. The transition between these states is fluid and poorly captured by these criteria: a. Individuals who have received antibiotic therapy for latent TB infection cannot be differentiated from those who are treatment naïve. b. Individuals who progress subclinically from latent infection to active disease (5-10%) and those who regress or remain asymptomatic (>90%) are indistinguishable. c. After successful treatment with antibiotics for active TB disease, individuals no longer have detectable bacteria as captured by standard assays but may have residual positive IGRA. Moreover, emerging epidemiological and immune correlates data suggest that beyond these classical states, there are groups who are highly exposed to *Mtb* who potentially represent an alternative state to latent TB infection not yet clearly defined.

the inherent caveats is that models imprecisely phenocopy human *Mtb* infection and disease. For example, the wildly used inbred C57BL6 mouse model does not form the same granuloma pathology (23) and have different antibody and Fc receptor (FcR) repertoires compared to humans (24). For human studies, power is limited by access to relevant tissues containing *Mtb* and heterogenous clinical manifestations requiring years in duration for evaluation. For studies of humoral immunity, these difficulties are compounded by the persistence of residual antibodies and B cells despite pharmacologic depletion of plasma and B cells in humans (25, 26). As such, the potential of antibodies and B cells to influence the course of TB is inescapably stitched from studies that identify correlates of protection and disease in humans and evaluate mechanisms in model systems. Here, we extrapolate from the literature to understand the capacity of antibodies and B cells to: (1) modulate initial interactions between *Mtb* and host cells, (2) guide the development of adaptive immunity, and (3) contribute to protection and disease across the spectrum of clinical TB.

FUNCTIONAL DIVERSITY IN ANTIBODIES AND B CELLS

Antigen Binding Fraction (Fab) Domain

Computational analyses of high throughput sequencing data estimate that the human antibody repertoire has the capacity to bind to 10^{13} unique molecules *via* the antigen binding fragment Fab domain (27). Targeted molecules span proteins, glycans, lipids and nucleic acids from self and non-self, contributing to specific and broad recognition patterns. For *Mtb*, potential antigens recognized by antibodies emanate from the over 4000 open reading frames (28) as well as carbohydrates and lipids that comprise ~60% of the bacterial cell envelope (29). Because of molecular mimicry between microbial and human glyco- and lipo- conjugates, broadly reactive antibodies even at low affinity and avidity have the potential to influence *Mtb*-host interactions. As such, somatic recombination of V(D)J gene segments and hypermutation in the naïve variable gene region following antigen recognition generate diverse Fab domains with the potential to induce different antibody mediated immune responses and clinical outcomes. Yet efforts to develop antibody-based diagnostics demonstrate that titers poorly capture the spectrum of TB (22). Thus, the search continues for *Mtb* antigens that induce relevant immune correlates *via* new combinations of protein, carbohydrate and lipid targets such as lipoarabinomannan (LAM). Moreover, the inability of indirect measures of mycobacterial antigenic burden, such as that by the antibody Fab domain to capture the complexity of *Mtb* infection and disease, compel the pursuit of immune responses beyond direct target detection.

Crystallizable Fraction (Fc) Domain

Antibody function is determined by the combination of the Fab and crystallizable (Fc) domains. The Fc domain can alter the structure of the Fab domain, impacting antigen recognition. Equally as important as antigen binding, the Fc domain is essential to recruiting innate and adaptive humoral and cellular immune responses. Diversity in the Fc domain is generated through different isotypes (IgM, IgG, IgA, IgE, IgD) and subclasses (IgG1, IgG2, IgG3, IgG4, IgA1, IgA2) (**Figure 2A**). Studies of polyclonal responses show that all are produced in

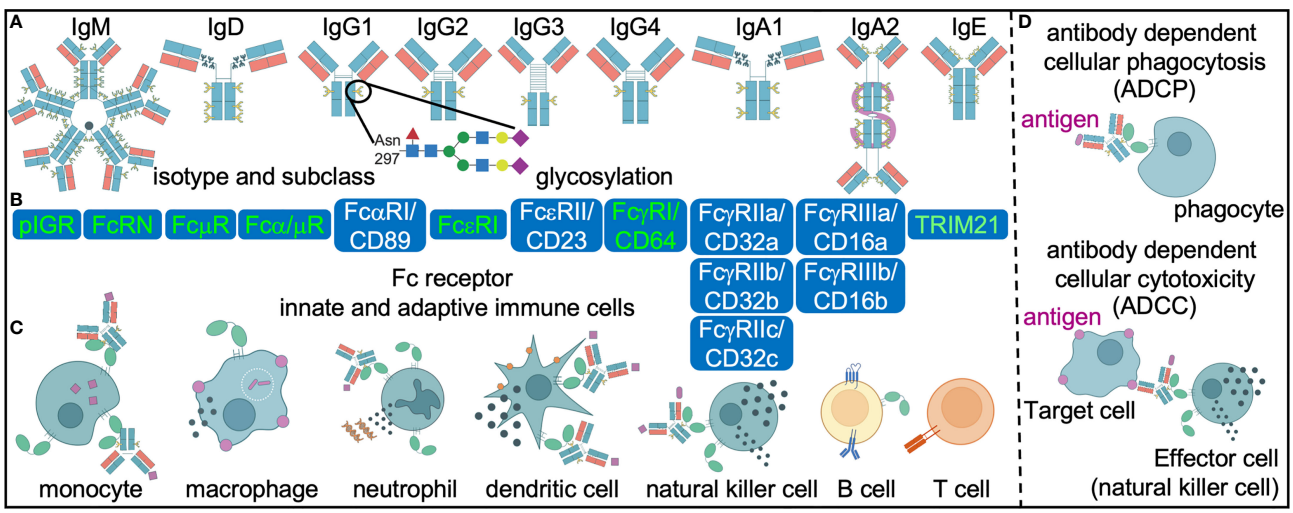

FIGURE 2 | Differential antibody engagement with Fc receptors mediate diverse innate and adaptive immune cell effector functions. Antibody diversity **(A)** in antigen specificity (theoretical n=10^{13}), isotype (n=5), subclass (n=6) and post-translational glycosylation (theoretical n=36 possible different moieties) influence engagement of Fc receptors. Subsequent differential activation of high (red) and low (white) affinity Fc receptors **(B)** expressed on innate and adaptive immune cells **(C)** have the potential to mediate effector functions such as antibody dependent cellular phagocytosis and cytotoxicity **(D)** that in concert determine the heterogenous outcomes in human TB.

response to *Mtb* infection with no one dominating correlate of disease or protection, although there are hints in some cohorts that decreased IgG3 is associated with recurrence (30) and increased IgG4 with active disease (18). Some monoclonal studies have suggested potential differential capacities between IgA, IgG and IgM to induce extra and intracellular host environments that restrict or enhance *Mtb* (31, 32). If these findings are confirmed by studies in polyclonal responses that influence clinical outcomes, the mechanisms likely involve differential immune complexing. With monomeric and multimeric antibodies, the affinity and avidity for microbial antigens in the Fab domain and host receptors and complement in the Fc domain can vary widely.

Antibody Post Translational Glycosylation

All antibodies are glycoproteins. These post translational modifications are made by glycosyltransferases and glycosidases during trafficking through the endoplasmic reticulum and Golgi apparatus of B cells. Some data suggest that further modification is possible in a B cell independent manner through glycosyltransferases secreted into the circulatory system (33–36). While all polyclonal IgG have a conserved asparagine residue 297 on the Fc domain that is glycosylated, only 15-20% are modified on the Fab domain (37). These N-linked glycan structures have a complex bi-antennary core composed of N acetylglucosamine and mannose residues (**Figure 2A**). The further addition and subtraction of N-acetylglucosamine, galactose, sialic acid and fucose extend the structural and functional heterogeneity of the Fc and Fab domains by altering affinity for FcRs and target antigens. O-linked glycosylation of proteins occurs on functional hydroxyl groups of serine and threonine, but site-specific analyses of O-glycans is challenged by the paucity of efficient proteolytic tools. Nevertheless the plethora of data on N-glycans within IgG show distinct and sometimes plastic glycosylation patterns in many physiological states: male versus female, age, pregnancy, infections such as those with HIV and SARS-CoV2, chronic non-infectious diseases such as diabetes and renal disease, autoimmune diseases and exacerbations (38). In some cases such as diabetes, passive transfer of antibodies into mice of differentially glycosylated IgG and the *in vivo* modification of glycosylation show that altered sialic acid is not merely associative but also contributes to non-immune processes such as glucose intolerance through FcR mediated insulin transport (39, 40).

For latent and active TB, the N-glycan profiles on IgG diverge and vary with antigen specificity (16–18, 41). However, some themes that emerge are that glycans associated with an anti-inflammatory state (galactose and sialic acid) are increased in individuals with latent compared to active TB (16). This is consistent with an overall decreased immune mediated inflammation in latent compared to active TB. In contrast, fucose is decreased in latent compared to active TB. The lack of fucose is generally associated with increased inflammation (42, 43). That afucosylated IgG is enhanced in latent TB indicates that this change is not a biomarker of inflammation but rather potentially reflective of an antibody function. Because studies using polyclonal and monoclonal antibodies show that changes in glycosylation influence FcR affinity and cellular effector functions such as antibody dependent cellular phagocytosis (ADCP) and cytotoxicity, differential modulation of immune responses are implicated for latent and active TB. Afucosylated IgG have increased affinity for FcγRIII/CD16 which mediates antibody dependent cellular cytotoxicity (ADCC). Both are enhanced with IgG purified from latent compared to active TB patients, implicating roles in potential protection for TB (16). If and how antibody glycosylation contributes to immune mediated outcomes in the context of HIV, diabetes and renal disease, the most significant risk factors for TB, remain uncharacterized (44). As biomarkers, direct comparison between *Mtb* reactive-IgG glycans and titers in a small cohort of individuals show that the former has enhanced ability to distinguish between latent and active TB (17). This is likely due to the ability of IgG glycans to capture the complexity of host immune responses that connect to pathology as compared to microbial burden alone by using antibody titers. As mediators of protection, one study showed that passive transfer of non-*Mtb* specific polyclonal human IgG into mice after enzymatic removal of glycans increases bacterial burden (45). Whether this applies to *Mtb* specific IgG and what species of glycans specifically are responsible are not known but could shed light into how differential IgG glycosylation is linked to pathology and protection.

IgA and IgM are also glycosylated, but because far more residues are involved, the deconvolution of these complex post translational modifications lags behind IgG. However, emerging data from the mouse model shows changes in IgM glycans with *Mtb* infection (46). With further definition, these post translational mechanisms of antibody diversification that contribute to the extent of the B cell antibody repertoire can be clarified across the clinical spectrum within and beyond the latent and active TB spectrum.

Neutralizing and Non-Neutralizing Antibody Functions

For infectious diseases, directly neutralizing and non-neutralizing antibody functions potentially impact microbial infection, replication and immune mediated pathology. Through the Fab domain, antibodies recognize and bind to microbial antigens. This could lead to direct neutralizing activity in which the organism is immediately sequestered after binding. In comparison, non-neutralizing antibody functions involve the Fc domain function to a greater extent. In conjunction with targeting an antigen *via* the Fab domain, the Fc domain engages complement and FcRs on immune cells that induce host responses to the microbe. Non-neutralizing antibody functions include cellular phagocytosis, cytotoxicity, activation (including NETosis and antigen presentation) and cytokine production, each of which could be protective or pathogenic based on the specific context of the microbe and host. Demonstration of consistent antibody-mediated direct neutralization of *Mtb* leading to prevention of infection has been elusive to date with monoclonal antibodies. While *in vitro* studies show different non-neutralizing cell mediated functions with polyclonal IgG isolated from individuals with latent TB, active TB (16), after antibiotic treatment (18), after BCG vaccination (32, 47, 48) and/or high exposure to *Mtb* (41, 49), it is less clear whether they are protective, inert or pathogenic *in vivo*.

Fc Receptors (FcR)

Beyond the antibody glycoprotein, FcR variations in copy number and single nucleotide polymorphisms (SNPs) generate diversity. These exist for receptors that have high (FcγRI/CD64, FcRN encoded by FCGRT, FcεRI), intermediate (polymeric immunoglobulin receptor pIGR and Fα/μ receptor) and low affinity (FcγRII/CD32, FcγRIII/CD16, FcαRI/CD89, FcεRII/CD23) for monomeric immunoglobulins (**Figure 2B**). High variation in copy number has been observed particularly in the *FCGR* loci. For FcγRII/CD32a, the polymorphism R131H (also described as 167) affects the membrane proximal Ig-like domain of the extracellular region and ablates the ability to bind and phagocytose IgG2 coated particles (50, 51). The R/R131 allotype is associated with more severe outcomes in disseminated meningococcal infection (52) and recurrent bacterial infections (53) in some human populations suggest that these FcR changes could have implications across multiple infectious diseases as well as vaccines. For FcγRIII/CD16a, valine at amino acid 158 (also described as 176) increases the affinity for IgG1 and IgG3 *via* interactions with the lower hinge region whereas phenylalanine in this same position enhances IgG4 binding (54, 55). The functional implications of this variation are most well-described with ADCC, where individuals with 158V/V compared to 158F/F have higher levels of this classic natural killer cell mediated function. Some human studies link these allelic variants to autoimmune diseases (56) and responses to monoclonal antibody therapies in cancer (57), though the extrapolated mechanisms and impacts may be obscured by the complexity of these conditions. For the only inhibitory FcR, a loss of function variant FcγRIIBT232 is associated with protection against severe malaria in an East African population and susceptibility to the autoimmune disease systemic lupus erythematosus in the Caucasian population (58). These functional impacts are conceptualized in the context of non-neutralizing antibody activity. However, studies in mice show that Fc-FcR binding is critical in enhancing monoclonal antibody mediated direct neutralization of pathogens including HIV (59, 60), influenza (61, 62) and SARS-CoV2 (63–66). Thus, FcR variations have the potential to influence directly neutralizing and non-neutralizing antibody functions.

For TB, studies focused on *FCGR* genetic variations show a mixed association with outcomes. Increased *FCGR1A/CD64* copy number in individuals with active disease indicates an association with poorer outcomes (67). Because the high affinity FcγRI/CD64 is also identified in the non-human primate model as a correlate of disease it could be simply a marker of general inflammation, or induce pathology (68). Beyond FcγRI/CD64, higher *FCGR3B* copy number in a subpopulation of Ethiopians is associated with the development of TB in people living with HIV, compared to those with HIV alone (69). The data from these two studies suggest that *FCGR* sequence heterogeneity is involved with inflammation in TB. Studies incorporating a larger clinical spectrum from high *Mtb* exposure to outcomes of antimicrobial treatment and recurrence could further clarify how *FCR* genetic variability impacts *Mtb* infection and disease.

In addition to pathology, data from both mouse models and human studies show that FcRs have the capacity to impart effects that protect the host against bacteria. Knockout of the immunoreceptor tyrosine-based activation motif (ITAM) responsible for activating signaling across FcRs in a low dose aerosol C57BL6 mouse model of *Mtb* infection leads to increased pulmonary *Mtb* burden and pathology along with decreased survival (14). Consistent with these findings, mouse knockout of the only the inhibitory FcγRIIb/CD32b leads to decreased pulmonary *Mtb* burden and pathology (14). Because FcγRIIb/CD32b is the only FcR functionally conserved between mice and humans, these findings could have relevance for translating findings. While *in vitro* blocking antibody studies show that *Mtb*-reactive IgG mediated opsonophagocytosis into human monocytes is FcγRII/CD32 dependent, the blocking antibody clone itself does not distinguish between the activating CD32a or inhibitory CD32b in these cells (47). Overcoming this limitation with FcγRIIb/CD32b specific tools could help clarify each respective role (70, 71). Apart from FcγRII/CD32, levels of the activating FcγRIII/CD16 correlate with latent compared to active TB across multiple cohorts (72). In addition, IgG purified from individuals with latent compared to active TB have higher affinity for FcγRIII/CD16 (16). However, the benefit of the activating FcγRIII/CD16 is likely cell type specific as CD16+ monocytes as opposed to macrophages and natural killer cells may be associated with disease severity (73). Finally, data from *in vitro* whole blood assays with blocking antibodies suggest that decreased bacterial replication mediated by polyclonal IgG from health care workers highly exposed to *Mtb* is in part due to FcγRIII/CD16 together with FcγRII/CD32 (49). Thus, the combinatorial engagement of low affinity inhibitory and activating FcRs (74) by differential immune complexes containing distinct antibody Fc determines signaling (75) contributes to immune response variability that could influence host outcomes.

Antibody Mediated Cellular Effector Functions

Antigen bound antibodies induce cell surface FcR aggregation and downstream signaling to induce effector functions (76) (**Figure 2C**). Antibody dependent cellular cytotoxicity (ADCC) is classically mediated by natural killer cells and macrophages that express FcγRIII/CD16 (**Figure 2D**). Granules containing perforin and granzyme from activated natural killer effector cells as measured by CD107a and IFNγ are released to mediate cytolysis of target cells with antigens present on the surface and recognized by the antibody. Following binding of IgG immune complexes to platelets, the release of serotonin stored in the granules is thought to contribute to systemic shock (77, 78). For FcεR, aggregation can lead to activation of mast cells, eosinophils and basophils with secretion of vasoactive amines and enzymes to generate allergic responses. Thus, the effect of granule release is dependent on the contents.

In addition to FcR aggregation, internalization of the antigen *via* antibody dependent cellular phagocytosis (ADCP) is an Fc effector function that can occur in neutrophils, monocytes, macrophages and dendritic cells (**Figure 2D**). Neutrophils express FcRs that engage IgG and IgA with phagocytosis (79), production of reactive oxygen species (80) and neutrophil extracellular traps (NETs) (81, 82) as potential consequences. Monocytes and macrophages can

respond to IgG, IgA and, sometimes, IgE mediated antigen uptake (62) with autophagy (83) and vesicular trafficking into the lysosome (84) as well as inflammasome activation (85, 86). In contrast, ADCP in dendritic cells induces antigen presentation, cytokine production and maturation (70, 87–89). Thus, FcR crosslinking induce multiple effector immune functions that are cell type specific.

In TB, antibody cellular effector functions have been described to potentially impact bacteria during initial acquisition of infection and in latent and active TB. *In vitro Mtb* infection studies show that opsonophagocytosis is influenced by antibodies from BCG vaccination (32, 48, 90). Because extracellular *Mtb* is thought to exist primarily during initial acquisition of infection and active TB, divergent cellular effector functions resulting from ADCP could be more relevant in these states. Differential macrophage phagolysosomal co-localization and inflammasome activation with intracellular bacteria are reported with polyclonal IgG from latent and active TB (16). Because intracellular *Mtb* is associated with latent infection, cellular effector functions that target an infected host cell as opposed to bacteria alone could be relevant. This could be ADCC but more broadly speaking, any effector cell function that could impact an infected target cell (for example granule or cytokine release, vesicular trafficking, the production of reactive oxygen species) in *cis* or *trans* is plausible. To this point, the discovery of new receptors that bind to antibodies such as the cytoplasmic TRIM21 brings opportunities to expand the repertoire of linked cellular effector functions such as ubiquitination and degradation of intracellular organisms (91). How cytoplasmic receptors, as opposed to cell surface expressing receptors, mediate responses to intracellular *Mtb* is not known but broadens the potential mechanisms by which antibodies modulate the immune response in TB.

B Cell Functions

T cell-B cell interactions in lymphoid follicles lead to the development of long-lived, antigen-specific humoral responses from plasma cells and plasmablasts (92) (**Figure 3A**). Expression of the CXCR5 chemokine receptor helps define the structure of B cell follicles by facilitating CD4 T cell trafficking to germinal centers. In secondary lymphoid organs such as lymph nodes and tertiary lymphoid structures in the *Mtb*-infected lung, CD4+ CXCR5+ T cells are thought to mediate host protective responses (93, 94). CCR7 regulates the trafficking of B cells toward the T cell zone, where they present endocytosed antigen in the form of peptide fragments loaded onto major histocompatibility complex type II (MHC-II) molecules to CD4 T cells (95). In addition, naïve and central memory CD4 T cells express CCR7, enabling circulation through lymphoid organs and interactions with antigen presenting cells (APCs). CCR7 knockout mice have a decreased ability to control *Mtb* growth after high but not low dose aerosol infection

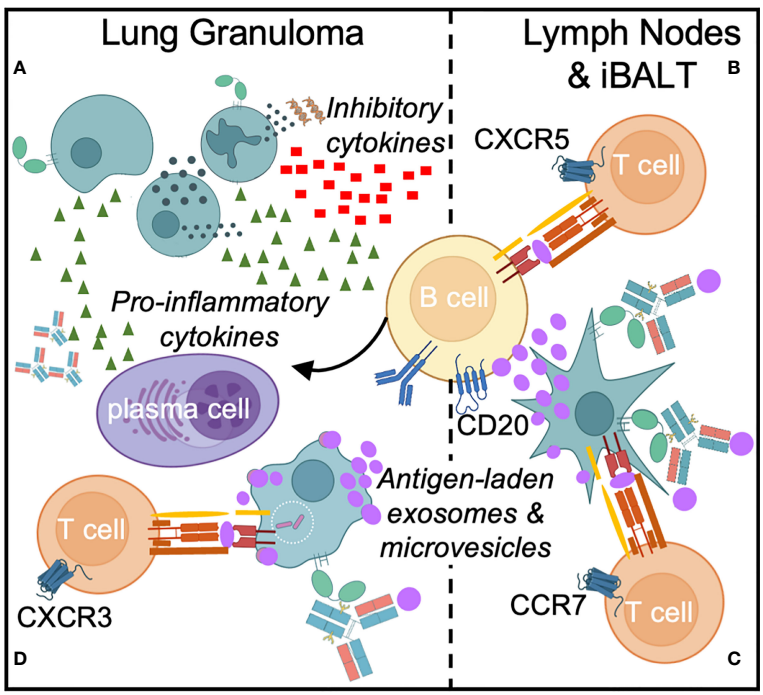

FIGURE 3 | Direct and indirect B cell responses occur in *Mtb* infection. Direct responses include cytokine production and differentiation of B cells specific into plasma cells that secrete *Mtb*-specific antibodies **(A)**. In response to *Mtb* infection in the lung, B cell effectors such as memory B cells, plasmablasts and plasma cells secrete pro-inflammatory cytokines (TNFα, IFNγ, IL2, IL6, GM-CSF and CCL3), while a subset of B cells can secrete inhibitory cytokines, such as IL10, which limits Th17 cell and neutrophil infiltration. In secondary and tertiary lymphoid organs such as lymph nodes and inducible bronchus-associated lymphoid tissue (iBALT), B cells facilitate antigen presentation to T cells **(B, C)**. B cells receive T cell help from Tfh cells to initiate germinal center responses **(B)** and might also participate in priming T cells through the transfer of *Mtb* antigens (purple) to dendritic cells via exosomes and extracellular microvesicles **(C)**. Finally, Fc-FcR interactions can enhance *Mtb* phagocytosis, macrophage and dendritic cell effecror functions, and antigen presentation to T cells in the lung granuloma **(D)**.

(51, 96). The T cell response is delayed in these knockout mice but whether this is due to a decreased CCR7 mediated B cell trafficking and maturation is less clear. Thus, the co-localization of T cells and B cells in secondary and tertiary lymphoid structures are opportunities for reciprocal interaction and synergy that could influence outcomes in TB (**Figures 3B, C**).

The presence of B cells and follicular structures in granulomas and inducible broncho-alveolar associated lymphoid tissue (iBALT) is described in humans, mouse and non-human primate models of TB. These pulmonary lesions are associated with protection against active disease in the non-human primate model (15, 93, 97–99). Furthermore, the identification of *Mtb*-specific antibody responses and their association with protection in latent infection and in other heavily exposed individuals indicate a protective role for B cells in TB (16, 41, 49), potentially through the activation of *Mtb*-specific T cell responses and regulation of inflammation (13).

While dendritic cells classically act as APCs to activate T cells in lymphoid organs, early experiments identified a role for B cells in the priming of antigen-specific CD4 T cell responses to vaccine antigens in mice (100). B cell depletion prior to vaccination ablates subsequent T cell proliferation upon *ex vivo* exposure to APCs and antigen. Interestingly, subcutaneous B cell supplementation proximal to draining lymph nodes at the time of vaccination rescues this muted T cell expansion. Moreover, B cells produce cytokines that regulate T cell responses during infection and persist as antigen-specific memory cells after the resolution of inflammation (101). While patients with active TB have dysfunctional circulating B cells (102–104), the implications for effector functions beyond antibody production and how they impact local (13, 15, 97) and systemic responses remains to be clarified. Because B cell depletion by anti-CD20 antibodies alters T cell activation, cytokine production and *Mtb* burden in pulmonary lesions (15), evaluation at the lesional level may afford the best appreciation of the diverse spectrum of B cell functions.

B cells were only recently observed to act as natural APCs for T cells, promoting their activation and proliferation when B cells were exposed to T follicular helper (Tfh) cell CD40L and IL4 signaling in contrast to IL21 signaling (105, 106). Colocalization at the T cell-B cell border of lymph nodes or within B cell follicles represent opportunities for B cell antigen presentation to T cells, facilitating T helper functions, B cell activation and clonal expansion. Furthermore, the distinct presence of B cell follicles and germinal centers in the lung as a feature of both granulomas and the adjacent iBALT raises the possibility of roles for B cells in local antigen presentation to T cells, either directly or *via* exosomes and microvesicles (107) (**Figures 3C, D**). CD40-activated B cells have been shown to prime at least transient effector CD8 T cell responses to intracellular bacteria such as *Listeria monocytogenes* (108). Dissecting the impact of B cell mediated antigen presentation for the intracellular *Mtb* could provide a path towards recognizing alternative mechanisms of T cell activation.

B cells and plasma cells produce pro-inflammatory cytokines (IFNγ, TNFα, IL2, IL6, CCL3, GM-CSF) that are balanced by the ability of certain subsets to produce anti-inflammatory IL10 and IL17 to regulate T cell responses (109). Exploitation of IL10 associated inhibitory properties by intracellular pathogens have been described with *Salmonella typhimurium* (110) and *Listeria* (111). In mouse models of these infections, stimulation of TLR2 and TLR4 induces IL10 production from B cells which, when inhibited, improves host control of bacterial burden. In non-human primate models of TB, IL10 is thought to regulate local immune responses to *Mtb* in lung granulomas where both T and B cells traffick (112). Thus, it is plausible that like *Salmonella* and *Listeria*, TLR2 signaling induced by *Mtb* (113) could modulate IL10 levels through B cells as well as macrophages to locally influence outcomes in TB lesions (114). Similarly, Th17 responses not only modulate B cell function by inducing class switching but B cells, particularly the regulatory subset, can in turn suppress Th17 responses (115, 116). In patients with more severe cavitary TB disease, CD19+ CD1d+ CD5+ B regulatory cells are increased, dampening IL17 (117, 118). Thus, IL10 and IL17 are additional conduits through which B cells can regulate T cell responses and subsequent protection as well as pathology.

AT THE INTERFACE OF INNATE HOST *Mtb* INTERACTIONS

Antibodies in the Respiratory Tract

Because antibodies are detected at the alveolar epithelia, the site of initial *Mtb* exposure in aerosol transmission, they are well-positioned to mediate the initial interactions with bacteria. In healthy humans, bronchial sampling by lavage demonstrates that IgG is present in the respiratory tract at levels equivalent to peripheral serum (119). During infection by the SARS-CoV2 virus, IgG levels increase even beyond those of IgA (120). In the widely used C57BL6 mouse model, IgG, IgA, and IgM are detected in the uninfected lung parenchyma with IgG2b levels in bronchoalveolar lavage (BAL) fluid higher than those of IgA (121). Thus, multiple isotypes and subclasses are likely present in the respiratory tract for these early events.

Cross Reactive and Specific Antibodies That Recognize *Mtb*

The repertoire of *Mtb* antigens recognized by antibodies in the respiratory tract, as well as systemically, remains a critical gap in knowledge. However, BCG vaccination (32, 47, 48, 122) and exposure to environmentally prevalent non-tuberculous mycobacteria likely introduce at minimum cell wall antigens that elicit antibodies cross-reactive to *Mtb* (32, 123, 124). As in the gut, symbiotic microbiota from the pulmonary compartment could induce systemic IgG responses that induce protection against pathogens (125). These antibodies arising from non-self antigens complement those from self. Natural IgM and IgG have the ability to engage with carbohydrate and lipid *Mtb* targets to influence initial host-microbial interactions and subsequent infectious challenge (126). As the products of B-1 cells (127) that arise during immune development independent

of exogenous antigens and T cells, natural IgM targeting self-antigens such as phosphorylcholine modulate autoimmunity and responses to virus *via* antibody mediated induction of complement (128) and efferocytosis of apoptotic cells (129, 130). In murine influenza studies, passive transfer of IgM from uninfected mice into those deficient in B-1 B cells or are unable to secrete IgM enhance survival and microbial specific IgG levels, suggestive of a role in modulating the development of the adaptive immune response in secondary lymphoid organs (131, 132). Beyond IgM, data from mouse studies suggest that natural IgG can aid in FcR mediated phagocytosis of ficolin coated gram negative and positive bacteria to impact susceptibility to infection (133, 134). Whether by specific and or cross-reactive antigen recognition, these studies suggest that localized and systemic antibodies are poised to recognize *Mtb* and mediate initial interactions within even an uninfected, naïve host.

In individuals who have developed an adaptive immune response to *Mtb* infection, the over 4000 open reading frames and the plethora of cell membrane and wall lipids and glycolipids provide a spectrum of *Mtb* targets to which antibodies can direct immune responses (28, 29). Because replicative and non-replicative *Mtb* states vary in relative abundance of these microbial antigens (135, 136), different specificities may be relevant for antibody functions in latent TB, active TB and with prior antimicrobial treatment. T cell responses to genes encoded by the dormancy regulon of *Mtb* are enhanced in latent infection (137) but the impact from the antibody standpoint is not known. Moreover, different clinical strains could mean that the Fab domain repertoire vary by geographical region (138). It is presumed that the majority of *Mtb* targets are expressed by live bacteria and infected host cells including epithelial cells (139) as well as macrophages (140). However, exosomes in the blood and granuloma also contain *Mtb* antigens that can activate immune cells *in vitro* and *in vivo* (141, 142). Thus, antigen specific antibody effector functions can be induced even in the absence of live *Mtb*.

FcRs in the Respiratory Epithelia

With aerosol transmission, the first encounter between *Mtb* and host likely occur with non-immune cells in the respiratory tract. At this earliest stage, the conditions that determine if the bacteria infect and cause disease are not known. Antibody Fc domain engagement of receptors aid in translocation across the lumen and induce non-immune cells to secrete local cytokines, activating resident immune cells such as alveolar macrophages. Thus, FcR on epithelial airway cells could be the first to encounter antibody-complexed *Mtb* to enable bacterial movement and initiate host responses. The two most abundant FcR in the respiratory tract are the neonatal FcR (FcRN) and polymeric immunoglobulin receptor (pIGR) though other FcRs that bind IgG, IgA and IgE are also expressed.

In the respiratory tract, FcRN facilitates transport of IgG across the mucosal surface (143). Its high affinity nature permits binding to monomeric IgG to guide through the endocytic excretion pathway and extend serum half-life by preventing lysosomal degradation. After low dose aerosol *Mtb* challenge, pulmonary bacterial burden is lower in FcRN knockout compared to wildtype mice at early but not late timepoints. However, there is an absence of differences in initial inoculum (121) and dissemination into the spleen and liver. These findings indicate that though uptake may be similar *via* non-*Mtb* specific antibodies, subsequent host responses and bacterial outcomes are transiently affected (121). Monoclonal *Mtb* specific IgG but not IgA increases opsinophagocytosis in FcRN expressing A549 human lung epithelial cell line (31). Thus, *in vivo* and *in vitro* data suggest that *Mtb* reactive IgG from prior mycobacterial exposure enhances early infection transiently *via* FcRN at the epithelium. The implications for outcomes in chronic disease and in the presence of *Mtb* reactive antibodies induced by BCG vaccination, prior *Mtb* or NTM infection are less clear but likely involve immune as well as epithelial cells.

Similar to FcRN, the polymeric immunoglobulin receptor (pIGR) is widely expressed in the respiratory tract. Unlike FcRN which focuses on IgG, pIGR supports the transport of dimeric IgA and, to a lesser extent, IgM from the interior basolateral surface of the epithelium to the exterior apical side. Interestingly, IgA levels are decreased in saliva but not bronchoalveolar lavage in a total mouse pIGR knockout (144). In these mice, there is an early and unsustained increase in pulmonary bacterial burden and decrease in IFNγ and TNFα after low dose aerosol infection with virulent *Mtb* strain H37Rv. These data suggest that the effects of non-specific IgA transported to upper respiratory tract by pIGR can be transiently protective in early infection.

Direct neutralization by *Mtb* specific compared to non-specific IgA in the mucosa that blocks bacterial uptake could mediate a more significant and durable effect. Monoclonal antibodies targeting the mycobacterial glycosylated lipoprotein phosphate transporter subunit PstS1 demonstrate this potential in human lung epithelial cells *in vitro* (31). Polyclonal antibodies induced after intranasal vaccination with PstS1 shows that *in vivo* protection in a high dose intranasal BCG challenge model can be generated in a pIGR dependent manner (31). That FcαR/CD89, the primary human IgA FcR, is not detected on human epithelial cells or expressed in mice points towards direct neutralization as one likely mechanism. However, other receptors for IgA including Fcα/μ receptors (145), asialoglycoprotein receptors (146), transferrin receptors (147) and M cell receptors (145, 148) have been reported to be able to bind to the IgA Fc domain. These receptors provide unexplored FcαR/CD89 independent mechanisms of non-neutralization by which *Mtb* specific IgA that could inhibit bacteria in the respiratory tract.

While the type I FcγRs are commonly described in cells of hematopoietic lineage, which consequently have been the focus of most functional studies, some data suggest that these FcRs can be found in non-immune cells, permitting IgG to induce non-neutralizing functions. The low affinity FcγRIII/CD16 is expressed in primary nasal epithelial cells and *in vitro* blocking antibody studies demonstrate a role in mediating IgG opsonized bacterial cytokine induction (149). The low affinity inhibitory FcγRIIb/CD32b but not the IgE receptor FcεRIII/CD23 is present in primary human airway smooth muscle cells (150). Understanding non-neutralizing Fc effector functions mediated

by non-immune cells in the airway lumen to *Mtb* could provide insight into the factors that determine whether colonization or deeper infection occurs.

FcRs Mediating Macrophage Environments That Permit and Restrict *Mtb* Growth

Macrophages represent a quintessential niche for *Mtb* where bacteria grow and die. In the high dose aerosol murine infection model, tissue resident, long-lived alveolar macrophages act as initial host cell targets for *Mtb* (151) and contribute to the development of immune conditions that permit *Mtb* replication and dissemination (151, 152). Bone marrow derived monocytes and macrophages are subsequently recruited to join their embryonic tissue resident counterparts. Further infection of these populations show heterogeneity between and within the groups. Initial studies suggested an M1 and M2 paradigm to describe macrophage restrictiveness and permissiveness to *Mtb* (153). However, more recent data from single cell mouse and human macrophage transcriptomics suggest that the determinants of bacterial outcomes are far more complex (154, 155). Whether or not FcR mediated signaling contribute to the heterogeneity of macrophage responses to *Mtb* is not known, but the combinatorial diversity from engagement of the multiple low and high affinity receptors expressed in this immune cell provides this potential.

Macrophages express a plethora of FcRs that enable responsiveness to antibodies found in the blood and tissue, including *Mtb* lesions such as granulomas (156). High affinity FcγRI/CD64 and FcRN allow monomeric IgG to influence macrophage phenotypes. The low affinity activating FcγRIIIa/CD16a and FcγRIIa/CD32a permit further tuning with IgG immune complexes, counterbalanced by the only inhibitory receptor FcγRIIb/CD32b. In being the only immune cell other than natural killer cells that expresses a significant level of FcγRIIIa/CD16a which classically mediates ADCC, macrophages have the potential to be both effector and target cells. In being like all other immune cells where the cytosolic FcR TRIM21 is expressed, antibodies may also enable the macrophage to target intracellular *Mtb*. For tissue macrophages including alveolar macrophages the activating low affinity FcγRIIIa/CD16 and high affinity FcγRI/CD64 are particularly highly expressed when compared to blood monocyte derived macrophages (157, 158). Examining the link between FcRs and cell population specific responses to *Mtb* could clarify how macrophages permit and restrict bacterial replication.

Classic experiments show that extracellular *Mtb* uptake mediated by live BCG immunized rabbit serum into mouse peritoneal macrophages direct bacteria into phagosomes, though the outcomes for the bacteria and host vary (159). Trafficking of *Mtb* into the phagolysomal and autophagosomal compartments, induction of pro- and anti- inflammatory cytokines and likely multiple other cellular effector functions collaboratively determine intracellular bacterial fate. Much of the literature has focused on opsonophagocytosis. Thus, classical FcRs at the cell surface involved in ADCP including FcγRI/CD64, FcγRII/CD32 and, to a significantly lesser extent, FcγRIII/CD16a (47) play roles in uptake of extracellular *Mtb* into monocytes and likely macrophages. For the intracellular bacteria *Legionella* (160), the initial steps of FcR mediated entry into the macrophage govern intracellular fate, but for *Mtb* this remains unknown.

As important as extracellular *Mtb*, *in vitro* data suggest that antibodies can also impact intracellular bacteria, the predominant state in infection. Addition of polyclonal IgG from latent compared to active TB patients to macrophages already infected with *Mtb* induce lower intracellular burden (16). That these antibodies have higher affinity for FcγRIIIa/CD16a and induce higher ADCC *in vitro* with natural killer cells that express FcγRIIIa/CD16a suggests that a similar mechanism could be occurring with *Mtb* infected macrophages as target and effector cells. An alternative and complementary mechanism could be *via* the cytosolic E3 ubiquitin ligase TRIM21. This FcR is able to ubiquitinate antibody bound intracellular viruses and bacteria such as *Salmonella* for degradation (91), though for *Mtb* this is not yet known. Thus, antibodies through surface and cytoplasmic FcRs can impact intracellular *Mtb* directly or indirectly to restrict growth.

Whether antibodies induce macrophages to restrict or permit *Mtb* infection and replication likely results from the sum of engaging multiple high and low affinity activating and inhibitory FcRs, which could differ for extracellular and intracellular bacteria. Additional immune cell signaling pathways could also contribute. For example, *Mtb* components interact with Toll like receptors (TLR) (161) to induce innate macrophage responses. Cross talk between TLR and FcR signals on macrophages have been described (162). Understanding the interactions of these pathways for *Mtb* could highlight macrophage diversity in the context of bacteria, antibodies and pathogen associated molecular patterns (PAMPs) that exist in concert throughout infection and disease.

FcR Mediated Neutrophil Inflammation in TB

Like in macrophages, much of the literature on neutrophils in TB have focused on inflammation in active TB (3, 163). Correlations between blood transcriptional signatures with disease suggest that neutrophils mediate or reflect pathogenic inflammation. While expression levels of the high affinity FcγRI/CD64 is consistent with this, additional low affinity receptors capable of binding to IgG and IgA provide the potential for antibody mediated protective effector functions *via* the peripheral blood and granuloma where neutrophils surround *Mtb* infected macrophages.

Neutrophils have a partially overlapping FcR repertoire with macrophages. Like macrophages, the low affinity activating FcγRIIa/CD32a, and inhibitory FcγRIIIb/CD32b, as well as high affinity FcRN and TRIM21 are constitutively expressed. Unlike macrophages, high FcαR/CD89 expression characterizes these granulocytes, permitting responses to IgA. The monomeric isoform FcγRIIIb/CD16b is constitutively expressed instead of the heterooligomeric FcγRIIIa/CD16a. FcγRI/CD64 expression is not constitutive but rather induced by IFNγ (164). Thus, baseline and induced FcR permit a spectrum of neutrophil phenotypes in *Mtb* infection.

Transcriptomics data show that FcγRI/CD64 expression and neutrophil activation are correlates of TB disease progression across multiple human cohorts (3, 165) and mouse and non-

human primate models (68). However, despite bearing the same names, murine and human CD64 differ in their binding abilities and expression patterns such that they are not functional homologues. Knockout in mice leads to a transient decrease in pulmonary *Mtb* at 60 days along with decreased neutrophil but not macrophage recruitment to the lungs, suggesting that FcγRI/CD64 enhances disease (68). Though there are limitations to extrapolating these mouse data to humans, increased *FCGR1/CD64* copy number in individuals with active disease shows association with poorer outcomes (67). Neutrophil FcγRI/CD64 expression is a biomarker for sepsis in children and adults with bacterial infections (166). As such, FcγRI/CD64 is likely similarly a correlate of inflammation for TB.

In contrast, the expression of FcγRIIa/CD32a and FcγRIIIb/CD16b on neutrophils suggests the potential existence of an IgG mediated protective function. While ADCC is typically described as a natural killer cell FcγRIIIa/CD16a function, neutrophils can also be effector cells with FcγRIIa/CD32a being the activating receptor, negatively regulated by FcγRIIIb/CD16b as shown in tumor models (167). In TB, higher *FCGR3B* copy number in a subpopulation of Ethiopians is associated with HIV-TB compared to HIV alone (69), suggesting that decreased neutrophil ADCC could be associated with more severe disease in dually infected individuals.

Beyond IgG, studies using human FcαR CD89 transgenic mice point towards the potential for IgA mediated FcR functions to impact *Mtb*. Opsonization of H37Rv with human monoclonal IgA targeting the alpha crystallin *Mtb* protein HspX prior to high dose intranasal challenge of these mice leads to decreased pulmonary bacterial burden early after infection compared to non-transgenic littermates. Thus, beyond direct binding, IgA Fc mediated non-neutralizing functions through FcαR/CD89 can impact events that affect the development of adaptive immunity (168). Whether protection occurs *via* neutrophils, monocytes/macrophages or other immune cells, the durability of such protection and how much can be translated into humans remain to be clarified (169). Intriguingly, IgA monoclonals can also induce neutrophil-mediated ADCC (170), providing a plausible mechanism by which antibodies can inhibit *Mtb*. In contrast, there is evidence that both IgA and IgG can induce neutrophil and monocyte mediated trogocytosis (171, 172), a phagocyte nibbling process which can contribute to the spread of intracellular organisms such as *Francisella tularensis* and *Salmonella* from infected to uninfected cells (173). Thus, some antibody induced neutrophil functions could contribute to *Mtb* pathogenesis. Indeed, NETosis is initiated by many receptors, amongst which FcγR (174, 175) and FcαR (81) are members. As NET formation is detected in necrotic lung lesions of TB patients which promote bacterial growth (163), antibody mediated neutrophil activation can be as locally pathologic as it is systemically.

FcRs Influencing Dendritic Cell Antigen Presentation

Dendritic cells are the most efficient professional APCs that prime T cells. As such, enhancement of dendritic cell functions in the context of vaccination can in animal models produce sterilizing protection for *Mtb* (176). Studies in other infectious disease and cancer models show that antibodies through FcR on dendritic cells bridge the gap between innate and adaptive responses, but how this can confer long lasting immune memory for TB in a physiologically relevant setting continues to be re-evaluated.

Similar to macrophages, dendritic cells express a plethora of receptors that permit responsiveness to antibodies in the lung upon recruitment in *Mtb* infection. Monocyte derived dendritic cells and macrophages express baseline high levels of activating FcγRs, and conventional and plasmacytoid dendritic cells can also express the only inhibitory FcγR FcγRIIb/CD32b (177). By engaging both activating FcγRIIa/CD32a and inhibitory FcγRIIb/CD32b low affinity signaling, IgG can influence antigen uptake and presentation, maturation and cytokine production. These activities likely direct priming either at the primary pulmonary site of *Mtb* infection or in the draining lymph nodes as adaptive immunity develops (70, 87–89, 178). Moreover, in addition to its recycling function, the high affinity FcRN in concert with FcγRIIa/CD32a can regulate cross presentation of IgG immune complexes (179). Exactly how this occurs in TB is unclear. FcRN knockout mice have enhanced *Mtb* infected CD103+ dendritic cells and CD4 T cell priming early at day 14 of infection, with decreased *Mtb* burden on days 14 and 28. However, it appears that this effect is transient, leading to similar pulmonary burdens on day 56 (121).

An anti-tumor T cell "vaccinal effect" through engagement of FcγRIIa/CD32a on dendritic cells can be induced in a human *FCGR* transgenic mouse model with monoclonal antibodies. This is in addition to the transient clearance of tumor cell targets by macrophage FcγRIIIa/CD16a mediated ADCC (180). This FcγRIIa/CD32a dendritic cell mediated effect is even more pronounced in the context of influenza infection. Fc engineered antibodies show that binding to FcγRIIa/CD32a on dendritic cells increases CD40, CD80 and CD86 expression that induces protective CD8 T cell activation while FcgRIIIa/CD16a on macrophages had a limited role (181). A direct link between antibody mediated effects on dendritic cell antigen presentation and B and T cell maturation have yet to be shown for *Mtb*. However, any protective *in vitro* effect of polyclonal IgG on dendritic cells from humans highly exposed to *Mtb* is dependent on the presence of MHC-II and CD4 T cells in whole blood (49). This suggests that the interaction is plausible in natural exposure and could be leveraged by vaccines.

Regulation by the Inhibitory FcγRIIb/CD32b

Activating FcR mediated immune responses in the absence of checks and balances lead to autoimmune induced pathology. Though there are multiple regulatory points, FcγRIIb/CD32b is the only inhibitory FcγR and is the only FcγR well conserved between humans and mice (182). The high sequence similarity between the extracellular domains of *FCGRIIB/CD32B*, *FCGRIIA/CD32A* and *FCGRIIC/CD32C* and the paucity of specific monoclonal antibody probes limit experimental designs. However, the knockout mouse model has provided some hints as to the importance of inhibitory FcγR regulation in TB.

In response to low dose *Mtb* aerosol infection, mice genetically deficient in FcγRIIb/CD32b have increased CD4 T

cell IFNγ production, decreased bacterial burden in the lungs and spleen, and decreased neutrophilic inflammation at day 30 (13). Thus, in early infection, activating FcR signaling that enhance CD4 T cells are protective. However, the implications for chronic disease, which is more characteristic of human TB, are unclear as the autoimmune phenotype of these knockout mice confound the interpretation of *Mtb* survival experiments that last over one year.

Because FcγRIIb/CD32b is detectable on dendritic cells and subpopulations of monocytes, macrophages and neutrophils, it is likely that the cumulative impact of the only inhibitory FcγR for TB reflects functions from all of these immune cells. In human (70) and mouse dendritic cells (88), FcγRIIb/CD32b counter balances FcγRIIa/CD32a activation of maturation, secretion of inflammatory cytokines and MHC-I and MHC-II antigen presentation (87). Thus, loss of FcγRIIb/CD32b in dendritic cells likely promotes the development of a Th1 response able to inhibit *Mtb*. However, FcγRIIb/CD32b in follicular dendritic cells counterintuitively enhances B cell activation by multimerizing antigens to crosslink multiple B cell receptors (BCRs) (183). The existence of this T cell independent mechanism of antibody induction suggests stark differences within dendritic cell subsets that could have implications for long lasting immunity. For monocytes, macrophages and other granulocytes, the presence of activating FcRs determine the impact of FcγRIIb/CD32b (74, 75, 156). This further argues that FcγRIIb/CD32b functions are likely highlighted primarily in the context of stimulatory factors as opposed to acting in isolation.

In B cells, FcγRIIb/CD32b negatively regulates BCR signaling, expansion and plasma cell differentiation (184), suggesting that antibody production is also inhibited. Thus, *Mtb* specific antibodies generated in knockout mice could be higher when compared to wildtype. Higher levels of IgG, IgM and IgA could enhance immune cell effector functions, further contributing to anti-*Mtb* activities in the absence of an inhibitory checkpoint.

Finally, there is emerging evidence from adoptive transfer experiments that FcγRIIb/CD32b can act as a CD8 T cell checkpoint inhibitor involved in anti-tumor immunity (185). Extrapolation for *Mtb* would implicate an involvement of the inhibitory FcR more directly in the regulation of cytotoxic T cell functions that could be protective.

INFLUENCING ADAPTIVE IMMUNITY

Fc Receptors on T Cells

While MHC-I and MHC-II antigen presentation and expression of co-stimulatory ligands by APCs and B cells represent the primary paths through which CD4 and CD8 T cells are activated, there is some data to suggest that activating FcR can more directly influence T cells. T cell activation and differentiation has been associated with expression of the low affinity FcR, FcγRII/CD32, including both CD4 (186–188) and CD8 T cells (181, 189). On a small subset of CD4 T cells from blood and lymphoid tissues of humans and Rhesus macaques with and without HIV/SIV infection, proliferation, differentiation and cytokine production could be enhanced by immune complex activation of FcγRIIa/CD32a (186, 187). Interestingly, IgM binding to the Fcμ receptor on peripheral human T cells increases T cell receptor (TCR) and CD28 coreceptor expression, thereby lowering the threshold for T cell activation (190). Thus, high levels of IgM such as that induced by intravenous BCG could provide co-stimulation through FcR binding and enhance early T cell responses to lead to protection against *Mtb* (32). Evaluation of these T cell subsets in TB would provide greater clarity as to whether FcR binding could serve a co-stimulatory function *in vivo* when T cells are activated naturally through TCR-dependent mechanisms.

B Cells in Antigen Presentation to T Cells

The interactions between naïve T cells and APCs within the T cell zones of secondary lymphoid organs determine the repertoire of TCRs, which is governed by antigen availability and TCR binding characteristics (191). B cells recognize and respond to the structure of 3-dimensional antigens, including the simultaneous binding of non-sequential, distant residues which become juxtaposed upon protein folding. However, T cells recognize sequential amino acids within short peptides only when they are presented in the context of the MHC molecule. Since antigens are bound to the BCR, endocytosed, processed and presented as peptides, antibodies produced by differentiated plasma cells might affect the activation of peptide-specific T cells targeting the same *Mtb* protein. Thus, B cells could present antigens for the purpose of activating conventional T cells in a manner similar to their presentation of antigens to T follicular helper (Tfh) cells (**Figure 3B**) (111).

The most well-characterized interactions between B cells and T cells occurs in the context of B cell antigen presentation to Tfh cells in secondary lymphoid organs. This facilitates B cell activation and differentiation into antibody-producing plasma cells. However, the professional antigen-presenting capacity of B cells together with their strategic localization in and around sites of T cell priming in secondary lymphoid organs, granulomas and iBALT after *Mtb* infection suggests a broader role, including participation in *Mtb*-specific T cell activation.

Classically, CD4 T cell priming in response to *Mtb* has been shown to occur when T cells are activated by conventional dendritic cells in lymph nodes after CCR2+ monocyte-derived APCs transport live *Mtb* from the lung to the draining lymph nodes (178, 192, 193). After priming, effector T cells traffick to the lungs and secrete IFNγ and cytokines in response to *Mtb*. However, depletion studies in animal models identified a role for B cell antigen presentation in supporting optimal T cell responses in infectious disease and autoimmune models, suggesting that this too could occur in the context of TB. In a mouse model of adjuvanted peptide vaccination, B cell presentation of peptides on MHC-II was found to be necessary to enhance CD4 T cell expansion and IL2 production (106). B cell depletion using an anti-CD20 monoclonal antibody in mice significantly reduces total baseline numbers of naïve, effector, and regulatory CD4 and CD8 T cells. In the context of lymphocytic choriomeningitis virus (LCMV) Armstrong infection, this leads to increased viral load, an effect which is

rescued by infusion of LCMV-specific TCR transgenic CD8 T cells (194). Similarly, B cell depletion prior to infection with *Trypanosoma cruzi* reduces subsequent induction of total and parasite-specific CD8 T cells (195), and B cells are critical in the development of antigen-specific effector and memory CD4 T cell responses to *Listeria* (196, 197) and *Salmonella* (198). Finally, at least two studies have shown a supporting role for B cells in priming autoreactive T cell responses in mouse models of autoimmune diabetes, arthritis and lupus independent of plasma cell differentiation and antibody production (197, 199). These data indicate that B cells assist antimicrobial and autoimmune T cell responses either directly or indirectly.

An indirect mechanism of antigen presentation to T cells by B cells is secretion of MHC-II containing exosomes or extracellular vesicles. In this scenario B cells activate T cells in an HLA-DR dependent manner (200–202). T cell stimulation by extracellular vesicles is dependent on expression of the costimulatory receptor CD28 (203). This mechanism of antigen presentation is of particular interest in TB as both extracellular microvesicles and exosomes from *Mtb* infected macrophages and dendritic cells are sources of antigen that can directly or indirectly activate antigen-specific CD4 and CD8 T cells (204–208). Though not yet studied in TB, B cell exosomes may serve a similar function to provide alternative ways to activate T cells to compensate for Mtb immune evasion in macrophages (209–211). It is also possible that B cell exosomes provide a means of transferring units of MHC class II-peptide complexes between different cells (212) (**Figure 3C**). Thus, MHC-II provides multiple lines of B cell-T cell communications.

In addition to T and B cells, tingible body macrophages (TBMs) are found in the germinal centers in lymph nodes, spleen and iBALT from the non-human primate model of TB (213). TBMs are specialized macrophages that engulf apoptotic B cells during affinity maturation (214, 215). In this manner, TBMs prevent the loading of self-antigens from cell debris immune complexes onto follicular dendritic cells that present to B cells (216, 217). Moreover, studies using ovalbumin-specific T cell hybridomas show that antigen-laden TBMs suppress the ability of B cells to activate T cells (215), thereby preventing autoimmune responses. In the mouse model of TB, dendritic cells uptake extracellular vesicles from apoptotic macrophages infected with *Mtb* and stimulate CD8 T cell responses in an MHC-I or CD1-dependent manner (218). These data imply a role for scavenger APCs in presenting *Mtb* antigens to regulate T cell responses. Cross-priming of CD8 T cells from APCs is likely important for the recognition and killing of many pathogen infected cells. In TB, acquisition of antigens *via* efferocytosis and uptake of extracellular vesicles enhances the number of antigen specific CD8 T cells that recognize *Mtb* infected macrophages (130, 219, 220). TBM mediated efferocytosis and T cell cross-priming could explain the association of B cell follicles with protection against active disease in the non-human primate model of TB (213).

B Cell Follicle-Like Structures

Like a granuloma, the iBALT is a tertiary lymphoid structures that enrich and facilitate interaction between myeloid cells, B cells, T cells and non-hematopoietic cells (107, 221). Adjacent to granulomas, the iBALT is a pulmonary structure consisting of B cell follicles and components of the lymph node including high endothelial venules and connection the lymphatic drainage (93, 99, 107, 222–225). Induced early after infection, the follicles contain IgD+ B cells clustered around a network of follicular dendritic cells. These stromal cells produce IL1α, express the lymphotoxin α (LTα) receptor and secrete CXCL13 (225) to help recruit immune cells to form the iBALT (226). The iBALT is associated with protection in the setting of *Mtb*, serving as both a lymphoid organ and a lung-resident source of locally-activated, antigen-specific T and B cells primed for rapid responses (107, 213).

The iBALT is a feature of type 1 immune responses and is reported to regulate type 2 and type 17 responses. A recent study in a mouse model of asthma found that pre-existing iBALT delayed the onset of Th2 trafficking and related inflammation (227). In a mouse model of influenza infection, the iBALT offers protection through supporting antigen specific CD8 T cells, humoral responses and the formation of immunological memory even in the absence of spleen and lymph nodes (228, 229). The iBALT has also been shown to recruit dendritic cells harboring antigens and naïve T cells, leading to co-localization and T cell priming (230). For TB, the association of iBALT formation with protective phenotypes in human lung tissue as well as in the mouse and non-human primate models point towards a protective feature against active disease (93, 213, 231, 232).

In TB, the extent of T and B cell priming in the iBALT versus lung-draining lymph nodes has been incompletely explored. The priming of naïve antigen specific CD8 T cells after non-replicating viral vector infection has been demonstrated in adoptive cell transfer models in mice (230). However, in the mouse model of TB, priming of naïve T cells in the lung is undetectable (178, 192, 233). Memory T cell priming in the lungs has only been shown after the intratracheal transfer of antigen-laden dendritic cells (234). Yet previously activated T and B cells do traffick through the iBALT in other infectious models (229). Tfh cells which are critical to germinal center formation and B cell differentiation into antibody-producing plasma cells are normally found in secondary lymphoid organs lymph node and spleen and may have the same role in iBALT (107, 235). T cells that express properties of both Th1 and Th17 cells, along with Tfh cells are found in the lung, express CXCR5, produce IFNγ and/or IL17 and are associated with iBALT formation and control of *Mtb* infection (93, 107). For protection against TB, Tfh cells in the lung support germinal center responses involved in (1) the development of memory B cells and differentiation into antibody producing plasma cells, (2) the regulation of pathologic immune responses such as neutrophilia and cavity formation, (3) the classical priming of T cells locally, and (4) the non-classical activation of CD8 and CD1-restricted T cells by cross-priming and efferocytosis (130, 218, 219).

The formation of iBALT near bronchi or in the lung interstitium is influenced by the infecting microbe and host response (236, 237). The recruitment of dendritic cells, macrophages, and innate lymphoid cells leads to cytokine and chemokine production that enlists B and T cells (223, 230). More

specifically, in early *Mtb* infection, type 3 innate lymphoid cells (ILC3s) (223) and production of IL23, IL17, IL22 and CXCL13 direct B and T cells into the lung of the mouse model (238). Within the iBALT, conventional dendritic cells and T cells localize around B cell follicles into germinal center-like structure. Over time distinct T cell and B cell zones are formed (228, 230). Thus, lymphocytes expressing CCR7 and CXCR5 traffick to and organize the iBALT (93, 239). In addition, CCL19, CCL21 and CXCL13 from follicular dendritic cells are critical to establishing structure (228). These same axes (CCR7-CCL19/CCL21 and CXCL13-CXCR5) are required for T and B cell homing, antigen presentation, T cell activation, IFNγ production and control of *Mtb* growth (93, 222, 240). Finally, a recent transposon mutagenesis screen in the non-human primate model of TB identified gene associated with production of *Mtb* cell wall lipids with the formation of iBALT (98). Together, these studies show that the extent of protection offered by the iBALT (241) is likely dependent on both the infecting organism and the host.

COMPLEXITY OF IMMUNITY IN TB

Protection and Sterilizing Immunity

One goal of an effective TB vaccine is to prevent infection or provide sterilizing immunity to the host. However, generating a sufficiently robust and durable immune response that neutralizes and eradicates *Mtb* could come at a survival cost to the host. To this point, enhancement of CD4 T cell responses at the level of immune checkpoints such as PD-1 counterintuitively enhances disease and decreases survival in mouse studies (242). In some patients, anti-PD-1 monoclonal antibodies used to treat cancer precipitated reactivation TB from latently infected individuals (242). Indeed, *post-hoc* analyses of the MVA85A clinical trials demonstrate that higher frequency of HLA-DR+ activated CD4 T cells can be associated with increased risk of TB while higher Ag85A IgG titers correlate with protection (243). Thus, strategies that release the break on T cells unilaterally could provide more harm than benefit. Nevertheless, a cytomegalovirus vectored vaccine generating antigen-specific T cell but no antibody responses prevented TB in nearly half of the *Mtb*-challenged non-human primates (244). Elucidating how immune responses can provide benefit with minimal cost will likely have broad applicability to vaccines across many infectious diseases.

Most TB vaccines in clinical development now incorporate both antibody and T cell responses, though which are correlates of protection and which of disease remain to be fully clarified. These vaccines include but are not limited to the M72-AS01e subunit vaccine containing a recombinant fusion protein of Mtb32a and Mtb39a (245) and BCG in multiple forms (246). While much has been evaluated involving the classic intradermal delivery, revaccination (247, 248) and the use of the recombinant VPM1002 expressing listerolysin-O to enhance CD8 T cell responses (249, 250) are variations currently in clinical trials. In pre-clinical models there is attention paid to delivery route- intravenous (32, 251), intranasal, aerosol, intratracheal and endobronchial (252). For both BCG and MTBVAC, an attenuated *Mtb* strain lacking the phoP and fadD26 virulence factors, antigen specific IgG are detected in pulmonary but not intradermal vaccinated animals and facilitate *Mtb* opsonophagocytosis *in vitro* (253). Thus, independent of what is induced during natural infection and disease, vaccine strategies that incorporate a greater breadth and depth of responses including B cells, antibodies and trained innate immunity (254, 255) could complement T cell responses to more effectively eradicate *Mtb* (32, 251, 256, 257).

Pathology and Disease

A second goal of an effective vaccine is to prevent TB disease and lung pathology. This, notably, does not necessarily imply eradication of the bacteria. In humans, there is increasing recognition that latent TB may represent a protective state (2, 258). Indeed only 5-10% of individuals progress to active disease. Yet the immune mechanisms by which the transition between latent and active disease occurs in humans and the corollary of how the remaining 90-95% of individuals maintain the asymptomatic latent state – whether this be with dormant or eradicated bacteria (2) – are not known. This phenotype has been difficult to study in animal models. The classic murine model recapitulates active TB but not latent infection. Furthermore, there is a disconnect between *Mtb* burden, dissemination and survival observed in passive antibody transfer studies of mice (259, 260). Thus, mechanisms by which asymptomatic *Mtb* latent infection is sustainably induced could be leveraged for vaccine design. To this point, antibodies have the potential to enhance disease whether directly through increased replication such as in Dengue hemorrhagic fever and *Leishmania* or indirectly through inducing a dysregulated immune response such as in COVID-19 (261). Understanding whether and how antibodies can enhance TB disease by mediating pathological inflammation in immune reconstitution inflammatory syndrome or simply supporting dissemination (262, 263) could provide novel host directed therapeutic targets.

Several candidate subunit TB vaccines aim to prevent not only initial infection but also pathology once infection has occurred. These include, but are not limited, to H56:IC31 that encompasses Ag85B, ESAT6 and Rv2660c (264), and the ID93 + GLA-SE vaccine which contains a TLR4 agonist formulated with a recombinant fusion protein of the *Mtb* virulence factors (esxV/Rv3619, esxW/Rv3620, PPE42/Rv2608) and *Mtb* latency associated protein Rv1813 (256, 265, 266). Administration of these vaccines in animal models induces robust antigen specific immune responses that, when combined with antibiotics, is linked to decreased bacterial burden and lung pathology in comparison to antibiotics alone. The highly effective mRNA vaccines BNT162b2 and mRNA-1273 successfully prevents both infection and serious disease with spike specific T cell and antibody responses against SARS-CoV2 (267, 268). As such, mRNA platforms provide promising avenues for TB vaccines in generating immune responses that both protect against *Mtb* infection and prevent disease pathology.

Challenges in Modeling Tuberculosis

Inherent differences between the widely used inbred mouse models and humans are critical to acknowledge when extrapolating data

(269). Antibody translocation and recycling functions of FcRN and pIGR in humans are recapitulated in the murine model. Similarly, the non-classical IgG binding TRIM21, the single IgM receptor (FcμR), the two receptors for IgM and IgA (pIGR and Fcα/μR/CD351) and the two receptors that bind to IgE (FcεRI and FcεRII) in humans are also found in mice. Unique to humans is FcαRI/CD89 which binds only IgA. For the classical IgG receptors (24), the expression of the activating FcγRI/CD64 in mice is limited to monocytes, macrophages and dendritic cells whereas in humans the spectrum also includes neutrophils. Conversely, FcγRIIIa/CD16 in humans is restricted to natural killer cells, monocytes and macrophages while in mice the spectrum also includes neutrophils, dendritic cells, basophils, eosinophils and mast cells. The only inhibitory Fc receptor, FcγRIIb/CD32b, is detected primarily on B cells and other myeloid lineage cells in mice but in a more limited capacity in humans. The activating FcγRIIa/CD32a, FcγRIIc/CD32c and FcγRIIIb/CD16b exist exclusively in humans while FcγRIV/CD16.2 is unique to mice. In addition, there is no clear equivalence between the FcR binding capacity of the human subclasses IgG1, 2, 3 and 4 and mouse IgG1, 2a/c, 2b and 3. Finally, the mouse IgG glycome partially overlaps with that of humans, with the functional implications of the differences not yet defined (36, 270). Mice with human FcR and signaling adaptors (271) as well as immunoglobulin genes (272) provide paths towards bridging the species gap. However, ensuring similarities in expression patterns to recapitulate immune effector functions at baseline and during infection remains to be fully flushed out as levels of each receptor influence each other.

For TB, the widely used low dose aerosol inbred mouse model does not recapitulate latent infection and poorly captures the phenotypic heterogeneity observed in humans (9, 273). The absence of some mechanisms of protection involved in latency may be one reason why results from vaccines studies in mice do not always directly translate to humans. For example, the promising 1-2 fold log reduction in colony forming units in the mouse model with BCG is reflected by reduction of disseminated TB in the pediatric population and variable impact on adult pulmonary TB, the most common form (274). Whether the aforementioned differences in antibody responses between mice and humans could be a factor in this gap is not known. Questions to this point could be addressed with diverse outbred mice and or new models of TB such as ultra-low dose aerosol infection that have the potential to reflect latent infection more closely than the current most widely used approach (275–277). Nevertheless, the canonical (and tractable) inbred mouse model has generated data that has formed the foundations of our understanding of antibody Fc effector functions in autoimmunity and monoclonal antibody fields. Building on this knowledge to address specific questions in the context of *Mtb* that could be orthogonally tested in non-human primates and or *ex vivo* work with patient samples provide paths to dissect physiologically relevant mechanisms of disease.

Challenges in Defining Human TB

The development and exploitation of robust imaging, microbiology and immune correlates techniques to characterize the spectrum of TB observed clinically has transformed the classic framework of uninfected, latent infection and active disease. Now it is possible to begin to better identify individuals with high exposure, initial infection, the quiescent bacterial state, subclinical infection, chronic smoldering disease that progresses and regresses, overt active disease, bacterial persistence after treatment and bacterial cure (41, 278–283).

Beyond pulmonary TB, extrapulmonary disease involving hematogenous dissemination to the central nervous system, bone marrow and other organs characterize a subset of cases. The risk of multiorgan involvement increases with immunosuppression. However, the precise mechanisms by which these additional TB states develop are largely unknown but likely involve both bacterial and host protective and pathologic immune factors (284).

Notably, not all immunosuppression leads to TB. Over 90% of TST+ individuals do not develop active TB after receiving anti-TNFα therapy, solid organ or hematopoietic stem cell transplantation (2). Clinical observations in heavily immunosuppressed adults such as these, particularly in the absence of routine antibiotic prophylaxis for TB, indicate that a proportion had elicited sterilizing immunity and cleared the infection. In neonates, accidental delivery of live virulent *Mtb* contaminating the BCG vaccine in the pre-antibiotic era led to death in only 29% of the cases and the surviving 70% had significant variation in clinical phenotypes (285). These observations demonstrate that there are likely multiple paths to protection that leverage a diverse array of innate and adaptive immune responses. Thus, in addition to CD4 T cell production of IFNγ, the distinct presence of B cells in granulomas in the *Mtb* infected lung as well as B cell follicles and germinal centers in the adjacent iBALT raise the possibility that their functions influence outcomes. Similarly, the presence of antibodies amidst the FcR bearing monocytes, macrophages, neutrophils, dendritic cells and T cells recruited to an *Mtb* lesion points towards Fab and Fc domain mediated effector functions that locally coordinate host responses to bacteria. In revisiting the paradigm of protection and disease, linking diverse immune responses that include antibodies, B and T cells will enable the re-examination of the heterogenous spectrum of human TB.

AUTHOR CONTRIBUTIONS

LL and SC drafted and wrote the manuscript, and approved the submitted version.

FUNDING

SC is supported by University Hospitals Cleveland Medical Center. LL is supported by the National Institutes of Health under Award Number R01AI158858 and the Disease Oriented Scholars Award at UT Southwestern Medical School.

ACKNOWLEDGMENTS

We thank Patricia Grace for her thoughtful review and comments, Taylor Buckholz for help with graphical illustrations and Ann Mcdonald for editorial and reference assistance.

REFERENCES

1. *Global Tuberculosis Report 2021*. Geneva: World Health Organization (2021).
2. Behr MA, Edelstein PH, Ramakrishnan L. Is Mycobacterium Tuberculosis Infection Life Long? *BMJ* (2019) 367:l5770. doi: 10.1136/bmj.l5770
3. Berry MP, Graham CM, McNab FW, Xu Z, Bloch SA, Oni T, et al. An Interferon-Inducible Neutrophil-Driven Blood Transcriptional Signature in Human Tuberculosis. *Nature* (2010) 466(7309):973–7. doi: 10.1038/nature09247
4. Malherbe ST, Shenai S, Ronacher K, Loxton AG, Dolganov G, Kriel M, et al. Persisting Positron Emission Tomography Lesion Activity and Mycobacterium Tuberculosis mRNA After Tuberculosis Cure. *Nat Med* (2016) 22(10):1094–100. doi: 10.1038/nm.4177
5. Beltran CGG, Heunis T, Gallant J, Venter R, du Plessis N, Loxton AG, et al. Investigating Non-Sterilizing Cure in TB Patients at the End of Successful Anti-TB Therapy. *Front Cell Infect Microbiol* (2020) 10:443. doi: 10.3389/fcimb.2020.00443
6. Lin PL, Maiello P, Gideon HP, Coleman MT, Cadena AM, Rodgers MA, et al. PET CT Identifies Reactivation Risk in Cynomolgus Macaques With Latent M. Tuberculosis. *PloS Pathog* (2016) 12(7):e1005739. doi: 10.1371/journal.ppat.1005739
7. Lin PL, Ford CB, Coleman MT, Myers AJ, Gawande R, Ioerger T, et al. Sterilization of Granulomas is Common in Active and Latent Tuberculosis Despite Within-Host Variability in Bacterial Killing. *Nat Med* (2014) 20(1):75–9. doi: 10.1038/nm.3412
8. Ordonez AA, Tucker EW, Anderson CJ, Carter CL, Ganatra S, Kaushal D, et al. Visualizing the Dynamics of Tuberculosis Pathology Using Molecular Imaging. *J Clin Invest* (2021) 131(5):e145107. doi: 10.1172/JCI145107
9. Barry CE 3rd, Boshoff HI, Dartois V, Dick T, Ehrt S, Flynn J, et al. The Spectrum of Latent Tuberculosis: Rethinking the Biology and Intervention Strategies. *Nat Rev Microbiol* (2009) 7(12):845–55. doi: 10.1038/nrmicro2236
10. Flynn JL, Chan J, Triebold KJ, Dalton DK, Stewart TA, Bloom BR. An Essential Role for Interferon Gamma in Resistance to Mycobacterium Tuberculosis Infection. *J Exp Med* (1993) 178(6):2249–54. doi: 10.1084/jem.178.6.2249
11. Orme IM, Roberts AD, Griffin JP, Abrams JS. Cytokine Secretion by CD4 T Lymphocytes Acquired in Response to Mycobacterium Tuberculosis Infection. *J Immunol* (1993) 151(1):518–25.
12. Nunes-Alves C, Booty MG, Carpenter SM, Jayaraman P, Rothchild AC, Behar SM. In Search of a New Paradigm for Protective Immunity to TB. *Nat Rev Microbiol* (2014) 12(4):289–99. doi: 10.1038/nrmicro3230
13. Maglione PJ, Xu J, Chan J. B Cells Moderate Inflammatory Progression and Enhance Bacterial Containment Upon Pulmonary Challenge With Mycobacterium Tuberculosis. *J Immunol* (2007) 178(11):7222–34. doi: 10.4049/jimmunol.178.11.7222
14. Maglione PJ, Xu J, Casadevall A, Chan J. Fc Gamma Receptors Regulate Immune Activation and Susceptibility During Mycobacterium Tuberculosis Infection. *J Immunol* (2008) 180(5):3329–38. doi: 10.4049/jimmunol.180.5.3329
15. Phuah J, Wong EA, Gideon HP, Maiello P, Coleman MT, Hendricks MR, et al. Effects of B Cell Depletion on Early Mycobacterium Tuberculosis Infection in Cynomolgus Macaques. *Infect Immun* (2016) 84(5):1301–11. doi: 10.1128/IAI.00083-16
16. Lu LL, Chung AW, Rosebrock TR, Ghebremichael M, Yu WH, Grace PS, et al. A Functional Role for Antibodies in Tuberculosis. *Cell* (2016) 167(2):433–43.e14. doi: 10.1016/j.cell.2016.08.072
17. Lu LL, Das J, Grace PS, Fortune SM, Restrepo BI, Alter G. Antibody Fc Glycosylation Discriminates Between Latent and Active Tuberculosis. *J Infect Dis* (2020) 222(12):2093–102. doi: 10.1093/infdis/jiz643
18. Grace PS, Dolatshahi S, Lu LL, Cain A, Palmieri F, Petrone L, et al. Antibody Subclass and Glycosylation Shift Following Effective TB Treatment. *Front Immunol* (2021) 12:679973. doi: 10.3389/fimmu.2021.679973
19. Glatman-Freedman A, Casadevall A. Serum Therapy for Tuberculosis Revisited: Reappraisal of the Role of Antibody-Mediated Immunity Against Mycobacterium Tuberculosis. *Clin Microbiol Rev* (1998) 11(3):514–32. doi: 10.1128/CMR.11.3.514
20. Kimby E. Tolerability and Safety of Rituximab (MabThera). *Cancer Treat Rev* (2005) 31(6):456–73. doi: 10.1016/j.ctrv.2005.05.007
21. Janssen LMA, van der Flier M, de Vries E. Lessons Learned From the Clinical Presentation of Common Variable Immunodeficiency Disorders: A Systematic Review and Meta-Analysis. *Front Immunol* (2021) 12:620709. doi: 10.3389/fimmu.2021.620709
22. Steingart KR, Henry M, Laal S, Hopewell PC, Ramsay A, Menzies D, et al. A Systematic Review of Commercial Serological Antibody Detection Tests for the Diagnosis of Extrapulmonary Tuberculosis. *Postgrad Med J* (2007) 83(985):705–12. doi: 10.1136/thx.2006.075754
23. Kramnik I, Beamer G. Mouse Models of Human TB Pathology: Roles in the Analysis of Necrosis and the Development of Host-Directed Therapies. *Semin Immunopathol* (2016) 38(2):221–37. doi: 10.1007/s00281-015-0538-9
24. Bruhns P. Properties of Mouse and Human IgG Receptors and Their Contribution to Disease Models. *Blood* (2012) 119(24):5640–9. doi: 10.1182/blood-2012-01-380121
25. Marco H, Smith RM, Jones RB, Guerry MJ, Catapano F, Burns S, et al. The Effect of Rituximab Therapy on Immunoglobulin Levels in Patients With Multisystem Autoimmune Disease. *BMC Musculoskelet Disord* (2014) 15:178. doi: 10.1186/1471-2474-15-178
26. Bergantini L, d'Alessandro M, Cameli P, Vietri L, Vagaggini C, Perrone A, et al. Effects of Rituximab Therapy on B Cell Differentiation and Depletion. *Clin Rheumatol* (2020) 39(5):1415–21. doi: 10.1007/s10067-020-04996-7
27. Greiff V, Miho E, Menzel U, Reddy ST. Bioinformatic and Statistical Analysis of Adaptive Immune Repertoires. *Trends Immunol* (2015) 36(11):738–49. doi: 10.1016/j.it.2015.09.006
28. Cole ST, Brosch R, Parkhill J, Garnier T, Churcher C, Harris D, et al. Deciphering the Biology of Mycobacterium Tuberculosis From the Complete Genome Sequence. *Nature* (1998) 393(6685):537–44. doi: 10.1038/31159
29. Daffe M, Draper P. The Envelope Layers of Mycobacteria With Reference to Their Pathogenicity. *Adv Microb Physiol* (1998) 39:131–203. doi: 10.1016/S0065-2911(08)60016-8
30. Fischinger S, Cizmeci D, Shin S, Davies L, Grace PS, Sivro A, et al. A Mycobacterium Tuberculosis Specific IgG3 Signature of Recurrent Tuberculosis. *Front Immunol* (2021) 12:729186. doi: 10.3389/fimmu.2021.729186
31. Zimmermann N, Thormann V, Hu B, Kohler AB, Imai-Matsushima A, Locht C, et al. Human Isotype-Dependent Inhibitory Antibody Responses Against Mycobacterium Tuberculosis. *EMBO Mol Med* (2016) 8(11):1325–39. doi: 10.15252/emmm.201606330
32. Irvine EB, O'Neil A, Darrah PA, Shin S, Choudhary A, Li W, et al. Robust IgM Responses Following Intravenous Vaccination With Bacille Calmette-Guerin Associate With Prevention of Mycobacterium Tuberculosis Infection in Macaques. *Nat Immunol* (2021) 22(12):1515–23. doi: 10.1038/s41590-021-01066-1
33. Jones MB, Oswald DM, Joshi S, Whiteheart SW, Orlando R, Cobb BA. B-Cell-Independent Sialylation of IgG. *Proc Natl Acad Sci USA* (2016) 113(26):7207–12. doi: 10.1073/pnas.1523968113
34. Dougher CWL, Buffone A Jr, Nemeth MJ, Nasirikenari M, Irons EE, Bogner PN, et al. The Blood-Borne Sialyltransferase ST6Gal-1 Is a Negative Systemic Regulator of Granulopoiesis. *J Leukoc Biol* (2017) 102(2):507–16. doi: 10.1189/jlb.3A1216-538RR
35. Manhardt CT, Punch PR, Dougher CWL, Lau JTY. Extrinsic Sialylation is Dynamically Regulated by Systemic Triggers In Vivo. *J Biol Chem* (2017) 292(33):13514–20. doi: 10.1074/jbc.C117.795138
36. Schaffert A, Hanic M, Novokmet M, Zaytseva O, Kristic J, Lux A, et al. Minimal B Cell Extrinsic IgG Glycan Modifications of Pro- and Anti-Inflammatory IgG Preparations In Vivo. *Front Immunol* (2019) 10:3024. doi: 10.3389/fimmu.2019.03024
37. van de Bovenkamp FS, Derksen NIL, Ooijevaar-de Heer P, van Schie KA, Kruithof S, Berkowska MA, et al. Adaptive Antibody Diversification Through N-Linked Glycosylation of the Immunoglobulin Variable Region. *Proc Natl Acad Sci USA* (2018) 115(8):1901–6. doi: 10.1073/pnas.1711720115
38. Cobb BA. The History of IgG Glycosylation and Where We are Now. *Glycobiology* (2020) 30(4):202–13. doi: 10.1093/glycob/cwz065

39. Tanigaki K, Sacharidou A, Peng J, Chambliss KL, Yuhanna IS, Ghosh D, et al. Hyposialylated IgG Activates Endothelial IgG Receptor FcgammaRIIB to Promote Obesity-Induced Insulin Resistance. *J Clin Invest* (2018) 128 (1):309–22. doi: 10.1172/JCI89333
40. Peng J, Vongpatanasin W, Sacharidou A, Kifer D, Yuhanna IS, Banerjee S, et al. Supplementation With the Sialic Acid Precursor N-Acetyl-D-Mannosamine Breaks the Link Between Obesity and Hypertension. *Circulation* (2019) 140(24):2005–18. doi: 10.1161/CIRCULATIONAHA.119.043490
41. Lu LL, Smith MT, Yu KKQ, Luedemann C, Suscovich TJ, Grace PS, et al. IFN-Gamma-Independent Immune Markers of Mycobacterium Tuberculosis Exposure. *Nat Med* (2019) 25(6):977–87. doi: 10.1038/s41591-019-0441-3
42. Thulin NK, Brewer RC, Sherwood R, Bournazos S, Edwards KG, Ramadoss NS, et al. Maternal Anti-Dengue IgG Fucosylation Predicts Susceptibility to Dengue Disease in Infants. *Cell Rep* (2020) 31(6):107642. doi: 10.1016/j.celrep.2020.107642
43. Wang TT, Sewatanon J, Memoli MJ, Wrammert J, Bournazos S, Bhaumik SK, et al. IgG Antibodies to Dengue Enhanced for FcgammaRIIIA Binding Determine Disease Severity. *Science* (2017) 355(6323):395–8. doi: 10.1126/science.aai8128
44. McLean MR, Wragg KM, Lopez E, Kiazyk SA, Ball TB, Bueti J, et al. Serological and Cellular Inflammatory Signatures in End-Stage Kidney Disease and Latent Tuberculosis. *Clin Transl Immunol* (2021) 10(11): e1355. doi: 10.1002/cti2.1355
45. Olivares N, Marquina B, Mata-Espinoza D, Zatarain-Barron ZL, Pinzon CE, Estrada I, et al. The Protective Effect of Immunoglobulin in Murine Tuberculosis is Dependent on IgG Glycosylation. *Pathog Dis* (2013) 69 (3):176–83. doi: 10.1111/2049-632X.12069
46. Kumagai T, Palacios A, Casadevall A, Garcia MJ, Toro C, Tiemeyer M, et al. Serum IgM Glycosylation Associated With Tuberculosis Infection in Mice. *mSphere* (2019) 4(2):e00684–18. doi: 10.1128/mSphere.00684-18
47. Chen T, Blanc C, Liu Y, Ishida E, Singer S, Xu J, et al. Capsular Glycan Recognition Provides Antibody-Mediated Immunity Against Tuberculosis. *J Clin Invest* (2020) 130(4):1808–22. doi: 10.1172/JCI128459
48. de Valliere S, Abate G, Blazevic A, Heuertz RM, Hoft DF. Enhancement of Innate and Cell-Mediated Immunity by Antimycobacterial Antibodies. *Infect Immun* (2005) 73(10):6711–20. doi: 10.1128/IAI.73.10.6711-6720.2005
49. Li H, Wang XX, Wang B, Fu L, Liu G, Lu Y, et al. Latently and Uninfected Healthcare Workers Exposed to TB Make Protective Antibodies Against Mycobacterium Tuberculosis. *Proc Natl Acad Sci USA* (2017) 114(19):5023–8. doi: 10.1073/pnas.1611776114
50. Warmerdam PA, van de Winkel JG, Gosselin EJ, Capel PJ. Molecular Basis for a Polymorphism of Human Fc Gamma Receptor II (Cd32). *J Exp Med* (1990) 172(1):19–25. doi: 10.1084/jem.172.1.19
51. Sanders LA, Feldman RG, Voorhorst-Ogink MM, de Haas M, Rijkers GT, Capel PJ, et al. Human Immunoglobulin G (IgG) Fc Receptor IIA (CD32) Polymorphism and IgG2-Mediated Bacterial Phagocytosis by Neutrophils. *Infect Immun* (1995) 63(1):73–81. doi: 10.1128/iai.63.1.73-81.1995
52. Platonov AE, Shipulin GA, Vershinina IV, Dankert J, van de Winkel JG, Kuijper EJ. Association of Human Fc Gamma RIIa (CD32) Polymorphism With Susceptibility to and Severity of Meningococcal Disease. *Clin Infect Dis* (1998) 27(4):746–50. doi: 10.1086/514935
53. Sanders LA, van de Winkel JG, Rijkers GT, Voorhorst-Ogink MM, de Haas M, Capel PJ, et al. Fc Gamma Receptor IIa (CD32) Heterogeneity in Patients With Recurrent Bacterial Respiratory Tract Infections. *J Infect Dis* (1994) 170(4):854–61. doi: 10.1093/infdis/170.4.854
54. Koene HR, Kleijer M, Algra J, Roos D, von dem Borne AE, de Haas M. Fc gammaRIIIa-158v/F Polymorphism Influences the Binding of IgG by Natural Killer Cell Fc gammaRIIIa, Independently of the Fc gammaRIIIa-48l/R/H Phenotype. *Blood* (1997) 90(3):1109–14. doi: 10.1182/blood.V90.3.1109
55. Wu J, Edberg JC, Redecha PB, Bansal V, Guyre PM, Coleman K, et al. A Novel Polymorphism of FcgammaRIIIa (CD16) Alters Receptor Function and Predisposes to Autoimmune Disease. *J Clin Invest* (1997) 100(5):1059–70. doi: 10.1172/JCI119616
56. Bournazos S, Woof JM, Hart SP, Dransfield I. Functional and Clinical Consequences of Fc Receptor Polymorphic and Copy Number Variants. *Clin Exp Immunol* (2009) 157(2):244–54. doi: 10.1111/j.1365-2249.2009.03980.x
57. Mellor JD, Brown MP, Irving HR, Zalcberg JR, Dobrovic A. A Critical Review of the Role of Fc Gamma Receptor Polymorphisms in the Response to Monoclonal Antibodies in Cancer. *J Hematol Oncol* (2013) 6:1. doi: 10.1186/1756-8722-6-1
58. Willcocks LC, Carr EJ, Niederer HA, Rayner TF, Williams TN, Yang W, et al. A Defunctioning Polymorphism in FCGR2B is Associated With Protection Against Malaria But Susceptibility to Systemic Lupus Erythematosus. *Proc Natl Acad Sci USA* (2010) 107(17):7881–5. doi: 10.1073/pnas.0915133107
59. Bournazos S, Klein F, Pietzsch J, Seaman MS, Nussenzweig MC, Ravetch JV. Broadly Neutralizing Anti-HIV-1 Antibodies Require Fc Effector Functions for In Vivo Activity. *Cell* (2014) 158(6):1243–53. doi: 10.1016/j.cell.2014.08.023
60. Halper-Stromberg A, Lu CL, Klein F, Horwitz JA, Bournazos S, Nogueira L, et al. Broadly Neutralizing Antibodies and Viral Inducers Decrease Rebound From HIV-1 Latent Reservoirs in Humanized Mice. *Cell* (2014) 158(5):989–99. doi: 10.1016/j.cell.2014.07.043
61. DiLillo DJ, Tan GS, Palese P, Ravetch JV. Broadly Neutralizing Hemagglutinin Stalk-Specific Antibodies Require FcgammaR Interactions for Protection Against Influenza Virus In Vivo. *Nat Med* (2014) 20(2):143–51. doi: 10.1038/nm.3443
62. He W, Chen CJ, Mullarkey CE, Hamilton JR, Wong CK, Leon PE, et al. Alveolar Macrophages are Critical for Broadly-Reactive Antibody-Mediated Protection Against Influenza A Virus in Mice. *Nat Commun* (2017) 8(1):846. doi: 10.1038/s41467-017-00928-3
63. Yamin R, Jones AT, Hoffmann HH, Schafer A, Kao KS, Francis RL, et al. Fc-Engineered Antibody Therapeutics With Improved Anti-SARS-CoV-2 Efficacy. *Nature* (2021) 599(7885):465–70. doi: 10.1038/s41586-021-04017-w
64. Ullah I, Prevost J, Ladinsky MS, Stone H, Lu M, Anand SP, et al. Live Imaging of SARS-CoV-2 Infection in Mice Reveals That Neutralizing Antibodies Require Fc Function for Optimal Efficacy. *Immunity* (2021) 54 (9):2143–58.e15. doi: 10.1016/j.immuni.2021.08.015
65. Suryadevara N, Shrihari S, Gilchuk P, VanBlargan LA, Binshtein E, Zost SJ, et al. Neutralizing and Protective Human Monoclonal Antibodies Recognizing the N-Terminal Domain of the SARS-CoV-2 Spike Protein. *Cell* (2021) 184(9):2316–31.e15. doi: 10.1016/j.cell.2021.03.029
66. Winkler ES, Gilchuk P, Yu J, Bailey AL, Chen RE, Chong Z, et al. Human Neutralizing Antibodies Against SARS-CoV-2 Require Intact Fc Effector Functions for Optimal Therapeutic Protection. *Cell* (2021) 184(7):1804–20.e16. doi: 10.1016/j.cell.2021.02.026
67. Sutherland JS, Loxton AG, Haks MC, Kassa D, Ambrose L, Lee JS, et al. Differential Gene Expression of Activating Fcgamma Receptor Classifies Active Tuberculosis Regardless of Human Immunodeficiency Virus Status or Ethnicity. *Clin Microbiol Infect* (2014) 20(4):O230–8. doi: 10.1111/1469-0691.12383
68. Ahmed M, Thirunavukkarasu S, Rosa BA, Thomas KA, Das S, Rangel-Moreno J, et al. Immune Correlates of Tuberculosis Disease and Risk Translate Across Species. *Sci Transl Med* (2020) 12(528):eaay0233. doi: 10.1126/scitranslmed.aay0233
69. Machado LR, Bowdrey J, Ngaimisi E, Habtewold A, Minzi O, Makonnen E, et al. Copy Number Variation of Fc Gamma Receptor Genes in HIV-Infected and HIV-Tuberculosis Co-Infected Individuals in Sub-Saharan Africa. *PloS One* (2013) 8(11):e78165. doi: 10.1371/journal.pone.0078165
70. Boruchov AM, Heller G, Veri MC, Bonvini E, Ravetch JV, Young JW. Activating and Inhibitory IgG Fc Receptors on Human DCs Mediate Opposing Functions. *J Clin Invest* (2005) 115(10):2914–23. doi: 10.1172/JCI24772
71. Veri MC, Gorlatov S, Li H, Burke S, Johnson S, Stavenhagen J, et al. Monoclonal Antibodies Capable of Discriminating the Human Inhibitory Fcgamma-Receptor IIB (CD32B) From the Activating Fcgamma-Receptor IIA (CD32A): Biochemical, Biological and Functional Characterization. *Immunology* (2007) 121(3):392–404. doi: 10.1111/j.1365-2567.2007.02588.x
72. Roy Chowdhury R, Vallania F, Yang Q, Lopez Angel CJ, Darboe F, Penn-Nicholson A, et al. A Multi-Cohort Study of the Immune Factors Associated With M. Tuberculosis Infection Outcomes. *Nature* (2018) 560(7720):644–8. doi: 10.1038/s41586-018-0439-x
73. Lastrucci C, Benard A, Balboa L, Pingris K, Souriant S, Poincloux R, et al. Tuberculosis Is Associated With Expansion of a Motile, Permissive and

Immunomodulatory CD16(+) Monocyte Population via the IL-10/STAT3 Axis. *Cell Res* (2015) 25(12):1333–51. doi: 10.1038/cr.2015.123
74. Nimmerjahn F, Ravetch JV. Divergent Immunoglobulin G Subclass Activity Through Selective Fc Receptor Binding. *Science* (2005) 310(5753):1510–2. doi: 10.1126/science.1118948
75. Clynes R, Maizes JS, Guinamard R, Ono M, Takai T, Ravetch JV. Modulation of Immune Complex-Induced Inflammation In Vivo by the Coordinate Expression of Activation and Inhibitory Fc Receptors. *J Exp Med* (1999) 189(1):179–85. doi: 10.1084/jem.189.1.179
76. Lu LL, Suscovich TJ, Fortune SM, Alter G. Beyond Binding: Antibody Effector Functions in Infectious Diseases. *Nat Rev Immunol* (2018) 18(1):46–61. doi: 10.1038/nri.2017.106
77. Cloutier N, Allaeys I, Marcoux G, Machlus KR, Mailhot B, Zufferey A, et al. Platelets Release Pathogenic Serotonin and Return to Circulation After Immune Complex-Mediated Sequestration. *Proc Natl Acad Sci USA* (2018) 115(7):E1550–9. doi: 10.1073/pnas.1720553115
78. Cui L, Lee YH, Thein TL, Fang J, Pang J, Ooi EE, et al. Serum Metabolomics Reveals Serotonin as a Predictor of Severe Dengue in the Early Phase of Dengue Fever. *PloS Negl Trop Dis* (2016) 10(4):e0004607. doi: 10.1371/journal.pntd.0004607
79. Sips M, Krykbaeva M, Diefenbach TJ, Ghebremichael M, Bowman BA, Dugast AS, et al. Fc Receptor-Mediated Phagocytosis in Tissues as a Potent Mechanism for Preventive and Therapeutic HIV Vaccine Strategies. *Mucosal Immunol* (2016) 9(6):1584–95. doi: 10.1038/mi.2016.12
80. Suh CI, Stull ND, Li XJ, Tian W, Price MO, Grinstein S, et al. The Phosphoinositide-Binding Protein P40phox Activates the NADPH Oxidase During FcgammaIIA Receptor-Induced Phagocytosis. *J Exp Med* (2006) 203(8):1915–25. doi: 10.1084/jem.20052085
81. Stacey HD, Golubeva D, Posca A, Ang JC, Novakowski KE, Zahoor MA, et al. IgA Potentiates NETosis in Response to Viral Infection. *Proc Natl Acad Sci USA* (2021) 118(27):e2101497118. doi: 10.1073/pnas.2101497118
82. Jonsson F, de Chaisemartin L, Granger V, Gouel-Cheron A, Gillis CM, Zhu Q, et al. An IgG-Induced Neutrophil Activation Pathway Contributes to Human Drug-Induced Anaphylaxis. *Sci Transl Med* (2019) 11(500): eaat1479. doi: 10.1126/scitranslmed.aat1479
83. Das M, Karnam A, Stephen-Victor E, Gilardin L, Bhatt B, Kumar Sharma V, et al. Intravenous Immunoglobulin Mediates Anti-Inflammatory Effects in Peripheral Blood Mononuclear Cells by Inducing Autophagy. *Cell Death Dis* (2020) 11(1):50. doi: 10.1038/s41419-020-2249-y
84. Bonnerot C, Briken V, Brachet V, Lankar D, Cassard S, Jabri B, et al. Syk Protein Tyrosine Kinase Regulates Fc Receptor Gamma-Chain-Mediated Transport to Lysosomes. *EMBO J* (1998) 17(16):4606–16. doi: 10.1093/emboj/17.16.4606
85. Hirako IC, Gallego-Marin C, Ataide MA, Andrade WA, Gravina H, Rocha BC, et al. DNA-Containing Immunocomplexes Promote Inflammasome Assembly and Release of Pyrogenic Cytokines by CD14+ CD16+ CD64high CD32low Inflammatory Monocytes From Malaria Patients. *mBio* (2015) 6 (6):e01605–15. doi: 10.1128/mBio.01605-15
86. Labzin LI, Bottermann M, Rodriguez-Silvestre P, Foss S, Andersen JT, Vaysburd M, et al. Antibody and DNA Sensing Pathways Converge to Activate the Inflammasome During Primary Human Macrophage Infection. *EMBO J* (2019) 38(21):e101365. doi: 10.15252/embj.2018101365
87. Dhodapkar KM, Kaufman JL, Ehlers M, Banerjee DK, Bonvini E, Koenig S, et al. Selective Blockade of Inhibitory Fcgamma Receptor Enables Human Dendritic Cell Maturation With IL-12p70 Production and Immunity to Antibody-Coated Tumor Cells. *Proc Natl Acad Sci USA* (2005) 102(8):2910–5. doi: 10.1073/pnas.0500014102
88. Regnault A, Lankar D, Lacabanne V, Rodriguez A, Thery C, Rescigno M, et al. Fcgamma Receptor-Mediated Induction of Dendritic Cell Maturation and Major Histocompatibility Complex Class I-Restricted Antigen Presentation After Immune Complex Internalization. *J Exp Med* (1999) 189(2):371–80. doi: 10.1084/jem.189.2.371
89. Hoffmann E, Kotsias F, Visentin G, Bruhns P, Savina A, Amigorena S. Autonomous Phagosomal Degradation and Antigen Presentation in Dendritic Cells. *Proc Natl Acad Sci USA* (2012) 109(36):14556–61. doi: 10.1073/pnas.1203912109
90. Chen T, Blanc C, Eder AZ, Prados-Rosales R, Souza AC, Kim RS, et al. Association of Human Antibodies to Arabinomannan With Enhanced Mycobacterial Opsonophagocytosis and Intracellular Growth Reduction. *J Infect Dis* (2016) 214(2):300–10. doi: 10.1093/infdis/jiw141
91. McEwan WA, Tam JC, Watkinson RE, Bidgood SR, Mallery DL, James LC. Intracellular Antibody-Bound Pathogens Stimulate Immune Signaling via the Fc Receptor TRIM21. *Nat Immunol* (2013) 14(4):327–36. doi: 10.1038/ni.2548
92. MacLennan IC. Germinal Centers. *Annu Rev Immunol* (1994) 12:117–39. doi: 10.1146/annurev.iy.12.040194.001001
93. Slight SR, Rangel-Moreno J, Gopal R, Lin Y, Fallert Junecko BA, Mehra S, et al. CXCR5(+) T Helper Cells Mediate Protective Immunity Against Tuberculosis. *J Clin Invest* (2013) 123(2):712–26. doi: 10.1172/JCI65728
94. Walker LS, Gulbranson-Judge A, Flynn S, Brocker T, Raykundalia C, Goodall M, et al. Compromised OX40 Function in CD28-Deficient Mice Is Linked With Failure to Develop CXC Chemokine Receptor 5-Positive CD4 Cells and Germinal Centers. *J Exp Med* (1999) 190(8):1115–22. doi: 10.1084/jem.190.8.1115
95. Mesin L, Ersching J, Victora GD. Germinal Center B Cell Dynamics. *Immunity* (2016) 45(3):471–82. doi: 10.1016/j.immuni.2016.09.001
96. Olmos S, Stukes S, Ernst JD. Ectopic Activation of Mycobacterium Tuberculosis-Specific CD4+ T Cells in Lungs of CCR7-/- Mice. *J Immunol* (2010) 184(2):895–901. doi: 10.4049/jimmunol.0901230
97. Phuah JY, Mattila JT, Lin PL, Flynn JL. Activated B Cells in the Granulomas of Nonhuman Primates Infected With Mycobacterium Tuberculosis. *Am J Pathol* (2012) 181(2):508–14. doi: 10.1016/j.ajpath.2012.05.009
98. Dunlap MD, Prince OA, Rangel-Moreno J, Thomas KA, Scordo JM, Torrelles JB, et al. Formation of Lung Inducible Bronchus Associated Lymphoid Tissue Is Regulated by Mycobacterium Tuberculosis Expressed Determinants. *Front Immunol* (2020) 11:1325. doi: 10.3389/fimmu.2020.01325
99. Ulrichs T, Kosmiadi GA, Trusov V, Jorg S, Pradl L, Titukhina M, et al. Human Tuberculous Granulomas Induce Peripheral Lymphoid Follicle-Like Structures to Orchestrate Local Host Defence in the Lung. *J Pathol* (2004) 204(2):217–28. doi: 10.1002/path.1628
100. Ron Y, Sprent J. T Cell Priming In Vivo: A Major Role for B Cells in Presenting Antigen to T Cells in Lymph Nodes. *J Immunol* (1987) 138 (9):2848–56.
101. Cyster JG, Allen CDC. B Cell Responses: Cell Interaction Dynamics and Decisions. *Cell* (2019) 177(3):524–40. doi: 10.1016/j.cell.2019.03.016
102. Joosten SA, van Meijgaarden KE, Del Nonno F, Baiocchini A, Petrone L, Vanini V, et al. Patients With Tuberculosis Have a Dysfunctional Circulating B-Cell Compartment, Which Normalizes Following Successful Treatment. *PloS Pathog* (2016) 12(6):e1005687. doi: 10.1371/journal.ppat.1005687
103. du Plessis WJ, Keyser A, Walzl G, Loxton AG. Phenotypic Analysis of Peripheral B Cell Populations During Mycobacterium Tuberculosis Infection and Disease. *J Inflammation (Lond)* (2016) 13:23. doi: 10.1186/s12950-016-0133-4
104. Abreu MT, Carvalheiro H, Rodrigues-Sousa T, Domingos A, Segorbe-Luis A, Rodrigues-Santos P, et al. Alterations in the Peripheral Blood B Cell Subpopulations of Multidrug-Resistant Tuberculosis Patients. *Clin Exp Med* (2014) 14(4):423–9. doi: 10.1007/s10238-013-0258-1
105. Possamai D, Page G, Panes R, Gagnon E, Lapointe R. CD40L-Stimulated B Lymphocytes Are Polarized Toward APC Functions After Exposure to IL-4 and IL-21. *J Immunol* (2021) 207(1):77–89. doi: 10.4049/jimmunol.2001173
106. Kleindienst P, Brocker T. Concerted Antigen Presentation by Dendritic Cells and B Cells is Necessary for Optimal CD4 T-Cell Immunity In Vivo. *Immunology* (2005) 115(4):556–64. doi: 10.1111/j.1365-2567.2005.02196.x
107. Marin ND, Dunlap MD, Kaushal D, Khader SA. Friend or Foe: The Protective and Pathological Roles of Inducible Bronchus-Associated Lymphoid Tissue in Pulmonary Diseases. *J Immunol* (2019) 202(9):2519–26. doi: 10.4049/jimmunol.1801135
108. Mathieu M, Cotta-Grand N, Daudelin JF, Boulet S, Lapointe R, Labrecque N. CD40-Activated B Cells can Efficiently Prime Antigen-Specific Naive CD8+ T Cells to Generate Effector But Not Memory T Cells. *PloS One* (2012) 7(1): e30139. doi: 10.1371/journal.pone.0030139
109. Shen P, Fillatreau S. Antibody-Independent Functions of B Cells: A Focus on Cytokines. *Nat Rev Immunol* (2015) 15(7):441–51. doi: 10.1038/nri3857
110. Neves P, Lampropoulou V, Calderon-Gomez E, Roch T, Stervbo U, Shen P, et al. Signaling via the MyD88 Adaptor Protein in B Cells Suppresses

Protective Immunity During Salmonella Typhimurium Infection. *Immunity* (2010) 33(5):777–90. doi: 10.1016/j.immuni.2010.10.016
111. Lee CC, Kung JT. Marginal Zone B Cell Is a Major Source of Il-10 in Listeria Monocytogenes Susceptibility. *J Immunol* (2012) 189(7):3319–27. doi: 10.4049/jimmunol.1201247
112. Wong EA, Evans S, Kraus CR, Engelman KD, Maiello P, Flores WJ, et al. IL-10 Impairs Local Immune Response in Lung Granulomas and Lymph Nodes During Early Mycobacterium Tuberculosis Infection. *J Immunol* (2020) 204 (3):644–59. doi: 10.4049/jimmunol.1901211
113. Richardson ET, Shukla S, Sweet DR, Wearsch PA, Tsichlis PN, Boom WH, et al. Toll-Like Receptor 2-Dependent Extracellular Signal-Regulated Kinase Signaling in Mycobacterium Tuberculosis-Infected Macrophages Drives Anti-Inflammatory Responses and Inhibits Th1 Polarization of Responding T Cells. *Infect Immun* (2015) 83(6):2242–54. doi: 10.1128/IAI.00135-15
114. Gideon HP, Phuah J, Myers AJ, Bryson BD, Rodgers MA, Coleman MT, et al. Variability in Tuberculosis Granuloma T Cell Responses Exists, But a Balance of Pro- and Anti-Inflammatory Cytokines Is Associated With Sterilization. *PloS Pathog* (2015) 11(1):e1004603. doi: 10.1371/journal.ppat.1004603
115. Carter NA, Vasconcellos R, Rosser EC, Tulone C, Munoz-Suano A, Kamanaka M, et al. Mice Lacking Endogenous IL-10-Producing Regulatory B Cells Develop Exacerbated Disease and Present With an Increased Frequency of Th1/Th17 But a Decrease in Regulatory T Cells. *J Immunol* (2011) 186(10):5569–79. doi: 10.4049/jimmunol.1100284
116. Flores-Borja F, Bosma A, Ng D, Reddy V, Ehrenstein MR, Isenberg DA, et al. CD19+CD24hiCD38hi B Cells Maintain Regulatory T Cells While Limiting TH1 and TH17 Differentiation. *Sci Transl Med* (2013) 5(173):173ra23. doi: 10.1126/scitranslmed.3005407
117. Zhang M, Zheng X, Zhang J, Zhu Y, Zhu X, Liu H, et al. CD19(+)CD1d(+) CD5(+) B Cell Frequencies are Increased in Patients With Tuberculosis and Suppress Th17 Responses. *Cell Immunol* (2012) 274(1-2):89–97. doi: 10.1016/j.cellimm.2012.01.007
118. Zhang M, Zeng G, Yang Q, Zhang J, Zhu X, Chen Q, et al. Anti-Tuberculosis Treatment Enhances the Production of IL-22 Through Reducing the Frequencies of Regulatory B Cell. *Tuberculosis (Edinb)* (2014) 94(3):238–44. doi: 10.1016/j.tube.2013.12.003
119. Reynolds HY. Immunoglobulin G and Its Function in the Human Respiratory Tract. *Mayo Clin Proc* (1988) 63(2):161–74. doi: 10.1016/S0025-6196(12)64949-0
120. Sterlin D, Mathian A, Miyara M, Mohr A, Anna F, Claer L, et al. IgA Dominates the Early Neutralizing Antibody Response to SARS-CoV-2. *Sci Transl Med* (2021) 13(577):eabd2223. doi: 10.1126/scitranslmed.abd2223
121. Vogelzang A, Lozza L, Reece ST, Perdomo C, Zedler U, Hahnke K, et al. Neonatal Fc Receptor Regulation of Lung Immunoglobulin and CD103+ Dendritic Cells Confers Transient Susceptibility to Tuberculosis. *Infect Immun* (2016) 84(10):2914–21. doi: 10.1128/IAI.00533-16
122. Reyes F, Tirado Y, Puig A, Borrero R, Reyes G, Fernandez S, et al. Immunogenicity and Cross-Reactivity Against Mycobacterium Tuberculosis of Proteoliposomes Derived From Mycobacterium Bovis BCG. *BMC Immunol* (2013) 14 Suppl 1:S7. doi: 10.1186/1471-2172-14-S1-S7
123. Shah JA, Lindestam Arlehamn CS, Horne DJ, Sette A, Hawn TR. Nontuberculous Mycobacteria and Heterologous Immunity to Tuberculosis. *J Infect Dis* (2019) 220(7):1091–8. doi: 10.1093/infdis/jiz285
124. Perley CC, Frahm M, Click EM, Dobos KM, Ferrari G, Stout JE, et al. The Human Antibody Response to the Surface of Mycobacterium Tuberculosis. *PloS One* (2014) 9(2):e98938. doi: 10.1371/journal.pone.0098938
125. Zeng MY, Cisalpino D, Varadarajan S, Hellman J, Warren HS, Cascalho M, et al. Gut Microbiota-Induced Immunoglobulin G Controls Systemic Infection by Symbiotic Bacteria and Pathogens. *Immunity* (2016) 44 (3):647–58. doi: 10.1016/j.immuni.2016.02.006
126. Ochsenbein AF, Fehr T, Lutz C, Suter M, Brombacher F, Hengartner H, et al. Control of Early Viral and Bacterial Distribution and Disease by Natural Antibodies. *Science* (1999) 286(5447):2156–9. doi: 10.1126/science.286.5447.2156
127. Griffin DO, Holodick NE, Rothstein TL. Human B1 Cells in Umbilical Cord and Adult Peripheral Blood Express the Novel Phenotype CD20+ CD27+ CD43+ Cd70. *J Exp Med* (2011) 208(1):67–80. doi: 10.1084/jem.20101499
128. Jayasekera JP, Moseman EA, Carroll MC. Natural Antibody and Complement Mediate Neutralization of Influenza Virus in the Absence of Prior Immunity. *J Virol* (2007) 81(7):3487–94. doi: 10.1128/JVI.02128-06
129. Vas J, Gronwall C, Silverman GJ. Fundamental Roles of the Innate-Like Repertoire of Natural Antibodies in Immune Homeostasis. *Front Immunol* (2013) 4:4. doi: 10.3389/fimmu.2013.00004
130. Martin CJ, Booty MG, Rosebrock TR, Nunes-Alves C, Desjardins DM, Keren I, et al. Efferocytosis is an Innate Antibacterial Mechanism. *Cell Host Microbe* (2012) 12(3):289–300. doi: 10.1016/j.chom.2012.06.010
131. Baumgarth N, Herman OC, Jager GC, Brown LE, Herzenberg LA, Chen J. B-1 and B-2 Cell-Derived Immunoglobulin M Antibodies are Nonredundant Components of the Protective Response to Influenza Virus Infection. *J Exp Med* (2000) 192(2):271–80. doi: 10.1084/jem.192.2.271
132. Boes M, Prodeus AP, Schmidt T, Carroll MC, Chen J. A Critical Role of Natural Immunoglobulin M in Immediate Defense Against Systemic Bacterial Infection. *J Exp Med* (1998) 188(12):2381–6. doi: 10.1084/jem.188.12.2381
133. Panda S, Ding JL. Natural Antibodies Bridge Innate and Adaptive Immunity. *J Immunol* (2015) 194(1):13–20. doi: 10.4049/jimmunol.1400844
134. Panda S, Zhang J, Tan NS, Ho B, Ding JL. Natural IgG Antibodies Provide Innate Protection Against Ficolin-Opsonized Bacteria. *EMBO J* (2013) 32 (22):2905–19. doi: 10.1038/emboj.2013.199
135. Schubert OT, Ludwig C, Kogadeeva M, Zimmermann M, Rosenberger G, Gengenbacher M, et al. Absolute Proteome Composition and Dynamics During Dormancy and Resuscitation of Mycobacterium Tuberculosis. *Cell Host Microbe* (2015) 18(1):96–108. doi: 10.1016/j.chom.2015.06.001
136. Gopinath V, Raghunandanan S, Gomez RL, Jose L, Surendran A, Ramachandran R, et al. Profiling the Proteome of Mycobacterium Tuberculosis During Dormancy and Reactivation. *Mol Cell Proteomics* (2015) 14(8):2160–76. doi: 10.1074/mcp.M115.051151
137. Leyten EM, Lin MY, Franken KL, Friggen AH, Prins C, van Meijgaarden KE, et al. Human T-Cell Responses to 25 Novel Antigens Encoded by Genes of the Dormancy Regulon of Mycobacterium Tuberculosis. *Microbes Infect* (2006) 8(8):2052–60. doi: 10.1016/j.micinf.2006.03.018
138. Coscolla M, Gagneux S. Consequences of Genomic Diversity in Mycobacterium Tuberculosis. *Semin Immunol* (2014) 26(6):431–44. doi: 10.1016/j.smim.2014.09.012
139. Cambier CJ, Banik SM, Buonomo JA, Bertozzi CR. Spreading of a Mycobacterial Cell-Surface Lipid Into Host Epithelial Membranes Promotes Infectivity. *Elife* (2020) 9:e60648. doi: 10.7554/eLife.60648
140. Beatty WL, Rhoades ER, Ullrich HJ, Chatterjee D, Heuser JE, Russell DG. Trafficking and Release of Mycobacterial Lipids From Infected Macrophages. *Traffic* (2000) 1(3):235–47. doi: 10.1034/j.1600-0854.2000.010306.x
141. Kruh-Garcia NA, Wolfe LM, Chaisson LH, Worodria WO, Nahid P, Schorey JS, et al. Detection of Mycobacterium Tuberculosis Peptides in the Exosomes of Patients With Active and Latent M. Tuberculosis Infection Using MRM-MS. *PloS One* (2014) 9(7):e103811. doi: 10.1371/journal.pone.0103811
142. Singh PP, Smith VL, Karakousis PC, Schorey JS. Exosomes Isolated From Mycobacteria-Infected Mice or Cultured Macrophages can Recruit and Activate Immune Cells In Vitro and In Vivo. *J Immunol* (2012) 189 (2):777–85. doi: 10.4049/jimmunol.1103638
143. Spiekermann GM, Finn PW, Ward ES, Dumont J, Dickinson BL, Blumberg RS, et al. Receptor-Mediated Immunoglobulin G Transport Across Mucosal Barriers in Adult Life: Functional Expression of FcRn in the Mammalian Lung. *J Exp Med* (2002) 196(3):303–10. doi: 10.1084/jem.20020400
144. Tjarnlund A, Rodriguez A, Cardona PJ, Guirado E, Ivanyi J, Singh M, et al. Polymeric IgR Knockout Mice Are More Susceptible to Mycobacterial Infections in the Respiratory Tract Than Wild-Type Mice. *Int Immunol* (2006) 18(5):807–16. doi: 10.1093/intimm/dxl017
145. Shibuya A, Sakamoto N, Shimizu Y, Shibuya K, Osawa M, Hiroyama T, et al. Fc Alpha/Mu Receptor Mediates Endocytosis of IgM-Coated Microbes. *Nat Immunol* (2000) 1(5):441–6. doi: 10.1038/80886
146. Stockert RJ, Kressner MS, Collins JC, Sternlieb I, Morell AG. IgA Interaction With the Asialoglycoprotein Receptor. *Proc Natl Acad Sci USA* (1982) 79 (20):6229–31. doi: 10.1073/pnas.79.20.6229
147. Moura IC, Centelles MN, Arcos-Fajardo M, Malheiros DM, Collawn JF, Cooper MD, et al. Identification of the Transferrin Receptor as a Novel Immunoglobulin (Ig)A1 Receptor and its Enhanced Expression on Mesangial Cells in IgA Nephropathy. *J Exp Med* (2001) 194(4):417–25. doi: 10.1084/jem.194.4.417
148. Mantis NJ, Cheung MC, Chintalacharuvu KR, Rey J, Corthesy B, Neutra MR. Selective Adherence of IgA to Murine Peyer's Patch M Cells: Evidence for a

Novel IgA Receptor. *J Immunol* (2002) 169(4):1844–51. doi: 10.4049/jimmunol.169.4.1844
149. Golebski K, Hoepel W, van Egmond D, de Groot EJ, Amatngalim GD, Beekman JM, et al. FcgammaRIII Stimulation Breaks the Tolerance of Human Nasal Epithelial Cells to Bacteria Through Cross-Talk With TLR4. *Mucosal Immunol* (2019) 12(2):425–33. doi: 10.1038/s41385-018-0129-x
150. Xia YC, Schuliga M, Shepherd M, Powell M, Harris T, Langenbach SY, et al. Functional Expression of IgG-Fc Receptors in Human Airway Smooth Muscle Cells. *Am J Respir Cell Mol Biol* (2011) 44(5):665–72. doi: 10.1165/rcmb.2009-0371OC
151. Cohen SB, Gern BH, Delahaye JL, Adams KN, Plumlee CR, Winkler JK, et al. Alveolar Macrophages Provide an Early Mycobacterium Tuberculosis Niche and Initiate Dissemination. *Cell Host Microbe* (2018) 24(3):439–46.e4. doi: 10.1016/j.chom.2018.08.001
152. Papp AC, Azad AK, Pietrzak M, Williams A, Handelman SK, Igo RP Jr, et al. AmpliSeq Transcriptome Analysis of Human Alveolar and Monocyte-Derived Macrophages Over Time in Response to Mycobacterium Tuberculosis Infection. *PloS One* (2018) 13(5):e0198221. doi: 10.1371/journal.pone.0198221
153. Verreck FA, de Boer T, Langenberg DM, Hoeve MA, Kramer M, Vaisberg E, et al. Human IL-23-Producing Type 1 Macrophages Promote But IL-10-Producing Type 2 Macrophages Subvert Immunity to (Myco)Bacteria. *Proc Natl Acad Sci USA* (2004) 101(13):4560–5. doi: 10.1073/pnas.0400983101
154. Pisu D, Huang L, Narang V, Theriault M, Le-Bury G, Lee B, et al. Single Cell Analysis of M. Tuberculosis Phenotype and Macrophage Lineages in the Infected Lung. *J Exp Med* (2021) 218(9):e20210615. doi: 10.1084/jem.20210615
155. Bryson BD, Rosebrock TR, Tafesse FG, Itoh CY, Nibasumba A, Babunovic GH, et al. Heterogeneous GM-CSF Signaling in Macrophages is Associated With Control of Mycobacterium Tuberculosis. *Nat Commun* (2019) 10(1):2329. doi: 10.1038/s41467-019-10065-8
156. Pincetic A, Bournazos S, DiLillo DJ, Maamary J, Wang TT, Dahan R, et al. Type I and Type II Fc Receptors Regulate Innate and Adaptive Immunity. *Nat Immunol* (2014) 15(8):707–16. doi: 10.1038/ni.2939
157. Bruggeman CW, Houtzager J, Dierdorp B, Kers J, Pals ST, Lutter R, et al. Tissue-Specific Expression of IgG Receptors by Human Macrophages Ex Vivo. *PloS One* (2019) 14(10):e0223264. doi: 10.1371/journal.pone.0223264
158. Li Y, Lee PY, Sobel ES, Narain S, Satoh M, Segal MS, et al. Increased Expression of FcgammaRI/CD64 on Circulating Monocytes Parallels Ongoing Inflammation and Nephritis in Lupus. *Arthritis Res Ther* (2009) 11(1):R6. doi: 10.1186/ar2591
159. Armstrong JA, Hart PD. Phagosome-Lysosome Interactions in Cultured Macrophages Infected With Virulent Tubercle Bacilli. Reversal of the Usual Nonfusion Pattern and Observations on Bacterial Survival. *J Exp Med* (1975) 142(1):1–16. doi: 10.1084/jem.142.1.1
160. Joller N, Weber SS, Muller AJ, Sporri R, Selchow P, Sander P, et al. Antibodies Protect Against Intracellular Bacteria by Fc Receptor-Mediated Lysosomal Targeting. *Proc Natl Acad Sci USA* (2010) 107(47):20441–6. doi: 10.1073/pnas.1013827107
161. Faridgohar M, Nikoueinejad H. New Findings of Toll-Like Receptors Involved in Mycobacterium Tuberculosis Infection. *Pathog Glob Health* (2017) 111(5):256–64. doi: 10.1080/20477724.2017.1351080
162. Vogelpoel LT, Hansen IS, Rispens T, Muller FJ, van Capel TM, Turina MC, et al. Fc Gamma Receptor-TLR Cross-Talk Elicits Pro-Inflammatory Cytokine Production by Human M2 Macrophages. *Nat Commun* (2014) 5:5444. doi: 10.1038/ncomms6444
163. Moreira-Teixeira L, Stimpson PJ, Stavropoulos E, Hadebe S, Chakravarty P, Ioannou M, et al. Type I IFN Exacerbates Disease in Tuberculosis-Susceptible Mice by Inducing Neutrophil-Mediated Lung Inflammation and NETosis. *Nat Commun* (2020) 11(1):5566. doi: 10.1038/s41467-020-19412-6
164. Schiff DE, Rae J, Martin TR, Davis BH, Curnutte JT. Increased Phagocyte Fc gammaRI Expression and Improved Fc Gamma-Receptor-Mediated Phagocytosis After In Vivo Recombinant Human Interferon-Gamma Treatment of Normal Human Subjects. *Blood* (1997) 90(8):3187–94. doi: 10.1182/blood.V90.8.3187
165. Zak DE, Penn-Nicholson A, Scriba TJ, Thompson E, Suliman S, Amon LM, et al. A Blood RNA Signature for Tuberculosis Disease Risk: A Prospective Cohort Study. *Lancet* (2016) 387(10035):2312–22. doi: 10.1016/S0140-6736(15)01316-1
166. Cid J, Aguinaco R, Sanchez R, Garcia-Pardo G, Llorente A. Neutrophil CD64 Expression as Marker of Bacterial Infection: A Systematic Review and Meta-Analysis. *J Infect* (2010) 60(5):313–9. doi: 10.1016/j.jinf.2010.02.013
167. Treffers LW, van Houdt M, Bruggeman CW, Heineke MH, Zhao XW, van der Heijden J, et al. FcgammaRIIIb Restricts Antibody-Dependent Destruction of Cancer Cells by Human Neutrophils. *Front Immunol* (2018) 9:3124. doi: 10.3389/fimmu.2018.03124
168. Balu S, Reljic R, Lewis MJ, Pleass RJ, McIntosh R, van Kooten C, et al. A Novel Human IgA Monoclonal Antibody Protects Against Tuberculosis. *J Immunol* (2011) 186(5):3113–9. doi: 10.4049/jimmunol.1003189
169. Tran AC, Diogo GR, Paul MJ, Copland A, Hart P, Mehta N, et al. Mucosal Therapy of Multi-Drug Resistant Tuberculosis With IgA and Interferon-Gamma. *Front Immunol* (2020) 11:582833. doi: 10.3389/fimmu.2020.582833
170. Otten MA, Rudolph E, Dechant M, Tuk CW, Reijmers RM, Beelen RH, et al. Immature Neutrophils Mediate Tumor Cell Killing via IgA But Not IgG Fc Receptors. *J Immunol* (2005) 174(9):5472–80. doi: 10.4049/jimmunol.174.9.5472
171. Matlung HL, Babes L, Zhao XW, van Houdt M, Treffers LW, van Rees DJ, et al. Neutrophils Kill Antibody-Opsonized Cancer Cells by Trogoptosis. *Cell Rep* (2018) 23(13):3946–59.e6. doi: 10.1016/j.celrep.2018.05.082
172. Richardson SI, Crowther C, Mkhize NN, Morris L. Measuring the Ability of HIV-Specific Antibodies to Mediate Trogocytosis. *J Immunol Methods* (2018) 463:71–83. doi: 10.1016/j.jim.2018.09.009
173. Steele S, Radlinski L, Taft-Benz S, Brunton J, Kawula TH. Trogocytosis-Associated Cell to Cell Spread of Intracellular Bacterial Pathogens. *Elife* (2016) 5:e10625. doi: 10.7554/eLife.10625
174. Chen K, Nishi H, Travers R, Tsuboi N, Martinod K, Wagner DD, et al. Endocytosis of Soluble Immune Complexes Leads to Their Clearance by FcgammaRIIIB But Induces Neutrophil Extracellular Traps via FcgammaRIIA In Vivo. *Blood* (2012) 120(22):4421–31. doi: 10.1182/blood-2011-12-401133
175. Aleman OR, Mora N, Cortes-Vieyra R, Uribe-Querol E, Rosales C. Differential Use of Human Neutrophil Fcgamma Receptors for Inducing Neutrophil Extracellular Trap Formation. *J Immunol Res* (2016) 2016:2908034. doi: 10.1155/2016/2908034
176. Griffiths KL, Ahmed M, Das S, Gopal R, Horne W, Connell TD, et al. Targeting Dendritic Cells to Accelerate T-Cell Activation Overcomes a Bottleneck in Tuberculosis Vaccine Efficacy. *Nat Commun* (2016) 7:13894. doi: 10.1038/ncomms13894
177. Guilliams M, Bruhns P, Saeys Y, Hammad H, Lambrecht BN. The Function of Fcgamma Receptors in Dendritic Cells and Macrophages. *Nat Rev Immunol* (2014) 14(2):94–108. doi: 10.1038/nri3582
178. Wolf AJ, Desvignes L, Linas B, Banaiee N, Tamura T, Takatsu K, et al. Initiation of the Adaptive Immune Response to Mycobacterium Tuberculosis Depends on Antigen Production in the Local Lymph Node, Not the Lungs. *J Exp Med* (2008) 205(1):105–15. doi: 10.1084/jem.20071367
179. Liu X, Lu L, Yang Z, Palaniyandi S, Zeng R, Gao LY, et al. The Neonatal FcR-Mediated Presentation of Immune-Complexed Antigen is Associated With Endosomal and Phagosomal pH and Antigen Stability in Macrophages and Dendritic Cells. *J Immunol* (2011) 186(8):4674–86. doi: 10.4049/jimmunol.1003584
180. DiLillo DJ, Ravetch JV. Differential Fc-Receptor Engagement Drives an Anti-Tumor Vaccinal Effect. *Cell* (2015) 161(5):1035–45. doi: 10.1016/j.cell.2015.04.016
181. Bournazos S, Ravetch JV, Corti D, Virgin HW. Fc-Optimized Antibodies Elicit CD8 Immunity to Viral Respiratory Infection. *Nature* (2020) 588(7838):485–90. doi: 10.1038/s41586-020-2838-z
182. Brooks DG, Qiu WQ, Luster AD, Ravetch JV. Structure and Expression of Human IgG FcRII(CD32). Functional Heterogeneity is Encoded by the Alternatively Spliced Products of Multiple Genes. *J Exp Med* (1989) 170(4):1369–85. doi: 10.1084/jem.170.4.1369
183. El Shikh ME, El Sayed RM, Sukumar S, Szakal AK, Tew JG. Activation of B Cells by Antigens on Follicular Dendritic Cells. *Trends Immunol* (2010) 31(6):205–11. doi: 10.1016/j.it.2010.03.002
184. Muta T, Kurosaki T, Misulovin Z, Sanchez M, Nussenzweig MC, Ravetch JV. A 13-Amino-Acid Motif in the Cytoplasmic Domain of Fc Gamma RIIB Modulates B-Cell Receptor Signalling. *Nature* (1994) 368(6466):70–3. doi: 10.1038/368070a0

185. Farley CR, Morris AB, Tariq M, Bennion KB, Potdar S, Kudchadkar R, et al. FcgammaRIIB is a T Cell Checkpoint in Antitumor Immunity. *JCI Insight* (2021) 6(4):e135623. doi: 10.1172/jci.insight.135623
186. Holgado MP, Sananez I, Raiden S, Geffner JR, Arruvito L. CD32 Ligation Promotes the Activation of CD4(+) T Cells. *Front Immunol* (2018) 9:2814. doi: 10.3389/fimmu.2018.02814
187. Abdel-Mohsen M, Kuri-Cervantes L, Grau-Exposito J, Spivak AM, Nell RA, Tomescu C, et al. CD32 is Expressed on Cells With Transcriptionally Active HIV But Does Not Enrich for HIV DNA in Resting T Cells. *Sci Transl Med* (2018) 10(437):eaar6759. doi: 10.1126/scitranslmed.aar6759
188. Engelhardt W, Matzke J, Schmidt RE. Activation-Dependent Expression of Low Affinity IgG Receptors Fc Gamma RII(CD32) and Fc Gamma RIII (CD16) in Subpopulations of Human T Lymphocytes. *Immunobiology* (1995) 192(5):297–320. doi: 10.1016/S0171-2985(11)80172-5
189. Virdi AK, Wallace J, Barbian H, Richards MH, Ritz EM, Sha B, et al. CD32 Is Enriched on CD4dimCD8bright T Cells. *PloS One* (2020) 15(9):e0239157. doi: 10.1371/journal.pone.0239157
190. Meryk A, Pangrazzi L, Hagen M, Hatzmann F, Jenewein B, Jakic B, et al. Fcmu Receptor as a Costimulatory Molecule for T Cells. *Cell Rep* (2019) 26 (10):2681–91.e5. doi: 10.1016/j.celrep.2019.02.024
191. Henrickson SE, von Andrian UH. Single-Cell Dynamics of T-Cell Priming. *Curr Opin Immunol* (2007) 19(3):249–58. doi: 10.1016/j.coi.2007.04.013
192. Carpenter SM, Yang JD, Lee J, Barreira-Silva P, Behar SM. Vaccine-Elicited Memory CD4+ T Cell Expansion is Impaired in the Lungs During Tuberculosis. *PloS Pathog* (2017) 13(11):e1006704. doi: 10.1371/journal.ppat.1006704
193. Samstein M, Schreiber HA, Leiner IM, Susac B, Glickman MS, Pamer EG. Essential Yet Limited Role for CCR2(+) Inflammatory Monocytes During Mycobacterium Tuberculosis-Specific T Cell Priming. *Elife* (2013) 2:e01086. doi: 10.7554/eLife.01086.013
194. Lykken JM, DiLillo DJ, Weimer ET, Roser-Page S, Heise MT, Grayson JM, et al. Acute and Chronic B Cell Depletion Disrupts CD4+ and CD8+ T Cell Homeostasis and Expansion During Acute Viral Infection in Mice. *J Immunol* (2014) 193(2):746–56. doi: 10.4049/jimmunol.1302848
195. Fiocca Vernengo F, Beccaria CG, Araujo Furlan CL, Tosello Boari J, Almada L, Gorosito Serran M, et al. CD8(+) T Cell Immunity Is Compromised by Anti-CD20 Treatment and Rescued by Interleukin-17a. *mBio* (2020) 11(3): e00447–20. doi: 10.1128/mBio.00447-20
196. Mollo SB, Zajac AJ, Harrington LE. Temporal Requirements for B Cells in the Establishment of CD4 T Cell Memory. *J Immunol* (2013) 191(12):6052–9. doi: 10.4049/jimmunol.1302033
197. Bouaziz JD, Yanaba K, Venturi GM, Wang Y, Tisch RM, Poe JC, et al. Therapeutic B Cell Depletion Impairs Adaptive and Autoreactive CD4+ T Cell Activation in Mice. *Proc Natl Acad Sci USA* (2007) 104(52):20878–83. doi: 10.1073/pnas.0709205105
198. Ugrinovic S, Menager N, Goh N, Mastroeni P. Characterization and Development of T-Cell Immune Responses in B-Cell-Deficient (Igh-6(-/-)) Mice With Salmonella Enterica Serovar Typhimurium Infection. *Infect Immun* (2003) 71(12):6808–19. doi: 10.1128/IAI.71.12.6808-6819.2003
199. Kroeger DR, Rudulier CD, Bretscher PA. Antigen Presenting B Cells Facilitate CD4 T Cell Cooperation Resulting in Enhanced Generation of Effector and Memory CD4 T Cells. *PloS One* (2013) 8(10):e77346. doi: 10.1371/journal.pone.0077346
200. Raposo G, Nijman HW, Stoorvogel W, Liejendekker R, Harding CV, Melief CJ, et al. B Lymphocytes Secrete Antigen-Presenting Vesicles. *J Exp Med* (1996) 183(3):1161–72. doi: 10.1084/jem.183.3.1161
201. Muntasell A, Berger AC, Roche PA. T Cell-Induced Secretion of MHC Class II-Peptide Complexes on B Cell Exosomes. *EMBO J* (2007) 26(19):4263–72. doi: 10.1038/sj.emboj.7601842
202. Saunderson SC, McLellan AD. Role of Lymphocyte Subsets in the Immune Response to Primary B Cell-Derived Exosomes. *J Immunol* (2017) 199 (7):2225–35. doi: 10.4049/jimmunol.1601537
203. Hwang I, Shen X, Sprent J. Direct Stimulation of Naive T Cells by Membrane Vesicles From Antigen-Presenting Cells: Distinct Roles for CD54 and B7 Molecules. *Proc Natl Acad Sci U.S.A.* (2003) 100(11):6670–5. doi: 10.1073/pnas.1131852100
204. Giri PK, Schorey JS. Exosomes Derived From M. Bovis BCG Infected Macrophages Activate Antigen-Specific CD4+ and CD8+ T Cells In Vitro and In Vivo. *PloS One* (2008) 3(6):e2461. doi: 10.1371/journal.pone.0002461
205. Ramachandra L, Qu Y, Wang Y, Lewis CJ, Cobb BA, Takatsu K, et al. Mycobacterium Tuberculosis Synergizes With ATP to Induce Release of Microvesicles and Exosomes Containing Major Histocompatibility Complex Class II Molecules Capable of Antigen Presentation. *Infect Immun* (2010) 78 (12):5116–25. doi: 10.1128/IAI.01089-09
206. Bhatnagar S, Shinagawa K, Castellino FJ, Schorey JS. Exosomes Released From Macrophages Infected With Intracellular Pathogens Stimulate a Proinflammatory Response In Vitro and In Vivo. *Blood* (2007) 110 (9):3234–44. doi: 10.1182/blood-2007-03-079152
207. Cheng Y, Schorey JS. Exosomes Carrying Mycobacterial Antigens can Protect Mice Against Mycobacterium Tuberculosis Infection. *Eur J Immunol* (2013) 43(12):3279–90. doi: 10.1002/eji.201343727
208. Smith VL, Cheng Y, Bryant BR, Schorey JS. Exosomes Function in Antigen Presentation During an In Vivo Mycobacterium Tuberculosis Infection. *Sci Rep* (2017) 7:43578. doi: 10.1038/srep43578
209. Yang JD, Mott D, Sutiwisesak R, Lu YJ, Raso F, Stowell B, et al. Mycobacterium Tuberculosis-Specific CD4+ and CD8+ T Cells Differ in Their Capacity to Recognize Infected Macrophages. *PloS Pathog* (2018) 14 (5):e1007060. doi: 10.1371/journal.ppat.1007060
210. Srivastava S, Grace PS, Ernst JD. Antigen Export Reduces Antigen Presentation and Limits T Cell Control of M. Tuberculosis. *Cell Host Microbe* (2016) 19(1):44–54. doi: 10.1016/j.chom.2015.12.003
211. Patankar YR, Sutiwisesak R, Boyce S, Lai R, Lindestam Arlehamn CS, Sette A, et al. Limited Recognition of Mycobacterium Tuberculosis-Infected Macrophages by Polyclonal CD4 and CD8 T Cells From the Lungs of Infected Mice. *Mucosal Immunol* (2020) 13(1):140–8. doi: 10.1038/s41385-019-0217-6
212. Wakim LM, Bevan MJ. Cross-Dressed Dendritic Cells Drive Memory CD8+ T-Cell Activation After Viral Infection. *Nature* (2011) 471(7340):629–32. doi: 10.1038/nature09863
213. Foreman TW, Mehra S, LoBato DN, Malek A, Alvarez X, Golden NA, et al. CD4+ T-Cell-Independent Mechanisms Suppress Reactivation of Latent Tuberculosis in a Macaque Model of HIV Coinfection. *Proc Natl Acad Sci USA* (2016) 113(38):E5636–44. doi: 10.1073/pnas.1611987113
214. Kranich J, Krautler NJ, Heinen E, Polymenidou M, Bridel C, Schildknecht A, et al. Follicular Dendritic Cells Control Engulfment of Apoptotic Bodies by Secreting Mfge8. *J Exp Med* (2008) 205(6):1293–302. doi: 10.1084/jem.20071019
215. Smith JP, Burton GF, Tew JG, Szakal AK. Tingible Body Macrophages in Regulation of Germinal Center Reactions. *Dev Immunol* (1998) 6(3-4):285–94. doi: 10.1155/1998/38923
216. Hanayama R, Tanaka M, Miyasaka K, Aozasa K, Koike M, Uchiyama Y, et al. Autoimmune Disease and Impaired Uptake of Apoptotic Cells in MFG-E8-Deficient Mice. *Science* (2004) 304(5674):1147–50. doi: 10.1126/science.1094359
217. Baumann I, Kolowos W, Voll RE, Manger B, Gaipl U, Neuhuber WL, et al. Impaired Uptake of Apoptotic Cells Into Tingible Body Macrophages in Germinal Centers of Patients With Systemic Lupus Erythematosus. *Arthritis Rheum* (2002) 46(1):191–201. doi: 10.1002/1529-0131(200201)46:1<191::AID-ART10027>3.0.CO;2-K
218. Schaible UE, Winau F, Sieling PA, Fischer K, Collins HL, Hagens K, et al. Apoptosis Facilitates Antigen Presentation to T Lymphocytes Through MHC-I and CD1 in Tuberculosis. *Nat Med* (2003) 9(8):1039–46. doi: 10.1038/nm906
219. Lauron EJ, Yang L, Elliott JI, Gainey MD, Fremont DH, Yokoyama WM. Cross-Priming Induces Immunodomination in the Presence of Viral MHC Class I Inhibition. *PloS Pathog* (2018) 14(2):e1006883. doi: 10.1371/journal.ppat.1006883
220. Sutiwisesak R, Hicks ND, Boyce S, Murphy KC, Papavinasasundaram K, Carpenter SM, et al. A Natural Polymorphism of Mycobacterium Tuberculosis in the esxH Gene Disrupts Immunodomination by the TB10.4-Specific CD8 T Cell Response. *PloS Pathog* (2020) 16(10): e1009000. doi: 10.1371/journal.ppat.1009000
221. Cadena AM, Fortune SM, Flynn JL. Heterogeneity in Tuberculosis. *Nat Rev Immunol* (2017) 17(11):691–702. doi: 10.1038/nri.2017.69
222. Kahnert A, Hopken UE, Stein M, Bandermann S, Lipp M, Kaufmann SH. Mycobacterium Tuberculosis Triggers Formation of Lymphoid Structure in Murine Lungs. *J Infect Dis* (2007) 195(1):46–54. doi: 10.1086/508894

223. Ardain A, Domingo-Gonzalez R, Das S, Kazer SW, Howard NC, Singh A, et al. Group 3 Innate Lymphoid Cells Mediate Early Protective Immunity Against Tuberculosis. *Nature* (2019) 570(7762):528–32. doi: 10.1038/s41586-019-1276-2
224. Foo SY, Phipps S. Regulation of Inducible BALT Formation and Contribution to Immunity and Pathology. *Mucosal Immunol* (2010) 3 (6):537–44. doi: 10.1038/mi.2010.52
225. Vinuesa CG, Linterman MA, Goodnow CC, Randall KL. T Cells and Follicular Dendritic Cells in Germinal Center B-Cell Formation and Selection. *Immunol Rev* (2010) 237(1):72–89. doi: 10.1111/j.1600-065X.2010.00937.x
226. Neyt K, GeurtsvanKessel CH, Deswarte K, Hammad H, Lambrecht BN. Early IL-1 Signaling Promotes iBALT Induction After Influenza Virus Infection. *Front Immunol* (2016) 7:312. doi: 10.3389/fimmu.2016.00312
227. Hwang JY, Silva-Sanchez A, Carragher DM, Garcia-Hernandez ML, Rangel-Moreno J, Randall TD. Inducible Bronchus-Associated Lymphoid Tissue (iBALT) Attenuates Pulmonary Pathology in a Mouse Model of Allergic Airway Disease. *Front Immunol* (2020) 11:570661. doi: 10.3389/fimmu.2020.570661
228. Moyron-Quiroz JE, Rangel-Moreno J, Kusser K, Hartson L, Sprague F, Goodrich S, et al. Role of Inducible Bronchus Associated Lymphoid Tissue (iBALT) in Respiratory Immunity. *Nat Med* (2004) 10(9):927–34. doi: 10.1038/nm1091
229. Moyron-Quiroz JE, Rangel-Moreno J, Hartson L, Kusser K, Tighe MP, Klonowski KD, et al. Persistence and Responsiveness of Immunologic Memory in the Absence of Secondary Lymphoid Organs. *Immunity* (2006) 25(4):643–54. doi: 10.1016/j.immuni.2006.08.022
230. Halle S, Dujardin HC, Bakocevic N, Fleige H, Danzer H, Willenzon S, et al. Induced Bronchus-Associated Lymphoid Tissue Serves as a General Priming Site for T Cells and is Maintained by Dendritic Cells. *J Exp Med* (2009) 206 (12):2593–601. doi: 10.1084/jem.20091472
231. Ulrichs T, Kosmiadi GA, Jorg S, Pradl L, Titukhina M, Mishenko V, et al. Differential Organization of the Local Immune Response in Patients With Active Cavitary Tuberculosis or With Nonprogressive Tuberculoma. *J Infect Dis* (2005) 192(1):89–97. doi: 10.1086/430621
232. Esaulova E, Das S, Singh DK, Choreno-Parra JA, Swain A, Arthur L, et al. The Immune Landscape in Tuberculosis Reveals Populations Linked to Disease and Latency. *Cell Host Microbe* (2021) 29(2):165–178 e8. doi: 10.1016/j.chom.2020.11.013
233. Carpenter SM, Nunes-Alves C, Booty MG, Way SS, Behar SM. A Higher Activation Threshold of Memory CD8+ T Cells Has a Fitness Cost That Is Modified by TCR Affinity During Tuberculosis. *PloS Pathog* (2016) 12(1): e1005380. doi: 10.1371/journal.ppat.1005380
234. Das S, Marin ND, Esaulova E, Ahmed M, Swain A, Rosa BA, et al. Lung Epithelial Signaling Mediates Early Vaccine-Induced CD4(+) T Cell Activation and Mycobacterium Tuberculosis Control. *mBio* (2021) 12(4): e0146821. doi: 10.1128/mBio.01468-21
235. Qin L, Waseem TC, Sahoo A, Bieerkehazhi S, Zhou H, Galkina EV, et al. Insights Into the Molecular Mechanisms of T Follicular Helper-Mediated Immunity and Pathology. *Front Immunol* (2018) 9:1884. doi: 10.3389/fimmu.2018.01884
236. Chiavolini D, Rangel-Moreno J, Berg G, Christian K, Oliveira-Nascimento L, Weir S, et al. Bronchus-Associated Lymphoid Tissue (BALT) and Survival in a Vaccine Mouse Model of Tularemia. *PloS One* (2010) 5(6):e11156. doi: 10.1371/journal.pone.0011156
237. Barone F, Nayar S, Campos J, Cloake T, Withers DR, Toellner KM, et al. IL-22 Regulates Lymphoid Chemokine Production and Assembly of Tertiary Lymphoid Organs. *Proc Natl Acad Sci USA* (2015) 112(35):11024–9. doi: 10.1073/pnas.1503315112
238. Treerat P, Prince O, Cruz-Lagunas A, Munoz-Torrico M, Salazar-Lezama MA, Selman M, et al. Novel Role for IL-22 in Protection During Chronic Mycobacterium Tuberculosis HN878 Infection. *Mucosal Immunol* (2017) 10 (4):1069–81. doi: 10.1038/mi.2017.15
239. Eddens T, Elsegeiny W, Garcia-Hernadez ML, Castillo P, Trevejo-Nunez G, Serody K, et al. Pneumocystis-Driven Inducible Bronchus-Associated Lymphoid Tissue Formation Requires Th2 and Th17 Immunity. *Cell Rep* (2017) 18(13):3078–90. doi: 10.1016/j.celrep.2017.03.016
240. Khader SA, Rangel-Moreno J, Fountain JJ, Martino CA, Reiley WW, Pearl JE, et al. In a Murine Tuberculosis Model, the Absence of Homeostatic Chemokines Delays Granuloma Formation and Protective Immunity. *J Immunol* (2009) 183(12):8004–14. doi: 10.4049/jimmunol.0901937
241. Kaushal D, Mehra S, Didier PJ, Lackner AA. The non-Human Primate Model of Tuberculosis. *J Med Primatol* (2012) 41(3):191–201. doi: 10.1111/j.1600-0684.2012.00536.x
242. Barber DL, Mayer-Barber KD, Feng CG, Sharpe AH, Sher A. CD4 T Cells Promote Rather Than Control Tuberculosis in the Absence of PD-1-Mediated Inhibition. *J Immunol* (2011) 186(3):1598–607. doi: 10.4049/jimmunol.1003304
243. Fletcher HA, Snowden MA, Landry B, Rida W, Satti I, Harris SA, et al. T-Cell Activation is an Immune Correlate of Risk in BCG Vaccinated Infants. *Nat Commun* (2016) 7:11290. doi: 10.1038/ncomms11290
244. Hansen SG, Zak DE, Xu G, Ford JC, Marshall EE, Malouli D, et al. Prevention of Tuberculosis in Rhesus Macaques by a Cytomegalovirus-Based Vaccine. *Nat Med* (2018) 24(2):130–43. doi: 10.1038/nm.4473
245. Tait DR, Hatherill M, van der Meeren O, Ginsberg AM, Van Brakel E, Salaun B, et al. Final Analysis of a Trial of M72/AS01E Vaccine to Prevent Tuberculosis. *N Engl J Med* (2019) 381(25):2429–39. doi: 10.1056/NEJMoa1909953
246. Tanner R, Villarreal-Ramos B, Vordermeier HM, McShane H. The Humoral Immune Response to BCG Vaccination. *Front Immunol* (2019) 10:1317. doi: 10.3389/fimmu.2019.01317
247. Bekker LG, Dintwe O, Fiore-Gartland A, Middelkoop K, Hutter J, Williams A, et al. A Phase 1b Randomized Study of the Safety and Immunological Responses to Vaccination With H4:IC31, H56:IC31, and BCG Revaccination in Mycobacterium Tuberculosis-Uninfected Adolescents in Cape Town, South Africa. *EClinicalMedicine* (2020) 21:100313. doi: 10.1016/j.eclinm.2020.100313
248. Luabeya AK, Kagina BM, Tameris MD, Geldenhuys H, Hoff ST, Shi Z, et al. First-In-Human Trial of the Post-Exposure Tuberculosis Vaccine H56:IC31 in Mycobacterium Tuberculosis Infected and non-Infected Healthy Adults. *Vaccine* (2015) 33(33):4130–40. doi: 10.1016/j.vaccine.2015.06.051
249. Loxton AG, Knaul JK, Grode L, Gutschmidt A, Meller C, Eisele B, et al. Safety and Immunogenicity of the Recombinant Mycobacterium Bovis BCG Vaccine VPM1002 in HIV-Unexposed Newborn Infants in South Africa. *Clin Vaccine Immunol* (2017) 24(2):e00439–16. doi: 10.1128/CVI.00439-16
250. Grode L, Ganoza CA, Brohm C, Weiner J 3rd, Eisele B, Kaufmann SH. Safety and Immunogenicity of the Recombinant BCG Vaccine VPM1002 in a Phase 1 Open-Label Randomized Clinical Trial. *Vaccine* (2013) 31(9):1340–8. doi: 10.1016/j.vaccine.2012.12.053
251. Darrah PA, Zeppa JJ, Maiello P, Hackney JA, Wadsworth MH 32nd, Hughes TK, et al. Prevention of Tuberculosis in Macaques After Intravenous BCG Immunization. *Nature* (2020) 577(7788):95–102. doi: 10.1038/s41586-019-1817-8
252. Dijkman K, Sombroek CC, Vervenne RAW, Hofman SO, Boot C, Remarque EJ, et al. Prevention of Tuberculosis Infection and Disease by Local BCG in Repeatedly Exposed Rhesus Macaques. *Nat Med* (2019) 25(2):255–62. doi: 10.1038/s41591-018-0319-9
253. Dijkman K, Aguilo N, Boot C, Hofman SO, Sombroek CC, Vervenne RAW, et al. Pulmonary MTBVAC Vaccination Induces Immune Signatures Previously Correlated With Prevention of Tuberculosis Infection. *Cell Rep Med* (2021) 2(1):100187. doi: 10.1016/j.xcrm.2020.100187
254. Divangahi M, Aaby P, Khader SA, Barreiro LB, Bekkering S, Chavakis T, et al. Trained Immunity, Tolerance, Priming and Differentiation: Distinct Immunological Processes. *Nat Immunol* (2021) 22(1):2–6. doi: 10.1038/s41590-020-00845-6
255. Vierboom MPM, Dijkman K, Sombroek CC, Hofman SO, Boot C, Vervenne RAW, et al. Stronger Induction of Trained Immunity by Mucosal BCG or MTBVAC Vaccination Compared to Standard Intradermal Vaccination. *Cell Rep Med* (2021) 2(1):100185. doi: 10.1016/j.xcrm.2020.100185
256. Coler RN, Day TA, Ellis R, Piazza FM, Beckmann AM, Vergara J, et al. The TLR-4 Agonist Adjuvant, GLA-SE, Improves Magnitude and Quality of Immune Responses Elicited by the ID93 Tuberculosis Vaccine: First-in-Human Trial. *NPJ Vaccines* (2018) 3:34. doi: 10.1038/s41541-018-0057-5
257. Prados-Rosales R, Carreno L, Cheng T, Blanc C, Weinrick B, Malek A, et al. Enhanced Control of Mycobacterium Tuberculosis Extrapulmonary Dissemination in Mice by an Arabinomannan-Protein Conjugate Vaccine. *PloS Pathog* (2017) 13(3):e1006250. doi: 10.1371/journal.ppat.1006250

258. Andrews JR, Noubary F, Walensky RP, Cerda R, Losina E, Horsburgh CR. Risk of Progression to Active Tuberculosis Following Reinfection With Mycobacterium Tuberculosis. *Clin Infect Dis* (2012) 54(6):784–91. doi: 10.1093/cid/cir951
259. Teitelbaum R, Glatman-Freedman A, Chen B, Robbins JB, Unanue E, Casadevall A, et al. A mAb Recognizing a Surface Antigen of Mycobacterium Tuberculosis Enhances Host Survival. *Proc Natl Acad Sci USA* (1998) 95(26):15688–93. doi: 10.1073/pnas.95.26.15688
260. Pethe K, Alonso S, Biet F, Delogu G, Brennan MJ, Locht C, et al. The Heparin-Binding Haemagglutinin of M. Tuberculosis is Required for Extrapulmonary Dissemination. *Nature* (2001) 412(6843):190–4. doi: 10.1038/35084083
261. Bournazos S, Gupta A, Ravetch JV. The Role of IgG Fc Receptors in Antibody-Dependent Enhancement. *Nat Rev Immunol* (2020) 20(10):633–43. doi: 10.1038/s41577-020-00410-0
262. Lenzini L, Rottoli P, Rottoli L. The Spectrum of Human Tuberculosis. *Clin Exp Immunol* (1977) 27(2):230–7.
263. Forget A, Benoit JC, Turcotte R, Gusew-Chartrand N. Enhancement Activity of Anti-Mycobacterial Sera in Experimental Mycobacterium Bovis (BCG) Infection in Mice. *Infect Immun* (1976) 13(5):1301–6. doi: 10.1128/iai.13.5.1301-1306.1976
264. Jenum S, Tonby K, Rueegg CS, Ruhwald M, Kristiansen MP, Bang P, et al. A Phase I/II Randomized Trial of H56:IC31 Vaccination and Adjunctive Cyclooxygenase-2-Inhibitor Treatment in Tuberculosis Patients. *Nat Commun* (2021) 12(1):6774. doi: 10.1038/s41467-021-27029-6
265. Penn-Nicholson A, Tameris M, Smit E, Day TA, Musvosvi M, Jayashankar L, et al. Safety and Immunogenicity of the Novel Tuberculosis Vaccine ID93 + GLA-SE in BCG-Vaccinated Healthy Adults in South Africa: A Randomised, Double-Blind, Placebo-Controlled Phase 1 Trial. *Lancet Respir Med* (2018) 6 (4):287–98. doi: 10.1016/S2213-2600(18)30077-8
266. Coler RN, Bertholet S, Pine SO, Orr MT, Reese V, Windish HP, et al. Therapeutic Immunization Against Mycobacterium Tuberculosis is an Effective Adjunct to Antibiotic Treatment. *J Infect Dis* (2013) 207(8):1242–52. doi: 10.1093/infdis/jis425
267. Polack FP, Thomas SJ, Kitchin N, Absalon J, Gurtman A, Lockhart S, et al. Safety and Efficacy of the BNT162b2 mRNA Covid-19 Vaccine. *N Engl J Med* (2020) 383(27):2603–15. doi: 10.1056/NEJMoa2034577
268. Baden LR, El Sahly HM, Essink B, Kotloff K, Frey S, Novak R, et al. Efficacy and Safety of the mRNA-1273 SARS-CoV-2 Vaccine. *N Engl J Med* (2021) 384(5):403–16. doi: 10.1056/NEJMoa2035389
269. Bruhns P, Jonsson F. Mouse and Human FcR Effector Functions. *Immunol Rev* (2015) 268(1):25–51. doi: 10.1111/imr.12350
270. de Haan N, Reiding KR, Kristic J, Hipgrave Ederveen AL, Lauc G, Wuhrer M. The N-Glycosylation of Mouse Immunoglobulin G (IgG)-Fragment Crystallizable Differs Between IgG Subclasses and Strains. *Front Immunol* (2017) 8:608. doi: 10.3389/fimmu.2017.00608
271. Smith P, DiLillo DJ, Bournazos S, Li F, Ravetch JV. Mouse Model Recapitulating Human Fcgamma Receptor Structural and Functional Diversity. *Proc Natl Acad Sci USA* (2012) 109(16):6181–6. doi: 10.1073/pnas.1203954109
272. Murphy AJ, Macdonald LE, Stevens S, Karow M, Dore AT, Pobursky K, et al. Mice With Megabase Humanization of Their Immunoglobulin Genes Generate Antibodies as Efficiently as Normal Mice. *Proc Natl Acad Sci USA* (2014) 111(14):5153–8. doi: 10.1073/pnas.1324022111
273. Flynn JL. Lessons From Experimental Mycobacterium Tuberculosis Infections. *Microbes Infect* (2006) 8(4):1179–88. doi: 10.1016/j.micinf.2005.10.033
274. Mangtani P, Abubakar I, Ariti C, Beynon R, Pimpin L, Fine PE, et al. Protection by BCG Vaccine Against Tuberculosis: A Systematic Review of Randomized Controlled Trials. *Clin Infect Dis* (2014) 58(4):470–80. doi: 10.1093/cid/cit790
275. Kurtz SL, Rossi AP, Beamer GL, Gatti DM, Kramnik I, Elkins KL. The Diversity Outbred Mouse Population Is an Improved Animal Model of Vaccination Against Tuberculosis That Reflects Heterogeneity of Protection. *mSphere* (2020) 5(2):e00097–20. doi: 10.1128/mSphere.00097-20
276. Smith CM, Proulx MK, Olive AJ, Laddy D, Mishra BB, Moss C, et al. Tuberculosis Susceptibility and Vaccine Protection Are Independently Controlled by Host Genotype. *mBio* (2016) 7(5):e01516–16. doi: 10.1128/mBio.01516-16
277. Plumlee CR, Duffy FJ, Gern BH, Delahaye JL, Cohen SB, Stoltzfus CR, et al. Ultra-Low Dose Aerosol Infection of Mice With Mycobacterium Tuberculosis More Closely Models Human Tuberculosis. *Cell Host Microbe* (2021) 29(1):68–82 e5. doi: 10.1016/j.chom.2020.10.003
278. Colangeli R, Gupta A, Vinhas SA, Chippada Venkata UD, Kim S, Grady C, et al. Mycobacterium Tuberculosis Progresses Through Two Phases of Latent Infection in Humans. *Nat Commun* (2020) 11(1):4870. doi: 10.1038/s41467-020-18699-9
279. Warsinske HC, Rao AM, Moreira FMF, Santos PCP, Liu AB, Scott M, et al. Assessment of Validity of a Blood-Based 3-Gene Signature Score for Progression and Diagnosis of Tuberculosis, Disease Severity, and Treatment Response. *JAMA Netw Open* (2018) 1(6):e183779. doi: 10.1001/jamanetworkopen.2018.3779
280. Mulenga H, Zauchenberger CZ, Bunyasi EW, Mbandi SK, Mendelsohn SC, Kagina B, et al. Performance of Diagnostic and Predictive Host Blood Transcriptomic Signatures for Tuberculosis Disease: A Systematic Review and Meta-Analysis. *PloS One* (2020) 15(8):e0237574. doi: 10.1371/journal.pone.0237574
281. Mave V, Chandrasekaran P, Chavan A, Shivakumar S, Danasekaran K, Paradkar M, et al. Infection Free "Resisters" Among Household Contacts of Adult Pulmonary Tuberculosis. *PloS One* (2019) 14(7):e0218034. doi: 10.1371/journal.pone.0218034
282. Seshadri C, Sedaghat N, Campo M, Peterson G, Wells RD, Olson GS, et al. Transcriptional Networks are Associated With Resistance to Mycobacterium Tuberculosis Infection. *PloS One* (2017) 12(4):e0175844. doi: 10.1371/journal.pone.0175844
283. Kroon EE, Kinnear CJ, Orlova M, Fischinger S, Shin S, Boolay S, et al. An Observational Study Identifying Highly Tuberculosis-Exposed, HIV-1-Positive But Persistently TB, Tuberculin and IGRA Negative Persons With M. Tuberculosis Specific Antibodies in Cape Town, South Africa. *EBioMedicine* (2020) 61:103053. doi: 10.1016/j.ebiom.2020.103053
284. Jain SK, Tobin DM, Tucker EW, Venketaraman V, Ordonez AA, Jayashankar L, et al. Tuberculous Meningitis: A Roadmap for Advancing Basic and Translational Research. *Nat Immunol* (2018) 19(6):521–5. doi: 10.1038/s41590-018-0119-x
285. Fox GJ, Orlova M, Schurr E. Tuberculosis in Newborns: The Lessons of the "Lubeck Disaster" (1929-1933). *PloS Pathog* (2016) 12(1):e1005271. doi: 10.1371/journal.ppat.1005271

Conflict of Interest: The authors declare that the research was conducted in the absence of any commercial or financial relationships that could be construed as a potential conflict of interest.

Publisher's Note: All claims expressed in this article are solely those of the authors and do not necessarily represent those of their affiliated organizations, or those of the publisher, the editors and the reviewers. Any product that may be evaluated in this article, or claim that may be made by its manufacturer, is not guaranteed or endorsed by the publisher.

frontiers | Frontiers in Immunology

ORIGINAL RESEARCH
published: 19 April 2022
doi: 10.3389/fimmu.2022.873191

Influenza Vaccination Results in Differential Hemagglutinin Stalk-Specific Fc-Mediated Functions in Individuals Living With or Without HIV

*Boitumelo M. Motsoeneng[1,2], Nisha Dhar[3,4], Marta C. Nunes[3,4], Florian Krammer[5,6], Shabir A. Madhi[3,4,7], Penny L. Moore[1,2,7,8,9] and Simone I. Richardson[1,2]**

[1] HIV Virology Section, Centre for HIV and STIs, National Institute for Communicable Diseases of The National Health Laboratory Services, Johannesburg, South Africa, [2] South African Medical Research Council Antibody Immunity Research Unit, Faculty of Health Sciences, University of the Witwatersrand, Johannesburg, South Africa, [3] South African Medical Research Council Vaccines and Infectious Diseases Analytics Research Unit, Faculty of Health Sciences, University of the Witwatersrand, Johannesburg, South Africa, [4] Department of Science and Innovation/National Research Foundation, South African Research Chair Initiative in Vaccine Preventable Diseases Unit, Faculty of Health Sciences, University of the Witwatersrand, Johannesburg, South Africa, [5] Department of Microbiology, Icahn School of Medicine at Mount Sinai, New York, NY, United States, [6] Department of Pathology, Molecular and Cell based Medicine, Icahn School of Medicine at Mount Sinai, New York, NY, United States, [7] African Leadership in Vaccinology Expertise (ALIVE), Faculty of Health Sciences, University of the Witwatersrand, Johannesburg, South Africa, [8] Centre for the AIDS Programme of Research in South Africa (CAPRISA), University of KwaZulu Natal, Durban, South Africa, [9] Institute of Infectious Disease and Molecular Medicine, University of Cape Town, Cape Town, South Africa

OPEN ACCESS

Edited by:
R. Keith Reeves, Duke University, United States

Reviewed by:
Hillary Anne Vanderven, James Cook University, Australia
Marc Paul Girard, Université Paris Diderot, France

***Correspondence:**
Simone I. Richardson
simoner@nicd.ac.za

Specialty section:
This article was submitted to Viral Immunology, a section of the journal Frontiers in Immunology

Received: *10 February 2022*
Accepted: *28 March 2022*
Published: *19 April 2022*

Citation:
Motsoeneng BM, Dhar N, Nunes MC, Krammer F, Madhi SA, Moore PL and Richardson SI (2022) Influenza Vaccination Results in Differential Hemagglutinin Stalk-Specific Fc-Mediated Functions in Individuals Living With or Without HIV. Front. Immunol. 13:873191. doi: 10.3389/fimmu.2022.873191

Influenza virus hemagglutinin (HA) stalk-specific antibodies have been shown to potently induce Fc-mediated effector functions which are important in protection from disease. In placebo-controlled maternal influenza (MatFlu) vaccination trials of pregnant women living with or without HIV, reduced risk of influenza illness was associated with high HA stalk antibody titers following trivalent inactivated vaccination (TIV). However, the mechanisms of immunity conferred by the HA stalk antibodies were not well understood. Here, we investigated HA stalk-specific Fc effector functions including antibody-dependent cellular phagocytosis (ADCP), antibody-dependent cellular cytotoxicity (ADCC), antibody-dependent complement deposition (ADCD), and FcγRIIa and FcγRIIIa binding in response to seasonal influenza vaccination. These were measured pre- and 1-month post-vaccination in 141 HIV-uninfected women (67 TIV and 74 placebo recipients) and 119 women living with HIV (WLWH; 66 TIV and 53 placebo recipients). In contrast to HIV-uninfected women, where HA stalk-specific ADCP and FcγRIIa binding were significantly boosted, WLWH showed no increase in response to vaccination. HA stalk-specific ADCC potential and FcγRIIIa binding were not boosted regardless of HIV status but were higher in WLWH compared with HIV-uninfected women prior to vaccination. HA stalk-specific ADCD was significantly increased by vaccination in all women, but was significantly lower in the WLWH both pre- and post- vaccination. Co-ordination between HA stalk-specific ADCP and ADCD in WLWH was improved by vaccination. Fc polyfunctionality was enhanced by vaccination in HIV-uninfected women and driven by the HA stalk antibody titers. However, in the WLWH, higher pre-vaccination Fc polyfunctionality was maintained

post-vaccination but was decoupled from titer. Overall, we showed differential regulation of Fc effector HA stalk responses, suggesting that HIV infection results in unique humoral immunity in response to influenza vaccination, with relevance for future strategies that aim to target the HA stalk in this population.

Keywords: influenza vaccination, Fc effector functions, HIV co-infection, hemagglutinin stalk antibodies, antibody-dependent cellular phagocytosis (ADCP), antibody-dependent complement deposition (ADCD), antibody-dependent cellular cytotoxicity (ADCC)

INTRODUCTION

Seasonal influenza epidemics cause over 56,000 hospitalizations and 11,000 deaths annually in South Africa (1). Immunocompromised individuals such as pregnant women and people living with HIV (PLWH) are especially burdened with severe respiratory disease. Therefore seasonal trivalent inactivated influenza vaccines (TIV) are recommended for these high-risk individuals and have been shown to have a significant impact on public health (2). Whilst TIV efficacy has been confirmed in PLWH, vaccine immunogenicity was suboptimal in these individuals (3–8). Therefore, there is a need to further understand the mechanisms of immunity in PLWH, following seasonal influenza vaccination.

Humoral immune responses elicited by TIVs primarily target the viral hemagglutinin (HA), which is composed of a head and stalk domain. The ability of HA head-specific antibodies to neutralize influenza virus, detected using hemagglutination inhibition (HAI) assays, is considered a relative correlate of protection (9). However, the HA head domain continuously undergoes antigenic drift, allowing escape from HA head-specific antibodies induced from previous viral exposures and vaccinations (10). The immuno-subdominant, but conserved HA stalk domain is a target for the development of broadly protective influenza vaccines (11). In addition to having neutralizing activity, HA stalk antibodies confer protection through Fc-FcγR interactions (12).

Fc effector functions have been associated with protection against influenza virus infection, in experimental challenge models and after vaccination (13–17). Through the interaction of the antibody Fc region with cell surface Fc receptors or complement proteins, cytotoxic functions such as antibody-dependent cellular phagocytosis (ADCP), cellular cytotoxicity (ADCC) and complement deposition (ADCD) occur. In animal models, ADCP, ADCC and ADCD have been associated with protection against infection (18–21). In humans, seasonal influenza vaccination enhances cross-reactive ADCC and ADCP antibodies directed to the HA in healthy individuals and high-risk groups, such as older adults and PLWH (22–24). In these studies, TIV boosted Fc effector functions when head-specific HAI responses were low, highlighting the potential of HA stalk antibodies and their cytotoxic functions for protection in immunocompromised individuals.

In general, PLWH are at a higher risk of deaths associated with severe influenza disease (25). B-cell impairments and reduced HAI antibody levels in response to seasonal TIV have been observed in this group, with pregnancy further increasing susceptibility to severe influenza virus infections (26–30). PLWH on antiretroviral treatment (ART) have lower HAI responses in comparison to HIV-uninfected individuals even when TIV doses were increased or a second dose was administered (5, 6, 8, 31). However, studies focusing on the HA stalk are limited and detailed antibody responses and mechanisms of immunogenicity in this high-risk group are not well understood.

In two randomized, double-blind, placebo-controlled maternal influenza (MatFlu) vaccination trials, lower HAI titers were observed in pregnant women living with HIV (WLWH) compared with pregnant women living without HIV (6). However, the vaccine efficacy against confirmed influenza illness in WLWH trended to being higher (70.6%) than in HIV-uninfected women (54.4%) (6). This indicated that antibody responses to epitopes that lie beyond the HA head may be important in protection in this high-risk group. A follow up study showed that HA stalk antibody titers were associated with reduced risk of influenza virus infection (32). Given that HA stalk-specific antibodies mediate potent Fc effector functions and are known to be protective, we explored the Fc-mediated functions of HA stalk-specific antibodies in this cohort of WLWH.

In this study we observed higher HA stalk-specific *in vitro* ADCP and ADCC as measured by a reporter assay in WLWH prior to vaccination in comparison with HIV-uninfected women. ADCC potential directed at the HA stalk was not boosted regardless of HIV status, whereas ADCP was enhanced only in HIV-uninfected women. In both groups HA stalk-specific ADCD was increased although this function is compromised in WLWH. We also observed differences in the coordination of Fc effector functions post-vaccination. In WLWH the association between HA stalk-specific ADCP and ADCD was enhanced but in the HIV-uninfected women these functions were associated with HA stalk-specific ADCC potential. We also show that Fc polyfunctionality was higher in WLWH prior to vaccination and was not further enhanced, whereas in HIV-uninfected women it was improved. This study suggests that seasonal influenza vaccination may confer protection through different HA stalk targeted mechanisms which may include Fc effector functions for WLWH and HIV-uninfected women.

MATERIALS AND METHODS

Ethics Statement

The 2011 maternal influenza (MatFlu) vaccination trials (approval numbers: 101106 and 101107) and this sub-study

(approval number: M200444) were approved by the Human Research Ethics Committee of the University of the Witwatersrand. All study participants provided written informed consent to have their stored samples used for future studies. All healthy donors in this study provided written informed consent to obtain plasma, isolate IgG and have their samples stored for future use.

Influenza Vaccination Cohort

The two randomized, double-blind, placebo-controlled MatFlu vaccination trials conducted in Soweto, South Africa have been previously described (6). Briefly, women, all of whom were pregnant, between the ages of 18-38 years were stratified according to their HIV status and randomly assigned (1:1) to the placebo or vaccine groups. The trivalent inactivated vaccine (TIV) used in the trials was Vaxigrip, which contained 15 µg each of A/California/7/2009 (A/H1N1/pdm09), A/Victoria/210/2009 (A/H3N2), and a B/Brisbane/60/2008-like virus (B/Victoria) as recommended by the World Health Organization for the Southern Hemisphere in 2011. Active surveillance for respiratory illness and PCR-confirmed influenza-illness was performed. In this study, plasma samples from a sub-set of HIV-uninfected women (74 placebo-recipients and 67 vaccinees) and WLWH (53 placebo-recipients and 66 vaccinees), collected prior to vaccination and one-month post-vaccination, were tested. Data from participants with PCR-confirmed influenza-illness were excluded from this study.

Protein Expression and Pooled Plasma/IgG Preparation

A chimeric recombinant hemagglutinin (cHA) protein, composed of an H6 head and an H1 stalk (cH6/1) was produced as previously described (33). For use as a positive control in all the Fc assays, plasma was pooled from 5 healthy donors with high HA stalk IgG titers. From this pooled plasma IgG was isolated using Protein G (Pierce Biotechnology), according to the manufacturer's instructions and confirmed by IgG enzyme linked immunosorbent assay (ELISA). A cross-reactive HA stalk antibody CR9114 that mediates potent Fc effector function was expressed as a positive control (34). For antibody expression, plasmids encoding heavy or light chain genes were co-transfected into HEK293F cells with PEI-MAX 40,000 (Polysciences) head-to-head. Cells were cultured for six days in 293F Freestyle media at 37°C, 10% CO_2, then harvested supernatants were filtered and purified using Protein G (Thermo Scientific). Antibody concentration was quantified by nanodrop using sequence-specific extinction coefficients as determined by ProtParam (ExPASy) and confirmed by ELISA.

Hemagglutinin Inhibition (HAI) Assay

Modified HAI assays were previously performed (6, 35). Briefly, plasma samples instead of serum were treated with receptor-destroying enzyme (RDE) from *Vibrio cholera* (Denka-Seiken). Then these were diluted 1:10 in saline and subsequent serial 2-fold dilutions of the plasma were used in a standard HAI assay using 4 hemagglutinating units of the antigen and 0.75% turkey red blood cells. Plasma samples with titers ≥10 were considered indicative of immune responses. The antigen used in the assays was A/H1N1/pdm09.

Hemagglutinin Stalk (H1/stalk) IgG ELISA

H1/stalk IgG ELISAs were performed as previously described (32). The cH6/1 recombinant protein described above was utilized and binding against this protein measures antibodies against the H1 stalk domain. Plates were coated with cH6/1 diluted to 2 µg/ml overnight at 4°C. Plates were washed and subsequently blocked with 3% fetal bovine serum (Biowest), 0.5% non-fat dry milk powder (Bio-Rad) for 2 hours at room temperature (RT). After washing, plasma samples were added to the plate diluted to a starting concentration of 1:40, followed by two-fold serial dilution and incubated for 2 hours at RT. Following a wash, anti-human IgG (Fab specific)-peroxidase antibody (Sigma, USA) diluted to 1:3000 in blocking solution was added to the plate. After 1-hour incubation at RT, plates were washed and developed using SigmaFast *o*-phenylenediamine dichloride (OPD) (Sigma, USA) for 10 min at RT. The reaction was stopped by adding 3M HCl and the optical density (OD) was measured at 490 nm. The antibody concentration was quantified against the standard curve included on each plate that consisted of polyvalent human normal immunoglobulin (Polygam) (National Bioproducts Institute, South Africa) with an assigned arbitrary value of 1000 arbitrary units (AU)/ml.

Antibody-Dependent Cellular Phagocytosis (ADCP)

The ADCP assay was performed as previously described (36). Briefly The EZ-Link Sulfo-NHS-LC-Biotin kit (Thermo Scientific) was used to biotinylate cH6/1, which was coated onto fluorescent neutravidin beads (Invitrogen). The coated beads were incubated for 2 hours with mAbs at a final concentration of 50 µg/ml or a 1:100 dilution of plasma sample, prior to overnight incubation with a monocytic cell line, THP-1 cells. The THP-1 cells were obtained from the NIH AIDS Reagent Program and cultured at 37°C, 5% CO_2 in Roswell Park Memorial Institute (RPMI) 1640 media supplemented with 10% fetal bovine serum (FBS), 100 units/ml Penicillin and 100 ug/ml Streptomycin (Gibco), referred to as R10, and not allowed to exceed 4 x 10^5 cells/ml. This assay was completed on a FACS Aria II (BD Biosciences). Phagocytic scores were calculated as the geometric mean fluorescent intensity (MFI) of the beads multiplied by the percentage bead uptake minus the no antibody control as background. For this and all functional Fc assays, pooled plasma from 5 healthy donors with previous exposures to influenza, screened for H1 stalk antibodies and CR9114 were used as positive controls and Palivizumab (RSV mAb; MedImmune, LLC) and VRC01 (In house HIV mAb) were used as negative controls. In order to normalize across plates and runs, the pooled plasma positive scores were averaged, divided by the pooled plasma score per plate and this normalizing factor multiplied across the scores.

Antibody-Dependent Cellular Cytotoxicity (ADCC) Reporter Assay

The ability of plasma antibodies to cross-link cH6/1 HA stalk antigen and activate FcγRIIIa on Jurkat-Lucia™ NFAT-CD16 cells (*In vivo*gen) was measured as a proxy for ADCC or cell lysis. These cells *In vivo* were cultured according to the manufacturer's instructions. Adapted from elsewhere (37), high-binding 96 well plates were coated with 1 µg/mL cH6/1 and incubated at 4°C overnight. Plates were then washed with phosphate buffered saline (PBS) and blocked at room temperature for 1 hour with 2.5% bovine serum albumin (BSA)/PBS. After washing, mAbs at a starting concentration of 1 mg/ml or a 1:10 dilution of plasma sample was added and incubated for 1 hour at 37°C. Subsequently, 2x 10^5 cells/well in R10 were added and incubated for 24 hours at 37°C, 5% CO_2. Then 25 µl of supernatant was transferred to a white 96-well plate with 75 µl of reconstituted QUANTI-Luc secreted luciferase and read immediately on a Victor 3 luminometer (PerkinElmer) with 1s integration time. Relative light units (RLU) of a no antibody control were subtracted as background. The pooled plasma and CR9114 were used as positive controls and Palivizumab and VRC01 were used as negative controls. The reported values are the mean of three kinetic reads taken at 0, 2.5, and 5 min. To induce the transgene 1x cell stimulation cocktail (Thermo Scientific) and 2 µg/ml ionomycin in R10 was added as a positive control to confirm sufficient expression of the CD16 Fc receptor. ADCC RLUs were normalised across plates and runs, by averaging the pooled plasma RLUs and multiplying the RLUs across the samples with the normalizing factor.

Antibody-Dependent Complement Deposition (ADCD)

ADCD was measured using a previously described high-throughput bead-based assay (38). Biotinylated cH6/1 was coated 1:1 onto fluorescent neutravidin beads (Invitrogen) for 2 hours at 37°C. The antigen-coated beads were incubated with a 1:10 plasma sample dilution or mAbs at a starting concentration of 100 µg/ml for 2 hours and incubated with guinea pig complement diluted 1 in 50 with gelatin/veronal buffer for 15 minutes at 37°C. Beads were washed in PBS and stained with anti-guinea pig C3b-FITC, fixed and interrogated on a FACS Aria II (BD Biosciences). Complement deposition scores were calculated as the percentage of C3b-FITC positive beads multiplied by the geometric MFI of FITC in this population minus the no antibody or heat inactivated controls. The pooled plasma and CR9114 were used as positive controls and Palivizumab and VRC01 were used as negative controls. ADCD scores were normalised between plates and runs, by dividing the ADCD score of the pooled plasma by the average across the plates and multiplying the scores with this normalizing factor.

Dimeric Fc Gamma Receptor Binding ELISAs

High-binding 96 well ELISA plates were coated with 1 ug/ml cH6/1 in PBS overnight at 4°C. Three wells on each plate were directly coated with 5 ug/ml IgG, isolated from healthy donors, signals from these wells were used to normalize the FcR activity of the plasma samples and pooled plasma was used as a positive control. Plates were washed with PBS and blocked with PBS/1 mM ethylenediaminetetraacetic acid (EDTA)/1% BSA for 1 hour at 37°C. Plates were then washed and incubated with 1:10 diluted plasma for 1 hour at 37°C and then with 0.2 ug/ml of biotinylated FcγRIIa dimer or 0.1 ug/ml of biotinylated FcγRIIIa dimer for 1 hour at 37°C. The dimeric FcγRs were provided by Prof. Mark Hogarth from the Burnet Institute, Melbourne, Australia (39). Subsequently, a 1:10000 dilution of Pierce high-sensitivity streptavidin-horseradish peroxidase (Thermo Scientific) was added for a final incubation of 1 hour at 37°C. Lastly, TMB (3,3,5,5-tetramethylbenzidine) substrate (Sigma-Aldrich) was added, colour development was stopped with 1 M sulfuric acid and absorbance read at 450 nm.

Statistical Analysis

Data were analyzed in Prism (v9; GraphPad Software Inc., San Diego, CA, USA). Non-parametric tests were used for all comparisons. The Mann-Whitney and Wilcoxon tests were used for unmatched and paired samples, respectively. Fc polyfunctionality Z-scores were calculated by subtracting the mean of the Fc function from the individual value and divided by the standard deviation of the mean and then adding all the Z-scores for each function per individual. The proportions of responders and non-responders in each group and the proportions of participants with high or low Fc polyfunctionality Z-scores were compared by Fisher's exact tests. All correlations reported are non-parametric Spearman's correlations. *P* values less than 0.05 were considered statistically significant.

RESULTS

Women Living With HIV (WLWH) Have Lower HAI and H1 Stalk Antibody Titers in Response to Seasonal Influenza Vaccination

In our previous study, HAI titers were significantly boosted by vaccination regardless of HIV status, but WLWH showed significantly lower HAI titers post-vaccination compared to HIV-uninfected women (6). We confirmed this finding in a subset of plasma samples from pregnant vaccinated participants from the MatFlu cohort, including 67 HIV-uninfected women and 66 WLWH, matched in age with a median of 25 years (range 18-39) and 27 years (range 18-38) respectively, and excluded all PCR-confirmed influenza virus infection cases. Plasma samples were collected pre-vaccination and post-vaccination at a median of 31 days (range 28-33) for HIV-uninfected and 30 days (range 28-31) for WLWH (**Supplementary Table 1**). Post-vaccination HAI titers were significantly lower in WLWH compared with HIV-uninfected women (medians 80 vs. 320 A/H1N1 HAI titer) (**Figure 1A**), coupled with decreased boosting levels following vaccination (median fold change 1.5 vs. 4) (**Supplementary Figure 1A**). In these samples, we also confirmed that post-

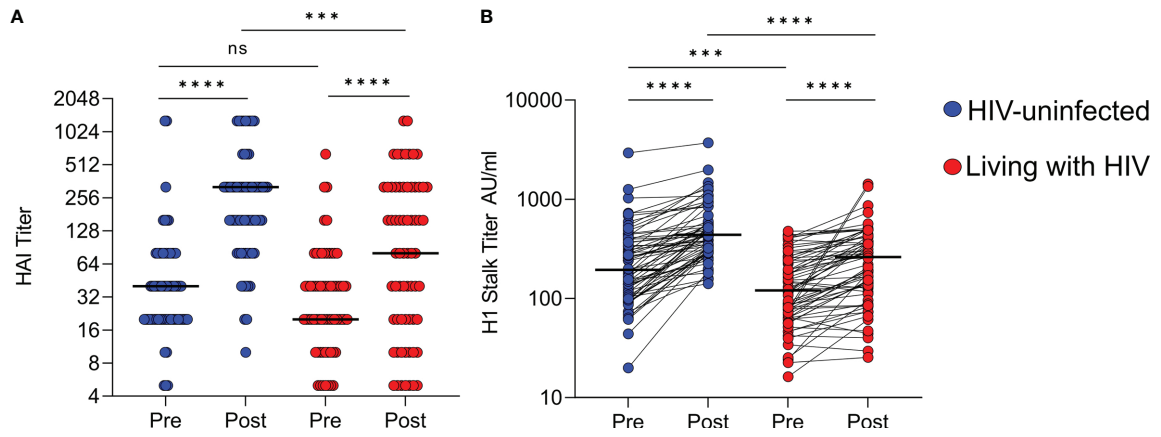

FIGURE 1 | A/H1N1 HAI and H1 stalk antibody responses amongst vaccinated women. **(A)** Pre-vaccination and 1-month post-vaccination hemagglutination inhibition (HAI) titers against A/H1N1 and **(B)** H1 stalk titers by ELISA, with HIV-uninfected participants (n=67), shown in blue and participants living with HIV (n=66), shown in red. The lines represent the median. Wilcoxon matched-pairs signed rank test used to compare pre- and post-vaccination titers. Mann Whitney U test used to compare responses between vaccine groups. Significant associations shown as ****p < 0.0001; ***p < 0.001; ns,not significant.

vaccination H1 stalk antibody titers were significantly lower in WLWH compared with HIV-uninfected women (medians 259.3 vs. 433.5 AU/ml) (**Figure 1B**). This was despite vaccine boosting H1 stalk antibody titers in both groups, which was consistent with the parent study (32). Furthermore, we also confirmed that in contrast to HAI titers, the HIV-uninfected women and WLWH had more comparable fold increases in the H1 stalk antibody titer boosting (median fold change 1.9 vs. 1.7) (**Supplementary Figure 1B**). As expected, no changes in HAI and H1 stalk antibody titers amongst placebo recipients living with or without HIV were observed (**Supplementary Figure 2**).

Women Living With HIV Have Higher Pre-Vaccination ADCP and ADCC Reporter Activity, but These Are Not Boosted by Seasonal TIV

We first assessed whether WLWH differ in terms of pre- and post-vaccination HA stalk antibody Fc-mediated effector functions. To do this, we measured HA stalk-specific ADCP, ADCC reporter activity and ADCD using a chimeric recombinant HA protein with an H6 head, to which humans are generally naïve, and an H1 stalk. TIV administration resulted in significant boosting of HA stalk-specific ADCP in HIV-uninfected women but not in WLWH (**Figure 2A**). Despite this, post-vaccination ADCP activity between the two groups was similar, a consequence of pre-vaccination HA stalk-specific ADCP being significantly higher in WLWH (medians 348.6 vs. 189.7). No ADCP boosting was observed in the placebo groups indicating that these responses were TIV specific (**Supplementary Figure 2**). For ADCC, which was measured using a high throughput FcγRIIIa activation assay, previously shown to correlate with NK degranulation assays (40), there was no significant boosting in either HIV-uninfected women or WLWH (**Figure 2B**). However, like ADCP, pre-vaccination ADCC was significantly higher in the WLWH (medians 154.5 vs. 73.5), and therefore also post-vaccination (medians 170 vs. 83.2). The ADCC activity amongst the vaccinated and placebo groups were similar and remained unchanged since there was no vaccine-mediated boosting of this function (**Supplementary Figure 2**).

To assess Fc-FcγR engagement required for ADCP and ADCC activity, plasma samples were tested for the capacity to bind cH6/1 antigen and cross-link recombinant soluble dimeric FcγRIIa or FcγRIIIa, respectively (39). No boosting in FcγRIIa and FcγRIIIa binding was observed in placebo recipients (**Supplementary Figure 2**). However, as observed in the cell-based functional and reporter assays, FcγRIIa binding was boosted by TIV in HIV-uninfected women but not WLWH, whereas for FcγRIIIa binding, no boosting was observed in either group (**Supplementary Figures 3A, B**). Furthermore, strong positive Spearman's correlations were noted between FcγRIIa binding and ADCP scores (r=0.44; p<0.0001), and between FcγRIIIa binding and ADCC RLUs (r=0.55; p<0.0001) (**Supplementary Figures 3C, D**).

Seasonal TIV Substantially Boosts ADCD but Women Living With HIV Have Lower Responses Both Pre- and Post-Vaccination

Since ADCD has been shown to confer protection from influenza virus infection (16, 21), we examined this function in WLWH and HIV-uninfected women, before and after TIV vaccination. ADCD, measured using a bead-based flow cytometry assay, was significantly boosted by TIV in all participants irrespective of HIV status (**Figure 2C**). However, ADCD was substantially impaired in WLWH prior to vaccination and post-vaccination remained significantly lower in comparison to the HIV-uninfected women after TIV boosting (medians 16.2 vs. 225). Placebo recipients showed no increase in ADCD activity (**Supplementary Figure 2**).

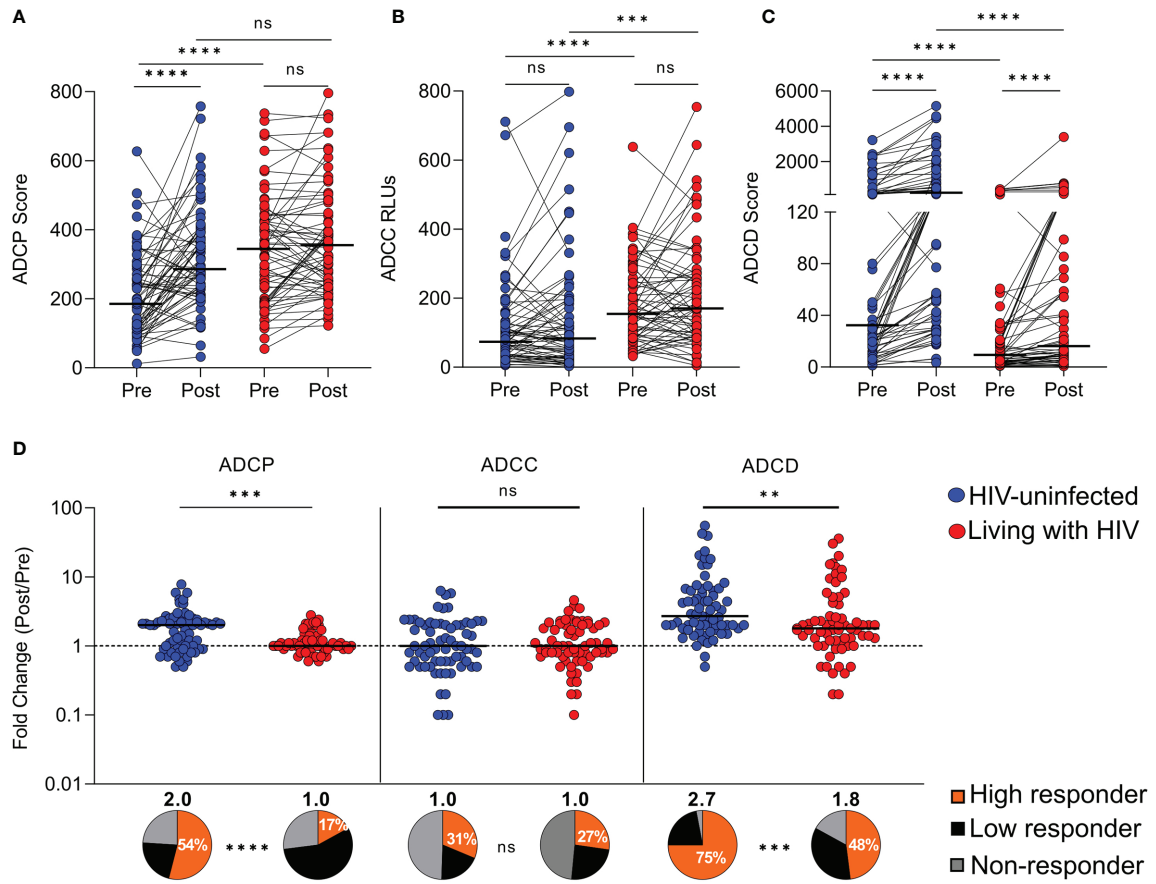

FIGURE 2 | Differential boosting of HA stalk-specific Fc-mediated antibody functions amongst vaccinated women. Pre-vaccination and 1-month post-vaccination H1 stalk-specific **(A)** antibody-dependent cellular phagocytosis (ADCP), **(B)** antibody-dependent cellular cytotoxicity (ADCC) or FcγRIIIa activation and **(C)** antibody-dependent complement deposition (ADCD) are shown where HIV-uninfected participants (n=67), shown in blue and participants living with HIV (n=66), shown in red.**(D)** The fold increases for each of the functions and the proportion (%) of high responders that exceed a 2-fold increase in Fc activity are shown in orange. Low responders, who show reduced enhancement that does not reach a 2-fold increase are shown in black, whilst those not boosted (non-responders) are shown in grey. The lines represent the median. Wilcoxon matched-pairs signed rank tests were used to compare pre-vaccination and post-vaccination functional scores within groups. Mann Whitney U test was used to compare functional scores between the vaccine groups. Fischer's exact tests were used to compare the proportions of high responders. Significant associations are shown as ****p < 0.0001; ***p < 0.001; **p < 0.01; ns,not significant.

The Magnitude of Vaccine-Mediated Boosting of ADCP and ADCD Is Lower in Women Living With HIV

When we compared Fc-mediated functions, we observed differential boosting across the HIV-uninfected women and WLWH for ADCP and ADCD following vaccination (**Figure 2D**). For ADCP the WLWH were not boosted, and the proportion of high responders (individuals that exceeded a 2-fold increase in Fc activity) was significantly lower than in the HIV-uninfected group (17% vs. 54%). Since there was no boosting of ADCC potential, the proportion of high responders was similar between HIV-uninfected women and WLWH (31% vs. 27%). However, for ADCD, in the WLWH the TIV boosting and the proportion of high responders was significantly lower (median fold change 1.8 and high responders 48%) than in the HIV-uninfected women (median fold change 2.7 and high responders 75%). Thus, while ADCD activity was boosted in both groups in response to TIV vaccination, this function was substantially impaired in WLWH prior to vaccination.

Seasonal TIV Does Not Improve Overall Co-Ordination of the Fc-Mediated Responses, Irrespective of HIV Status

Co-ordinated antibody responses elicited by vaccines against other diseases have been associated with increased efficacy (41). We therefore assessed the correlations between HAI titers, stalk-specific responses and Fc-mediated effector functions at baseline and after TIV vaccination and compared these in HIV-uninfected women and WLWH. Prior to vaccination, there was a significant correlation between HAI and HA stalk titers in HIV-uninfected women, but the significant boosting of HAI

antibodies resulted in loss of this correlation post-vaccination (**Figures 3A, B**). In contrast in WLWH, while there was a strong correlation between HA stalk and HAI pre-vaccination (**Figure 3C**), HA stalk titers were boosted simultaneously with HAI titers, as previously reported (32) and remained significantly correlated (**Figure 3D**). In the HIV-uninfected women, ADCP, ADCC, ADCD and FcγRIIa and FcγRIIIa binding were significantly associated with the HA stalk titers before vaccination, and these associations improved slightly following vaccination (**Figures 3A, B**). In WLWH, ADCP, ADCD and FcγRIIa and FcγRIIIa binding were associated with HA stalk titers pre-vaccination, with the FcγRIIIa binding been the only association to not improve, after TIV vaccination (**Figures 3C, D**). We also observed varying relationships amongst the Fc-mediated effector functions. In the HIV-uninfected women, we observed a significant correlation between ADCP and ADCD pre-vaccination, but not post-vaccination. Instead, after vaccination we observed a correlation between ADCC potential and both ADCP and ADCD. The FcγRIIa and FcγRIIIa binding correlated with all the Fc functions both pre- and post-vaccination in the HIV-uninfected women. In contrast, in WLWH the existing association between ADCD and ADCP prior to vaccination was strengthened post-vaccination. There was also an in increase in the FcγRIIa and FcγRIIIa binding associations with all the Fc functions, following vaccination in this group. Therefore, vaccination resulted in nuanced improvements of particular functional relationships that differed between WLWH and HIV-uninfected women, but overall co-ordination of antibody responses and Fc-mediated functions was not significantly improved.

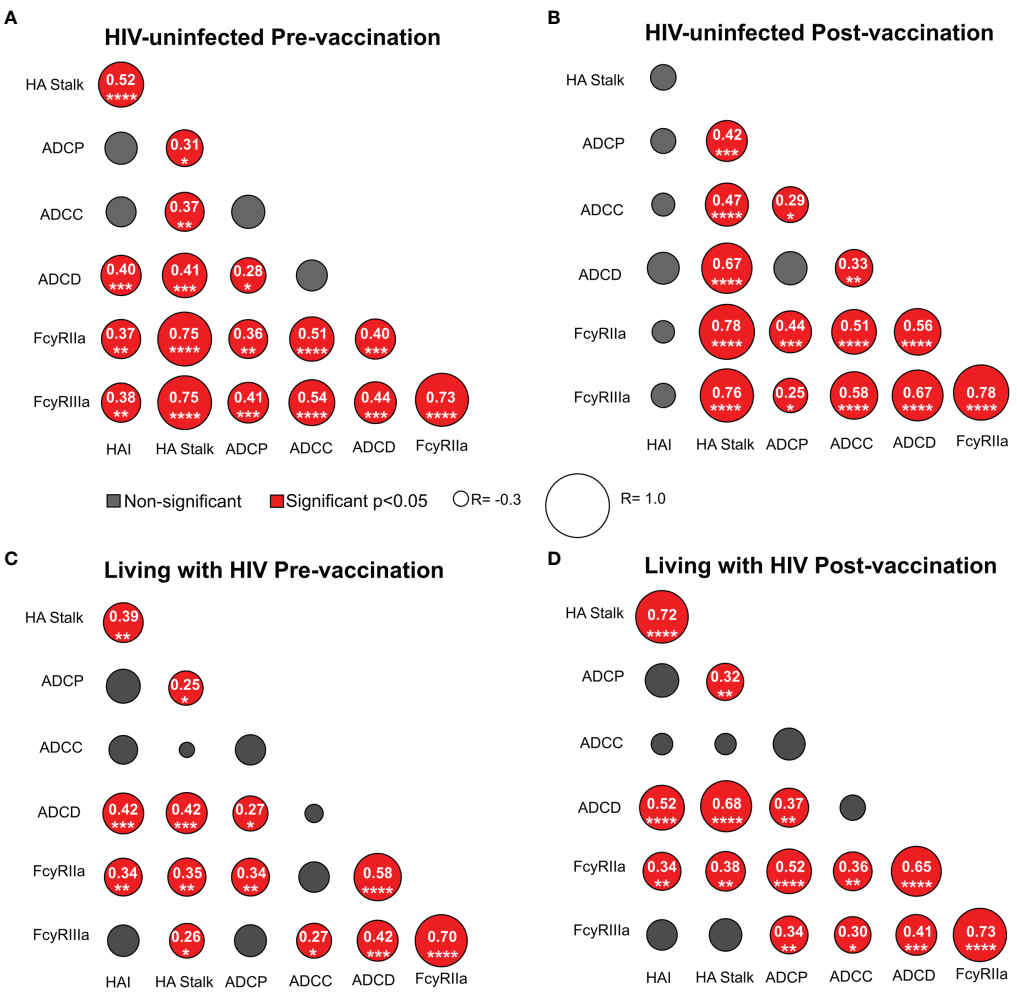

FIGURE 3 | Co-ordination between HAI titers, HA stalk antibodies and HA stalk-specific Fc-mediated functions in response to vaccination. Spearman correlations of Fc effector function and titers in **(A)** HIV-uninfected pre-vaccination, **(B)** HIV-uninfected post-vaccination, **(C)** WLWH pre-vaccination and **(D)** WLWH post-vaccination groups. The asterisks indicate the following statistical significance, ****p < 0.0001; ***p < 0.001; **p < 0.01; *p < 0.05; ns,not significant. Significant correlations are displayed in red. Non-significant correlations are in grey. The size of the circle is proportional to the Spearman correlation coefficients -0.3 been the smallest and 1 been the largest, indicated inside of circles for correlations that were significant.

Stalk-Specific Fc Polyfunctionality of Women Living With HIV Is Not Improved by Vaccination and Is Not Driven by H1 Stalk Antibody Titer

Fc polyfunctionality has been shown to be associated with protective immunity and broader responses in other diseases (41–44). We calculated HA stalk-specific Fc polyfunctionality scores by summing the z-scores of ADCP, ADCC and ADCD for each of the participants. Prior to vaccination, WLWH showed significantly higher Fc polyfunctionality directed at the HA stalk than HIV-uninfected women, as a result of their baseline higher ADCC and ADCP responses (medians 0.89 vs. -0.26) (**Figure 4A**). The proportion of participants with high HA stalk-specific Fc polyfunctionality (the sum of z-scores greater than 0) was also higher for WLWH (76%) than for HIV-uninfected group (45%). Following vaccination, HA stalk-specific Fc polyfunctionality in the HIV-uninfected women significantly increased, reaching the same levels observed in WLWH at baseline. In contrast, WLWH did not show improvement of overall HA stalk-specific Fc-mediated functionality following vaccination.

We next assessed the influence of H1 stalk titer on stalk-specific Fc polyfunctionality after vaccination. In the HIV-uninfected group there was a strong correlation between the HA stalk antibody titers and HA stalk- specific Fc polyfunctionality (r=0,71; p<0.0001) (**Figure 4B**). However, in WLWH we observed no correlation between H1 stalk titers and HA stalk-specific Fc polyfunctionality (r=0,19; p=0.26) (**Figure 4C**). The lack of association in WLWH suggests that in this group, the potency of the Fc–mediated functions is mediated through qualitatively different HA stalk-specific antibodies to those occurring in HIV-uninfected women. Overall, these data indicate a fundamentally different humoral response in WLWH in response to vaccination.

DISCUSSION

HA stalk-specific Fc effector functions have an important complementary role to neutralization in protection against influenza virus infection (45, 46). Therefore, understanding their role in vaccination of high-risk groups, such as PLWH, is crucial but have not been previously studied. In the cohort described here, we observed lower HAI titers and lower HA stalk-specific titers in WLWH than in HIV-uninfected women in response to seasonal influenza vaccination, as reported in our previous studies (6, 32). Despite these lower antibody titers, the vaccine efficacy was higher in WLWH (6). Here, we examined differences in HA stalk-specific Fc-mediated functions between pregnant women living with or without HIV in response to seasonal influenza vaccination in a cohort where the HA stalk antibody titers were previously shown to be protective (32). We observed significant differences in responses; WLWH showed only HA stalk-specific ADCD boosting, whereas in HIV-uninfected women both ADCP and ADCD were significantly enhanced. We also assessed the association between Fc effector functions post-vaccination and found that ADCC or FcγRIIIa activation was coordinated with ADCP and ADCD in HIV-uninfected women but in WLWH only ADCP and ADCD showed improved correlation following vaccination. Furthermore, in HIV-uninfected women overall Fc polyfunctionality was improved following vaccination and was driven by HA stalk antibody titers. In contrast, in WLWH the higher Fc polyfunctionality was not associated with the titers of the HA stalk-specific antibodies. Overall, HA stalk-specific Fc functions were differentially mediated in WLWH in response to seasonal

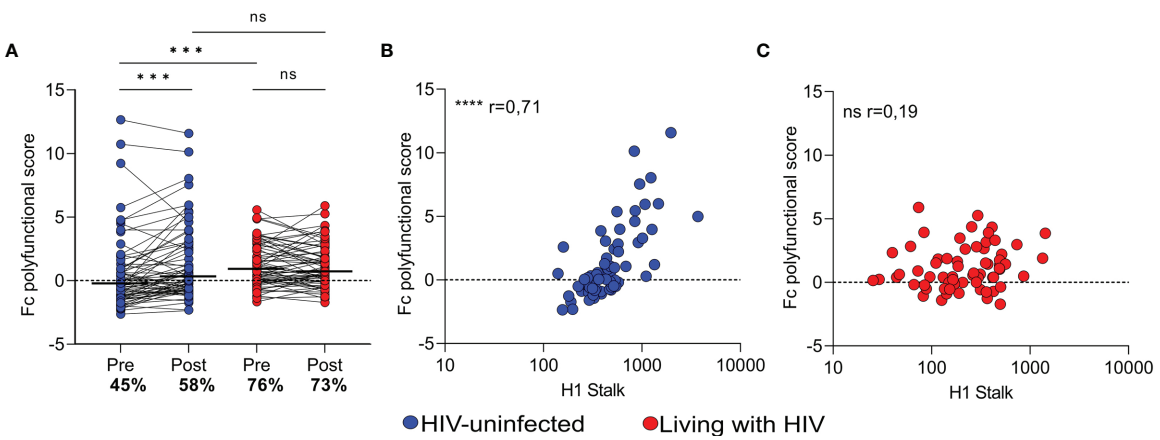

FIGURE 4 | HA stalk-specific Fc polyfunctionality scores of Fc-mediated functions amongst vaccinated women. **(A)** Fc polyfunctionality (determined by the addition of individual standardized Fc function scores), prior to and following vaccination. Dots above 0 indicate Fc polyfunctional individuals, while those below indicate poor Fc polyfunctionality below the mean. The proportion (%) of individuals with Fc polyfunctionality is indicated on the plot. Spearman´s correlation between the Fc polyfunctionality score and HA stalk response in **(B)** HIV-uninfected women and **(C)** WLWH. Wilcoxon matched-pairs signed rank test was used to compare pre-vaccination and post-vaccination polyfunctionality scores within groups. Mann Whitney U test was used to compare polyfunctionality scores between the vaccine groups. Significant associations are shown as ****p < 0.0001; ***p < 0.001; ns,not significant.

influenza vaccination, despite similar boosting of HA stalk antibodies.

Although the WLWH and HIV-uninfected groups were matched for age, there were substantial differences in their baseline responses, prior to vaccination. Both ADCP and ADCC potential were higher in WLWH pre-vaccination. This may be due to increased previous exposures to influenza virus infections in WLWH prior to vaccination, which may have broadened the HA stalk-specific Fc-mediated functions (6, 45). Multiple exposures to divergent influenza virus strains has been shown to prime HA-specific antibodies with the ability to mediate ADCP and ADCC (47). Several studies have provided evidence of this concept, with H7N9 infection and vaccination of healthy people, inducing cross-reactive, ADCC mediating HA stalk antibodies (13, 18, 48). In addition, the WLWH were on ART and this may have allowed for the partial restoration of past HA stalk-specific Fc functionality and together with the vaccine, provided sufficient immunity against influenza virus infections (22).

In this trial, irrespective of HIV status, HA stalk-specific ADCC (measured either through a reporter assay or binding to dimeric FcγRIIIa) was not boosted following vaccination. TIV has elicited variable ADCC responses in humans, with similar findings to ours reported in healthy individuals (49–51), but moderate ADCC boosting has been reported in older adults and PLWH (22, 24, 52). The lack of boosting of ADCC potential in our study, compared to others, may be a consequence of high pre-existing levels of ADCC responses from prior infections in both groups. These responses may be at a "ceiling" and cannot be further significantly boosted following vaccination. The reporter assay that we use in this study has been shown to correlate with traditionally used CD107a NK degranulation assays (40) and is therefore unlikely the reason for the observed lack of boosting.

We observed differences in functions that were boosted in response to vaccination by HIV status. Specifically, ADCP and binding to dimeric FcγRIIa were only boosted in HIV-uninfected women, similar to previous studies (22). However, WLWH had ADCP levels prior to vaccination that exceeded that of HIV-uninfected women. Similarly, a weaker ADCP vaccine response directed at HA has been previously associated with higher baseline levels, similar to those observed here in HIV-uninfected women (23). Post-vaccination ADCP levels in HIV-uninfected women did not exceed the levels in the WLWH, indicating a maximum threshold in HA stalk ADCP activity. In contrast, ADCD was boosted regardless of HIV status, but was significantly lower in the WLWH both pre and post-vaccination suggesting that the ability of antibodies to perform this function was impaired in this group. Despite similar increasing of HA stalk antibody boosting in response to vaccination there were distinct differences in the ability to boost stalk-specific Fc responses associated with HIV co-infection. Overall, these differences show distinct Fc function between WLWH and HIV-uninfected women in response to vaccination.

Vaccination that induces coordinated Fc effector responses has been associated with efficacy in other infectious diseases (41). We observed a loss in the association between HA stalk titers and HAI activity post-vaccination in the HIV-uninfected group but it was strengthened in the WLWH group, as shown previously (32). While the simultaneous elicitation of both head and stalk directed antibodies in WLWH post-vaccination may indicate that the antibody functions behave in a synergistic manner in this group, how HA stalk-specific Fc effector function is affected by broad HAI antibodies was not investigated in this study. This was also observed through the Fc-mediated functions correlating with both HAI and HA stalk titers in WLWH, whilst the Fc effector functions and FcγR binding did not correlate at all with HAI post-vaccination in HIV-uninfected women (previously shown for ADCD pre-vaccination). This, coupled with the observation that HA stalk antibody titer alone did not correlate with overall Fc polyfunctionality in WLWH, suggests that the quality of the Fc responses may have been impacted by both HAI and HA stalk responses in this group which requires further investigation. In addition, it is possible that modulators of Fc effector function such as isotype or glycosylation may differ as a result of HIV infection (53–55). These differences may drive polyfunctionality more robustly than titer in WLWH. This further highlights the differences between WLWH and HIV-uninfected women HA stalk mediated Fc effector functions, of which the differences in response to seasonal influenza vaccination may explain the elevated protection observed for WLWH.

Chimeric hemagglutinin-based vaccines aimed at eliciting cross-reactive HA stalk antibodies have the potential to be developed as universal vaccines. Correlates of protection for this approach should include HA stalk-specific Fc-mediated functions (56). In this cohort, levels of HA stalk antibodies were protective however only ADCP and ADCD were boosted in response to the vaccine in HIV-uninfected women and only ADCD in WLWH, suggesting that these antibody functions may be more important than ADCC in protection. Future studies should determine whether the higher levels of HA stalk-specific ADCP and ADCC potential in the WLWH were enough to confer protection against influenza virus infection or disease severity. In summary, we showed that although HIV-uninfected women exhibited significantly improved Fc polyfunctionality post-vaccination that was driven by HA stalk titer, WLWH mounted fundamentally different HAI and HA stalk coordinated responses, likely impacted by high baseline HA stalk-specific Fc effector function. Our study highlights the need to include, in future clinical trials, high-risk groups who may have different responses.

DATA AVAILABILITY STATEMENT

The original contributions presented in the study are included in the article/**Supplementary Material**. Further inquiries can be directed to the corresponding author.

ETHICS STATEMENT

The studies involving human participants were reviewed and approved by Human Research Ethics Committee of the University of the Witwatersrand. The patients/participants

provided their written informed consent to participate in this study.

AUTHOR CONTRIBUTIONS

BM, PM, and SR conceptualized the study. BM performed experiments, analyzed data, generated the figures and wrote the manuscript. ND performed H1 stalk ELISAs. MN and SM established the trials, collected and provided participant samples and the HAI data. FK provided the chimeric hemagglutinin protein (cH6/1). PM and SR assisted in data interpretation, reviewed and edited the manuscript and supervised the research. All authors contributed to the manuscript and approved the submitted version.

FUNDING

This sub-study is funded by the African Leadership in Vaccinology Expertise (ALIVE) research grant of the University of the Witwatersrand. BM is a recipient of bursaries from the South African National Research Foundation, the Poliomyelitis Research Foundation (grant 20/36) and the University of the Witwatersrand postgraduate merit award. PM is supported by the South African Research Chairs Initiative of the Department of Science and Innovation and National Research Foundation of South Africa, the SA Medical Research Council SHIP program (grant 98341), the Centre for the AIDS Program of Research (CAPRISA). SR is a L'Oreal/ UNESCO Women in Science South Africa Young Talents awardee. The funders were not involved in the study design, collection, analysis, interpretation of data, the writing of this article or the decision to submit it for publication. Related research by the authors is conducted as part of the DST-NRF Centre of Excellence in HIV Prevention, which is supported by the Department of Science and Technology and the National Research Foundation. Generation of reagents in the Krammer laboratory was supported by Centers of Excellence for influenza Research and Response (75N93021C00014) and Collaborative Influenza Vaccine Innovation Centers (75N93019C00051).

ACKNOWLEDGMENTS

We thank Prof. Mark Hogarth (Burnet Institute, Melbourne, Australia) for the dimeric FcγR constructs. The authors acknowledge Dr. Adriana Weinberg (University of Colorado, Denver) for testing of HAI titers. We thank all the trial participants, clinical staff and the Maternal Flu trial team.

SUPPLEMENTARY MATERIAL

The Supplementary Material for this article can be found online at: https://www.frontiersin.org/articles/10.3389/fimmu.2022.873191/full#supplementary-material

REFERENCES

1. Tempia S, Walaza S, Moyes J, Cohen AL, McMorrow ML, Treurnicht FK, et al. Quantifying How Different Clinical Presentations, Levels of Severity, and Healthcare Attendance Shape the Burden of Influenza-Associated Illness: A Modeling Study From South Africa. *Clin Infect Dis* (2019) 69:1036–48. doi: 10.1093/CID/CIY1017
2. McMorrow ML, Tempia S, Walaza S, Treurnicht FK, Ramkrishna W, Azziz-Baumgartner E, et al. Prioritization of Risk Groups for Influenza Vaccination in Resource Limited Settings - A Case Study From South Africa. *Vaccine* (2019) 37:25–33. doi: 10.1016/J.VACCINE.2018.11.048
3. Tasker SA, Treanor JJ, Paxton WB, Wallace MR. Efficacy of Influenza Vaccination in HIV-Infected Persons. *Ann Intern Med* (1999) 131:430–3. doi: 10.7326/0003-4819-131-6-199909210-00006
4. Tebas P, Frank I, Lewis M, Quinn J, Zifchak L, Thomas A, et al. Poor Immunogenicity of the H1N1 2009 Vaccine in Well Controlled HIV-Infected Individuals. *AIDS* (2010) 24:2187–92. doi: 10.1097/QAD.0B013E32833C6D5C
5. Madhi SA, Maskew M, Koen A, Kuwanda L, Besselaar TG, Naidoo D, et al. Trivalent Inactivated Influenza Vaccine in African Adults Infected With Human Immunodeficient Virus: Double Blind, Randomized Clinical Trial of Efficacy, Immunogenicity, and Safety. *Clin Infect Dis* (2011) 52:128–37. doi: 10.1093/CID/CIQ004
6. Madhi SA, Cutland CL, Kuwanda L, Weinberg A, Hugo A, Jones S, et al. Influenza Vaccination of Pregnant Women and Protection of Their Infants. *N Engl J Med* (2014) 371:918–31. doi: 10.1056/NEJMoa1401480
7. Lau YF, Tang LH, Chien Lye D, Ooi EE, Leo YS. Serological Response to Trivalent Inactivated Influenza Vaccine in HIV-Infected Adults in Singapore. *Hum Vaccin Immunother* (2017) 13:551–60. doi: 10.1080/21645515.2016.1246636
8. Nunes MC, Cutland CL, Moultrie A, Jones S, Ortiz JR, Neuzil KM, et al. Immunogenicity and Safety of Different Dosing Schedules of Trivalent Inactivated Influenza Vaccine in Pregnant Women With HIV: A Randomised Controlled Trial. *Lancet HIV* (2020) 7:e91–103. doi: 10.1016/S2352-3018(19)30322-4
9. Ohmit SE, Petrie JG, Cross RT, Johnson E, Monto AS. Influenza Hemagglutination-Inhibition Antibody Titer as a Correlate of Vaccine-Induced Protection. *J Infect Dis* (2011) 204:1879–85. doi: 10.1093/infdis/jir661
10. Kirkpatrick E, Qiu X, Wilson PC, Bahl J, Krammer F. The Influenza Virus Hemagglutinin Head Evolves Faster Than the Stalk Domain. *Sci Rep* (2018) 8:1–14. doi: 10.1038/s41598-018-28706-1
11. Estrada LD, Schultz-Cherry S. Development of a Universal Influenza Vaccine. *J Immunol* (2019) 202:392–8. doi: 10.4049/JIMMUNOL.1801054
12. DiLillo DJ, Tan GS, Palese P, Ravetch JV. Broadly Neutralizing Hemagglutinin Stalk–Specific Antibodies Require Fcγr Interactions for Protection Against Influenza Virus *in Vivo*. *Nat Med* (2014) 20:143–51. doi: 10.1038/nm.3443
13. Vanderven HA, Liu L, Ana-Sosa-Batiz F, Nguyen THO, Wan Y, Wines B, et al. Fc Functional Antibodies in Humans With Severe H7N9 and Seasonal Influenza. *JCI Insight Clin Med* (2017) 13:e92750. doi: 10.1172/jci.insight.92750
14. Arunkumar AG, Ioannou A, Wohlbold TJ, Meade P, Aslam S, Amanat F, et al. Broadly Cross-Reactive, Nonneutralizing Antibodies Against Influenza B Virus Hemagglutinin Demonstrate Effector Function-Dependent Protection Against Lethal Viral Challenge in Mice. *J Virol* (2019) 93:e01696-18. doi: 10.1128/JVI.01696-18
15. Boudreau CM, Yu WH, Suscovich TJ, Talbot HK, Edwards KM, Alter G. Selective Induction of Antibody Effector Functional Responses Using MF59-Adjuvanted Vaccination. *J Clin Invest* (2020) 130:662–72. doi: 10.1172/JCI129520
16. Terajima M, Ennis FA, Terajima M, Cruz J, Lee J-H, Wrammert J, et al. Complement-Dependent Lysis of Influenza A Virus-Infected Cells by Broadly Cross-Reactive Human Monoclonal Antibodies. *J Virol* (2012) 86:1901–1. doi: 10.1128/jvi.06884-11
17. Mullarkey CE, Bailey MJ, Golubeva DA, Tan GS, Nachbagauer R, He W, et al. Broadly Neutralizing Hemagglutinin Stalk-Specific Antibodies Induce Potent

Phagocytosis of Immune Complexes by Neutrophils in an Fc-Dependent Manner. *MBio* (2016) 7:e01624-16. doi: 10.1128/mBio.01624-16
18. Dunand HCJ, Leon PE, Huang M, Choi A, Chromikova V, Ho IY, et al. Both Neutralizing and Non-Neutralizing Human H7N9 Influenza Vaccine-Induced Monoclonal Antibodies Confer Protection. *Cell Host Microbe* (2016) 19:800–13. doi: 10.1016/J.CHOM.2016.05.014
19. Florek NW, Weinfurter JT, Jegaskanda S, Brewoo JN, Powell TD, Young GR, et al. Modified Vaccinia Virus Ankara Encoding Influenza Virus Hemagglutinin Induces Heterosubtypic Immunity in Macaques. *J Virol* (2014) 88:13418–28. doi: 10.1128/JVI.01219-14
20. Tan G, Leon PE, Albrecht RA, Margine I, Hirsh A, Bahl J, et al. Broadly-Reactive Neutralizing and Non-Neutralizing Antibodies Directed Against the H7 Influenza Virus Hemagglutinin Reveal Divergent Mechanisms of Protection. *PloS Pathog* (2016) 12:e1005578. doi: 10.1371/JOURNAL.PPAT.1005578
21. Rattan A, Pawar SD, Nawadkar R, Kulkarni N, Lal G, Mullick J, et al. Synergy Between the Classical and Alternative Pathways of Complement is Essential for Conferring Effective Protection Against the Pandemic Influenza A(H1N1) 2009 Virus Infection. *PloS Pathog* (2017) 13:e1006248. doi: 10.1371/JOURNAL.PPAT.1006248
22. Kristensen AB, Lay WN, Ana-Sosa-Batiz F, Vanderven HA, Madhavi V, Laurie KL, et al. Antibody Responses With Fc-Mediated Functions After Vaccination of HIV-Infected Subjects With Trivalent Influenza Vaccine. *J Virol* (2016) 90:5724–34. doi: 10.1128/JVI.00285-16
23. Ana-Sosa-Batiz F, Johnston APR, Hogarth PM, Wines BD, Barr I, Wheatley AK, et al. Antibody-Dependent Phagocytosis (ADP) Responses Following Trivalent Inactivated Influenza Vaccination of Younger and Older Adults. *Vaccine* (2017) 35:6451–8. doi: 10.1016/j.vaccine.2017.09.062
24. Vanderven HA, Barr I, Reynaldi A, Wheatley AK, Wines BD, Davenport MP, et al. Fc Functional Antibody Responses to Adjuvanted Versus Unadjuvanted Seasonal Influenza Vaccination in Community-Dwelling Older Adults. *Vaccine* (2020) 38:2368–77. doi: 10.1016/j.vaccine.2020.01.066
25. Tempia S, Walaza S, Viboud C, Cohen AL, Madhi SA, Venter M, et al. Deaths Associated With Respiratory Syncytial and Influenza Viruses Among Persons ≥5 Years of Age in HIV-Prevalent Area, South Africa, 1998–2009. *Emerg Infect Dis* (2015) 21:600. doi: 10.3201/EID2104.141033
26. Louie JK, Acosta M, Jamieson DJ, Honein MA. Severe 2009 H1N1 Influenza in Pregnant and Postpartum Women in California. *N Engl J Med* (2010) 362:27–35. doi: 10.1056/NEJMOA0910444
27. Cohen C, Simonsen L, Sample J, Kang J-W, Miller M, Madhi SA, et al. Influenza-Related Mortality Among Adults Aged 25–54 Years With AIDS in South Africa and the United States of America. *Clin Infect Dis* (2012) 55:996. doi: 10.1093/CID/CIS549
28. Kroon FP, van Dissel JT, de Jong JC, van Furth R. Antibody Response to Influenza, Tetanus and Pneumococcal Vaccines in HIV-Seropositive Individuals in Relation to the Number of CD4+ Lymphocytes. *AIDS* (1994) 8:469–76. doi: 10.1097/00002030-199404000-00008
29. Malaspina A, Moir S, Orsega SM, Vasquez J, Miller NJ, Donoghue ET, et al. Compromised B Cell Responses to Influenza Vaccination in HIV-Infected Individuals. *J Infect Dis* (2005) 191:1442–50. doi: 10.1086/429298
30. Pallikkuth S, De Armas LR, Pahwa R, Rinaldi S, George VK, Sanchez CM, et al. Impact of Aging and HIV Infection on Serologic Response to Seasonal Influenza Vaccination. *AIDS* (2018) 32:1085. doi: 10.1097/QAD.0000000000001774
31. Cooper C, Thorne A, Klein M, Conway B, Boivin G, Haase D, et al. Immunogenicity Is Not Improved by Increased Antigen Dose or Booster Dosing of Seasonal Influenza Vaccine in a Randomized Trial of HIV Infected Adults. *PloS One* (2011) 6:e17758. doi: 10.1371/JOURNAL.PONE.0017758
32. Dhar N, Kwatra G, Nunes MC, Cutland C, Izu A, Nachbagauer R, et al. Hemagglutinin Stalk Antibody Responses Following Trivalent Inactivated Influenza Vaccine Immunization of Pregnant Women and Association With Protection From Influenza Virus Illness. *Clin Infect Dis* (2020) 71:1072–9. doi: 10.1093/cid/ciz927
33. Miller MS, Tsibane T, Krammer F, Hai R, Rahmat S , Basler CF, et al. 1976 and 2009 H1N1 Influenza Virus Vaccines Boost Anti-Hemagglutinin Stalk Antibodies in Humans. *J Infect Dis* (2013) 207:98–105. doi: 10.1093/infdis/jis652
34. Dreyfus C, Laursen NS, Kwaks T, Zuijdgeest D, Khayat R, Ekiert DC, et al. Highly Conserved Protective Epitopes on Influenza B Viruses. *Sci (80-)* (2012) 337:1343–8. doi: 10.1126/science.1222908
35. Weinberg A, Song L-Y, Walker R, Allende M, Fenton T, Patterson-Bartlett J, et al. Anti-Influenza Serum and Mucosal Antibody Responses After Administration of Live Attenuated or Inactivated Influenza Vaccines to HIV-Infected Children. *JAIDS J Acquir Immune Defic Syndr* (2010) 55:189–96. doi: 10.1097/QAI.0b013e3181e46308
36. Ackerman ME, Moldt B, Wyatt RT, Dugast A-S, McAndrew E, Tsoukas S, et al. A Robust, High-Throughput Assay to Determine the Phagocytic Activity of Clinical Antibody Samples. *J Immunol Methods* (2011) 366:8–19. doi: 10.1016/j.jim.2010.12.016
37. Butler SE, Crowley AR, Natarajan H, Xu S, Weiner JA, Bobak CA, et al. Distinct Features and Functions of Systemic and Mucosal Humoral Immunity Among SARS-CoV-2 Convalescent Individuals. *Front Immunol* (2021) 11:618685. doi: 10.3389/fimmu.2020.618685
38. Fischinger S, Fallon JK, Michell AR, Broge T, Suscovich TJ, Streeck H, et al. High-Throughput, Bead-Based, Antigen-Specific Assay to Assess the Ability of Antibodies to Induce Complement Activation. *J Immunol Methods* (2019) 473:112630. doi: 10.1016/j.jim.2019.07.002
39. Wines BD, Vanderven HA, Esparon SE, Kristensen AB, Kent SJ, Hogarth PM. Dimeric Fcγr Ectodomains as Probes of the Fc Receptor Function of Anti-Influenza Virus IgG. *J Immunol* (2016) 197:1507–16. doi: 10.4049/jimmunol.1502551
40. Chromikova V, Tan J, Aslam S, Rajabhathor A, Bermudez-Gonzalez M, Ayllon J, et al. Activity of Human Serum Antibodies in an Influenza Virus Hemagglutinin Stalk-Based ADCC Reporter Assay Correlates With Activity in a CD107a Degranulation Assay. *Vaccine* (2020) 38:1953–61. doi: 10.1016/J.VACCINE.2020.01.008
41. Chung AW, Ghebremichael M, Robinson H, Brown E, Choi I, Lane S, et al. Polyfunctional Fc-Effector Profiles Mediated by IgG Subclass Selection Distinguish RV144 and VAX003 Vaccines. *Sci Transl Med* (2014) 6:38. doi: 10.1126/scitranslmed.3007736
42. Gunn BM, Yu WH, Karim MM, Brannan JM, Herbert AS, Wec AZ, et al. A Role for Fc Function in Therapeutic Monoclonal Antibody-Mediated Protection Against Ebola Virus. *Cell Host Microbe* (2018) 24:221–233.e5. doi: 10.1016/J.CHOM.2018.07.009
43. Richardson SI, Chung AW, Natarajan H, Mabvakure B, Mkhize NN, Garrett N, et al. HIV-Specific Fc Effector Function Early in Infection Predicts the Development of Broadly Neutralizing Antibodies. *PloS Pathog* (2018) 14:e1006987. doi: 10.1371/journal.ppat.1006987
44. Natarajan H, Crowley AR, Butler SE, Xu S, Weiner JA, Bloch EM, et al. Markers of Polyfunctional SARS-CoV-2 Antibodies in Convalescent Plasma. *Am Soc Microbiol* (2021) 12:e00765–21. doi: 10.1128/mBio
45. Vanderven HA, Jegaskanda S, Wheatley AK, Kent SJ. Antibody-Dependent Cellular Cytotoxicity and Influenza Virus. *Curr Opin Virol* (2017) 22:89–96. doi: 10.1016/j.coviro.2016.12.002
46. Boudreau CM, Alter G. Extra-Neutralizing FcR-Mediated Antibody Functions for a Universal Influenza Vaccine. *Front Immunol* (2019) 10:440. doi: 10.3389/fimmu.2019.00440
47. Ana-Sosa-Batiz F, Vanderven H, Jegaskanda S, Johnston A, Rockman S, Laurie K, et al. Influenza-Specific Antibody-Dependent Phagocytosis. *PloS One* (2016) 11:e0154461. doi: 10.1371/journal.pone.0154461
48. Koup RA, Narpala SR, Joyce MG, Boyington JC, Leung K, Chambers MJ, et al. Preferential Induction of Cross-Group Influenza A Hemagglutinin Stem–Specific Memory B Cells After H7N9 Immunization in Humans. *Sci Immunol* (2017) 2:eaan2676. doi: 10.1126/sciimmunol.aan2676
49. Jegaskanda S, Luke C, Hickman HD, Sangster MY, Wieland-Alter WF, McBride JM, et al. Generation and Protective Ability of Influenza Virus–Specific Antibody-Dependent Cellular Cytotoxicity in Humans Elicited by Vaccination, Natural Infection, and Experimental Challenge. *J Infect Dis* (2016) 214:945–52. doi: 10.1093/infdis/jiw262
50. Vanderven HA, Jegaskanda S, Wines BD, Hogarth PM, Carmuglia S, Rockman S, et al. Antibody-Dependent Cellular Cytotoxicity Responses to Seasonal Influenza Vaccination in Older Adults. *J Infect Dis* (2018) 217:12–23. doi: 10.1093/infdis/jix554
51. Hashimoto G, Wright PF, Karzon DT. Antibody-Dependent Cell-Mediated Cytotoxicity Against Influenza Virus-Infected Cells. *J Infect Dis* (1983) 148:785–94. doi: 10.1093/INFDIS/148.5.785
52. Jegaskanda S, Laurie KL, Amarasena TH, Winnall WR, Kramski M, De Rose R, et al. Age-Associated Cross-Reactive Antibody-Dependent

Cellular Cytotoxicity Toward 2009 Pandemic Influenza A Virus Subtype H1n1. *J Infect Dis* (2013) 208:1051–61. doi: 10.1093/infdis/jit294

53. Ackerman ME, Crispin M, Yu X, Baruah K, Boesch AW, Harvey DJ, et al. Natural Variation in Fc Glycosylation of HIV-Specific Antibodies Impacts Antiviral Activity. *J Clin Invest* (2013) 123:2183–92. doi: 10.1172/JCI65708
54. Cheng HD, Dowell KG, Bailey-Kellogg C, Goods BA, Love JC, Ferrari G, et al. Diverse Antiviral IgG Effector Activities are Predicted by Unique Biophysical Antibody Features. *Retrovirology* (2021) 18:1–12. doi: 10.1186/S12977-021-00579-9/FIGURES/4
55. Alter G, Ottenhoff THM, Joosten SA. Antibody Glycosylation in Inflammation, Disease and Vaccination. *Semin Immunol* (2018) 39:102–10. doi: 10.1016/J.SMIM.2018.05.003
56. Nachbagauer R, Feser J, Naficy A, Bernstein DI, Guptill J, Walter EB, et al. A Chimeric Hemagglutinin-Based Universal Influenza Virus Vaccine Approach Induces Broad and Long-Lasting Immunity in a Randomized, Placebo-Controlled Phase I Trial. *Nat Med* (2020) 27:106–14. doi: 10.1038/s41591-020-1118-7

Conflict of Interest: FK reports royalties (Avimex), consulting fees (Pfizer, Seqirus, Third Rock Ventures and Avimex), and payment for academic lectures during the past two years. FK is also named as inventor on IP filed by the Icahn School of Medicine at Mount Sinai for influenza virus vaccines and therapeutics, SARS-CoV-2 vaccines and SARS-CoV-2 serological assays.

The remaining authors declare that the research was conducted in the absence of any commercial or financial relationships that could be construed as a potential conflict of interest.

Publisher's Note: All claims expressed in this article are solely those of the authors and do not necessarily represent those of their affiliated organizations, or those of the publisher, the editors and the reviewers. Any product that may be evaluated in this article, or claim that may be made by its manufacturer, is not guaranteed or endorsed by the publisher.

Frontiers in Immunology

Explores novel approaches and diagnoses to treat immune disorders.

The official journal of the International Union of Immunological Societies (IUIS) and the most cited in its field, leading the way for research across basic, translational and clinical immunology.

Discover the latest Research Topics

See more →

Frontiers

Avenue du Tribunal-Fédéral 34
1005 Lausanne, Switzerland
frontiersin.org

Contact us

+41 (0)21 510 17 00
frontiersin.org/about/contact